

Metal-catalyzed Approaches to the Synthesis of Indolizine Derivatives from 2-Pyridinyl-substituted *para*-Quinone Methides and/or 2-(2-Enynyl)pyridines

FEROZ AHMAD

*A thesis submitted for the partial fulfillment of
the degree of Doctor of Philosophy*



Department of Chemical Sciences

**Indian Institute of Science Education and Research (IISER) Mohali
Knowledge City, Sector 81, S. A. S. Nagar, Manauli PO, Mohali, 140306, Punjab, India.**

November 2023

Dedicated

To

My beloved Parents

&

My Friends

Declaration

The work presented in this thesis has been carried out by me under the guidance of **PROF. R. VIJAYA ANAND** at the Indian Institute of Science Education and Research Mohali. This work has not been submitted in part or in full for a degree, a diploma, or a fellowship to any other university or institute. Whenever contributions of others are involved, every effort is made to indicate this clearly, with due acknowledgement of collaborative research and discussions. This thesis is a bonafide record of original work done by me and all sources listed within have been detailed in the bibliography.

FEROZ AHMAD

In my capacity as the supervisor of the candidate's thesis work, I certify that the above statements by the candidate are true to the best of my knowledge.

PROF. R. VIJAYA ANAND

Acknowledgments

First and foremost, I would like to express my gratitude to Almighty God for His blessings and guidance. Without His unwavering support, I would not have been able to achieve this milestone. As I am writing this acknowledgment section, I am overwhelmed with emotions. Completing my Ph.D. journey has been an incredible experience, full of challenges, triumphs, and moments of self-doubt. But through it all, I have been blessed with the support, encouragement, and love of many incredible people, and I am eternally grateful.

First, I would like to express my sincere appreciation and gratitude to my Ph.D. thesis supervisor, **Prof. R. Vijaya Anand**, for his invaluable guidance, encouragement, and constant support throughout my Ph.D. I am incredibly thankful for his excellent guidance, invaluable discussions, and wisdom. Though I have minimal exposure to fundamental lab techniques from industry, his teaching improved my practical skills to a higher level during my research period. I am forever thankful and indebted to him for allowing me to work in his lab and for sharing his knowledge, expertise, guidance, and consistent encouragement throughout this journey. Without his guidance and constant support, I would never have been able to complete this journey. Further, the daily discussions with his active participation and scientific liberty in the lab sharpened my intellectual ability. They stimulated a positive attitude to enhance my growth as a human, for which I am indebted to him. I feel privileged to submit my Ph.D. thesis under his unconditional supervision.

Further, I extend my gratitude to my Doctoral Committee Members, Dr. Sugumar Venkataramani and Dr. Ujjal K. Gautam, for their invaluable discussions, feedback, and constructive advice and for evaluating my research progress on yearly bases by spending their valuable time. They have provided insightful comments on my research that have substantially aided this accomplishment.

I want to thank former Directors of IISER Mohali, Professor N. Sathyamurthy and Professor Debi P. Sarkar, and the Current Director, Professor Gauri Shankar, for providing the world-class infrastructure and facilities at IISER Mohali. I want to thank former Heads of Department (HOD) of chemical sciences IISER Mohali, Prof. K. S. Viswanathan, Prof. S. Arulananda Babu, and current Head of Department (HOD), Prof. Sanjay Singh, for providing the necessary facilities at the Department of Chemical Sciences. I also acknowledge IISER Mohali for NMR, HRMS, IR, XRD, and other facilities.

Furthermore, I am also obliged to my lab mates Dr. Dilip K. Paluru, Dr. Sriram Mahesh, Dr. Abhijeet S. Jadhav, Dr. Prithwish Goswami, Dr. Priya Gosh, Dr. Akshi Tyagi, Mrs. Guddi Kant, Mr. Pavit K. Ranga, Dr. Yogesh A. Pankhade, Dr. Gurdeep Singh, Dr. Rajat Panday, Dr. Sonam Sharma, Dr. Rekha Yadav, Shaheen Fatma, Akshay, Arun, Shruthy, Athira, Divyanshu, Tarunjeet, Vaibhav Kumar, Piyush Saini, Munnu Kumar for their valuable discussions, co-operation and for creating a healthy environment around me. I am whole-heartedly thankful to them for their moral boost and support. I am grateful to Dr. Gurdeep Singh, Ashrumochan Gouda, and Jyotiranjana for their help and assistance during the projects. I am also obliged to Dr. Sandeep Kumar Thakur for his help in solving the crystal structure. I am very thankful to Dr. Gurdeep Singh for his generous support in correcting my thesis. I also acknowledge all the summer trainees who worked with me in our lab.

I am also thankful to Mr. Balbir and Mr. Triveni for their help. I want to acknowledge the chemistry teaching lab assistants, especially Mr. Mangat, Mr. Bahadur, and Mr. Satwinder, for their co-operation during my research period.

Words are inadequate to explain my gratitude to all my friends, especially Dr. Basharat Ali, Dr. Mohd Javed, Dr. Mohd Shareef, Dr. Hadi Ali, Dr. Jaskaran Singh, Dr. Bara Singh, Dr. Gurdeep Singh, Dr. Mayank, Dr. Gaurav, Dr. Sandeep Kumar Thakur, Ms. Chandarkala Negi, Mr. Prateek Ahuja, Mr. Prabhakar Singh, Dr. Ankit Kumar Gaur, Mr. Himanshu Kumar, Dr. Pravesh Kumar, Dr. Mayank Joshi and all the friends at IISER-Mohali who are always with me through good and bad phases of my life. To my friends, both old and new, thank you all for being there for me during all the ups and downs of this journey. Your support, encouragement, and laughter have kept me going, even on the most challenging days. I am grateful for every moment we spend together and look forward to many more.

I must also acknowledge the University grants commission (UGC), New Delhi, for my research fellowship during my doctoral study. I would also like to thank the Department of Science and Technology (DST), India, and IISER Mohali for funding and allowing me to complete my Ph.D.

I would also like to acknowledge the Chemistry Ph.D. cricket team for their support, encouragement, and friendship throughout these years. They have been a source of inspiration and motivation, not only on the field but also in my academic pursuits. Their friendship and camaraderie have made this journey more enjoyable and memorable.

I am also grateful to all my teachers from the bottom of my heart for their guidance and inspiration from the tender stage of my career. I wish to express my sincere gratitude to my beloved parents (Mr. **Mohd Solah** and Mrs. **Nissa Banoo**) and siblings (**Fayaz Ahmad, Nargis Banoo, Shahar Banoo**, and **Suqra Banoo**) who have always believed in me, stood with me, and supported me in all circumstances with unconditional love throughout my life. Their love, encouragement, and unwavering belief in me have been a constant source of strength, inspiration, and motivation, and I am deeply grateful for their love and support. Their continuous prayers for me and my progress have allowed me to complete this journey.

Lastly, I want to thank everyone who has supported me on this journey. Your love, encouragement, and belief in me have meant more than words can express. Thank you all for being a part of this unforgettable journey.

Abstract

The research work presented in this thesis primarily focuses on *Metal-catalyzed Approaches to the Synthesis of Indolizine Derivatives from 2-Pyridinyl-substituted para-Quinone Methides (p-QMs) and/or 2-(2-Enynyl)pyridines*. This thesis is divided into two parts, namely Part A and Part B. Part A describes the synthesis of indolizine-based heterocycles from 2-pyridinyl substituted *para*-quinone methides using suitable coupling partners such as terminal alkynes and *N,N*-dimethyl enaminones; Part B involves the synthesis of indolizine-based unsymmetrical triarylmethane derivatives through copper-catalyzed reactions between 2-(2-enynyl)pyridines and boronic acids or 2-hydroxyphenyl-substituted *N,N*-dimethyl enaminones.

Part A: Synthesis of Indolizine-based heterocycles from 2-pyridinyl-substituted para-quinone methides (p-QMs)

Part A is subdivided into three chapters.

Chapter 1: General introduction to the synthesis of heterocycles from functionalized para-quinone methides

In this Chapter, the synthetic applications of functionalized *para*-quinone methides for the syntheses of oxygen and nitrogen-containing heterocycles have been briefly discussed.

Chapter 2: Pd(II)-Catalyzed annulation of terminal alkynes with 2-pyridinyl-substituted para-quinone methides: Direct access to indolizines

This chapter describes the synthesis of 1,3-disubstituted indolizine derivatives from 2-pyridinyl substituted *p*-QMs through a Pd(II)-catalyzed regiospecific [3+2]-annulation with terminal alkynes. The indolizine scaffold is widely found in many natural products and biologically active molecules, and several of them display a variety of pharmacological activities such as anti-cancer, anti-bacterial, anti-oxidant, and cytotoxic properties. Besides these, they have also found application in material science as fluorescent probes, dye for dye-sensitized solar cells (DSSC), and as a material in organic light-emitting diodes (OLEDs) and in the agricultural sector as herbicide and fungicide (Figure 1). Although numerous synthetic approaches to efficiently access the indolizine moiety have been reported in the literature, most of them require pre-functionalized starting material and multistep synthesis of starting materials. As a result, both economically and in terms of reaction conditions, an easy and atom-economical approach to the synthesis of indolizine derivatives is highly desirable. While working in the field of *p*-QMs as a 1,6-conjugate acceptor and its utilization for the synthesis of various

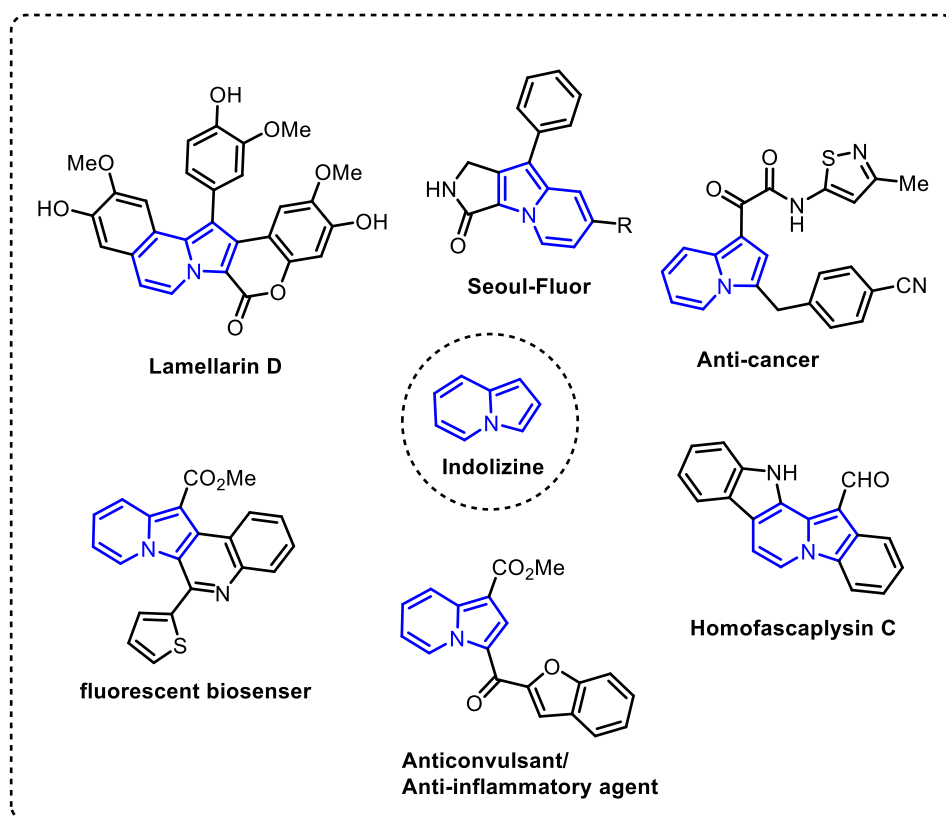
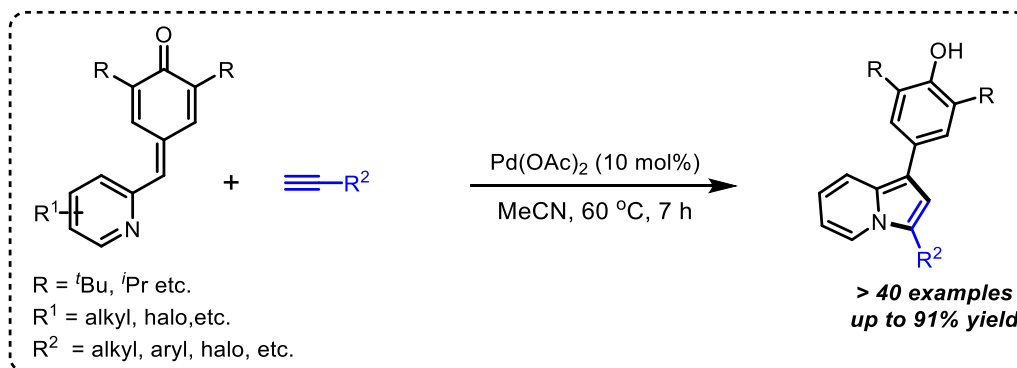


Figure 1. Representative examples of natural products and bioactive indolizine derivatives

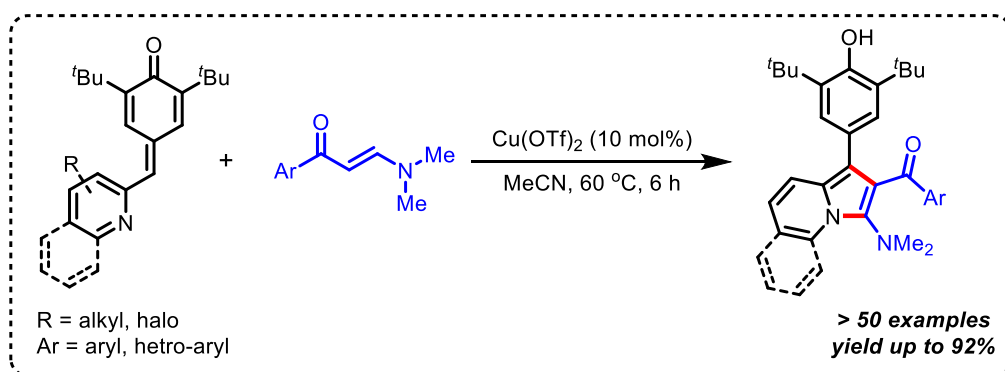
carbocycles and heterocycles, we hypothesized that the 2-pyridinyl substituted *p*-QMs could be used as a three-atom synthon for the synthesis of substituted indolizine derivatives through a [3+2]-annulation with terminal alkynes (Scheme 1). This protocol worked well with most of the terminal alkynes, and the corresponding indolizine derivatives were obtained in moderate to good yields. Control experiments revealed that the reaction takes place through a regioselective [3+2]-annulation of terminal alkynes with 2-pyridinyl substituted *para*-quinone methides.



Scheme 1. Synthesis of 1, 3-disubstituted indolizines from *p*-QMs and terminal alkynes

Chapter 3: Cu(II)-Catalyzed [3+2]-annulation of 2-pyridinyl-substituted *p*-quinone methides with enaminones: Access to functionalized indolizine derivatives

This chapter describes the synthesis of 3-amino-1,2-disubstituted indolizine derivatives from *p*-QMs. While exploring the synthesis of indolizine heterocycles from *p*-QMs, we have further



Scheme 2. Synthesis of 3-amino-1,2-disubstituted indolizine derivatives from *p*-QMs

hypothesized that *N,N*-dimethyl enaminones could be utilized as a two-carbon synthon for the synthesis of functionalized indolizines through the initial 1,6-conjugate addition of enaminone to *p*-QMs followed by a 5-*exo*-trig-cyclization and subsequent aromatization to afford the functionalized indolizine derivatives (Scheme 2). In line with this concept, we have developed a Cu[II]-catalyzed one-pot approach for the synthesis of 3-amino-2,3-disubstituted indolizine derivatives from 2-pyridinyl substituted *p*-QMs and *N,N*-dimethyl enaminones as the reaction partners.

Part B: Synthesis of indolizine-based unsymmetrical triarylmethanes from 2-(2-enynyl)pyridines

Part B is further subdivided into two chapters.

Chapter 1: Copper-catalyzed synthesis of indolizine containing unsymmetrical triarylmethane derivatives from 2-(2-enynyl)pyridines

This chapter deals with the synthesis of indolizine-based unsymmetrical triarylmethane derivatives. In recent years, triarylmethanes (TAMs) have emerged as important and integral scaffolds in many pharmaceuticals and biologically active molecules (Figure 2). Several of them, especially the unsymmetrical ones, exhibit important therapeutic activities and are being explored as anti-breast cancer, anti-viral and anti-TB, and anti-fungal agents. Besides the

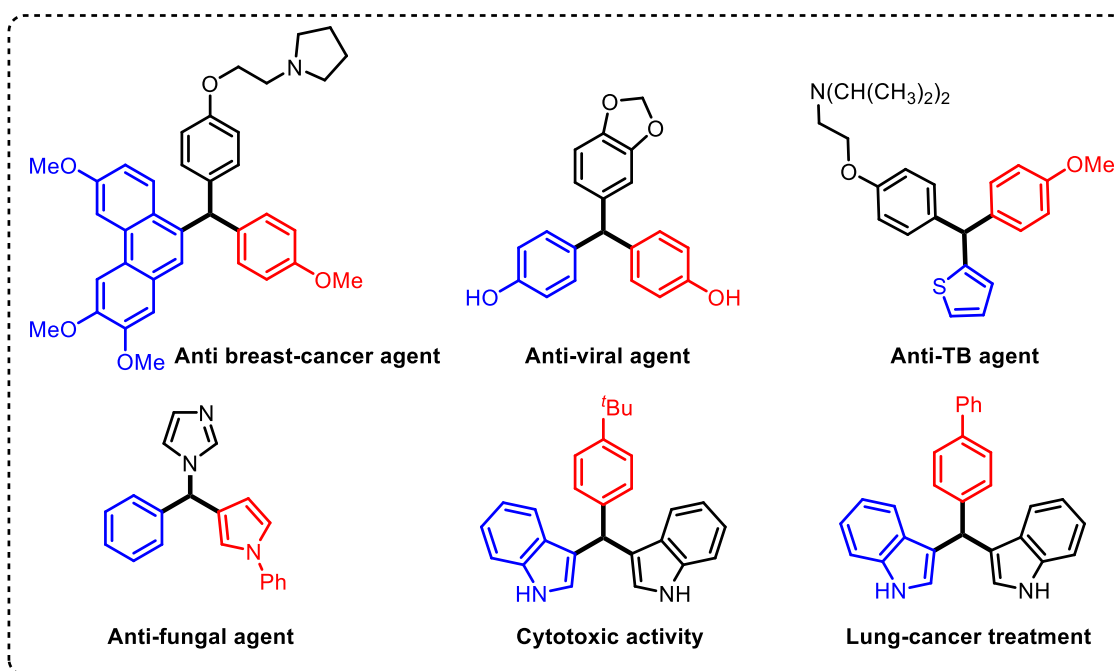
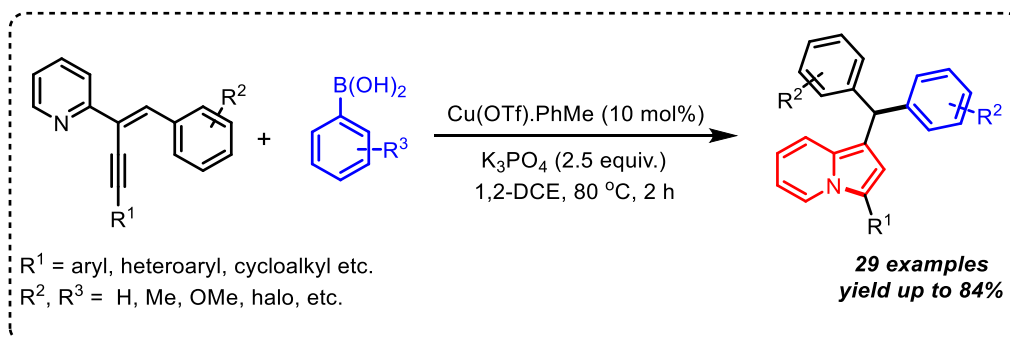


Figure 2. Some biologically active triarylmethane derivatives

medicinal applications, triarylmethanes have also found remarkable applications in the dye industry and materials science. These significant applications of triarylmethanes have attracted the scientific community toward the development of different easily accessible routes for the synthesis of functionalized triarylmethanes derivatives. Therefore we became interested in synthesizing indolizine-based unsymmetrical triarylmethane derivatives using 2-(2-enynyl)pyridine and boronic acids as the reaction partners (Scheme 3). The reaction proceeds through the Cu-catalysed 5-*endo*-dig-cyclization of 2-(2-enynyl)pyridine, followed by the addition of boronic acid.



Scheme 3. Synthesis of indolizine-based unsymmetrical triarylmethanes from 2-(2-enynyl)pyridines and boronic acids

Chapter 2: Copper-catalyzed synthesis of chromone and indolizine-based unsymmetrical triarylmethanes from 2-(2-enynyl)pyridines

This chapter deals with the synthesis of chromone and indolizine-based unsymmetrical triarylmethane derivatives. Chromones are naturally occurring compounds mainly found in plants. This class of oxygen-containing heterocycles are found as an integral part of many natural products and bioactive molecules, and they are known to show various pharmacological

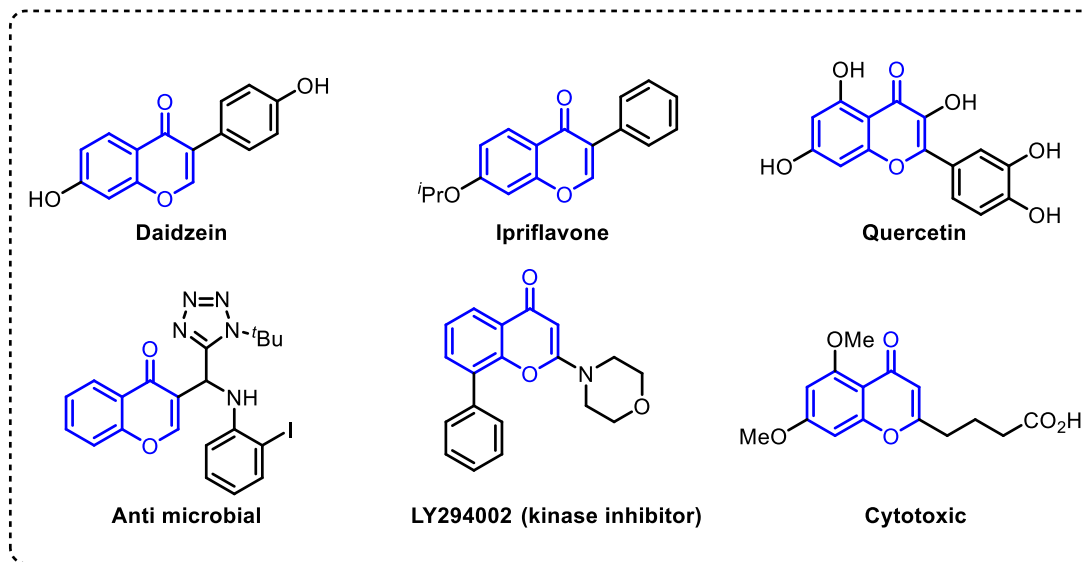
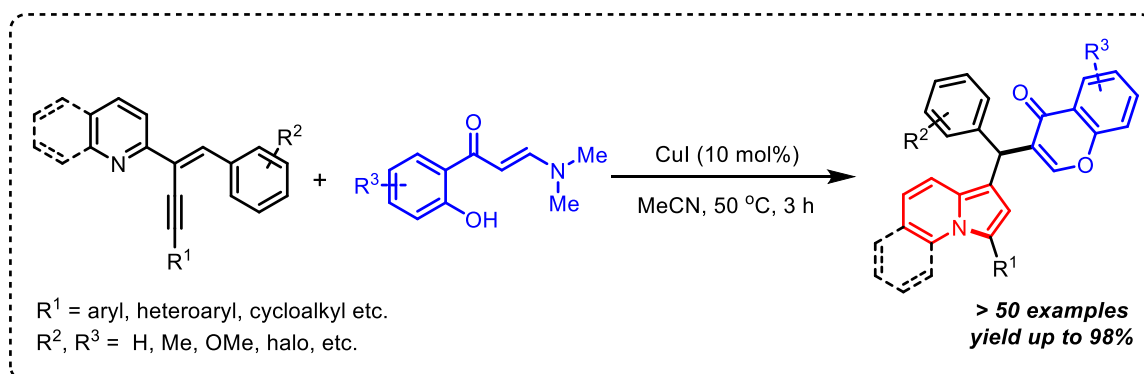


Figure 3. Chromone-based natural products and bioactive compounds

activities, such as anti-cancer, anti-oxidant, anti-fungal, etc. (Figure 3). Due to the importance of both indolizine and chromone derivatives, we developed a metal catalyzed protocol to access unsymmetrical triarylmethanes containing chromone and the indolizine scaffold in the same molecule using 2-hydroxyphenyl-substituted *N,N*-dimethylenaminones and 2-(2-enynyl)pyridines (Scheme 4).



Scheme 4. Synthesis of indolizine and chromone containing unsymmetrical triarylmethanes

Abbreviations

Acac	Acetylacetone
Ac	Acetyl
MeCN	Acetonitrile
aq	Aqueous
B ₂ Pin ₂	Bis(pinacolato)diboron
Bz	Benzoyl
Bn	Benzyl
OBn	Benzyloxy
BINAP	2,2'-Bis(diphenylphosphino)-1,1'-binaphthalene
dppf	1,1'-Bis(diphenylphosphino)ferrocene
DPPPe	1,5-Bis(diphenylphosphino)pentane
<i>n</i> -Bu	Butyl
calcd	Calculated
CDI	1,1'-Carbonyldiimidazole
Cbz	Carboxybenzyl
cm	Centimeter
δ	Chemical shift
CDCl ₃	Chloroform-D
TMSCl	Chlorotrimethylsilane
J	Coupling constant
Cy	Cyclohexyl
cod	1,5-Cyclooctadiene
CPME	Cyclopentyl methyl ether
°C	Degree celsius
DMP	Dess-Martin periodinane
dr	Diastereomeric ratio
DABCO	1,4-diazabicyclo[2.2.2]octane
DBU	1,8-Diazabicyclo(5.4.0)undec-7-ene
DDQ	2,3-Dichloro-5,6-dicyano-1,4-benzoquinone
DCE	1,2-Dichloroethane
DCM	Dichloromethane
Xphos	2-Dicyclohexylphosphino-2',4',6'-triisopropylbiphenyl
Et ₂ O	Diethyl ether
DEAD	Diethylazodicarboxylate
DIPEA	Diisopropylethylamine
DME	Dimethoxyethane
DMAc	Dimethylacetamide
DMF	<i>N,N'</i> -Dimethyl formamide
d	Doublet
dd	Doublet of doublet
ddd	Doublet of doublet of doublet

dt	Doublet of triplets
EWG	Electron withdrawing
ESI	Electrospray ionization
ee	Enantiomeric excess
er	Enantiomeric ratio
EtOH	Ethanol
EtOAc	Ethylacetate
EDCI	1-Ethyl-3-(3-dimethylaminopropyl)carbodiimide
equiv	Equivalents
FT-IR	Fourier transform infrared spectroscopy
HEH	Hantzschester
Hz	Hertz
HMPA	Hexamethylphosphoramide
HRMS	High-resolution Mass Spectrum
HFIP	Hexafluoroisopropanol
h	Hour(s)
<i>i</i> -Pr	<i>iso</i> -Propyl
LiHMDS	Lithium bis(trimethylsilyl)amide
LDA	Lithium diisopropylamide
^t BuOLi	Lithium- <i>tert</i> -butoxide
<i>m/z</i>	Mass/Charge
MHz	Mega Hertz
m.p.	Melting point
Mes	Mesityl
MeOH	Methanol
MOM	Methoxymethyl
MPPIM	Methyl 1-(3-phenylpropanoyl)-2-oxaimidazolidine-4(<i>S</i>)-carboxylate
mg	Milligram(s)
mL	Milliliter(s)
mmol	Millimole(s)
min	Minute(s)
M.S.	Molecular sieves
m	Multiplet
NHC	<i>N</i> -heterocyclic carbene
NMR	Nuclear Magnetic Resonance
Nu	Nucleophile
POCl ₃	Phosphoryl chloride
Phen	1,10-Phenanthroline
Piv	Pivaloyl
^t BuOK	Potassium- <i>tert</i> -butoxide
PEG	Polyethyleneglycol

q	Quartet
R _f	Retention factor
RT	Room temperature
SIPr	1,3-Bis(2,6-diisopropylphenyl)imidazolinium
s	Singlet
sept	Septet
<i>tert</i>	Tertiary
^t Bu	<i>tert</i> -Butyl
Boc	<i>tert</i> -Butyloxycarbonyl
TBDMS	<i>tert</i> -Butyldimethylsilyl
TBDPS	<i>tert</i> -Butyldiphenylsilyl
TBS	<i>tert</i> -butylsilyl
OTBS	<i>tert</i> -butylsilyloxy
TBAI	Tetrabutylammonium iodide
TBAF	Tetrabutylammonium fluoride
THF	Tetrahydrofuran
TMS	Tetramethylsilane
TPCD	Tetra Pyridine Cobalt (II) Dichromate
TIPS	Triisopropylsilyl
TFSA/TfOH	Trifluoromethanesulfonic acid
TFE	Trifluoroethanol
TFA	Trifluoroacetic acid
t	Triplet
td	Triplet of doublets
tt	Triplet of triplet

Contents

Declaration	i
Acknowledgments	ii
Abstract	v
Abbreviations	x

The thesis work is divided into two parts, **Part A** and **Part B**

Part A: Synthesis of indolizine-based heterocycles from 2-pyridinyl-substituted *para*-quinone methides (*p*-QMs)

Part A is sub-divided into three chapters

Chapter 1: General introduction to the chemistry of *para*-quinone methides (*p*-QMs)

1.1 Introduction	4
1.2 Literature reports on the synthesis of oxygen-containing heterocycles	6
1.3 Literature reports on the synthesis of nitrogen-containing heterocycles	10
1.4 Miscellaneous reports of functionalized <i>p</i> -QMs	15
1.5 References	21

Chapter 2: Pd(II)-catalyzed annulation of terminal alkynes with 2-pyridinyl-substituted *para*-quinone methides: Direct access to indolizines

2.1 Introduction	23
2.2 Literature reports on the synthesis of indolizine derivatives	24
2.3 Background	31
2.4 Results and Discussions	31
2.5 Conclusion	40
2.6 Experimental Section	40
2.7 References	70

Chapter 3: Cu(II)-catalyzed [3+2]-annulation of 2-pyridinyl-substituted *para*-quinone methides with enaminones: Access to functionalized indolizine derivatives

3.1 Introduction	73
3.2 Literature reports on <i>N,N</i> -dimethyl enaminones	75
3.3 Background	80
3.4 Results and Discussions	81
3.5 Conclusion	89
3.6 Experimental Section	90
3.7 References	130

Part B: Synthesis of indolizine-based unsymmetrical triarylmethanes from 2-(2-enynyl)pyridines

Part B is sub-divided into two chapters

Chapter 1: Copper-catalyzed synthesis of indolizine containing unsymmetrical triarylmethane derivatives from 2-(2-enynyl)pyridines

1.1 Introduction	133
1.2 Literature reports on the synthesis of triarylmethane derivatives	134
1.3 Literature reports on 2-(2-enynyl)pyridines in organic synthesis	148
1.4 Background	151
1.5 Results and Discussions	152
1.6 Conclusion	159
1.7 Experimental Section	159
1.8 References	178

Chapter 2: Copper-catalyzed synthesis of chromone and indolizine-based unsymmetrical triarylmethanes from 2-(2-enynyl)pyridines

2.1 Introduction	181
2.2 Literature reports on the synthesis of chromone derivatives	182
2.3 Background	192
2.4 Results and Discussions	193
2.5 Conclusion	202

2.6 Experimental Section	202
2.7 References	227
Summary	230
Curriculum Vitae	232

1. General Introduction to the Chemistry of *para*-Quinone Methides (*p*-QMs)

1.1 Introduction:

In the past few years, *para*-quinone methides (*p*-QMs) chemistry has been extensively explored to synthesize a diverse range of organic structural moieties, such as diaryl/triarylmethanes, carbocycles, heterocycles, and spiro-cycles, etc.^[1] *p*-QMs are not only valuable for synthetic applications, but are also commonly found in nature, where they function as intermediates in various biological and biosynthesis pathways.^[2] Structurally, *p*-QMs are analogues of 1,4-benzoquinone (**I**), but with one of the carbonyl groups replaced by a methylene group. Unlike 1,4-benzoquinone, which has carbonyl groups at opposite ends that counterbalance each other's polarizability effect, *p*-QMs have different entities at both ends that alter their dipole moment and polarizability.^[3] As a result, *p*-QMs exist in a zwitterionic form **III**,^[4] which stabilizes the *para*-quinone methide via aromatization of cyclohexadiene ring and also directs the incoming nucleophile to attack the benzylic carbocation, leading to the formation of more stable neutral aromatic compounds (Figure 1).

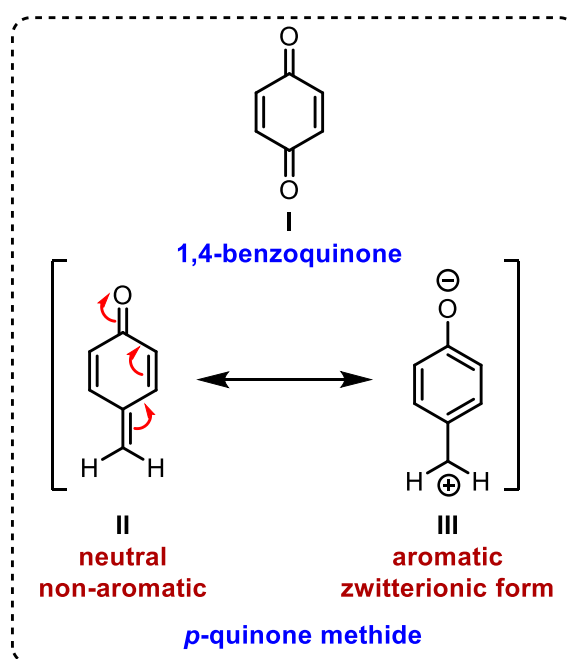


Figure 1. Zwitterionic form of *para*-quinone methide

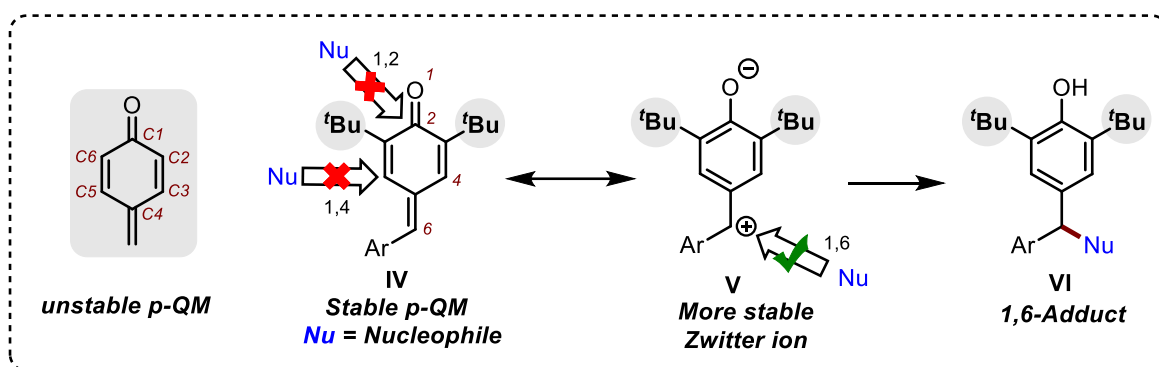


Figure 2. Reactivity of *para*-Quinone methide

Studies have shown that the unsubstituted *p*-QMs are highly reactive and unstable intermediates. However, it was observed that the presence of bulky alkyl substituents (such as a *tert*-butyl group) at C-2 and C-6 positions was found to enhance the stability of *p*-QM. Moreover, these bulky substituents also hinder the nucleophilic attack at the C-1 (1,2-addition) and C-3 (1,4-addition) positions (IV). As a result, only the *exo*-cyclic methylene carbon, which

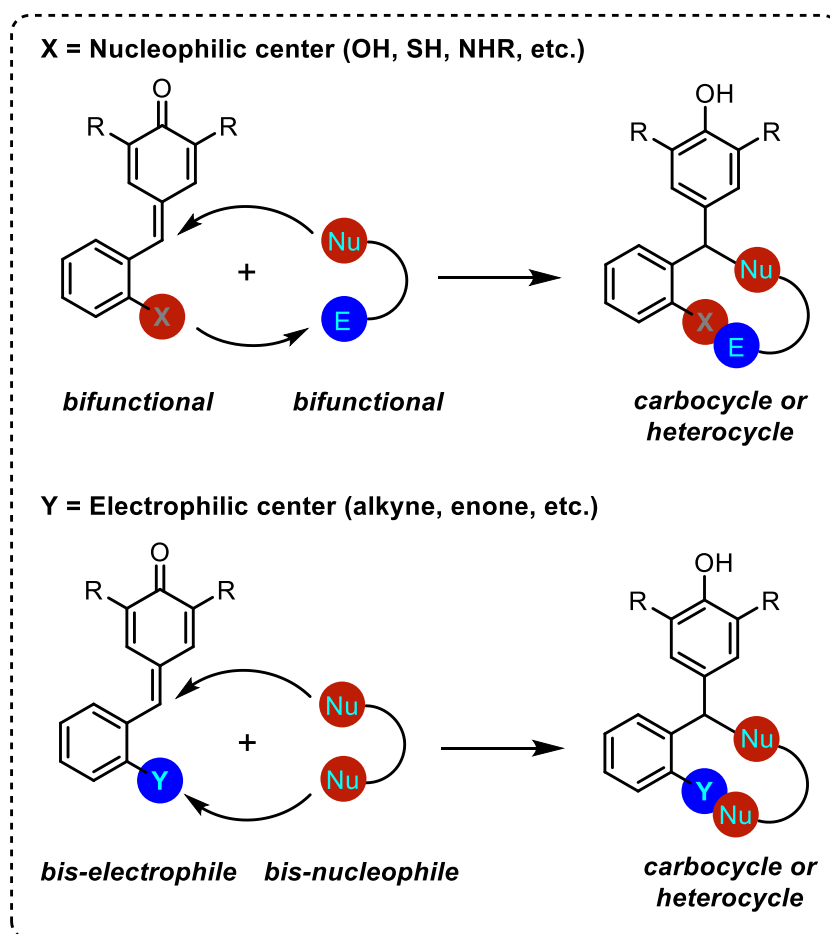


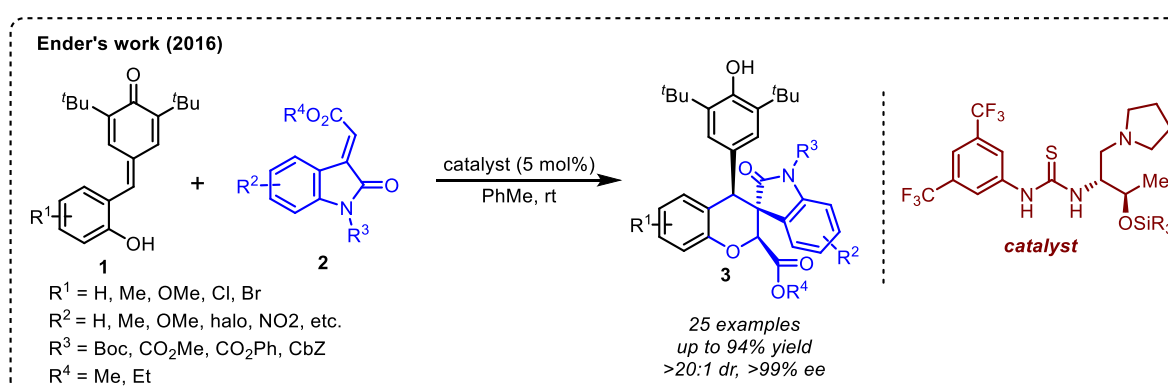
Figure 3. Hypothesis for the synthesis of carbocycles/heterocycles from *p*-QMs

typically exists as a carbocation during the zwitterionic form, is susceptible to nucleophilic attack (**V**). This unique reactivity makes *p*-QMs an ideal substrate for regiospecific 1,6-conjugate addition reactions with various nucleophiles (**VI**) [Figure 2], and numerous synthetic protocols have been documented in the literature on the utilization of stable *p*-QMs as a 1,6-acceptors to access various diaryl and triarylmethane derivatives.^[1]

Recently, it was hypothesized that if some modifications are made at the ortho position of the aryl group with a nucleophilic or an electrophilic substituent in the basic structure of *p*-QM, then it can be transformed into a bifunctional molecule. Depending on the substitution, this functionalized *p*-QM can react with another bifunctional molecule to produce fused carbocycles and heterocycles (Figure 3). This chapter focuses mainly on the syntheses of oxygen and nitrogen-containing heterocycles using structurally modified *para*-quinone methides.

1.2. Literature reports on the synthesis of oxygen-containing heterocycles:

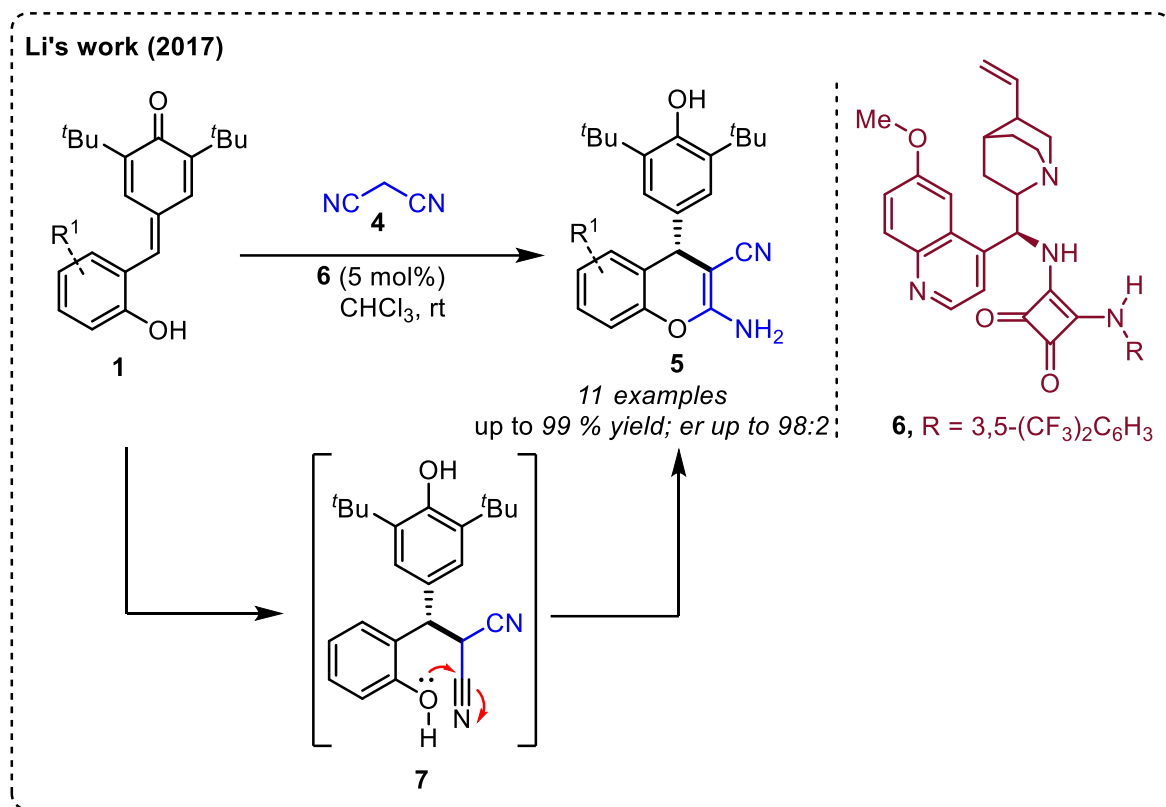
For the first time, in 2016, Enders and co-workers utilized 2-hydroxyphenyl substituted *p*-QMs (**1**) for the synthesis of enantiomerically pure *spiro*-cyclic chromane derivatives (**3**). A wide range of chiral *spiro*-cyclic chromanes have been synthesized with excellent yields and stereoselectivity by using **1** and isatin-derived enoates **2** in the presence of a chiral thiourea catalyst. According to the proposed reaction mechanism, the thiourea catalyst activates both **1** and **2**, followed by an *oxa*-Michael/1,6-conjugate addition reaction to produce the product **3** (Scheme 1).^[5]



Scheme 1. Synthesis of chiral *spiro*-cyclic chromanes using isatin-derived enoates

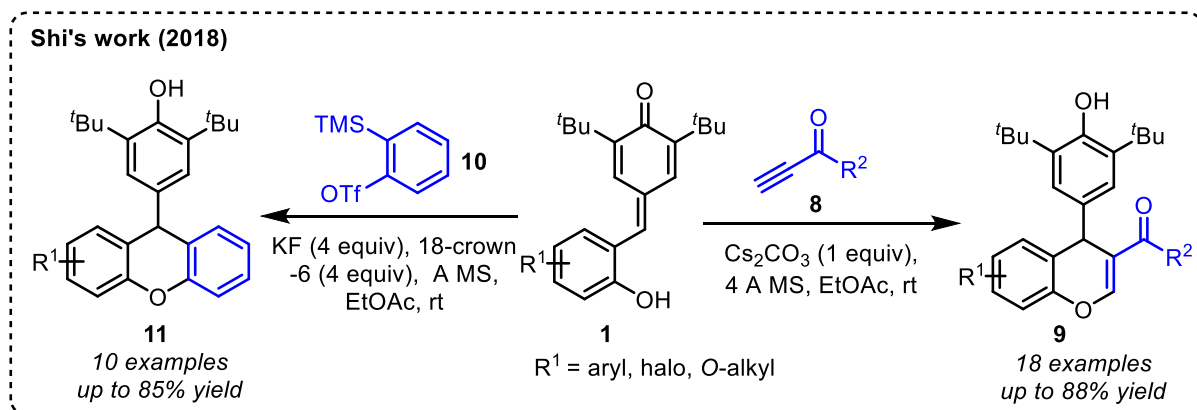
Li's group in 2017 reported an enantioselective synthesis of chromene derivatives (**5**) in good yields with excellent enantioselectivities by the reaction of 2-hydroxyphenyl

substituted *p*-QMs (**1**) and malononitrile **4**, in the presence of a bifunctional chiral squaramide-based catalyst **6**. According to the proposed reaction mechanism, the reaction proceeds



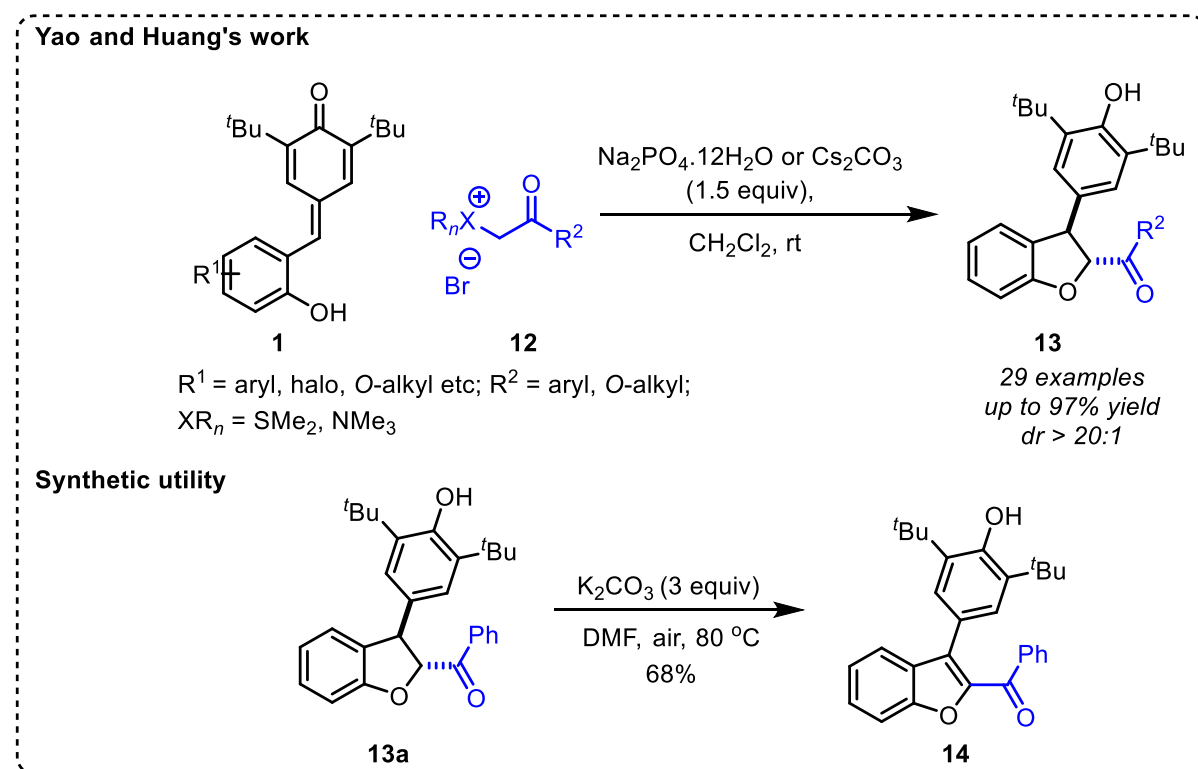
Scheme 2. Synthesis of 4H-chromenes using malononitrile

through the initial 1,6-Conjugate addition of **4** to *p*-QM **1** to give intermediate **7**. The intermediate **7** undergoes subsequent intramolecular cyclization and isomerization to produce enantiomerically pure chromene derivatives **5** (Scheme 2).^[6]



Scheme 3. [4+2]-annulation with *o*-hydroxyphenyl-substituted *p*-QMs

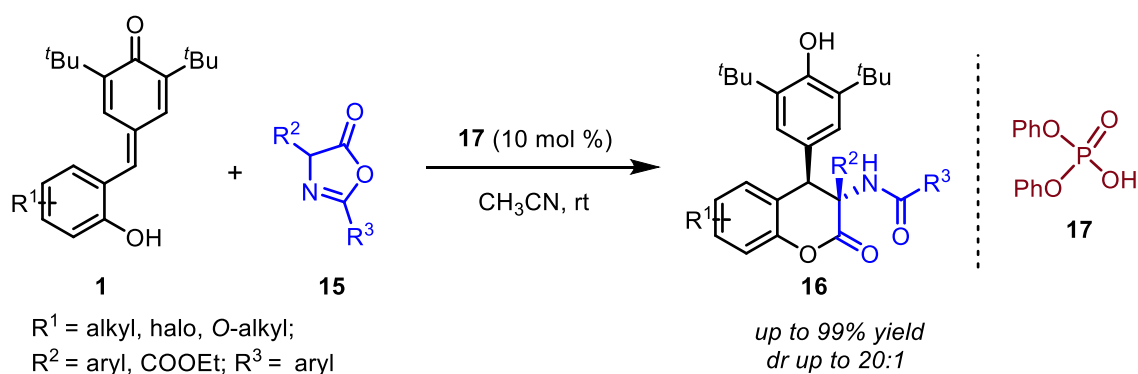
In 2018, Shi and co-workers developed a [4+2] cyclization reaction of *o*-hydroxyphenyl substituted *p*-QMs (**1**) with alkynone **8** or benzyne **10** for the synthesis of chromene derivatives (**9**) and xanthene scaffolds (**11**), respectively. The reaction mechanism involves the nucleophilic attack of the hydroxylic group on the alkynone **8** or the in situ-generated benzyne from **10**, followed by intramolecular 1,6-conjugate addition to give the final chromene **9** and xanthene derivatives **11**, respectively (Scheme 3).^[7]



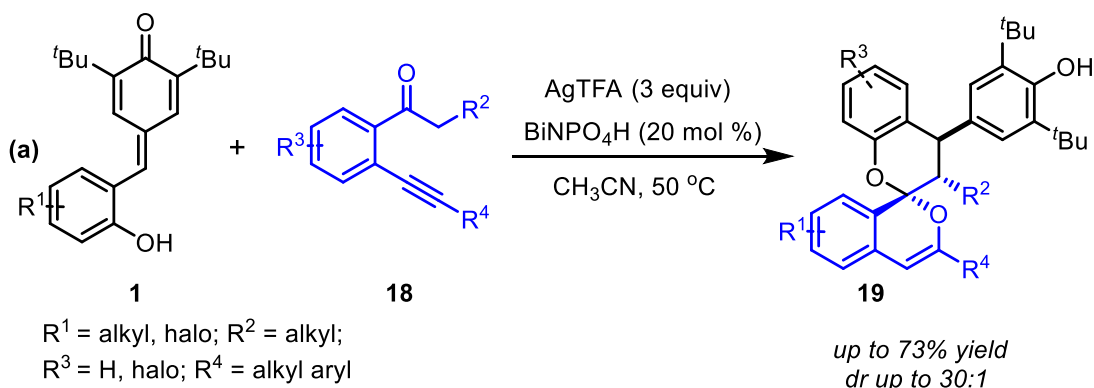
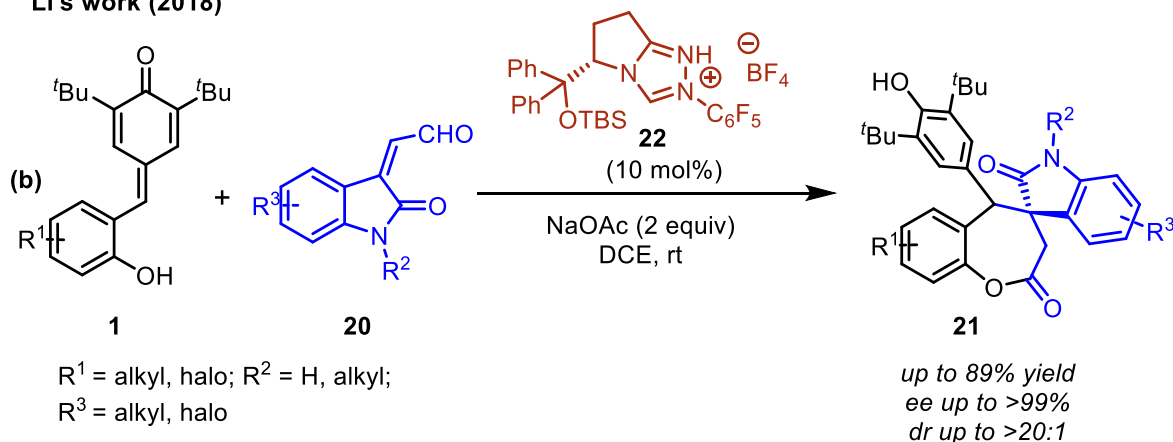
Scheme 4. [4+1]-annulation with *o*-hydroxyphenyl-substituted *p*-QMs

Yao and Huang's research group developed an interesting approach for the synthesis of 2,3-dihydrobenzofurans (**13**) in moderate to excellent diastereoselectivity, through a formal [4+1]-annulation of 2-hydroxyphenyl substituted *p*-QMs (**1**) and ammonium or sulfonium bromides (**12**). This protocol was further extended for the synthesis of benzofuran derivative **14** under basic conditions (Scheme 4).^[8]

Mei and co-workers reported an efficient approach for the synthesis of biologically important dihydrocoumarin derivatives (**16**) in excellent yield and diastereoselectivity through the addition of azalactone **15** to *p*-QMs (**1**) under Brønsted acid catalysis. In this reaction, the Brønsted acid **17** was found to catalyze both the addition as well as cyclization steps through hydrogen bonding (Scheme 5).^[9]

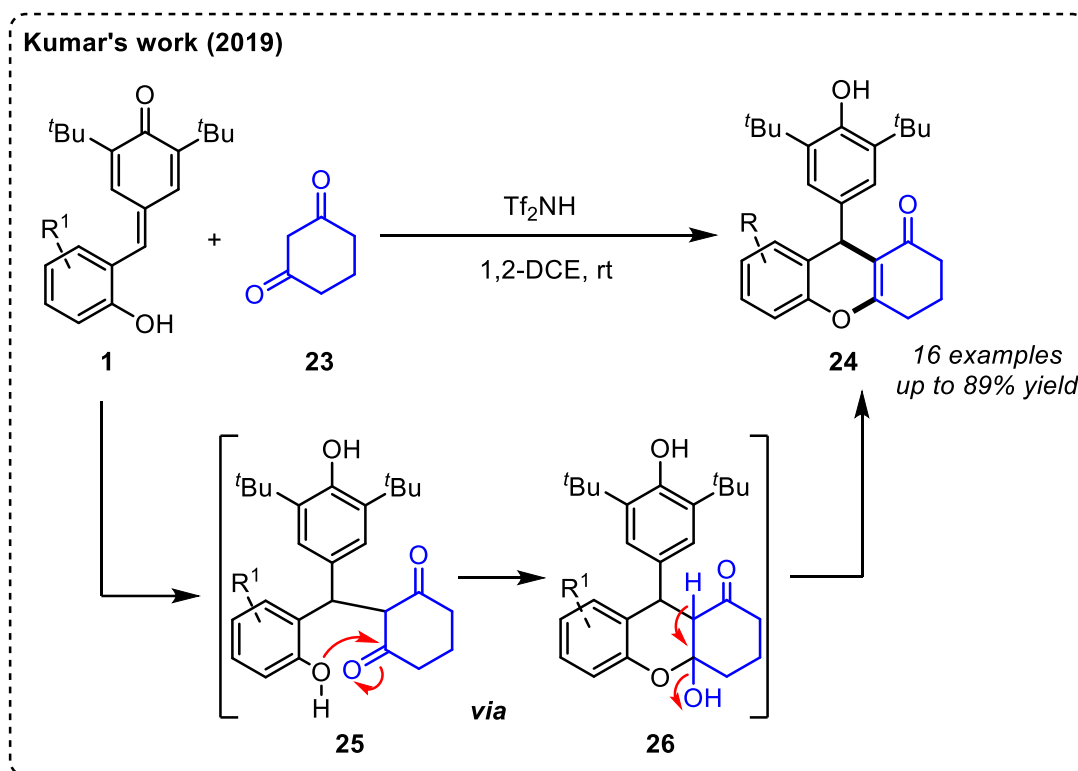
Mei's work (2018)**Scheme 5.** Addition of azalactone to *o*-hydroxyphenyl-substituted *p*-QMs

Jiang and co-workers reported a Silver/Brønsted acid co-catalyzed method for synthesizing spiro[chromane-2,1-isochromene] derivatives (**19**). This reaction occurs through multiple C–O and C–C bond-formation reactions between *o*-hydroxy substituted *p*- QMs (**1**)

Jiang's work (2018)**Li's work (2018)****Scheme 6.** Annulation reactions with *o*-hydroxyphenyl-substituted *p*-QMs

and β -alkynyl ketones **18** (Scheme 6a).^[10] Enantioenriched spirobenzoxopinones (**21**) bearing an oxindole moiety has been constructed through *N*-heterocyclic carbene (**22**) catalyzed cycloaddition between *o*-hydroxy substituted *p*-QMs (**1**) and isatin-derived enals (**20**) by Li's group. Most of the spirobenzoxopinones, bearing an oxindole derivative, were isolated in excellent yields and enantioselectivities (Scheme 6b).^[11]

Kumar and co-workers recently reported a metal-free approach to prepare xanthenone derivatives (**24**) from 2-hydroxyphenyl substituted *p*-QMs (**1**) and β -functionalized ketones (**23**) using Tf₂NH as a Brønsted acid catalyst (Scheme 7).^[12] According to the authors, the reaction proceeds through a 1,6-addition of **23** to **1** to generate the intermediate **25**, followed by an intramolecular cyclization/dehydration to give the desired product **24** in moderate to good yields.

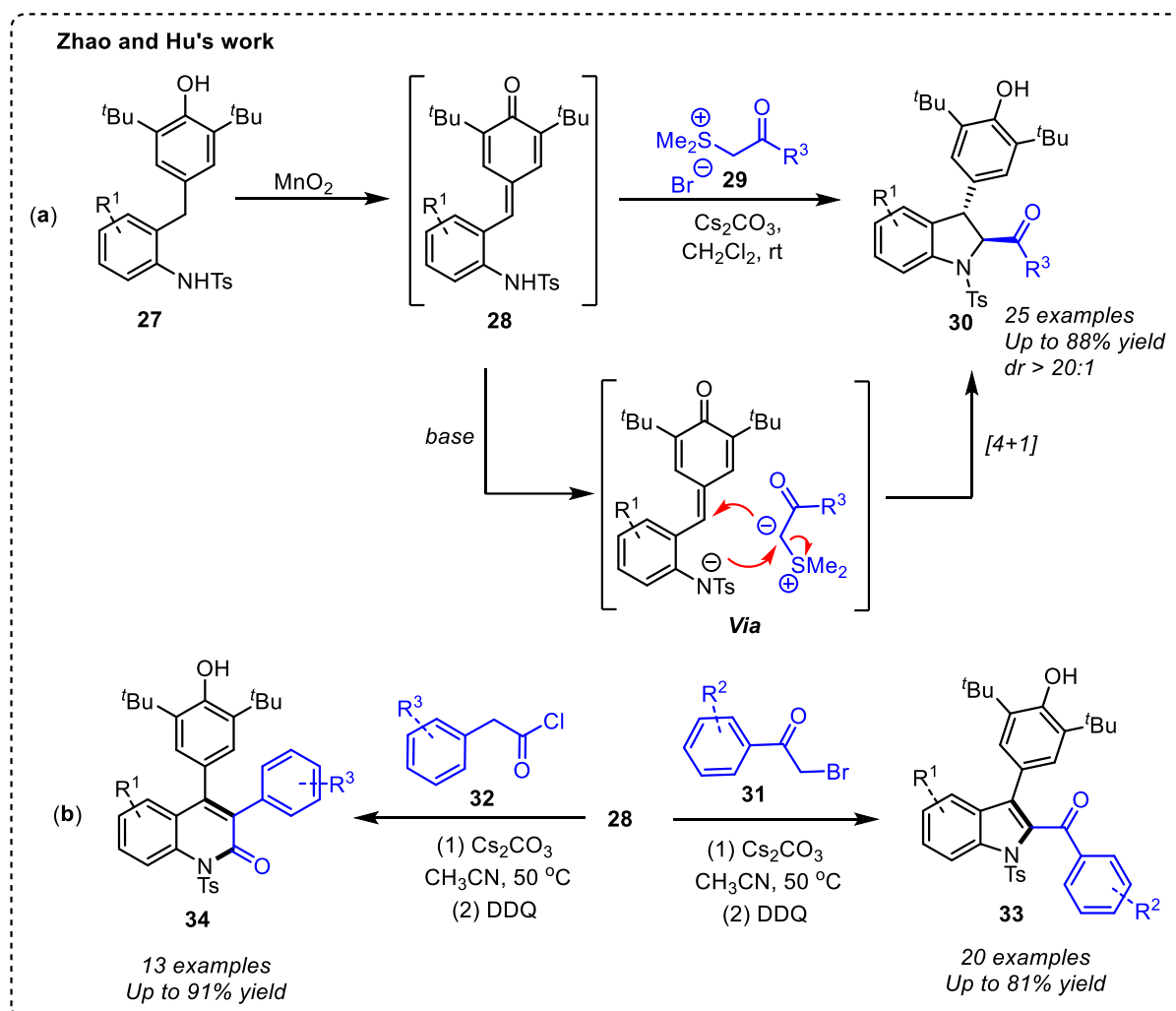


Scheme 7. Addition of β -functionalized ketones to *o*-hydroxyphenyl-substituted *p*-QMs

1.3. Literature reports on the synthesis of nitrogen-containing heterocycles:

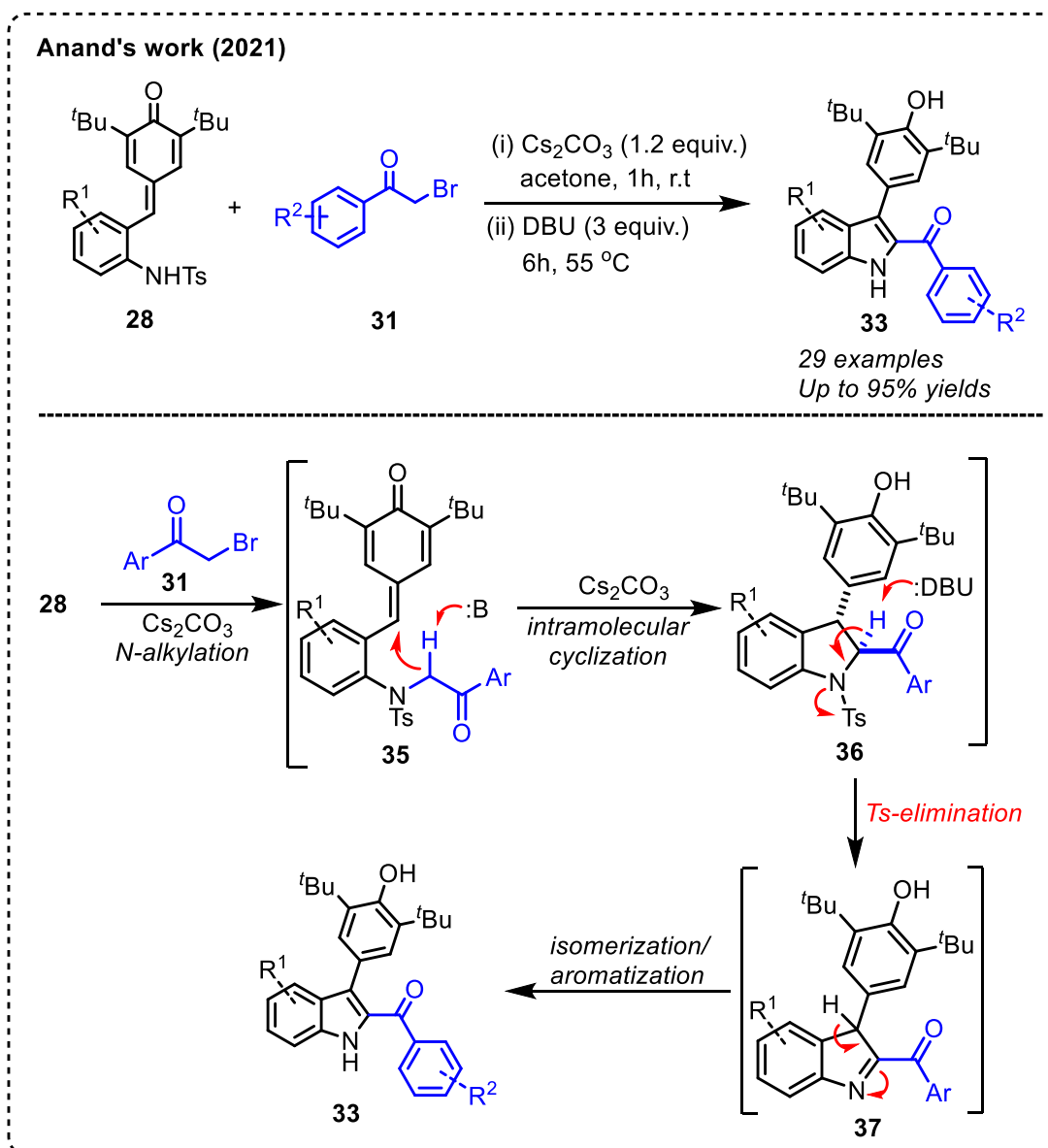
In 2019, Zhao, Hu, and co-workers reported an effective method for the synthesis of 2,3-dihydroindoles (**30**) through a base-mediated [4+1]-annulation of in situ generated *o*-tosylaminophenyl substituted *p*-QMs (**28**) with sulfonium ylides (**29**) [Scheme 8a].^[13] A wide range of 2,3-dihydroindoles could be accessed in good yields and excellent diastereoselectivities (*dr*

> 20:1). Later, the same group developed a one-pot approach for the synthesis 2,3-disubstituted indoles (**33**) and 3,4-diaryl-substituted quinolinones (**34**) through a base-mediated reaction of **28** with α -halo ketones (**31**) and arylacetyl halides (**32**) respectively, followed by DDQ-mediated oxidation to give the respective products **33** and **34** in good yields (Scheme 8b).^[14]



Scheme 8. Annulation of *o*-tosylaminophenyl-substituted *p*-QMs

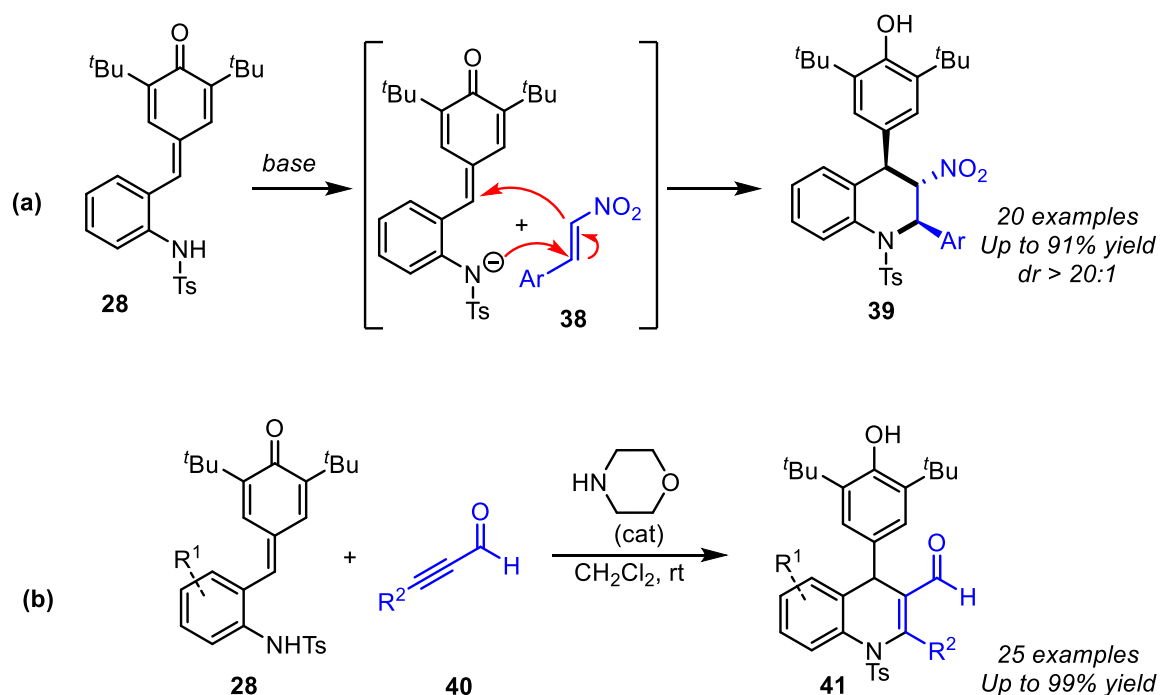
Similarly, Anand's group reported a combination of inorganic and organic base-mediated approach for the synthesis of 2,3-disubstituted indole derivatives (**33**) using *o*-tosylaminophenyl-substituted *p*-QMs (**28**) and substituted phenacyl bromides (**31**) [Scheme 9].^[15] According to the proposed mechanism, the inorganic base Cs_2CO_3 initially abstracts the NH-Ts proton of **28**, and the resulting anion reacts with **31** to give the *N*-alkylated *p*-QM **35**. Under the basic condition, this intermediate **35** undergoes an intramolecular cyclization to generate another intermediate **36**, which further undergoes Tosyl group elimination with the help of organic base (DBU) followed by isomerization to form the indole derivative **33**.



Scheme 9. Annulation of *o*-tosylaminophenyl substituted *p*-QMs

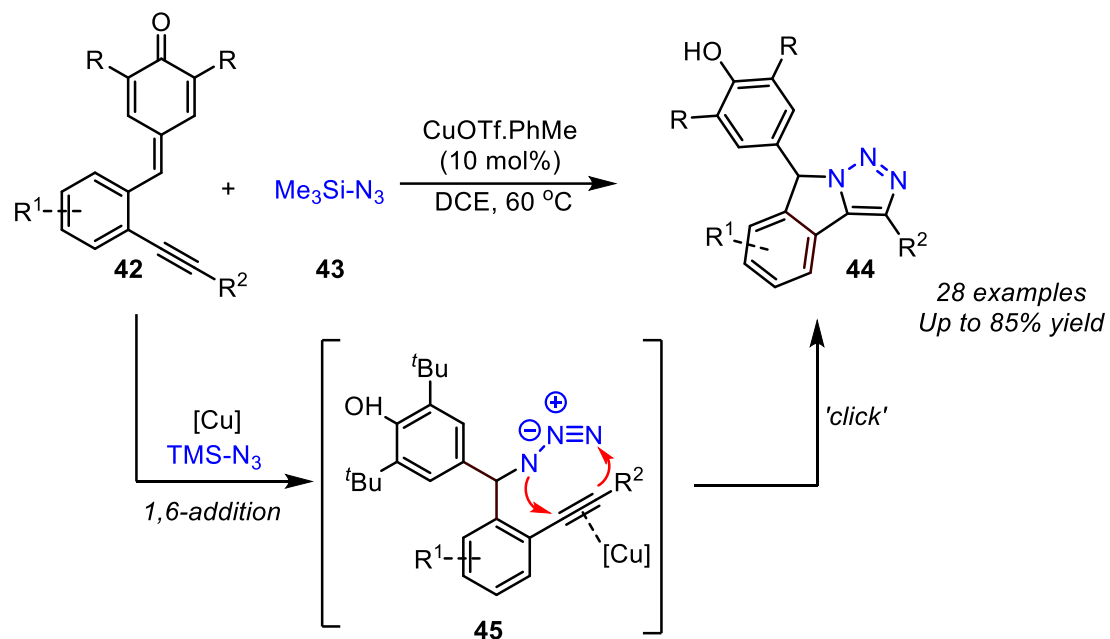
In 2018, Zhao, Hu, and co-workers reported a base-mediated synthesis of 4-aryl-substituted tetrahydroquinolines (**39**) through an aza-Michael addition of nitrostyrene (**38**) to the *in situ* generated *o*-tosylaminophenyl-substituted *p*-QMs (**28**), followed by an intramolecular 1,6-conjugate addition. Many 4-aryl-substituted tetrahydroquinolines (**39**) could be accessed in good yields and excellent diastereoselectivity ($dr = > 20:1$) [Scheme 10a].^[16] Later, the same group also reported an organocatalytic method for the synthesis of 1,4-dihydroquinolines (**41**) through an aza-Michael type addition reaction of **28** with ynals (**40**) followed by intramolecular 1,6-addition/cyclization sequence (Scheme 10b).^[17]

Zhao and Hu's work



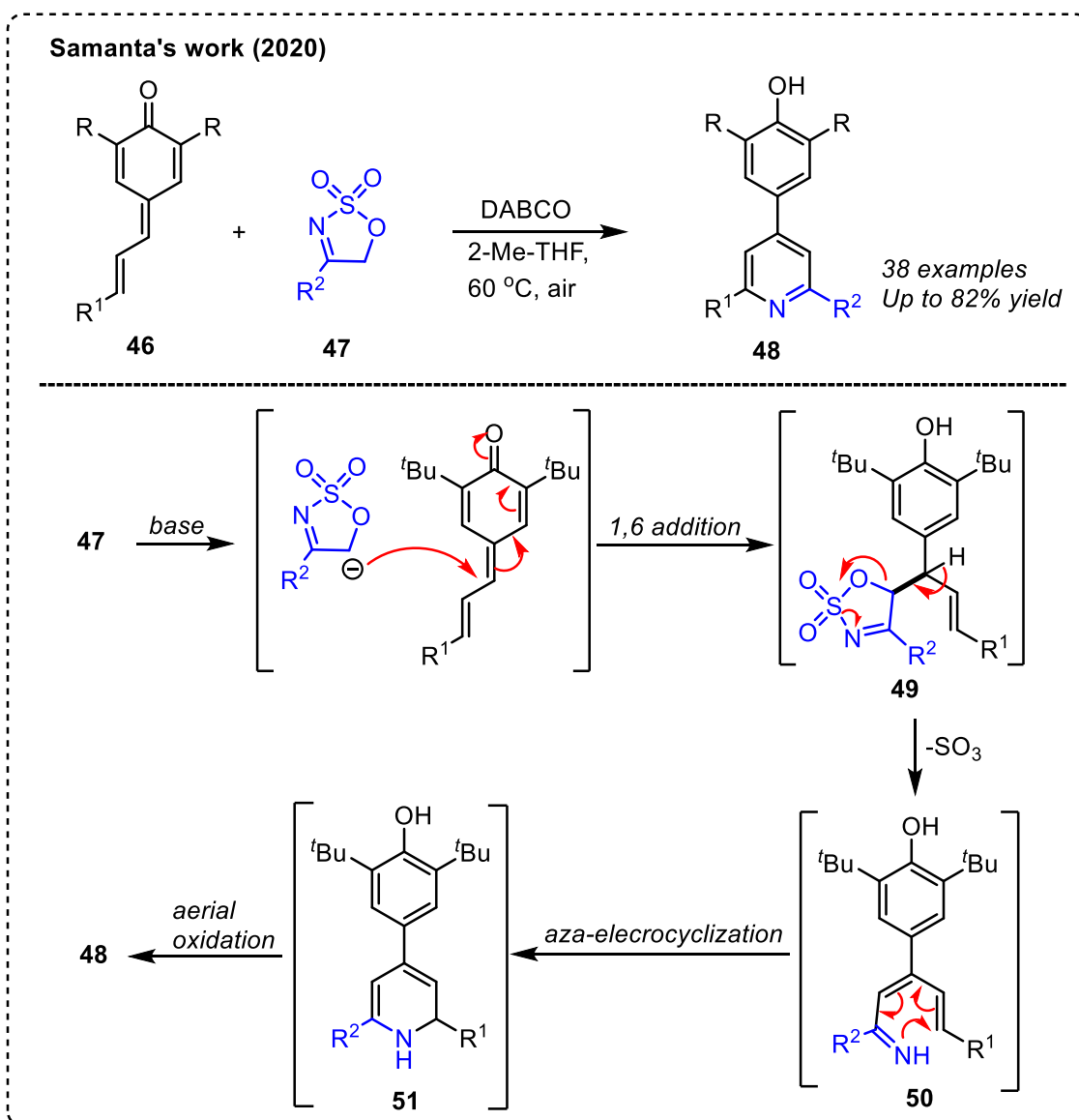
Scheme 10. Synthesis of tetrahydroquinolines from *p*-QMs

Anand's work (2018)



Scheme 11. Cu-catalyzed synthesis of 1,2,3-triazole-fused isoindolines from *p*-QMs

Anand's group in 2018 reported a Cu-catalyzed synthesis of 1,2,3-triazole-fused isoindolines (**44**) from 2-(alkynyl) phenyl-substituted *p*-QMs (**42**) and trimethylsilyl azide (**43**) [Scheme 11].^[18] Through control experiments, the authors proposed that initially, the 1,6-conjugate addition of **43** to **42** takes place to form a 1,6-adduct **45**, which then undergoes copper-catalyzed intramolecular click reaction to produce the final product **44**.



Scheme 12. DABCO-mediated synthesis of substituted pyridines from *p*-QMs

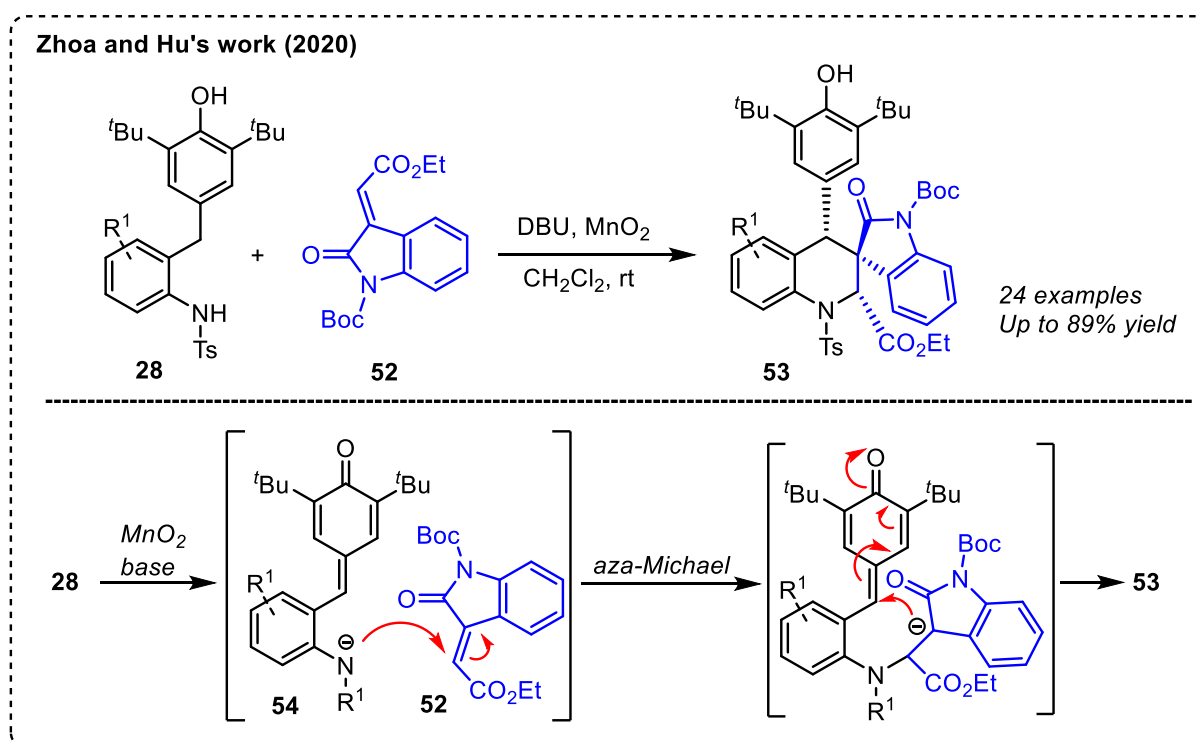
Samanta and co-workers disclosed an interesting 1,4-diazabicyclo [2.2.2] octane (DABCO)-mediated protocol for the synthesis of substituted pyridines (**48**) from vinyl-substituted *p*-QMs (**46**) and cyclic sulfamidate-imines (**47**) [Scheme 12].^[19] According to the proposed reaction mechanism, the reaction proceeds through the abstraction of a proton from **47** by the base (DABCO) to generate the corresponding anion, which then adds to **46** in a 1,6-

fashion to generate an adduct **49**. The intermediate **49**, on the elimination of $-\text{SO}_3$ followed by isomerization and aza-electrocyclization, forms the dihydropyridine intermediate **51**, which, further on aerobic oxidation, generates the product **48**.

1.4. Miscellaneous reports of functionalized *p*-QMs

1.4.1. Literature reports on the synthesis of spirocyclic nitrogen-containing heterocycles

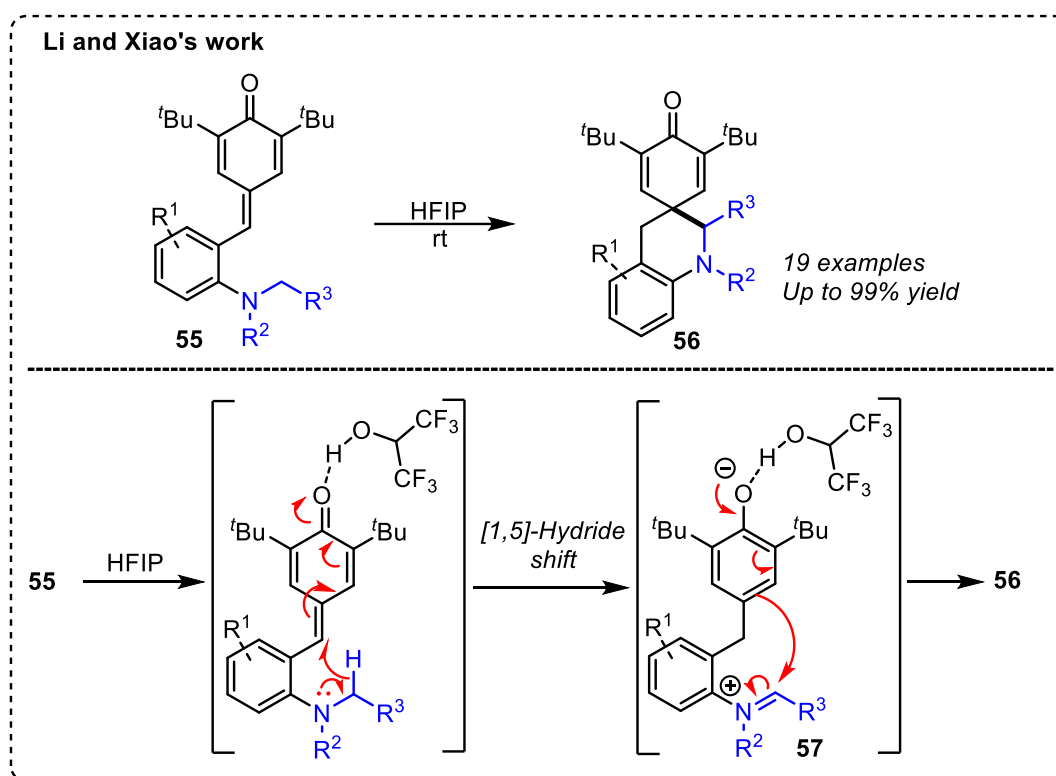
Apart from dihydro- and tetrahydro-isoquinolines, a few reports are available for the synthesis of spirocyclic nitrogen-containing heterocycles from structurally modified *p*-QMs. For example, Zhao and Hu reported the synthesis of spirocyclic tetrahydroquinolines (**53**) through a base-mediated aza-Michael addition of in situ-generated *o*-tosylaminophenyl-substituted *p*-QMs (**54**) to isatin derivatives (**52**) followed by intramolecular 1,6-conjugate addition to afford the final product **53** (Scheme 13).^[20]



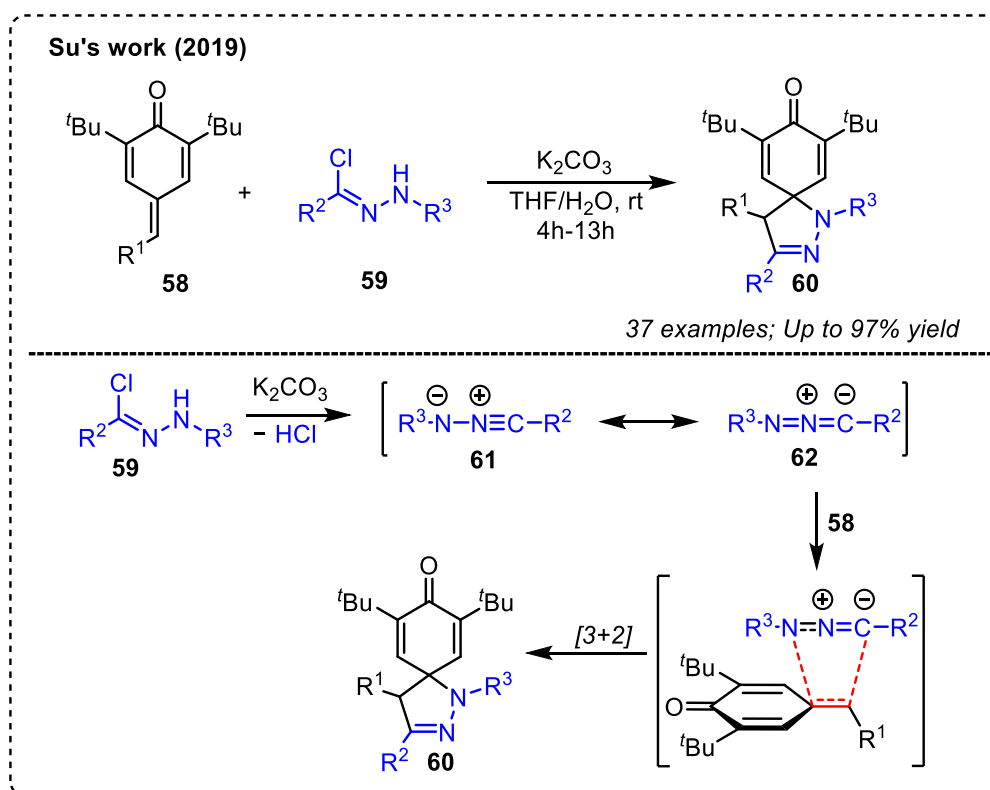
Scheme 13. Base mediated synthesis of tetrahydroquinolines from *p*-QMs

Later, Li and Xiao reported an interesting hexafluoroisopropanol (HFIP)-mediated intramolecular cyclization strategy for the synthesis of spirocyclic tetrahydroquinolines (**56**) from 2-aminophenyl-substituted *p*-QMs (**55**). The authors believe that HFIP initially activates

55 and triggers the 1,5-hydride shift to generate an iminium intermediate (**57**), which



Scheme 14. Synthesis of tetrahydroquinoline derivatives from *p*-QMs



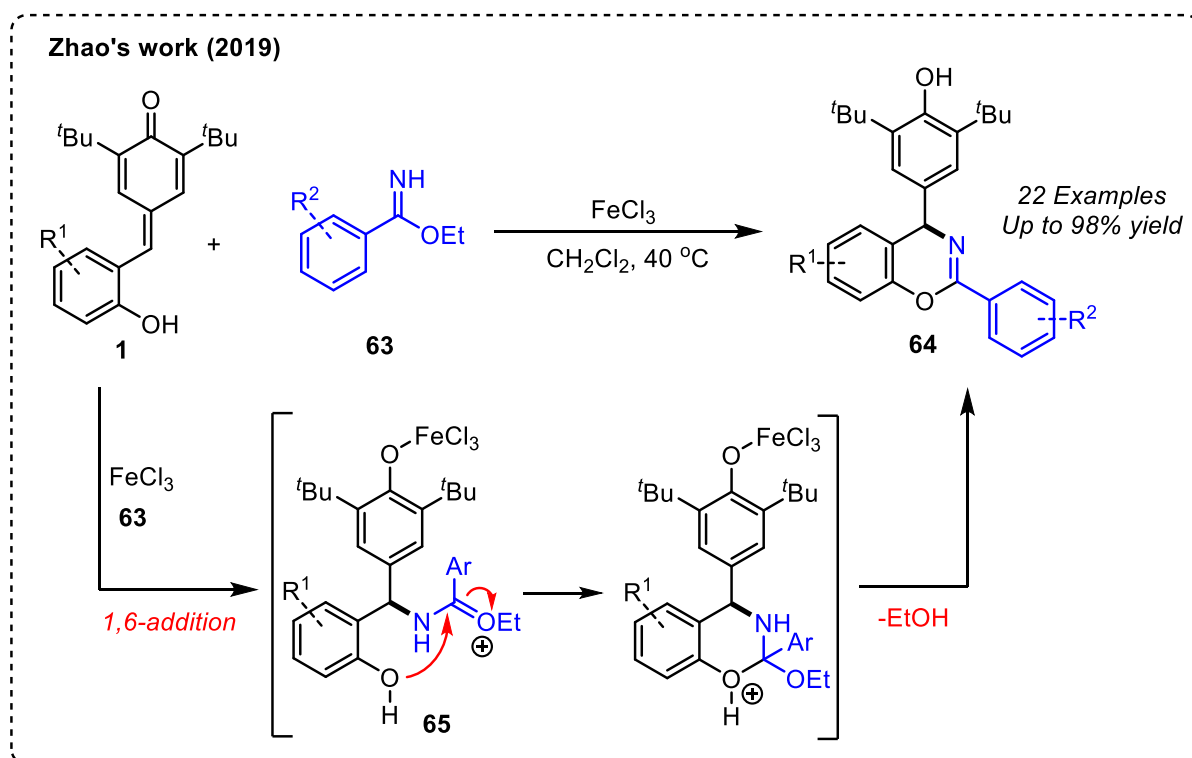
Scheme 15. Synthesis of pyrazoline derivatives from *p*-QMs

subsequently undergoes dearomative cyclization to produce the spirocyclic tetrahydroquinolines (**56**) [Scheme 14].^[21]

The synthesis of spirocyclic pyrazoline derivatives (**60**) through a [3+2]-cycloaddition of hydrazonoyl chlorides (**59**) to *p*-QMs (**58**) has been reported by Su and co-workers. It was proposed that the base initially reacts with **59** and generates a nitrile imine intermediate with two resonance forms, propargylic (**61**) and allenic (**62**), of which **62** undergoes a formal [3+2]-cycloaddition with **58** to furnish the product **60** (Scheme 15).^[22]

1.4.2. Literature reports on the synthesis of both oxygen and nitrogen-containing heterocycles

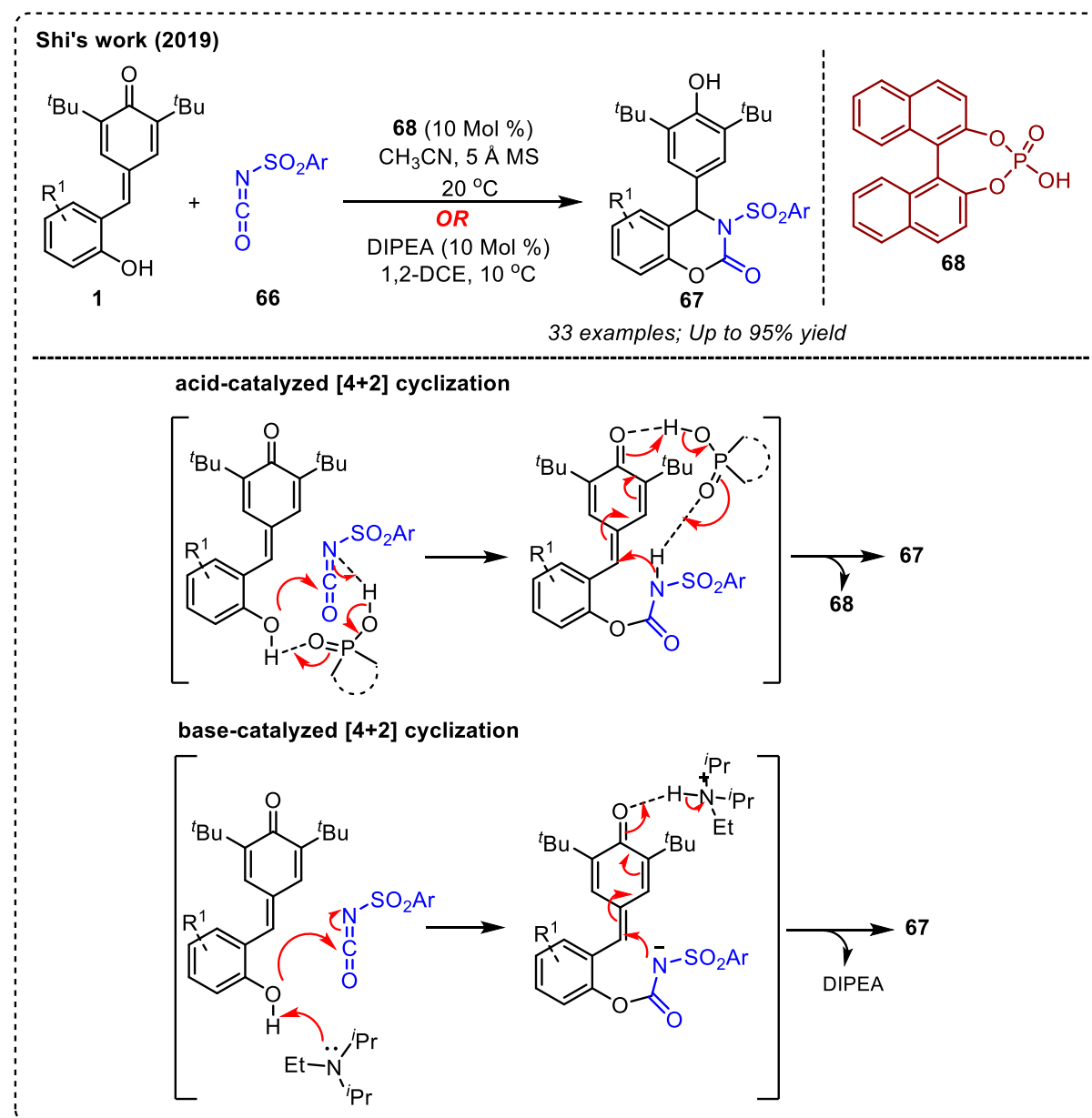
Zhao's group demonstrated a Fe-catalyzed [4+2]-annulation approach to access 2,4-diaryl-1,3-benzoxazine derivatives (**64**) from 2-hydroxyphenyl-substituted *p*-QMs (**1**) and imidates (**63**). The reaction proceeds through the activation of **1** with FeCl₃ followed by 1,6-addition of **63** to generate an intermediate **65**, which then undergoes an intramolecular cyclization, followed by elimination to produce the product **64** (Scheme 16).^[23]



Scheme 16. Fe(III)-catalyzed synthesis of 1,3-benzoxazine derivatives from *p*-QMs

In 2019, Gao, Jiao, and Shi reported an organocatalytic method to access benzoxazin-2-ones (**67**) via a [4+2]-cycloaddition of benzenesulfonyl isocyanates (**66**) with 2-

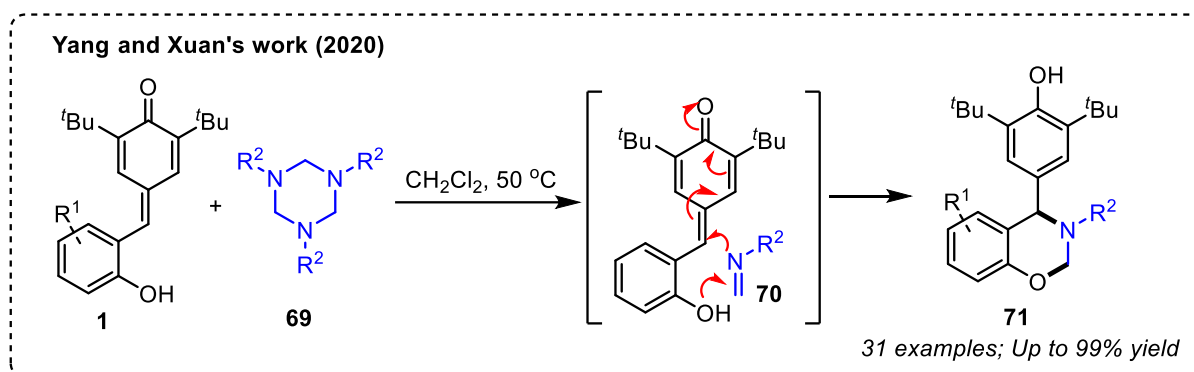
hydroxyphenyl-substituted *p*-QMs (**1**). Interestingly, the reaction worked very well in the presence of catalytic amounts of a Brønsted acid or a Brønsted base. In the acid-catalyzed transformation, the acid **68** initially triggers the reaction between **1** and **66** and forms an intermediate, which on intramolecular 1,6-conjugate addition, generates the product **67**. In the case of base-mediated reaction, the base first abstracts the phenolic proton of **1**, and the resulting phenolate anion reacts with **66** to generate the carbamate intermediate, which then undergoes intramolecular 1,6- addition affording the product **67** (Scheme 17).^[24]



Scheme 17. [4+2]-annulation of *p*-QMs for the synthesis of benzoxazin-2-ones

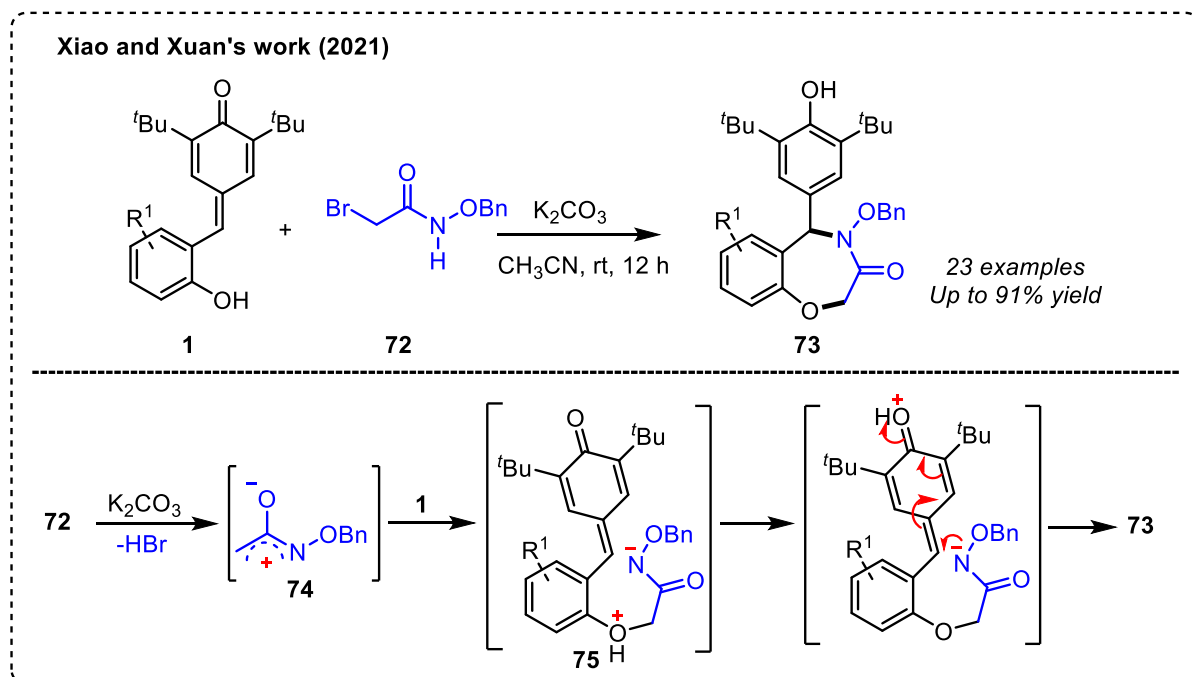
Yang and Xuan developed a catalyst-free strategy for the synthesis of 1,3-benzoxazine derivatives (**71**) through a [4+ 2] cycloaddition between **1** and hexahydro-1,3,5-triazines (**69**).

The authors proposed that initially, **69** undergoes fragmentation to produce an imine **70**, which then undergoes a formal [4+2]-annulation with **1** to form the 1,3-benzoxazine derivative **71** (Scheme 18).^[25]



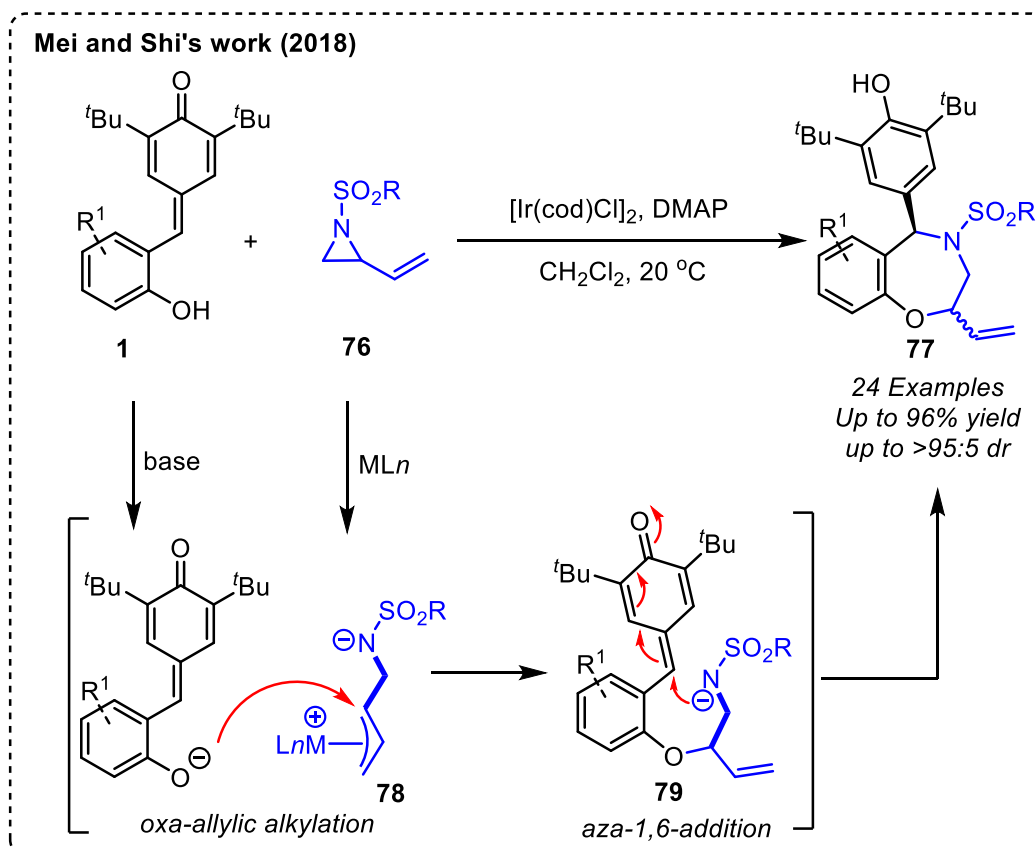
Scheme 18. Synthesis of 1,3-benzoxazine derivatives from *o*-hydroxy substituted *p*-QMs

Another base-mediated protocol for the synthesis of 1,4-benzoxazepines (**73**) from **1** and α -bromohydroxamate (**72**) has been disclosed by Xiao and Xuan. According to the proposed mechanism, the base initially reacts with **72** and generates an azaoxyallyl cation intermediate **74**, which then reacts with **1** to generate **75**. The intermediate **75** then undergoes an intramolecular 1,6-addition to form the desired product **73** (Scheme 19).^[26]



Scheme 19. Synthesis of 1,4-benzoxazepine derivatives from *o*-hydroxy substituted *p*-QMs

Mei, Shi, and co-workers have established a [4+3]- annulation between vinyl aziridines (**76**) and **1** in the presence of a Ir-catalyst to access benzoxazepine derivatives (**77**) in moderate to good yields and excellent diastereoselectivity (up to 95: 5 *dr*). When the metal catalyst reacts with vinyl aziridine, a zwitterionic π -allyl metal complex **78** is formed and subsequently reacts with **1** to form another intermediate **79**, which then undergoes intramolecular cyclization to generate the product **77** (Scheme 20).^[27]



Scheme 20. Synthesis of benzoxazepine derivatives from *o*-hydroxy substituted *p*-QMs

1.5. References

1. Parra, A.; Tortosa, M. *ChemCatChem* **2015**, *7*, 1524. (b) Caruana, L.; Fochi, M.; Bernardi, L. *Molecules* **2015**, *20*, 11733. (c) Li, W.; Xu, X.; Zhang, P.; Li, P. *Chem. Asian J.* **2018**, *13*, 2350. (d) Wang, J. Y.; Hao, W. J.; Tu, S. J.; Jiang, B. *Org. Chem. Front.* **2020**, *7*, 1743. (e) Lima, C. G. S.; Pauli, F. P.; Costa, D. C. S.; de Souza, A. S.; Forezi, L. S. M.; Ferreira, V. F.; de Carvalho da Silva, F. *European J. Org. Chem.* **2020**, 2020, 2650.
2. For selected references: (a) Larsen, A. A. *Nature* **1969**, *224*, 25. (b) Messiano, G. B.; da Silva, T.; Nascimento, I. R.; Lopes, L. M. X. *Phytochemistry* **2009**, *70*, 590. (c) Dehn, R.; Katsuyama, Y.; Weber, A.; Gerth, K.; Jansen, R.; Steinmetz, H.; Hçfle, G.; Müller, R.; Kirschning, A. *Angew. Chem. Int. Ed.* **2011**, *50*, 3882. (d) Wang, L. L.; Candito, D.; Dräger, G.; Herrmann, J.; Müller R.; Kirschning, A. *Chem. Eur. J.* **2017**, *23*, 5291.
3. Koutek, B.; Pišová, M.; Souček, M.; Exner, O. *Collect. Czech. Chem. Commun.* **1976**, *41*, 1676.
4. (a) Toteva, M. M.; Richard, J. P. *J. Am. Chem. Soc.* **2000**, *122*, 11073. (b) Richard, J. P.; Toteva, M. M.; Crugeiras, J. *J. Am. Chem. Soc.* **2000**, *122*, 1664. (c) Toteva, M. M.; Moran, M.; Amyes, T. L.; Richard, J. P. *J. Am. Chem. Soc.* **2003**, *125*, 8814. (d) Toteva, M. M.; Richard, J. P. *The Generation and Reactions of Quinone Methides. In Advances in Physical Organic Chemistry*; Richard, J. P., Ed.; Academic Press, Elsevier, **2011**; Vol. 45, pp 39–91.
5. Zhao, K.; Zhi, Y.; Shu, T.; Valkonen, A.; Rissanen, K.; Enders, D. *Angew. Chemie - Int. Ed.* **2016**, *55*, 12104.
6. Zhang, L.; Zhou, X.; Li, P.; Liu, Z.; Liu, Y.; Sun, Y.; Li, W. *RSC Adv.* **2017**, *7*, 39216.
7. Su, Y.; Zhao, Y.; Chang, B.; Zhao, X.; Zhang, R.; Liu, X.; Huang, D.; Wang, K.-H.; Huo, C.; Hu, Y.; *J. Org. Chem.* **2019**, *84*, 6719.
8. Zhang, J.-R.; Jin, H.-S.; Wang, R.-B.; Zhao, L.-M. *Adv. Synth. Catal.* **2019**, *361*, 4811.
9. Cao, Z.; Zhou, G.-X.; Ma, C.; Jiang, K.; Mei, G.-J. *Synthesis* **2018**, *50*, 1307.
10. Liu, S.; Lan, X.-C.; Chen, K.; Hao, W.-J.; Li, G.; Tu, S.-J.; Jiang, B. *Org. Lett.* **2017**, *19*, 3831.

11. Li, W.; Yuan, H.; Liu, Z.; Zhang, Z.; Cheng, Y.; Li, P. *Adv. Synth. Catal.* **2018**, *360*, 2460.
12. Satbhaiya, S.; Khonde, N. S.; Rathod, J.; Gonnade, R.; Kumar, P. *Eur. J. Org. Chem.* **2019**, 3127.
13. Wang, J.; Pan, X.; Zhao, L.; Zhao, L.; Liu, J. Wang, Y.; Zhao, K.; Hu, L. *Org. Biomol. Chem.* **2019**, *17*, 10158.
14. Wang, J.; Pan, X.; Rong, Q.; Zhao, L.; Zhao, L.; Dai, W.; Zhao, K.; Hu, L. *RSC Adv.* **2020**, *10*, 33455.
15. Pandey, R.; Singh, G.; Gour, V.; Anand, R. V. *Tetrahedron* **2021**, *82*, 131950.
16. J. Wang, X. Pan, J. Liu, L. Zhao, Y. Zhi, K. Zhao, L. Hu, *Org. Lett.* **2018**, *20*, 5995.
17. J. Wang, Q. Rong, L. Zhao, X. Pan, L. Zhao, K. Zhao, L. Hu, *J. Org. Chem.* **2020**, *85*, 11240.
18. Jadhav, S. A.; Pankhade, Y. A.; Anand, R. V. *J. Org. Chem.* **2018**, *83*, 8596.
19. Guin, S.; Gudimella, S. K.; Samanta, S. *Org. Biomol. Chem.* **2020**, *18*, 1337.
20. Wang, J.; Zhao, L.; Zhao, L.; Pan, X.; Lv, C.; Zhi, Y.; Wang, A.; Zhao, K.; Hu, L. *Adv. Synth. Catal.* **2020**, *362*, 2755.
21. (a) X. Lv, F. Hu, K. Duan, S.-S. Li, Q. Liu, J. Xiao, *J. Org. Chem.* **2019**, *84*, 1833.;
(b) S.-S. Li, X. Lv, D. Ren, C.-L. Shao, Q. Liuc, J. Xiao, *Chem. Sci.* **2018**, *9*, 8253.
22. Su, Y.; Zhao, Y.; Chang, B.; Zhao, X., Zhang, R.; Liu, X.; Huang, D.; Wang, K.-H.; Huo, C.; Hu, Y.; *J. Org. Chem.* **2019**, *84*, 6719.
23. Zhang, J.-R.; Jin, H.-S.; Wang, R.-B.; Zhao, L.-M. *Adv. Synth. Catal.* **2019**, *361*, 4811.
24. Cheng, Y.-C.; Wang, C.-S.; Li, T.-Z.; Gao, F.; Jiao, Y.; Shi, F. *Org. Biomol. Chem.* **2019**, *17*, 6662
25. Cheng, X.; Zhou, S.-J.; Xu, G.-Y.; Wang, L.; Yang, Q.-Q.; Xuan, J. *Adv. Synth. Catal.* **2020**, *362*, 523.
26. Zhou, S.-T.; Cheng, X.; Hu, C.-X.; Xu, G.-Y.; Xiao, W.-J.; Xuan, J. *Sci. China Chem.* **2021**, *64*, 61.
27. Jiang, F.; Yuan, F.-R.; Jin, L.-W.; Mei, G.-J.; Shi, F. *ACS Catal.* **2018**, *8*, 10234.

2. Pd(II)-catalyzed Annulation of Terminal Alkynes with 2-Pyridinyl-substituted *para*-Quinone Methides: Direct Access to Indolizines

2.1. Introduction:

Indolizine is recognized as one of the privileged cores by synthetic chemists as it is found in many naturally occurring alkaloids,^[1] agrochemicals^[2] and other biologically significant molecules.^[3] Numerous natural/unnatural indolizine derivatives have been found to show incredible therapeutic activities such as anti-tubercular, anti-bacterial, anti-neoplastic, anti-inflammatory and anti-oxidant properties (Figure 1).^[4] Besides, other notable applications of these compounds as fluorescent probes, dyes for dye sensitized solar cells and also as materials in organic light emitting devices (OLEDs) have also been realized.^[5]

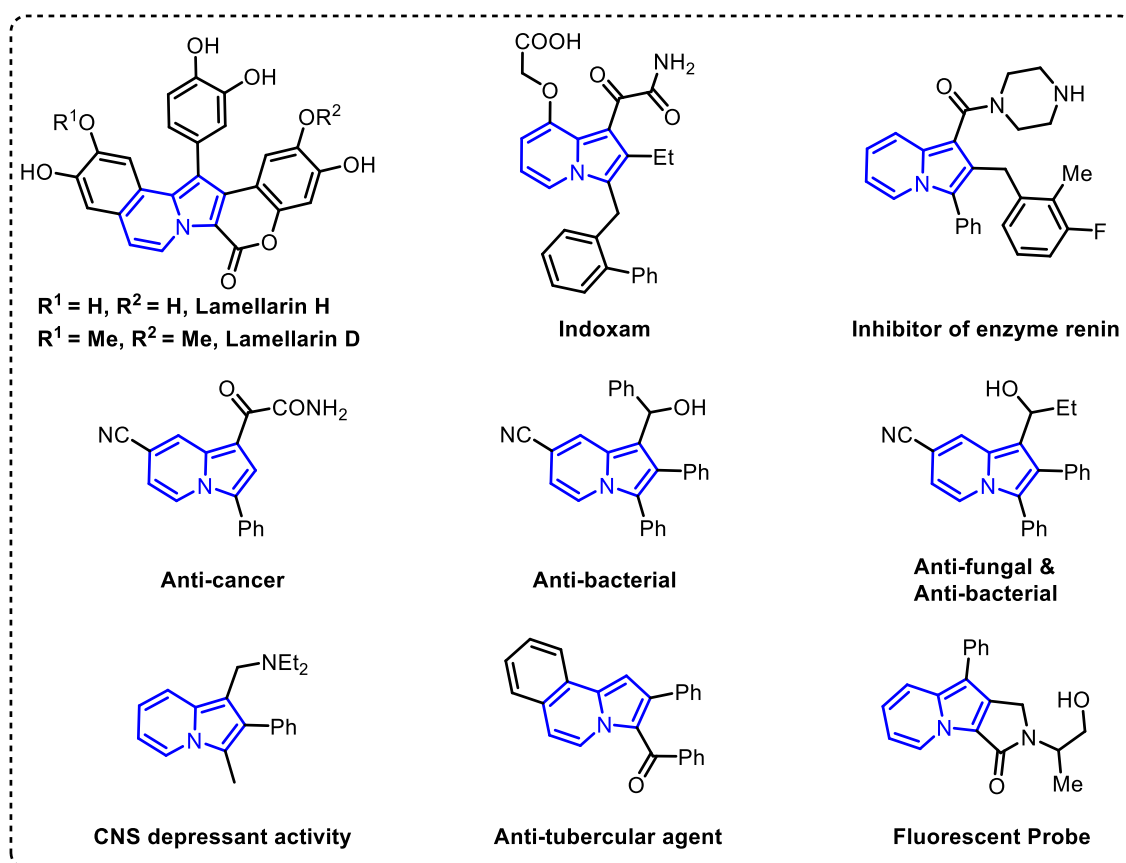
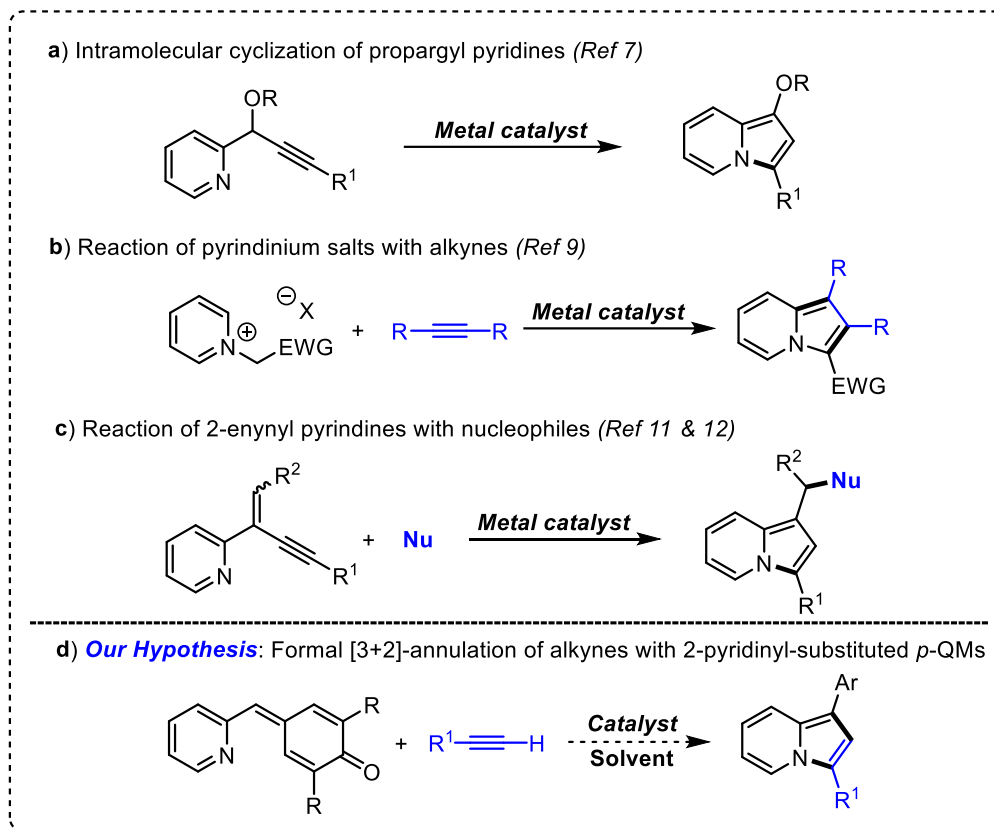


Figure 1. Biologically active natural and unnatural indolizine derivatives.

The diverse range of properties and applications of these molecules made them attractive targets for synthetic as well as materials chemists, and, as a result, many synthetic approaches have been established to access these heterocycles.^[6] The most common protocols involve either metal-catalyzed intramolecular cyclization of propargylic pyridines^[7] or

intermolecular reactions between pyridine^[8] or pyridinium salts^[9] or pyrrole derivatives^[10] with suitable coupling partners (**a** & **b**, Scheme 1). Very recently, 2-(2-enynyl) pyridine derivatives have also been explored as precursors for the synthesis of highly-substituted indolizines by a few research groups,^[11] including ours (**c**, Scheme 1).^[12]

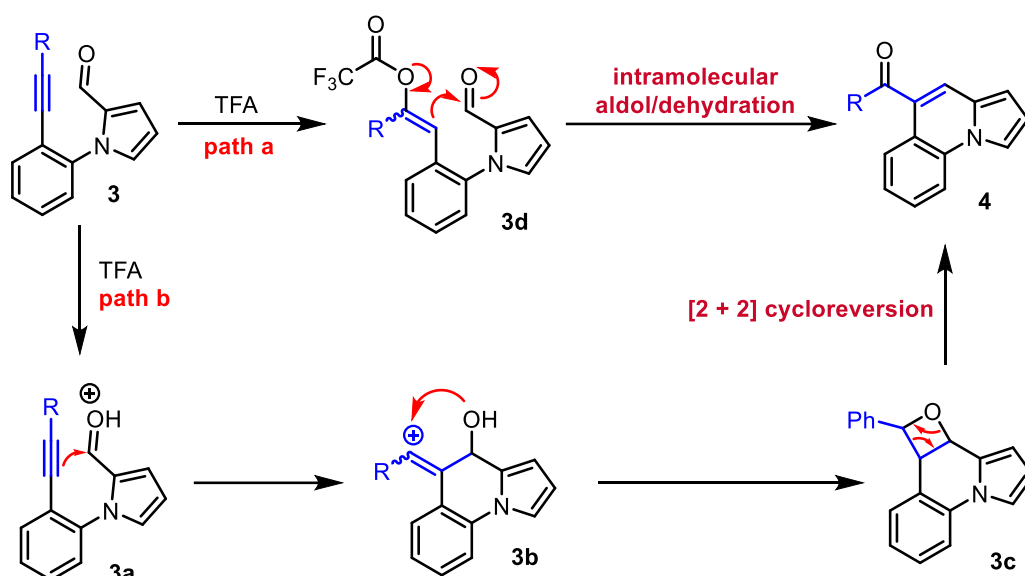
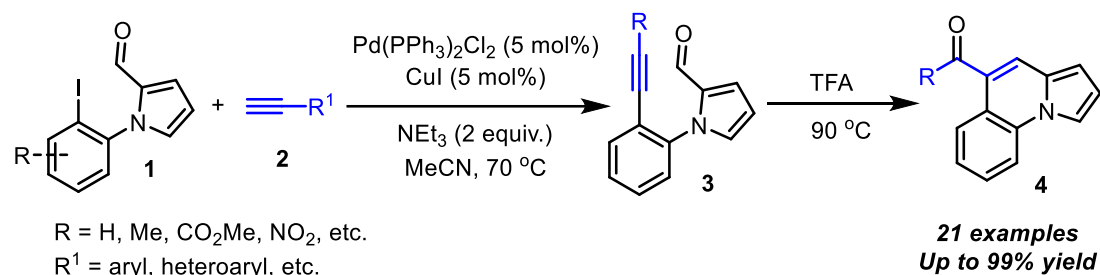


Scheme 1. Reported protocols to access indolizines.

2.2. Literature reports on the synthesis of indolizine derivatives:

In 2015 Kim and co-workers reported the synthesis of benzo-fused indolizine derivatives (**4**) in good to excellent yields from 1-(2-haloaryl)-1H-pyrrole-2-carbaldehydes (**1**) and terminal alkynes (**2**) through a sequential Sonogashira cross-coupling followed by an intramolecular alkyne–carbonyl metathesis (ACM). The authors proposed two possible pathways for this protocol. After the formation of **3** by the Sonogashira cross-coupling of **1** and **2**, it either undergoes an intramolecular aldol/dehydration to give rise to **4** in the presence of TFA through the intermediate **3d**. The other possibility is that **3** undergoes an alkyne addition to aldehyde promoted by the protonation of **3** to provide the intermediate **3b**. The neighbouring hydroxyl group present in **3b** then attacks the resulting carbocation to produce **3c**, which is followed by [2+2] cycloreversion, leading to the final product **4** (scheme 2)^[13]

Kim's work (2015)

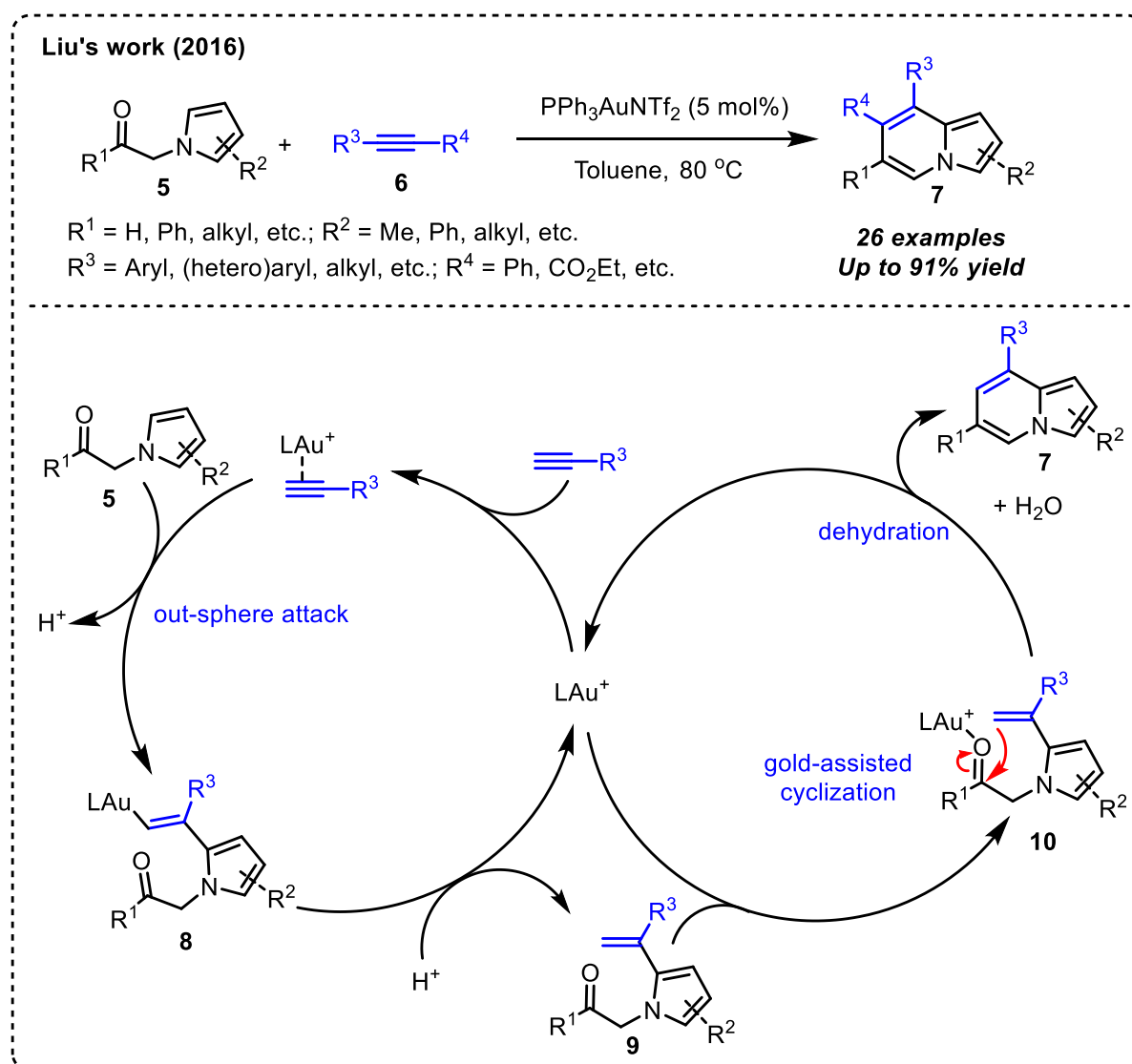


Scheme 2. Synthesis of Indolizine derivatives from pyrrole-2-carbaldehyde

The Liu group in 2016 developed an efficient and atom-economic method for synthesizing multi-substituted indolizines (**7**) from α -(*N*-pyrrolyl)ketones (**5**) and alkynes (**6**) *via* a gold-catalyzed cascade hydroarylation/cyclo-aromatization reaction. According to the proposed mechanism, the reaction proceeds through the regioselective hydroarylation of the pyrrole ring at the α -position to produce the intermediate **8**, which upon protodeauration generates **9**. The intermediate **9** then undergoes gold assisted cyclization and subsequent dehydration, leading to the final product **7** (scheme 3)^[14]

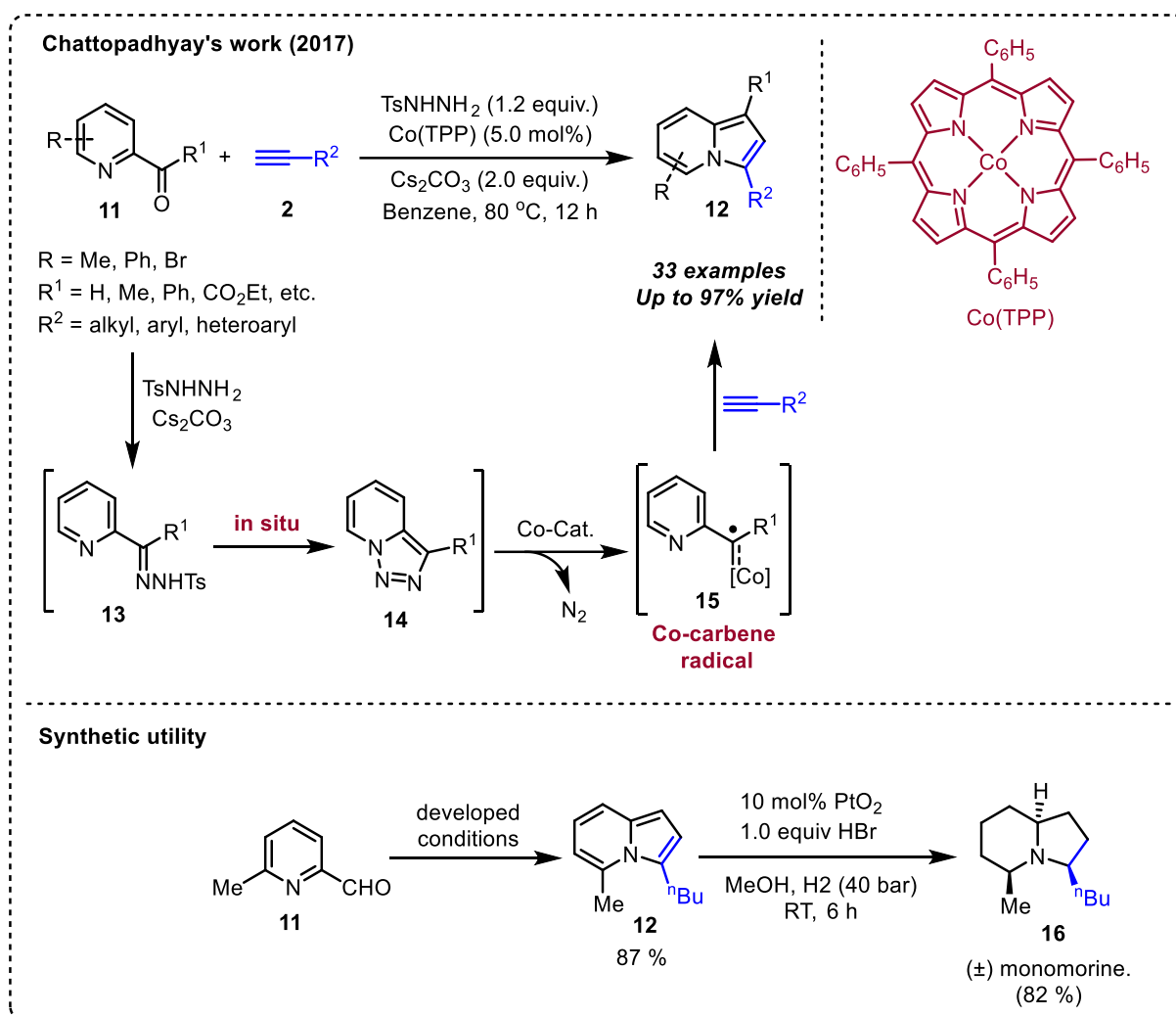
In 2017 Chattopadhyay and co-workers reported a Cobalt(II)-catalyzed radical-activation protocol for the synthesis of indolizine derivatives (**12**) from 2-pyridine carboxaldehyde (**11**) and terminal alkynes. A wide range of terminal alkynes was successfully utilized to get the respective indolizine products in good to excellent yields. According to the authors, the reaction proceeds through the generation of a Co(III)-carbene radical intermediate

15, from the *in situ*-generated pyridotriazole **14**. Notably, they have utilized this protocol for the total synthesis of the (±) monomorine **16** (scheme 4)^[15]



Scheme 3. Gold-catalyzed hydroarylation/cycloaromatization for indolizine synthesis

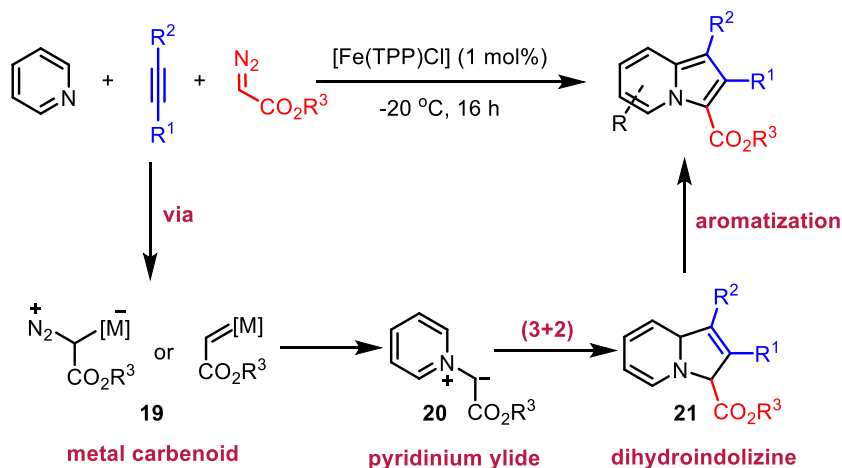
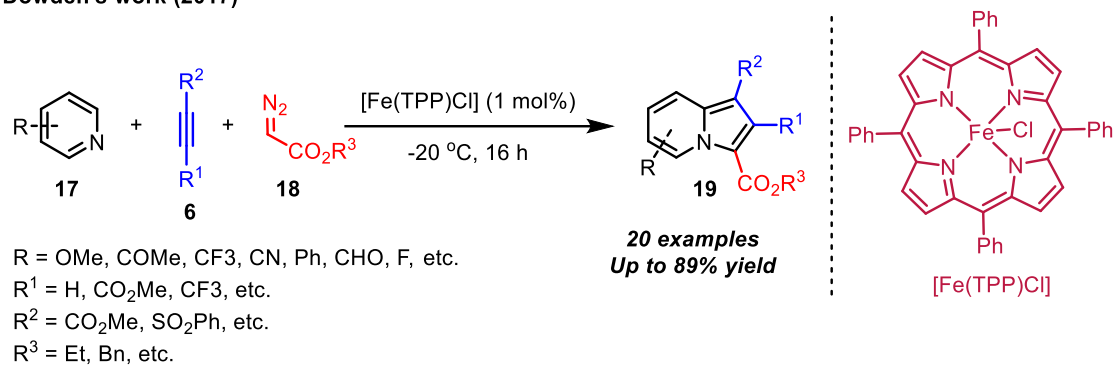
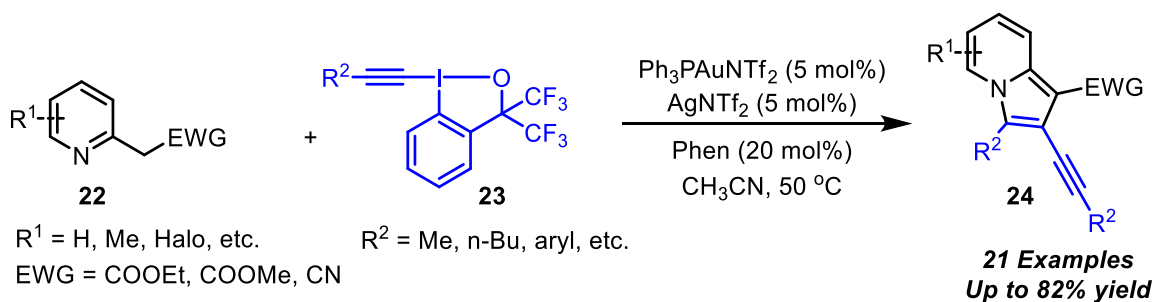
Dowden group in 2017 developed a Fe(III) catalyzed, one-pot multi-component reaction for synthesizing indolizine compounds (**19**) from pyridines (**17**), alkynes (**6**), and a diazo precursor **18**. The authors proposed that the reaction proceeds through the formation of an electrophilic metal carbenoid **19** from the diazo precursor **18**, which is attacked by the pyridine to give the pyridinium ylide **20**, which through a [3+2] cycloaddition reaction with the electrophilic alkyne **6** generates the dihydroindolizine **21**, which then undergoes aromatization to give the final indolizine product **19** (scheme 5).^[16]



Scheme 4. Synthesis of indolizine from 2-pyridine carboxaldehyde

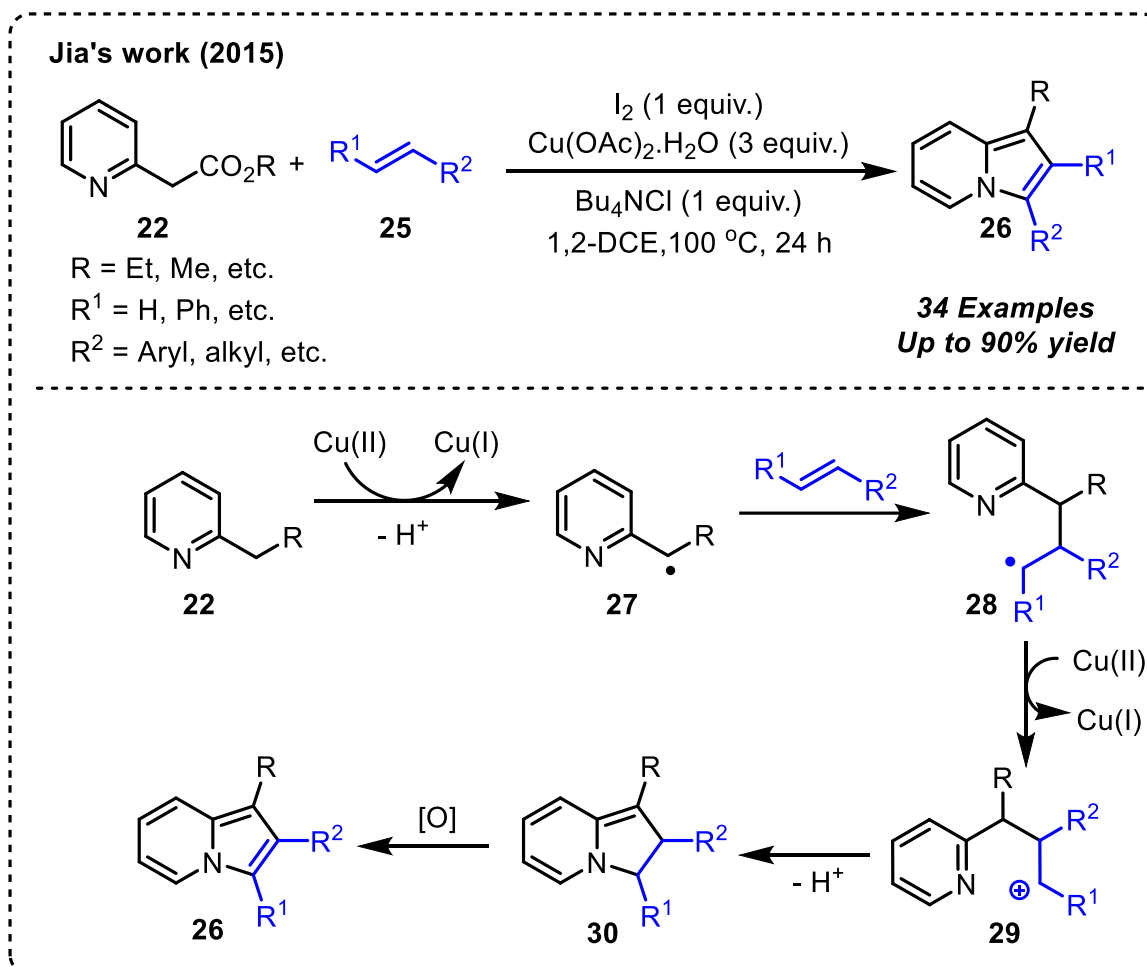
In 2021 Hashmi and co-workers reported a dual Au/Ag catalyzed cascade reaction for the synthesis of 2-alkynyl indolizine derivatives (**24**) from the reaction of 2-substituted pyridines (**22**) and hypervalent iodine (III) reagent (**23**). A series of indolizines bearing diverse functionalities were prepared in good to excellent yield (scheme 6).^[17]

Jia and co-workers developed a copper/ I_2 -mediated oxidative cross-coupling/cyclization of 2-(pyridin-2-yl)acetate derivatives (**22**) and olefins (**25**) to access polysubstituted indolizines **26**. Based on some control experiments the authors proposed a radical mechanism for this transformation. Initially, the single-electron oxidation of 2-(pyridin-2-yl)acetate **22** generates the radical intermediate **27**. Subsequent radical addition of **27** to alkene **25** produces another radical intermediate **28**. The radical intermediate **28** is then oxidized by Cu(II) to carbocation intermediate **29**, followed by an intramolecular cyclization and subsequent aromatization to afford the final product **26** (scheme 7).^[18]

Dowden's work (2017)**Scheme 5.** Fe(III)-catalyzed multicomponent reaction for indolizine synthesis**Hashmi's work (2021)****Scheme 6.** Synthesis of indolizine using hypervalent iodine (III) reagent

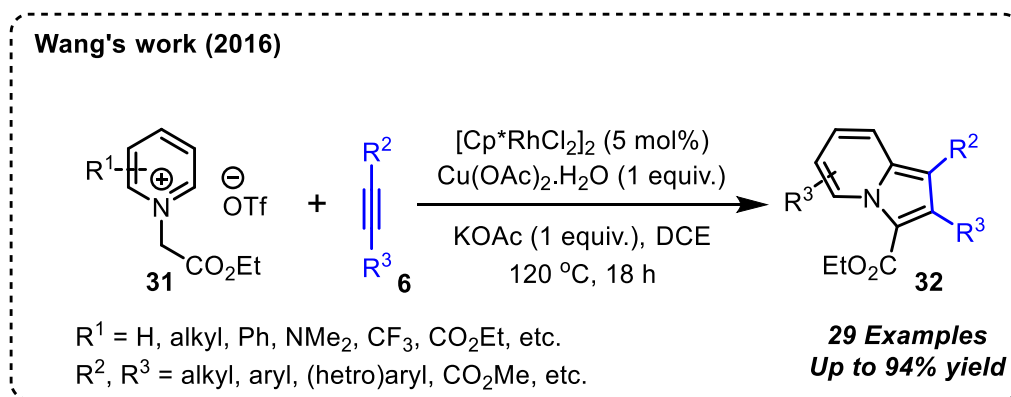
Wang's group in 2016 reported a Rh(III)-catalyzed oxidative annulation of pyridinium salt (**31**) with alkynes (**6**) to access polysubstituted indolizine derivatives (**32**). A stoichiometric amount of $\text{Cu}(\text{OAc})_2 \cdot \text{H}_2\text{O}$ was used as the oxidant in the presence of KOAc as the base. The

reaction did not work in the absence of KOAc, which suggests that the presence of the base is essential to drive this transformation (scheme 8).^[19]



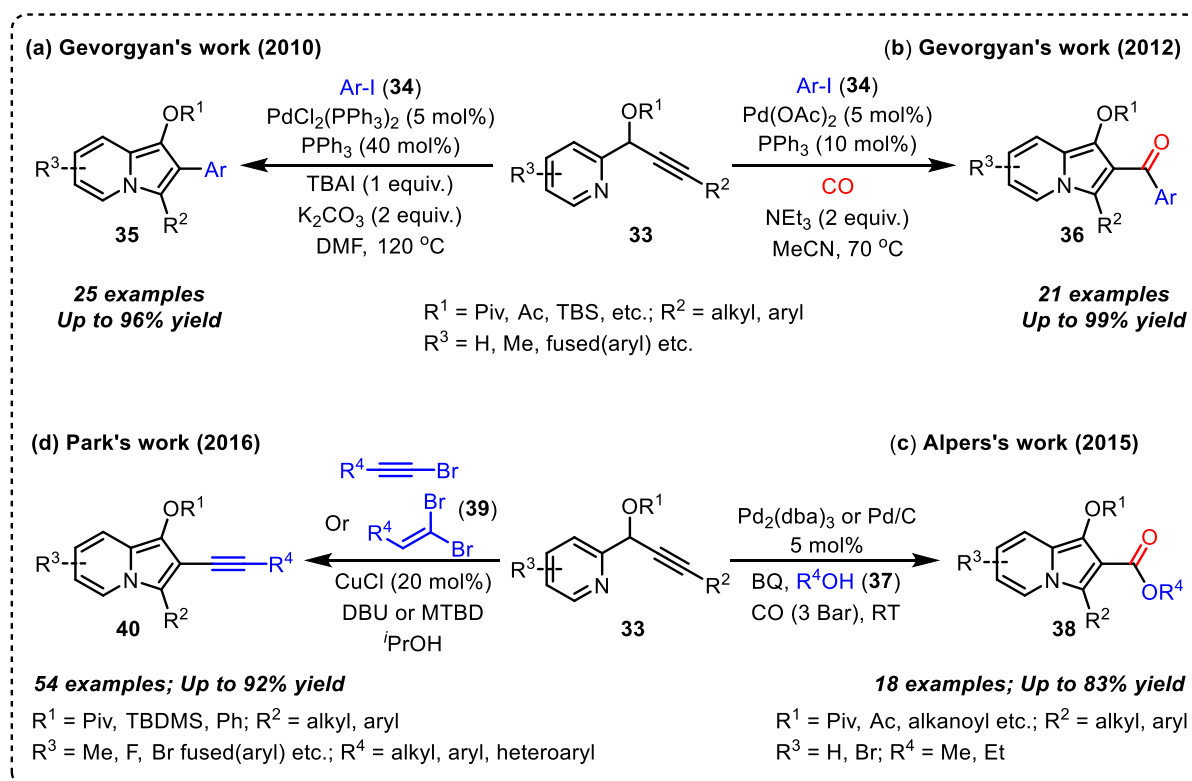
Scheme 7. copper/I₂-mediated oxidative cross-coupling/cyclization to access indolizines

One-pot approaches for synthesizing C2-substituted indolizine have become an attractive research area, which primarily involve cycloisomerization of propargyl pyridine derivatives followed by trapping with an electrophile. For instance, Gevorgyan's group disclosed a Pd-catalyzed coupling of aryl halides (**34**) with propargylic pyridines (**33**), followed by the 5-*endo*-dig cyclization approach for the synthesis of a variety of 2-aryl substituted indolizines **35** (Scheme 9a).^[20a] Later, the same group in 2012 reported a Pd-catalyzed carbonylative cyclization/arylation strategy for the synthesis of 2-arylindolizines (**36**) in good to excellent yields from propargylic pyridines (**33**), triggered by in situ generated aryl Pd-complex (Scheme 9b).^[20b]



Scheme 8. Rh(III)-catalyzed synthesis of indolizine derivatives

Similarly, Alper and co-workers disclosed a Pd-catalyzed oxidative carbonylation of propargylic pyridines (**33**) for the synthesis of indolizine. This method was successfully utilized to access a broad range of heavily substituted indolizines (**38**) under mild reaction conditions (Scheme 9c).^[20c] Further, a base-controlled and Cu-catalyzed tandem cyclization followed by alkynylation was reported by Park and co-workers in 2016. According to the proposed mechanism, the reaction proceeds through a 5-*endo*-dig amino-cupration of **33** followed by a



Scheme 9. Synthesis of indolizines from the cycloisomerization of propargyl pyridine

Cu-catalyzed coupling with alkynyl bromide or alkenyl bromides (**39**) to provide the functionalized indolizine derivatives (**40**) in good to excellent yields [Scheme 9d].^[20d]

2.3. Background:

Although all the above-mentioned approaches are elegant, there is a demand for simpler and more practical approaches to synthesize indolizine derivatives. To the best of our knowledge there are currently no reports available on the synthesis of indolizine heterocycles from *p*-quinone methides. While working on the synthesis of carbocycles/heterocycles^[21] from *p*-quinone methides (*p*-QMs),^[22] we envisioned that 2-pyridinyl-substituted *p*-QMs could be used as synthons for 1,3-disubstituted indolizines (**d**, Scheme 1). Herein, we report an unprecedented protocol involving a Pd (II)-catalyzed highly regiospecific intermolecular [3+2]-annulation reactions between 2-pyridinyl substituted *p*-QMs and terminal alkynes to access a variety of 1,3-disubstituted indolizines.

2.4. Result and discussion:

To optimize the reaction conditions, we have chosen readily available *para*-quinone methide **41a** and phenylacetylene **2a** as model substrates and, the results of optimization study are shown in Table 1. Initially, a couple of reactions between **41a** and **2a** were performed using 10 mol% of Cu(OTf)₂ in MeCN or THF at room temperature, but no product formation was seen as the starting material was remained as such even after 24 hours (entries 1 & 2). When the same reaction was conducted in toluene at room temperature, only trace amount of the product formation was observed (entry 3). However, interestingly, when the temperature of the reaction was raised to 50 °C, the desired product **42a** was obtained in 30% yield after 12 hours (entry 4). The isolated product **42a** was comprehensively characterised by ¹H NMR, ¹³C NMR, IR spectroscopy, and mass spectrometry. In ¹H NMR (see figure 2) presence of a singlets at δ 5.18 ppm and the singlet at δ 1.52 ppm is due to the phenolic OH and due to two symmetric *tert*-butyl groups respectively. In ¹³C NMR (see figure 3), the absence of carbonyl peak from **40a** and the presence of two peaks at δ 34.6 ppm and δ 30.6 ppm due to symmetric *tert*-butyl carbon peak confirmed the formation of **42a**. The formation of OH in product **42a** was also confirmed by IR peak at 3635 cm⁻¹. Further the HRMS (ESI): *m/z* calcd for C₂₈H₃₂NO [M+H]⁺ : 398.2492 also confirms the formation of **42a**. At this point, we thought addition of stoichiometric amounts of base would help in improving the yield of **42a**. Thus, a couple of experiments have been

Figure 2: ^1H NMR (400 MHz, CDCl_3) spectrum of **42a**

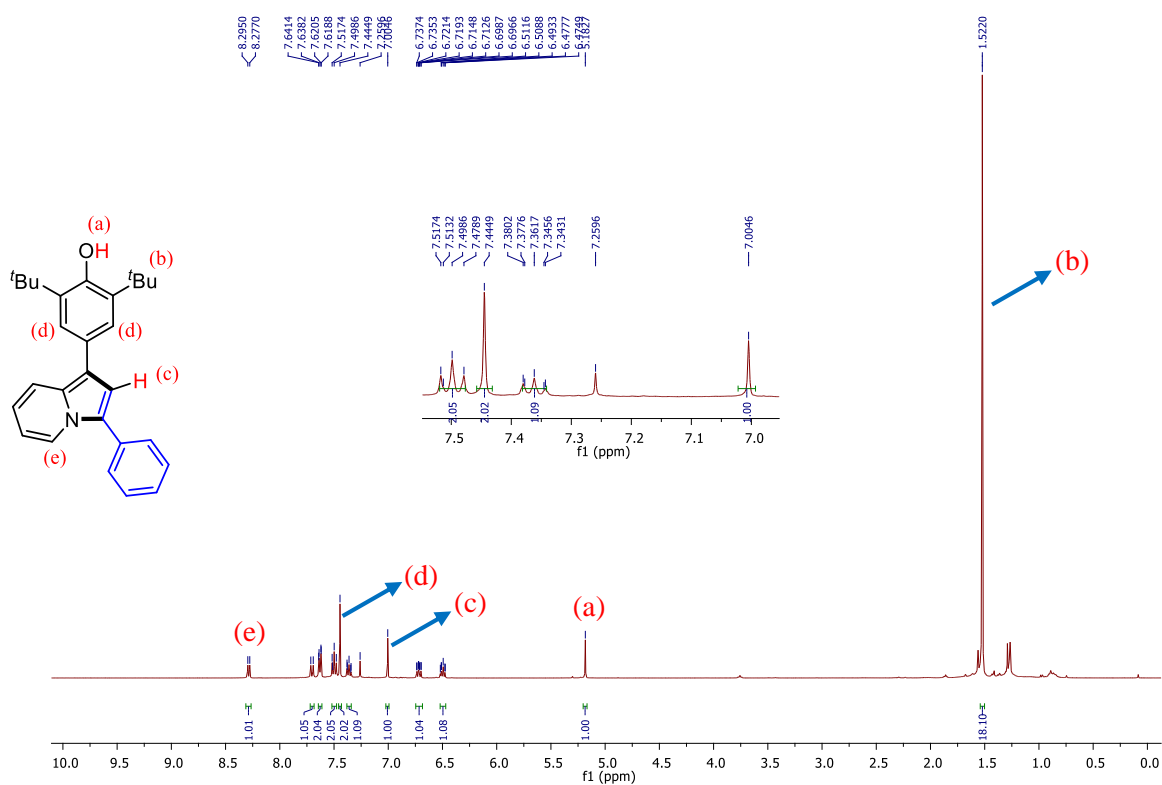


Figure 3: $^{13}\text{C}\{^1\text{H}\}$ NMR (100 MHz, CDCl_3) spectrum of **42a**

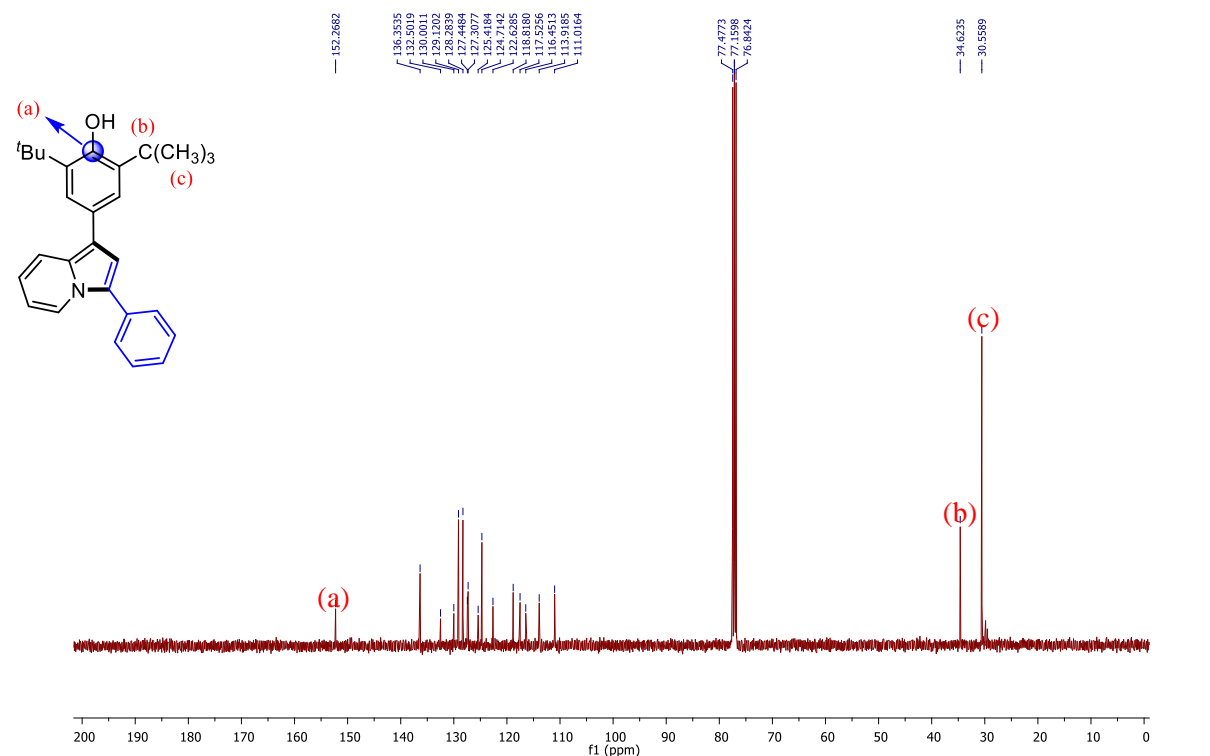
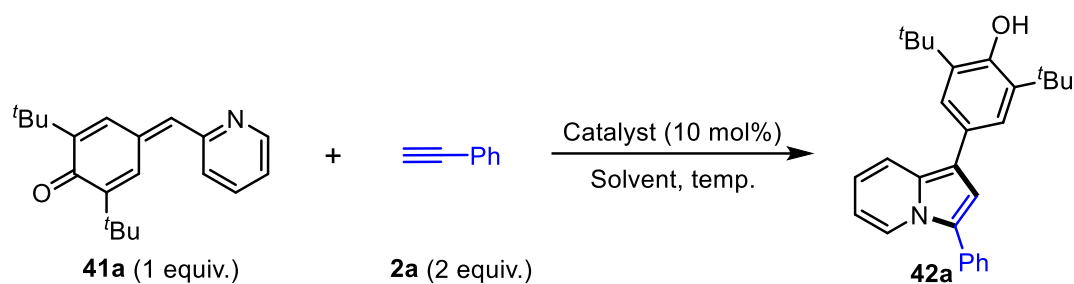


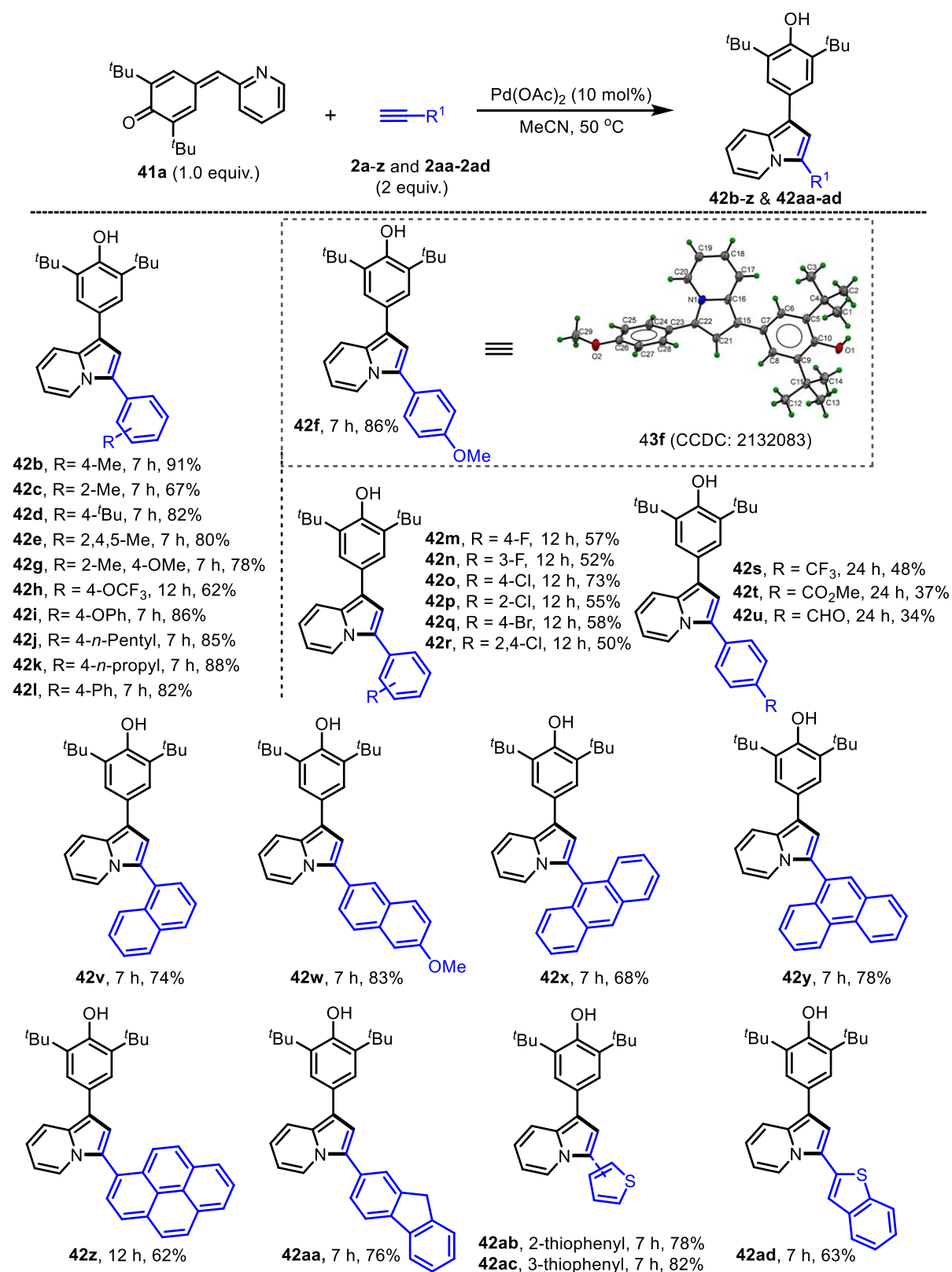
Table 1. Optimization Study^a

Entry	Catalyst	Solvent	Temp. [°C]	Time [h]	Yield [%] ^b
1	Cu(OTf) ₂	MeCN	RT	24	n.r.
2	Cu(OTf) ₂	THF	RT	24	n.r.
3	Cu(OTf) ₂	PhMe	RT	24	Trace
4	Cu(OTf) ₂	PhMe	50	12	30
5 ^c	Cu(OTf) ₂	PhMe	50	12	32
6 ^d	Cu(OTf) ₂	PhMe	50	12	30
7	CuOTf·PhMe	PhMe	50	12	25
8	Pd(OAc) ₂	PhMe	50	12	56
9	Pd(OAc) ₂	1,2-DCE	50	12	73
10	Pd(OAc) ₂	1,4-Dioxane	50	10	75
11	Pd(OAc) ₂	THF	50	24	59
12	Pd(OAc)₂	MeCN	50	7	90
13	PdCl ₂	MeCN	50	24	62
14	Pd(PPh ₃) ₄	MeCN	50	24	n.r.
15	AgOCOCF ₃	MeCN	50	24	n.r.
16	AgSbF ₆	MeCN	50	24	n.r.
17	AgOAc	MeCN	50	24	n.r.
18	Pd(OAc) ₂	MeCN	RT	24	52
19	---	MeCN	50	48	n.r.
20	Ni(C ₅ H ₅) ₂	MeCN	50	24	n.r.
21	[(C ₆ H ₅) ₃ P] ₃ RhCl	MeCN	50	24	n.r.
22	Cu(OAc) ₂	MeCN	50	24	Trace
23	CuBr ₂	MeCN	50	24	n.r.
24	FeCl ₂	MeCN	50	24	n.r.
25	Fe(OAc) ₂	MeCN	50	24	n.r.

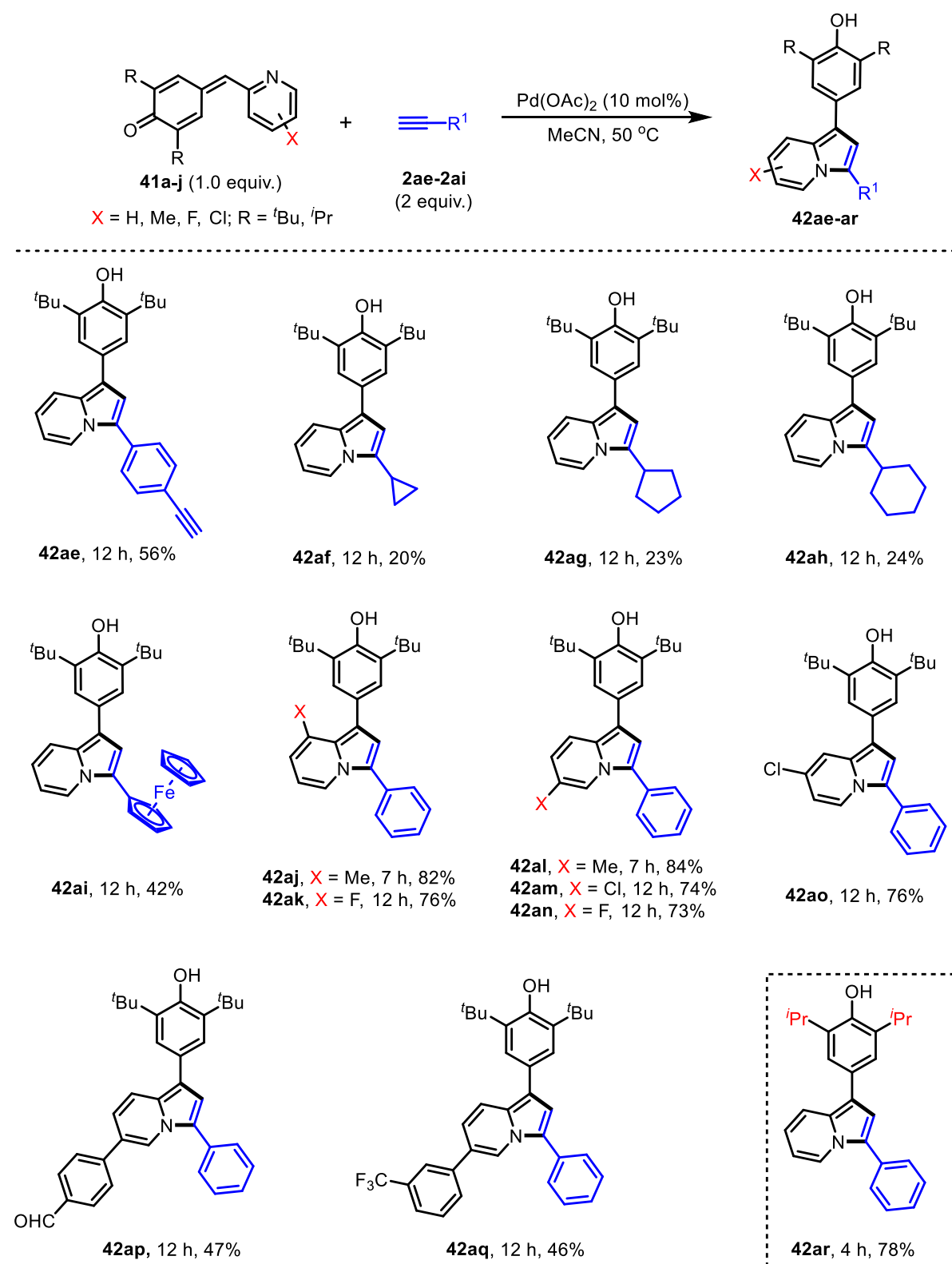
^aReaction conditions: Reactions were carried out with 0.10 mmol of **41a**, 2 equiv. of **2a** with respect to **41a** and 10 mol % catalyst. ^bYields reported are isolated yields. ^c2 equiv. of NEt₃ was used, ^d2 equiv. of ⁱPr₂NEt was used. 1,2-DCE = 1,2-Dichloroethane; n.r. = No reaction).

performed using 2 equivalents of base such as NEt₃ and *i*Pr₂NEt. However, in both the cases, no further improvement in the yield of **42a** was observed (entries 5 & 6). In addition, the Cu(I)-catalyst, i.e., Cu(OTf).PhMe also yielded the product **44a** only in 25% yield (entry 7). Interestingly, a significant improvement in the yield of **42a** was noticed, when Pd(OAc)₂ was as a catalyst (entry 8). Therefore, further optimization studies were carried out using Pd(OAc)₂ as a catalyst under different conditions (entries 9-12). In fact, the reaction worked well in almost all the solvents examined, but, out of these solvents, MeCN was found to be the best solvent as **42a** was obtained in 90% yield in that case (entry 12). Although PdCl₂ was also found to drive this transformation (entry 13), the yield of **42a** was much lower when compared to the reaction catalyzed by Pd(OAc)₂ (entry 12). Interestingly, the Pd(0) and Ag(I) catalysts, which are known to activate alkynes, were found to be ineffective for this transformation (entries 14-17). When the reaction was carried out in MeCN at rt with Pd(OAc)₂ as a catalyst, **42a** was obtained only in 52% yield (entry 18). So, the reaction at 50 °C, i.e., entry 12 seemed to be the ideal condition for this transformation. No product was formed when the reaction was performed without the catalyst, which clearly indicates a catalyst is required for this transformation (entry 19). Other metal catalysts such as salts of Fe, Rh, Ni and Cu failed to catalyze this transformation (entries 20-25).

To investigate the substrate scope of this transformation, the reaction between a wide range of terminal alkynes (**2a-z** & **2aa-ai**) and 2-pyridinyl-substituted *p*-QMs (**41a-j**) were carried out under optimal conditions (entry 12, Table 1) and the results are summarized in Table 2 & 3. The reaction worked well with alkynes, substituted with electron-rich arenes and halo-substituted arenes and, the corresponding products **42b-r** were isolated in moderate to good yields (50-91%). However, the reactions between alkynes, substituted with electron-poor arenes (**2s-u**), with **41a** were found to be sluggish and, in those cases, the products **42s-u** were obtained in relatively lower yields (34-48%). Otherwise, the alkynes (**2v-2z** & **2aa**) substituted with naphthalene, anthracene and pyrene etc., reacted smoothly with **41a** to provide the products **42v-42z** and **42aa** in acceptable isolated yields (62-83%). The indolizine derivatives **42ab-ad** were obtained in the range of 72-83% yields, when the reaction was carried out between **1a** and alkynes bearing heteroaromatic substituents (**2ab-ad**). Interestingly, when a reaction was carried out between 1,4-diacetylenebenzene **2ae** and **41a**, the product **42ae** was obtained in 56% yield. Reactions of alkyl-substituted alkynes **2af-ah** with **41a**, also took place under the optimal conditions, however, the corresponding products **42af-ah** were isolated in low yields (20-24%). The reaction of ethynylferrocene **2ai** and **41a** also worked well and the

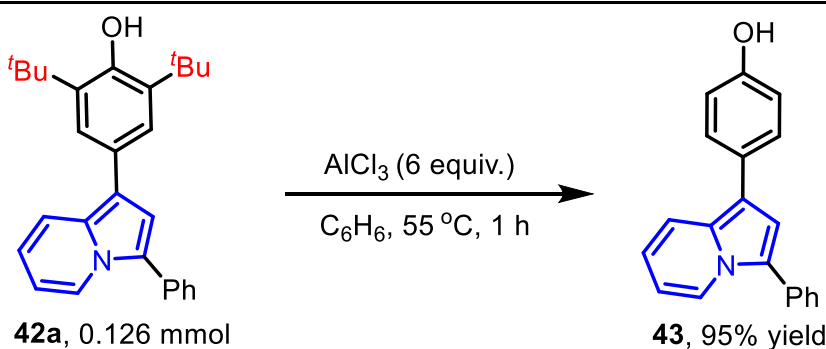
Table 2. Substrate Scope^b

^aReactions were carried out with 30 mg of **41a** and 2.0 equiv. of **2(a-z & aa-ad)** in 1.5 mL of MeCN. ^bYields reported are isolated yields.

Table 3. Substrate Scope^b

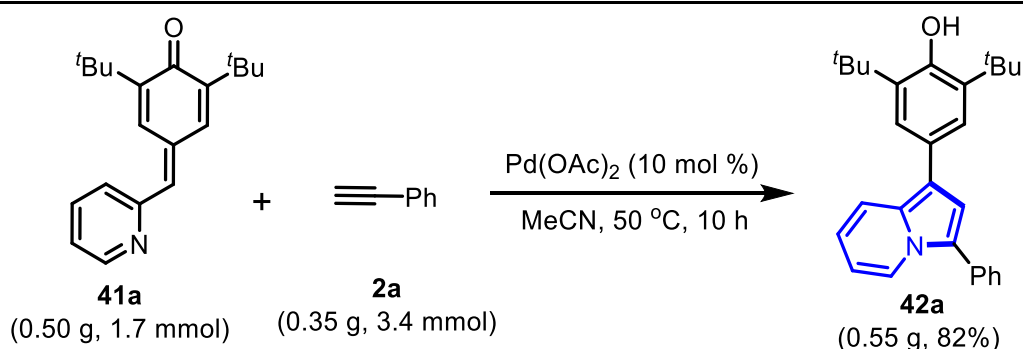
^aReactions were carried out with 30 mg of **41a-k** and 2.0 equiv. of **2(a & ae-ai)** in 1.5 mL of MeCN. ^bYields reported are isolated yields.

corresponding product **42ai** was obtained in 42% yield. The *p*-QMs **41b-41g** (derived from substituted 2-pyridine carboxaldehydes) were also subjected to react with **2a** and, in those cases, the indolizines **42aj-42ao** were isolated in the range of 74-84% yields. The *p*-QMs **41h** and **41i**, substituted with relatively electron-poor substituents on the pyridine ring, were also subjected to react with **2a** and, in those cases, the indolizines **42ap** and **42aq** were isolated in 46% and 47% yields, respectively. The *p*-QMs **41j**, with isopropyl groups in place of *t*-butyl groups, also reacted smoothly with **2a** and, the corresponding product **42ar** was isolated in 78% yield. To further improve the substrate-scope of this transformation, **42a** was subjected to de-*tert*-butylation reaction with AlCl₃ (6 equiv.) in benzene at 55 °C and, the resultant product **43** was obtained in 95% yield in an hour (scheme 10).



Scheme 10. De-*tert*-butylation Reaction

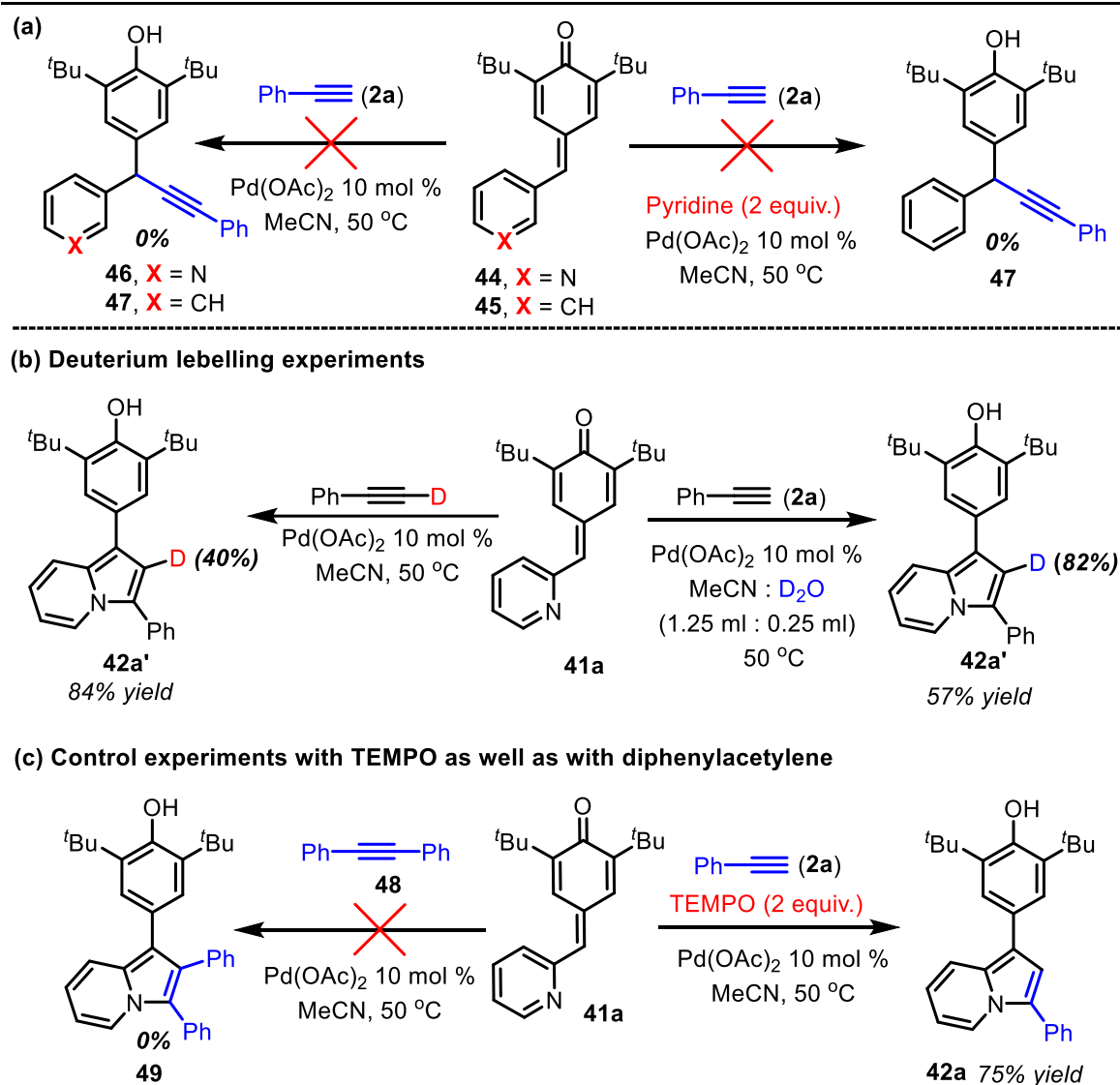
In addition, to show the practical applicability of this transformation, a relatively large-scale reaction between **41a** (0.5 g scale) and **2a** was performed, and the desired product **42a** was obtained in 85% yield (0.55 g) in 10 hours (scheme 11).



Scheme 11. Relatively large-scale reaction

To understand the mechanistic aspects of this protocol, a few control experiments were performed. In one of the experiments, the *p*-quinone methide **44** (derived from pyridine-3-carboxaldehyde), was treated with phenyl acetylene **2a** under the standard reaction conditions;

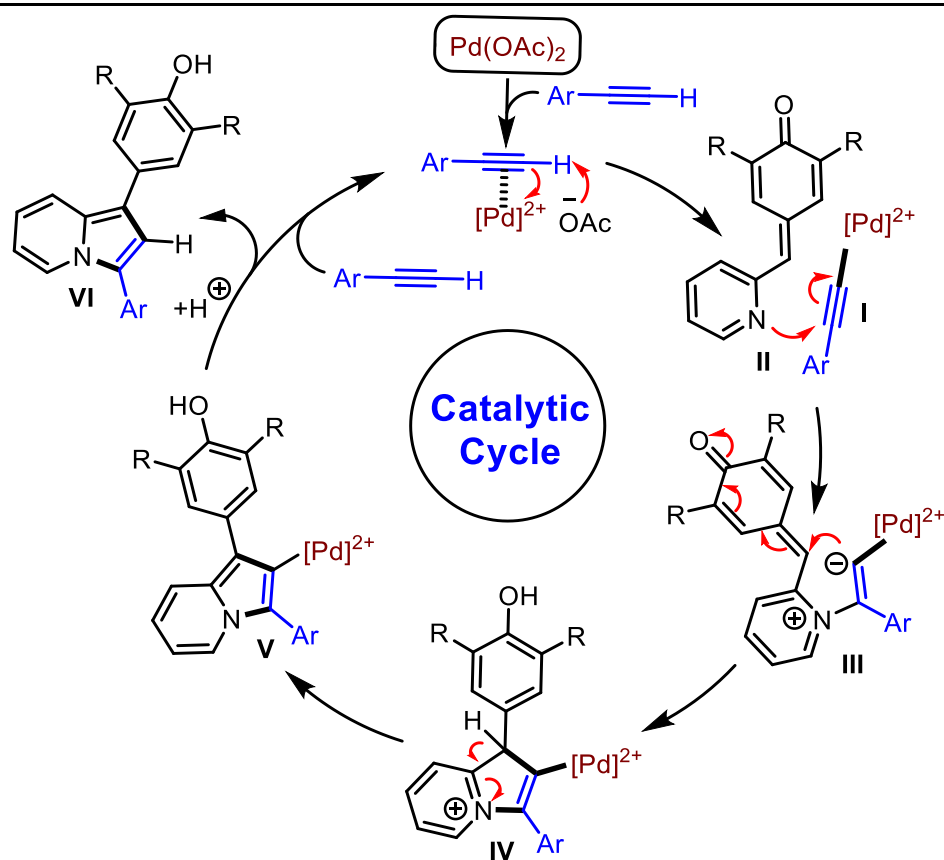
however, the formation of 1,6-adduct **46** was not observed [Scheme 12, (a)].¹⁵ In another set of experiments, *p*-quinone methide **45** was treated with **2a** under the optimized reaction conditions as well as in the presence of pyridine (2.0 equiv.). In both the cases, no formation of 1,6-adduct **47** was observed. These control experiments clearly indicate that this transformation is not proceeding through the 1,6-conjugate addition of alkyne to *p*-QM.



Scheme 12. Control Experiments

Interestingly, when the reaction between **41a** and **2a** was performed in a mixture of MeCN and D₂O, the product **42a'** was obtained in 57% yield with 82% Deuterium incorporation at C-2 of indolizine ring [Scheme 12, (b)]. In another experiment, **41a** was treated with deuterated phenylacetylene (Ph-C≡C-D) under standard conditions and, in this case, **42a'** was obtained in 84% yield with only 40% D incorporation at C-2 of indolizine [Scheme 12, (b)]. It is evident

from these experiments that the alkynyl proton of **2a** is getting removed during the reaction. The reaction did take place even in the presence of excess of TEMPO, which indicates that the reaction does not proceed through radical intermediate(s) [Scheme 12, (c)]. Another interesting observation was that the internal alkyne, diphenylacetylene (**48**) failed to provide the respective indolizine **49** under standard conditions even after 48 h [Scheme 12, (c)]. This result and the deuterium labelling experiments [Scheme 12, (b)] clearly indicate that the acetylenic hydrogen ($\equiv\text{C-H}$) is playing an important role in the reaction and, during the course of the reaction, this proton is getting removed as observed in the labelling experiments.



Scheme 13. Plausible Mechanism

On the basis of the above-mentioned control experiments, a plausible mechanism for this transformation has been proposed (Scheme 13). Initially, the reaction proceeds through the activation of alkyne by palladium (II) catalyst followed by the removal of the alkyne proton to give the intermediate **I**. The nucleophilic attack of pyridine to intermediate **I** generates a salt **III**, which then undergoes an intramolecular cyclization/1,6-addition to generate a Pd-complex **IV**. Subsequently, **IV** undergoes proton isomerization followed by protodepalladation to generate the product **VI** (Scheme 13).

2.5. Conclusion:

In conclusion, we have developed a facile strategy for the synthesis of a wide range of 1,3-disubstituted indolizine derivatives in moderate to good yields through a Pd(II)-catalyzed regiospecific formal [3+2]-annulation of terminal alkynes and 2-pyridinyl substituted *p*-quinone methides. Most of the alkynes, especially the aryl-substituted ones, reacted with 2-pyridinyl substituted *p*-quinone methides smoothly and provided the respective 1,3-disubstituted indolizines in good to excellent yields. We believe the inherent advantages of the present method such as 100% atom-economy, relatively milder reaction conditions and regiospecificity will make this method practically attractive.

2.6. Experimental section:

General information

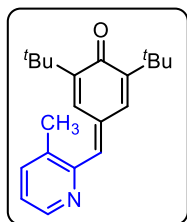
All reactions were carried out in an oven dried round bottom flask. All the solvents were distilled before use and stored under argon atmosphere. Most of the reagents, starting materials were purchased from commercial sources and used as such. Melting points were recorded on SMP20 melting point apparatus and are uncorrected. ^1H , ^{13}C and ^{19}F spectra were recorded in CDCl_3 (400, 100 and 376 MHz respectively) on Bruker FT-NMR spectrometer. Chemical shift (δ) values are reported in parts per million relative to TMS and the coupling constants (J) are reported in Hz. High resolution mass spectra were recorded on Waters Q-TOF Premier-HAB213 spectrometer. FT-IR spectra were recorded on a Perkin-Elmer FTIR spectrometer. Thin layer chromatography was performed on Merck silica gel 60 F₂₅₄ TLC pellets and visualised by UV irradiation and KMnO_4 stain. Column chromatography was carried out through silica gel (100–200 mesh) using EtOAc/hexane as an eluent.

General procedure for the reaction between terminal alkynes to 2-pyridinyl-substituted p-quinone methides:

Anhydrous MeCN (1.5 mL) was added to the mixture of *p*-quinone methide [*p*-QM] (30 mg, 1.0 equiv.), terminal alkyne (2.0 equiv.) and $\text{Pd}(\text{OAc})_2$ (10 mol %) under argon atmosphere and the resulting suspension was stirred at 50 °C until the *p*-QM was completely consumed (based on TLC analysis). The reaction mixture was concentrated under reduced pressure and the residue was purified through a silica gel chromatography, using EtOAc/Hexane mixture as an eluent, to get the pure 1,3-disubstituted indolizine.

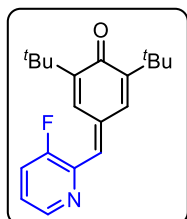
The 2-pyridinyl-substituted *p*-quinone methides **41b-f** were prepared by following a literature procedure.^[23] The 2-pyridinyl-substituted *p*-quinone methides **1h-i** were prepared by following a literature procedure^[24] by the coupling of corresponding boronic acid and *p*-QM (**41f**). The 2-pyridinyl-substituted *p*-quinone methide **1i** was prepared by following a literature procedure.^[25]

2,6-di-*tert*-butyl-4-[(3-methylpyridin-2-yl)-methylene]-cyclohexa-2,5-dien-1-one (**41b**)



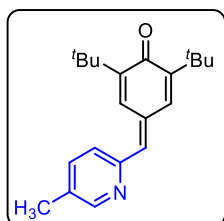
The reaction was performed at 4.127 mmol scale of 3-methylpicolinaldehyde; $R_f = 0.5$ (5% EtOAc in hexane); yellow solid (794 mg, 62% yield); m. p. = 154 – 156 °C; ^1H NMR (400 MHz, CDCl_3) δ 8.57 – 8.56 (m, 1H), 8.34 (d, $J = 1.9$ Hz, 1H), 7.54 – 7.52 (m, 1H), 7.15 (dd, $J = 7.7, 4.7$ Hz, 1H), 7.12 (s, 1H), 7.00 (d, $J = 2.0$ Hz, 1H), 2.43 (s, 3H), 1.32 (s, 9H), 1.30 (s, 9H); ^{13}C NMR (100 MHz, CDCl_3) δ 186.8, 153.7, 149.8, 148.6, 147.5, 138.3, 136.1, 135.5, 134.7, 134.4, 129.6, 123.1, 35.6, 35.2, 29.7, 29.67, 19.5; FT-IR (thin film, neat): 2952, 2857, 1739, 1604, 1540, 1372, 1237, 1045, 931, 740, 590 cm^{-1} ; HRMS (ESI): m/z calcd for $\text{C}_{21}\text{H}_{28}\text{NO}$ $[\text{M}+\text{H}]^+$: 310.2171; found : 310.2176.

2,6-di-*tert*-butyl-4-[(3-fluoropyridin-2-yl)-methylene]-cyclohexa-2,5-dien-1-one (**41c**)



The reaction was performed at 3.997 mmol scale of 3-fluoropicolinaldehyde; $R_f = 0.5$ (5% EtOAc in hexane); orange solid (826 mg, 66% yield); m. p. = 130 – 132 °C; ^1H NMR (400 MHz, CDCl_3) δ 8.75 (d, $J = 2.2$ Hz, 1H), 8.53 (d, $J = 4.5$ Hz, 1H), 7.44 – 7.39 (m, 1H), 7.27 – 7.23 (m, 1H), 7.13 (d, $J = 2.2$ Hz, 1H), 6.98 (d, $J = 2.2$ Hz, 1H), 1.33 (s, 9H), 1.32 (s, 9H); ^{13}C NMR (100 MHz, CDCl_3) δ 186.8, 158.9 (d, $J_{\text{C-F}} = 263.4$ Hz), 150.3, 149.0, 145.7 (d, $J_{\text{C-F}} = 5.4$ Hz), 144.1 (d, $J_{\text{C-F}} = 9.0$ Hz), 135.7 (d, $J_{\text{C-F}} = 1.6$ Hz), 135.5, 129.4, 128.8, 124.5 (d, $J_{\text{C-F}} = 4.1$ Hz), 123.3 (d, $J_{\text{C-F}} = 19.5$ Hz), 35.8, 35.2, 29.7, 29.69; $^{19}\text{F}\{^1\text{H}\}$ NMR (376 MHz, CDCl_3) δ -120.4; FT-IR (thin film, neat): 2983, 1738, 1618, 1451, 1372, 1235, 1044, 936, 787, 536 cm^{-1} ; HRMS (ESI): m/z calcd for $\text{C}_{20}\text{H}_{25}\text{FNO}$ $[\text{M}+\text{H}]^+$: 314.1920; found : 314.1913.

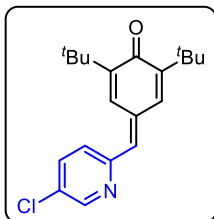
2,6-di-*tert*-butyl-4-[(5-methylpyridin-2-yl)-methylene]-cyclohexa-2,5-dien-1-one (**41d**)



The reaction was performed at 0.102 mmol scale of 5-methylpicolinaldehyde; $R_f = 0.5$ (5% EtOAc in hexane); yellow solid (820 mg, 64% yield); m. p. = 152 – 154 °C; ^1H NMR (400 MHz, CDCl_3) δ 8.69 (d, $J = 1.6$ Hz, 1H), 8.57 (brs, 1H), 7.52 – 7.49 (m, 1H), 7.29 (d, $J = 8.0$ Hz

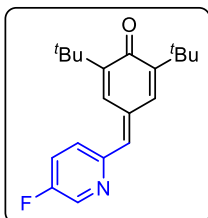
1H), 6.95 (d, $J = 1.8$ Hz, 1H), 6.92 (s, 1H), 2.36 (s, 3H), 1.33 (s, 9H), 1.31 (s, 9H); ^{13}C NMR (100 MHz, CDCl_3) δ 186.8, 152.7, 150.9, 149.6, 148.4, 138.7, 136.9, 135.6, 133.9, 133.0, 129.3, 126.9, 35.7, 35.1, 29.7, 29.69, 18.6; FT-IR (thin film, neat): 3090, 2954, 2864, 2734, 1951, 1762, 1606, 1541, 1382, 1251, 1023, 950, 705, 644, 535 cm^{-1} ; HRMS (ESI): m/z calcd for $\text{C}_{21}\text{H}_{28}\text{NO}$ $[\text{M}+\text{H}]^+$: 310.2171; found: 310.2180.

2,6-di-*tert*-butyl-4-[(5-chloropyridin-2-yl)-methylene]-cyclohexa-2,5-dien-1-one (41e)



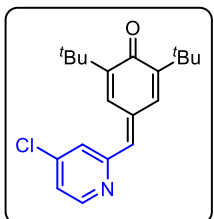
The reaction was performed at 3.532 mmol scale of 5-chloropicolinaldehyde; $R_f = 0.5$ (5% EtOAc in hexane); yellow solid (842 mg, 72% yield); m. p. = 154 – 156 $^{\circ}\text{C}$; ^1H NMR (400 MHz, CDCl_3) δ 8.68 (d, $J = 2.2$ Hz, 1H), 8.63 (d, $J = 1.7$ Hz, 1H), 7.68 (dd, $J = 8.4, 2.4$ Hz 1H), 7.33 (d, $J = 8.4$ Hz, 1H), 6.93 (d, $J = 1.8$ Hz, 1H), 6.86 (s, 1H), 1.32 (s, 9H), 1.31 (s, 9H); ^{13}C NMR (100 MHz, CDCl_3) δ 186.7, 153.5, 150.2, 149.2, 149.0, 136.5, 136.3, 135.3, 135.1, 131.3, 128.8, 127.7, 35.8, 35.2, 29.7, 29.69; FT-IR (thin film, neat): 2984, 2925, 1737, 1618, 1448, 1372, 1234, 1044, 937, 736, 607, 512 cm^{-1} ; HRMS (ESI): m/z calcd for $\text{C}_{20}\text{H}_{25}\text{ClNO}$ $[\text{M}+\text{H}]^+$: 330.1625; found : 330.1624.

2,6-di-*tert*-butyl-4-((5-fluoropyridin-2-yl)methylene)cyclohexa-2,5-dien-1-one (41f)



The reaction was performed at 3.997 mmol scale of 5-fluoropicolinaldehyde; $R_f = 0.5$ (5% EtOAc in hexane); yellow solid (852 mg, 68% yield); m. p. = 136 – 138 $^{\circ}\text{C}$; ^1H NMR (400 MHz, CDCl_3) δ 8.62 (d, $J = 2.0$ Hz, 1H), 8.58 (s, 1H), 7.42 – 7.40 (m, 2H), 6.93 (d, $J = 2.0$ Hz, 1H), 6.89 (s, 1H), 1.32 (s, 9H), 1.31 (s, 9H); $^{13}\text{C}\{^1\text{H}\}$ NMR (100 MHz, CDCl_3) δ 186.7, 158.4 (d, $J_{\text{C-F}} = 259.6$ Hz), 151.7 (d, $J_{\text{C-F}} = 4.6$ Hz), 150.1, 148.7, 138.8 (d, $J_{\text{C-F}} = 23.8$ Hz), 136.6, 135.4, 134.3 (d, $J_{\text{C-F}} = 2.2$ Hz), 128.9, 128.3 (d, $J_{\text{C-F}} = 4.4$ Hz), 123.3 (d, $J_{\text{C-F}} = 18.5$ Hz), 35.7, 35.2, 29.71, 29.67; $^{19}\text{F}\{^1\text{H}\}$ NMR (376 MHz, CDCl_3) δ -125.41; FT-IR (thin film, neat): 2982, 1740, 1622, 1455, 1373, 1236, 1044, 938, 785, 532 cm^{-1} ; HRMS (ESI): m/z calcd for $\text{C}_{20}\text{H}_{25}\text{FNO}$ $[\text{M}+\text{H}]^+$: 314.1920; found : 314.1914.

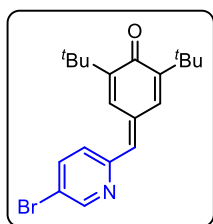
2,6-di-*tert*-butyl-4-((4-chloropyridin-2-yl)methylene)cyclohexa-2,5-dien-1-one (41g)



The reaction was performed at 3.532 mmol scale of 4-chloropicolinaldehyde; $R_f = 0.5$ (5% EtOAc in hexane); yellow solid (830 mg, 71% yield); m. p. = 158 – 160 $^{\circ}\text{C}$; ^1H NMR (400 MHz, CDCl_3) δ 8.65 (d, $J = 1.9$ Hz, 1H), 8.59 (d, $J = 5.2$ Hz, 1H), 7.36 (d, $J = 1.8$ Hz, 1H), 7.19

(dd, $J = 5.2, 1.8$ Hz, 1H), 6.91 (d, $J = 2.2$ Hz, 1H), 6.80 (s, 1H), 1.31 (s, 9H), 1.30 (s, 9H); $^{13}\text{C}\{^1\text{H}\}$ NMR (100 MHz, CDCl_3) δ 186.7, 156.7, 150.9, 150.3, 149.1, 144.5, 136.3, 135.8, 135.2, 128.9, 127.0, 122.8, 35.7, 35.2, 29.7, 29.6; FT-IR (thin film, neat): 3052, 2982, 2862, 1730, 1607, 1458, 1332, 1225, 1022, 740, 532 cm^{-1} ; HRMS (ESI): m/z calcd for $\text{C}_{20}\text{H}_{25}\text{ClNO}$ $[\text{M}+\text{H}]^+$: 330.1625; found : 330.1621.

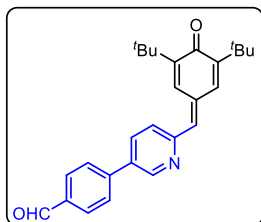
4-[(5-bromopyridin-2-yl)methylene]-2,6-di-*tert*-butylcyclohexa-2,5-dien-1-one (41h)



The reaction was performed at 2.855 mmol scale of 5-bromopicolinaldehyde; $R_f = 0.5$ (5% EtOAc in hexane); yellow solid (760 mg, 75% yield); m. p. = 168 – 170 °C; ^1H NMR (400 MHz, CDCl_3) δ 8.78 (d, $J = 2.3$ Hz, 1H), 8.63 (d, $J = 2.3$ Hz, 1H), 7.83 (dd, $J = 8.3, 2.4$ Hz, 1H), 7.27 (d, $J = 8.2$ Hz, 1H), 6.93 (d, $J = 2.2$ Hz, 1H), 6.84 (s, 1H), 1.32 (s, 9H),

1.31 (s, 9H); ^{13}C NMR (100 MHz, CDCl_3) δ 186.8, 153.7, 151.3, 150.2, 149.0, 139.2, 136.6, 135.3, 135.1, 128.8, 128.1, 120.2, 35.8, 35.2, 29.72, 29.68; FT-IR (thin film, neat): 3053, 2917, 2865, 1733, 1607, 1455, 1329, 1232, 1022, 742, 534 cm^{-1} ; HRMS (ESI): m/z calcd for $\text{C}_{20}\text{H}_{25}\text{BrNO}$ $[\text{M}+\text{H}]^+$: 374.1120; found : 374.1109.

4-{6-[(3,5-di-*tert*-butyl-4-oxocyclohexa-2,5-dien-1-ylidene)methyl]-pyridin-3-yl}-benzaldehyde (41i)

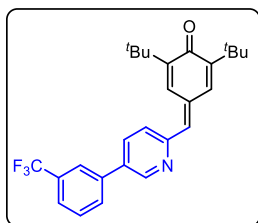


The reaction was performed at 0.801 mmol scale of **41h**; $R_f = 0.3$ (10% EtOAc in hexane); yellow solid (134mg, 41% yield); m. p. = 174 – 176 °C; ^1H NMR (400 MHz, CDCl_3) δ 10.1 (s, 1H), 9.04 (d, $J = 2.2$ Hz, 1H), 8.79 (d, $J = 2.0$ Hz, 1H), 8.01 (d, $J = 8.4$ Hz, 2H), 7.97 (dd, $J = 8.2, 2.4$ Hz, 1H), 7.82 (d, $J = 8.2$ Hz, 2H), 7.51 (d, $J = 8.1$ Hz, 1H), 6.98 (d, $J =$

2.2 Hz 1H), 6.97 (s, 1H), 1.35 (s, 9H), 1.33 (s, 9H); ^{13}C NMR (100 MHz, CDCl_3) δ 191.7, 186.8, 155.3, 150.2, 148.9, 148.8, 143.1, 137.3, 136.1, 135.5, 134.9, 135.3, 133.9, 130.7, 129.1, 127.7, 127.4, 35.8, 35.3, 29.8, 29.7; FT-IR (thin film, neat): 2998, 2955, 2866, 2731, 1699, 1604, 1535, 1359, 1251, 1089, 953, 818, 738 cm^{-1} ; HRMS (ESI): m/z calcd for $\text{C}_{27}\text{H}_{30}\text{NO}_2$ $[\text{M}+\text{H}]^+$: 400.2277; found: 400.2257.

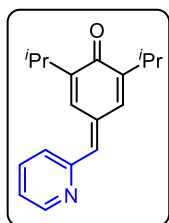
2,6-di-*tert*-butyl-4-{(5-[3-(trifluoromethyl)phenyl]pyridin-2-yl)methylene}-cyclohexa-2,5-dien-1-one (41j)

The reaction was performed at 0.801 mmol scale of **41h**; $R_f = 0.5$ (5% EtOAc in hexane); yellow solid (138 mg, 39% yield); m. p. = 122– 124 °C; ^1H NMR (400 MHz, CDCl_3) δ 9.00



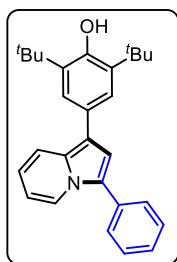
(d, $J = 2.2$ Hz, 1H), 8.81 (d, $J = 2.2$ Hz, 1H), 7.93 (dd, $J = 8.1, 2.4$ Hz, 1H), 7.88 (s, 1H), 7.85 (d, $J = 7.6$ Hz, 1H), 7.69 – 7.68 (m, 1H), 7.62 (t, $J = 7.7$ Hz, 1H), 7.50 (d, $J = 8.1$ Hz, 1H), 6.98 (d, $J = 2.2$ Hz, 1H), 6.97 (s, 1H), 1.36 (s, 9H), 1.33 (s, 9H); ^{13}C NMR (100 MHz, CDCl_3) δ 186.8, 155.0, 150.2, 148.9, 148.7, 138.1, 137.4, 135.5, 135.1, 134.7, 134.0, 13.8 (q, $J_{\text{C-F}} = 32.2$ Hz), 130.42, 130.41, 129.9, 127.4, 125.2 (q, $J_{\text{C-F}} = 3.7$ Hz), 124.1 (q, $J_{\text{C-F}} = 270.8$ Hz), 123.9 (q, $J_{\text{C-F}} = 3.8$ Hz), 35.8, 35.2, 29.8, 29.7; $^{19}\text{F}\{^1\text{H}\}$ NMR (376 MHz, CDCl_3) δ -62.7; FT-IR (thin film, neat): 2956, 2866, 1613, 1537, 1440, 1360, 1265, 1129, 1048, 933, 737 cm^{-1} ; HRMS (ESI): m/z calcd for $\text{C}_{27}\text{H}_{29}\text{F}_3\text{NO}$ $[\text{M}+\text{H}]^+$: 440.2201; found: 440.2187.

2,6-di-*iso*-propyl-4-(pyridin-2-ylmethylene)-cyclohexa-2,5-dien-1-one (41k)



$R_f = 0.3$ (10% EtOAc in hexane); greenish gummy solid; ^1H NMR (400 MHz, CDCl_3) δ 8.74 – 8.73 (m, 1H), 8.64 – 8.63 (m, 1H), 7.71 (td, $J = 7.7, 1.8$ Hz, 1H), 7.39 (d, $J = 7.8$ Hz, 1H), 7.22 – 7.19 (m, 1H), 6.96 (s, 1H), 6.92 (d, $J = 2.3$ Hz, 1H), 3.20 – 3.13 (m, 2H), 1.16 (d, $J = 6.9$ Hz, 6H), 1.14 (d, $J = 6.9$ Hz, 6H); ^{13}C NMR (100 MHz, CDCl_3) δ 185.6, 155.2, 150.3, 147.8, 146.6, 138.7, 136.6, 135.3, 134.6, 128.9, 127.4, 123.0, 27.3, 26.6, 22.13, 22.12; FT-IR (thin film, neat): 3053, 2961, 2867, 1611, 1590, 1464, 1383, 1265, 1115, 993, 735, 703 cm^{-1} ; HRMS (ESI): m/z calcd for $\text{C}_{18}\text{H}_{21}\text{NNaO}$ $[\text{M}+\text{Na}]^+$: 290.1521; found: 290.1518.

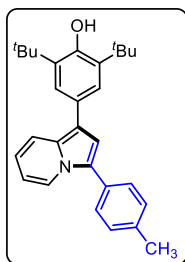
2,6-di-*tert*-butyl-4-(3-phenylindolizin-1-yl)-phenol (42a)



The reaction was performed at 0.102 mmol scale of **41a**; $R_f = 0.6$ (5% EtOAc in hexane); pale green solid (36.4 mg, 90% yield); m. p. = 108 – 110 $^{\circ}\text{C}$; ^1H NMR (400 MHz, CDCl_3) δ 8.29 (d, $J = 7.2$ Hz, 1H), 7.70 (d, $J = 9.1$ Hz, 1H), 7.64 – 7.62 (m, 2H), 7.52 – 7.48 (m, 3H), 7.44 (s, 2H), 7.38 – 7.34 (m, 1H), 7.00 (s, 1H), 6.74 – 6.70 (m, 1H), 6.52 – 6.47 (m, 1H), 5.18 (s, 1H), 1.52 (s, 18H); ^{13}C NMR (100 MHz, CDCl_3) δ 152.3, 136.4, 132.5, 130.0, 129.1, 128.3, 127.4, 127.3, 125.4, 124.7, 122.6, 118.8, 117.5, 116.5, 113.9, 111.0, 34.6, 30.6; FT-IR (thin film, neat): 3635, 2956, 1600, 1407, 1302, 1233, 1155, 1013, 737, 699 cm^{-1} ; HRMS (ESI): m/z calcd for $\text{C}_{28}\text{H}_{32}\text{NO}$ $[\text{M}+\text{H}]^+$: 398.2484; found: 398.2492.

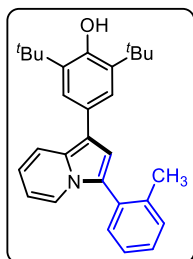
2,6-di-*tert*-butyl-4-[3-(*p*-tolyl)-indolizin-1-yl]-phenol (42b)

The reaction was performed at 0.102 mmol scale of **41a**; $R_f = 0.6$ (5% EtOAc in hexane); green solid (38.1 mg, 91% yield); m. p. = 180 – 182 $^{\circ}\text{C}$; ^1H NMR (400 MHz, CDCl_3) δ 8.25 (d, $J =$



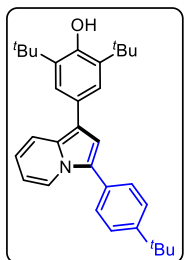
7.2 Hz, 1H), 7.70 (d, $J = 9.1$ Hz, 1H), 7.52 (d, $J = 8$ Hz, 2H), 7.44(s, 2H), 7.31 (d, $J = 7.9$ Hz, 2H), 7.00 (s, 1H), 6.72 – 6.68 (m, 1H), 6.50 – 6.46 (m, 1H), 5.18 (s, 1H), 2.44 (s, 3H), 1.52 (s, 18H) ; ^{13}C NMR (100 MHz, CDCl_3) δ 152.2, 137.2, 136.3, 129.8, 129.78, 129.6, 128.3, 127.5, 125.5, 124.7, 122.7, 118.8, 117.3, 116.3, 113.6, 110.9, 34.6, 30.6, 21.5; FT-IR (thin film, neat): 3451, 2956, 2870, 1641, 1451, 1360, 1233, 1154, 1119, 886, 738 cm^{-1} ; HRMS (ESI): m/z calcd for $\text{C}_{29}\text{H}_{34}\text{NO}$ $[\text{M}+\text{H}]^+$: 412.2640; found : 412.2631.

2,6-di-tert-butyl-4-[3-(*o*-tolyl)-indolizin-1-yl]-phenol (42c)



The reaction was performed at 0.102 mmol scale of **41a**; $R_f = 0.6$ (5% EtOAc in hexane); green solid (28.1 mg, 67% yield); m. p. = 128 – 130 $^{\circ}\text{C}$; ^1H NMR (400 MHz, CDCl_3) δ 7.73 (d, $J = 9.1$ Hz, 1H), 7.56 (d, $J = 7.1$ Hz, 1H), 7.47 (s, 2H), 7.43 (d, $J = 7.2$ Hz, 1H), 7.37 – 7.36 (m, 2H), 7.34 – 7.29 (m, 1H), 6.93 (s, 1H); 6.73 – 6.70 (m, 1H), 6.45 (t, $J = 6.6$ Hz, 1H), 5.17 (s, 1H), 2.20 (s, 3H) 1.53 (s, 18H); ^{13}C NMR (100 MHz, CDCl_3) δ 152.1, 138.4, 136.4, 131.7, 131.4, 130.6, 128.8, 128.5, 127.7, 126.2, 124.5, 123.1, 118.6, 117.0, 115.49, 115.48, 114.0, 110.6, 34.6, 30.6, 20.0; FT-IR (thin film, neat): 3635, 2957, 2869, 1601, 1550, 1455, 1330, 1233, 1147, 884, 699, 599 cm^{-1} ; HRMS (ESI): m/z calcd for $\text{C}_{29}\text{H}_{34}\text{NO}$ $[\text{M}+\text{H}]^+$: 412.2640; found : 412.2620.

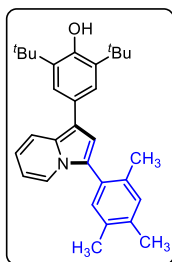
2,6-di-tert-butyl-4-{3-[4-(*tert*-butyl) phenyl] indolizin-1-yl}-phenol (42d)



The reaction was performed at 0.102 mmol scale of **41a**; $R_f = 0.6$ (5% EtOAc in hexane); brown solid (38.1 mg, 82% yield); m. p. = 112 – 114 $^{\circ}\text{C}$; ^1H NMR (400 MHz, CDCl_3) δ 8.31 (d, $J = 7.2$ Hz, 1H), 7.73 (d, $J = 9.1$ Hz, 1H), 7.59 (d, $J = 8.4$ Hz 2H) 7.55 (d, $J = 8.5$ Hz 2H) 7.48 (s, 2H), 7.02 (s, 1H), 6.74 – 6.71 (m, 1H), 6.52 – 6.48 (m, 1H) 5.20 (s, 1H), 1.55 (s, 18H), 1.42 (s, 9H); ^{13}C NMR (100 MHz, CDCl_3) δ 152.2, 150.3, 136.3, 129.8, 129.6, 128.0, 127.6, 126.0, 125.4, 124.7, 122.8, 118.8, 117.3, 116.3, 113.7, 110.8, 34.8, 34.6, 31.5, 30.6; FT-IR (thin film, neat): 3640, 2961, 1737, 1604, 1515, 1407, 1362, 1262, 1146, 1097, 1022, 826, 708 cm^{-1} ; HRMS (ESI): m/z calcd for $\text{C}_{32}\text{H}_{40}\text{NO}$ $[\text{M}+\text{H}]^+$: 454.3110; found : 454.3109.

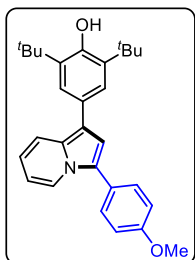
2,6-di-tert-butyl-4-[3-(2,4,5-trimethylphenyl)-indolizin-1-yl]-phenol (42e)

The reaction was performed at 0.102 mmol scale of **41a**; $R_f = 0.6$ (5% EtOAc in hexane); green solid (36.1 mg, 80% yield); m. p. = 118–120 $^{\circ}\text{C}$; ^1H NMR (400 MHz, CDCl_3) δ 7.74 (d, $J = 9.1$ Hz, 1H), 7.59 (d, $J = 7.1$ Hz, 1H), 7.50 (s, 2H), 7.22 (s, 1H), 7.17 (s, 1H), 6.92 (s, 1H), 6.73 – 6.70 (m, 1H), 6.47 – 6.44 (m, 1H), 5.18 (s, 1H), 2.35 (s, 3H), 2.31 (s, 3H), 2.15 (s, 3H), 1.55



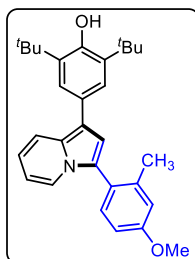
(s, 18H); ^{13}C NMR (100 MHz, CDCl_3) δ 152.0, 136.9, 136.3, 135.6, 134.2, 132.5, 131.9, 129.0, 128.7, 127.8, 124.7, 124.5, 123.2, 118.5, 116.8, 115.4, 113.9, 110.4, 34.6, 30.6, 19.7, 19.4 (2C); FT-IR (thin film, neat): 3639, 2956, 2869, 1602, 1515, 1451, 1410, 1360, 1304, 1264, 1199, 1150, 1114, 1009, 885, 831, 740, 726 cm^{-1} ; HRMS (ESI): m/z calcd for $\text{C}_{31}\text{H}_{38}\text{NO}$ $[\text{M}+\text{H}]^+$: 440.2953; found: 440.2955.

2,6-di-tert-butyl-4-[3-(4-methoxyphenyl)-indolizin-1-yl]-phenol (42f)



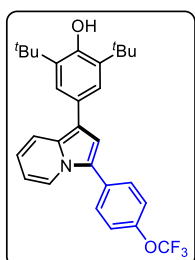
The reaction was performed at 0.102 mmol scale of **41a**; $R_f = 0.5$ (5% EtOAc in hexane); pale green solid (37.5 mg, 86% yield); m. p. = 148–150 $^\circ\text{C}$; ^1H NMR (400 MHz, CDCl_3) δ 8.18 (d, $J = 7.2$ Hz, 1H), 7.69 (d, $J = 9.1$ Hz, 1H), 7.56 – 7.52 (m, 2H), 7.45 (s, 2H), 7.10 – 7.03 (m, 2H), 6.94 (s, 1H), 6.71 – 6.67 (m, 1H), 6.49 – 6.45 (m, 1H), 5.18 (s, 1H), 3.89 (s, 3H), 1.52 (s, 18H); ^{13}C NMR (100 MHz, CDCl_3) δ 159.0, 152.2, 136.3, 129.8, 129.5, 127.6, 125.2, 124.9, 124.7, 122.6, 118.7, 117.2, 116.1, 114.5, 113.4, 110.8, 55.5, 34.6, 30.6; FT-IR (thin film, neat): 3632, 2962, 1732, 1601, 1504, 1462, 1291, 1258, 1169, 1096, 830, 799 cm^{-1} ; HRMS (ESI): m/z calcd for $\text{C}_{29}\text{H}_{34}\text{NO}_2$ $[\text{M}+\text{H}]^+$: 428.2590; found: 428.2597.

2,6-di-tert-butyl-4-[3-(4-methoxy-2-methylphenyl)-indolizin-1-yl]-phenol (42g)



The reaction was performed at 0.102 mmol scale of **41a**; $R_f = 0.5$ (5% EtOAc in hexane); green solid (35.0 mg, 78% yield); m. p. = 157–159 $^\circ\text{C}$; ^1H NMR (400 MHz, CDCl_3) δ 7.74 (d, $J = 9.1$ Hz, 1H), 7.55 (d, $J = 7.1$ Hz, 1H), 7.49 (s, 1H), 7.34 (d, $J = 8.4$ Hz, 1H), 6.93 (d, $J = 2.3$ Hz, 1H), 6.91 (s, 2H), 6.88 (dd, $J = 8.4, 2.5$ Hz, 1H), 6.71 (dd, $J = 8.9, 6.4$ Hz, 1H), 6.45 (t, $J = 6.8$ Hz, 1H), 5.18 (s, 1H), 3.89 (s, 3H), 2.17 (s, 3H), 1.54 (s, 18H); ^{13}C NMR (100 MHz, CDCl_3) δ 159.8, 152.1, 140.1, 136.3, 132.6, 128.6, 127.7, 124.5, 124.3, 124.1, 123.0, 118.5, 116.9, 115.9, 115.3, 114.0, 111.5, 110.4, 55.4, 34.6, 30.6, 20.2; FT-IR (thin film, neat): 3635, 2956, 2870, 1607, 1567, 1515, 1463, 1413, 1304, 1238, 1160, 1119, 1045, 885, 819, 741 cm^{-1} ; HRMS (ESI): m/z calcd for $\text{C}_{30}\text{H}_{36}\text{NO}_2$ $[\text{M}+\text{H}]^+$: 442.2746; found: 442.2746.

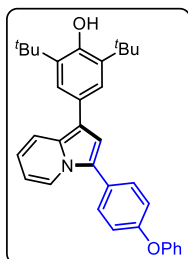
2,6-di-tert-butyl-4-[3-[4-(trifluoromethoxy)phenyl]indolizin-1-yl]-phenol (42h)



The reaction was performed at 0.102 mmol scale of **41a**; $R_f = 0.5$ (5% EtOAc in hexane); green solid (30.3 mg, 62% yield); m. p. = 178–180 $^\circ\text{C}$; ^1H NMR (400 MHz, CDCl_3) δ 8.22 (d, $J = 7.2$ Hz, 1H), 7.70 (d, $J = 9.1$ Hz, 1H), 7.64 (d, $J = 8.6$ Hz, 2H), 7.43 (s, 2H), 7.34 (d, $J = 8.2$ Hz, 2H), 7.00 (s, 1H), 6.76 – 6.72 (m, 1H), 6.52 (t, $J = 6.9$ Hz, 1H), 5.19 (s, 1H), 1.52 (s, 18H); $^{13}\text{C}\{^1\text{H}\}$

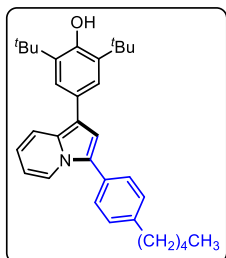
NMR (100 MHz, CDCl₃) δ 152.4, 148.2 (q, $J_{\text{C-F}} = 1.8$ Hz), 136.4, 131.3, 130.3, 129.5, 127.2, 124.7, 123.9, 122.3, 121.7, 120.7 (q, $J_{\text{C-F}} = 255.7$ Hz), 118.9, 117.8, 116.7, 114.2, 111.4, 34.6, 30.6; $^{19}\text{F}\{^1\text{H}\}$ NMR (376 MHz, CDCl₃) δ -57.78; FT-IR (thin film, neat): 3641, 2957, 2871, 1603, 1548, 1481, 1407, 1340, 1258, 1164, 1119, 1013, 921, 854, 780, 738 cm⁻¹; HRMS (ESI): m/z calcd for C₂₉H₃₁F₃NO₂ [M+H]⁺ : 482.2307; found : 482.2284.

2,6-di-*tert*-butyl-4-[3-(4-phenoxyphenyl)indolizin-1-yl]-phenol (42i)



The reaction was performed at 0.102 mmol scale of **41a**; $R_f = 0.5$ (5% EtOAc in hexane); brown solid (43.2 mg, 86% yield); m. p. = 110–112 °C; ^1H NMR (400 MHz, CDCl₃) δ 8.24 (d, $J = 7.1$ Hz, 1H), 7.71 (d, $J = 9.1$ Hz, 1H), 7.6 (d, $J = 8.6$ Hz, 2H), 7.46 (s, 2H), 7.42 – 7.38 (m, 2H), 7.18 – 7.16 (m, 2H), 7.13 – 7.11 (m, 3H), 7.00 (s, 1H), 6.74 – 6.70 (m, 1H), 6.53 – 6.48 (m, 1H), 5.19 (s, 1H), 1.54 (s, 18H); ^{13}C NMR (100 MHz, CDCl₃) δ 157.1, 156.7, 152.3, 136.4, 130.0, 129.84, 129.79, 129.4, 127.5, 127.4, 124.8, 124.7, 123.7, 122.5, 119.3, 118.8, 117.4, 116.3, 113.7, 111.0, 34.6, 30.6; FT-IR (thin film, neat): 3449, 2958, 1640, 1484, 1338, 1145, 828, 762, 739, 696 cm⁻¹; HRMS (ESI): m/z calcd for C₃₄H₃₆NO₂ [M-H]⁺ : 490.2746; found : 490.2758.

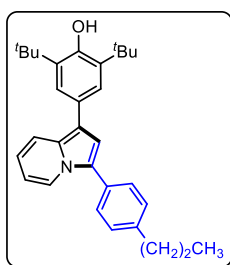
2,6-di-*tert*-butyl-4-[3-(4-pentylphenyl)indolizin-1-yl]-phenol (42j)



The reaction was performed at 0.102 mmol scale of **41a**; $R_f = 0.6$ (5% EtOAc in hexane); green solid (34.4 mg, 85% yield); m. p. = 116 – 118 °C; ^1H NMR (400 MHz, CDCl₃) δ 8.28 (d, $J = 7.2$ Hz, 1H), 7.71 (d, $J = 9.1$ Hz, 1H), 7.55 (d, $J = 8.0$ Hz, 2H), 7.46 (s, 1H), 7.32 (d, $J = 8.1$ Hz, 2H), 7.0 (s, 1H), 6.73 – 6.69 (m, 1H), 6.51 – 6.47 (m, 1H), 5.19 (s, 1H), 2.69 (t, $J = 7.6$ Hz, 2H), 1.74 – 1.67 (m, 2H), 1.54 (s, 18H), 1.43 – 1.38 (m, 4H), 0.95 (t, $J = 7.1$ Hz, 3H); ^{13}C NMR (100 MHz, CDCl₃) δ 152.2, 142.2, 136.3, 129.8, 129.1, 128.2, 127.5, 125.5, 124.7, 122.7, 118.8, 117.3, 116.3, 113.7, 110.8, 35.9, 34.6, 31.7, 31.3, 30.6, 22.7, 14.2; FT-IR (thin film, neat): 3451, 2956, 1641, 1451, 1407, 1304, 1233, 1143, 1012, 827, 739 cm⁻¹; HRMS (ESI): m/z calcd for C₃₃H₄₂NO [M+H]⁺ : 468.3266; found : 468.3270.

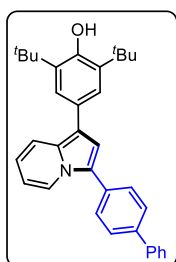
2,6-di-*tert*-butyl-4-[3-(4-propylphenyl)indolizin-1-yl]-phenol (42k)

The reaction was performed at 0.102 mmol scale of **41a**; $R_f = 0.6$ (5% EtOAc in hexane); brown solid (39.4 mg, 88% yield); m. p. = 124–126 °C; ^1H NMR (400 MHz, CDCl₃) δ 8.28 (d, $J = 7.2$ Hz, 1H), 7.71 (d, $J = 9.1$ Hz, 1H), 7.55 (d, $J = 7.9$ Hz, 2H), 7.46 (s, 2H), 7.32 (d, $J = 8.0$ Hz, 2H), 7.01 (s, 1H), 6.73 – 6.69 (m, 1H), 6.49 (t, $J = 6.6$ Hz, 1H), 5.19 (s, 1H), 2.68 (t, $J = 7.5$



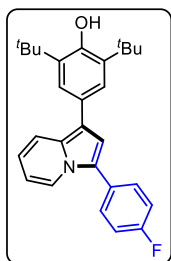
Hz, 2H), 1.78 – 1.68 (m, 2H), 1.54 (s, 18H), 1.02 (t, $J = 7.3$ Hz, 3H); ^{13}C NMR (100 MHz, CDCl_3) δ 152.2, 142.0, 136.3, 129.81, 129.78, 129.2, 128.2, 127.6, 125.5, 124.7, 122.7, 118.8, 117.3, 116.3, 113.7, 110.8, 38.0, 34.6, 30.6, 24.7, 14.1; FT-IR (thin film, neat): 3633, 2955, 2859, 1654, 1547, 1453, 1408, 1304, 1233, 1152, 1017, 965, 887, 737, 591, 535, 512 cm^{-1} ; HRMS (ESI): m/z calcd for $\text{C}_{31}\text{H}_{38}\text{NO}$ $[\text{M}+\text{H}]^+$: 440.2953; found: 440.2953.

4-{3-[(1,1'-biphenyl)-4-yl]-indolizin-1-yl}-2,6-di-*tert*-butylphenol (42l)



The reaction was performed at 0.102 mmol scale of **41a**; $R_f = 0.6$ (5% EtOAc in hexane); green solid (39.7 mg, 82% yield); m. p. = 248–250 °C; ^1H NMR (400 MHz, CDCl_3) δ 8.37 (d, $J = 7.2$ Hz, 1H), 7.77 – 7.71 (m, 5H), 7.70 – 7.68 (m, 2H), 7.52 – 7.48 (m, 4H), 7.42 – 7.38 (m, 1H), 7.10 (s, 1H), 6.77 – 6.73 (m, 1H), 6.56 – 6.52 (m, 1H), 5.21 (s, 1H), 1.55 (s, 18H); ^{13}C NMR (100 MHz, CDCl_3) δ 152.3, 140.8, 140.0, 136.4, 131.4, 130.2, 129.0, 128.5, 127.8, 127.5, 127.4, 127.1, 125.1, 124.7, 122.7, 118.9, 117.6, 116.7, 114.0, 111.1, 34.6, 30.6; FT-IR (thin film, neat): 3449, 2957, 1640, 1484, 1446, 1360, 1306, 1233, 1145, 1007, 885, 696 cm^{-1} ; HRMS (ESI): m/z calcd for $\text{C}_{34}\text{H}_{36}\text{NO}$ $[\text{M}+\text{H}]^+$: 474.2797; found: 474.2780.

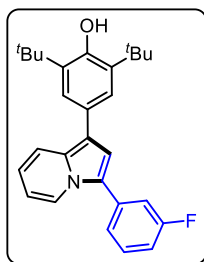
2,6-di-*tert*-butyl- 4-[3-(4-fluorophenyl)-indolizin-1-yl]-phenol (42m)



The reaction was performed at 0.102 mmol scale of **41a**; $R_f = 0.6$ (5% EtOAc in hexane); off white solid (24.2 mg, 57% yield); m. p. = 176–178 °C; ^1H NMR (400 MHz, CDCl_3) δ 8.18 (d, $J = 7.2$ Hz, 1H), 7.72 (d, $J = 9.1$ Hz, 1H), 7.61 – 7.57 (m, 2H), 7.45 (s, 2H), 7.23 – 7.18 (m, 2H), 7.00 (s, 1H), 6.75 – 6.71 (m, 1H), 6.52 – 6.49 (m, 1H), 5.20 (s, 1H), 1.54 (s, 18H); ^{13}C NMR (100 MHz, CDCl_3) δ 162.1 (d, $J_{\text{C-F}} = 245.5$ Hz), 152.3, 136.4, 130.5 (d, $J_{\text{C-F}} = 7.9$ Hz), 129.9, 128.6 (d, $J_{\text{C-F}} = 3.2$ Hz), 127.3, 124.7, 124.3, 122.4, 118.8, 117.5, 116.4, 116.1 (d, $J_{\text{C-F}} = 21.4$ Hz), 113.9, 111.1, 34.6, 30.6; $^{19}\text{F}\{^1\text{H}\}$ NMR (376 MHz, CDCl_3) δ -114.32; FT-IR (thin film, neat): 3636, 3440, 2957, 1603, 1521, 1451, 1360, 1304, 1233, 1157, 1119, 1013, 887, 739 cm^{-1} ; HRMS (ESI): m/z calcd for $\text{C}_{28}\text{H}_{31}\text{FNO}$ $[\text{M}+\text{H}]^+$: 416.2390; found: 416.2378.

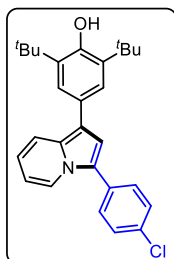
2,6-di-*tert*-butyl-4-[3-(3-fluorophenyl)indolizin-1-yl]-phenol (42n)

The reaction was performed at 0.102 mmol scale of **41a**; $R_f = 0.6$ (5% EtOAc in hexane); brown solid (22.0 mg, 52% yield); m. p. = 152–154 °C; ^1H NMR (400 MHz, CDCl_3) δ 8.29 (d, $J = 7.2$ Hz, 1H), 7.70 (d, $J = 9.1$ Hz, 1H), 7.46 – 7.40 (m, 4H), 7.34 – 7.31 (m, 1H), 7.06 – 7.01 (m, 2H), 6.76 – 6.72 (m, 1H), 6.53 (t, $J = 7.0$ Hz, 1H), 5.19 (s, 1H), 1.52 (s, 18H); ^{13}C NMR (100



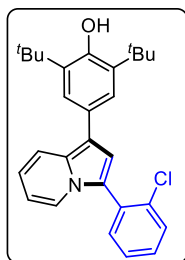
MHz, CDCl₃) δ 163.3 (d, $J_{\text{C-F}} = 244.8$ Hz), 152.4, 136.4, 134.6 (d, $J_{\text{C-F}} = 8.3$ Hz), 130.6, (d, $J_{\text{C-F}} = 8.7$ Hz), 130.5, 127.2, 124.7, 124.1 (d, $J_{\text{C-F}} = 2.4$ Hz), 123.6 (d, $J_{\text{C-F}} = 2.7$ Hz), 122.5, 118.9, 117.9, 116.8, 114.8 (d, $J_{\text{C-F}} = 21.9$ Hz), 114.3 (d, $J_{\text{C-F}} = 1.1$ Hz), 114.0, (d, $J_{\text{C-F}} = 21.0$ Hz), 111.4, 34.6, 30.6; $^{19}\text{F}\{^1\text{H}\}$ NMR (376 MHz, CDCl₃) δ -112.35; FT-IR (thin film, neat): 3636, 2924, 1603, 1521, 1482, 1408, 1304, 1233, 1119, 887, 739 cm⁻¹; HRMS (ESI): m/z calcd for C₂₈H₃₁FNO [M+H]⁺: 416.2390; found : 416.2387.

2,6-di-*tert*-butyl-4-[3-(4-chlorophenyl)indolizin-1-yl]-phenol (42o)



The reaction was performed at 0.102 mmol scale of **41a**; $R_f = 0.6$ (5% EtOAc in hexane); green solid (32.1 mg, 73% yield); m. p. = 216 – 218 °C; ^1H NMR (400 MHz, CDCl₃) δ 8.22 (d, $J = 7.2$ Hz, 1H), 7.72 – 7.69 (m, 1H), 7.59 – 7.56 (m, 1H), 7.55 – 7.54 (m, 1H), 7.48 – 7.45 (m, 2H) 7.43 (s, 2H), 7.00 (s, 1H); 6.75 – 6.71 (m, 1H), 6.53 – 7.50 (m, 1H), 5.19 (s, 1H), 1.52 (s, 18H); ^{13}C NMR (100 MHz, CDCl₃) δ 152.4, 136.4, 132.9, 130.9, 130.3, 129.4, 129.3, 127.2, 124.7, 124.1, 122.4, 118.9, 117.8, 116.7, 114.1, 111.3, 34.6, 30.5; FT-IR (thin film, neat): 3627, 2954, 1511, 1450, 1304, 1231, 1141, 1009, 829, 726 cm⁻¹; HRMS (ESI): m/z calcd for C₂₈H₃₁ClNO [M+H]⁺ : 432.2094; found : 432.2097.

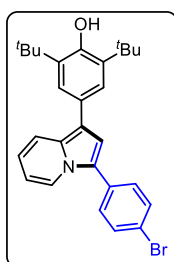
2,6-di-*tert*-butyl-4-[3-(2-chlorophenyl)indolizin-1-yl]-phenol (42p)



The reaction was performed at 0.102mmol scale of **41a**; $R_f = 0.6$ (5% EtOAc in hexane); brown solid (24.4 mg, 55% yield); m. p. = 165–167 °C; ^1H NMR (400 MHz, CDCl₃) δ 7.77 – 7.74 (m, 1H), 7.67 – 7.66 (m, 1H), 7.58 – 7.53 (m, 2H), 7.48 (s, 2H), 7.40 – 7.37 (m, 2H), 7.04 (s, 1H); 6.80 – 6.76 (m, 1H), 6.55 – 6.51 (m, 1H), 5.19 (s, 1H), 1.54 (s, 18H); ^{13}C NMR (100 MHz, CDCl₃) δ 152.2, 136.3, 134.8, 133.1, 131.3, 130.2, 129.6, 129.5, 127.4, 127.1, 124.7, 123.7, 122.3, 118.5, 117.6, 115.9, 114.9, 110.6, 34.6, 30.6; FT-IR (thin film, neat): 3634, 2957, 1598, 1443, 1306, 1262, 1150, 1034, 833, 654 cm⁻¹; HRMS (ESI): m/z calcd for C₂₈H₃₁ClNO [M+H]⁺ : 432.2094; found : 432.2094.

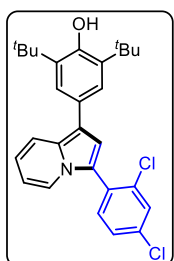
4-[3-(4-bromophenyl)-indolizin-1-yl]-2,6-di-*tert*-butylphenol (42q)

The reaction was performed at 0.102 mmol scale of **41a**; $R_f = 0.5$ (5% EtOAc in hexane); green solid (28.3 mg, 58% yield); m. p. = 230–232 °C; ^1H NMR (400 MHz, CDCl₃) δ 8.22 (d, $J = 7.2$ Hz, 1H), 7.70 (d, $J = 9.1$ Hz, 1H), 7.63 – 7.60 (m, 2H), 7.51 – 7.48 (m, 2H), 7.42 (s, 2H), 6.98 (s, 1H), 6.75 – 6.71 (m, 1H), 6.53 – 6.50 (m, 1H), 5.19 (s, 1H), 1.52 (s, 18H); ^{13}C NMR (100



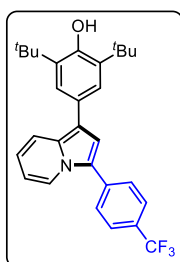
MHz, CDCl₃) δ 152.4, 136.4, 132.3, 131.4, 130.3, 129.7, 127.2, 124.7, 124.1, 122.4, 121.0, 118.9, 117.8, 116.8, 114.1, 111.4, 34.6, 30.5; FT-IR (thin film, neat): 3437, 2956, 2850, 1633, 1510, 1485, 1450, 1361, 1304, 1233, 1144, 1071, 1009, 822, 723 cm⁻¹; HRMS (ESI): m/z calcd for C₂₈H₃₁BrNO [M+H]⁺ : 476.1589; found : 476.1570.

2,6-di-tert-butyl-4-[3-(2,4-dichlorophenyl)-indolizin-1-yl]-phenol (42r)



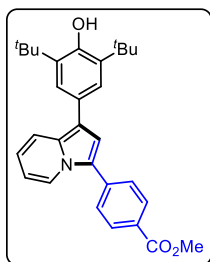
The reaction was performed at 0.102 mmol scale of **41a**; R_f = 0.5 (5% EtOAc in hexane); brown solid (24.0 mg, 50% yield); m. p. = 152–154 °C; ¹H NMR (400 MHz, CDCl₃) δ 7.74 (d, J = 9.1 Hz, 1H), 7.62 (d, J = 7.1 Hz, 1H), 7.58 (d, J = 2.1 Hz, 1H), 7.48 – 7.45 (m, 3H), 7.37 (dd, J = 8.2, 1.9 Hz, 1H), 7.00 (s, 1H), 6.80 – 6.76 (m, 1H), 6.55 – 6.51 (m, 1H), 5.19 (s, 1H), 1.52 (s, 18H); ¹³C NMR (100 MHz, CDCl₃) δ 152.3, 136.4, 135.4, 134.6, 133.7, 130.1, 130.0, 129.9, 127.5, 127.2, 124.7, 123.5, 121.0, 118.6, 117.9, 116.1, 115.1, 110.9, 34.6, 30.6; FT-IR (thin film, neat): 3635, 3452, 2956, 2870, 1631, 1548, 1443, 1408, 1360, 1233, 1154, 1101, 1056, 822, 724 cm⁻¹; HRMS (ESI): m/z calcd for C₂₈H₃₀Cl₂NO [M+H]⁺ : 466.1704; found : 466.1687.

2,6-di-tert-butyl-4-{3-[4-(trifluoromethyl)phenyl]indolizin-1-yl}-phenol (42s)



The reaction was performed at 0.102 mmol scale of **41a**; R_f = 0.6 (5% EtOAc in hexane); off white solid (23.0 mg, 48% yield); m. p. = 220–222 °C; ¹H NMR (400 MHz, CDCl₃) δ 8.30 (d, J = 7.2 Hz, 1H), 7.74 – 7.71 (m, 5H), 7.43 (s, 2H), 7.05 (s, 1H), 6.79 – 6.75 (m, 1H), 6.57 – 6.53 (m, 1H), 5.21 (s, 1H), 1.52 (s, 18H); ¹³C NMR (100 MHz, CDCl₃) δ 152.5, 136.4, 136.0 (apparent q, J_{C-F} = 0.9 Hz), 130.9, 128.8 (q, J_{C-F} = 32.4 Hz), 127.9, 127.0, 126.1 (q, J_{C-F} = 3.7 Hz), 124.7, 124.3 (q, J_{C-F} = 270.2 Hz), 123.9, 122.4, 119.0, 118.3, 117.2, 114.8, 111.7, 34.6, 30.5; ¹⁹F{¹H} NMR (376 MHz, CDCl₃) δ -62.41; FT-IR (thin film, neat): 3453, 2957, 2855, 1615, 1456, 1408, 1324, 1235, 1167, 1127, 1067, 1017, 841, 722, 684 cm⁻¹; HRMS (ESI): m/z calcd for C₂₉H₃₁F₃NO [M+H]⁺ : 466.2358; found : 466.2349.

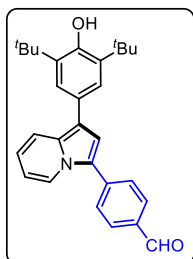
methlyl 4-[1-(3,5-di-tert-butyl-4-hydroxyphenyl)indolizin-3-yl]-benzoate (42t)



The reaction was performed at 0.102 mmol scale of **41a**; R_f = 0.4 (5% EtOAc in hexane); brown solid (17.3 mg, 37% yield); m. p. = 204–206 °C; ¹H NMR (400 MHz, CDCl₃) δ 8.36 (d, J = 7.2 Hz, 1H), 8.15 (d, J = 8.3 Hz, 2H), 7.71 (d, J = 8.3 Hz, 3H), 7.42 (s, 2H), 7.07 (s, 1H), 6.79 – 6.75 (m, 1H), 6.57 – 6.54 (m, 1H), 5.20 (s, 1H), 3.96 (s, 3H), 1.52 (s, 18H); ¹³C NMR (100 MHz,

CDCl₃) δ 167.0, 152.5, 136.9, 136.4, 131.2, 130.5, 128.2, 127.2, 127.0, 124.7, 124.3, 122.7, 119.0, 118.4, 117.3, 114.9, 111.7, 52.3, 34.6, 30.5; FT-IR (thin film, neat): 3633, 3078, 2955, 1719, 1605, 1517, 1407, 1235, 1146, 1014, 832, 704 cm⁻¹; HRMS (ESI): m/z calcd for C₃₀H₃₄NO₃ [M+H]⁺ : 456.2539; found : 456.2541.

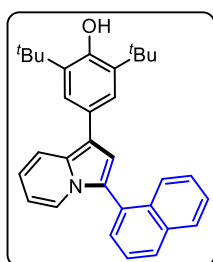
4-[1-(3,5-di-*tert*-butyl-4-hydroxyphenyl)indolizin-3-yl]-benzaldehyde (42u)



The reaction was performed at 0.102 mmol scale of **41a**; R_f = 0.4 (5% EtOAc in hexane); brown solid (14.8 mg, 34% yield); m. p. = 234–236 °C; ¹H NMR (400 MHz, CDCl₃) δ 10.04 (s, 1H), 8.41 (d, J = 7.2 Hz, 1H), 8.00 (d, J = 8.3 Hz, 2H), 7.81 (d, J = 8.2 Hz, 2H), 7.73 (d, J = 9.1 Hz, 1H), 7.43 (s, 2H), 7.12 (s, 1H), 6.82 – 6.78 (m, 1H), 6.61 – 6.58 (m, 1H), 5.22 (s, 1H), 1.52 (s, 18H);

¹³C NMR (100 MHz, CDCl₃) δ 191.6, 152.6, 138.5, 136.5, 134.5, 131.7, 130.7, 127.5, 126.8, 124.8, 124.1, 122.7, 119.1, 118.8, 117.7, 115.4, 112.0, 34.6, 30.5; FT-IR (thin film, neat): 3522, 2924, 2864, 2730, 1685, 1591, 1458, 1401, 1291, 1222, 1103, 1023, 943, 822, 730, 666 cm⁻¹; HRMS (ESI): m/z calcd for C₂₉H₃₂NO₂ [M+H]⁺ : 426.2433; found : 426.2443.

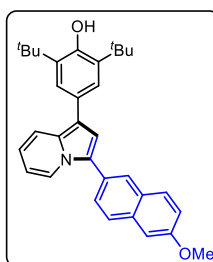
2,6-di-*tert*-butyl-4-[3-(naphthalen-1-yl)-indolizin-1-yl]-phenol (42v)



The reaction was performed at 0.102 mmol scale of **41a**; R_f = 0.6 (5% EtOAc in hexane); green solid (33.7 mg, 74% yield); m. p. = 139–141 °C; ¹H NMR (400 MHz, CDCl₃) δ 8.0 (d, J = 8.1 Hz, 2H), 7.80 (d, J = 9.1 Hz, 1H), 7.70 – 7.66 (m, 2H), 7.63 – 7.59 (m, 2H), 7.56 – 7.52 (m, 3H), 7.47 – 7.43 (m, 1H), 7.14 (s, 1H), 6.78 – 6.74 (m, 1H), 6.42 – 6.39 (m, 1H), 5.21 (s, 1H),

1.56 (s, 18H); ¹³C NMR (100 MHz, CDCl₃) δ 152.2, 136.4, 134.1, 132.4, 129.9, 129.4, 129.0, 128.8, 128.7, 127.6, 126.7, 126.3, 126.1, 125.8, 124.6, 123.5, 123.3, 118.6, 117.4, 115.9, 115.4, 110.6, 34.6, 30.6; FT-IR (thin film, neat): 3633, 3056, 2957, 2870, 1599, 1545, 1451, 1410, 1361, 1303, 1264, 1234, 1154, 1112, 1017, 886, 777, 740 cm⁻¹; HRMS (ESI): m/z calcd for C₃₂H₃₄NO [M+H]⁺ : 448.2640; found : 448.2644.

2,6-di-*tert*-butyl-4-[3-(6-methoxynaphthalen-2-yl)indolizin-1-yl]-phenol (42w)

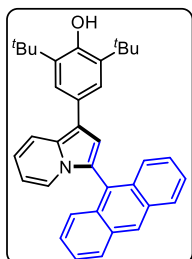


The reaction was performed at 0.102 mmol scale of **41a**; R_f = 0.5 (5% EtOAc in hexane); brown solid (40.4 mg, 83% yield); m. p. = 190–192 °C; ¹H NMR (400 MHz, CDCl₃) δ 8.38 (d, J = 7.2 Hz, 1H), 8.03 (s, 1H), 7.87 (d, J = 8.5 Hz, 1H), 7.81 (d, J = 8.6 Hz, 1H), 7.78 – 7.72 (m, 2H), 7.52 (s, 2H), 7.25 – 7.22 (m, 2H), 7.12 (s, 1H), 6.78 – 6.74 (m, 1H), 6.55 – 6.51 (m,

1H), 5.22 (s, 1H), 3.98 (s, 3H), 1.39 (s, 18H); ¹³C NMR (100 MHz, CDCl₃) δ 158.0, 152.2,

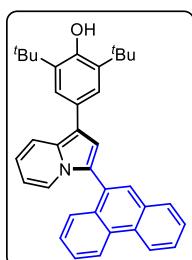
136.4, 133.8, 130.0, 129.6, 129.3, 127.6, 127.54, 127.51, 127.1, 126.6, 125.5, 124.7, 122.6, 119.4, 118.8, 117.5, 116.5, 114.0, 111.1, 105.9, 55.5, 34.6, 30.6; FT-IR (thin film, neat): 3630, 2956, 1732, 1606, 1494, 1302, 1220, 1135, 890, 739 cm^{-1} ; HRMS (ESI): m/z calcd for $\text{C}_{33}\text{H}_{36}\text{NO}_2$ $[\text{M}+\text{H}]^+$: 478.2746; found : 478.2742.

4-[3-(anthracen-9-yl)-indolizin-1-yl]-2,6-di-*tert*-butylphenol (42x)



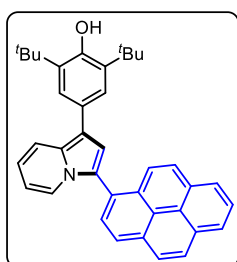
The reaction was performed at 0.102 mmol scale of **41a**; $R_f = 0.5$ (5% EtOAc in hexane); green solid (34.4 mg, 68% yield); m. p. = 154–156 °C; ^1H NMR (400 MHz, CDCl_3) δ 8.62 (s, 1H), 8.12 (d, $J = 8.4$ Hz, 2H), 7.91 (d, $J = 9.1$ Hz, 1H), 7.69 (d, $J = 8.7$ Hz, 2H), 7.64 (s, 2H), 7.53 – 7.49 (m, 2H), 7.43 – 7.38 (m, 2H), 7.28 (s, 1H), 7.18 (d, $J = 7.1$ Hz, 1H), 6.81 – 6.77 (m, 1H), 6.35 – 6.31 (m, 1H), 5.23 (s, 1H), 1.58 (s, 18H); ^{13}C NMR (100 MHz, CDCl_3) δ 152.2, 136.5, 132.0, 131.8, 129.3, 128.8, 128.4, 127.7, 126.6, 126.5, 126.1, 125.6, 124.5, 123.5, 120.3, 118.6, 117.4, 116.8, 115.9, 110.6, 34.7, 30.6; FT-IR (thin film, neat): 3633, 3401, 2957, 2870, 1622, 1511, 1454, 1361, 1324, 1233, 1152, 1115, 1013, 887, 791, 737 cm^{-1} ; HRMS (ESI): m/z calcd for $\text{C}_{36}\text{H}_{35}\text{NNaO}$ $[\text{M}+\text{Na}]^+$: 520.2616; found : 520.2596.

2,6-di-*tert*-butyl-4-[3-(phenanthren-9-yl) indolizin-1-yl]-phenol (42y)



The reaction was performed at 0.102 mmol scale of **41a**; $R_f = 0.5$ (5% EtOAc in hexane); green solid (39.6 mg, 78% yield); m. p. = 136–138 °C; 8.83 (d, $J = 8.2$ Hz, 1H), 8.78 (d, $J = 8.2$ Hz, 1H), 8.00 (s, 1H), 7.95 (dd, $J = 7.8, 0.9$ Hz, 1H), 7.83 (d, $J = 9.2$ Hz, 1H), 7.76 – 7.73 (m, 1H), 7.72 – 7.71 (m, 1H), 7.70 – 7.68 (m, 1H), 7.67 – 7.65 (m, 1H), 7.60 – 7.53 (m, 4H), 7.21 (s, 1H), 6.80 – 6.75 (m, 1H), 6.42 – 6.39 (m, 1H), 5.22 (s, 1H), 1.57 (s, 18H); ^{13}C NMR (100 MHz, CDCl_3) δ 152.2, 136.4, 131.8, 131.2, 130.9, 130.6, 130.3, 129.4, 129.0, 128.6, 127.6, 127.3, 127.2, 127.1, 127.0, 126.9, 124.6, 123.7, 123.3, 123.2, 122.8, 118.6, 117.4, 115.9, 115.3, 110.6, 34.7, 30.6; FT-IR (thin film, neat): 3635, 3450, 2957, 1642, 1450, 1442, 1336, 1233, 1153, 886, 727 cm^{-1} ; HRMS (ESI): m/z calcd for $\text{C}_{36}\text{H}_{36}\text{NO}$ $[\text{M}+\text{H}]^+$: 498.2797; found : 498.2788.

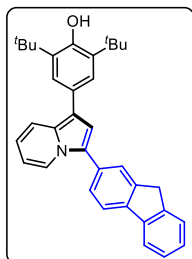
2,6-di-*tert*-butyl-4-[3-(pyren-1-yl)indolizin-1-yl]-phenol (42z)



The reaction was performed at 0.102 mmol scale of **41a**; $R_f = 0.5$ (5% EtOAc in hexane); green solid (33.1 mg, 62% yield); m. p. = 128–130 °C; ^1H NMR (400 MHz, CDCl_3) δ 8.30 (d, $J = 7.9$ Hz, 1H), 8.24 (d, $J = 7.6$ Hz, 1H), 8.21 – 8.16 (m, 2H), 8.15 (s, 2H), 8.06 – 8.02 (m, 2H), 7.92 (d, $J = 9.2$ Hz, 1H), 7.83 (d, $J = 9.1$ Hz, 1H), 7.69 (d, $J = 7.1$ Hz, 1H), 7.56 (s, 2H), 7.25 (s, 1H), 6.80 – 6.76 (m, 1H), 6.43 – 6.40 (m, 1H), 5.21 (s, 1H), 1.55 (s, 18H) ^{13}C

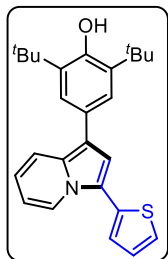
NMR (100 MHz, CDCl₃) δ 152.3, 136.5, 131.5, 131.3, 131.1, 129.9, 129.7, 128.8, 128.2, 127.9, 127.6, 127.5, 127.0, 126.3, 125.52, 125.49, 125.4, 125.3, 125.1, 124.9, 124.7, 123.7, 123.2, 118.7, 117.6, 116.3, 115.9, 110.8, 34.7, 30.6; FT-IR (thin film, neat): 3465, 2924, 1640, 1462, 1432, 1303, 1234, 1116, 844, 716 cm⁻¹; HRMS (ESI): m/z calcd for C₃₈H₃₆NO [M+H]⁺ : 522.2797; found : 522.2772.

4-[3-(9H-fluoren-2-yl)indolizin-1-yl]-2,6-di-*tert*-butylphenol (42aa)



The reaction was performed at 0.102 mmol scale of **41a**; R_f = 0.6 (5% EtOAc in hexane); light green solid (37.6 mg, 76% yield); m. p. = 196–198 °C; ¹H NMR (400 MHz, CDCl₃) δ 8.36 (d, J = 7.1 Hz, 1H), 7.91 (d, J = 7.8 Hz, 1H), 7.85 (d, J = 7.5 Hz, 1H), 7.81 (s, 1H), 7.74 (d, J = 9.1 Hz, 1H), 7.67 (d, J = 7.9, Hz, 1H), 7.60 (d, J = 7.4 Hz, 1H), 7.50 (s, 2H), 7.43 (t, J = 7.4 Hz, 1H), 7.35 (t, J = 7.4, Hz, 1H), 7.10 (s, 1H), 6.76 – 6.73 (m, 1H), 6.53 (t, J = 6.8 Hz, 1H), 5.21 (s, 1H), 4.01 (s, 2H), 1.55 (s, 18H); ¹³C NMR (100 MHz, CDCl₃) δ 152.3, 144.1, 143.5, 141.5, 140.9, 136.4, 130.8, 130.0, 127.5, 127.0, 126.9 (2C), 125.8, 125.2, 124.8, 124.7, 122.8, 120.4, 120.0, 118.8, 117.5, 116.5, 113.9, 111.0, 37.1, 34.6, 30.6; FT-IR (thin film, neat): 3633, 2957, 2870, 1612, 1547, 1422, 1337, 1152, 1014, 827, 703, 653 cm⁻¹; HRMS (ESI): m/z calcd for C₃₅H₃₆NO [M+H]⁺ : 486.2797; found : 486.2785.

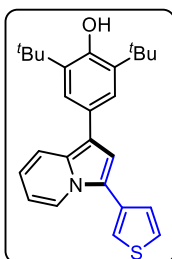
2,6-di-*tert*-butyl-4-[3-(thiophen-2-yl)-indolizin-1-yl]-phenol (42ab)



The reaction was performed at 0.102 mmol scale of **41a**; R_f = 0.5 (5% EtOAc in hexane); brown solid (32.0 mg, 78% yield); m. p. = 138 – 140 °C; ¹H NMR (400 MHz, CDCl₃) δ 8.38 (d, J = 7.2 Hz, 1H), 7.72 (d, J = 9.1 Hz, 1H), 7.45 (s, 2H), 7.37 (dd, J = 5.2, 1.0 Hz, 1H), 7.31 – 7.30 (m, 1H), 7.20 – 7.18 (m, 1H), 7.10 (s, 1H), 6.79 – 6.75 (m, 1H), 6.61 – 6.57 (m, 1H), 5.21 (s, 1H) 1.54 (s, 18H); ¹³C NMR (100 MHz, CDCl₃) δ 152.4, 136.4, 134.0, 130.5, 127.7, 127.1, 124.8, 124.74, 124.70, 123.2, 118.7, 118.3, 117.8, 116.6, 115.0, 111.4, 34.6, 30.6, FT-IR (thin film, neat): 3633, 3452, 2870, 1758, 1566, 1416, 1399, 1248, 1139, 853, 724, 664 cm⁻¹; HRMS (ESI): m/z calcd for C₂₆H₃₀NOS [M+H]⁺ : 404.2048; found : 404.2034.

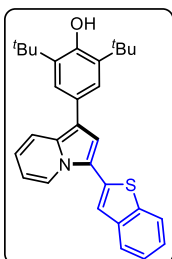
2,6-di-*tert*-butyl-4-[3-(thiophen-3-yl)indolizin-1-yl]-phenol (42ac)

The reaction was performed at 0.102 mmol scale of **41a**; R_f = 0.5 (5% EtOAc in hexane); brown solid (33.6 mg, 82% yield); m. p. = 140–142 °C; ¹H NMR (400 MHz, CDCl₃) δ 8.25 (d, J = 7.2 Hz, 1H), 7.71 (d, J = 9.1 Hz, 1H), 7.49 – 7.47 (m, 2H), 7.44 (s, 2H), 7.40 (dd, J = 4.7, 1.4 Hz, 1H), 7.03 (s, 1H), 6.74 – 6.70 (m, 1H), 6.56 – 6.52 (m, 1H), 5.19 (s, 1H), 1.53 (s, 18H); ¹³C



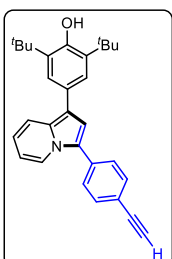
NMR (100 MHz, CDCl_3) δ 152.3, 136.4, 132.8, 129.8, 127.7, 127.4, 126.2, 124.7, 123.0, 121.2, 120.8, 118.7, 117.3, 116.2, 113.8, 111.2, 34.6, 30.6; FT-IR (thin film, neat): 3632, 3452, 2956, 2870, 1642, 1566, 1452, 1416, 1399, 1360, 1331, 1264, 1248, 1139, 887, 783, 663 cm^{-1} ; HRMS (ESI): m/z calcd for $\text{C}_{26}\text{H}_{30}\text{NOS}$ $[\text{M}+\text{H}]^+$: 404.2048; found: 404.2037.

4-{3-(benzo[b]thiophen-2-yl)indolizin-1-yl}-2,6-di-tert-butylphenol (42ad)



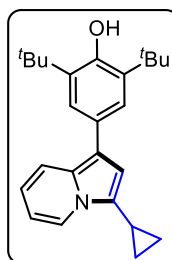
The reaction was performed at 0.102 mmol scale of **41a**; R_f = 0.5 (5% EtOAc in hexane); brown solid (29.1 mg, 63% yield); m. p. = 126–128 $^\circ\text{C}$; ^1H NMR (400 MHz, CDCl_3) δ 8.55 (d, J = 7.2 Hz, 1H), 7.85 (d, J = 8.0 Hz, 1H), 7.80 (d, J = 7.5 Hz, 1H), 7.73 (d, J = 9.0 Hz, 1H), 7.50 (s, 1H), 7.43 (s, 1H), 7.41 – 7.31 (m, 3H), 7.19 (s, 1H), 6.82 – 6.78 (m, 1H), 6.67 – 6.63 (m, 1H), 5.22 (s, 1H) 1.53 (s, 18H); ^{13}C NMR (100 MHz, CDCl_3) δ 152.5, 140.6, 138.9, 136.4, 134.4, 131.3, 126.9, 124.8, 124.7, 124.3, 123.5, 123.3, 122.1, 119.7, 118.8, 118.5, 118.3, 117.2, 115.8, 111.9, 34.6, 30.6; FT-IR (thin film, neat): 3632, 2957, 2922, 2871, 1597, 1578, 1434, 1360, 1238, 1157, 1025, 889, 748, 665 cm^{-1} ; HRMS (ESI): m/z calcd for $\text{C}_{30}\text{H}_{32}\text{NOS}$ $[\text{M}+\text{H}]^+$: 454.2205; found: 454.2226.

2,6-di-tert-butyl-4-[3-(4-ethynylphenyl)indolizin-1-yl]-phenol (42ae)



The reaction was performed at 0.102 mmol scale of **41a**; R_f = 0.5 (5% EtOAc in hexane); brown solid (24.0 mg, 56% yield); m. p. = 118–120 $^\circ\text{C}$; ^1H NMR (400 MHz, CDCl_3) δ 8.29 (d, J = 7.2 Hz, 1H), 7.70 (d, J = 9.1 Hz, 1H), 7.63 – 7.58 (m, 4H), 7.43 (s, 2H), 7.02 (s, 1H), 6.76 – 6.72 (m, 1H), 6.55 – 6.51 (m, 1H), 5.19 (s, 1H), 3.16 (s, 1H), 1.52 (s, 18H); ^{13}C NMR (100 MHz, CDCl_3) δ 152.4, 136.4, 132.91, 132.88, 130.6, 127.6, 127.2, 124.7, 124.6, 122.6, 120.5, 118.9, 118.0, 117.0, 114.4, 111.4, 83.7, 77.9, 34.6, 30.6; FT-IR (thin film, neat): 3643, 3306, 3267, 3066, 2923, 2870, 1657, 1484, 1365, 1243, 1154, 1025, 918, 684 cm^{-1} ; HRMS (ESI): m/z calcd for $\text{C}_{30}\text{H}_{32}\text{NO}$ $[\text{M}+\text{H}]^+$: 422.2484; found: 422.2472.

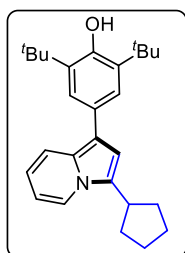
2,6-di-tert-butyl-4-(3-cyclopropylindolizin-1-yl)-phenol (42af)



The reaction was performed at 0.102 mmol scale of **41a**; R_f = 0.6 (5% EtOAc in hexane); brown gummy solid (7.6 mg, 20% yield); ^1H NMR (400 MHz, CDCl_3) δ 8.07 (d, J = 7.1 Hz, 1H), 7.64 (d, J = 9.1 Hz, 1H), 7.37 (s, 2H), 6.71 – 6.66 (m, 2H), 6.57 – 6.53 (m, 1H), 5.12 (s, 1H), 1.91 – 1.85 (m, 1H), 1.50 (s, 18H), 1.03 – 0.98 (m, 2H), 0.76 – 0.72 (m, 2H); ^{13}C NMR (100 MHz, CDCl_3)

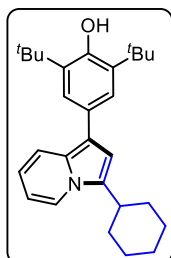
δ 152.0, 136.3, 128.7, 127.9, 126.1, 124.5, 122.7, 118.4, 116.7, 114.3, 111.4, 110.2, 34.6, 30.6, 6.3, 5.5; FT-IR (thin film, neat): 3630, 3500, 3055, 2871, 1605, 1499, 1407, 1338, 1301, 1157, 1030, 928, 808, 676, 556 cm^{-1} ; HRMS (ESI): m/z calcd for $\text{C}_{25}\text{H}_{32}\text{NO}$ $[\text{M}+\text{H}]^+$: 362.2484; found : 362.2498.

2,6-di-tert-butyl-4-(3-cyclopentylindolizin-1-yl)phenol (42ag)



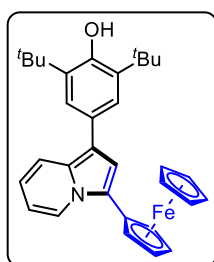
The reaction was performed at 0.087 mmol scale of **41a**; R_f = 0.6 (5% EtOAc in hexane); brown gummy solid (9.2 mg, 23% yield); ^1H NMR (400 MHz, CDCl_3) δ 7.80 (d, J = 7.2 Hz, 1H), 7.64 (d, J = 9.1 Hz, 1H), 7.38 (s, 2H), 6.72 (s, 1H), 6.64 (ddd, J = 9.0, 6.4, 0.72 Hz, 1H), 6.52 – 6.48 (m, 1H), 5.13 (s, 1H), 3.29 (quintet, J = 7.7, 7.5 Hz, 1H), 1.86 – 1.68 (m, 8H), 1.50 (s, 18H); $^{13}\text{C}\{^1\text{H}\}$ NMR (100 MHz, CDCl_3) δ 152.0, 136.3, 128.9, 128.7, 128.0, 124.6, 122.5, 118.6, 116.0, 114.6, 110.2, 109.6, 36.6, 34.6, 31.5, 30.6, 25.3; FT-IR (thin film, neat): 3628, 3450, 2930, 2870, 1642, 1622, 1445, 1232, 1165, 735, 722 cm^{-1} ; HRMS (ESI): m/z calcd for $\text{C}_{27}\text{H}_{36}\text{NO}$ $[\text{M}+\text{H}]^+$: 390.2797; found : 390.2794.

2,6-di-tert-butyl-4-(3-cyclohexylindolizin-1-yl)-phenol (42ah)



The reaction was performed at 0.102 mmol scale of **41a**; R_f = 0.6 (5% EtOAc in hexane); brown gummy solid (10.1 mg, 24% yield); ^1H NMR (400 MHz, CDCl_3) δ 7.78 (d, J = 7.2 Hz, 1H), 7.64 (d, J = 9.1 Hz, 1H), 7.38 (s, 2H), 6.69 (s, 1H), 6.65 – 6.61 (m, 1H), 6.52 – 6.47 (m, 1H), 5.12 (s, 1H), 2.86 – 2.80 (m, 1H), 2.18 – 2.13 (m, 4H), 1.92 – 1.80 (m, 3H), 1.61 – 1.54 (m, 3H), 1.50 (s, 18H); ^{13}C NMR (100 MHz, CDCl_3) δ 151.9, 136.2, 130.1, 128.4, 128.0, 124.6, 122.1, 118.8, 115.9, 114.8, 110.2, 109.4, 35.4, 34.6, 31.9, 30.6, 29.9, 26.8; FT-IR (thin film, neat): 3451, 2927, 2853, 1644, 1453, 1407, 1360, 1336, 1234, 1155, 1118, 888, 735, 721 cm^{-1} ; HRMS (ESI): m/z calcd for $\text{C}_{28}\text{H}_{38}\text{NO}$ $[\text{M}+\text{H}]^+$: 404.2953; found : 404.2960.

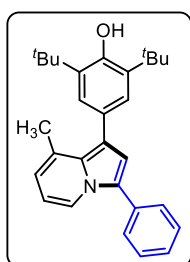
2,6-di-tert-butyl-4-(3-(ferrocenyl)indolizin-1-yl)phenol (42ai)



The reaction was performed at 0.102 mmol scale of **41a**; R_f = 0.6 (5% EtOAc in hexane); brown solid (22.0 mg, 42% yield); m. p. = 96–98 $^{\circ}\text{C}$; ^1H NMR (400 MHz, CDCl_3) δ 8.59 (d, J = 7.2 Hz, 1H), 7.69 (d, J = 9.0 Hz, 1H), 7.44 (s, 2H); 6.97 (s, 1H); 6.75 – 6.71 (m, 1H), 6.63 – 6.59 (m, 1H),

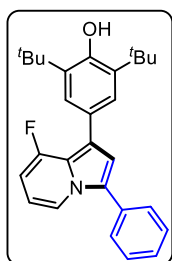
5.18 (s, 1H); 4.62 (t, $J = 1.8$ Hz, 2H), 4.39 (t, $J = 1.8$ Hz, 2H), 4.24 (s, 5H), 1.54 (s, 18H); ^{13}C NMR (100 MHz, CDCl_3) δ 152.2, 136.3, 129.9, 127.5, 124.7, 123.9, 121.4, 118.6, 116.5, 116.0, 113.9, 110.5, 78.2, 69.1, 68.4, 66.9, 34.6, 30.6; FT-IR (thin film, neat): 3450, 3095, 2961, 1655, 1513, 1460, 1431, 1362, 1261, 1106, 1025, 819, 739, 498 cm^{-1} ; HRMS (ESI): m/z calcd for $\text{C}_{32}\text{H}_{36}\text{FeNO}$ $[\text{M}+\text{H}]^+$: 506.2146; found : 506.2138

2,6-di-*tert*-butyl-4-(8-methyl-3-phenylindolizin-1-yl)-phenol (42aj)



The reaction was performed at 0.0969 mmol scale of **41b**; $R_f = 0.6$ (5% EtOAc in hexane); green solid (32.8 mg, 82% yield); m. p. = 158–160 °C; ^1H NMR (400 MHz, CDCl_3) δ 8.23 (d, $J = 6.3$ Hz, 1H), 7.66 – 7.64 (m, 2H); 7.53 – 7.49 (m, 2H); 7.40 – 7.35 (m, 1H), 7.30 (s, 2H), 6.89 (s, 1H), 6.47 – 6.42 (m, 2H), 5.22 (s, 1H), 2.18 (s, 3H), 1.53 (s, 18H); ^{13}C NMR (100 MHz, CDCl_3) δ 152.6, 134.8, 132.7, 130.0, 129.8, 129.1, 128.8, 128.5, 127.8, 127.2, 124.7, 120.7, 118.0, 117.8, 116.5, 110.6, 34.5, 30.6, 20.9; FT-IR (thin film, neat): 3635, 2955, 2870, 1601, 1544, 1395, 1333, 1231, 1154, 1026, 833, 736, 627, 590 cm^{-1} ; HRMS (ESI): m/z calcd for $\text{C}_{29}\text{H}_{34}\text{NO}$ $[\text{M}+\text{H}]^+$: 412.2640; found : 412.2638.

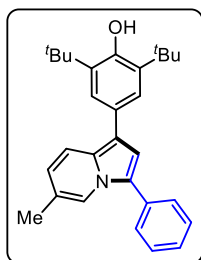
2,6-di-*tert*-butyl-4-(8-fluoro-3-phenylindolizin-1-yl)-phenol (42ak)



The reaction was performed at 0.0957 mmol scale of **41c**; $R_f = 0.6$ (5% EtOAc in hexane); brown solid (30.3 mg, 76% yield); m. p. = 160–160 °C; ^1H NMR (400 MHz, CDCl_3) δ 8.07 – 8.05 (m, 1H), 7.63 – 7.61 (m, 2H), 7.54 – 7.50 (m, 2H), 7.46 (d, $J = 3.3$ Hz, 2H), 7.43 – 7.39 (m, 1H), 7.00 (s, 1H), 6.42 – 6.38 (m, 2H), 5.21 (s, 1H), 1.53 (s, 18H); ^{13}C NMR (100 MHz, CDCl_3) δ 155.9 (d, $J_{\text{C-F}} = 247.9$ Hz) 152.6, 135.5, 132.1, 129.2, 128.6, 127.8, 127.4, 126.7, 126.3 (d, $J_{\text{C-F}} = 4.1$ Hz), 121.0 (d, $J_{\text{C-F}} = 32.1$ Hz), 119.1 (d, $J_{\text{C-F}} = 4.0$ Hz), 117.1 (d, $J_{\text{C-F}} = 4.7$ Hz), 115.5, 109.5 (d, $J_{\text{C-F}} = 8.1$ Hz), 100.1 (d, $J_{\text{C-F}} = 19.4$ Hz), 34.6, 30.6; ^{19}F $\{^1\text{H}\}$ NMR (376 MHz, CDCl_3) δ –120.04; FT-IR (thin film, neat): 3638, 2941, 2856, 2742, 1601, 1527, 1437, 1396, 1264, 1152, 1078, 924, 831, 731, 623, 516 cm^{-1} ; HRMS (ESI): m/z calcd for $\text{C}_{28}\text{H}_{30}\text{NaFNO}$ $[\text{M}+\text{H}]^+$: 438.2209; found : 438.2204.

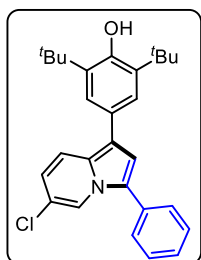
2,6-di-*tert*-butyl-4-(6-methyl-3-phenylindolizin-1-yl)-phenol (42al)

The reaction was performed at 0.0969 mmol scale of **41d**; $R_f = 0.6$ (5% EtOAc in hexane); brown solid (33.6 mg, 84% yield); m. p. = 146–148 °C; ^1H NMR (400 MHz, CDCl_3) δ 8.09 (s,



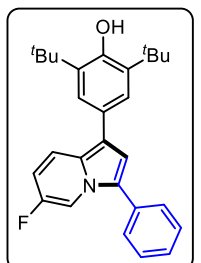
1H), 7.66 – 7.63 (m, 3H), 7.53 – 7.49 (m, 2H), 7.46 (s, 2H), 7.39 – 7.35 (m, 1H), 7.00 (s, 1H), 6.61 (d, $J = 9.1$ Hz, 1H), 5.18 (s, 1H), 2.23 (s, 3H), 1.53 (s, 18H); ^{13}C NMR (100 MHz, CDCl_3) δ 152.2, 136.3, 132.7, 129.1, 129.0, 128.3, 127.6, 127.2, 125.1, 124.6, 120.9, 120.3, 120.0, 118.3, 116.2, 113.4, 34.6, 30.6, 18.7; FT-IR (thin film, neat): 3633, 3056, 2954, 2869, 1884, 1729, 1514, 1413, 1301, 1199, 1072, 884, 785, 698, 627, 574, 536 cm^{-1} ; HRMS (ESI): m/z calcd for $\text{C}_{29}\text{H}_{34}\text{NO}$ $[\text{M}+\text{H}]^+$: 412.2640; found: 412.2644.

2,6-di-tert-butyl-4-(6-chloro-3-phenylindolizin-1-yl)-phenol (42am)



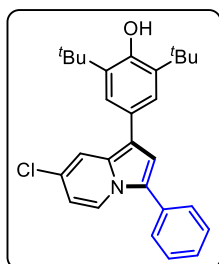
The reaction was performed at 0.0909 mmol scale of **41e**; $R_f = 0.6$ (5% EtOAc in hexane); brown gummy solid (29.2 mg, 74% yield); ^1H NMR (400 MHz, CDCl_3) δ 8.293 – 8.287 (m, 1H), 7.66 – 7.60 (m, 3H), 7.55 – 7.51 (m, 2H), 7.42 – 7.38 (m, 3H), 7.00 (s, 1H), 6.68 (dd, $J = 9.5, 1.7$ Hz, 1H), 5.23 (s, 1H), 1.53 (s, 18H); ^{13}C NMR (100 MHz, CDCl_3) δ 152.6, 136.5, 131.8, 129.3, 128.6, 128.3, 127.8, 126.8, 126.1, 124.7, 120.2, 119.5, 119.4, 118.7, 117.9, 114.4, 34.6, 30.5; FT-IR (thin film, neat): 3633, 2955, 2869, 1601, 1455, 1313, 1233, 1152, 1112, 887, 757, 671 cm^{-1} ; HRMS (ESI): m/z calcd for $\text{C}_{28}\text{H}_{31}\text{ClNO}$ $[\text{M}+\text{H}]^+$: 432.2094; found: 432.2084.

2,6-di-tert-butyl-4-(6-fluoro-3-phenylindolizin-1-yl)phenol (42an)



The reaction was performed at 0.0957 mmol scale of **41f**; $R_f = 0.6$ (5% EtOAc in hexane); brown gummy solid (29.0 mg, 73% yield); ^1H NMR (400 MHz, CDCl_3) δ 8.20 – 8.18 (m, 1H), 7.67 – 7.62 (m, 2H), 7.60 (s, 1H), 7.51 (t, $J = 7.6$ Hz, 2H), 7.40 (s, 2H), 7.38 – 7.34 (m, 1H), 7.00 (s, 1H), 6.68 – 6.63 (m, 1H), 5.20 (s, 1H), 1.51 (s, 18H); $^{13}\text{C}\{^1\text{H}\}$ NMR (100 MHz, CDCl_3) δ 153.6 (d, $J_{\text{C-F}} = 232.0$ Hz), 152.5, 136.5, 132.1, 129.3, 128.2, 128.1, 127.7, 127.0, 126.6 (d, $J_{\text{C-F}} = 1.6$ Hz), 124.7, 119.6 (d, $J_{\text{C-F}} = 9.4$ Hz), 118.0, 114.3 (d, $J_{\text{C-F}} = 2.0$ Hz), 109.8 (d, $J_{\text{C-F}} = 25.9$ Hz), 108.5 (d, $J_{\text{C-F}} = 41.4$ Hz), 34.6, 30.5; $^{19}\text{F}\{^1\text{H}\}$ NMR (376 MHz, CDCl_3) δ -142.88; FT-IR (thin film, neat): 3638, 3442, 2955, 2744, 1756, 1608, 1522, 1436, 1258, 1169, 1036, 836, 632 cm^{-1} ; HRMS (ESI): m/z calcd for $\text{C}_{28}\text{H}_{31}\text{FNO}$ $[\text{M}+\text{H}]^+$: 416.2390; found: 416.2387.

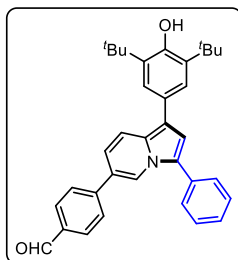
2,6-di-tert-butyl-4-(7-chloro-3-phenylindolizin-1-yl)phenol (42ao)



The reaction was performed at 0.0909 mmol scale of **41g**; $R_f = 0.6$ (5% EtOAc in hexane); brown gummy solid (30.0 mg, 76% yield); ^1H NMR (400 MHz, CDCl_3) δ 8.18 (d, $J = 7.6$ Hz, 1H), 7.64 (d, $J = 1.8$ Hz, 1H), 7.60 – 7.58 (m, 2H), 7.50 (t, $J = 7.5$ Hz, 2H), 7.40 – 7.38 (m, 3H), 7.00 (s, 1H), 6.44 (dd, $J = 7.6, 2.2$ Hz, 1H), 5.22 (s, 1H), 1.52 (s, 18H); $^{13}\text{C}\{^1\text{H}\}$ NMR (100 MHz, CDCl_3) δ 152.6, 136.5, 132.0, 129.6, 129.2, 128.3, 127.7, 126.8, 125.9, 124.7,

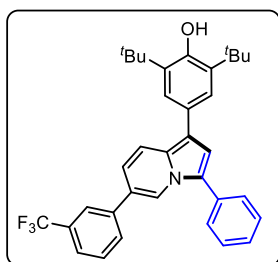
123.6, 123.4, 117.4, 116.7, 114.8, 112.3, 34.6, 30.5; FT-IR (thin film, neat): 3634, 2952, 2866, 1607, 1452, 1232, 1114, 885, 755, 673 cm^{-1} ; HRMS (ESI): m/z calcd for $\text{C}_{28}\text{H}_{31}\text{ClNO}$ $[\text{M}+\text{H}]^+$: 432.2094; found : 432.2089.

4-[1-(3,5-di-*tert*-butyl-4-hydroxyphenyl)-3-phenyl-indolizin-6-yl]-benzaldehyde (42ap)



The reaction was performed at 0.075 mmol scale of **41i**; $R_f = 0.3$ (10% EtOAc in hexane); brown solid (18.0 mg, 47% yield); m. p. = 102–104 $^{\circ}\text{C}$; ^1H NMR (400 MHz, CDCl_3) δ 10.04 (s, 1H), 8.56 (s, 1H), 7.94 (d, $J = 8.3$ Hz, 1H), 7.81 (dd, $J = 9.3, 0.5$ Hz, 1H), 7.71 (d, $J = 8.2$ Hz, 2H), 7.68 – 7.65 (m, 2H), 7.54 (t, $J = 7.6$ Hz, 2H), 7.47 (s, 2H), 7.43 – 7.39 (m, 1H), 7.06 (s, 1H), 7.04 (dd, $J = 7.8, 1.6$ Hz, 1H), 5.23 (s, 1H), 1.54 (s, 18H); ^{13}C NMR (100 MHz, CDCl_3) δ 191.8, 152.5, 144.8, 136.5, 135.2, 132.1, 130.6, 129.3, 129.0, 128.4, 127.7, 127.0, 126.5, 124.7, 123.8, 121.1, 119.3, 117.4, 117.2, 115.07, 115.05, 34.6, 30.5; FT-IR (thin film, neat): 3627, 2955, 2826, 1701, 1603, 1565, 1462, 1396, 1265, 839, 702, cm^{-1} ; HRMS (ESI): m/z calcd for $\text{C}_{35}\text{H}_{34}\text{NO}_2$ $[\text{M}-\text{H}]^-$: 500.2590; found: 500.2586.

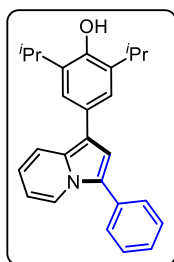
2,6-di-*tert*-butyl-4-{3-phenyl-6-[3-(trifluoromethyl)phenyl]-indolizin-1-yl}-phenol (42aq)



The reaction was performed at 0.068 mmol scale of **41j**; $R_f = 0.5$ (5% EtOAc in hexane); brown gummy solid (17 mg, 46% yield); ^1H NMR (400 MHz, CDCl_3) δ 8.48 (s, 1H), 7.81 (dd, $J = 8.6, 0.7$ Hz, 1H), 7.78 (s, 1H), 7.71 (d, $J = 7.6$ Hz, 1H), 7.68 – 7.66 (m, 2H), 7.59 (d, $J = 7.8$ Hz, 1H), 7.76– 7.52 (m, 3H), 7.48 (s, 2H), 7.43 – 7.38 (m, 1H), 7.06 (s, 1H), 7.00 (dd, $J = 9.4, 1.5$ Hz, 1H), 5.22 (s, 1H), 1.54 (s, 18H); ^{13}C NMR (100 MHz, CDCl_3) δ 152.5, 139.7, 136.5, 132.2, 131.6, 131.3, 130.0, 129.5, 129.3, 129.1, 128.4, 127.7, 127.1, 126.3, 124.7, 124.0 (q, $J_{\text{C-F}} = 5.1$ Hz), 124.2 (q, $J_{\text{C-F}} = 270.8$ Hz), 123.5 (q, $J_{\text{C-F}} = 3.8$ Hz), 120.5, 119.3, 117.7, 117.0, 114.9, 34.7, 30.6; $^{19}\text{F}\{^1\text{H}\}$ NMR (376 MHz, CDCl_3) δ -62.6; FT-IR (thin film, neat): 3641, 2956, 2859, 1736, 1602, 1517, 1458, 1364, 1235, 1038, 889, 788, 701 cm^{-1} ; HRMS (ESI): m/z calcd for $\text{C}_{35}\text{H}_{33}\text{F}_3\text{NO}$ $[\text{M}-\text{H}]^-$: 540.2514; found : 540.2518.

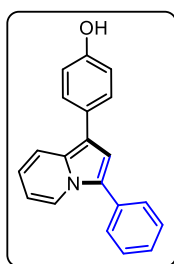
2,6-di-*iso*-propyl-4-(3-phenylindolizin-1-yl)-phenol (42ar)

The reaction was performed at 0.112 mmol scale of **41k**; $R_f = 0.3$ (5% EtOAc in hexane); brown gummy solid (32.3 mg, 78% yield); ^1H NMR (400 MHz, CDCl_3) δ 8.32 (d, $J = 7.0$ Hz, 1H), 7.74 (d, $J = 9.1$ Hz, 1H), 7.67 (d, $J = 7.3$ Hz, 2H), 7.53 (t, $J = 7.5$ Hz, 1H), 7.40 (d, $J = 7.4$



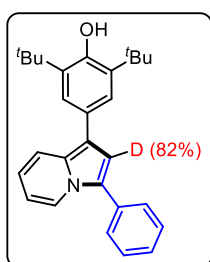
Hz, 1H), 7.37 (s, 2H), 7.07 (s, 1H), 6.76 (t, $J = 7.1$ Hz, 1H), 6.54 – 6.51 (m, 1H), 4.83 (s, 1H), 3.28 (septet, $J = 5.8$ Hz, 2H), 1.39 (d, $J = 6.8$ Hz, 12H); ^{13}C NMR (100 MHz, CDCl_3) δ 148.4, 134.1, 132.5, 130.0, 129.1, 128.6, 128.3, 127.3, 125.5, 123.2, 122.6, 118.8, 117.6, 116.2, 113.9, 111.0, 27.4, 23.0; FT-IR (thin film, neat): 3053, 2960, 2869, 1654, 1601, 1547, 1341, 1263, 1014, 938, 833, 700 cm^{-1} ; HRMS (ESI): m/z calcd for $\text{C}_{26}\text{H}_{26}\text{NO}$ $[\text{M}-\text{H}]^-$: 368.2014; found: 368.2014.

Experimental procedure for the de-tert-butylation of **42a**:



AlCl_3 (100.6 mg, 0.755 mmol) was added to a solution of **42a** (50 mg, 0.126 mmol) in benzene (2.0 mL) and the mixture was stirred at 55 °C for 1 h. The reaction mixture was then quenched with cold ice water and extracted with Ethyl acetate, and the organic part was concentrated under reduced pressure. The residue was purified through a neutral alumina column using EtOAc/Hexane mixture as an eluent to get the pure product **43** (34.2 mg, 95%) as brown gummy solid; $R_f = 0.5$ (50% EtOAc in hexane); ^1H NMR (400 MHz, $\text{DMSO}-d_6$) δ 9.32 (s, 1H), 8.29 (d, $J = 7.2$ Hz, 1H), 7.64 (d, $J = 9.1$ Hz, 1H), 7.57 (d, $J = 7.3$ Hz, 2H), 7.45 (t, $J = 7.5$ Hz, 2H), 7.37 (d, $J = 8.4$ Hz, 2H), 7.31 (t, $J = 7.4$ Hz, 1H), 7.00 (s, 1H), 6.80 (d, $J = 8.5$ Hz, 2H), 6.73 – 7.70 (m, 1H), 6.54 (t, $J = 6.9$ Hz, 1H); ^{13}C NMR (100 MHz, $\text{DMSO}-d_6$) δ 155.5, 131.6, 129.2, 129.1, 128.3, 127.7, 127.2, 126.4, 124.7, 122.6, 118.3, 118.0, 115.7, 114.8, 113.5, 111.4; FT-IR (thin film, neat): 3386, 3255, 2956, 2257, 1653, 1552, 1515, 1267, 1023, 572 cm^{-1} ; HRMS (ESI): m/z calcd for $\text{C}_{20}\text{H}_{16}\text{NO}$ $[\text{M}+\text{H}]^+$: 286.1232; found: 286.1227.

Experimental Procedure for the reaction between phenylacetylene to **1a** in a mixture of MeCN and D_2O :

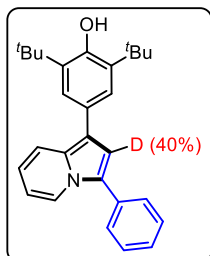


Anhydrous MeCN (1.25 mL) and D_2O (0.25 mL) was added to the mixture of *p*-quinone methide **41a** (30 mg, 1.0 equiv.), phenylacetylene (2.0 equiv.) and $\text{Pd}(\text{OAc})_2$ (10 mol %) under argon atmosphere and the resulting suspension was stirred at 50 °C until the *p*-QM **41a** was completely consumed (based on TLC analysis). The reaction mixture was concentrated under reduced pressure and the residue was purified through a silica gel chromatography, using EtOAc/Hexane mixture as an eluent, to get the pure **3a'** (23.0 mg, 57% yield) as a brown solid; $R_f = 0.5$ (5% EtOAc in hexane); m. p. = 104–106 °C; ^1H NMR (400 MHz, CDCl_3) δ 8.30 (d, $J = 7.2$ Hz, 1H), 7.72 (d, $J = 9.1$ Hz, 1H), 7.65 – 7.63 (m, 2H), 7.51 (t, $J = 7.5$ Hz, 2H), 7.46 (s, 2H), 7.39 – 7.35 (m, 1H), 7.02 (s, 0.18H), 6.75 – 6.71 (m, 1H) 6.50 (td, $J = 7.4, 1.2$ Hz, 1H),

5.20 (s,1H), 1.54 (s, 18H); ^{13}C NMR (100 MHz, CDCl_3) δ 152.3, 136.4, 132.5, 130.0, 129.1, 128.3, 127.4, 127.3, 125.3, 124.7, 122.6, 118.8, 117.5, 116.4, 113.9, 111.0, 34.6, 30.6.

Experimental Procedure for the reaction between phenylacetylene-d to **41a:**

The phenylacetylene-d was prepared by following a literature procedure^[26]

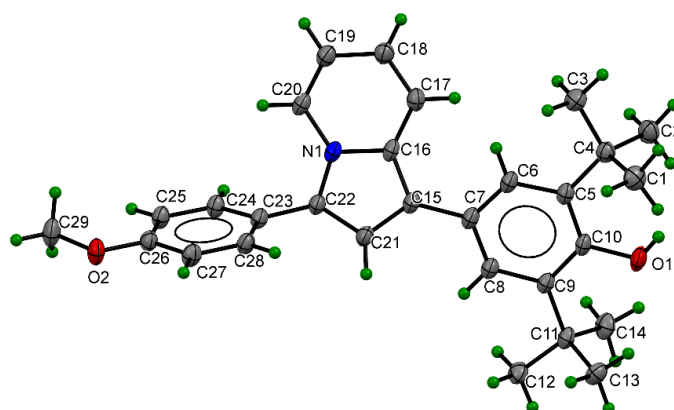


Anhydrous MeCN (1.5 mL) was added to the mixture of *p*-quinone methide **41a** (30 mg, 0.102 mmol, 1.0 equiv.), phenylacetylene-d (2.0 equiv.) and $\text{Pd}(\text{OAc})_2$ (10 mol %) under argon atmosphere and the resulting suspension was stirred at 50 °C until the *p*-QM **41a** was completely consumed (based on TLC analysis). The reaction mixture was concentrated under reduced pressure and the residue was purified through a silica gel chromatography, using EtOAc/Hexane mixture as an eluent, to get the pure **3a'** (34.2 mg, 84% yield) as a brown gummy solid; R_f = 0.5 (5% EtOAc in hexane); ^1H NMR (400 MHz, CDCl_3) δ 8.30 (d, J = 7.2 Hz, 1H), 7.72 (d, J = 9.1 Hz, 1H), 7.65 – 7.63 (m, 2H), 7.51 (t, J = 7.5 Hz, 2H), 7.46 (s, 2H), 7.39 – 7.35 (m, 1H), 7.02 (s, 0.60H), 6.75 – 6.71 (m, 1H), 6.50 (td, J = 7.4, 1.2 Hz, 1H), 5.20 (s,1H), 1.54 (s, 18H); ^{13}C NMR (100 MHz, CDCl_3) δ 152.3, 136.4, 132.5, 130.0, 129.1, 128.3, 127.4, 127.3, 125.4, 124.7, 122.6, 118.8, 117.5, 116.4, 113.9, 111.0, 34.6, 30.6.

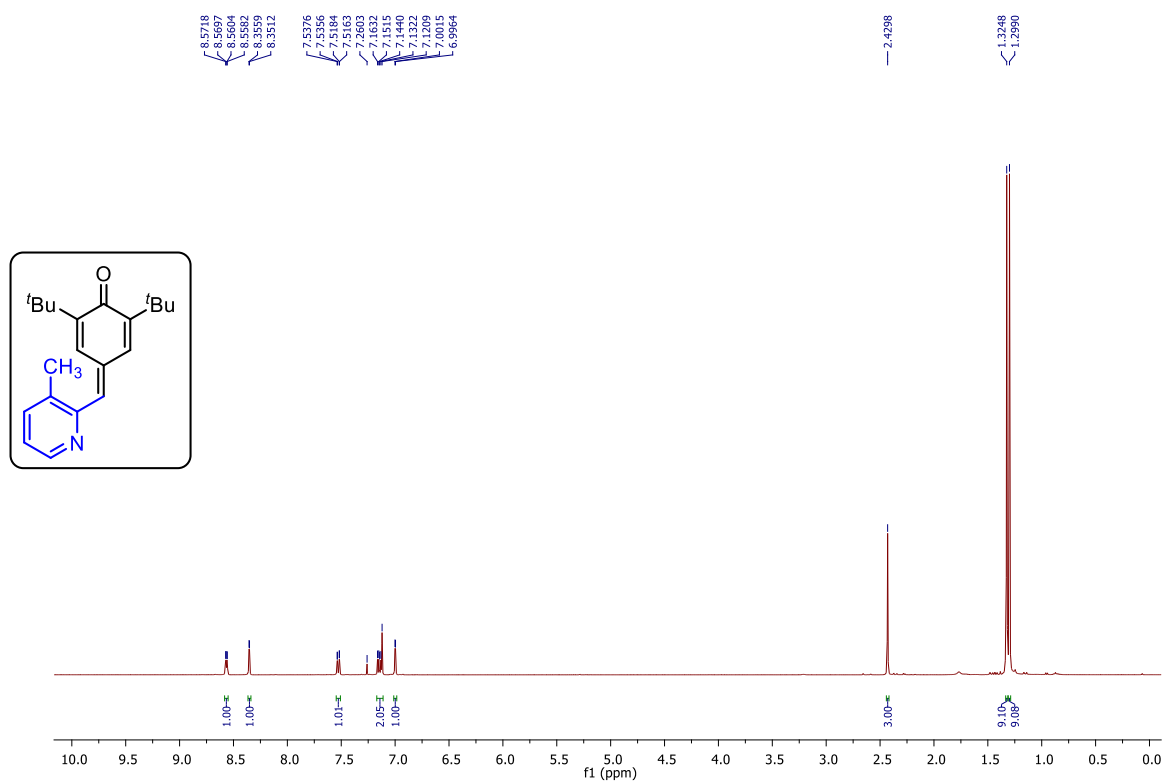
X-ray crystallographic analysis for compound 42f:

Table 2. Crystal data and structure refinement for compound 42f (CCDC 2132083)

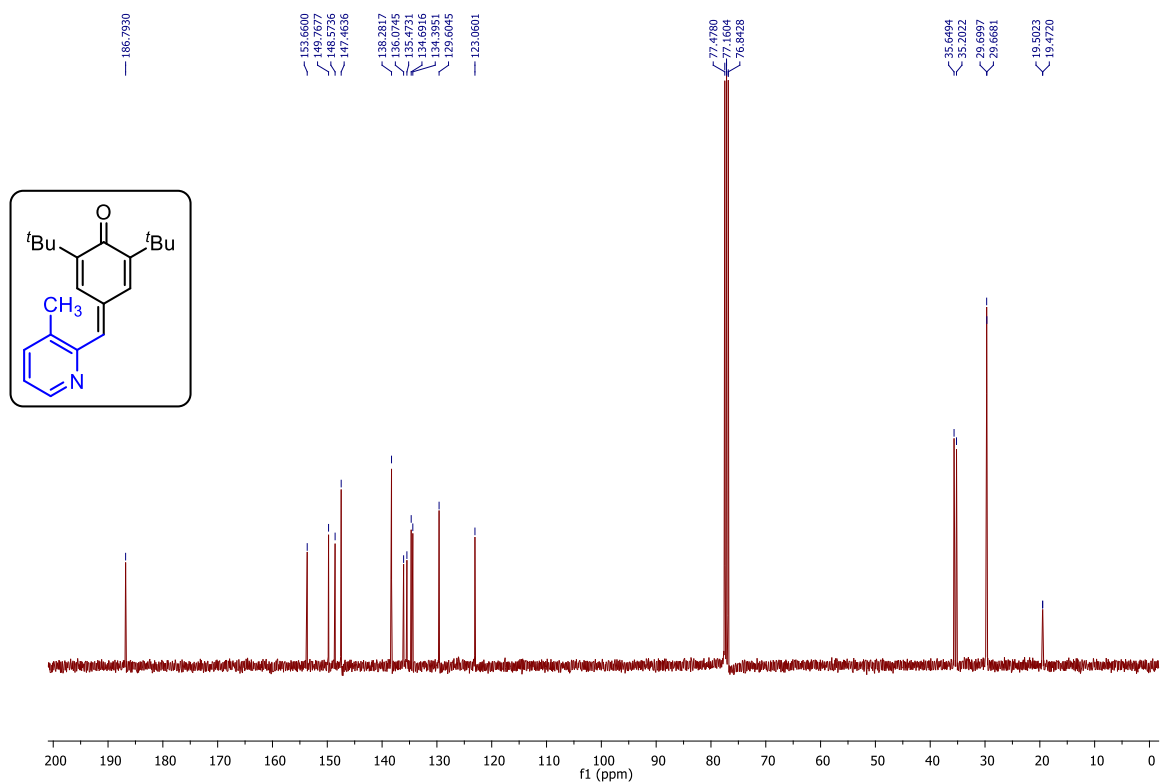
Complex	XII-FZ-23
Chemical formula	C ₂₉ H ₃₃ NO ₂
molar mass	427.56
Crystal system	Monoclinic
Space group	<i>P</i> 2 ₁ / <i>c</i>
<i>T</i> [K]	150.02(10)
<i>a</i> [Å]	12.5189(4)
<i>b</i> [Å]	10.2586(4)
<i>c</i> [Å]	18.1361(7)
α [°]	90.00
β [°]	97.843(4)
γ [°]	90.00
<i>V</i> [Å ³]	2307.37(15)
<i>Z</i>	4
<i>D</i> (calcd.) [g·cm ⁻³]	1.231
μ (Mo-K α) [mm ⁻¹]	0.076
Reflections collected	16666
Independent reflections	7963
Data/restraints/parameters	7963/0/300
<i>R</i> 1, <i>wR</i> ₂ [<i>I</i> > 2 σ (<i>I</i>)] ^[a]	0.0708, 0.1848
<i>R</i> 1, <i>wR</i> ₂ (all data) ^[a]	0.0955, 0.2251
GOF	1.062
CCDC	2132083



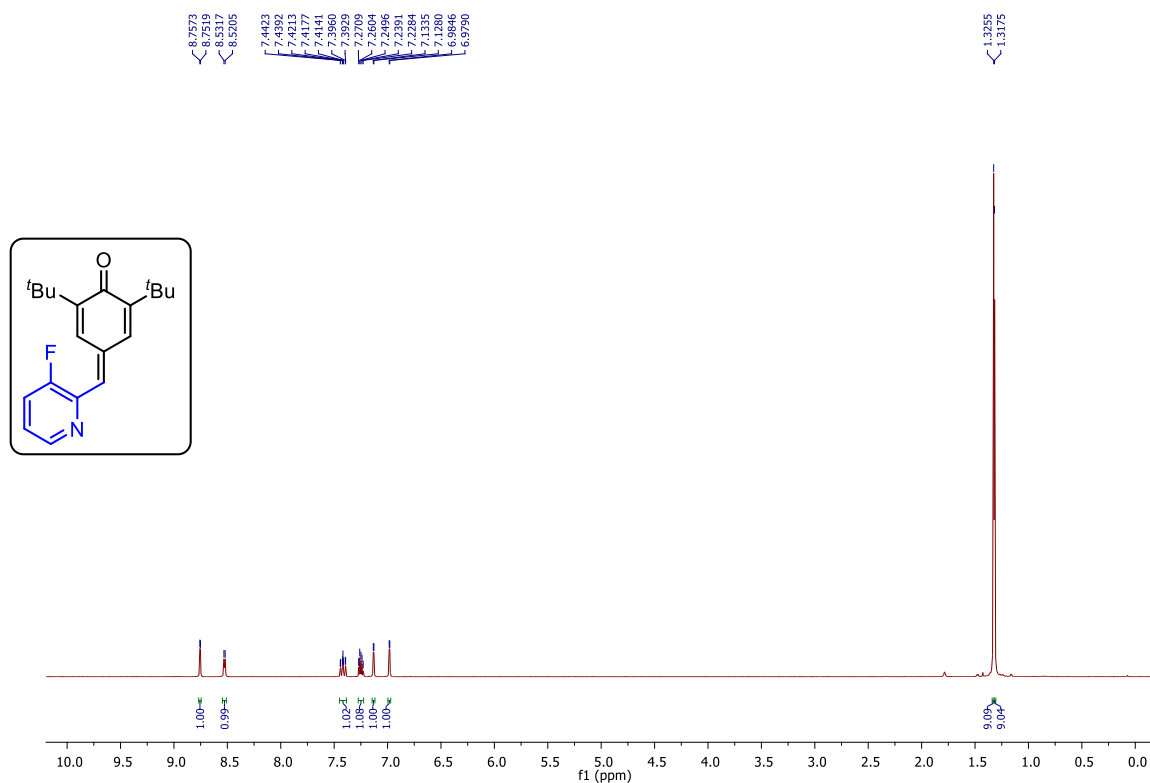
^1H NMR (400 MHz, CDCl_3) spectrum of (**41b**)



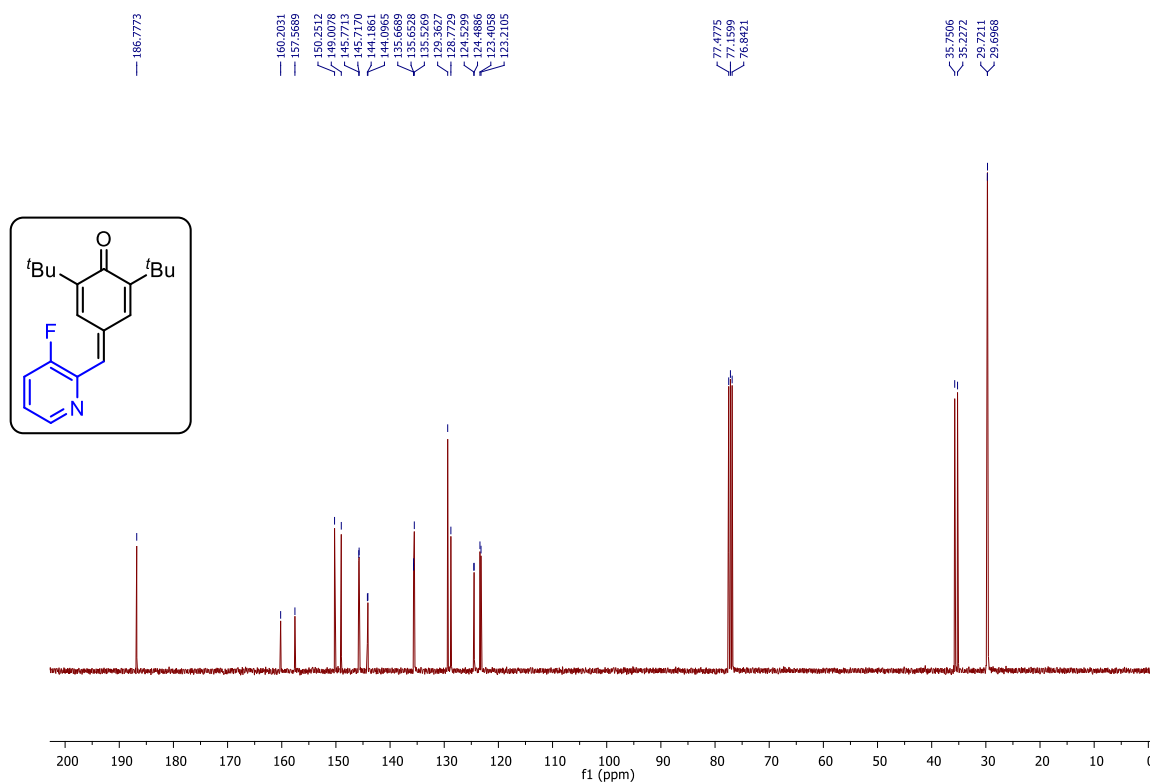
$^{13}\text{C}\{^1\text{H}\}$ NMR (100 MHz, CDCl_3) spectrum of (**41b**)



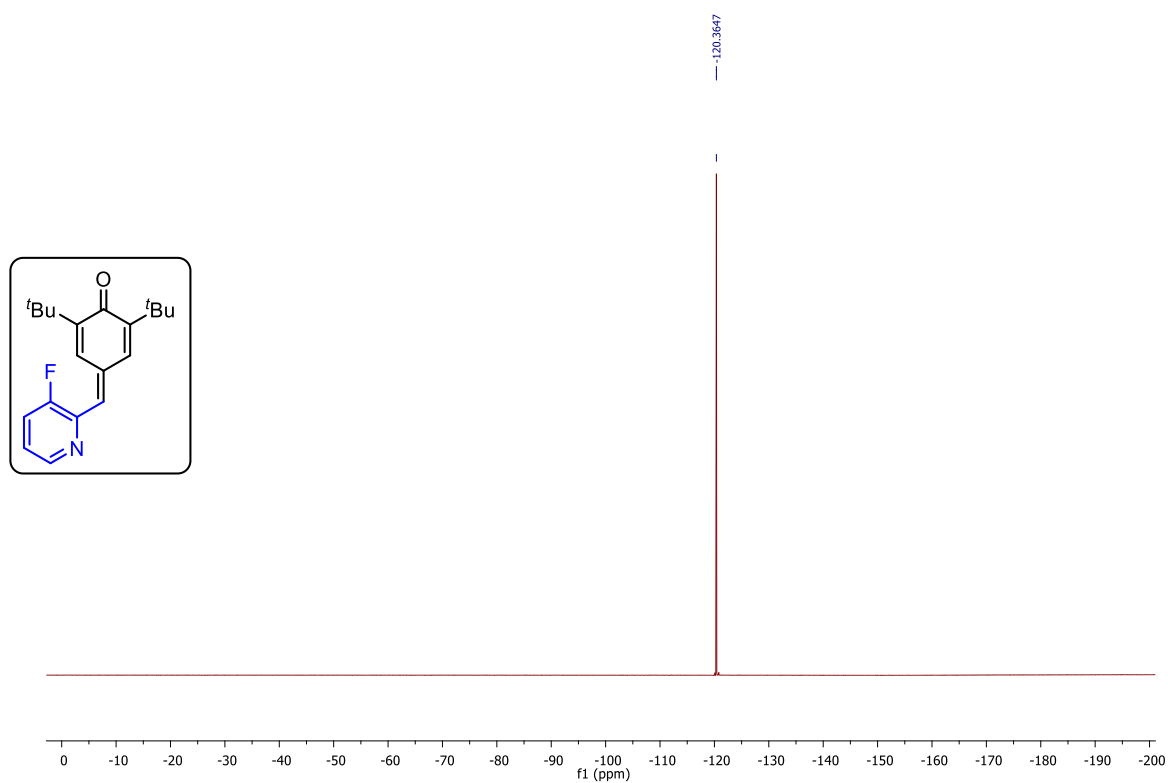
^1H NMR (400 MHz, CDCl_3) spectrum of (**41c**)



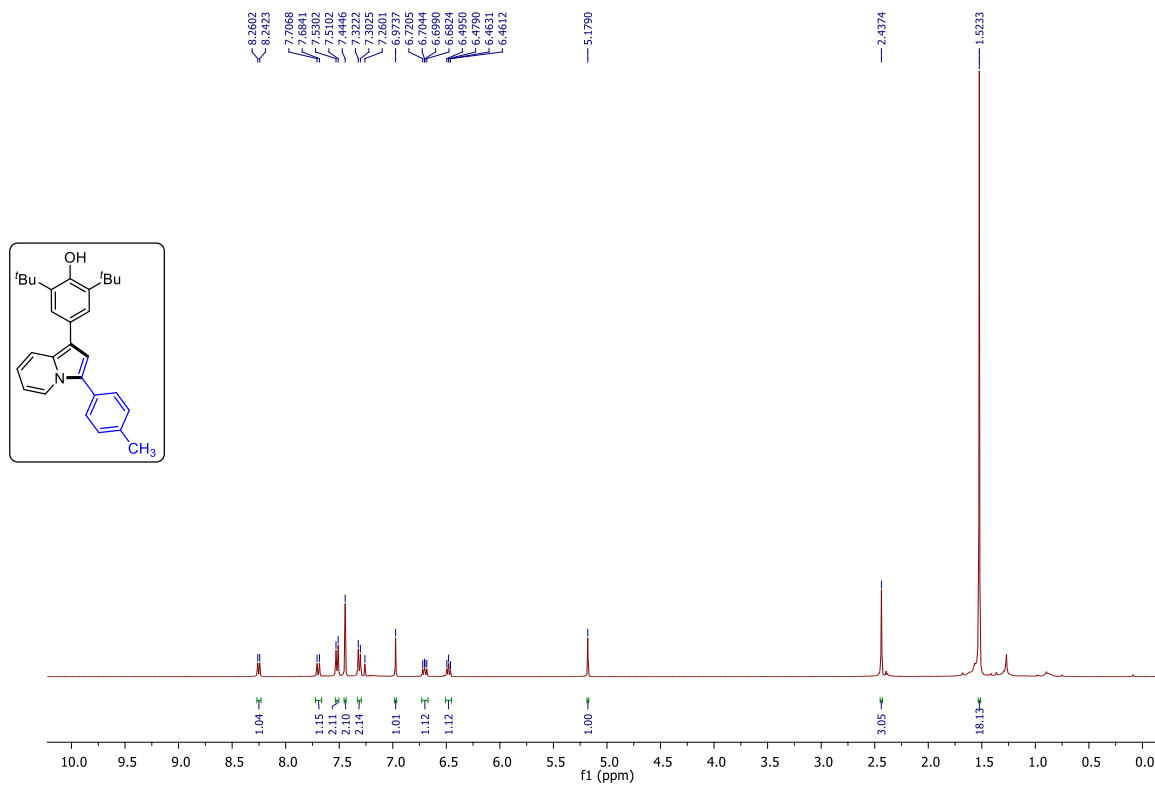
$^{13}\text{C}\{^1\text{H}\}$ NMR (100 MHz, CDCl_3) spectrum of (**41c**)



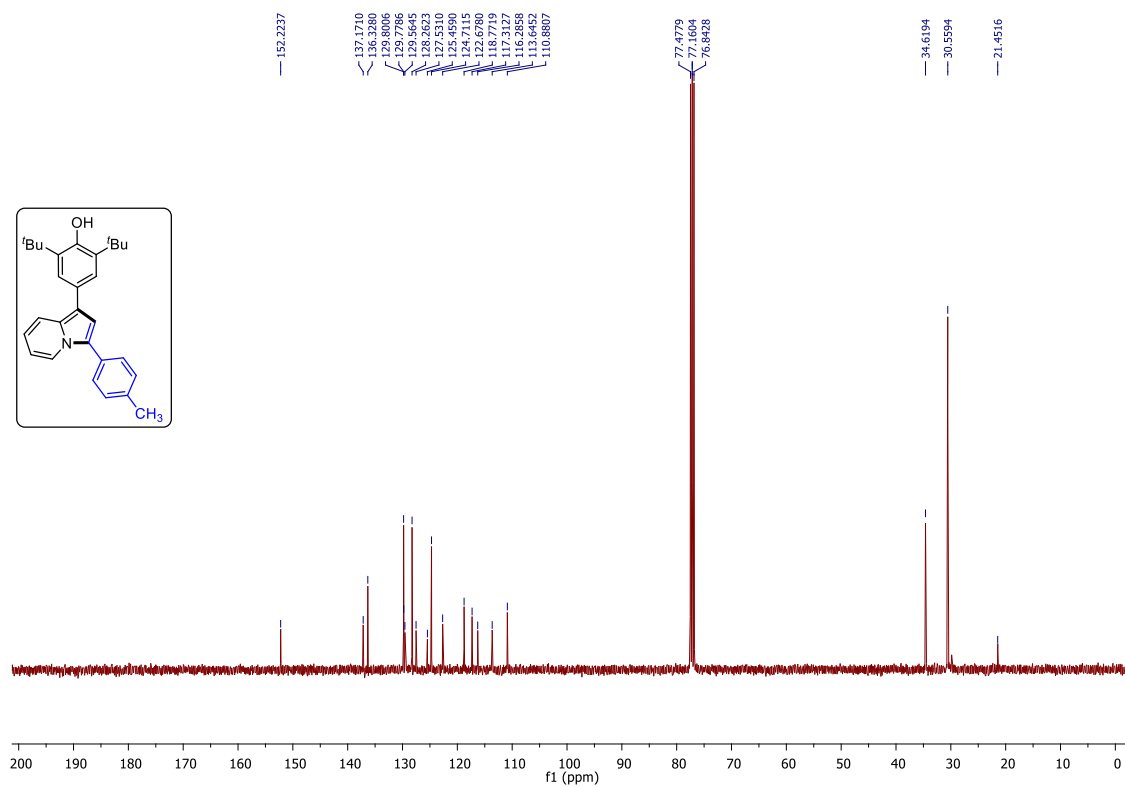
$^{19}\text{F}\{^1\text{H}\}$ NMR (376 MHz, CDCl_3) spectrum of (**41c**)



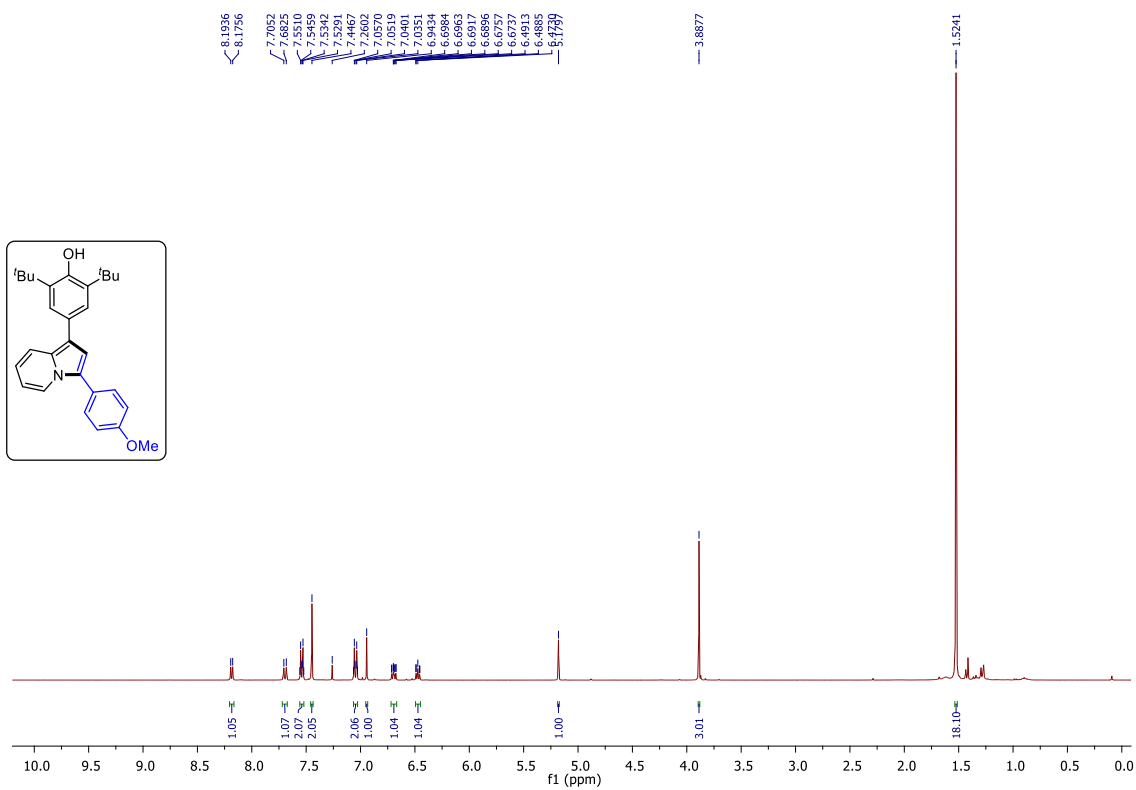
^1H NMR (400 MHz, CDCl_3) spectrum of (**42b**)



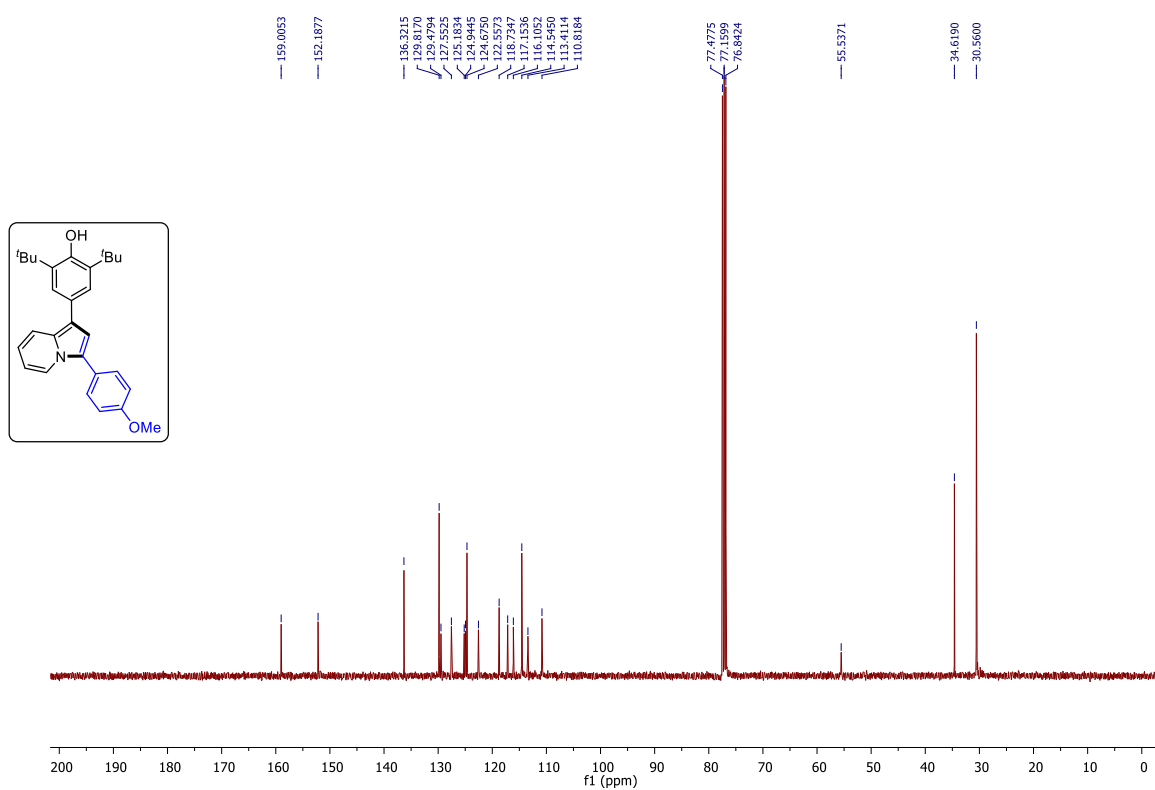
$^{13}\text{C}\{^1\text{H}\}$ NMR (100 MHz, CDCl_3) spectrum of (**42b**)



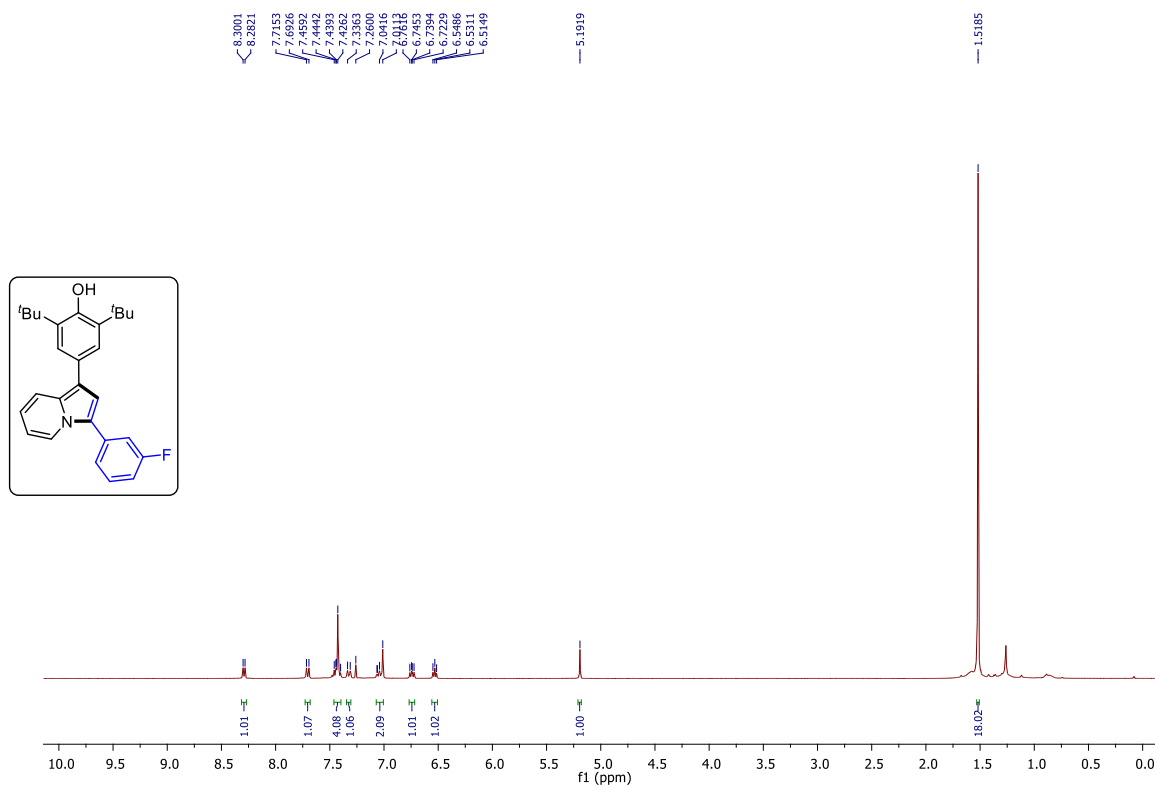
^1H NMR (400 MHz, CDCl_3) spectrum of (**42f**)



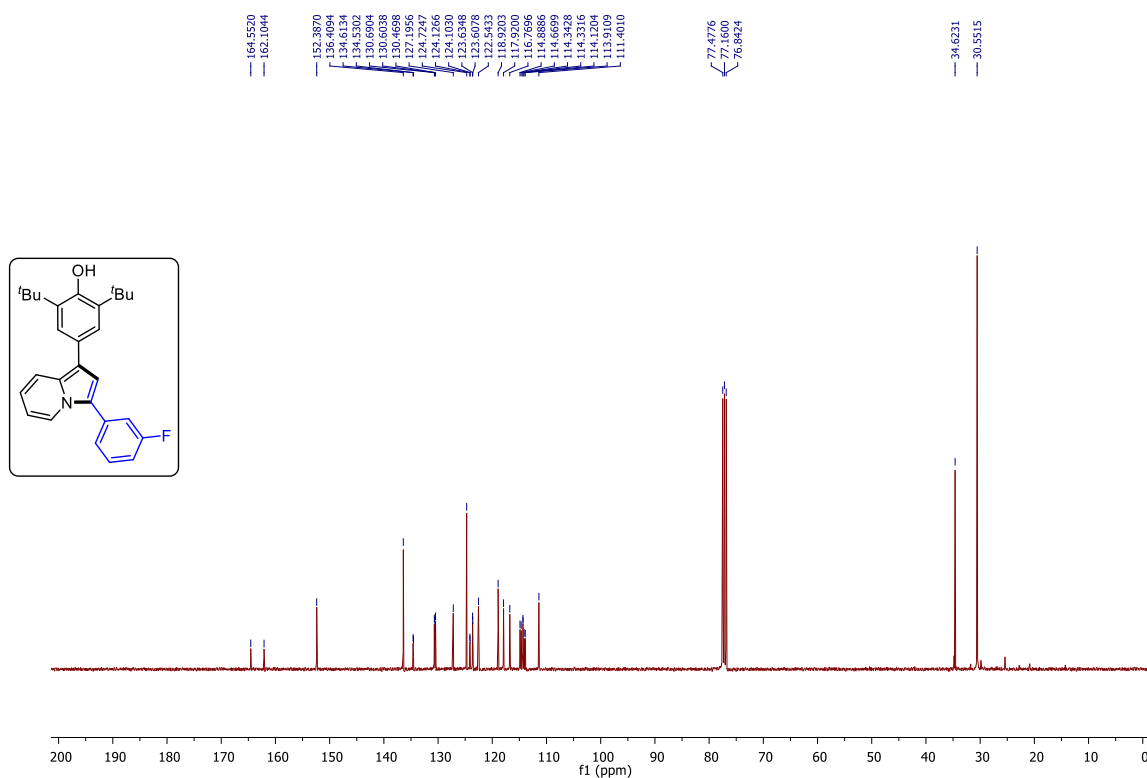
$^{13}\text{C}\{^1\text{H}\}$ NMR (100 MHz, CDCl_3) spectrum of (**42f**)



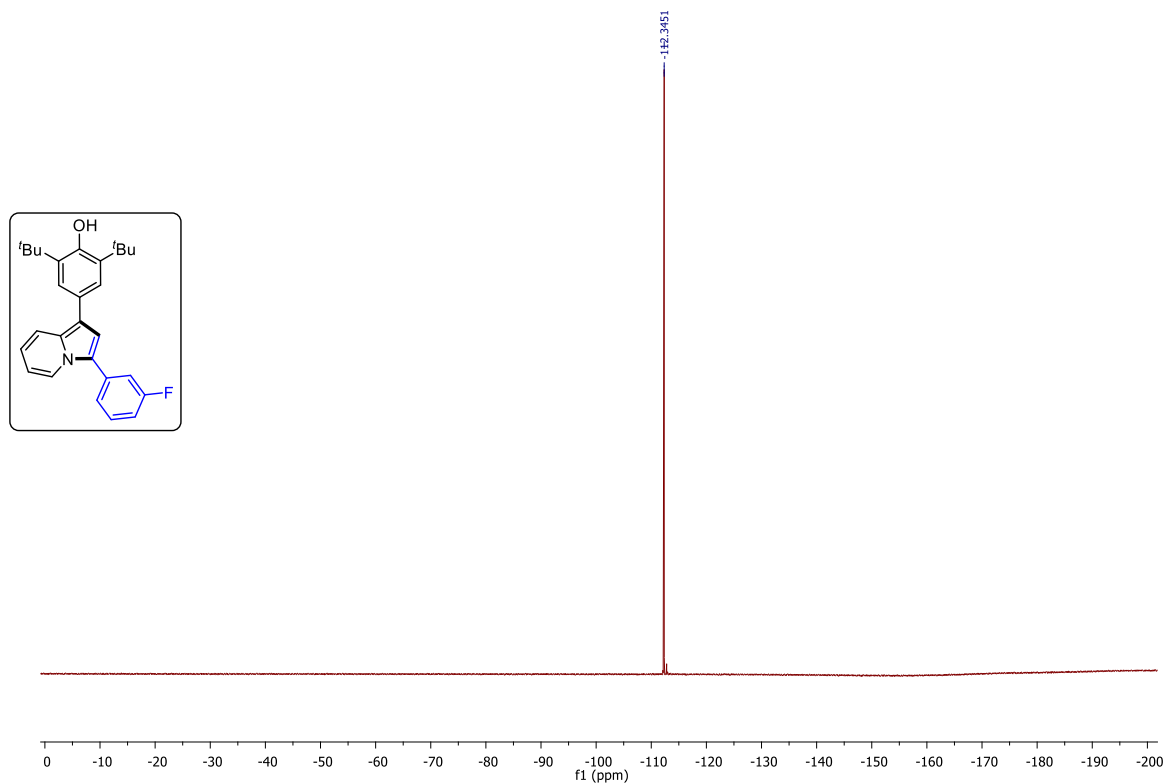
^1H NMR (400 MHz, CDCl_3) spectrum of (**42n**)



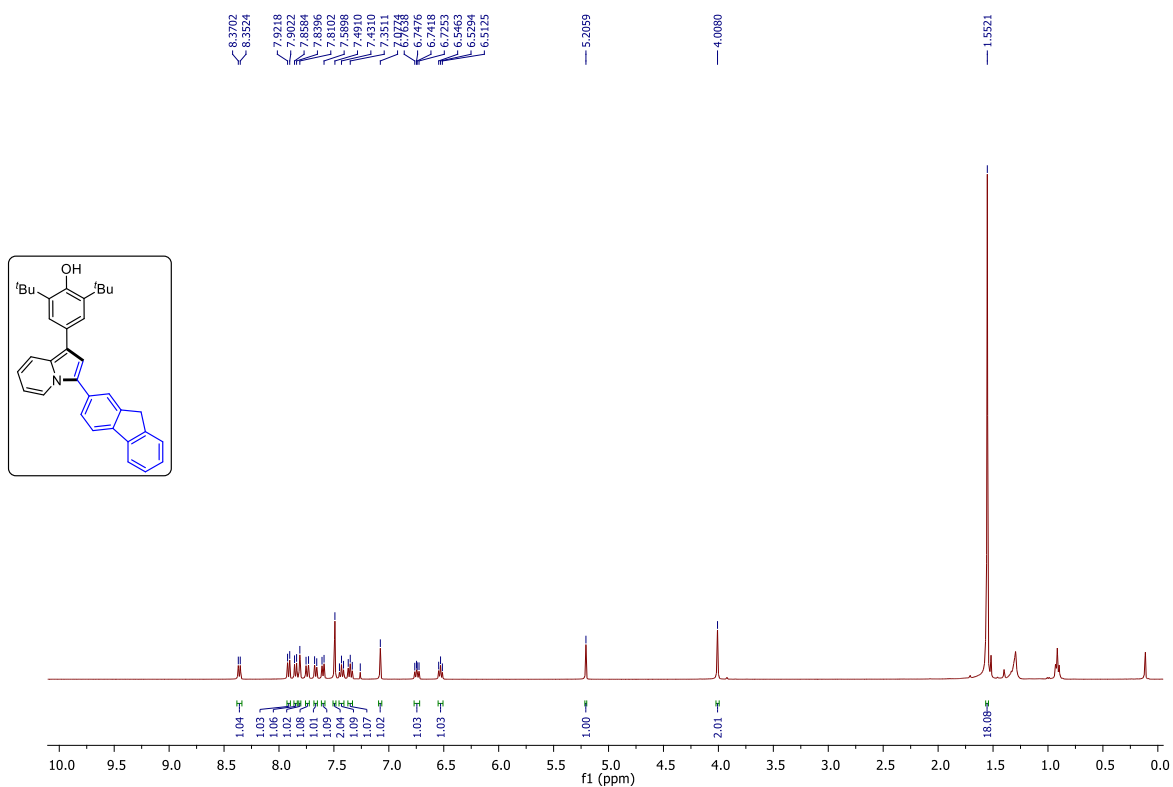
$^{13}\text{C}\{^1\text{H}\}$ NMR (100 MHz, CDCl_3) spectrum of (**42n**)



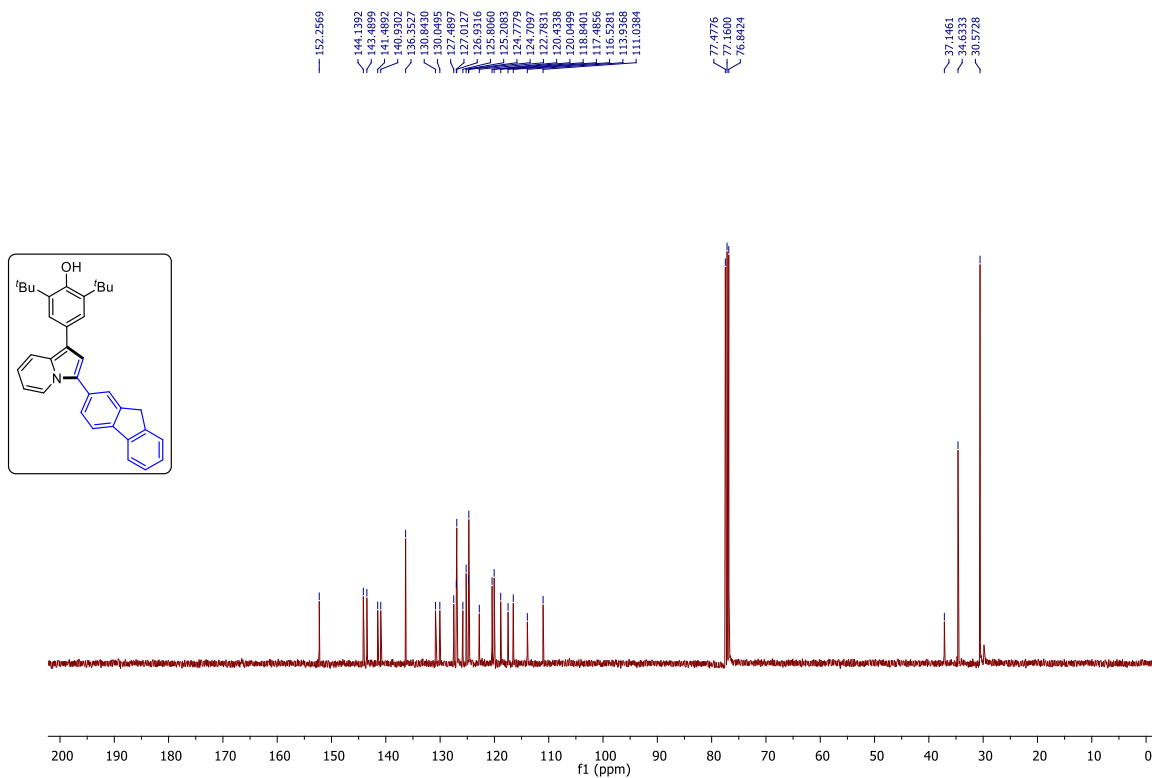
$^{19}\text{F}\{^1\text{H}\}$ NMR (376 MHz, CDCl_3) spectrum of (**42n**)



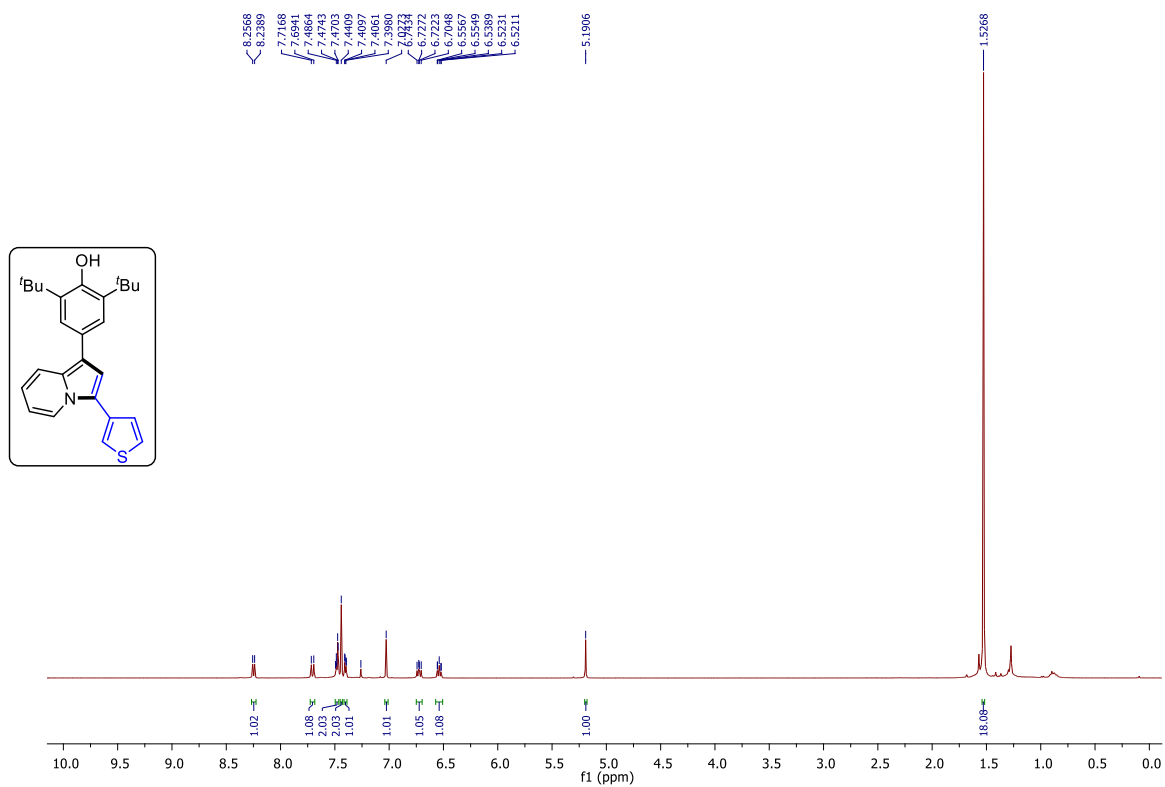
¹H NMR (400 MHz, CDCl₃) spectrum of (**42aa**)



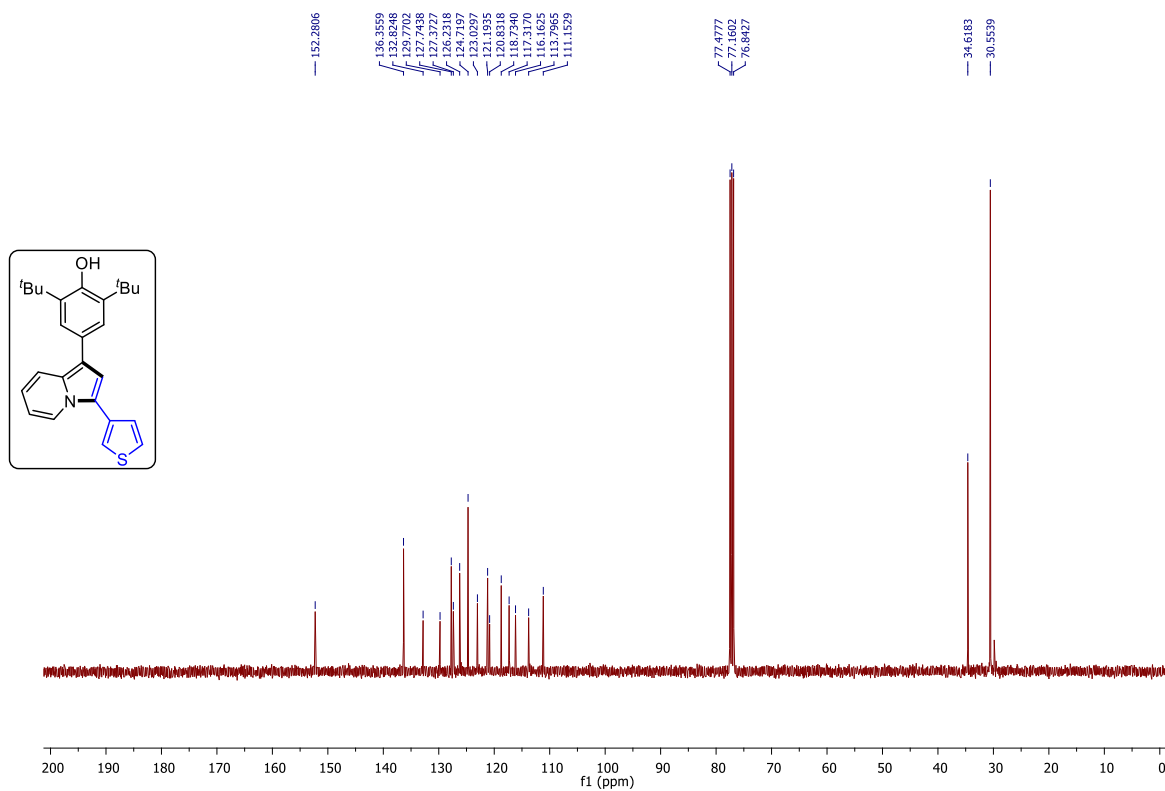
¹³C{¹H} NMR (100 MHz, CDCl₃) spectrum of (**42aa**)



¹H NMR (400 MHz, CDCl₃) spectrum of (**42ac**)



¹³C{¹H} NMR (100 MHz, CDCl₃) spectrum of (**42ac**)



2.7. References:

1. (a) Iwao, M.; Fukuda, T.; Ishibashi, F. *Heterocycles*, **2011**, 83, 491; (b) Michael, J. P. *Nat. Prod. Rep.*, **2005**, 22, 603 (c) Bailly, C. *Mar. Drugs*, **2015**, 13, 1105.
2. Smith, S. C.; Clarke, E. D.; Ridley, S. M.; Bartlett, D.; Greenhow, D. T.; Glithro, H.; Klong, A. Y.; Mitchell, G.; Mullier, G. W. *Pest Manage. Sci.*, **2005**, 61, 16.
3. (a) Arvin-Berod, M.; Desroches-Castan, A.; Bonte, S.; Brugière, S.; Couté, Y.; Guyon, L.; Feige, J.-J.; Baussanne I.; Demeunynck, M. *ACS Omega*, **2017**, 2, 9221; (b) Weide, T.; Arve, L.; Prinz, H.; Waldmann, H.; Kessler, H. *Bioorg. Med. Chem. Lett.*, **2006**, 16, 59.
4. (a) Dawood, K. M.; Abbas, A. A. *Expert Opin. Ther. Pat.*, **2020**, 30, 695 (b) Hazra, A.; Mondal, S.; Maity, A.; Naskar, S.; Saha, P.; Paira, R.; Sahu, K. B.; Paira, P.; Ghosh, S.; Sinha, C.; Samanta, A.; Banerjee, S.; Mondal, N. B. *Eur. J. Med. Chem.*, **2011**, 46, 2132 (c) Bloch, W. M.; Derwent-Smith, S. M.; Issa, F.; Morris, J. C.; Rendina, L. M.; Sumby, C. J. *Tetrahedron*, **2011**, 67, 9368. (d) Østby, O. B.; Dalhus, B.; Gundersen, L.-L.; Rise, F.; Bast, A.; Haenen, G. R. M. M. *Eur. J. Org. Chem.*, **2000**, 3763.
5. (a) Kim, E.; Koh, M.; Lim, B. J.; Park, S. B. *J. Am. Chem. Soc.*, **2011**, 133, 6642 (b) Ge, Y.; Liu, A. Dong, J.; Duan, G.; Cao, X.; Li, F. *Sens. Actuators B*, **2017**, 247, 46 (c) Delcamp, J. H.; Yella, A.; Holcombe, T. W.; Nazeeruddin, M. K.; Gratzel, M. *Angew. Chem. Int. Ed.*, **2013**, 52, 376.
6. For recent reviews: (a) Sadowski, B.; Klajn, J.; Gryko, D. T. *Org. Biomol. Chem.*, **2016**, 14, 7804 (b) Hui, J.; Ma, Y.; Zhao, J.; Cao, H. *Org. Biomol. Chem.*, **2021**, 19, 10245.
7. For selected examples: (a) Seregin, I. V.; Gevorgyan, V. *J. Am. Chem. Soc.*, **2006**, 128, 12050. (b) Xu, T.; Alper, H. *Org. Lett.*, **2015**, 17, 4526 (c) Oh, K. H.; Kim, S. M.; Park, S. Y.; Park, J. K. *Org. Lett.*, **2016**, 18, 2204.
8. For selected examples: (a) Marchalin, S.; Baumlovà, B.; Baran, P.; Oulyadi, H. Daïch, A. *J. Org. Chem.*, **2006**, 71, 9114. (b) Albaladejo, M. J.; Alonso, F.; Yus, M. *Chem. - Eur. J.*, **2013**, 19, 5242 (c) Kim, H.; Lee, K.; Kim, S.; Lee, P. H. *Chem. Commun.*, **2010**, 46, 6341 (d) Yan, B.; Liu, Y. *Org. Lett.*, **2007**, 9, 4323.
9. For selected recent examples: (a) Chen, Y.; Shatskiy, A.; Liu, J. -Q.; Kärkäs, M. D.; Wang, X. -S. *Org. Lett.*, **2021**, 23, 7555 (b) Dong, S.; Huang, J.; Sha, H.; Qiu, L.; Hub, W.; Xu, X. *Org. Biomol. Chem.*, **2020**, 18, 1926 (c) Lu, C. J.; Yu, X.; Chen, Y. T.; Song, Q. B.; Wang, H. *Org. Chem. Front.*, **2020**, 7, 2313 (d) Xiao, X.; Han, P.; Zhou,

- H.; Liu, J. *J. Org. Chem.*, **2021**, 86, 18179 (e) Kim, H.; Kim, S.; Kim, J.; Son, J. Y.; Baek, Y.; Um, K.; Lee, P. H. *Org. Lett.*, **2017**, 19, 5677.
10. For selected recent examples: (a) Escalante, C. H.; Hernández, F. A. C.; López, A. H.; Mora, E. I. M.; Delgado, F.; Tamariz, J. *Org. Biomol. Chem.*, **2022**, 20, 396 (b) Joshi, D. R.; Kim, I. *J. Org. Chem.*, **2021**, 86, 10235 (c) Joshi, D. R.; Kim, I. *Adv. Synth. Catal.*, **2021**, 363, 5330 (d) Kim, S.; Lee, J. H.; Yoon, S. H.; Kim, I. *Org. Biomol. Chem.*, **2021**, 19, 5806 (e) Liu, R.; Wang, Q.; Wei, Y.; Shi, M. *Chem. Commun.*, **2018**, 54, 1225 (f) Patel, R. K.; Chauhan A.; Jha, P.; Kant, R.; Kumar, R. *Org. Lett.* **2022**, 24, 542.
11. (a) Liu, R. -R.; Lu, C. -J.; Zhang, M. -D.; Gao, J. R.; Jia, Y. -X. *Chem. Eur. J.*, **2015**, 21, 7057 (b) Bagle, P. N.; Mane, M. V.; Venka, K.; Shinde, D. R.; Shaikh, S. R.; Gonnade, R. G.; Patil, N. T. *Chem. Commun.*, **2016**, 52, 14462 (c) Pathipati, S. R.; Werf, A. van der; Selander, N. *Org. Lett.*, **2018**, 20, 3691.
12. (a) Paluru, D. K.; Mahesh, S.; Ahmad, F.; Anand, R. V. *Chem. Asian. J.*, **2019**, 14, 4688; (b) Mahesh, S.; Anand, R. V. *Eur. J. Org. Chem.*, **2017**, 2698 (c) Mahesh, S.; Paluru, D. K.; Ahmad, F.; Patil, S.; Kant, G.; Anand, R. V. *Asian J. Org. Chem.*, **2017**, 6, 1857.
13. Nayak, M.; kim, I. *Org. Biomol. Chem.*, **2015**, 13, 9697.
14. Li, X.; Xie, X.; Liu, Y. *J. Org. Chem.* **2016**, 81, 3688.
15. Roy, S. Das, S. K.; Chattopadhyay, B. *Angew. Chem. Int. Ed.* **2018**, 57, 2238.
16. Douglas, T.; Pordia, A.; Dowden, J. *Org. Lett.* **2017**, 19, 6396.
17. Han, C.; Liu, Y.; Tian, X.; Rominger, F.; Hashmi, A. S. K. *Org. Lett.* **2021**, 23, 9480.
18. Liu, R. R.; Hong, J. J.; Lu, C. J.; Xu, M.; Gao, J. R.; Jia, Y. X. *Org. Lett.* **2015**, 17, 3050.
19. Shen, B.; Li, B.; Wang, B. *Org. Lett.* **2016**, 18, 2816.
20. (a) Chernyak, D.; Skontos, C.; Gevorgyan, V. *Org. Lett.* **2010**, 12, 3242; (b) Li, Z.; Chernyak, D.; Gevorgyan, V. *Org. Lett.* **2012**, 14, 6056; (c) Xu, T.; Alper, H. *Org. Lett.* **2015**, 17, 4526. (d) Oh, K. H.; Kim, S. M.; Park, S. Y.; Park, J. K. *Org. Lett.* **2016**, 18, 2204.
21. For selected reports, please see: (a) Pankhade, Y. A.; Pandey, R.; Fatma, S.; Ahmad, F.; Anand, R. V. *J. Org. Chem.*, **2022**, 87, 3363. (b) Jadhav, A. S.; Pankhade, Y. A.; Hazra, R.; Anand, R. V. *J. Org. Chem.*, **2018**, 83, 10107. (c) Singh, G.; Goswami, P.; Sharma, S.; Anand, R. V. *J. Org. Chem.*, **2018**, 83, 10546. (d) Jadhav, A. S.; Pankhade, Y. A.; Anand, R. V. *J. Org. Chem.*, **2018**, 83, 8615.

22. For recent reviews on *para*-quinone methide chemistry: (a) Li, W.; Xu, X.; Zhang, P.; Li, P. *Chem. Asian J.*, **2018**, *17*, 2350 (b) Lima, C. G. S.; Pauli, F. P.; Costa, D. C. S.; de Souza, A. S.; Forezi, L. S. M.; Ferriera, V. F.; de Carvalho da Silva, F. *Eur. J. Org. Chem.*, **2020**, *18*, 2650 (c) Wang, J. -Y.; Hao, W. -J.; Tu, S. -J.; Jiang, B. *Org. Chem. Front.*, **2020**, *7*, 1743. (d) Singh, G.; Pandey, R.; Pankhade, Y. A.; Fatma, S.; Anand, R. V. *Chem. Rec.*, **2021**, *21*, 4150.
23. (a) Reddy, V.; Anand, R. V. *Org. Lett.*, **2015**, *17*, 3390; (b) Chu, W. -D.; Zhang, L. -F.; Bao, X.; Zhao, X. -H.; Zeng, C.; Du, J. -Y.; Zhang, G. -B.; Wang, F. -X.; Ma, X. -Y.; Fan, C. -A. *Angew. Chem., Int. Ed.*, **2013**, *52*, 9229.
24. Pankhade, Y. A.; Pandey, R.; Fatma, S.; Ahmad F.; Anand, R. V. *J. Org. Chem.* **2022**, *87*, 3363
25. Lopez, A.; Parra, A.; Jarava-Barrera, C.; Tortosa, M. *Chem. Commun.*, **2015**, *51*, 17684.
26. Chen, H.; Yang, M.; Wang, G.; Gao, L.; Ni, Z.; Zou, J.; Li, S. *Org. Lett.* **2021**, *23*, 5533.

3. Copper[II]-catalyzed [3+2]-Annulation of 2-Pyridinyl-substituted *p*-Quinone Methides with Enaminones: Access to Functionalized Indolizine Derivatives

3.1. Introduction:

The *N*-containing heterocycles are often found as an integral part of many bioactive natural products and synthetic biologically active compounds.^[1] Among the nitrogen-containing heterocycles, indolizine is one of the significant skeletons (figure 1), which consists of a six-membered pyridine ring fused with a five-membered pyrrole ring. Indolizine core serve as an integral part in many natural products,^[2] agrochemicals,^[3] and bioactive molecules.^[4] In addition, they have also found applications in material science.^[5]

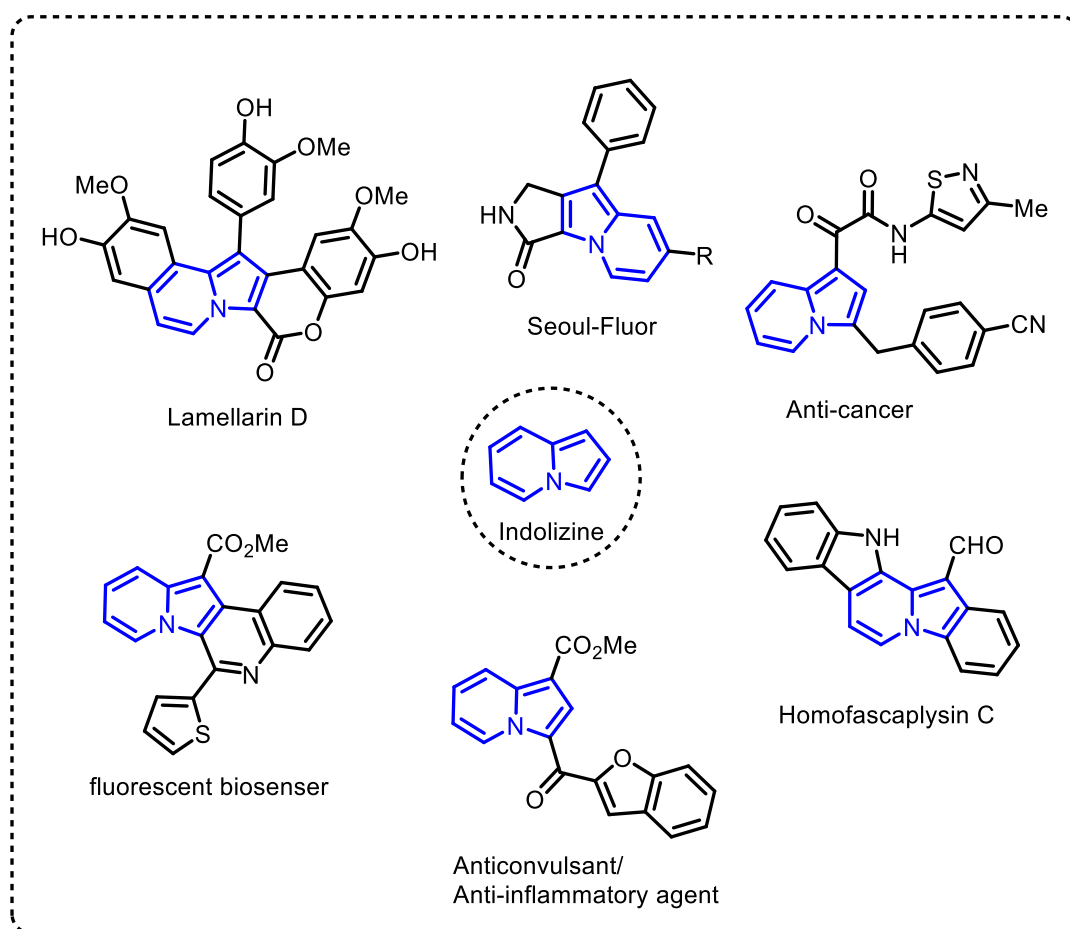
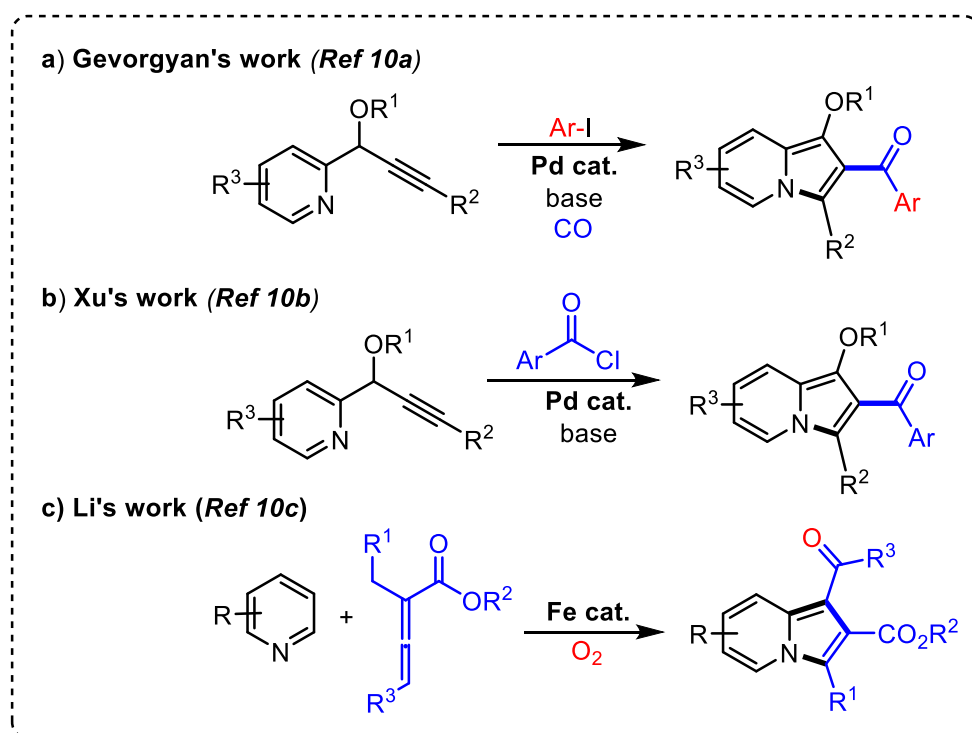


Figure 1. Natural products and bioactive indolizine derivatives

Due to the diverse range of properties, from medicinal chemistry to material science, it is highly desirable to discover practical synthetic methods to quickly access these substituted indolizine derivatives. Of course, numerous synthetic approaches have been developed for the synthesis of these heterocycles.^[6] The most common methods to access indolizines are (i) intermolecular cyclization of pyridiniums or C2-substituted pyridines with various coupling partners,^[7] and (ii) intramolecular cyclization of propargylic pyridines through transition metal-catalyzed cycloisomerization reactions.^[8] Recently, 2-(2-enynyl) pyridines have been recognized as an alternative synthons for highly substituted indolizine derivatives.^[9]



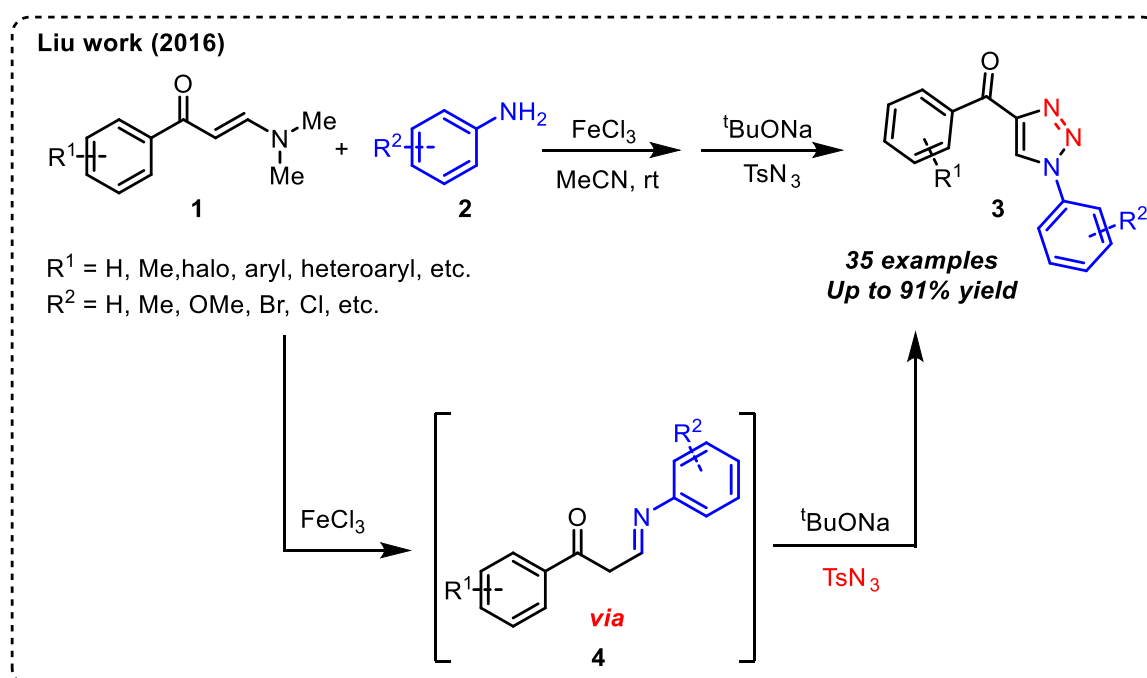
Scheme 1: Previous Protocols to Access 2-Aroyl Indolizines.

Although there are several reports appeared in the literature for the synthesis of 1,2-diary/dialkyl substituted indolizines, only a few direct protocols are available at this point in time for the synthesis of 1- or 2-acyl substituted indolizines. For example, Gevorgyan's group reported a palladium-catalyzed carbonylative cyclization/arylation approach for the synthesis of 2-aryloindolizines from propargylic pyridines and aryl halides (**a**, Scheme 1).^[10a] Similarly, Xu's group reported a palladium-catalyzed synthesis of 2-aryloindolizine derivatives through cyclization of propargylic pyridines with aroyl chlorides (**b**, Scheme 1).^[10b] In addition, Li's group reported an iron-catalyzed reaction of pyridine and substituted allenoate towards functionalized indolizine derivatives (**c**, Scheme 1).^[10c]

3.2. Literature reports on the synthesis heterocycles using *N,N*-dimethyl enaminones:

In recent years, enaminones and analogous stable enamines have been widely used in the construction of diverse heterocyclic scaffolds, especially, *N*-heterocycles.^[11] Some of them are discussed below.

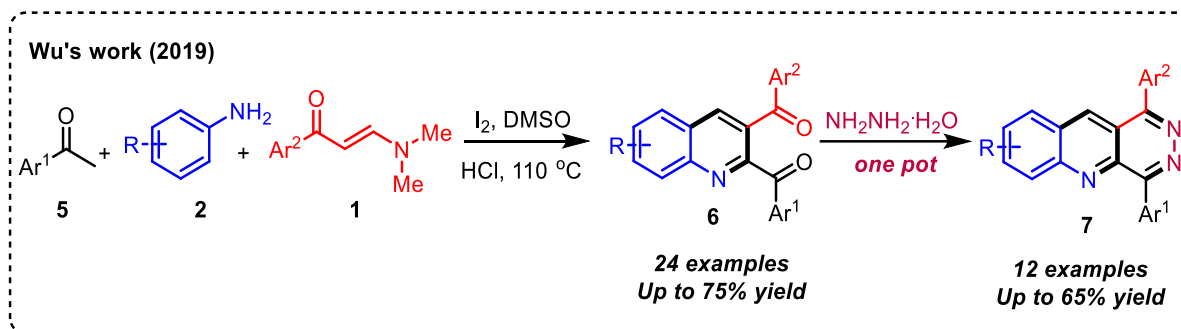
In 2016 Liu group reported the synthesis of various *N*-substituted 1,2,3-triazoles through a domino reaction between NH-based secondary enaminones and tosyl azide by using FeCl₃ and *t*-BuONa as the base promoter. The reactions proceed efficiently at room temperature with good substrate tolerance. According to the proposed mechanism the reaction proceeds via cycloaddition reactions through a key Regitz diazo-transfer process with tosyl azide (scheme 2).^[12]



Scheme 2: Synthesis of *N*-substituted 1,2,3-triazoles using enaminone

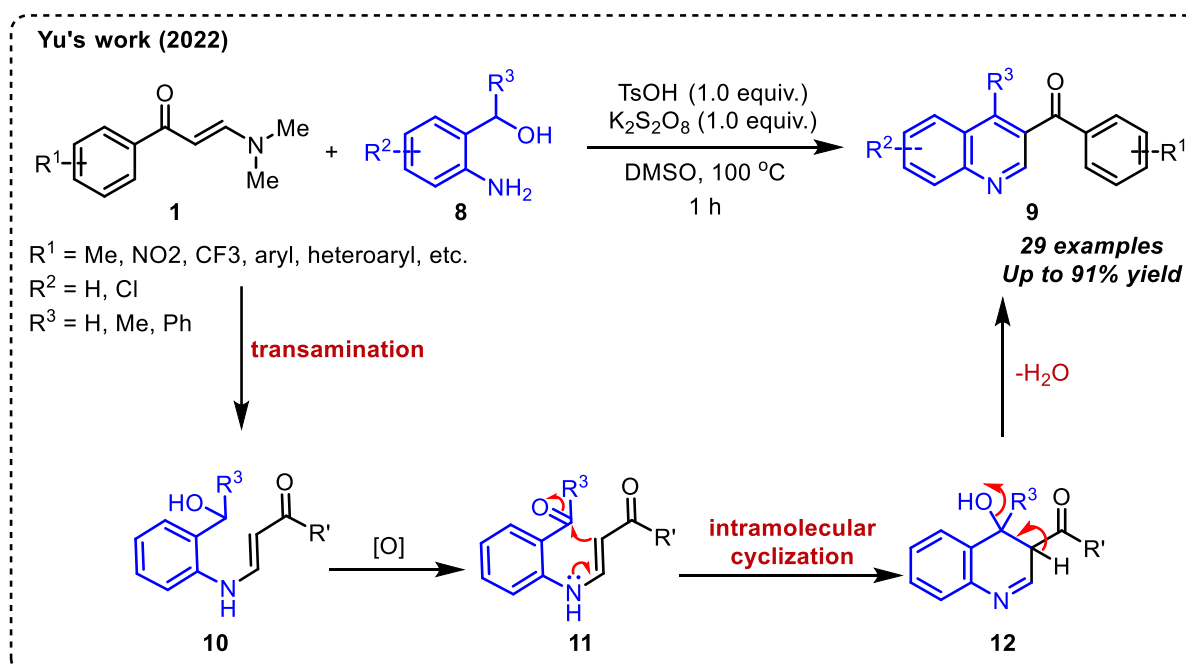
Wu's group in 2019 developed an I₂-promoted one-pot multicomponent reaction for the synthesis of 2,3-diaroyl quinolines (6) via a formal [3+2+1] cycloaddition of aryl methyl ketones (5), aryl amines (2) and enaminones (1). A variety of substituted aryl ketones, anilines and enaminones were reacted smoothly under the optimized reaction conditions and the corresponding 2,3-diaroyl quinolines (6) were obtained in moderate to good yields. The alkyl reactants such as alkyl ketones, alkyl amines, and alkyl enaminones were not compatible with

this transformation. Furthermore they have successfully transformed the 1,4-dicarbonyl scaffold in **6** to prepare pyridazino[4,5-b]quinoline skeletons (**7**) in one-pot (scheme 3).^[13]



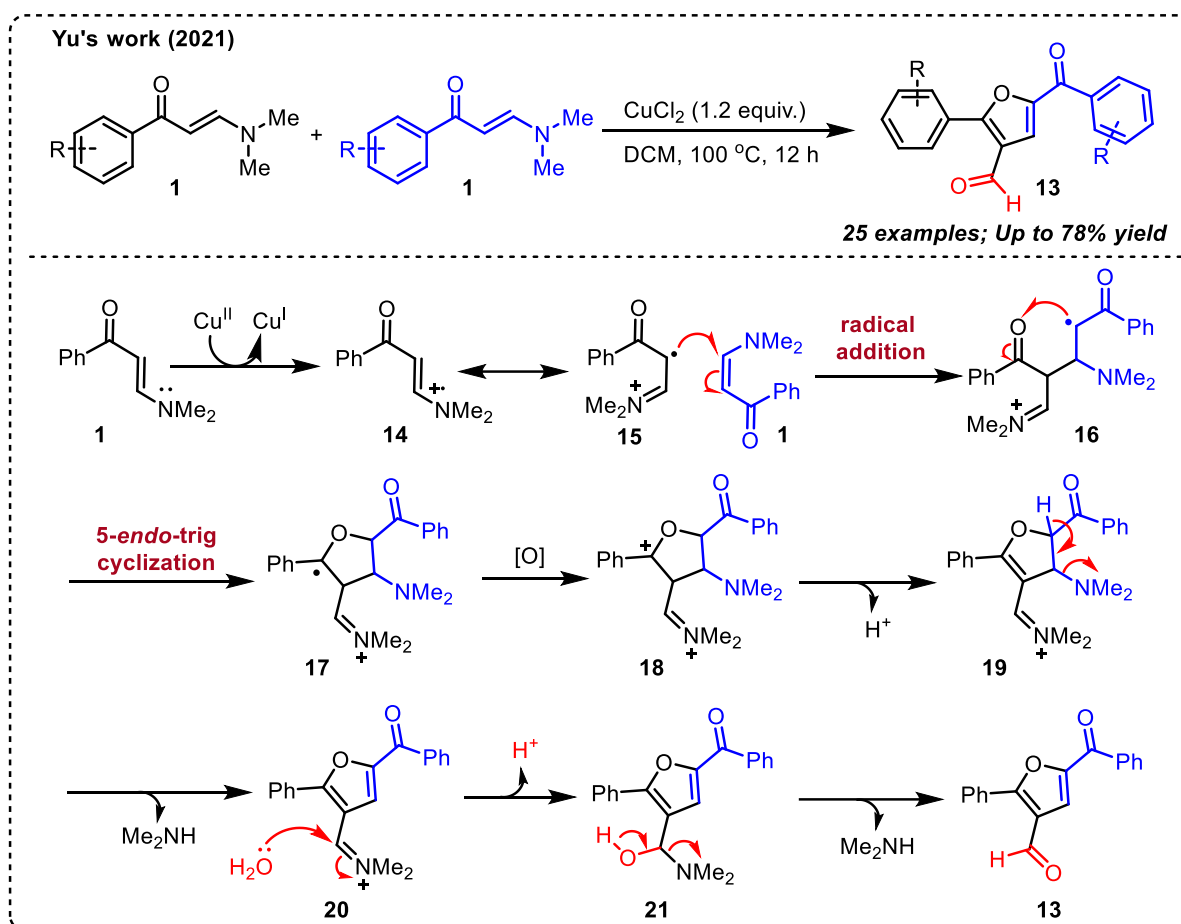
Scheme 3: I₂-promoted one-pot multicomponent synthesis of quinolines using enaminones

In 2022 Yu's group reported a transition-metal free approach for the synthesis of quinoline derivatives (**9**) in moderate to excellent yields through an oxidative cyclocondensation reaction of *o*-aminobenzyl alcohols (**8**) and enaminones (**1**) promoted by



Scheme 4: TsOH promoted oxidative cyclocondensation reaction of enaminones

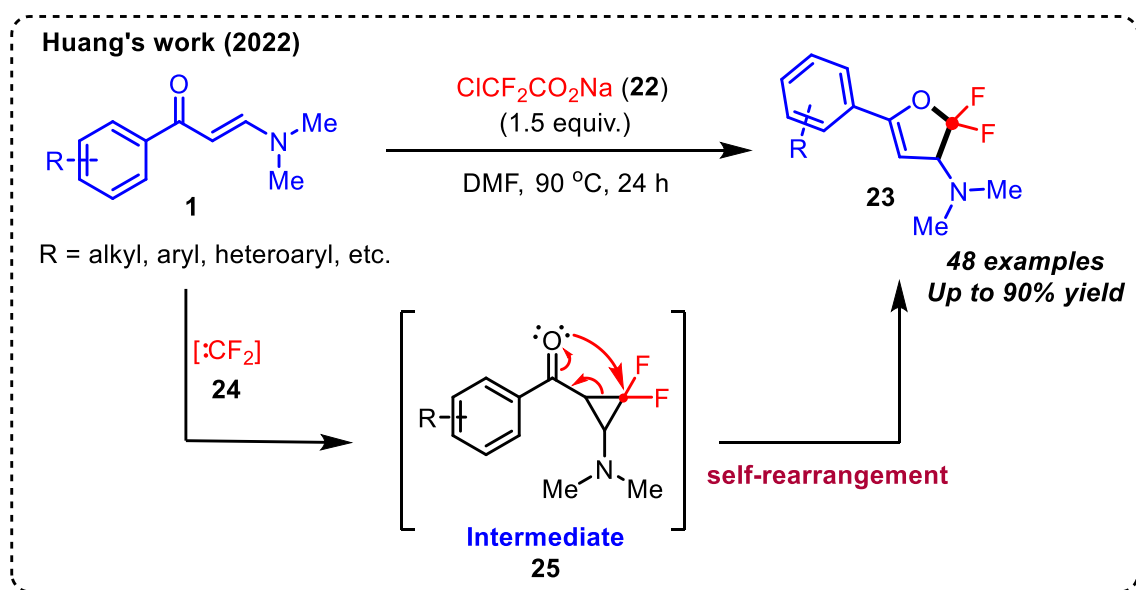
TsOH and K₂S₂O₈. Based on the control experiments the authors proposed that the reaction proceeds through a TsOH promoted transamination reaction of enaminone **1** and *o*-aminobenzyl alcohols (**8**) to generate an intermediate **10**, which subsequently undergoes a K₂S₂O₈-assisted oxidation to form **11**. The intermediate **11** on intramolecular cyclization and aromatization produces the final quinoline product **9** (scheme 4).^[14]



Scheme 5: Cu(II)-mediated radical annulation of *N,N*-dimethyl enaminone

Yu and co-workers in 2021 reported the synthesis of diverse 5-acyl-3-furancarboxaldehydes (**13**) through a radical cascade [3+2] annulation of two molecules of *N,N*-dimethyl enaminones (**1**) mediated by copper(II) chloride. On the basis of control experiments the authors proposed that this intermolecular radical transformation proceeds through the oxidation of *N,N*-dimethyl enaminones **1** by Cu(II) to generate the radical cation intermediate **14**, which then further tautomerizes to generate the carbon centered radical intermediate **15**. Subsequently, the radical addition of **15** across a C=C bond in another molecule of *N,N*-dimethyl enaminone **1** generates the radical intermediate **16**, followed by 5-*endo*-trig radical cyclization with the carbonyl oxygen to afford the radical intermediate **17**. The intermediate **17** is oxidized to produce the cation intermediate **18**, which then undergoes a successive deprotonation and deamination to give aromatic furan intermediate **20**. Finally, the imine of intermediate **20** is attacked by water to produce the hydroxylated intermediate **21**, which loses one molecule of dimethylamine to yield the final product **13** (scheme 5).^[15]

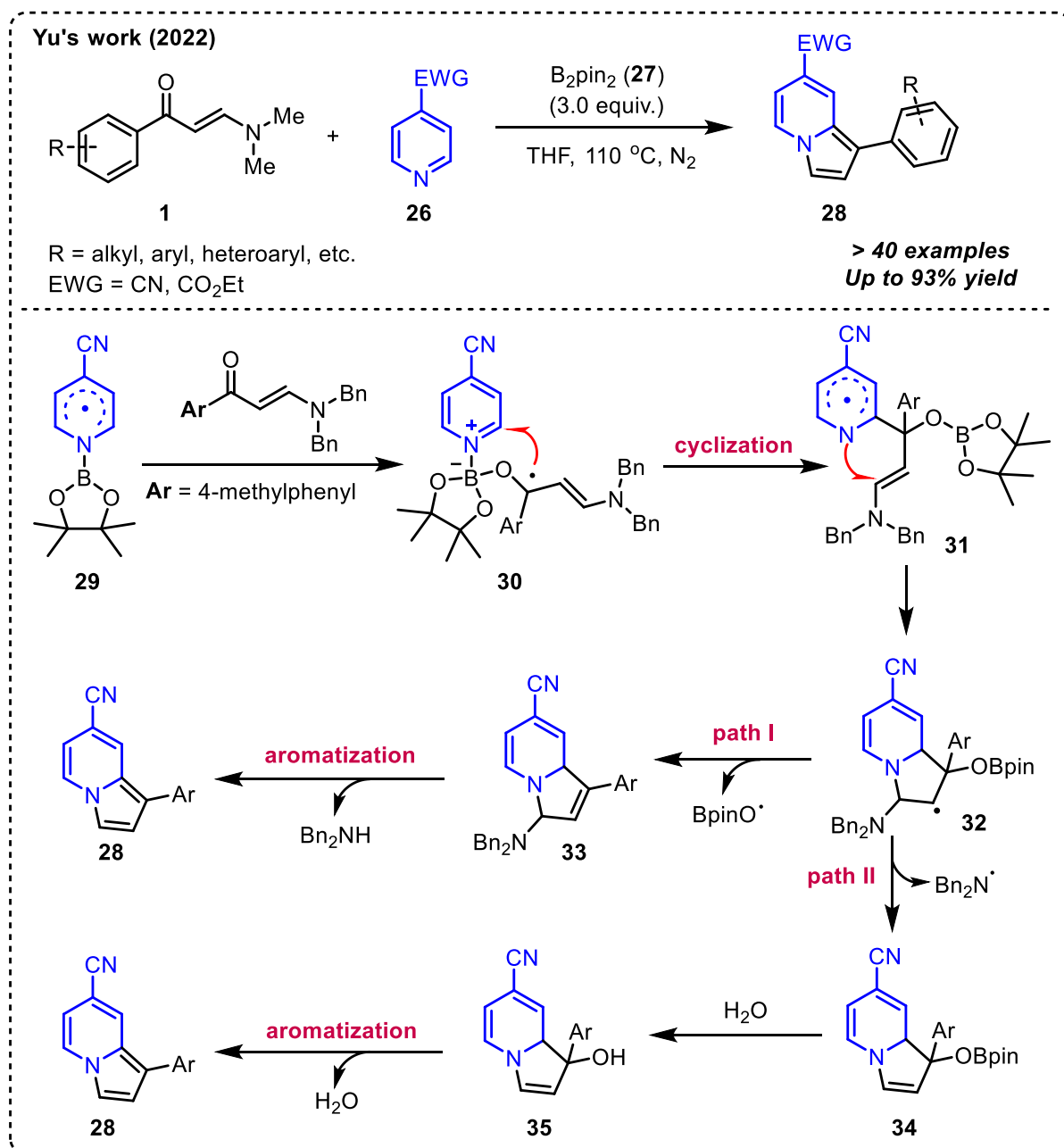
Huang group in 2022 reported an approach to synthesize monocyclic 2,2-difluoro-2,3-dihydrofuran derivatives (**23**) by the cycloaddition reaction of enaminones (**1**) and a difluorocarbene generated from sodium chlorodifluoroacetate ($\text{ClCF}_2\text{CO}_2\text{Na}$) **22**. Mechanistic investigation of this transformation revealed that *N,N*-dimethylformamide (DMF) promoted the formation of difluorocarbene **24** from $\text{ClCF}_2\text{CO}_2\text{Na}$ **22**. The difluorocarbene **24** generated then reacts with the carbon–carbon double bond of enaminone **1** to form a donor–acceptor cyclopropane intermediate **25**, which upon self-rearrangement produces the final product **23** (scheme 6).^[16]



Scheme 6: Synthesis of dihydrofuran derivatives using *N,N*-dimethyl enaminones

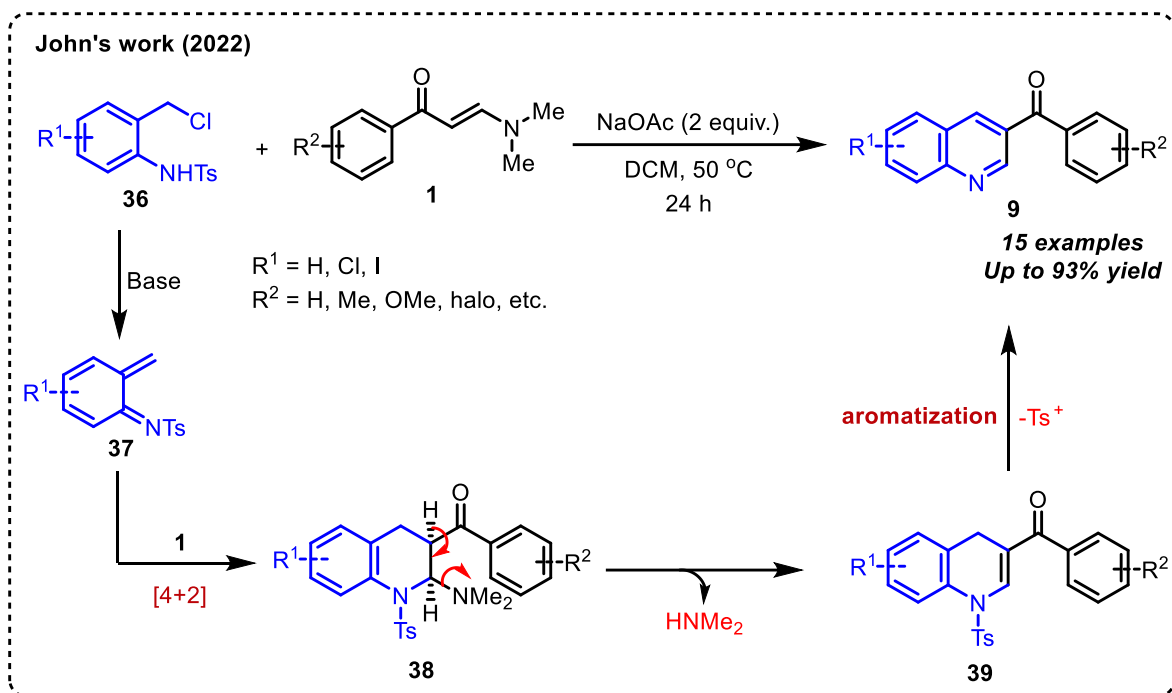
Yu and co-workers in 2022 developed an efficient B_2pin_2 (**27**) mediated radical cascade cyclization/aromatization reaction of enaminones (**1**) and pyridines (**26**) to synthesize various functionalized indolizine derivatives (**28**) in moderate to excellent yields. The control experiments indicated that the pyridine-boryl radical **29** formed in situ triggered the reaction to occur. According to the proposed mechanism 4-cyanopyridine-boryl radical **29** is generated from direct homolytic cleavage of B_2pin_2 **27** assisted by 4-cyanopyridine **26**. The intermediate **29** then couples with enaminone **1** to form intermediate **30**, which through a series of radical intermediate and aromatization generates the final indolizine product **28** (scheme 7).^[17]

In 2022 John and co-workers reported a Diels Alder cycloaddition route for the synthesis of 3-aryl quinolones (**9**) from enaminones (**1**) and *in situ*-generated aza-*o*-quinone methides



Scheme 7: Bin_2pin_2 -mediated synthesis of indolizines from *N,N*-dimethyl enaminones

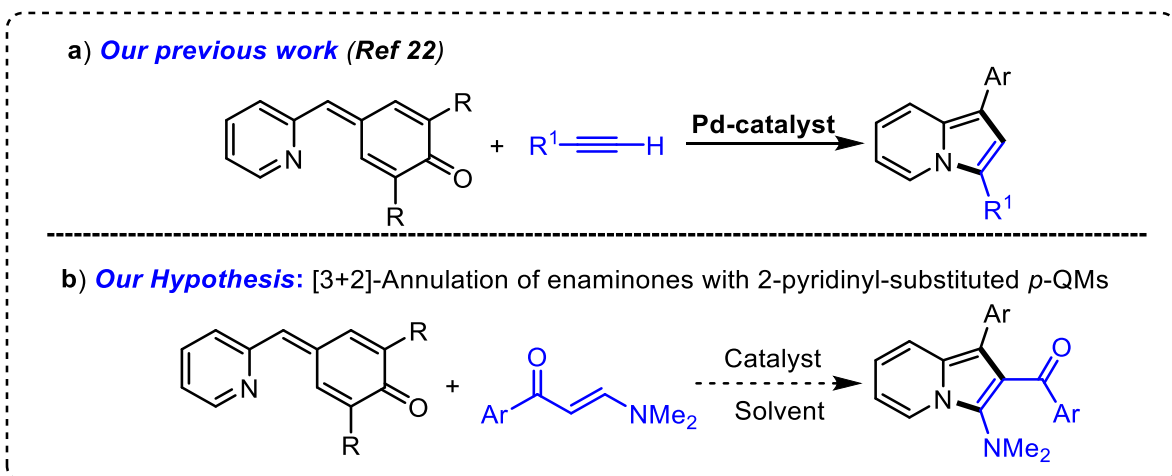
(37). A wide range of enaminone was utilized, affording the corresponding quinoline derivatives in good to excellent yields. According to the proposed reaction mechanism, this transformation proceeds through the base-mediated generation of aza-*o*-quinone methide **37** from *o*-aminobenzyl chloride **36**, which undergoes [4+2]-annulation with **1** to generate intermediate **38**. The elimination of HNMe_2 from intermediate **38** affords another intermediate **39**, which upon a base/oxidizing agent-mediated aromatization affords the final 3-aryl quinolones **9** (scheme 8).^[18]



Scheme 8: Synthesis of 3-aryl quinolone derivatives using *N,N*-dimethyl enaminones

3.3. Background:

In the past few years our research group is involved in the synthesis of *O*- and *N*-heterocycles using *p*-quinone methides (*p*-QMs) as synthons.^[19,20] We also utilized 2-enynyl pyridines to prepare various indolizine derivatives.^[21] In line with this, very recently, our research group developed a palladium-catalyzed [3+2]-annulation of terminal alkynes with 2-pyridinyl-substituted *p*-QMs to synthesize 1,3-disubstituted indolizine derivatives (**a**, Scheme 9).^[22] In fact, this was the first and only report available on the utilization of 2-pyridinyl-substituted *p*-QMs as synthons for fused *N*-heterocycles. Since our primary interest is inclined



Scheme 9: Our hypothesis

towards developing new protocols to access various *O*- and *N*-heterocycles from *p*-QMs, we hypothesized that it could be possible to access indolizine derivatives through [3+2] annulation of 2-pyridinyl substituted *p*-quinone methides and enaminones (**b**, Scheme 9).

3.4. Result and discussion:

Our initial investigations on the optimization began with a reaction between 2-pyridinyl-substituted *p*-QM **40a** and *N,N*-dimethyl enaminone **41a** as model substrates under different conditions, and the results are shown in (Table 1). The preliminary experiment was performed with Cu(OTf)₂ as a catalyst in MeCN at room temperature, but no product formation was seen as the starting materials remained as such even after 24 hours (entry 1). However, interestingly, when the temperature of the reaction was increased to 60 °C, almost complete conversion of **40a** was observed (TLC) in 6 h (entry 2). Since in most of the reported reactions of *N,N*-dimethyl enaminones,¹¹ the dimethyl amino group generally gets eliminated as dimethylamine in the last step under Lewis/Brønsted acidic conditions we expected the formation of **42a'**. However, to our surprise, the oxidized product **42a** was obtained in 88% isolated yield (entry 2). The structure of **42a** was confirmed from ¹H NMR, ¹³C NMR, IR spectroscopy and mass spectrometry. In ¹H NMR (see figure 2) the presence of singlet of (1H) at δ 4.93 ppm due to phenolic OH, singlet of (6H) at δ 2.85 ppm due to two methyl groups attached to nitrogen and the singlet of (18H) at δ 1.29 ppm due to two symmetric *tert*-butyl group protons supported the formation of product **42a**. In ¹³C NMR (see figure 3) disappearance of carbonyl peak from **40a**, and the aliphatic peak observed at δ 43.4 ppm for two methyl groups attached to nitrogen and two peaks at δ 34.3 ppm and 30.3 ppm for the two symmetric *tert*-butyl groups also supported the formation of **42a**. Further in IR peak observed at 3634 cm⁻¹ supported the formation of phenolic OH in product **42a**. Further the formation of **42a** was also confirmed by the HRMS (ESI): *m/z* calcd for C₃₁H₃₇N₂O₂ [M+H]⁺ : 469.2847. Since amino-substituted indolizines are also considered as privileged entries in medicinal chemistry,^{6,23} and not many general synthetic approaches are reported for their syntheses,²⁴ we decided to move forward with the optimization studies to further improve the yield of **42a**. When the reaction was conducted with Cu(OTf).PhMe as the catalyst, **42a** was formed in 67% after 6 hours (entry 3). The reaction also worked with CuI (entry 4) but the yield of **42a** was inferior when compared to Cu(OTf)₂. When CuBr₂ and Cu(OAc)₂ were used, the yield of **42a** were 35% and 65%, respectively (entries 5 & 6). Switching to Pd-based catalysts such as Pd(OAc)₂ and PdCl₂ did not improve the yield of **42a** (entries 7 & 8). Similarly, other Lewis acids such as Bi(OTf)₃ and Sc(OTf)₃

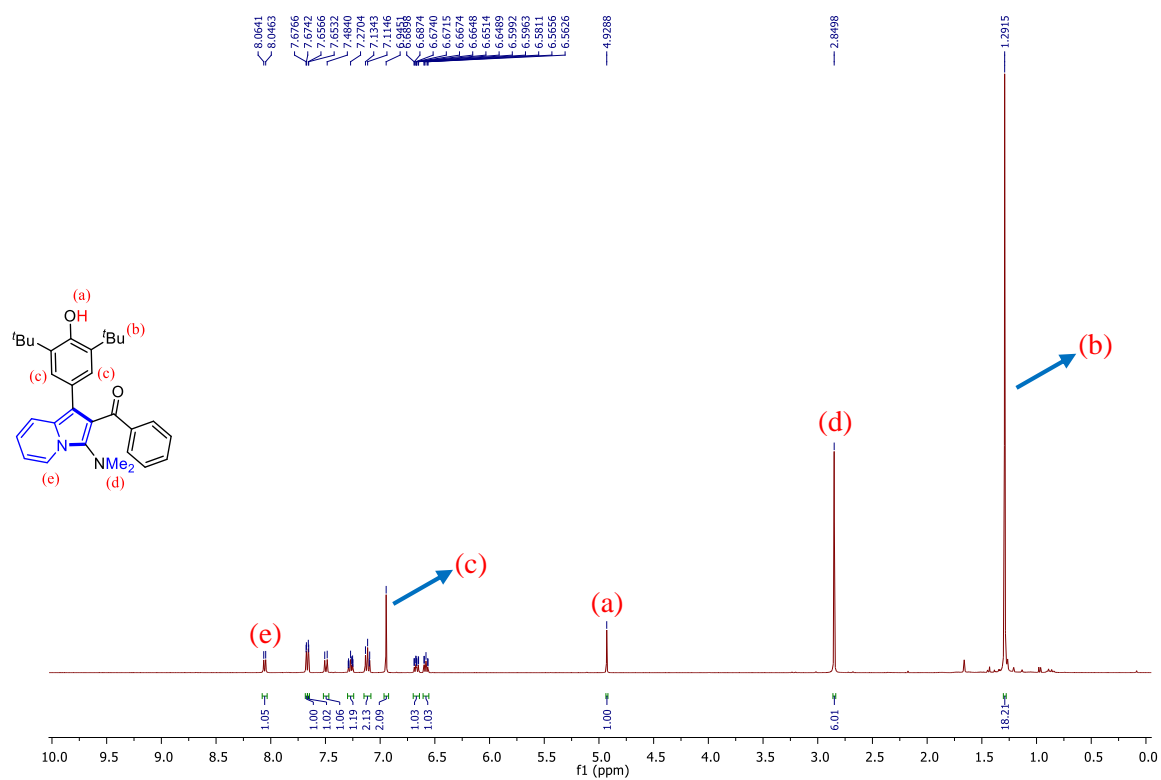


Figure 2: ¹H NMR (400 MHz, CDCl₃) spectrum of **42a**

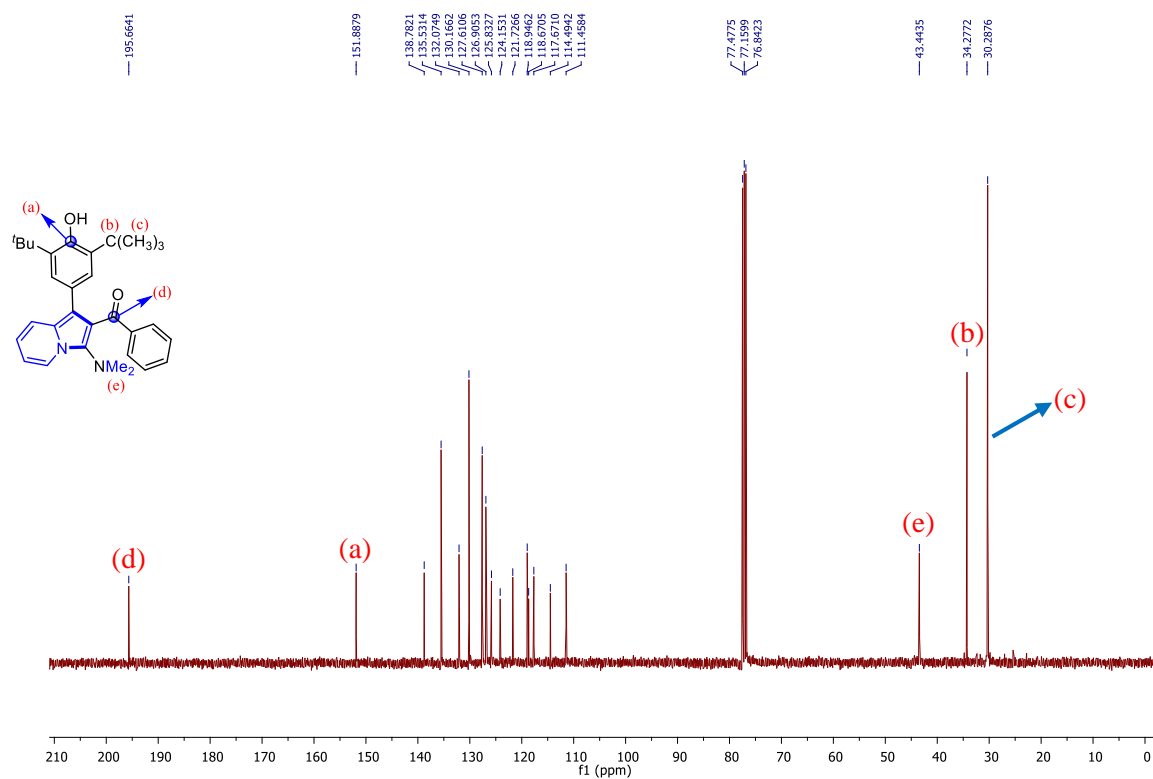
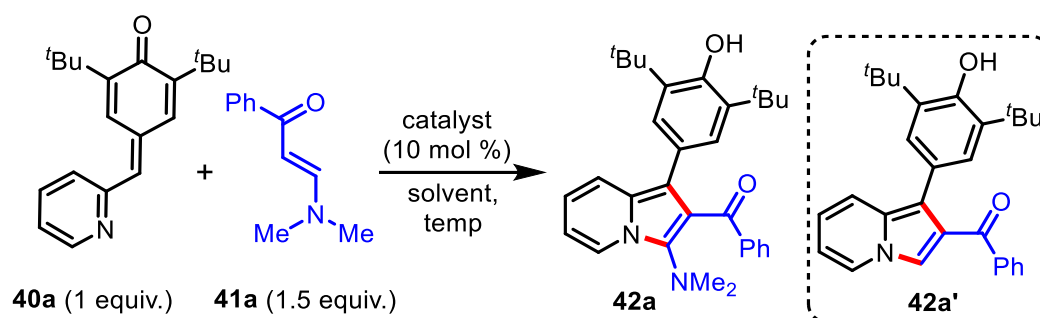


Figure 3: ¹³C{¹H} NMR (100 MHz, CDCl₃) spectrum of **42a**

Table 1. Optimization Study^a

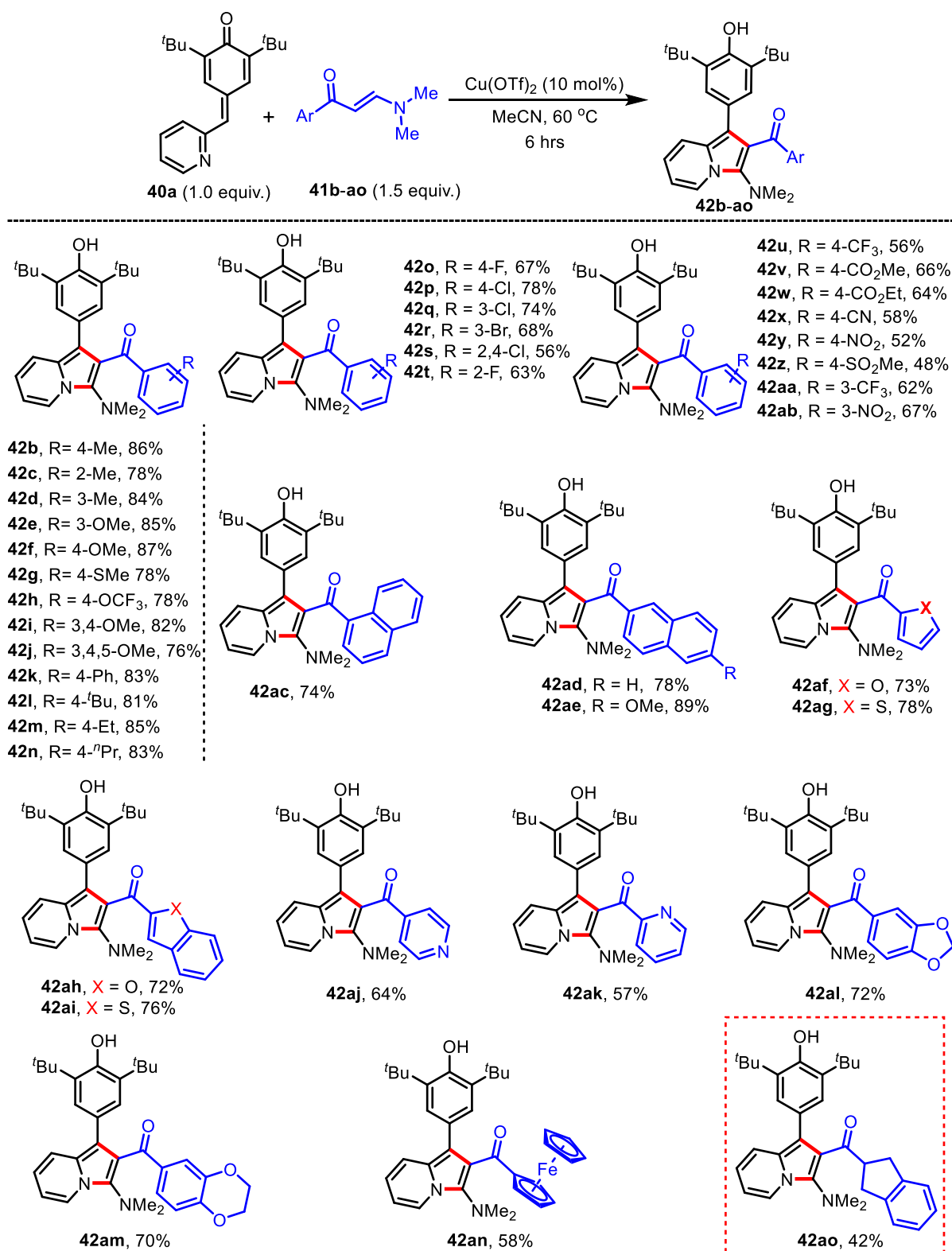
Entry	Catalyst	Solvent	Temp. [°C]	Time [h]	Yield of 42a ^b
1	Cu(OTf) ₂	MeCN	RT	24	ND
2	Cu(OTf)₂	MeCN	60	6	88
3	Cu(OTf) ₂ .PhMe	MeCN	60	6	67
4	CuI	MeCN	60	12	63
5	CuBr ₂	MeCN	60	12	35
6	Cu(OAc) ₂	MeCN	60	12	65
7	Pd(OAc) ₂	MeCN	60	12	42
8	PdCl ₂	MeCN	60	12	40
9	Bi(OTf) ₃	MeCN	60	12	52
10	Sc(OTf) ₃	MeCN	60	12	31
11	Cu(OTf) ₂	PhMe	60	12	42
12	Cu(OTf) ₂	THF	60	12	56
13	Cu(OTf) ₂	1,2-DCE	60	12	73
14	Cu(OTf) ₂	1,4-Dioxane	60	12	37
15	---	MeCN	60	24	ND
16 ^c	Cu(OTf) ₂	MeCN	60	6	67
17 ^d	TsOH	MeCN	60	24	ND
18 ^e	TsOH/Cu(OTf) ₂	MeCN	60	36	13

^aReaction conditions: Reactions were carried out with 0.10 mmol of **40a**, 1.5 equiv. of **41a** with respect to **40a** and 10 mol % catalyst. ^bYields reported are isolated yields. ^c2 equiv. of TEMPO was used, ^d2 equiv. of TsOH was used, ^e2 equiv. of TsOH and 10 mol% of Cu(OTf)₂ was used. 1,2-DCE = 1,2-Dichloroethane; ND. = Not detected).

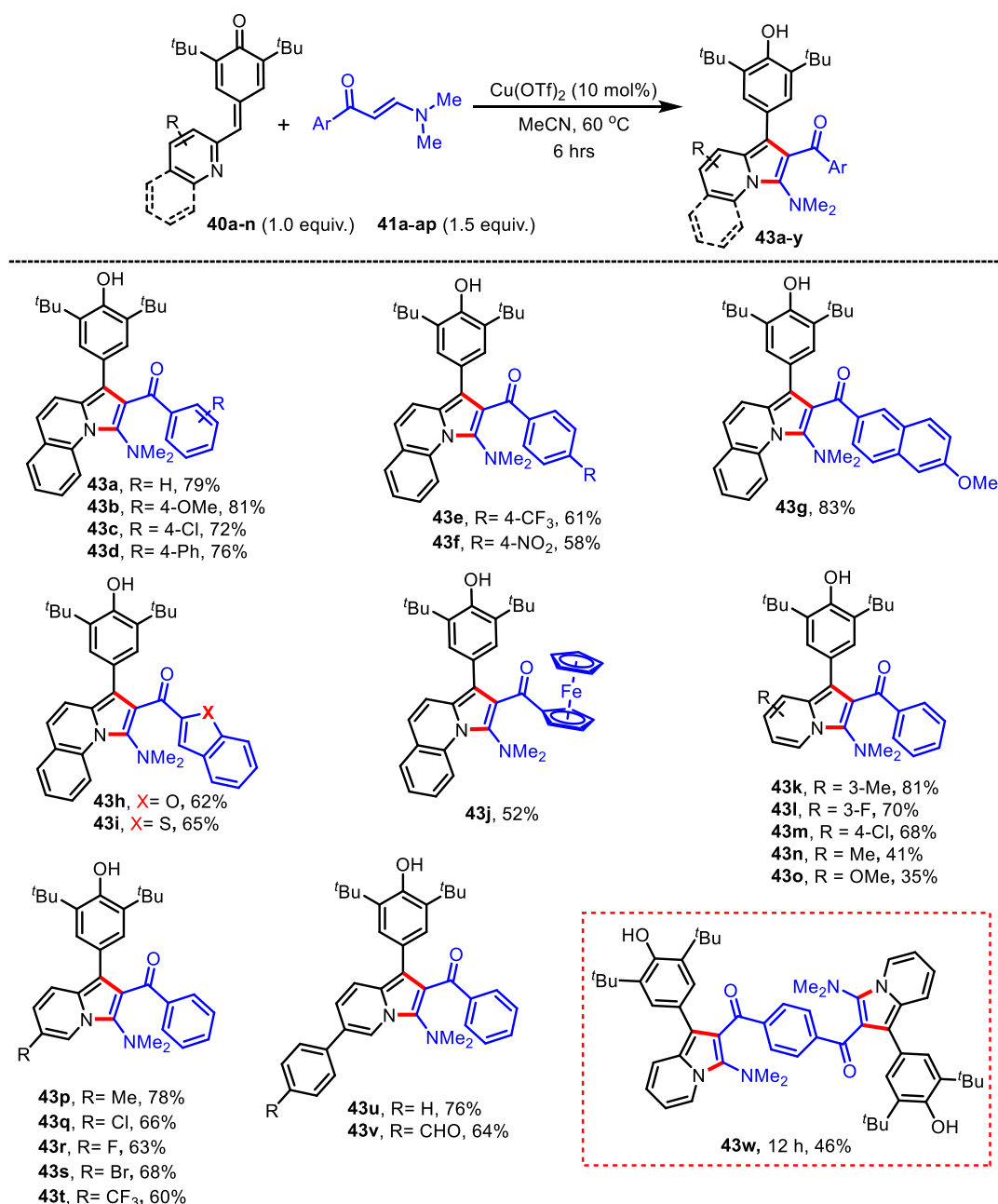
were found to be less effective for this transformation (entries 9 & 10). Since Cu(OTf)₂ was found to be the most effective catalyst in MeCN (entry 2), we thought of screening the effectiveness of Cu(OTf)₂ in other solvents (entries 11-14). However, although the reaction was taking place in all the other solvents screened, the yield of **42a** was found to be in the range of 37-73%. No product formation was seen in the absence of a catalyst, which shows that a catalyst is required to achieve this transformation (entry 15). The reaction did take place even in the presence of excess of TEMPO (entry 16), which indicates that the reaction does not

proceed through any radical intermediate(s). In our earlier work on the synthesis of chromene derivatives through TsOH mediated reactions between enaminones and 2-hydroxyphenyl-substituted *p*-QMs,²⁵ we noticed that TsOH was acting as a promoter for the dehydroamination in the last step. Therefore, we assumed that the use of stoichiometric amounts of TsOH would promote the formation of **42a'**. However, unfortunately, TsOH (2.0 equiv. with respect to **40a**) failed to produce **42a'** (entry 17). Another experiment was set up with a combination of 10 mol% of Cu(OTf)₂ and 2.0 equiv. of TsOH and, in that case, the formation of **42a'** was not observed at all; in fact, in this reaction only 13% of **42a** was obtained (entry 18). Most likely, in those two cases, TsOH interacts with pyridine nitrogen of **40a** and probably deactivates it by making the C-6 position relatively less electrophilic.

With the optimized reaction conditions in hand, we then turned our attention towards examining the substrate scope with different substituted enaminones. The reactions proceeded efficiently under the optimal reaction conditions, furnishing the desired products in moderate to good yields, and the results are summarized in (Table 2). For different substituted (electron donating) enaminone moiety in substrates **41b–41n**, the desired products **42b–42n** was obtained in 76–87% yields. Introducing a halogen substituent on the enaminone moiety afforded the desired products **42o–42t** in 56–78% yields. However, when electron-withdrawing substituents like (–CF₃, –CO₂Me, –CN, –NO₂, etc.) were introduced on the enaminone moiety, the products **42u–42ab** were obtained in the range of 48–67%. The lower yields in those cases are presumably due the presence of electron-withdrawing substituent on the enaminone reduces its nucleophilicity to attack the *p*-quinone methide. The reaction also worked well with enaminones having bulky aromatic substituents, and the desired products **42ac–42ae** were obtained in 74–89% yields. In the case of the enaminones with heteroaromatic substituents, the products **42af–42am** were obtained in the range of 57–78% yields. The reaction also worked with enaminone having a ferrocene and indane substituent, and in those cases, the products **42an** and **42ao** were isolated in 58% and 42% yield, respectively. *p*-QM (**40b**) derived from quinoline-2-carboxaldehyde also reacted well with **41a** to give the product **43a** in 79% yields. Different substituted (halo, EWG, EDG, heteroaromatic, etc.) enaminones also reacted smoothly with **40b**, and the corresponding products **43b–43j** were isolated in the range of 52–83% yields as summarized in (Table 3). *p*-QMs (**40c–e**) derived from 3- & 4-substituted 2-pyridine carboxaldehyde also reacted well with **41a** to give the respective products **43k–43m** in good yields. *p*-QMs (**40f–g**) having a substituent at the sixth position of pyridine furnished the products in poor yields, and the respective products **43n–43o** were obtained in the range of

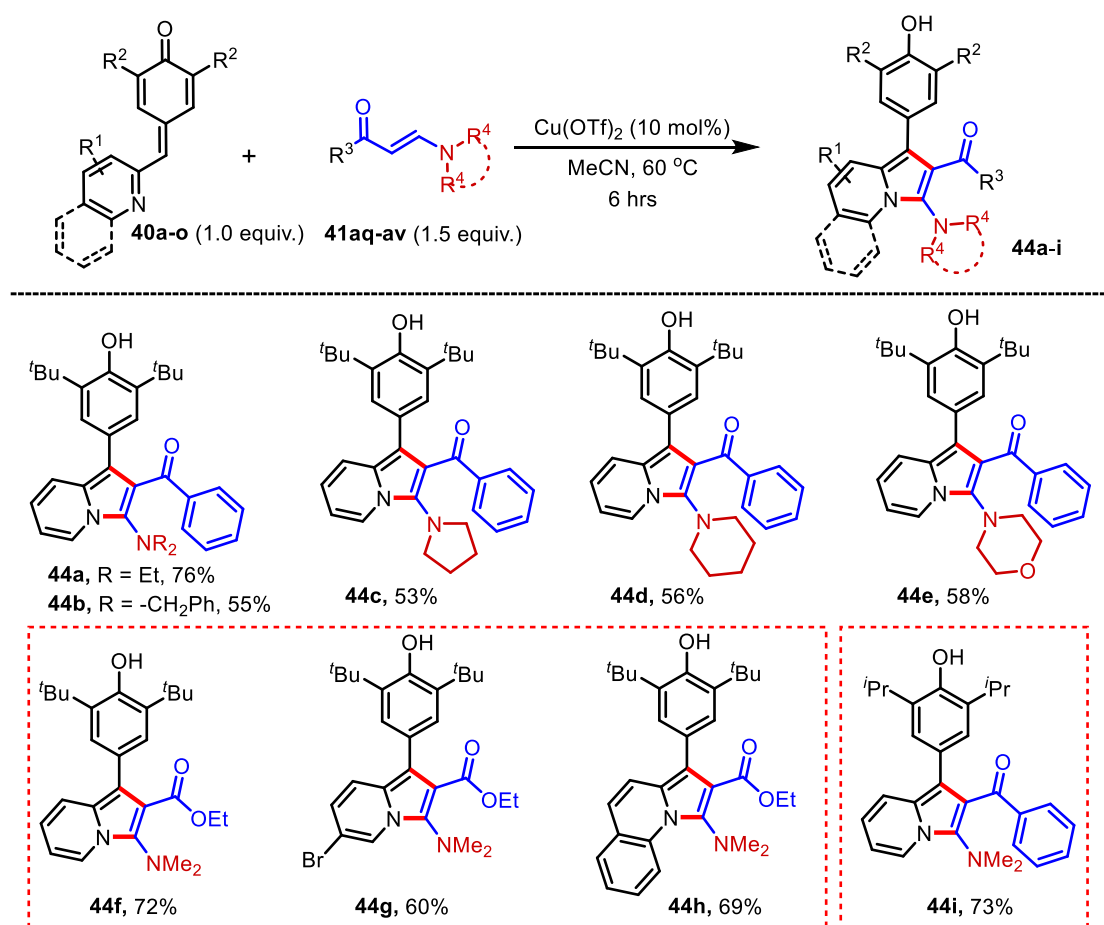
Table 2. Substrate Scope^b

^aReactions were carried out with 30 mg of **40a** and 1.5 equiv. of **41b-ao** in 1.5 mL of MeCN. ^bYields reported are isolated yields.

Table 3. Substrate Scope^b

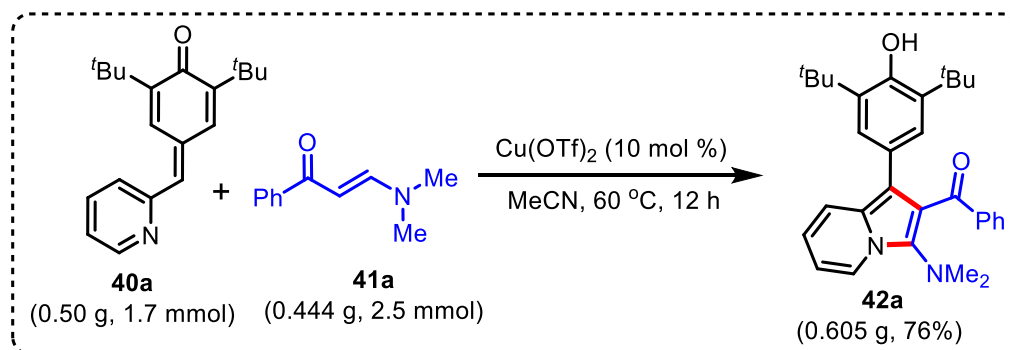
^aReactions were carried out with 30 mg of **40a-l** and 1.5 equiv. of enaminones in 1.5 mL of MeCN. ^bYields reported are isolated yields.

35–41% yields. *p*-QMs (**40h-n**) derived from 5-substituted 2-pyridine carboxaldehyde also reacted well with **41a** to give the respective products **43p-43v** in 60–78% yields. Later a reaction of the *p*-QM **40a** with 1,4-dienaminone **41ap** in the ratio (2.2:1 equiv.) was performed under the standard optimized reaction conditions, and the desired product **43w** was isolated in 46% yield after 12 hours. Enaminones substituted with different amine groups (such as diethylamine, dibenzylamine, pyrrole, pyridine and morpholine) based enaminone also reacted

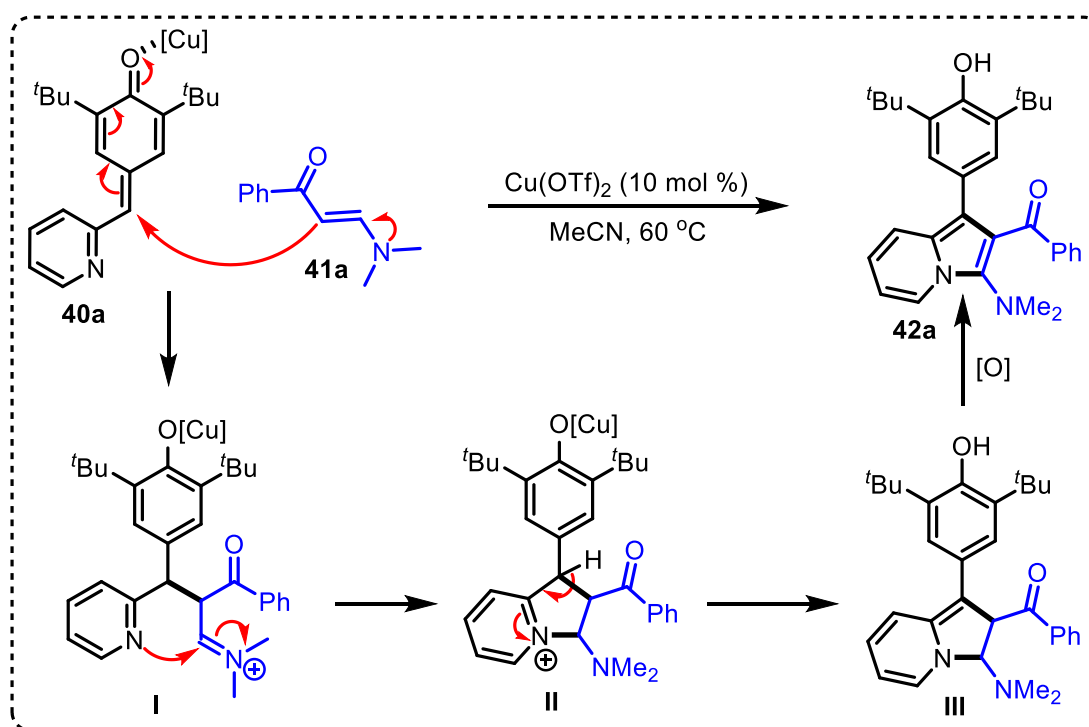
Table 4. Substrate Scope^b

^aReactions were carried out with 30 mg of **40a-o** and 1.5 equiv. of enaminones in 1.5 mL of MeCN. ^bYields reported are isolated yields.

smoothly with **40a** and the corresponding products **44a-44e** were isolated in 53–76% yields (Table 4). Enaminone **41av**, substituted with an ester group, also reacted well with different *p*-QMs and provided the respective products **44f-44h** in 60–72% yields. The *p*-QMs **40m**, substituted with *iso*-propyl groups (in place of tert-butyl groups) also reacted smoothly with **41a** to afford the corresponding product **44i** in 73% isolated yield.

**Scheme 10:** Gram Scale Reaction of **40a**

To show the practical applicability of this transformation, a relatively large-scale reaction of **40a** with **41a** was performed under the optimized reaction conditions, and the desired product was obtained in 76% yield after 12 hours (Scheme 10).

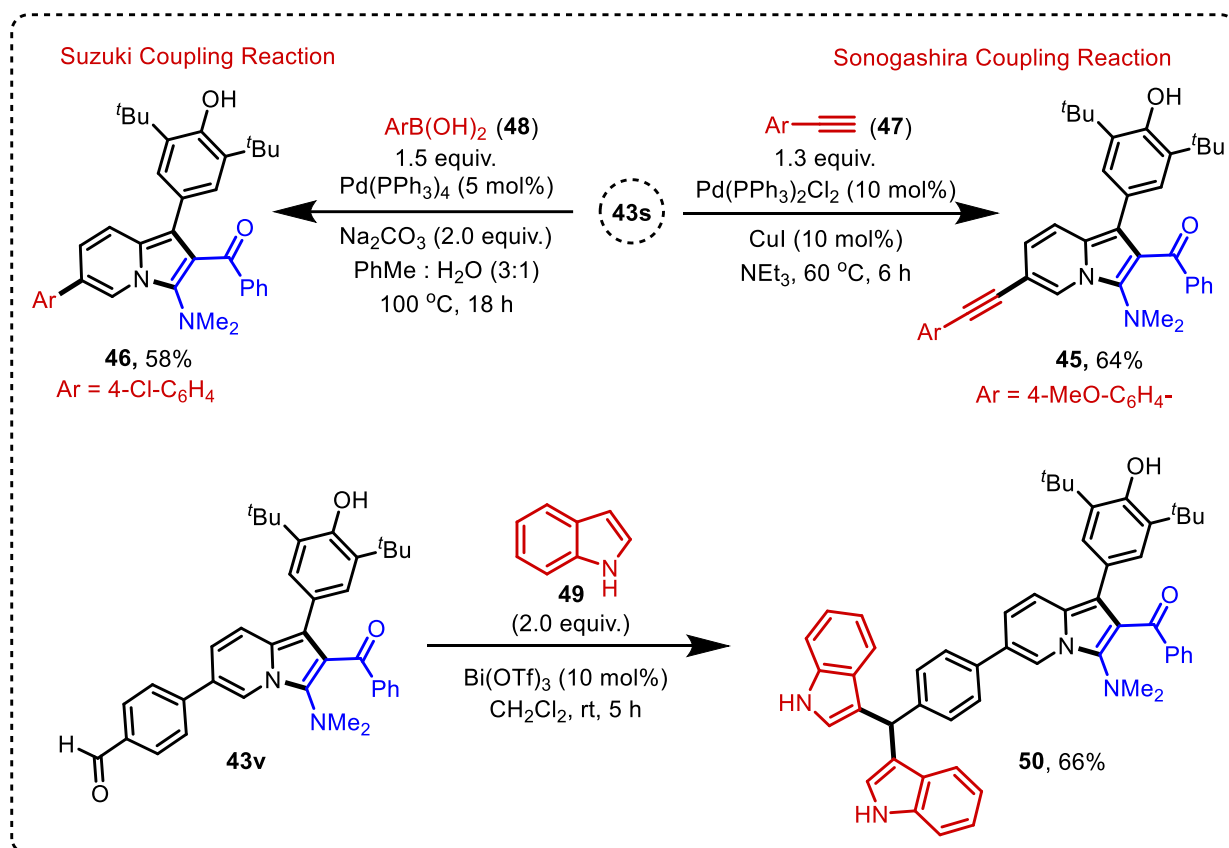


Scheme 11: Plausible Mechanism

Based on the outcome of the reaction, a plausible mechanism for this catalytic transformation was proposed in (Scheme 11). The catalytic cycle starts with activation of the carbonyl group of **40a** by the copper catalyst and making **40a** more susceptible for nucleophilic attack. Subsequently, the intermolecular 1,6-conjugate addition of **41a** takes place to generate an intermediate **I**, which then undergoes an intramolecular 5-*exo*-trig cyclization to generate another intermediate **II**. This intermediate **II**, upon deprotonation followed by protonation of Cu(II)-phenolate complex provides the dihydro-indolizine intermediate **III**, which readily gets oxidized in air to form the final product **42a**.

Furthermore, to show the synthetic utility of this transformation, one of the indolizine derivatives **43s** was subjected to react with 4-methoxy phenylacetylene under Sonogashira cross coupling reaction conditions to give the alkynylated indolizine **45** in 64% yield. In another experiment **43s** was treated with 4-chloro phenyl boronic acid under Suzuki cross coupling reaction conditions to afford the arylated indolizine **46** in 58% yield (Scheme 12). Since diindolylmethane derivatives are known to possess various biological properties,²⁶ we

thought of elaborating one of the indolizine product **43v** to the respective diindolylmethane analogue **50** by treating **43v** with 2 equivalents of indole in the presence of 10 mol% of Bi(OTf)₃. In that case, the indolizine based unsymmetrical triarylmethane derivative **50** was obtained in 66% yield (Scheme 12).



Scheme 12: Synthetic Elaborations

3.5. Conclusion:

In conclusion, we have developed an efficient method for the synthesis of various 2-acyl-3-amino-substituted indolizine derivatives through a copper(II) catalyzed [3+2]-annulation of enaminones with 2-pyridinyl substituted *p*-quinone methide. The generality of this transformation was examined using a wide range of enaminones and 2-pyridyl-substituted *p*-quinone methide. This general methodology displayed an excellent functional group tolerance in terms of substrate scope, providing the corresponding indolizine products in moderate to good yields. Since indolizines are considered as an important class of heterocycles from medicinal chemistry to materials science, we believe this methodology would find some applications in near future.

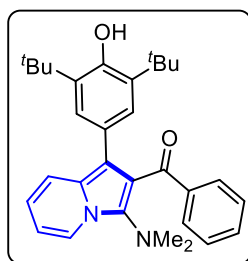
3.6. Experimental section:

General information. All reactions were carried out in an oven dried round bottom flask. All the solvents were distilled before use and stored under argon atmosphere. Most of the reagents, starting materials were purchased from commercial sources and used as such. Melting points were recorded on SMP20 melting point apparatus and are uncorrected. ^1H , ^{13}C and ^{19}F spectra were recorded in CDCl_3 (400, 100 and 376 MHz respectively) on Bruker FT-NMR spectrometer. Chemical shift (δ) values are reported in parts per million relative to TMS and the coupling constants (J) are reported in Hz. High resolution mass spectra were recorded on Waters Q-TOF Premier-HAB213 spectrometer. FT-IR spectra were recorded on a Perkin-Elmer FTIR spectrometer. Thin layer chromatography was performed on Merck silica gel 60 F₂₅₄ TLC pellets and visualised by UV irradiation and KMnO_4 stain. Column chromatography was carried out through silica gel (100–200 mesh) using EtOAc/hexane as an eluent.

General procedure for the reaction between enaminones and 2-pyridinyl-substituted p-quinone methides:

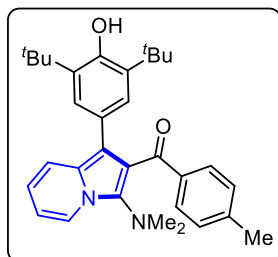
Anhydrous MeCN (1.5 mL) was added to the mixture of *p*-quinone methide [*p*-QM] (30 mg, 1.0 equiv.), enaminone (1.5 equiv.) and $\text{Cu}(\text{OTf})_2$ (10 mol %) and the resulting suspension was stirred at 60 °C until the *p*-QM was completely consumed (based on TLC analysis). The reaction mixture was concentrated under reduced pressure and the residue was purified through silica gel chromatography, using EtOAc/Hexane mixture as an eluent, to get the pure indolizine derivatives.

{1-[3,5-di-tert-butyl-4-hydroxyphenyl]-3-(dimethylamino)-indolizin-2-yl}(phenyl)-methanone (42a)



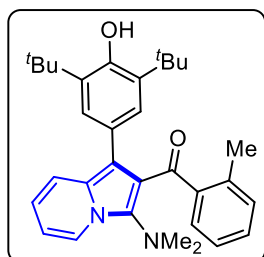
The reaction was performed at 0.102 mmol scale of **40a**; $R_f = 0.4$ (5% EtOAc in hexane); brown solid (42.2 mg, 88% yield); m. p. = 132–134 °C; ^1H NMR (400 MHz, CDCl_3) δ 8.06 (d, $J = 7.1$ Hz, 1H), 7.68 – 7.65 (m, 2H), 7.50 (d, $J = 9.0$ Hz, 1H), 7.29 – 7.25 (m, 1H), 7.13 – 7.10 (m, 2H), 6.95 (s, 2H), 6.69 – 6.65 (m, 1H), 6.60 – 6.56 (m, 1H), 4.93 (s, 1H), 2.85 (s, 6H), 1.29 (s, 18H); $^{13}\text{C}\{^1\text{H}\}$ NMR (100 MHz, CDCl_3) δ 195.7, 151.9, 138.8, 135.5, 132.1, 130.2 (2C), 127.6, 126.9, 125.8, 124.2, 121.7, 118.9, 118.7, 117.7, 114.5, 111.5, 43.4, 34.3, 30.3; FT-IR (thin film, neat): 3634, 2956, 1646, 1578, 1450, 1358, 1234, 1118, 733 cm^{-1} ; HRMS (ESI): m/z calcd for $\text{C}_{31}\text{H}_{37}\text{N}_2\text{O}_2$ $[\text{M}+\text{H}]^+$: 469.2855; found : 469.2847.

{1-[3,5-di-tert-butyl-4-hydroxyphenyl]-3-(dimethylamino)-indolizin-2-yl}(p-tolyl)-methanone (42b)



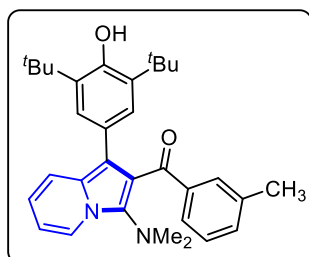
The reaction was performed at 0.102 mmol scale of **40a**; $R_f = 0.4$ (5% EtOAc in hexane); brown solid (42.4 mg, 86% yield); m. p. = 162–164 °C; ^1H NMR (400 MHz, CDCl_3) δ 8.04 (d, $J = 7.2$ Hz, 1H), 7.57 (d, $J = 8.2$ Hz, 2H), 7.49 (d, $J = 9.0$ Hz, 1H), 6.95 (s, 2H), 6.92 (d, $J = 8.0$ Hz, 2H), 6.68 – 6.64 (m, 1H), 6.59 – 6.55 (m, 1H), 4.94 (s, 1H), 2.84 (s, 6H), 2.24 (s, 3H), 1.30 (s, 18H); $^{13}\text{C}\{^1\text{H}\}$ NMR (100 MHz, CDCl_3) δ 195.4, 151.9, 142.7, 136.3, 135.5, 135.2, 130.4, 128.3, 126.9, 125.9, 124.1, 121.7, 118.92, 118.90, 117.6, 114.4, 111.3, 43.5, 34.3, 30.3, 21.6; FT-IR (thin film, neat): 3635, 2954, 1733, 1647, 1286, 1152, 758 cm^{-1} ; HRMS (ESI): m/z calcd for $\text{C}_{32}\text{H}_{39}\text{N}_2\text{O}_2$ $[\text{M}+\text{H}]^+$: 483.3012; found : 483.3013.

{1-[3,5-di-tert-butyl-4-hydroxyphenyl]-3-(dimethylamino)-indolizin-2-yl}-(o-tolyl)-methanone (42c)



The reaction was performed at 0.102 mmol scale of **40a**; $R_f = 0.4$ (5% EtOAc in hexane); brown gummy solid (38.4 mg, 78% yield); ^1H NMR (400 MHz, CDCl_3) δ 8.06 (d, $J = 6.8$ Hz, 1H), 7.32 – 7.26 (m, 2H), 7.06 (td, $J = 7.5, 1.2$ Hz, 1H), 6.96 – 6.94 (m, 1H), 6.84 – 6.81 (m, 3H), 6.63 – 6.55 (m, 2H), 4.93 (s, 1H), 2.89 (s, 6H), 2.46 (s, 3H), 1.32 (s, 18H); $^{13}\text{C}\{^1\text{H}\}$ NMR (100 MHz, CDCl_3) δ 197.0, 152.0, 139.2, 137.8, 135.5, 135.0, 131.8, 130.8, 130.5, 127.1, 125.6, 124.9, 124.8, 121.7, 120.5, 119.1, 117.5, 115.1, 111.6, 43.0, 34.2, 30.3, 21.5; FT-IR (thin film, neat): 3634, 2955, 1734, 1640, 1250, 1198, 743 cm^{-1} ; HRMS (ESI): m/z calcd for $\text{C}_{32}\text{H}_{39}\text{N}_2\text{O}_2$ $[\text{M}+\text{H}]^+$: 483.3012; found : 483.3015.

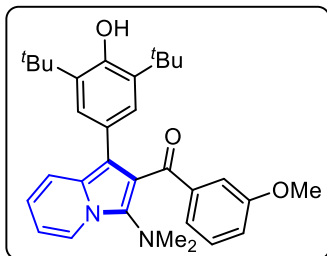
{1-[3,5-di-tert-butyl-4-hydroxyphenyl]-3-(dimethylamino)-indolizin-2-yl}-(m-tolyl)-methanone (42d)



The reaction was performed at 0.102 mmol scale of **40a**; $R_f = 0.4$ (5% EtOAc in hexane); brown gummy solid (41.4 mg, 84% yield); ^1H NMR (400 MHz, CDCl_3) δ 8.06 (d, $J = 7.2$ Hz, 1H), 7.53 – 7.48 (m, 2H), 7.42 (s, 1H), 7.09 – 7.01 (m, 2H), 6.93 (s, 2H), 6.69 – 6.65 (m, 1H), 6.60 – 6.56 (m, 1H), 4.92 (s, 1H), 2.85 (s, 6H), 2.14 (s, 3H), 1.29 (s, 18H); $^{13}\text{C}\{^1\text{H}\}$ NMR (100 MHz, CDCl_3) δ 195.7, 151.8, 138.7, 137.1, 135.7, 135.5, 132.8, 131.3, 127.6, 127.1, 126.8, 126.0, 124.1, 121.8, 119.0, 118.7, 117.7, 114.6, 111.5, 43.4,

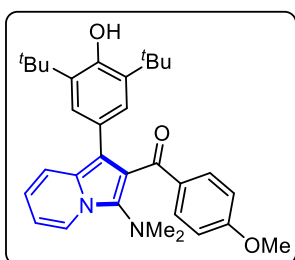
34.3, 30.3, 21.2; FT-IR (thin film, neat): 3629, 2952, 1736, 1635, 1245, 1118, 733 cm^{-1} ; HRMS (ESI): m/z calcd for $\text{C}_{32}\text{H}_{39}\text{N}_2\text{O}_2$ $[\text{M}+\text{H}]^+$: 483.3012; found : 483.3021.

{1-[3,5-di-tert-butyl-4-hydroxyphenyl]-3-(dimethylamino)-indolizin-2-yl}-(3-methoxyphenyl)-methanone (42e)



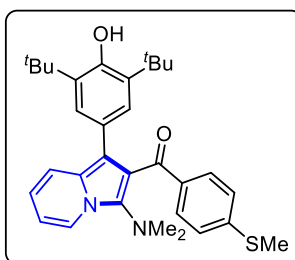
The reaction was performed at 0.102 mmol scale of **40a**; $R_f = 0.3$ (5% EtOAc in hexane); brown solid (43.3 mg, 85% yield); m. p. = 118–120 $^{\circ}\text{C}$; ^1H NMR (400 MHz, CDCl_3) δ 8.06 (d, $J = 7.0$ Hz, 1H), 7.5 (d, $J = 9.0$ Hz, 1H), 7.31 – 7.29 (m, 1H), 7.20 – 7.19 (m, 1H), 7.04 (t, $J = 7.9$ Hz, 1H), 6.96 (s, 2H), 6.85 – 6.82 (m, 1H), 6.69 – 6.66 (m, 1H), 6.60 – 6.57 (m, 1H), 4.96 (s, 1H), 3.67 (s, 3H), 2.86 (s, 6H), 1.31 (s, 18H); $^{13}\text{C}\{^1\text{H}\}$ NMR (100 MHz, CDCl_3) δ 195.3, 159.0, 151.9, 140.1, 135.8, 135.5, 128.7, 126.8, 125.9, 124.1, 123.0, 121.7, 119.0, 118.9, 118.6, 117.7, 114.5, 114.1, 111.5, 55.3, 43.4, 34.3, 30.2; FT-IR (thin film, neat): 3635, 2955, 2872, 2230, 1647, 1448, 1238, 855, 741 cm^{-1} ; HRMS (ESI): m/z calcd for $\text{C}_{32}\text{H}_{39}\text{N}_2\text{O}_3$ $[\text{M}+\text{H}]^+$: 499.2961; found : 499.2956.

{1-[3,5-di-tert-butyl-4-hydroxyphenyl]-3-(dimethylamino)-indolizin-2-yl}(4-methoxyphenyl)-methanone (42f)



The reaction was performed at 0.102 mmol scale of **40a**; $R_f = 0.3$ (5% EtOAc in hexane); brown solid (44.3 mg, 87% yield); m. p. = 136–138 $^{\circ}\text{C}$; ^1H NMR (400 MHz, CDCl_3) δ 8.05 – 8.03 (m, 1H), 7.69 – 7.65 (m, 2H), 7.52 – 7.49 (m, 1H), 6.97 (s, 2H), 6.68 – 6.64 (m, 1H), 6.63 – 6.60 (m, 2H), 6.59 – 6.55 (m, 1H), 4.96 (s, 1H), 3.72 (s, 3H), 2.84 (s, 6H), 1.31 (s, 18H); $^{13}\text{C}\{^1\text{H}\}$ NMR (100 MHz, CDCl_3) δ 194.3, 162.9, 151.8, 135.6, 135.1, 132.5, 131.8, 126.8, 126.0, 124.1, 121.7, 118.9, 118.8, 117.5, 114.2, 112.9, 111.3, 55.4, 43.5, 34.3, 30.3; FT-IR (thin film, neat): 3634, 3381, 2955, 1734, 1599, 1450, 1357, 1250, 1108, 1031, 701, 606 cm^{-1} ; HRMS (ESI): m/z calcd for $\text{C}_{32}\text{H}_{39}\text{N}_2\text{O}_3$ $[\text{M}+\text{H}]^+$: 499.2961; found : 499.2952.

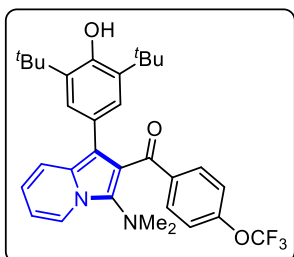
{1-[3,5-di-tert-butyl-4-hydroxyphenyl]-3-(dimethylamino)-indolizin-2-yl}-[4-(methylthio)phenyl]-methanone (42g)



The reaction was performed at 0.102 mmol scale of **40a**; $R_f = 0.4$ (5% EtOAc in hexane); brown solid (41.1 mg, 78% yield); m. p. = 138–140 $^{\circ}\text{C}$; ^1H NMR (400 MHz, CDCl_3) δ 8.05 (d, $J = 7.1$ Hz, 1H), 7.60 – 7.57 (m, 2H), 7.50 (d, $J = 9.0$ Hz, 1H), 6.95 – 6.93 (m, 4H), 6.69 – 6.65 (m, 1H), 6.59 – 6.56 (m, 1H), 4.97 (s, 1H), 2.85 (s, 6H), 2.38 (s,

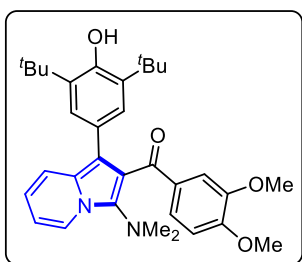
3H), 1.31 (s, 18H); $^{13}\text{C}\{^1\text{H}\}$ NMR (100 MHz, CDCl_3) δ 194.5, 151.9, 144.5, 135.6, 135.4, 135.2, 130.6, 126.9, 125.9, 124.4, 124.1, 121.7, 118.9, 118.6, 117.7, 114.3, 111.4, 43.4, 34.3, 30.3, 15.0; FT-IR (thin film, neat): 3632, 2958, 1736, 1640, 1284, 847, 743 cm^{-1} ; HRMS (ESI): m/z calcd for $\text{C}_{32}\text{H}_{39}\text{N}_2\text{O}_2\text{S}$ $[\text{M}+\text{H}]^+$: 515.2732; found : 515.2746.

{1-[3,5-di-tert-butyl-4-hydroxyphenyl]-3-(dimethylamino)-indolizin-2-yl}-[4-(trifluoromethoxy)-phenyl]-methanone (42h)



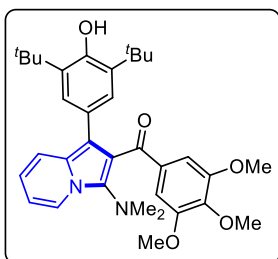
The reaction was performed at 0.102 mmol scale of **40a**; R_f = 0.3 (5% EtOAc in hexane); brown solid (44.2 mg, 78% yield); m. p. = 144–146 °C; ^1H NMR (400 MHz, CDCl_3) δ 8.07 (d, J = 7.1 Hz, 1H), 7.71 – 7.67 (m, 2H), 7.49 (d, J = 9.0 Hz, 1H), 6.93 – 6.92 (m, 4H), 6.70 – 6.67 (m, 1H), 6.61 – 6.58 (m, 1H), 4.97 (s, 1H), 2.87 (s, 6H), 1.30 (s, 18H); $^{13}\text{C}\{^1\text{H}\}$ NMR (100 MHz, CDCl_3) δ 193.7, 152.1, 151.7 (q, $J_{\text{C-F}}$ = 1.7 Hz), 137.2, 136.0, 135.8, 131.9, 127.0, 125.7, 124.3, 121.8, 120.3 (q, $J_{\text{C-F}}$ = 256.7 Hz), 119.6, 119.0, 118.1, 118.0, 114.5, 111.7, 43.4, 34.3, 30.2; $^{19}\text{F}\{^1\text{H}\}$ NMR (376 MHz, CDCl_3) δ –57.65; FT-IR (thin film, neat): 3632, 2965, 1648, 1421, 1046, 893, 734 cm^{-1} ; HRMS (ESI): m/z calcd for $\text{C}_{32}\text{H}_{36}\text{F}_3\text{N}_2\text{O}_3$ $[\text{M}+\text{H}]^+$: 553.2678; found : 553.2686.

{1-[3,5-di-tert-butyl-4-hydroxyphenyl]-3-(dimethylamino)-indolizin-2-yl}-(3,4-dimethoxyphenyl)-methanone (42i)



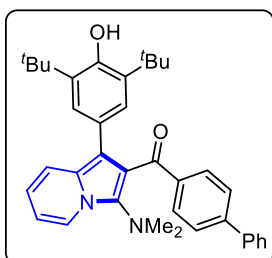
The reaction was performed at 0.102 mmol scale of **40a**; R_f = 0.3 (10% EtOAc in hexane); green solid (44.3 mg, 82% yield); m. p. = 114–116 °C; ^1H NMR (400 MHz, CDCl_3) δ 8.04 (d, J = 7.1 Hz, 1H), 7.54 – 7.51 (m, 1H), 7.34 – 7.30 (m, 2H), 6.98 (s, 2H), 6.69 – 6.65 (m, 1H), 6.59 – 6.55 (m, 2H), 4.96 (s, 1H), 3.80 (s, 3H), 3.74 (s, 3H), 2.84 (s, 6H) 1.30 (s, 18H); $^{13}\text{C}\{^1\text{H}\}$ NMR (100 MHz, CDCl_3) δ 194.2, 152.5, 151.8, 148.2, 135.6, 135.4, 131.7, 126.7, 126.0, 125.3, 124.0, 121.7, 118.9, 118.6, 117.6, 114.1, 112.1, 111.3, 109.6, 56.0, 55.9, 43.4, 34.3, 30.3; FT-IR (thin film, neat): 3625, 2957, 1735, 1640, 1612, 1450, 1251, 752, 643 cm^{-1} ; HRMS (ESI): m/z calcd for $\text{C}_{33}\text{H}_{41}\text{N}_2\text{O}_4$ $[\text{M}+\text{H}]^+$: 529.3066; found : 529.3053.

{1-[3,5-di-tert-butyl-4-hydroxyphenyl]-3-(dimethylamino)-indolizin-2-yl}-(3,4,5-trimethoxyphenyl)-methanone (42j)



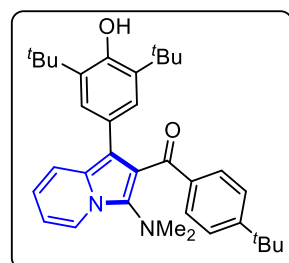
The reaction was performed at 0.102 mmol scale of **40a**; $R_f = 0.2$ (10% EtOAc in hexane); brown solid (43.3 mg, 76% yield); m. p. = 140–142 °C; ^1H NMR (400 MHz, CDCl_3) δ 8.07 (d, $J = 7.1$ Hz, 1H), 7.52 (d, $J = 9.0$ Hz, 1H), 6.97 (s, 2H), 6.94 (s, 2H), 6.70 – 6.66 (m, 1H), 6.60 (t, $J = 6.8$ Hz, 1H), 4.96 (s, 1H), 3.73 (s, 3H), 3.70 (s, 6H), 2.87 (s, 6H), 1.30 (s, 18H); $^{13}\text{C}\{^1\text{H}\}$ NMR (100 MHz, CDCl_3) δ 194.2, 152.4, 151.8, 141.5, 136.3, 135.6, 133.9, 126.7, 126.0, 124.1, 121.8, 119.0, 118.2, 117.8, 114.3, 111.6, 107.5, 60.8, 56.1, 43.4, 34.3, 30.3; FT-IR (thin film, neat): 3630, 3418, 2952, 1758, 1732, 1612, 1573, 1436, 1253, 1031, 742 cm^{-1} ; HRMS (ESI): m/z calcd for $\text{C}_{34}\text{H}_{43}\text{N}_2\text{O}_5$ $[\text{M}+\text{H}]^+$: 559.3172; found: 559.3163.

[1,1'-biphenyl]-4-yl(1-(3,5-di-tert-butyl-4-hydroxyphenyl)-3-(dimethylamino)indolizin-2-yl)methanone (42k)



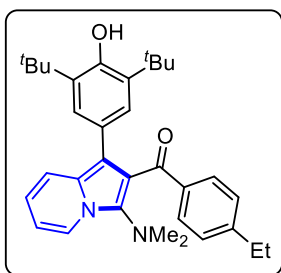
The reaction was performed at 0.102 mmol scale of **40a**; $R_f = 0.4$ (5% EtOAc in hexane); light brown solid (46.2 mg, 83% yield); m. p. = 184–186 °C; ^1H NMR (400 MHz, CDCl_3) δ 8.08 (d, $J = 7.1$ Hz, 1H), 7.56 – 7.34 (m, 2H), 7.53 (d, $J = 9.0$ Hz, 1H), 7.47 – 7.45 (m, 2H), 7.43 – 7.39 (m, 2H), 7.37 – 7.32 (m, 3H), 7.00 (s, 2H), 6.71 – 6.67 (m, 1H), 6.62 – 6.58 (m, 1H), 4.93 (s, 1H), 2.89 (s, 6H), 1.30 (s, 18H); $^{13}\text{C}\{^1\text{H}\}$ NMR (100 MHz, CDCl_3) δ 195.0, 152.0, 144.9, 140.5, 137.5, 135.64, 135.61, 130.8, 128.9, 127.9, 127.3, 127.0, 126.4, 125.9, 124.2, 121.7, 119.0, 118.7, 117.2, 114.5, 111.5, 43.4, 34.3, 30.3; FT-IR (thin film, neat): 3632, 3408, 2954, 1733, 1645, 1232, 1154, 758 cm^{-1} ; HRMS (ESI): m/z calcd for $\text{C}_{37}\text{H}_{41}\text{N}_2\text{O}_2$ $[\text{M}+\text{H}]^+$: 545.3168; found: 545.3159.

(4-(tert-butyl)phenyl)(1-(3,5-di-tert-butyl-4-hydroxyphenyl)-3-(dimethylamino)indolizin-2-yl)methanone (42l)



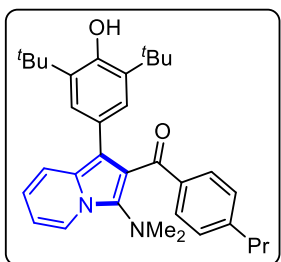
The reaction was performed at 0.102 mmol scale of **40a**; $R_f = 0.4$ (10% EtOAc in hexane); brown gummy solid (43.4 mg, 81% yield); ^1H NMR (400 MHz, CDCl_3) δ 8.07 (d, $J = 6.9$ Hz, 1H), 7.59 – 7.57 (m, 2H), 7.50 (d, $J = 8.9$ Hz, 1H), 7.12 – 7.09 (m, 2H), 6.93 (s, 2H), 6.67 (t, $J = 6.6$ Hz, 1H), 6.58 (t, $J = 6.6$ Hz, 1H), 4.91 (s, 1H), 2.87 (s, 6H), 1.29 (s, 18H), 1.19 (s, 9H); $^{13}\text{C}\{^1\text{H}\}$ NMR (100 MHz, CDCl_3) δ 195.1, 155.5, 151.8, 136.1, 135.7, 135.4, 130.1, 127.0, 126.0, 124.5, 124.0, 121.7, 118.94, 118.88, 117.6, 114.6, 111.4, 43.5, 34.9, 34.3, 31.1, 30.3; FT-IR (thin film, neat): 3632, 3442, 2958, 1736, 1642, 1232, 1179, 1034, 838, 635 cm^{-1} ; HRMS (ESI): m/z calcd for $\text{C}_{35}\text{H}_{45}\text{N}_2\text{O}_2$ $[\text{M}+\text{H}]^+$: 525.3481; found: 525.3483.

(1-(3,5-di-tert-butyl-4-hydroxyphenyl)-3-(dimethylamino)indolizin-2-yl)(4-ethylphenyl)methanone (42m)



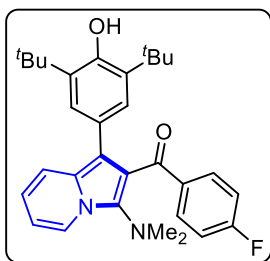
The reaction was performed at 0.102 mmol scale of **40a**; $R_f = 0.4$ (10% EtOAc in hexane); brown gummy solid (43.2 mg, 85% yield); ^1H NMR (400 MHz, CDCl_3) δ 8.05 (d, $J = 6.9$ Hz, 1H), 7.58 (d, $J = 8.2$ Hz, 2H), 7.50 (d, $J = 9.0$ Hz, 1H), 6.94 – 6.92 (m, 4H), 6.67 (t, $J = 6.6$ Hz, 1H), 6.57 (t, $J = 6.7$ Hz, 1H), 4.92 (s, 1H), 2.85 (s, 6H), 2.52 (q, $J = 7.6$ Hz, 2H), 1.29 (s, 18H), 1.12 (t, $J = 7.6$ Hz, 3H); $^{13}\text{C}\{^1\text{H}\}$ NMR (100 MHz, CDCl_3) δ 195.3, 151.8, 148.9, 136.5, 135.4, 130.5, 127.2, 127.0, 125.9, 124.1, 121.75, 121.71, 118.9, 117.6, 117.5, 114.5, 111.4, 43.5, 34.3, 30.3, 29.0, 15.4; FT-IR (thin film, neat): 3634, 3448, 2958, 1756, 1730, 1436, 1252, 1034, 836, 632 cm^{-1} ; HRMS (ESI): m/z calcd for $\text{C}_{33}\text{H}_{41}\text{N}_2\text{O}_2$ $[\text{M}+\text{H}]^+$: 497.3168; found : 497.3179.

(1-(3,5-di-tert-butyl-4-hydroxyphenyl)-3-(dimethylamino)indolizin-2-yl)(4-propylphenyl)methanone (42n)



The reaction was performed at 0.102 mmol scale of **40a**; $R_f = 0.4$ (10% EtOAc in hexane); brown gummy solid (43.3 mg, 83% yield); ^1H NMR (400 MHz, CDCl_3) δ 8.05 (d, $J = 7.0$ Hz, 1H), 7.58 (d, $J = 8.1$ Hz, 2H), 7.50 (d, $J = 9.0$ Hz, 1H), 6.95 (s, 2H), 6.91 (d, $J = 8.0$ Hz, 2H), 6.67 (t, $J = 6.6$ Hz, 1H), 6.57 (t, $J = 6.7$ Hz, 1H), 4.91 (s, 1H), 2.85 (s, 6H), 2.46 (t, $J = 7.4$ Hz, 2H), 1.54 – 1.48 (m, 2H), 1.29 (s, 18H), 0.82 (t, $J = 7.3$ Hz, 3H); $^{13}\text{C}\{^1\text{H}\}$ NMR (100 MHz, CDCl_3) δ 195.4, 151.9, 147.4, 136.6, 135.5, 135.4, 130.3, 127.8, 126.9, 126.0, 124.1, 121.7, 118.9, 117.62, 117.57, 114.5, 111.4, 43.5, 38.0, 34.3, 30.3, 24.3, 13.8; FT-IR (thin film, neat): 3632, 3442, 2956, 1758, 1612, 1436, 1250, 1178, 1034, 836, 635 cm^{-1} ; HRMS (ESI): m/z calcd for $\text{C}_{34}\text{H}_{43}\text{N}_2\text{O}_2$ $[\text{M}+\text{H}]^+$: 511.3325; found : 511.3328.

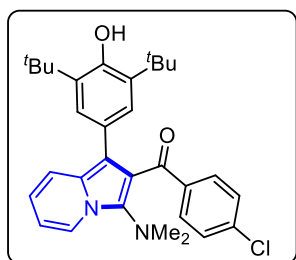
{1-[3,5-di-tert-butyl-4-hydroxyphenyl]-3-(dimethylamino)-indolizin-2-yl}-(4-fluorophenyl)-methanone (42o)



The reaction was performed at 0.102 mmol scale of **40a**; $R_f = 0.4$ (5% EtOAc in hexane); brown solid (33.3 mg, 67% yield); m. p. = 138–140 °C; ^1H NMR (400 MHz, CDCl_3) δ 8.05 (d, $J = 6.9$ Hz, 1H), 7.69 (t, $J = 6.5$ Hz, 2H), 7.49 (d, $J = 8.9$ Hz, 1H), 6.94 (s, 2H), 6.78 (t, $J = 8.0$ Hz, 2H), 6.68 (t, $J = 7.3$ Hz, 1H), 6.58 (t, $J = 6.7$ Hz, 1H), 4.98 (s, 1H), 2.85 (s, 6H), 1.31 (s, 18H); $^{13}\text{C}\{^1\text{H}\}$ NMR (100 MHz, CDCl_3) δ 193.9, 165.1 (d, $J = 252.0$ Hz),

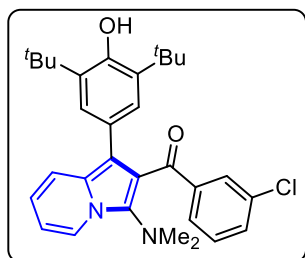
152.0, 135.7, 135.6, 135.2 (d, $J = 2.8$ Hz), 132.6 (d, $J = 9.2$ Hz), 126.9, 125.7, 124.2, 121.7, 118.9, 118.4, 117.8, 114.7, 114.6 (d, $J = 21.7$ Hz), 111.6, 43.4, 34.3, 30.3; $^{19}\text{F}\{^1\text{H}\}$ NMR (376 MHz, CDCl_3) δ -107.12; FT-IR (thin film, neat): 3634, 3469, 2956, 1732, 1648, 1236, 1120, 758 cm^{-1} ; HRMS (ESI): m/z calcd for $\text{C}_{31}\text{H}_{36}\text{FN}_2\text{O}_2$ $[\text{M}+\text{H}]^+$: 487.2761; found : 487.2771.

{4-chlorophenyl}-[1-(3,5-di-tert-butyl-4-hydroxyphenyl)-3-(dimethylamino)-indolizin-2-yl]-methanone (42p)



The reaction was performed at 0.102 mmol scale of **40a**; $R_f = 0.4$ (5% EtOAc in hexane); light brown solid (40.1 mg, 78% yield); m. p. = 198–200 °C; ^1H NMR (400 MHz, CDCl_3) δ 8.07 – 8.04 (m, 1H), 7.60 – 7.56 (m, 2H), 7.49 – 7.46 (m, 1H), 7.09 – 7.05 (m, 2H), 6.91 (s, 2H), 6.70 – 6.65 (m, 1H), 6.61 – 6.57 (m, 1H), 4.99 (s, 1H), 2.85 (s, 6H), 1.31 (s, 18H); $^{13}\text{C}\{^1\text{H}\}$ NMR (100 MHz, CDCl_3) δ 194.2, 152.1, 138.3, 137.3, 135.8, 135.7, 131.5, 127.8, 127.0, 125.7, 124.3, 121.8, 119.0, 118.3, 117.9, 114.5, 111.7, 43.4, 34.3, 30.3; FT-IR (thin film, neat): 3633, 2960, 1732, 1645, 1448, 1264, 736 cm^{-1} ; HRMS (ESI): m/z calcd for $\text{C}_{31}\text{H}_{36}\text{ClN}_2\text{O}_2$ $[\text{M}+\text{H}]^+$: 503.2465; found : 503.2449.

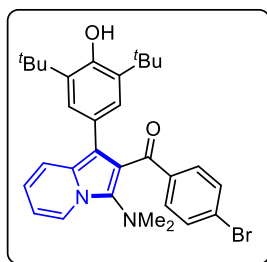
(3-chlorophenyl)-[1-[3,5-di-tert-butyl-4-hydroxyphenyl]-3-(dimethylamino)-indolizin-2-yl]-methanone (42q)



The reaction was performed at 0.102 mmol scale of **40a**; $R_f = 0.4$ (5% EtOAc in hexane); brown solid (38.0 mg, 74% yield); m. p. = 148–150 °C; ^1H NMR (400 MHz, CDCl_3) δ 8.07 (d, $J = 7.2$ Hz, 1H), 7.60 (d, $J = 7.7$ Hz, 1H), 7.52 – 7.47 (m, 2H), 7.22 – 7.20 (m, 1H), 7.08 (t, $J = 7.8$ Hz 1H), 6.92 (s, 2H), 6.70 – 6.67 (m, 1H), 6.61 – 6.58 (m, 1H), 4.98 (s, 1H), 2.87 (s, 6H), 1.32 (s, 18H); $^{13}\text{C}\{^1\text{H}\}$ NMR (100 MHz, CDCl_3) δ 193.9, 152.0, 140.5, 136.1, 135.7, 133.7, 131.7, 130.7, 129.0, 127.6, 126.9, 125.7, 124.3, 121.8, 119.0, 118.0, 117.9, 114.7, 111.8, 43.4, 34.3, 30.2; film, neat): 3634, 2959, 1755, 1587, 1436, 1262, 893, 736 cm^{-1} ; HRMS (ESI): m/z calcd for $\text{C}_{31}\text{H}_{36}\text{ClN}_2\text{O}_2$ $[\text{M}+\text{H}]^+$: 503.2465; found : 503.2445.

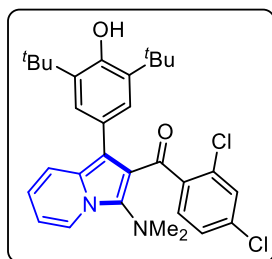
(4-bromophenyl)-[1-[3,5-di-tert-butyl-4-hydroxyphenyl]-3-(dimethylamino)-indolizin-2-yl]-methanone (42r)

The reaction was performed at 0.102 mmol scale of **40a**; $R_f = 0.4$ (5% EtOAc in hexane); light brown solid (42.4 mg, 76% yield); m. p. = 182 – 184 °C; ^1H NMR (400 MHz, CDCl_3) δ 8.07 (d, $J = 7.1$ Hz, 1H), 7.66 – 7.64 (m, 2H), 7.48 (d, $J = 9.0$ Hz 1H), 7.36 (d, $J = 8.0$ Hz 1H), 7.02 (t, $J = 7.8$ Hz 1H), 6.92 (s, 2H), 6.70 – 6.67 (m, 1H), 6.61 – 6.58 (m, 1H), 4.97 (s, 1H), 2.86 (s,



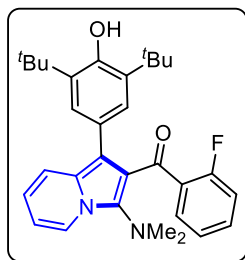
547.1935.

{1-[3,5-di-tert-butyl-4-hydroxyphenyl]-3-(dimethylamino)-indolizin-2-yl}-(2,4-dichlorophenyl)-methanone (42s)



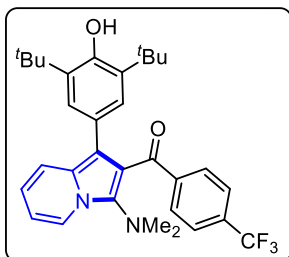
The reaction was performed at 0.102 mmol scale of **40a**; $R_f = 0.4$ (5% EtOAc in hexane); brown solid (31.1 mg, 56% yield); m. p. = 152 – 154 °C; ^1H NMR (400 MHz, CDCl_3) δ 8.08 – 8.06 (m, 1H), 7.20 – 7.18 (m, 1H), 7.17 – 7.15 (m, 1H), 7.01 (d, $J = 1.9$ Hz, 1H), 6.90 – 6.88 (m, 1H), 6.82 (s, 2H), 6.61 – 6.55 (m, 2H), 5.00 (s, 1H), 2.91 (s, 6H), 1.35 (s, 18H); $^{13}\text{C}\{^1\text{H}\}$ NMR (100 MHz, CDCl_3) δ 191.9, 152.4, 138.1, 136.4, 136.1, 135.1, 133.0, 132.3, 129.6, 127.5, 126.3, 125.5, 125.1, 121.8, 119.4, 119.3, 117.8, 115.6, 112.2, 42.6, 34.2, 30.3; FT-IR (thin film, neat): 3633, 2960, 1646, 1358, 1264, 893, 736 cm^{-1} ; HRMS (ESI): m/z calcd for $\text{C}_{31}\text{H}_{35}\text{Cl}_2\text{N}_2\text{O}_2$ $[\text{M}+\text{H}]^+$: 537.2076; found : 537.2062.

{1-[3,5-di-tert-butyl-4-hydroxyphenyl]-3-(dimethylamino)-indolizin-2-yl}-(2-fluorophenyl)-methanone (42t)



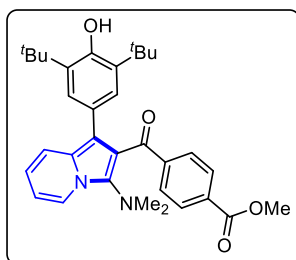
The reaction was performed at 0.102 mmol scale of **40a**; $R_f = 0.4$ (5% EtOAc in hexane); brown gummy solid (31.3 mg, 63% yield); ^1H NMR (400 MHz, CDCl_3) δ 8.08 – 8.06 (m, 1H), 7.37 – 7.30 (m, 2H), 7.16 – 7.10 (m, 1H), 6.89 (s, 2H), 6.85 – 6.81 (m, 1H), 6.71 – 6.66 (m, 1H), 6.63 – 6.54 (m, 2H), 4.94 (s, 1H), 2.90 (s, 6H), 1.32 (s, 18H); $^{13}\text{C}\{^1\text{H}\}$ NMR (100 MHz, CDCl_3) δ 191.6, 160.4 (d, $J_{\text{C-F}} = 253.4$ Hz), 152.1, 135.9, 135.1, 132.7 (d, $J_{\text{C-F}} = 8.7$ Hz), 131.5 (d, $J_{\text{C-F}} = 1.9$ Hz), 129.1 (d, $J_{\text{C-F}} = 11.4$ Hz), 127.3, 125.3, 124.8, 123.3 (d, $J_{\text{C-F}} = 3.3$ Hz), 121.8, 119.9, 119.2, 117.7, 115.8 (d, $J_{\text{C-F}} = 21.9$ Hz), 115.3 (d, $J_{\text{C-F}} = 1.1$ Hz), 111.8, 43.0, 34.2, 30.3; $^{19}\text{F}\{^1\text{H}\}$ NMR (376 MHz, CDCl_3) δ -112.5; FT-IR (thin film, neat): 3634, 3469, 2956, 1732, 1644, 1236, 1042, 758, 665 cm^{-1} ; HRMS (ESI): m/z calcd for $\text{C}_{31}\text{H}_{36}\text{FN}_2\text{O}_2$ $[\text{M}+\text{H}]^+$: 487.2761; found : 487.2756.

{1-[3,5-di-tert-butyl-4-hydroxyphenyl]-3-(dimethylamino)-indolizin-2-yl}-[4-(trifluoromethyl)phenyl]-methanone (42u)



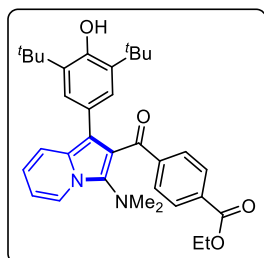
The reaction was performed at 0.102 mmol scale of **40a**; $R_f = 0.4$ (5% EtOAc in hexane); brown solid (31.0 mg, 56% yield); m. p. = 156–158 °C; ^1H NMR (400 MHz, CDCl_3) δ 8.09 (d, $J = 7.1$ Hz, 1H), 7.72 – 7.70 (m, 2H), 7.47 – 7.45 (m, 1H), 7.34 – 7.32 (m, 2H), 6.87 (s, 2H), 6.70 – 6.67 (m, 1H), 6.62 – 6.59 (m, 1H), 4.95 (s, 1H), 2.88 (s, 6H), 1.29 (s, 18H); $^{13}\text{C}\{^1\text{H}\}$ NMR (100 MHz, CDCl_3) δ 194.0, 152.1, 141.79, 141.78, 136.4, 135.7, 133.0 (q, $J_{\text{C-F}} = 32.2$ Hz), 130.3 (2C), 127.1, 125.6, 124.5 (q, $J_{\text{C-F}} = 4.2$ Hz), 123.8 (q, $J_{\text{C-F}} = 270.9$ Hz), 121.8, 191.0, 118.1, 114.8, 111.9, 43.3, 34.2, 30.2; $^{19}\text{F}\{^1\text{H}\}$ NMR (376 MHz, CDCl_3) δ –63.23; FT-IR (thin film, neat): 3630, 2965, 1648, 1451, 12562, 1166, 893, 736 cm^{-1} ; HRMS (ESI): m/z calcd for $\text{C}_{32}\text{H}_{36}\text{F}_3\text{N}_2\text{O}_2$ $[\text{M}+\text{H}]^+$: 537.2729; found : 537.2744.

methyl 4-(1-(3,5-di-tert-butyl-4-hydroxyphenyl)-3-(dimethylamino)indolizine-2-carbonyl)benzoate (42v)



The reaction was performed at 0.102 mmol scale of **40a**; $R_f = 0.4$ (10% EtOAc in hexane); brown solid (35.5 mg, 66% yield); m. p. = 178–180 °C; ^1H NMR (400 MHz, CDCl_3) δ 8.06 (d, $J = 7.1$ Hz, 1H), 7.78 – 7.75 (m, 2H), 7.68 – 7.65 (m, 2H), 7.46 (d, $J = 9.0$ Hz, 1H), 6.90 (s, 2H), 6.69 – 6.66 (m, 1H), 6.61 – 6.57 (m, 1H), 4.93 (s, 1H), 3.86 (s, 3H), 2.85 (s, 6H), 1.28 (s, 18H); $^{13}\text{C}\{^1\text{H}\}$ NMR (100 MHz, CDCl_3) δ 194.8, 166.4, 152.0, 142.5, 135.9, 135.7, 132.5, 129.9, 128.8, 127.0, 125.7, 124.4, 121.8, 119.0, 118.4, 118.0, 114.6, 111.8, 52.3, 43.3, 34.3, 30.3; FT-IR (thin film, neat): 3631, 3054, 2953, 1723, 1645, 1357, 1234, 1152, 1011, 733 cm^{-1} ; HRMS (ESI): m/z calcd for $\text{C}_{33}\text{H}_{39}\text{N}_2\text{O}_4$ $[\text{M}+\text{H}]^+$: 527.2910; found : 527.2914.

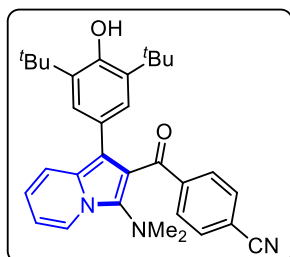
Ethyl 4-(1-(3,5-di-tert-butyl-4-hydroxyphenyl)-3-(dimethylamino)indolizine-2-carbonyl)benzoate (42w)



The reaction was performed at 0.102 mmol scale of **40a**; $R_f = 0.4$ (10% EtOAc in hexane); brown solid (35.3 mg, 64% yield); m. p. = 174–176 °C; ^1H NMR (400 MHz, CDCl_3) δ 8.07 (d, $J = 7.1$ Hz, 1H), 7.77 – 7.75 (m, 2H), 7.66 – 7.64 (m, 2H), 7.45 (d, $J = 9.0$ Hz, 1H), 6.90 – 6.89 (m, 2H), 6.69 – 6.65 (m, 1H), 6.61 – 6.57 (m, 1H), 4.93 (s, 1H), 4.32 (q, $J = 7.1$ Hz, 2H), 2.86 (s, 6H), 1.33 (t, $J = 7.1$ Hz, 1H), 1.28 (s, 18H); $^{13}\text{C}\{^1\text{H}\}$ NMR (100 MHz, CDCl_3) δ 194.8, 165.9, 152.0, 142.4, 136.0, 135.6, 132.9, 129.8, 128.8, 127.1, 125.7, 124.4, 121.8, 119.0, 118.4, 117.9, 114.7, 111.8, 61.2, 43.3, 34.2, 30.2, 14.4; FT-IR (thin film, neat):

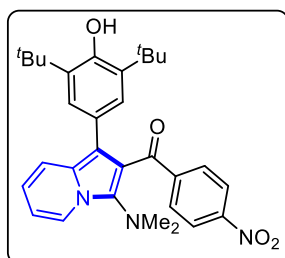
3632, 3052, 2956, 1725, 1643, 1437, 1234, 1153, 732 cm^{-1} ; HRMS (ESI): m/z calcd for $\text{C}_{34}\text{H}_{41}\text{N}_2\text{O}_4$ $[\text{M}+\text{H}]^+$: 541.3066; found : 541.3063.

4-(1-(3,5-di-tert-butyl-4-hydroxyphenyl)-3-(dimethylamino)indolizine-2-carbonyl)benzonitrile (42x)



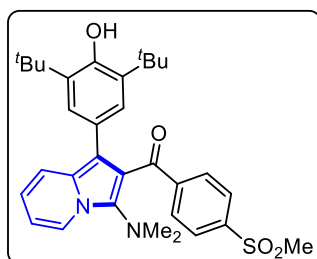
The reaction was performed at 0.102 mmol scale of **40a**; R_f = 0.2 (5% EtOAc in hexane); brown solid (29.3 mg, 58% yield); m. p. = 156–158 $^{\circ}\text{C}$; ^1H NMR (400 MHz, CDCl_3) δ 8.07 (d, J = 7.1 Hz, 1H), 7.68 (d, J = 8.4 Hz, 2H), 7.45 (d, J = 9.0 Hz, 1H), 7.37 (d, J = 8.4 Hz, 2H), 6.87 (s, 2H), 6.71 – 6.67 (m, 1H), 6.63 – 6.59 (m, 1H), 4.99 (s, 1H), 2.85 (s, 6H), 1.30 (s, 18H); $^{13}\text{C}\{^1\text{H}\}$ NMR (100 MHz, CDCl_3) δ 193.6, 152.2, 142.4, 136.4, 135.8, 131.3, 130.3 (2C), 127.1, 125.5, 124.5, 121.8, 119.0, 118.3, 117.7, 114.7, 114.5, 112.0, 43.3, 34.3, 30.3; FT-IR (thin film, neat): 3631, 2955, 2230, 1647, 1429, 1238, 1198, 975, 741 cm^{-1} ; HRMS (ESI): m/z calcd for $\text{C}_{32}\text{H}_{36}\text{N}_3\text{O}_2$ $[\text{M}+\text{H}]^+$: 494.2808; found : 494.2829.

{1-[3,5-di-tert-butyl-4-hydroxyphenyl]-3-(dimethylamino)-indolizin-2-yl}-[4-nitrophenyl]-methanone (42y)



The reaction was performed at 0.102 mmol scale of **40a**; R_f = 0.4 (10% EtOAc in hexane); brown solid (27.3 mg, 52% yield); m. p. = 136–138 $^{\circ}\text{C}$; ^1H NMR (400 MHz, CDCl_3) δ 8.08 (d, J = 7.1 Hz, 1H), 7.92 – 7.90 (m, 2H), 7.74 – 7.71 (m, 2H), 7.44 (d, J = 9 Hz, 1H), 6.86 (s, 2H), 6.71 – 6.67 (m, 1H), 6.63 – 6.60 (m, 1H), 4.95 (s, 1H), 2.87 (s, 6H), 1.28 (s, 18H); $^{13}\text{C}\{^1\text{H}\}$ NMR (100 MHz, CDCl_3) δ 193.2, 152.2, 149.2, 144.0, 136.5, 135.9, 130.8, 127.2, 125.5, 124.6, 122.6, 121.8, 119.0, 118.4, 117.8, 114.7, 112.1, 43.2, 34.3, 30.3; FT-IR (thin film, neat): 3633, 2959, 1650, 1525, 1349, 1264, 1150, 737 cm^{-1} ; HRMS (ESI): m/z calcd for $\text{C}_{31}\text{H}_{36}\text{N}_3\text{O}_4$ $[\text{M}+\text{H}]^+$: 514.2706; found : 514.2719.

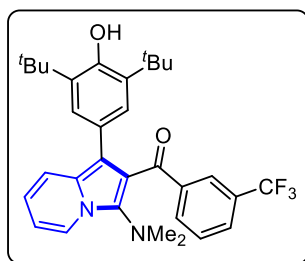
{1-[3,5-di-tert-butyl-4-hydroxyphenyl]-3-(dimethylamino)-indolizin-2-yl}-[4-(methylsulfonyl)-phenyl]-methanone (42z)



The reaction was performed at 0.102 mmol scale of **40a**; R_f = 0.3 (10% EtOAc in hexane); brown solid (27.1 mg, 48% yield); m. p. = 164–166 $^{\circ}\text{C}$; ^1H NMR (400 MHz, CDCl_3) δ 8.09 (d, J = 7.1 Hz, 1H), 7.77 – 7.75 (m, 2H), 7.65 – 7.63 (m, 2H), 7.44 (d, J = 9.0 Hz, 1H), 6.88 (s, 2H), 6.72 – 6.68 (m, 1H), 6.64 – 6.60 (m, 1H), 4.94 (s, 1H),

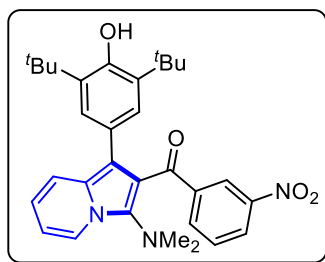
2.29 (s, 3H), 2.87 (s, 6H), 1.29 (s, 18H); $^{13}\text{C}\{^1\text{H}\}$ NMR (100 MHz, CDCl_3) δ 193.5, 152.1, 143.3, 142.6, 136.6, 135.8, 130.7, 127.2, 126.6, 125.8, 124.5, 121.9, 119.0, 118.4, 117.8, 114.6, 112.1, 44.5, 43.2, 34.3, 30.3; FT-IR (thin film, neat): 3630, 3442, 2957, 2872, 1756, 1601, 1349, 1236, 1145, 736 cm^{-1} ; HRMS (ESI): m/z calcd for $\text{C}_{32}\text{H}_{39}\text{N}_2\text{O}_4\text{S}$ $[\text{M}+\text{H}]^+$: 547.2631; found : 547.2604.

{1-[3,5-di-tert-butyl-4-hydroxyphenyl]-3-(dimethylamino)-indolizin-2-yl}-(3-(trifluoromethyl)-phenyl)-methanone (42aa)



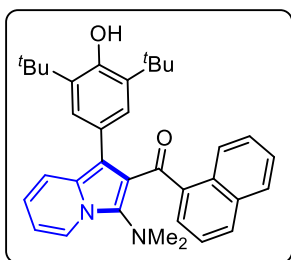
The reaction was performed at 0.102 mmol scale of **40a**; R_f = 0.4 (5 % EtOAc in hexane); brown solid (34.2 mg, 62% yield); m. p. = 154–156 °C; ^1H NMR (400 MHz, CDCl_3) δ 8.09 – 8.07 (m, 1H), 7.95 (d, J = 7.8 Hz, 1H), 7.81 (s, 1H), 7.52 – 7.47 (m, 2H), 7.32 – 7.28 (m, 1H), 6.90 (s, 2H), 6.71 – 6.67 (m, 1H), 6.63 – 6.59 (m, 1H), 4.95 (s, 1H), 2.87 (s, 6H), 1.27 (s, 18H); $^{13}\text{C}\{^1\text{H}\}$ NMR (100 MHz, CDCl_3) δ 193.7, 152.1, 139.3, 136.4, 135.8, 132.8, 130.3, 130.0, 128.3 (q, $J_{\text{C-F}}$ = 4.0 Hz), 127.4 (q, $J_{\text{C-F}}$ = 4.0 Hz), 127.0, 125.4, 124.4, 123.8 (q, $J_{\text{C-F}}$ = 271.0 Hz), 121.8, 119.1, 118.1, 117.7, 114.5, 111.9, 43.4, 34.2, 30.2; $^{19}\text{F}\{^1\text{H}\}$ NMR (376 MHz, CDCl_3) δ –62.5; FT-IR (thin film, neat): 3632, 3054, 2964, 1648, 1264, 1121, 893, 734 cm^{-1} ; HRMS (ESI): m/z calcd for $\text{C}_{32}\text{H}_{36}\text{F}_3\text{N}_2\text{O}_2$ $[\text{M}+\text{H}]^+$: 537.2729; found : 537.2734.

{1-[3,5-di-tert-butyl-4-hydroxyphenyl]-3-(dimethylamino)-indolizin-2-yl}-(3-nitrophenyl)-methanone (42ab)



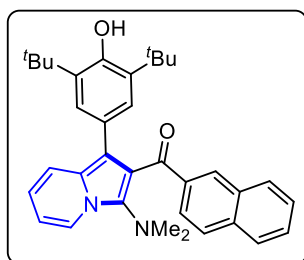
The reaction was performed at 0.102 mmol scale of **40a**; R_f = 0.3 (5% EtOAc in hexane); brown solid (35.2 mg, 67% yield); m. p. = 176–178 °C; ^1H NMR (400 MHz, CDCl_3) δ 8.25 (t, J = 1.8 Hz, 1H), 8.13 – 8.07 (m, 3H), 7.46 – 7.43 (m, 1H), 7.40 – 7.36 (m, 1H), 6.88 (s, 2H), 6.72 – 6.69 (m, 1H), 6.64 – 6.61 (m, 1H), 4.94 (s, 1H), 2.89 (s, 6H), 1.25 (s, 18H); $^{13}\text{C}\{^1\text{H}\}$ NMR (100 MHz, CDCl_3) δ 192.3, 152.1, 147.2, 140.3, 136.8, 135.8, 134.7, 128.8, 127.2, 126.1, 125.9, 125.5, 124.7, 121.9, 119.1, 118.4, 117.3, 114.7, 112.2, 43.2, 34.2, 30.2; FT-IR (thin film, neat): 3632, 2958, 1650, 1523, 1449, 1262, 1236, 976, 737 cm^{-1} ; HRMS (ESI): m/z calcd for $\text{C}_{31}\text{H}_{36}\text{N}_3\text{O}_4$ $[\text{M}+\text{H}]^+$: 514.2706; found : 514.2692.

{1-[3,5-di-tert-butyl-4-hydroxyphenyl]-3-(dimethylamino)indolizin-2-yl}-(naphthalen-1-yl)-methanone (42ac)



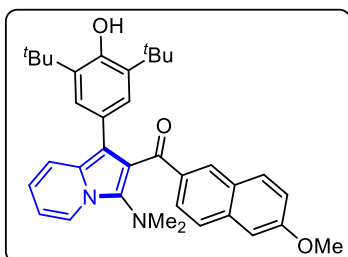
The reaction was performed at 0.102 mmol scale of **40a**; $R_f = 0.4$ (5% EtOAc in hexane); brown solid (39.2 mg, 74% yield); m. p. = 145–147 °C; ^1H NMR (400 MHz, CDCl_3) δ 8.10 (d, $J = 7.1$ Hz, 1H), 8.05 (s, 1H), 7.92 – 7.90 (m, 1H), 7.72 – 7.70 (m, 1H), 7.66 – 7.63 (m, 1H), 7.61 – 7.59 (m, 1H), 7.54 – 7.51 (m, 1H), 7.47 – 7.43 (m, 1H), 7.39 – 7.35 (m, 1H), 6.96 (s, 2H), 6.72 – 6.68 (m, 1H), 6.63 – 7.60 (m, 1H), 4.73 (s, 1H), 2.90 (s, 6H), 1.17 (s, 18H); $^{13}\text{C}\{^1\text{H}\}$ NMR (100 MHz, CDCl_3) δ 195.4, 151.7, 136.0, 135.8, 135.5, 135.1, 133.1, 132.1, 129.4, 128.0, 127.52, 127.51, 126.9, 126.2, 126.0, 125.2, 124.3, 121.8, 119.0, 118.8, 117.7, 114.8, 111.5, 34.4, 34.1, 30.1; FT-IR (thin film, neat): 3634, 2955, 2871, 1736, 1641, 1448, 1356, 1253, 1123, 891, 740 cm^{-1} ; HRMS (ESI): m/z calcd for $\text{C}_{35}\text{H}_{39}\text{N}_2\text{O}_2$ $[\text{M}+\text{H}]^+$: 519.3012; found: 519.3011.

[1-(3,5-di-tert-butyl-4-hydroxyphenyl)-3-(dimethylamino)indolizin-2-yl](naphthalen-2-yl)methanone (42ad)



The reaction was performed at 0.102 mmol scale of **40a**; $R_f = 0.4$ (5% EtOAc in hexane); brown solid (41.4 mg, 78% yield); m. p. = 142–144 °C; ^1H NMR (400 MHz, CDCl_3) δ 8.10 (d, $J = 7.1$ Hz, 1H), 8.04 (s, 1H), 7.92 – 7.90 (m, 1H), 7.72 – 7.70 (m, 1H), 7.66 – 7.63 (m, 1H), 7.61 – 7.59 (m, 1H), 7.52 (d, $J = 9.0$ Hz, 1H), 7.47 – 7.43 (m, 1H), 7.38 – 7.35 (m, 1H), 6.96 (s, 2H), 6.72 – 6.68 (m, 1H), 6.63 – 6.60 (m, 1H), 4.73 (s, 1H), 2.89 (s, 6H), 1.17 (s, 18H); $^{13}\text{C}\{^1\text{H}\}$ NMR (100 MHz, CDCl_3) δ 195.4, 151.7, 136.0, 135.8, 135.4 (2C), 135.1, 133.1, 132.1, 129.4, 128.0, 127.5, 126.9, 126.2, 125.9, 125.1, 124.2, 121.8, 119.0, 118.8, 117.7, 114.8, 111.5, 43.4, 34.1, 30.1; FT-IR (thin film, neat): 3635, 2954, 2875, 1734, 1642, 1446, 1353, 1255, 1126, 742 cm^{-1} ; HRMS (ESI): m/z calcd for $\text{C}_{35}\text{H}_{39}\text{N}_2\text{O}_2$ $[\text{M}+\text{H}]^+$: 519.3012; found: 519.3018.

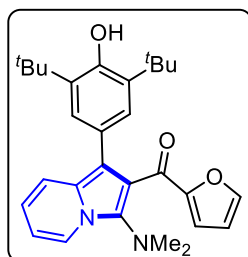
{1-[3,5-di-tert-butyl-4-hydroxyphenyl]-3-(dimethylamino)-indolizin-2-yl}-(6-methoxynaphthalen-2-yl)-methanone (42ae)



The reaction was performed at 0.102 mmol scale of **40a**; $R_f = 0.2$ (5% EtOAc in hexane); brown solid (50.1 mg, 89% yield); m. p. = 162–164 °C; ^1H NMR (400 MHz, CDCl_3) δ 8.09 (d, $J = 7.1$ Hz, 1H), 7.99 (s, 1H), 7.92 – 7.90 (m, 1H), 7.56 – 7.53 (m, 2H), 7.50 – 7.48 (m, 1H), 7.05 – 6.99 (m, 4H), 6.71 – 6.68 (m, 1H), 6.62 – 6.59 (m, 1H), 4.77 (s, 1H), 3.88 (s, 3H), 2.88 (s, 6H), 1.19 (s, 18H); $^{13}\text{C}\{^1\text{H}\}$ NMR (100 MHz,

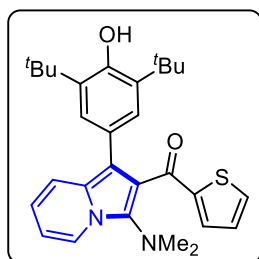
CDCl₃) δ 195.2, 159.4, 151.7, 136.8, 135.48, 135.46, 134.0, 133.1, 131.0, 127.5, 126.8, 126.3, 126.0, 125.9, 124.2, 121.7, 119.0, 118.9, 118.8, 117.6, 114.6, 111.4, 105.6, 55.4, 43.5, 34.1, 30.2; FT-IR (thin film, neat): 3629, 2957, 1756, 1732, 1622, 1513, 1448, 1264, 1030, 732 cm⁻¹; HRMS (ESI): m/z calcd for C₃₆H₄₁N₂O₃ [M+H]⁺ : 549.3117; found : 549.3114.

{1-[3,5-di-tert-butyl-4-hydroxyphenyl]-3-(dimethylamino)-indolizin-2-yl}-(furan-2-yl)-methanone (42af)



The reaction was performed at 0.102 mmol scale of **40a**; R_f = 0.3 (5% EtOAc in hexane); brown gummy solid (34.2 mg, 73% yield); ¹H NMR (400 MHz, CDCl₃) δ 8.01 (d, J = 7.1 Hz, 1H), 7.53 (d, J = 9.0 Hz, 1H), 7.26 (s, 1H), 7.07 (s, 2H), 6.70 – 6.69 (m, 1H), 6.68 – 6.65 (m, 1H), 6.58 – 6.55 (m, 1H), 6.21 – 6.20 (m, 1H), 5.03 (s, 1H), 2.85 (s, 6H), 1.36 (s, 18H); ¹³C{¹H} NMR (100 MHz, CDCl₃) δ 182.3, 153.8, 151.9, 145.9, 135.9, 135.5, 126.4, 126.1, 124.2, 121.7, 119.4, 119.0, 117.9, 117.8, 114.0, 111.8, 111.6, 43.5, 34.4, 30.4; FT-IR (thin film, neat): 3633, 2958, 1630, 1521, 1357, 1264, 1152, 893, 734 cm⁻¹; HRMS (ESI): m/z calcd for C₂₉H₃₅N₂O₃ [M+H]⁺ : 459.2648; found : 459.2642.

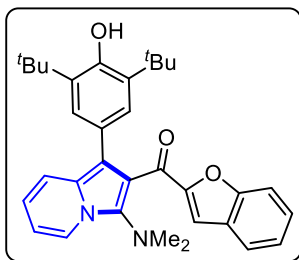
{1-[3,5-di-tert-butyl-4-hydroxyphenyl]-3-(dimethylamino)-indolizin-2-yl}-(thiophen-2-yl)-methanone (42ag)



The reaction was performed at 0.102 mmol scale of **40a**; R_f = 0.3 (5% EtOAc in hexane); brown solid (38.0 mg, 78% yield); m. p. = 178–180 °C; ¹H NMR (400 MHz, CDCl₃) δ 8.03 (d, J = 7.1 Hz, 1H), 7.54 (d, J = 9 Hz, 1H), 7.43 – 7.41 (m, 1H), 7.11 – 7.10 (m, 1H), 7.08 (s, 2H), 6.73 – 6.70 (m, 1H), 6.68 – 6.66 (m, 1H), 6.60 – 6.56 (m, 1H), 5.01 (s, 1H), 2.85 (s, 6H), 1.35 (s, 18H); ¹³C{¹H} NMR (100 MHz, CDCl₃) δ 187.6, 152.0, 145.9, 135.9, 135.3, 134.9, 133.1, 127.4, 126.6, 126.0, 124.1, 121.7, 118.9, 118.6, 117.7, 113.7, 111.5, 43.5, 34.4, 30.4; FT-IR (thin film, neat): 3632, 2953, 2869, 1629, 1518, 1449, 1235, 1153, 870, 741 cm⁻¹; HRMS (ESI): m/z calcd for C₂₉H₃₅N₂O₂S [M+H]⁺ : 475.2419; found : 475.2420.

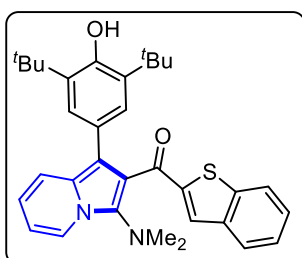
benzofuran-2-yl-{1-[3,5-di-tert-butyl-4-hydroxyphenyl]-3-(dimethylamino)-indolizin-2-yl}-methanone (42ah)

The reaction was performed at 0.102 mmol scale of **40a**; R_f = 0.4 (10% EtOAc in hexane); brown solid (37.4 mg, 72% yield); m. p. = 184–186 °C; ¹H NMR (400 MHz, CDCl₃) δ 8.05 (d, J = 7.1 Hz, 1H), 7.55 (d, J = 9.1 Hz, 1H), 7.42 (d, J = 7.8 Hz, 1H), 7.33 – 7.26 (m, 2H), 7.16 –



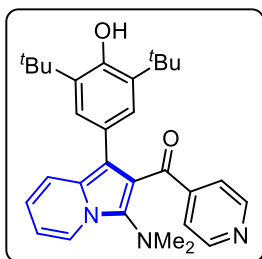
7.12 (m, 1H), 7.09 (s, 2H), 7.04 (s, 1H), 6.71 – 6.67 (m, 1H), 6.61 – 6.57 (m, 1H), 4.84 (s, 1H), 2.89 (s, 6H), 1.25 (s, 18H); $^{13}\text{C}\{^1\text{H}\}$ NMR (100 MHz, CDCl_3) δ 183.7, 155.3, 153.9, 151.9, 136.1, 135.9, 127.5, 127.1, 126.4, 126.2, 124.4, 123.5, 122.8, 121.8, 119.1, 118.0, 117.8, 115.1, 114.4, 112.2, 111.8, 43.4, 34.2, 30.3; FT-IR (thin film, neat): 3632, 2957, 2925, 1629, 1516, 1430, 1356, 1152, 1090, 872, 743 cm^{-1} ; HRMS (ESI): m/z calcd for $\text{C}_{33}\text{H}_{37}\text{N}_2\text{O}_3$ $[\text{M}+\text{H}]^+$: 509.2804; found : 509.2807.

benzo[b]thiophen-2-yl-{1-[3,5-di-tert-butyl-4-hydroxyphenyl]-3-(dimethylamino)-indolizin-2-yl}-methanone (42ai)



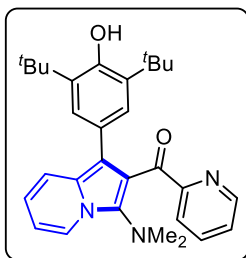
The reaction was performed at 0.102 mmol scale of **40a**; R_f = 0.4 (10% EtOAc in hexane); brown solid (41.1 mg, 76% yield); m. p. = 172–174 $^{\circ}\text{C}$; ^1H NMR (400 MHz, CDCl_3) δ 8.06 (d, J = 7.0 Hz, 1H), 7.76 (dd, J = 8.1, 0.6 Hz, 1H), 7.56 (d, J = 9.0 Hz, 1H), 7.47 – 7.45 (m, 1H), 7.34 – 7.29 (m, 2H), 7.24 – 7.20 (m, 1H), 7.10 (s, 2H), 6.71 (t, J = 6.6 Hz, 1H), 6.60 (t, J = 6.6 Hz, 1H), 4.86 (s, 1H), 2.88 (s, 6H), 1.26 (s, 18H); $^{13}\text{C}\{^1\text{H}\}$ NMR (100 MHz, CDCl_3) δ 188.9, 152.0, 144.9, 142.3, 139.1, 135.9, 135.3, 133.3, 127.0, 126.7, 126.0, 125.7, 124.6, 124.3, 122.7, 121.8, 119.0, 118.3, 117.9, 114.0, 111.7, 43.5, 34.3, 30.3; FT-IR (thin film, neat): 3632, 2954, 2923, 1628, 1517, 1428, 1254, 868, 743 cm^{-1} ; HRMS (ESI): m/z calcd for $\text{C}_{33}\text{H}_{37}\text{N}_2\text{O}_2\text{S}$ $[\text{M}+\text{H}]^+$: 525.2576; found : 525.2570.

{1-[3,5-di-tert-butyl-4-hydroxyphenyl]-3-(dimethylamino)-indolizin-2-yl}-(pyridin-4-yl)-methanone (42aj)



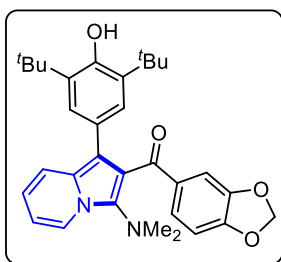
The reaction was performed at 0.102 mmol scale of **40a**; R_f = 0.4 (10% EtOAc in hexane); red solid (31.0 mg, 64% yield); m. p. = 126–128 $^{\circ}\text{C}$; ^1H NMR (400 MHz, CDCl_3) δ 8.40 – 8.39 (m, 2H), 8.07 (d, J = 7.1 Hz, 1H), 7.45 (d, J = 9.0 Hz, 1H), 7.38 – 7.37 (m, 2H), 6.88 (s, 2H), 6.70 – 6.67 (m, 1H), 6.62 – 6.59 (m, 1H), 4.99 (s, 1H), 2.86 (s, 6H), 1.30 (s, 18H); $^{13}\text{C}\{^1\text{H}\}$ NMR (100 MHz, CDCl_3) δ 194.0, 152.3, 149.7, 145.2, 136.5, 135.9, 127.1, 125.5, 124.5, 123.0, 121.8, 191.1, 118.2, 117.6, 114.7, 112.1, 43.2, 34.3, 30.3; FT-IR (thin film, neat): 3635, 2956, 1734, 1648, 1524, 1450, 1356, 1238, 1156, 759 cm^{-1} ; HRMS (ESI): m/z calcd for $\text{C}_{30}\text{H}_{36}\text{N}_3\text{O}_2$ $[\text{M}+\text{H}]^+$: 470.2808; found : 470.2820.

(1-(3,5-di-tert-butyl-4-hydroxyphenyl)-3-(dimethylamino)indolizin-2-yl)(pyridin-2-yl)methanone (42ak)



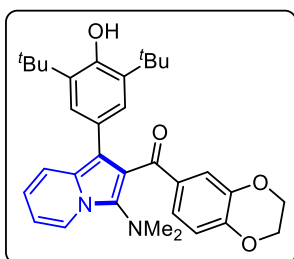
The reaction was performed at 0.102 mmol scale of **40a**; $R_f = 0.4$ (10% EtOAc in hexane); red solid (27.4 mg, 57% yield); m. p. = 132–134 °C; ^1H NMR (400 MHz, CDCl_3) δ 8.23 (d, $J = 4.7$ Hz, 1H), 8.03 (d, $J = 7.1$ Hz, 1H) 7.84 (d, $J = 7.8$ Hz, 1H), 7.61 – 7.57 (m, 1H), 7.43 (d, $J = 9.0$ Hz, 1H), 7.10 – 7.07 (m, 1H), 6.93 (s, 2H), 6.64 – 6.60 (m, 1H), 6.53 (t, $J = 6.6$ Hz, 1H), 4.91 (s, 1H), 2.90 (s, 6H), 1.30 (s, 18H); $^{13}\text{C}\{^1\text{H}\}$ NMR (100 MHz, CDCl_3) δ 194.4, 156.1, 151.6, 148.5, 136.5, 136.0, 135.3, 126.9, 126.5, 125.3, 124.8, 123.7, 121.8, 119.1, 118.0, 117.8, 115.0, 111.7, 43.1, 34.3, 30.3; FT-IR (thin film, neat): 3635, 3442, 2956, 1732, 1648, 1522, 1446, 1250, 1042, 756, 637 cm^{-1} ; HRMS (ESI): m/z calcd for $\text{C}_{30}\text{H}_{36}\text{N}_3\text{O}_2$ $[\text{M}+\text{H}]^+$: 470.2808; found : 470.2809.

benzo[d]-[1,3]-dioxol-5-yl-{1-[3,5-di-tert-butyl-4-hydroxyphenyl]-3-(dimethylamino)indolizin-2-yl}-methanone (42al)



The reaction was performed at 0.102 mmol scale of **40a**; $R_f = 0.4$ (10% EtOAc in hexane); brown gummy solid (38.1 mg, 72% yield); ^1H NMR (400 MHz, CDCl_3) δ 8.03 (d, $J = 7.1$ Hz, 1H), 7.49 (d, $J = 9.0$ Hz, 1H), 7.28 – 7.25 (m, 1H), 7.17 – 7.16 (m, 1H), 6.97 (s, 2H), 6.68 – 6.64 (m, 1H), 6.59 – 6.55 (m, 1H), 6.53 – 6.51 (m, 1H), 5.86 (s, 2H), 4.98 (s, 1H), 2.84 (s, 6H), 1.32 (s, 18H); $^{13}\text{C}\{^1\text{H}\}$ NMR (100 MHz, CDCl_3) δ 193.8, 151.9, 151.0, 147.3, 135.6, 135.2, 133.7, 126.8, 126.7, 126.0, 124.1, 121.7, 118.9, 118.7, 117.6, 114.3, 111.4, 109.9, 107.3, 101.5, 43.5, 34.3, 30.3; FT-IR (thin film, neat): 3629, 2958, 1642, 1386, 1262, 974, 856, 732 cm^{-1} ; HRMS (ESI): m/z calcd for $\text{C}_{32}\text{H}_{37}\text{N}_2\text{O}_4$ $[\text{M}+\text{H}]^+$: 513.2753; found : 513.2740.

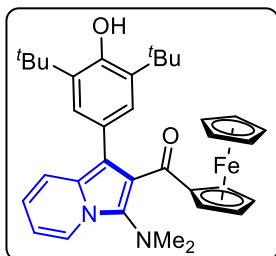
{1-[3,5-di-tert-butyl-4-hydroxyphenyl]-3-(dimethylamino)indolizin-2-yl}{2,3-dihydrobenzo[b][1,4]dioxin-6-yl}methanone (42am)



The reaction was performed at 0.102 mmol scale of **40a**; $R_f = 0.4$ (10% EtOAc in hexane); brown gummy solid (38.0 mg, 70% yield); ^1H NMR (400 MHz, CDCl_3) δ 8.03 (d, $J = 7.0$ Hz, 1H), 7.49 (d, $J = 9.0$ Hz, 1H), 7.27 – 7.24 (m, 1H), 7.16 (d, $J = 2.0$ Hz, 1H), 6.96 (s, 2H), 6.67 – 6.55 (m, 3H), 4.97 (s, 1H), 4.16 – 4.14 (m, 2H), 4.10 – 4.08 (m, 2H), 2.83 (s, 6H), 1.32 (s, 18H); $^{13}\text{C}\{^1\text{H}\}$ NMR (100 MHz, CDCl_3) δ 194.1, 151.8, 147.2, 142.5, 135.5, 132.6, 132.4, 126.9, 126.0, 124.1, 121.7, 120.1, 118.9, 118.7, 117.6, 116.5, 114.3, 113.6, 111.3, 64.7, 64.1, 43.4, 34.3, 30.3; FT-IR (thin film, neat): 3632, 2953, 1642,

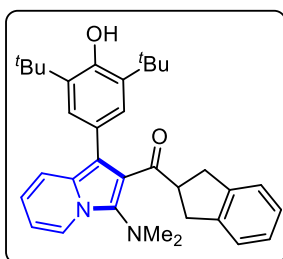
1575, 1452, 1354, 1237, 1115, 732 cm^{-1} ; HRMS (ESI): m/z calcd for $\text{C}_{33}\text{H}_{39}\text{N}_2\text{O}_4$ $[\text{M}+\text{H}]^+$: 527.2910; found : 527.2916.

{1-[3,5-di-tert-butyl-4-hydroxyphenyl]-3-(dimethylamino)-indolizin-2-yl}-(ferrocenyl)-methanone (42an)



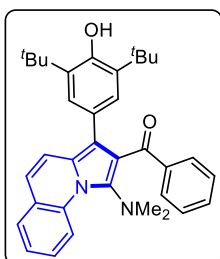
The reaction was performed at 0.102 mmol scale of **40a**; $R_f = 0.5$ (5% EtOAc in hexane); brown solid (34.2 mg, 58% yield); m. p. = 184–186 °C; ^1H NMR (400 MHz, CDCl_3) δ 7.96 (d, $J = 7.0$ Hz, 1H), 7.50 (d, $J = 9.0$ Hz, 1H), 7.15 (s, 2H), 6.64 (t, $J = 8.7$ Hz, 1H), 6.58 – 6.54 (m, 1H), 5.03 (s, 1H), 4.50 – 4.49 (m, 2H), 4.20 – 4.18 (m, 2H), 3.94 (s, 5H), 2.90 (s, 6H), 1.39 (s, 18H); $^{13}\text{C}\{^1\text{H}\}$ NMR (100 MHz, CDCl_3) δ 199.1, 152.2, 135.6, 133.3, 127.4, 126.3, 124.3, 121.6, 120.2, 119.0, 117.1, 114.0, 111.3, 82.6, 71.2, 70.8, 69.5, 43.2, 34.4, 30.5; FT-IR (thin film, neat): 3633, 2954, 2870, 1634, 1521, 1451, 1254, 1110, 894, 738 cm^{-1} ; HRMS (ESI): m/z calcd for $\text{C}_{35}\text{H}_{41}\text{FeN}_2\text{O}_2$ $[\text{M}+\text{H}]^+$: 577.2517; found : 577.2504.

{1-[3,5-di-tert-butyl-4-hydroxyphenyl]-3-(dimethylamino)-indolizin-2-yl}-(2,3-dihydro-1H-inden-2-yl)-methanone (42ao)



The reaction was performed at 0.102 mmol scale of **40a**; $R_f = 0.4$ (10% EtOAc in hexane); brown gummy solid (22.2 mg, 42% yield); ^1H NMR (400 MHz, CDCl_3) δ 8.07 (d, $J = 7.1$ Hz, 1H), 7.39 (d, $J = 9.0$ Hz, 1H), 7.22 – 7.18 (m, 2H), 7.13 – 7.09 (m, 4H), 6.68 – 6.64 (m, 1H), 6.59 – 6.55 (m, 1H), 5.20 (s, 1H), 3.69 (quintet, $J = 8.6$ Hz, 1H), 3.30 – 3.23 (m, 2H), 2.90 – 2.84 (m, 2H), 2.83 (s, 6H), 1.48 (s, 18H); $^{13}\text{C}\{^1\text{H}\}$ NMR (100 MHz, CDCl_3) δ 204.9, 152.8, 142.2, 141.6, 136.1, 134.4, 126.9, 126.8, 126.4, 126.0, 125.2, 124.6, 124.4, 121.9, 120.5, 118.9, 117.9, 113.5, 111.6, 50.5, 43.1, 36.7, 35.1, 34.6, 30.6; FT-IR (thin film, neat): 3634, 3440, 2958, 1732, 1612, 1436, 1250, 1036, 838, 637 cm^{-1} ; HRMS (ESI): m/z calcd for $\text{C}_{34}\text{H}_{41}\text{N}_2\text{O}_2$ $[\text{M}+\text{H}]^+$: 509.3168; found : 509.3162.

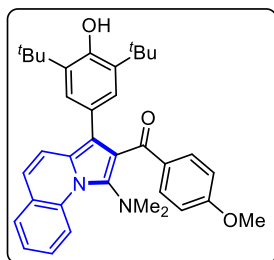
{3-[3,5-di-tert-butyl-4-hydroxyphenyl]-1-(dimethylamino)-pyrrolo[1,2-a]-quinolin-2-yl}-(phenyl)-methanone (43a)



The reaction was performed at 0.0868 mmol scale of **40b**; $R_f = 0.3$ (5% EtOAc in hexane); light yellow solid (35.6 mg, 79% yield); m. p. = 158 – 160 °C; ^1H NMR (400 MHz, CDCl_3) δ 9.33 (d, $J = 8.6$ Hz, 1H), 7.68 – 7.66 (m, 2H), 7.60 – 7.57 (m, 1H), 7.51 – 7.46 (m, 1H), 7.35 – 7.32 (m, 2H), 7.29 – 7.25 (m, 1H), 7.12 (t, $J = 7.8$ Hz, 2H), 6.94 – 6.92 (m, 3H), 4.95 (s,

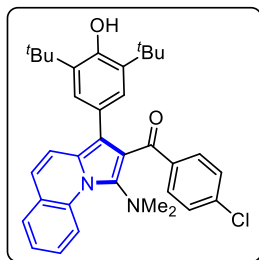
1H), 2.92 (s, 6H), 1.30 (s, 18H); $^{13}\text{C}\{^1\text{H}\}$ NMR (100 MHz, CDCl_3) δ 195.5, 152.2, 142.3, 138.9, 135.5, 135.4, 132.1, 130.1, 128.1, 127.6, 127.3, 127.2, 126.3, 125.3, 124.1, 123.3, 119.8, 119.5, 118.5, 118.0, 117.9, 43.5, 34.3, 30.3; FT-IR (thin film, neat): 3633, 3409, 2957, 2872, 1646, 1450, 1155, 891, 740 cm^{-1} ; HRMS (ESI): m/z calcd for $\text{C}_{35}\text{H}_{39}\text{N}_2\text{O}_2$ $[\text{M}+\text{H}]^+$: 519.3012; found : 519.3021.

{3-[3,5-di-tert-butyl-4-hydroxyphenyl]-1-(dimethylamino)-pyrrolo[1,2-a]-quinolin-2-yl}-(4-methoxyphenyl)-methanone (43b)



The reaction was performed at 0.0868 mmol scale of **40b**; R_f = 0.3 (10% EtOAc in hexane); brown solid (39.0 mg, 81% yield); m. p. = 152–154 °C; ^1H NMR (400 MHz, CDCl_3) δ 9.34 (d, J = 8.6 Hz, 1H), 7.70 – 7.67 (m, 2H), 7.59 – 7.57 (m, 1H), 7.50 – 7.46 (m, 1H), 7.38 – 7.31 (m, 2H), 6.97 – 6.96 (m, 2H), 6.94 – 6.92 (m, 1H), 6.64 – 6.61 (m, 2H), 4.99 (s, 1H), 3.73 (s, 3H), 2.91 (s, 6H), 1.32 (s, 18H); $^{13}\text{C}\{^1\text{H}\}$ NMR (100 MHz, CDCl_3) δ 194.2, 162.9, 152.2, 141.8, 135.6, 135.5, 135.4, 132.4, 131.9, 128.0, 127.2, 127.1, 126.2, 125.3, 124.0, 123.2, 119.6, 118.5, 118.0, 117.7, 112.9, 55.4, 43.6, 34.3, 30.3; FT-IR (thin film, neat): 3628, 2958, 2870, 1644, 1386, 1172, 1032, 738 cm^{-1} ; HRMS (ESI): m/z calcd for $\text{C}_{36}\text{H}_{41}\text{N}_2\text{O}_3$ $[\text{M}+\text{H}]^+$: 549.3117; found : 549.3116.

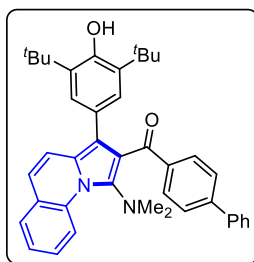
(4-chlorophenyl)-{3-[3,5-di-tert-butyl-4-hydroxyphenyl]-1-(dimethylamino)-pyrrolo(1,2-a)quinolin-2-yl}-methanone (43c)



The reaction was performed at 0.0868 mmol scale of **40b**; R_f = 0.3 (5% EtOAc in hexane); yellow solid (35.0 mg, 72% yield); m. p. = 154–156 °C; ^1H NMR (400 MHz, CDCl_3) δ 9.32 (d, J = 8.6 Hz, 1H), 7.60 – 7.57 (m, 3H), 7.51 – 7.47 (m, 1H), 7.36 – 7.31 (m, 2H), 7.09 – 7.06 (m, 2H), 6.94 (d, J = 9.4 Hz, 1H), 6.91 – 6.89 (m, 2H), 5.01 (s, 1H), 2.91 (s, 6H), 1.32 (s, 18H); $^{13}\text{C}\{^1\text{H}\}$ NMR (100 MHz, CDCl_3) δ 194.1, 152.4, 142.5, 138.3, 137.3, 135.7, 135.4, 131.4, 128.1, 127.9, 127.4, 127.3, 126.3, 125.1, 124.3, 123.4, 120.0, 119.1, 118.4, 118.1, 117.9, 43.4, 34.3, 30.3; FT-IR (thin film, neat): 3633, 2960, 2872, 1644, 1524, 1262, 736, 667 cm^{-1} ; HRMS (ESI): m/z calcd for $\text{C}_{35}\text{H}_{38}\text{ClN}_2\text{O}_2$ $[\text{M}+\text{H}]^+$: 553.2622; found : 553.2628.

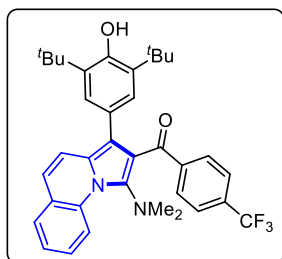
[1,1'-biphenyl]-4-yl-{3-[3,5-di-tert-butyl-4-hydroxyphenyl]-1-(dimethylamino)-pyrrolo[1,2-a]quinolin-2-yl}-methanone (43d)

The reaction was performed at 0.0868 mmol scale of **40b**; R_f = 0.3 (5% EtOAc in hexane); brown solid (39.3 mg, 76% yield); m. p. = 158–160 °C; ^1H NMR (400 MHz, CDCl_3) δ 9.37



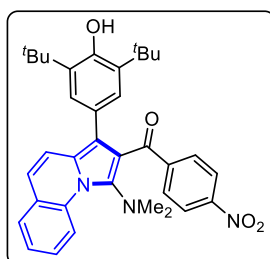
(d, $J = 8.6$ Hz, 1H), 7.77 (d, $J = 8.2$ Hz, 2H), 7.62 – 7.60 (m, 1H), 7.53 – 7.48 (m, 2H), 7.46 – 7.34 (m, 9H), 7.01 (s, 2H), 6.97 – 6.95 (m, 1H), 4.97 (s, 1H), 2.97 (s, 6H), 1.31 (s, 18H); $^{13}\text{C}\{^1\text{H}\}$ NMR (100 MHz, CDCl_3) δ 194.9, 152.3, 144.9, 142.4, 140.5, 137.6, 135.6, 135.4, 130.7, 128.9, 128.1, 127.9, 127.29, 127.26, 126.4, 126.3, 125.3, 124.1, 124.2, 123.3, 119.8, 119.5, 118.5, 118.0, 117.9, 43.5, 34.3, 30.3; FT-IR (thin film, neat): 3634, 2956, 1644, 1547, 1232, 1118, 748, 665 cm^{-1} ; HRMS (ESI): m/z calcd for $\text{C}_{41}\text{H}_{43}\text{N}_2\text{O}_2$ $[\text{M}+\text{H}]^+$: 595.3325; found : 595.3321.

{3-[3,5-di-tert-butyl-4-hydroxyphenyl]-1-(dimethylamino)-pyrrolo[1,2-a]quinolin-2-yl]-[4-(trifluoromethyl)-phenyl]-methanone (43e)}



The reaction was performed at 0.0868 mmol scale of **40b**; $R_f = 0.3$ (5% EtOAc in hexane); brown solid (31.2 mg, 61% yield); m. p. = 166–168 °C; ^1H NMR (400 MHz, CDCl_3) δ 9.35 (d, $J = 8.6$ Hz, 1H), 7.73 (d, $J = 8.0$ Hz, 2H), 7.61 – 7.59 (m, 1H), 7.53 – 7.49 (m, 1H), 7.38 – 7.33 (m, 3H), 7.32 – 7.30 (m, 1H), 6.95 (d, $J = 9.4$ Hz, 1H), 6.88 (s, 2H), 4.98 (s, 1H), 2.96 (s, 6H), 1.30 (s, 18H); $^{13}\text{C}\{^1\text{H}\}$ NMR (100 MHz, CDCl_3) δ 193.8, 152.4, 143.2, 141.0 (q, $J_{\text{C-F}} = 4.1$ Hz), 135.7, 135.3, 133.0 (q, $J_{\text{C-F}} = 32.3$ Hz), 130.2, 128.2, 127.5, 127.4, 126.4, 125.0, 124.6 (d, $J_{\text{C-F}} = 3.7$ Hz), 124.4, 123.7 (q, $J_{\text{C-F}} = 271.0$ Hz), 123.6, 120.2, 118.9, 118.3, 118.15, 118.11, 43.3, 34.2, 30.2; $^{19}\text{F}\{^1\text{H}\}$ NMR (376 MHz, CDCl_3) δ -63.21; FT-IR (thin film, neat): 3632, 2965, 1649, 1390, 1263, 1123, 736, 668 cm^{-1} ; HRMS (ESI): m/z calcd for $\text{C}_{36}\text{H}_{38}\text{F}_3\text{N}_2\text{O}_2$ $[\text{M}+\text{H}]^+$: 587.2885; found : 587.2883.

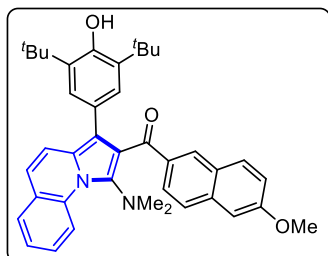
{3-[3,5-di-tert-butyl-4-hydroxyphenyl]-1-(dimethylamino)-pyrrolo[1,2-a]quinolin-2-yl]-[4-nitrophenyl]-methanone (43f)}



The reaction was performed at 0.0868 mmol scale of **40b**; $R_f = 0.4$ (10% EtOAc in hexane); dark brown solid (28.4 mg, 58% yield); m. p. = 186–188 °C; ^1H NMR (400 MHz, CDCl_3) δ 9.33 (d, $J = 8.6$ Hz, 1H), 7.94 – 7.91 (m, 2H), 7.75 – 7.73 (m, 2H), 7.61 – 7.59 (m, 1H), 7.54 – 7.49 (m, 1H), 7.39 – 7.35 (m, 1H), 7.29 – 7.27 (m, 1H), 6.97 – 6.95 (m, 1H), 6.87 (s, 2H), 4.99 (s, 1H), 2.95 (s, 6H), 1.29 (s, 18H); $^{13}\text{C}\{^1\text{H}\}$ NMR (100 MHz, CDCl_3) δ 193.0, 152.5, 149.2, 144.1, 143.3, 135.9, 135.3, 130.7, 128.2, 127.6, 127.4, 126.4, 124.9, 124.6, 123.8, 122.7, 120.5, 118.6, 118.2, 118.1, 118.0, 43.2, 34.3, 30.3; FT-IR (thin film, neat): 3632,

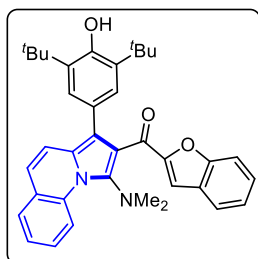
2957, 1653, 1523, 1347, 1264, 1148, 894, 738 cm^{-1} ; HRMS (ESI): m/z calcd for $\text{C}_{35}\text{H}_{38}\text{N}_3\text{O}_4$ $[\text{M}+\text{H}]^+$: 564.2862; found : 564.2853.

(3-(3,5-di-tert-butyl-4-hydroxyphenyl)-1-(dimethylamino)pyrrolo[1,2-a]quinolin-2-yl)(6-methoxynaphthalen-2-yl)methanone (43g)



The reaction was performed at 0.087 mmol scale of **40b**; R_f = 0.4 (10% EtOAc in hexane); brown solid (43.2 mg, 83% yield); ^1H NMR (400 MHz, CDCl_3) δ 9.37 (d, J = 8.6 Hz, 1H), 8.00 (s, 1H), 7.90 (dd, J = 8.6, 1.6 Hz, 1H), 7.60 (dd, J = 7.8, 1.3 Hz, 1H), 7.55 – 7.53 (m, 1H), 7.51 – 7.48 (m, 2H), 7.39 – 7.33 (m, 2H), 7.05 – 7.00 (m, 2H), 6.97 – 6.94 (m, 3H), 4.78 (s, 1H), 3.89 (s, 3H), 2.95 (s, 6H), 1.19 (s, 18H); $^{13}\text{C}\{^1\text{H}\}$ NMR (100 MHz, CDCl_3) δ 195.1, 159.5, 152.1, 142.2, 136.8, 135.5, 135.4, 134.2, 133.0, 131.0, 130.0, 128.0, 127.5, 127.3, 127.1, 126.4, 126.3, 125.8, 125.4, 124.1, 123.3, 119.7, 119.1, 118.5, 118.1, 118.0, 105.6, 55.5, 43.6, 34.2, 30.2; FT-IR (thin film, neat): 3628, 2957, 1642, 1621, 1449, 1359, 1264, 1172, 1030, 733, 703 cm^{-1} ; HRMS (ESI): m/z calcd for $\text{C}_{40}\text{H}_{43}\text{N}_2\text{O}_3$ $[\text{M}+\text{H}]^+$: 599.3274; found : 599.3272.

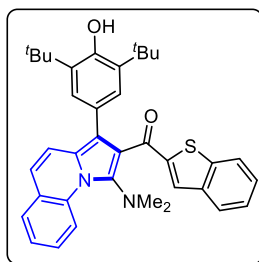
benzofuran-2-yl-{3-[3,5-di-tert-butyl-4-hydroxyphenyl]-1-(dimethylamino)-pyrrolo[1,2-a]quinolin-2-yl}-methanone (43h)



The reaction was performed at 0.0868 mmol scale of **40b**; R_f = 0.4 (10% EtOAc in hexane); brown solid (30.1 mg, 62% yield); m. p. = 178–170 $^{\circ}\text{C}$; ^1H NMR (400 MHz, CDCl_3) δ 9.33 (d, J = 8.6 Hz, 1H), 7.60 – 7.58 (m, 1H), 7.51 – 7.47 (m, 1H), 7.43 – 7.38 (m, 2H), 7.37 – 7.27 (m, 3H), 7.16 – 7.13 (m, 1H), 7.09 (s, 2H), 7.04 (s, 1H), 6.96 – 6.94 (m, 1H), 4.86 (s, 1H), 2.96 (s, 6H), 1.26 (s, 18H); $^{13}\text{C}\{^1\text{H}\}$ NMR (100 MHz, CDCl_3) δ 183.6, 155.3, 153.9, 152.3, 143.0, 135.8, 135.4, 128.1, 127.5, 127.4, 127.1, 126.7, 126.4, 125.5, 124.3, 123.6, 123.5, 122.8, 120.1, 118.6, 118.5, 118.1, 117.9, 114.9, 112.2, 43.4, 34.2, 30.3; FT-IR (thin film, neat): 3634, 2956, 1628, 1522, 1435, 1356, 1262, 1157, 874, 736 cm^{-1} ; HRMS (ESI): m/z calcd for $\text{C}_{37}\text{H}_{39}\text{N}_2\text{O}_3$ $[\text{M}+\text{H}]^+$: 559.2961; found : 559.2957.

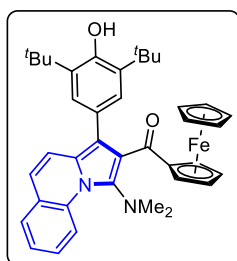
benzo[b]-thiophen-2-yl-{3-[3,5-di-tert-butyl-4-hydroxyphenyl]-1-(dimethylamino)-pyrrolo[1,2-a]quinolin-2-yl}-methanone (43i)

The reaction was performed at 0.0868 mmol scale of **40b**; R_f = 0.4 (10% EtOAc in hexane); brown solid (32.4 mg, 65% yield); m. p. = 184–186 $^{\circ}\text{C}$; ^1H NMR (400 MHz, CDCl_3) δ 9.34 (d,



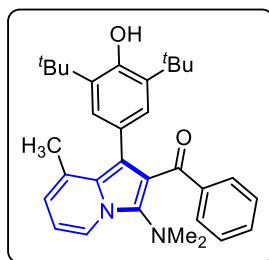
$J = 8.6$ Hz, 1H), 7.76 (d, $J = 8.1$ Hz, 1H), 7.61 – 7.59 (m, 1H), 7.52 – 7.46 (m, 2H), 7.42 – 7.40 (m, 1H), 7.37 – 7.33 (m, 2H), 7.31 (s, 1H), 7.24 – 7.20 (m, 1H), 7.10 (s, 2H), 6.98 – 6.96 (m, 1H), 4.89 (s, 1H), 2.95 (s, 6H), 1.27 (s, 18H); $^{13}\text{C}\{^1\text{H}\}$ NMR (100 MHz, CDCl_3) δ 188.8, 152.3, 145.1, 142.3, 142.0, 139.1, 135.9, 135.4, 133.1, 128.1, 127.4, 127.0 (2C), 126.3, 125.7, 125.4, 124.6, 124.2, 123.4, 122.7, 120.0, 119.1, 118.5, 118.0, 117.6, 43.6, 34.3, 30.3; FT-IR (thin film, neat): 3632, 2953, 1631, 1521, 1432, 1238, 1152, 1093, 856, 743 cm^{-1} ; HRMS (ESI): m/z calcd for $\text{C}_{37}\text{H}_{39}\text{N}_2\text{O}_2\text{S}$ $[\text{M}+\text{H}]^+$: 575.2732; found : 575.2734.

{3-[3,5-di-tert-butyl-4-hydroxyphenyl]-1-(dimethylamino)-pyrrolo[1,2-a]-quinolin-2-yl}-(ferrocenyl)-methanone (43j)



The reaction was performed at 0.0868 mmol scale of **40b**; $R_f = 0.4$ (5% EtOAc in hexane); brown solid (28.3 mg, 52% yield); m. p. = 186–188 °C; ^1H NMR (400 MHz, CDCl_3) δ 9.23 (d, $J = 8.6$ Hz, 1H), 7.58 – 7.55 (m, 1H), 7.48 – 7.44 (m, 1H), 7.36 – 7.30 (m, 2H), 7.10 (s, 2H), 6.89 (d, $J = 9.4$ Hz, 1H), 5.06 (s, 1H), 4.49 (t, $J = 1.9$ Hz, 2H), 4.17 (t, $J = 1.9$ Hz, 2H), 3.96 (s, 5H), 2.96 (s, 6H), 1.39 (s, 18H); $^{13}\text{C}\{^1\text{H}\}$ NMR (100 MHz, CDCl_3) δ 199.1, 152.5, 140.30, 135.5, 135.4, 128.0, 127.7, 127.1, 126.4, 125.7, 123.9, 123.4, 120.9, 119.3, 118.6, 117.8, 117.6, 83.0, 71.3, 70.7, 69.5, 43.3, 34.4, 30.5; FT-IR (thin film, neat): 3633, 2955, 2873, 1636, 1452, 1354, 1026, 892, 787 738 cm^{-1} ; HRMS (ESI): m/z calcd for $\text{C}_{39}\text{H}_{43}\text{FeN}_2\text{O}_2$ $[\text{M}+\text{H}]^+$: 627.2674; found : 627.2670.

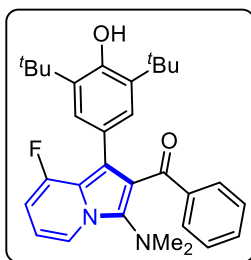
{1-[3,5-di-tert-butyl-4-hydroxyphenyl]-3-(dimethylamino)-8-methylindolizin-2-yl}-(phenyl)-methanone (43k)



The reaction was performed at 0.097 mmol scale of **40c**; $R_f = 0.3$ (5% EtOAc in hexane); brown solid (38.1 mg, 81% yield); m. p. = 168–170 °C; ^1H NMR (400 MHz, CDCl_3) δ 7.98 (d, $J = 7.0$ Hz, 1H), 7.54 – 7.52 (m, 2H), 7.26 – 7.21 (m, 1H), 7.11 – 7.08 (m, 2H), 6.86 (s, 2H), 6.50 (t, $J = 6.9$ Hz, 1H), 6.41 – 6.39 (m, 1H), 4.87 (s, 1H), 2.83 (s, 6H), 2.05 (s, 3H), 1.27 (s, 18H); $^{13}\text{C}\{^1\text{H}\}$ NMR (100 MHz, CDCl_3) δ 196.6, 152.0, 139.4, 135.2, 134.0, 131.7, 130.2, 129.8, 129.0, 127.5, 126.6, 123.7, 120.2, 119.9, 117.9, 115.3, 110.8, 43.5, 34.2, 30.3, 20.8; FT-IR (thin film, neat): 3635, 2955, 1733, 1647, 1522, 1448, 1399, 1236, 1155, 758 cm^{-1} ; HRMS (ESI): m/z calcd for $\text{C}_{32}\text{H}_{39}\text{N}_2\text{O}_2$ $[\text{M}+\text{H}]^+$: 483.3012; found : 483.2995.

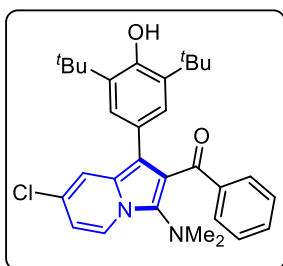
{1-[3,5-di-tert-butyl-4-hydroxyphenyl]-3-(dimethylamino)-8-fluoroindolizin-2-yl}-(phenyl)-methanone (43l)

The reaction was performed at 0.096 mmol scale of **40d**; $R_f = 0.4$ (5% EtOAc in hexane);



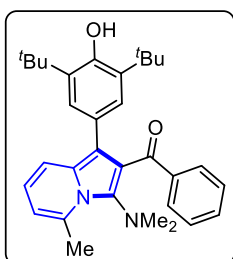
brown solid (33.0 mg, 70% yield); m. p. = 124–126 °C; ^1H NMR (400 MHz, CDCl_3) δ 7.89 (d, $J = 7.0$ Hz, 1H), 7.64 – 7.62 (m, 2H), 7.29 – 7.26 (m, 1H), 7.12 (t, $J = 7.8$ Hz, 2H), 6.97 (d, $J = 2.9$ Hz, 2H), 6.51 – 6.47 (m, 1H), 6.37 – 6.32 (m, 1H), 4.92 (s, 1H), 2.84 (s, 6H), 1.29 (s, 18H); $^{13}\text{C}\{^1\text{H}\}$ NMR (100 MHz, CDCl_3) δ 195.4, 156.1 (d, $J_{\text{C-F}} = 249.5$ Hz), 152.2, 138.4, 136.9, 134.6, 132.2, 130.0, 127.8 (d, $J_{\text{C-F}} = 2.2$ Hz), 127.6, 125.1, 119.9, 118.2 (d, $J_{\text{C-F}} = 4.1$ Hz), 115.3 (d, $J_{\text{C-F}} = 31.4$ Hz), 114.4 (d, $J_{\text{C-F}} = 4.7$ Hz), 109.7 (d, $J_{\text{C-F}} = 7.9$ Hz), 100.0 (d, $J_{\text{C-F}} = 18.9$ Hz), 43.4, 34.2, 30.3; $^{19}\text{F}\{^1\text{H}\}$ NMR (376 MHz, CDCl_3) δ -121.52; FT-IR (thin film, neat): 3634, 3469, 2956, 1732, 1646, 1598, 1448, 1354, 1295, 1120, 1071, 1042, 887, 692 cm^{-1} ; HRMS (ESI): m/z calcd for $\text{C}_{31}\text{H}_{36}\text{FN}_2\text{O}_2$ $[\text{M}+\text{H}]^+$: 487.2761; found: 487.2758.

(7-chloro-1-(3,5-di-tert-butyl-4-hydroxyphenyl)-3-(dimethylamino)indolizin-2-yl)(phenyl)methanone (43m)



The reaction was performed at 0.0909 mmol scale of **40e**; $R_f = 0.4$ (5% EtOAc in hexane); brown gummy solid (31.2 mg, 68% yield); ^1H NMR (400 MHz, CDCl_3) δ 8.01 (d, $J = 7.2$ Hz, 1H), 7.67 – 7.65 (m, 2H), 7.47 (s, 1H), 7.32 – 7.28 (m, 1H), 7.14 (t, $J = 7.8$ Hz, 2H), 6.92 (s, 2H), 6.55 (d, $J = 6.8$ Hz, 1H), 4.97 (s, 1H), 2.85 (s, 6H), 1.31 (s, 18H); $^{13}\text{C}\{^1\text{H}\}$ NMR (100 MHz, CDCl_3) δ 195.3, 152.2, 138.6, 135.7, 132.3, 130.1, 128.9, 127.7, 127.5, 126.8, 125.2, 122.6, 119.4, 119.3, 117.3, 114.5, 113.0, 43.5, 34.3, 30.3; FT-IR (thin film, neat): 3632, 3442, 2958, 1732, 1436, 1303, 1236, 1036, 838, 637 cm^{-1} ; HRMS (ESI): m/z calcd for $\text{C}_{31}\text{H}_{36}\text{ClN}_2\text{O}_2$ $[\text{M}+\text{H}]^+$: 503.2465; found: 503.2468.

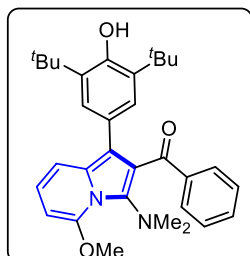
{1-[3,5-di-tert-butyl-4-hydroxyphenyl]-3-(dimethylamino)-5-methylindolizin-2-yl}-(phenyl)-methanone (43n)



The reaction was performed at 0.0969 mmol scale of **40f**; $R_f = 0.4$ (5% EtOAc in hexane); brown solid (18.1 mg, 38% yield); m. p. = 142–144 °C; ^1H NMR (400 MHz, CDCl_3) δ 7.64 – 7.62 (m, 2H), 7.42 – 7.40 (m, 1H), 7.27 – 7.23 (m, 1H), 7.10 (t, $J = 7.8$ Hz, 2H), 6.94 (s, 2H), 6.60 – 6.56 (m, 1H), 6.28 – 6.27 (m, 1H), 4.91 (s, 1H), 2.86 (s, 3H), 2.84 (s, 6H), 1.29 (s, 18H); $^{13}\text{C}\{^1\text{H}\}$ NMR (100 MHz, CDCl_3) δ 196.1, 151.9, 138.8, 137.5, 135.5, 135.2, 131.9, 130.0, 127.6, 127.0, 126.0, 125.8, 121.6, 118.0, 117.0, 115.1, 113.8, 45.5, 34.3, 30.3, 20.8; FT-

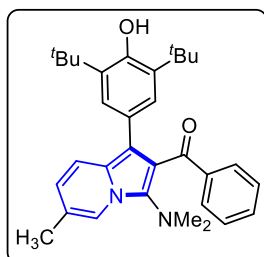
IR (thin film, neat): 3634, 2954, 1732, 1446, 1352, 1238, 1152, 756 cm^{-1} ; HRMS (ESI): m/z calcd for $\text{C}_{32}\text{H}_{39}\text{N}_2\text{O}_2$ $[\text{M}+\text{H}]^+$: 483.3012; found : 483.3010.

{1-[3,5-di-tert-butyl-4-hydroxyphenyl]-3-(dimethylamino)-5-methoxyindolizin-2-yl}-(phenyl)-methanone (43o)



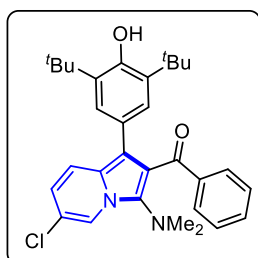
The reaction was performed at 0.0922 mmol scale of **40g**; R_f = 0.4 (10% EtOAc in hexane); yellow solid (16.2 mg, 35% yield); m. p. = 146–148 $^{\circ}\text{C}$; ^1H NMR (400 MHz, CDCl_3) δ 8.04 (d, J = 7.1 Hz, 1H), 7.69 – 7.65 (m, 2H), 7.51 (d, J = 9.0 Hz, 1H), 6.98 (s, 2H), 6.68 – 6.64 (m, 1H), 6.63 – 6.60 (m, 2H), 6.59 – 6.55 (m, 1H), 4.95 (s, 1H), 3.72 (s, 3H), 2.84 (s, 6H), 1.31 (s, 18H); $^{13}\text{C}\{^1\text{H}\}$ NMR (100 MHz, CDCl_3) δ 194.3, 162.9, 151.8, 135.6, 135.1, 132.5, 131.9, 126.8, 126.0, 124.1, 121.7, 118.9, 117.5, 114.2, 112.9 (2C), 111.3, 55.4, 43.5, 34.3, 30.3; FT-IR (thin film, neat): 3628, 2958, 1644, 1451, 1263, 1171, 1033, 858, 734 cm^{-1} ; HRMS (ESI): m/z calcd for $\text{C}_{32}\text{H}_{38}\text{NaN}_2\text{O}_3$ $[\text{M}+\text{Na}]^+$: 521.2780; found : 521.2800.

(1-(3,5-di-tert-butyl-4-hydroxyphenyl)-3-(dimethylamino)-6-methylindolizin-2-yl)(phenyl)methanone (43p)



The reaction was performed at 0.0969 mmol scale of **40h**; R_f = 0.4 (10% EtOAc in hexane); light brown gummy solid (36.5 mg, 78% yield); ^1H NMR (400 MHz, CDCl_3) δ 7.85 (s, 1H), 7.66 – 7.64 (m, 2H), 7.42 (d, J = 9.2 Hz, 1H), 7.28 – 7.24 (m, 1H), 7.12 – 7.08 (m, 2H), 6.93 (s, 2H), 6.55 (d, J = 9.1 Hz, 1H), 4.92 (s, 1H), 2.85 (s, 6H), 2.29 (s, 3H), 1.29 (s, 18H); $^{13}\text{C}\{^1\text{H}\}$ NMR (100 MHz, CDCl_3) δ 195.6, 151.8, 138.9, 135.5, 135.3, 132.0, 130.2, 127.6, 126.9, 126.0, 123.3, 121.2, 120.9, 118.9, 118.5, 118.4, 114.5, 43.4, 34.3, 30.3, 18.8; FT-IR (thin film, neat): 3633, 2956, 1732, 1646, 1524, 1446, 1386, 1238, 1154, 754 cm^{-1} ; HRMS (ESI): m/z calcd for $\text{C}_{32}\text{H}_{39}\text{N}_2\text{O}_2$ $[\text{M}+\text{H}]^+$: 483.3012; found : 483.3009.

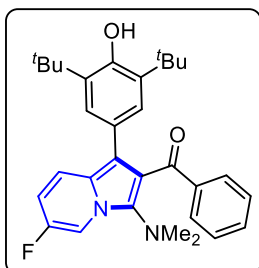
(6-chloro-1-(3,5-di-tert-butyl-4-hydroxyphenyl)-3-(dimethylamino)indolizin-2-yl)(phenyl)methanone (43q)



The reaction was performed at 0.0909 mmol scale of **40i**; R_f = 0.4 (5% EtOAc in hexane); brown solid (30.2 mg, 66% yield); m. p. = 152–154 $^{\circ}\text{C}$; ^1H NMR (400 MHz, CDCl_3) δ 8.09 (d, J = 0.8 Hz, 1H), 7.65 – 7.62 (m, 2H), 7.43 (d, J = 9.5 Hz, 1H), 7.30 – 7.26 (m, 1H), 7.14 – 7.10 (m, 2H), 6.91 (s, 2H), 6.62 (dd, J = 9.5, 1.8 Hz, 1H), 4.96 (s, 1H), 2.83 (s,

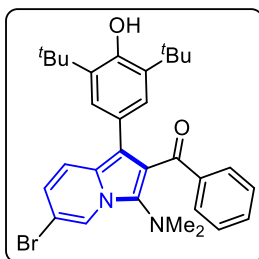
6H), 1.28 (s, 18H); $^{13}\text{C}\{^1\text{H}\}$ NMR (100 MHz, CDCl_3) δ 195.2, 152.2, 138.5, 135.8, 135.7, 132.3, 130.1, 127.7, 126.8, 125.2, 122.5, 120.3, 119.7, 119.3, 119.2, 119.1, 116.0, 43.4, 34.3, 30.3; FT-IR (thin film, neat): 3632, 2958, 1524, 1446, 1357, 1235, 1086, 743 cm^{-1} ; HRMS (ESI): m/z calcd for $\text{C}_{31}\text{H}_{36}\text{ClN}_2\text{O}_2$ $[\text{M}+\text{H}]^+$: 503.2465; found : 503.2466.

(1-(3,5-di-tert-butyl-4-hydroxyphenyl)-3-(dimethylamino)-6-fluoroindolizin-2-yl)(phenyl)methanone (43r)



The reaction was performed at 0.096 mmol scale of **40j**; R_f = 0.4 (10% EtOAc in hexane); brown solid (29.6 mg, 63% yield); m. p. = 126–128 $^{\circ}\text{C}$; ^1H NMR (400 MHz, CDCl_3) δ 8.00 (dd, J = 5.2, 1.8 Hz, 1H), 7.65 – 7.63 (m, 2H), 7.46 (dd, J = 9.8, 5.5 Hz, 1H), 7.29 – 7.25 (m, 1H), 7.12 (t, J = 7.9 Hz, 2H), 6.91 (s, 2H), 6.63 – 6.58 (m, 1H), 4.95 (s, 1H), 2.84 (s, 6H), 1.28 (s, 18H); $^{13}\text{C}\{^1\text{H}\}$ NMR (100 MHz, CDCl_3) δ 195.2, 154.2 (d, $J_{\text{C-F}}$ = 233.4 Hz), 152.2, 138.6, 136.5 (d, $J_{\text{C-F}}$ = 2.6 Hz), 135.7, 132.2, 130.1, 127.7, 126.9, 125.4, 122.3, 120.2 (d, $J_{\text{C-F}}$ = 9.3 Hz), 119.4 (d, $J_{\text{C-F}}$ = 2.5 Hz), 116.2, 110.5 (d, $J_{\text{C-F}}$ = 26.9 Hz), 107.4 (d, $J_{\text{C-F}}$ = 41.6 Hz), 43.2, 34.3, 30.3; $^{19}\text{F}\{^1\text{H}\}$ NMR (376 MHz, CDCl_3) δ -141.24; FT-IR (thin film, neat): 3632, 3442, 2958, 1732, 1520, 1434, 1352, 1258, 1015, 892, 736 cm^{-1} ; HRMS (ESI): m/z calcd for $\text{C}_{31}\text{H}_{36}\text{FN}_2\text{O}_2$ $[\text{M}+\text{H}]^+$: 487.2761; found : 487.2766.

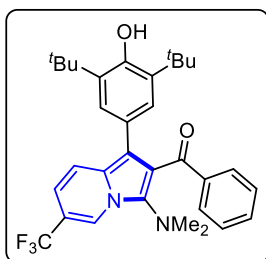
{6-bromo-1-[3,5-di-tert-butyl-4-hydroxyphenyl]-3-(dimethylamino)-indolizin-2-yl}-(phenyl)-methanone (43s)



The reaction was performed at 0.0801 mmol scale of **40k**; R_f = 0.2 (5% EtOAc in hexane); brown solid (30.1 mg, 68% yield); m. p. = 178–180 $^{\circ}\text{C}$; ^1H NMR (400 MHz, CDCl_3) δ 8.19 (d, J = 0.7 Hz, 1H), 7.64 – 7.61 (m, 2H), 7.39 – 7.36 (m, 1H), 7.30 – 7.26 (m, 1H), 7.11 (t, J = 7.9 Hz, 2H), 6.90 (s, 2H), 6.72 – 6.69 (m, 1H), 4.95 (s, 1H), 2.83 (s, 6H), 1.28 (s, 18H); $^{13}\text{C}\{^1\text{H}\}$ NMR (100 MHz, CDCl_3) δ 195.2, 152.2, 138.5, 135.7, 132.3, 130.1, 128.0, 127.7, 126.9, 125.2, 122.5, 121.6, 121.1, 119.9, 119.1, 116.1, 107.2, 43.4, 34.3, 30.3; FT-IR (thin film, neat): 3630, 2961, 1648, 1523, 1357, 1262, 1012, 893, 738 cm^{-1} ; HRMS (ESI): m/z calcd for $\text{C}_{31}\text{H}_{36}\text{BrN}_2\text{O}_2$ $[\text{M}+\text{H}]^+$: 547.1960; found : 547.1942.

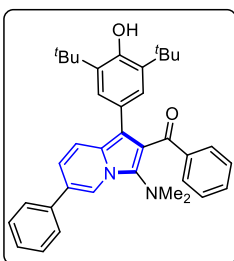
(1-(3,5-di-tert-butyl-4-hydroxyphenyl)-3-(dimethylamino)-6-(trifluoromethyl)indolizin-2-yl)(phenyl)methanone (43t)

The reaction was performed at 0.0825 mmol scale of **40l**; R_f = 0.4 (5% EtOAc in hexane); light brown gummy solid (27.1 mg, 61% yield); ^1H NMR (400 MHz, CDCl_3) δ 8.42 (s, 1H), 7.65 –



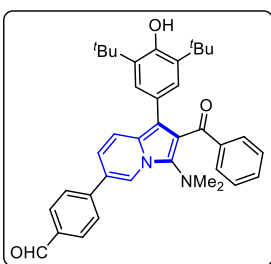
7.63 (m, 2H), 7.56 (d, $J = 9.4$ Hz, 1H), 7.30 (t, $J = 7.4$ Hz, 1H), 7.14 (t, $J = 7.7$ Hz, 2H), 6.93 (s, 2H), 6.78 – 6.75 (m, 1H), 4.99 (s, 1H), 2.85 (s, 6H), 1.29 (s, 18H); $^{13}\text{C}\{^1\text{H}\}$ NMR (100 MHz, CDCl_3) δ 195.1, 152.4, 138.3, 136.8, 135.8, 132.5, 130.1, 127.8, 126.8, 124.9, 124.4 (q, $J_{\text{C-F}} = 268.9$ Hz), 123.5, 121.1 (q, $J_{\text{C-F}} = 6.5$ Hz), 120.5, 119.9, 116.2, 115.7 (q, $J_{\text{C-F}} = 33.2$ Hz), 113.1 (q, $J_{\text{C-F}} = 2.4$ Hz), 43.6, 34.3, 30.2; $^{19}\text{F}\{^1\text{H}\}$ NMR (376 MHz, CDCl_3) δ -62.74; FT-IR (thin film, neat): 3633, 2964, 1649, 1324, 1262, 1154, 736 cm^{-1} ; HRMS (ESI): m/z calcd for $\text{C}_{32}\text{H}_{36}\text{F}_3\text{N}_2\text{O}_2$ $[\text{M}+\text{H}]^+$: 537.2729; found : 537.2744.

1-[3,5-di-tert-butyl-4-hydroxyphenyl]-3-(dimethylamino)-6-phenylindolizin-2-yl(phenyl)methanone (43u)



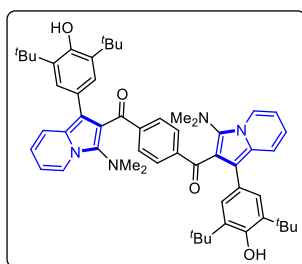
The reaction was performed at 0.1077 mmol scale of **40m**; $R_f = 0.4$ (5% EtOAc in hexane); pale yellow gummy solid (44.6 mg, 76% yield); ^1H NMR (400 MHz, CDCl_3) δ 8.29 (s, 1H), 7.71 – 7.65 (m, 4H), 7.59 (d, $J = 9.3$ Hz, 1H), 7.49 (t, $J = 7.6$ Hz, 2H), 7.39 (t, $J = 7.4$ Hz, 1H), 7.28 (dd, $J = 13.4, 6.0$ Hz, 2H), 7.14 (t, $J = 7.7$ Hz, 2H), 6.99 (s, 2H), 4.96 (s, 1H), 2.89 (s, 6H), 1.32 (s, 18H); $^{13}\text{C}\{^1\text{H}\}$ NMR (100 MHz, CDCl_3) δ 195.5, 152.0, 138.8, 138.7, 136.1, 135.6, 132.1, 130.2, 129.1, 127.6, 127.5, 126.9, 126.8, 125.7, 125.6, 123.4, 119.2, 119.1, 119.0, 118.6, 114.7, 43.5, 34.3, 30.3; FT-IR (thin film, neat): 3633, 2962, 2871, 1734, 1644, 1562, 1452, 1242, 706, cm^{-1} ; HRMS (ESI): m/z calcd for $\text{C}_{37}\text{H}_{41}\text{N}_2\text{O}_2$ $[\text{M}+\text{H}]^+$: 545.3168; found : 545.3173.

4-[2-benzoyl-1-(3,5-di-tert-butyl-4-hydroxyphenyl)-3-(dimethylamino)indolizin-6-yl]benzaldehyde (43v)



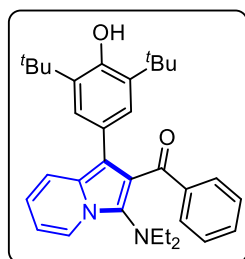
The reaction was performed at 0.100 mmol scale of **40n**; $R_f = 0.4$ (10% EtOAc in hexane); brown solid (37.0 mg, 64% yield); m. p. = 154–156 °C; ^1H NMR (400 MHz, CDCl_3) δ 10.07 (s, 1H), 8.38 – 8.37 (m, 1H), 8.00 – 7.98 (m, 2H), 7.83 (d, $J = 8.3$ Hz, 2H), 7.68 (dd, $J = 8.2, 1.1$ Hz, 2H), 7.61 (dd, $J = 9.4, 0.8$ Hz, 1H), 7.31 – 7.27 (m, 1H), 7.13 (t, $J = 7.7$ Hz, 2H), 7.01 (dd, $J = 9.4, 1.6$ Hz, 1H), 6.97 (s, 2H), 4.98 (s, 1H), 2.88 (s, 6H), 1.30 (s, 18H); $^{13}\text{C}\{^1\text{H}\}$ NMR (100 MHz, CDCl_3) δ 195.4, 191.9, 152.1, 144.8, 138.5, 136.4, 135.7, 135.3, 132.3, 130.6, 130.1, 127.7, 127.1, 126.8, 125.4, 124.2, 123.3, 120.1, 119.7, 119.5, 117.6, 115.3, 43.6, 34.3, 30.3; FT-IR (thin film, neat): 3634, 2870, 1700, 1646, 1390, 1170, 890, 738 cm^{-1} ; HRMS (ESI): m/z calcd for $\text{C}_{38}\text{H}_{41}\text{N}_2\text{O}_3$ $[\text{M}+\text{H}]^+$: 573.3117; found : 573.3127.

1,4-phenylenebis[[1-(3,5-di-tert-butyl-4-hydroxyphenyl)-3-(dimethylamino)indolizin-2-yl]methanone} (43w)



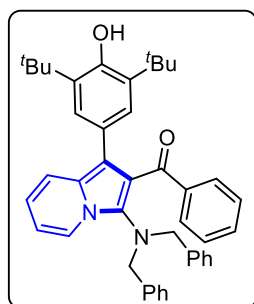
The reaction was performed at 0.1141 mmol scale of **2ap**; $R_f = 0.4$ (10% EtOAc in hexane); red solid (45.3 mg, 46% yield); m. p. = 156–158 °C; ^1H NMR (400 MHz, CDCl_3) δ 8.02 (d, $J = 7.1$ Hz, 2H), 7.45 (d, $J = 9.0$ Hz, 2H), 7.37 (s, 4H), 6.83 (s, 4H), 6.67 – 6.63 (m, 2H), 6.58 – 6.55 (m, 2H), 4.87 (s, 2H), 2.76 (s, 12H), 1.22 (s, 36H); $^{13}\text{C}\{^1\text{H}\}$ NMR (100 MHz, CDCl_3) δ 194.8, 151.9, 141.0, 135.6, 135.5, 129.2, 126.8, 125.5, 124.1, 121.7, 118.9, 118.4, 117.7, 114.3, 111.5, 43.3, 34.2, 30.2; FT-IR (thin film, neat): 3659, 3631, 2959, 1645, 1430, 1359, 1265, 1117, 738 cm^{-1} ; HRMS (ESI): m/z calcd for $\text{C}_{56}\text{H}_{67}\text{N}_4\text{O}_4$ $[\text{M}+\text{H}]^+$: 859.5162; found : 859.5160.

(1-(3,5-di-tert-butyl-4-hydroxyphenyl)-3-(diethylamino)indolizin-2-yl)(phenyl)methanone (44a)



The reaction was performed at 0.102 mmol scale of **40a**; $R_f = 0.4$ (5% EtOAc in hexane); pale yellow gummy solid (38.6 mg, 76% yield); ^1H NMR (400 MHz, CDCl_3) δ 8.27 (d, $J = 7.1$ Hz, 1H), 7.60 (d, $J = 7.3$ Hz, 2H), 7.50 (d, $J = 9.0$ Hz, 1H), 7.26 – 7.21 (m, 1H), 7.07 (t, $J = 7.8$ Hz, 2H), 6.94 (s, 2H), 6.68 (t, $J = 6.4$ Hz, 1H), 6.56 (t, $J = 6.5$ Hz, 1H), 4.90 (s, 1H), 3.18 (q, $J = 7.0$ Hz, 4H), 1.29 (s, 18H), 1.00 (t, $J = 7.2$ Hz, 6H); $^{13}\text{C}\{^1\text{H}\}$ NMR (100 MHz, CDCl_3) δ 195.7, 151.8, 138.8, 135.5, 132.7, 131.9, 130.0, 127.5, 126.9, 126.0, 124.7, 122.3, 120.9, 118.7, 118.0, 115.1, 111.3, 49.6, 34.3, 30.3, 14.2; FT-IR (thin film, neat): 3634, 3446, 2958, 1758, 1436, 1303, 1250, 1036, 838, 636 cm^{-1} ; HRMS (ESI): m/z calcd for $\text{C}_{33}\text{H}_{41}\text{N}_2\text{O}_2$ $[\text{M}+\text{H}]^+$: 497.3168; found : 497.3174.

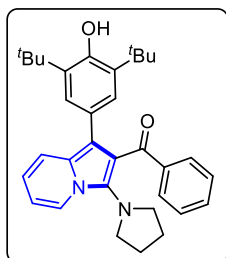
(1-(3,5-di-tert-butyl-4-hydroxyphenyl)-3-(dibenzylamino)indolizin-2-yl)(phenyl)methanone (44b)



The reaction was performed at 0.102 mmol scale of **40a**; $R_f = 0.4$ (5% EtOAc in hexane); pale brown gummy solid (35.1 mg, 55% yield); ^1H NMR (400 MHz, CDCl_3) δ 8.15 (d, $J = 7.2$ Hz, 1H), 7.50 – 7.48 (m, 2H), 7.40 (d, $J = 9.0$ Hz, 1H), 7.28 (dd, $J = 7.6, 1.6$ Hz, 4H), 7.24 – 7.20 (m, 4H), 7.18 – 7.16 (m, 3H), 7.06 (t, $J = 7.7$ Hz, 2H), 6.88 (s, 2H), 6.60 (ddd, $J = 9.0, 6.4, 0.8$ Hz, 1H), 6.47 – 6.43 (m, 1H), 4.91 (s, 1H), 4.35 (d, $J = 10.3$ Hz, 4H), 1.29 (s, 18H); $^{13}\text{C}\{^1\text{H}\}$ NMR (100 MHz, CDCl_3) δ 196.0, 151.8, 139.0,

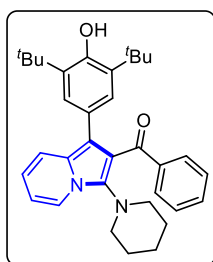
138.7, 135.5, 133.2, 131.9, 130.3, 129.0, 128.3, 127.4, 127.2, 127.0, 125.8, 124.5, 121.7, 120.7, 118.6, 118.0, 115.1, 111.5, 58.6, 34.3, 30.3; FT-IR (thin film, neat): 3632, 3442, 2956, 1758, 1434, 1303, 1250, 1034, 836, 634 cm^{-1} ; HRMS (ESI): m/z calcd for $\text{C}_{43}\text{H}_{45}\text{N}_2\text{O}_2$ $[\text{M}+\text{H}]^+$: 621.3481; found : 621.3493.

(1-(3,5-di-tert-butyl-4-hydroxyphenyl)-3-(pyrrolidin-1-yl)indolizin-2-yl)(phenyl)methanone (44c)



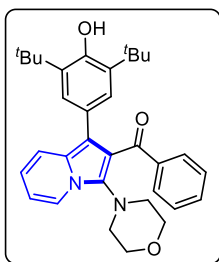
The reaction was performed at 0.102 mmol scale of **40a**; $R_f = 0.4$ (10% EtOAc in hexane); brown gummy solid (27.0 mg, 53% yield); ^1H NMR (400 MHz, CDCl_3) δ 8.05 (d, $J = 7.0$ Hz, 1H), 7.64 (d, $J = 7.4$ Hz, 2H), 7.49 (d, $J = 9.2$ Hz, 1H), 7.39 – 7.38 (m, 1H), 7.10 (t, $J = 7.7$ Hz, 2H), 6.95 (s, 2H), 6.67 (t, $J = 6.8$ Hz, 1H), 6.56 (t, $J = 6.7$ Hz, 1H), 4.91 (s, 1H), 3.27 (brs, 4H), 1.97 (brs, 4H), 1.29 (s, 18H); $^{13}\text{C}\{^1\text{H}\}$ NMR (100 MHz, CDCl_3) δ 195.7, 151.9, 139.0, 135.5, 132.0, 130.1, 129.2, 128.5, 128.4, 128.2, 128.0, 127.6, 126.9, 126.0, 122.2, 118.9, 111.4, 52.2, 34.3, 30.3, 25.9; FT-IR (thin film, neat): 3634, 3442, 2956, 1732, 1612, 1436, 1250, 1168, 1034, 638 cm^{-1} ; HRMS (ESI): m/z calcd for $\text{C}_{33}\text{H}_{39}\text{N}_2\text{O}_2$ $[\text{M}+\text{H}]^+$: 495.3012; found : 495.3017.

(1-(3,5-di-tert-butyl-4-hydroxyphenyl)-3-(piperidin-1-yl)indolizin-2-yl)(phenyl)methanone (44d)



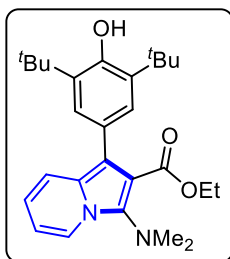
The reaction was performed at 0.102 mmol scale of **40a**; $R_f = 0.4$ (10% EtOAc in hexane); brown gummy solid (29.2 mg, 56% yield); ^1H NMR (400 MHz, CDCl_3) δ 8.05 (d, $J = 7.1$ Hz, 1H), 7.68 – 7.66 (m, 2H), 7.50 (d, $J = 9.0$ Hz, 1H), 7.30 – 7.26 (m, 1H), 7.12 (t, $J = 7.8$ Hz, 2H), 6.95 (s, 2H), 6.69 – 6.65 (m, 1H), 6.59 – 7.56 (m, 1H), 4.93 (s, 1H), 3.06 (brs, 4H), 1.71 – 1.67 (m, 4H), 1.30 (s, 18H), 1.27 (brs, 2H); $^{13}\text{C}\{^1\text{H}\}$ NMR (100 MHz, CDCl_3) δ 195.9, 151.9, 138.8, 135.5, 135.0, 132.1, 130.2, 127.6, 126.8, 125.9, 124.2, 121.7, 118.9, 118.7, 117.6, 114.4, 111.3, 52.2, 34.3, 30.3, 27.2, 24.2; FT-IR (thin film, neat): 3634, 3442, 2958, 1754, 1732, 1610, 1516, 1432, 1320, 1252, 1176, 1034, 838, 636 cm^{-1} ; HRMS (ESI): m/z calcd for $\text{C}_{33}\text{H}_{39}\text{N}_2\text{O}_2$ $[\text{M}+\text{H}]^+$: 495.3012; found : 495.3010.

(1-(3,5-di-tert-butyl-4-hydroxyphenyl)-3-morpholinoindolizin-2-yl)(phenyl)methanone (44e):



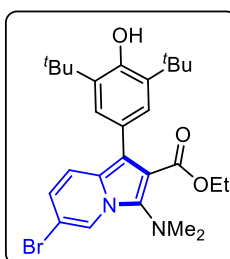
The reaction was performed at 0.102 mmol scale of **40a**; $R_f = 0.4$ (10% EtOAc in hexane); brown gummy solid (30.4 mg, 58% yield); ^1H NMR (400 MHz, CDCl_3) δ 8.12 (d, $J = 7.0$ Hz, 1H), 7.67 (d, $J = 7.8$ Hz, 2H), 7.52 (d, $J = 9.0$ Hz, 1H), 7.31 – 7.27 (m, 1H), 7.13 (t, $J = 7.6$ Hz, 2H), 6.95 (s, 2H), 6.70 (t, $J = 6.4$ Hz, 1H), 6.60 (t, $J = 6.8$ Hz, 1H), 4.94 (s, 1H), 3.84 (brs, 4H), 1.33 (d, $J = 3.9$ Hz, 4H), 1.28 (s, 18H); $^{13}\text{C}\{^1\text{H}\}$ NMR (100 MHz, CDCl_3) δ 195.6, 152.0, 138.6, 135.6, 132.8, 132.3, 130.2, 127.7, 126.8, 125.6, 124.6, 121.4, 119.5, 119.0, 118.0, 114.6, 111.7, 68.1, 51.3, 34.3, 30.3; FT-IR (thin film, neat): 3634, 3442, 2956, 1732, 1612, 1436, 1250, 1036, 834, 638 cm^{-1} ; HRMS (ESI): m/z calcd for $\text{C}_{33}\text{H}_{39}\text{N}_2\text{O}_3$ $[\text{M}+\text{H}]^+$: 511.2961; found : 511.2966.

ethyl 1-[3,5-di-tert-butyl-4-hydroxyphenyl]-3-(dimethylamino)indolizine-2-carboxylate (44f)



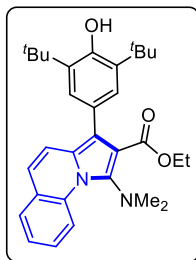
The reaction was performed at 0.102 mmol scale of **40a**; $R_f = 0.4$ (5% EtOAc in hexane); reddish brown gummy solid (32.3 mg, 72% yield); ^1H NMR (400 MHz, CDCl_3) δ 8.05 (d, $J = 3.6$ Hz, 1H), 7.38 (d, $J = 8.9$ Hz, 1H), 7.23 (s, 2H), 6.62 (s, 1H), 6.53 (t, $J = 6.6$ Hz, 1H), 5.18 (s, 1H), 4.22 (q, $J = 7.1$ Hz, 2H), 2.93 (s, 6H), 1.50 (s, 18H), 1.16 (t, $J = 7.1$ Hz, 3H); $^{13}\text{C}\{^1\text{H}\}$ NMR (100 MHz, CDCl_3) δ 166.4, 152.4, 135.4, 135.2, 126.9, 126.0, 125.4, 121.7, 119.0, 117.7, 114.4, 111.5, 111.2, 60.2, 42.8, 34.4, 30.6, 14.2; FT-IR (thin film, neat): 3640, 2956, 1706, 1617, 1447, 1262, 1179, 769, 662 cm^{-1} ; HRMS (ESI): m/z calcd for $\text{C}_{27}\text{H}_{37}\text{N}_2\text{O}_3$ $[\text{M}+\text{H}]^+$: 437.2804; found : 437.2796.

ethyl 6-bromo-1-[3,5-di-tert-butyl-4-hydroxyphenyl]-3-(dimethylamino)indolizine-2-carboxylate (44g)



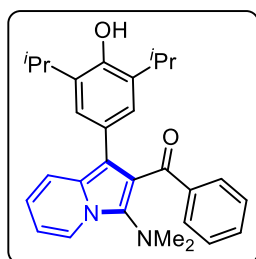
The reaction was performed at 0.107 mmol scale of **40k**; $R_f = 0.4$ (5% EtOAc in hexane); pale yellow gummy solid (33.2 mg, 60% yield); ^1H NMR (400 MHz, CDCl_3) δ 8.19 – 8.18 (m, 1H), 7.26 – 7.23 (m, 1H), 7.16 (s, 2H), 6.65 (dd, $J = 9.5, 1.7$ Hz, 1H), 5.19 (s, 1H), 4.20 (q, $J = 7.1$ Hz, 2H), 2.90 (s, 6H), 1.47 (s, 18H), 1.13 (t, $J = 7.1$ Hz, 3H); $^{13}\text{C}\{^1\text{H}\}$ NMR (100 MHz, CDCl_3) δ 165.9, 152.7, 135.6, 135.3, 126.9, 125.3, 123.8, 121.6, 121.1, 120.0, 116.1, 111.8, 107.3, 60.4, 42.8, 34.5, 30.6, 14.2; FT-IR (thin film, neat): 3640, 2958, 1704, 1519, 1391, 1179, 892, 737 cm^{-1} ; HRMS (ESI): m/z calcd for $\text{C}_{27}\text{H}_{36}\text{BrN}_2\text{O}_3$ $[\text{M}+\text{H}]^+$: 515.1909; found : 515.1900.

ethyl 3-[3,5-di-tert-butyl-4-hydroxyphenyl]-1-(dimethylamino)pyrrolo[1,2-a]quinoline-2-carboxylate (44h)



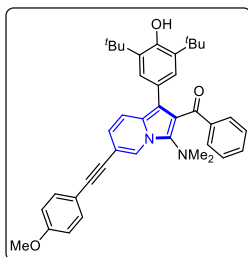
The reaction was performed at 0.101 mmol scale of **40b**; $R_f = 0.3$ (5% EtOAc in hexane); pale yellow gummy solid (34.0 mg, 69% yield); ^1H NMR (400 MHz, CDCl_3) δ 9.31 (d, $J = 8.6$ Hz, 1H), 7.55 (dd, $J = 7.7, 1.2$ Hz, 1H), 7.50 – 7.45 (m, 1H), 7.32 (t, $J = 7.4$ Hz, 1H), 7.23 (d, $J = 9.4$ Hz, 1H), 7.19 (s, 2H), 6.88 (d, $J = 9.4$ Hz, 1H), 5.19 (s, 1H), 4.20 (q, $J = 7.1$ Hz, 2H), 3.00 (s, 6H), 1.49 (s, 18H), 1.11 (t, $J = 7.1$ Hz, 3H); $^{13}\text{C}\{^1\text{H}\}$ NMR (100 MHz, CDCl_3) δ 166.4, 152.7, 142.0, 135.32 (d, $J = 9.2$ Hz), 128.1, 127.4, 127.0, 126.2, 125.6, 124.6, 124.2, 119.8, 118.5, 118.0, 117.8, 112.3, 60.3, 42.7, 34.5, 30.6, 14.2; FT-IR (thin film, neat): 3638, 2956, 1706, 1617, 1447, 1263, 1178, 768, 662 cm^{-1} ; HRMS (ESI): m/z calcd for $\text{C}_{31}\text{H}_{39}\text{N}_2\text{O}_3$ $[\text{M}+\text{H}]^+$: 487.2961; found : 487.2966.

{3-[dimethylamino]-1-(4-hydroxy-3,5-diisopropylphenyl)indolizin-2-yl}(phenyl)methanone (44i)



The reaction was performed at 0.1122 mmol scale of **40o**; $R_f = 0.3$ (5% EtOAc in hexane); red solid (36.0 mg, 73% yield); m. p. = 156–158 $^{\circ}\text{C}$; ^1H NMR (400 MHz, CDCl_3) δ 8.05 (d, $J = 6.6$ Hz, 1H), 7.72 (s, 1H), 7.70 (d, $J = 1.3$ Hz, 1H), 7.47 (d, $J = 8.8$ Hz, 1H), 7.30 – 7.26 (m, 1H), 7.13 (t, $J = 7.7$ Hz, 2H), 6.86 (s, 2H), 6.71 – 6.63 (m, 1H), 6.58 (t, $J = 6.5$ Hz, 1H), 4.67 (s, 1H), 3.06 – 2.97 (m, 2H), 2.84 (s, 6H), 1.11 (d, $J = 6.8$ Hz, 12H); $^{13}\text{C}\{^1\text{H}\}$ NMR (100 MHz, CDCl_3) δ 195.9, 147.9, 138.6, 135.34, 135.30, 133.5, 133.4, 132.3, 130.3, 127.7, 125.30, 125.29, 121.7, 118.85, 118.83, 114.0, 111.4, 43.5, 29.8, 27.0, 22.8; FT-IR (thin film, neat): 3444, 2960, 1644, 1356, 1150, 892, 728, 691 cm^{-1} ; HRMS (ESI): m/z calcd for $\text{C}_{29}\text{H}_{33}\text{N}_2\text{O}_2$ $[\text{M}+\text{H}]^+$: 441.2542; found : 441.2557.

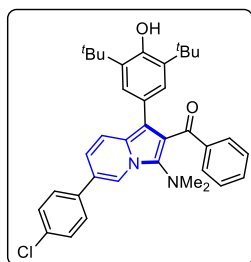
{1-[3,5-di-tert-butyl-4-hydroxyphenyl]-3-(dimethylamino)-6-[(4-methoxyphenyl)ethynyl]indolizin-2-yl}(phenyl)methanone (45)



The reaction was performed at 0.1096 mmol scale of **43s**; $R_f = 0.3$ (5% EtOAc in hexane); dark brown solid (42.0 mg, 64% yield); m. p. = 124–128 $^{\circ}\text{C}$; ^1H NMR (400 MHz, CDCl_3) δ 8.30 (s, 1H), 7.69 – 7.64 (m, 2H), 7.52 – 7.48 (m, 2H), 7.45 (dd, $J = 9.3, 0.7$ Hz, 1H), 7.28 (t, $J = 7.4$ Hz, 1H), 7.13 (t, $J = 7.7$ Hz, 2H), 6.94 (s, 2H), 6.90 (d, $J = 8.8$ Hz, 2H), 6.75 (dd, $J = 9.3, 1.4$ Hz, 1H), 4.96 (s, 1H), 3.84 (s, 3H), 2.86 (s, 6H), 1.29 (s, 18H); $^{13}\text{C}\{^1\text{H}\}$ NMR

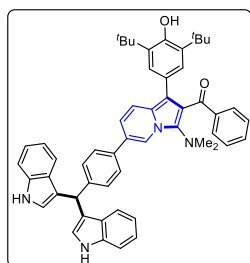
(100 MHz, CDCl₃) δ 195.3, 159.7, 152.1, 138.6, 135.9, 135.6, 133.1, 132.2, 130.1, 127.7, 126.8, 125.4, 124.9, 122.8, 120.3, 119.6, 118.6, 115.5, 115.4, 114.2, 108.1, 89.7, 86.1, 55.4, 43.5, 34.3, 30.3; FT-IR (thin film, neat): 3633, 2925, 1733, 1603, 1508, 1390, 1248, 1120, 791 cm⁻¹; HRMS (ESI): m/z calcd for C₄₀H₄₃N₂O₃ [M+H]⁺ : 599.3274; found : 599.3270.

{6-[4-chlorophenyl]-1-(3,5-di-tert-butyl-4-hydroxyphenyl)-3-(dimethylamino)indolizin-2-yl}(phenyl)methanone (46)



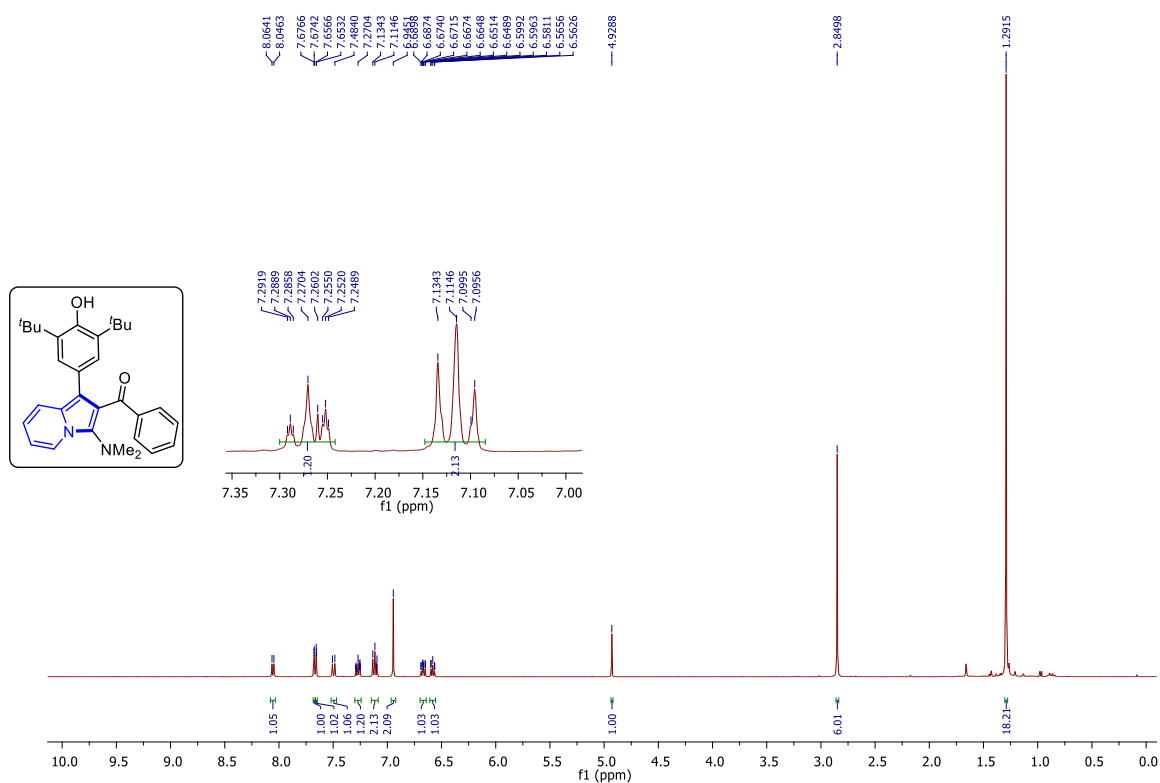
The reaction was performed at 0.1096 mmol scale of **43s**; R_f = 0.4 (5% EtOAc in hexane); brown solid (37.2 mg, 58% yield); m. p. = 134–136 °C; ¹H NMR (400 MHz, CDCl₃) δ 8.25 (s, 1H), 7.68 (d, J = 8.0 Hz, 2H), 7.58 (d, J = 8.6 Hz, 3H), 7.44 (d, J = 8.5 Hz, 2H), 7.29 (t, J = 7.4 Hz, 1H), 7.13 (t, J = 7.7 Hz, 2H), 6.97 (s, 2H), 6.93 (dd, J = 9.4, 1.5 Hz, 1H), 4.96 (s, 1H), 2.88 (s, 6H), 1.31 (s, 18H); ¹³C{¹H} NMR (100 MHz, CDCl₃) δ 195.4, 152.1, 138.7, 137.2, 136.2, 135.6, 133.4, 132.2, 130.1, 129.2, 128.0, 127.7, 126.9, 125.6, 124.5, 123.3, 119.4, 119.3, 119.0, 118.1, 115.0, 43.5, 34.3, 30.3; FT-IR (thin film, neat): 3633, 2960, 2872, 1736, 1644, 1558, 1448, 1242, 734, 665 cm⁻¹; HRMS (ESI): m/z calcd for C₃₇H₄₀ClN₂O₂ [M+H]⁺ : 579.2778; found : 579.2764.

{6-[4-(di(1H-indol-3-yl)methyl)phenyl]-1-(3,5-di-tert-butyl-4-hydroxyphenyl)-3-(dimethylamino)indolizin-2-yl}(phenyl)methanone (50)

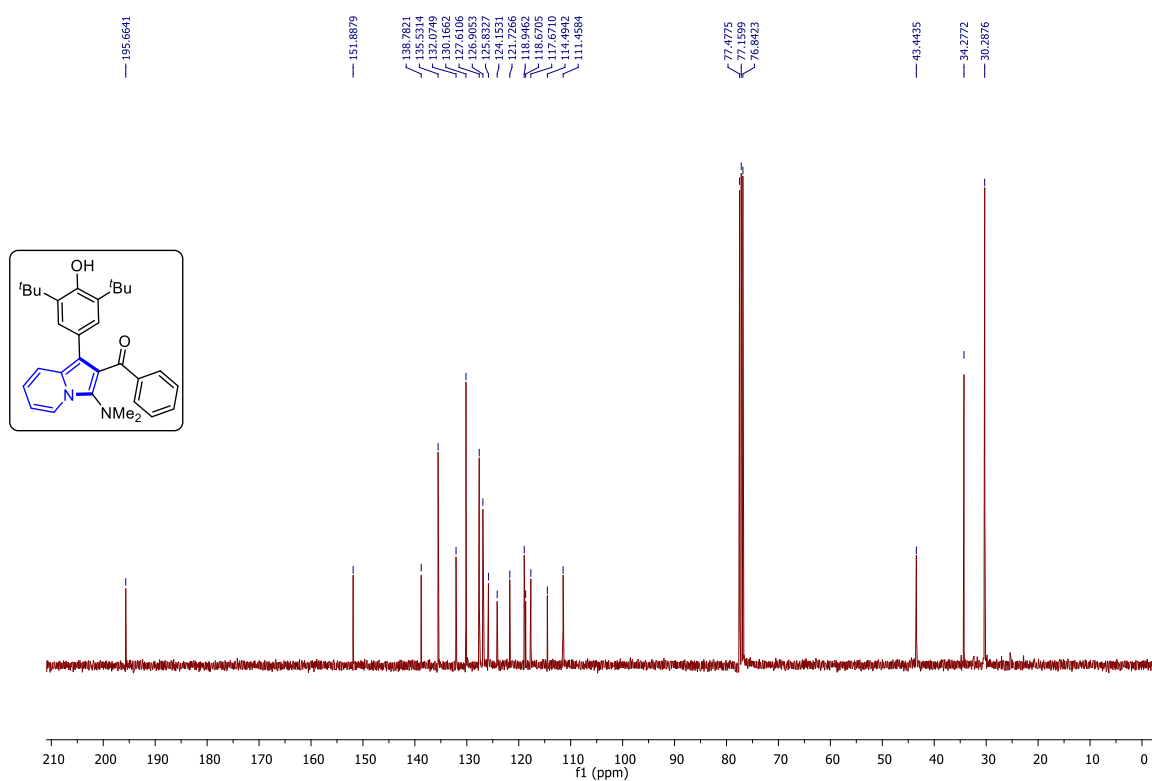


The reaction was performed at 0.105 mmol scale of **43v**; R_f = 0.2 (20% EtOAc in hexane); reddish brown solid (55.2 mg, 66% yield); m. p. = 150–152 °C; ¹H NMR (400 MHz, CDCl₃) δ 8.28 (s, 1H), 7.99 (d, J = 1.6 Hz, 2H), 7.72 – 7.70 (m, 2H), 7.59 – 7.56 (m, 3H), 7.46 (dd, J = 7.9, 5.1 Hz, 4H), 7.36 (d, J = 8.1 Hz, 2H), 7.29 (d, J = 7.4 Hz, 1H), 7.22 – 7.18 (m, 2H), 7.15 (t, J = 7.7 Hz, 2H), 7.05 (dd, J = 11.1, 3.9 Hz, 2H), 7.01 – 6.98 (m, 3H), 6.69 (d, J = 1.7 Hz, 2H), 5.97 (s, 1H), 4.97 (s, 1H), 2.88 (s, 6H), 1.32 (s, 18H); ¹³C{¹H} NMR (100 MHz, CDCl₃) δ 195.7, 151.9, 143.5, 138.8, 136.8, 136.3, 136.0, 135.6, 132.2, 130.2, 129.4, 127.6, 127.1, 126.9, 126.6, 125.8, 125.6, 123.8, 123.4, 122.1, 120.0, 119.5, 119.3, 119.1, 118.9, 118.8, 118.7, 114.6, 111.2, 43.5, 40.0, 34.3, 30.3; FT-IR (thin film, neat): 3632, 3414, 2926, 2870, 1640, 1450, 1235, 890, 739, 662 cm⁻¹; HRMS (ESI): m/z calcd for C₅₄H₅₃N₄O₂ [M+H]⁺ : 789.4169; found : 789.4125.

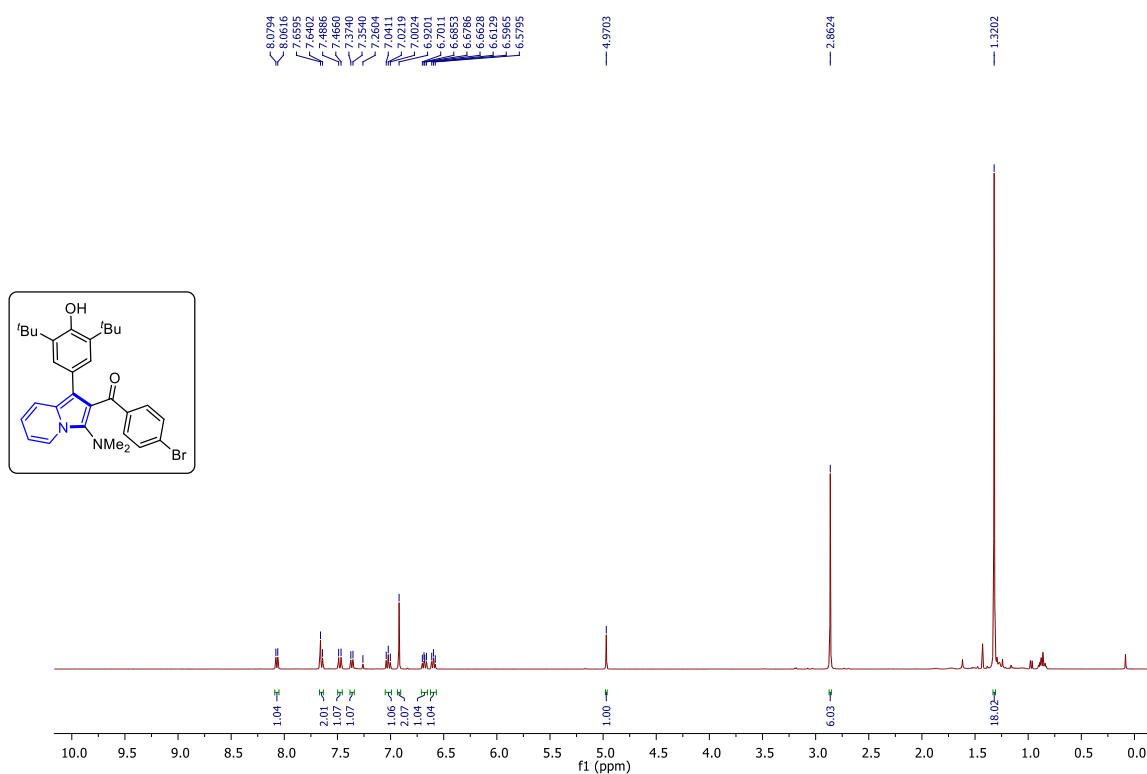
¹H NMR (400 MHz, CDCl₃) spectrum of (**42a**)



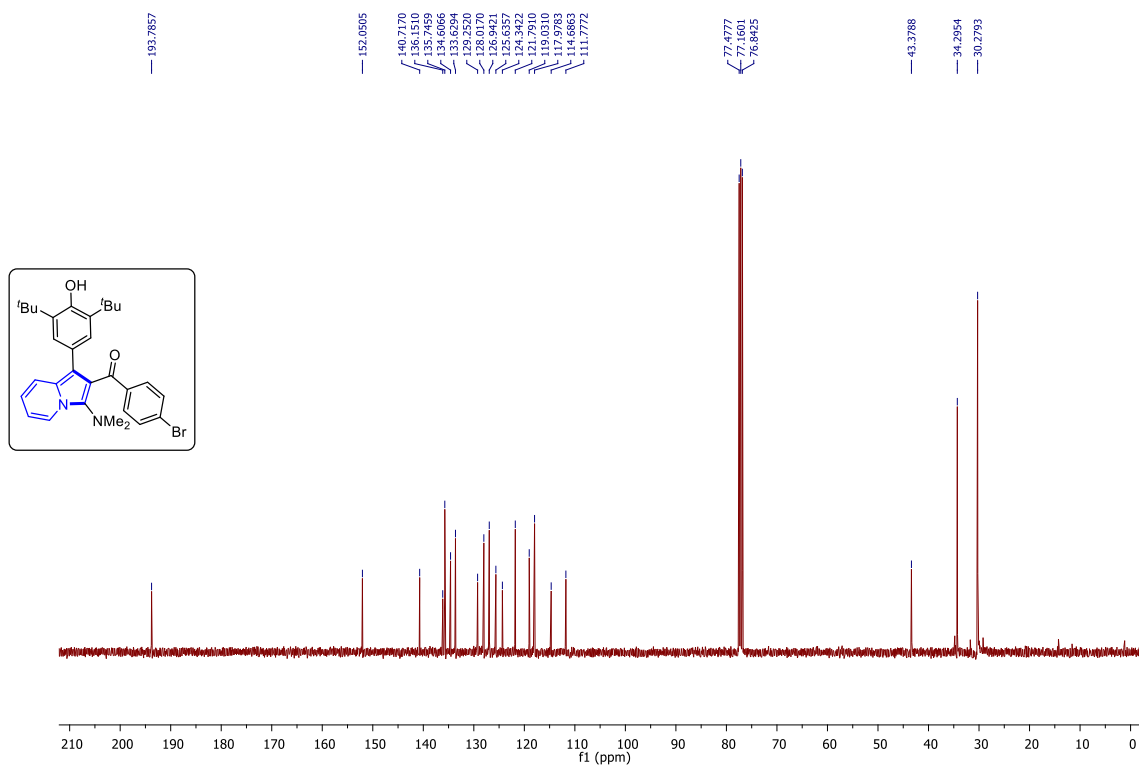
¹³C{¹H} NMR (100 MHz, CDCl₃) spectrum of (**42a**)



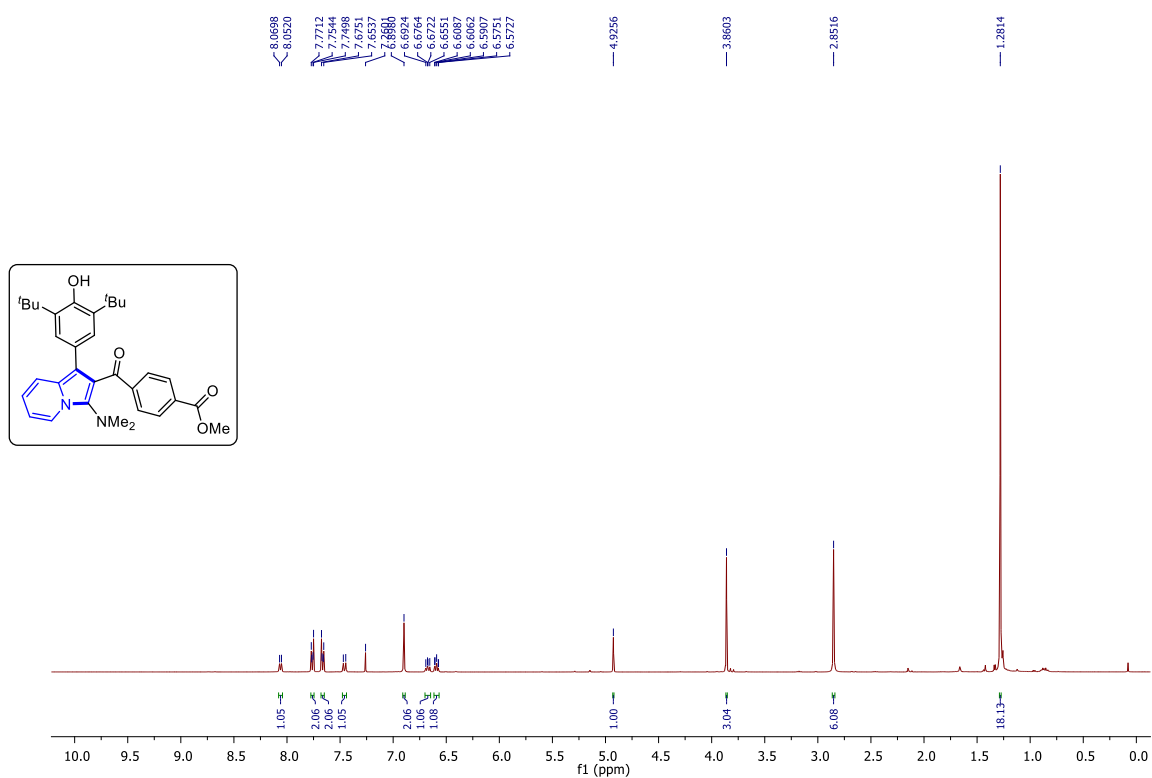
^1H NMR (400 MHz, CDCl_3) spectrum of (**42s**)



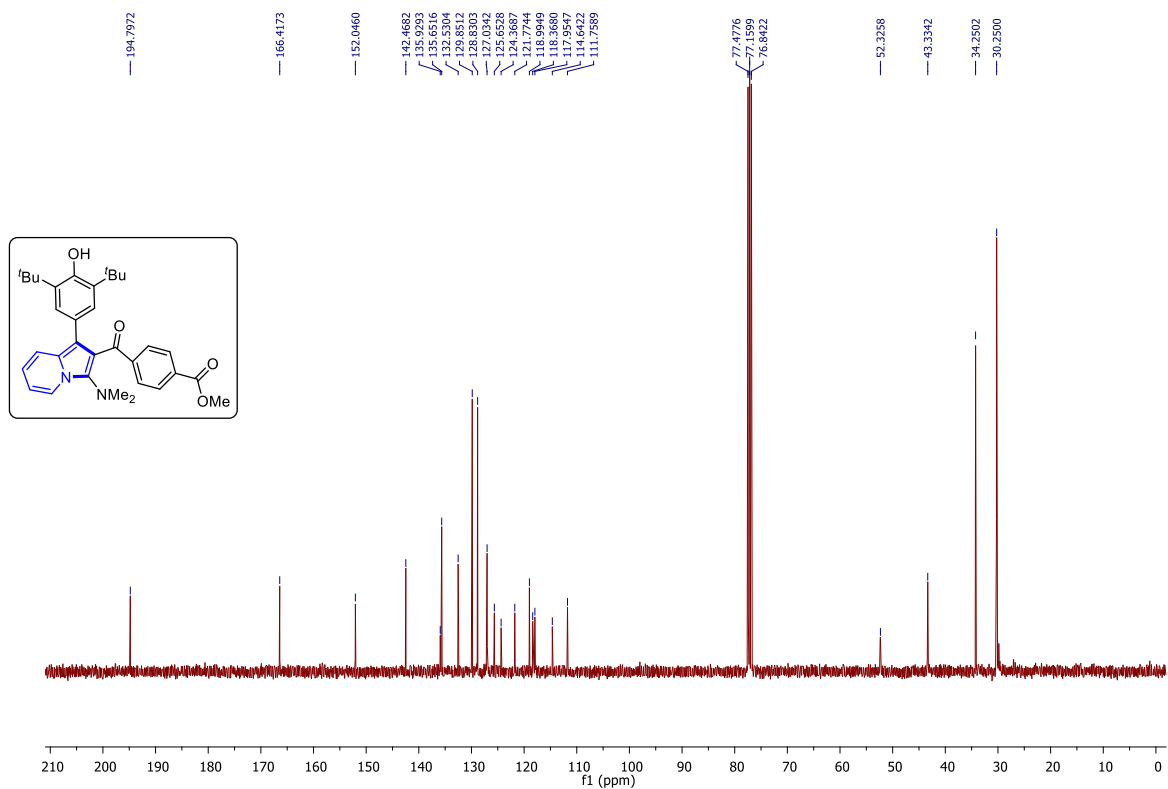
$^{13}\text{C}\{^1\text{H}\}$ NMR (100 MHz, CDCl_3) spectrum of (**42s**)



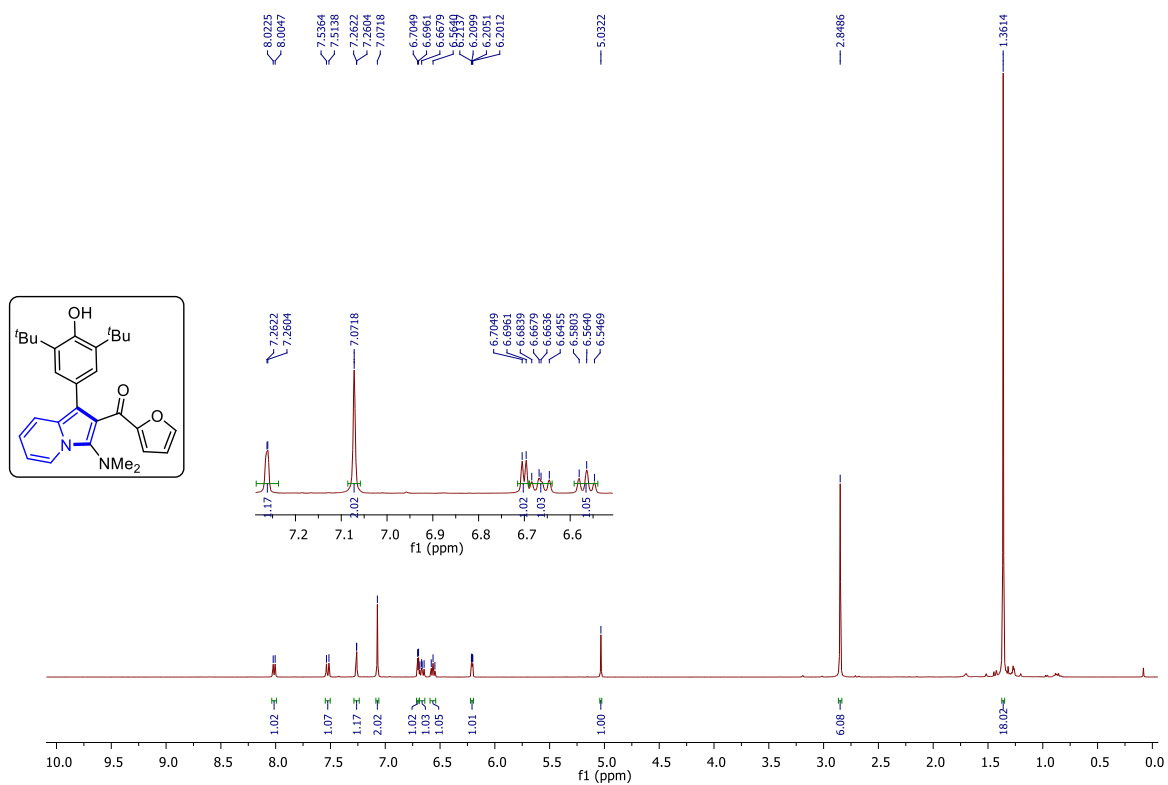
^1H NMR (400 MHz, CDCl_3) spectrum of (**42w**)



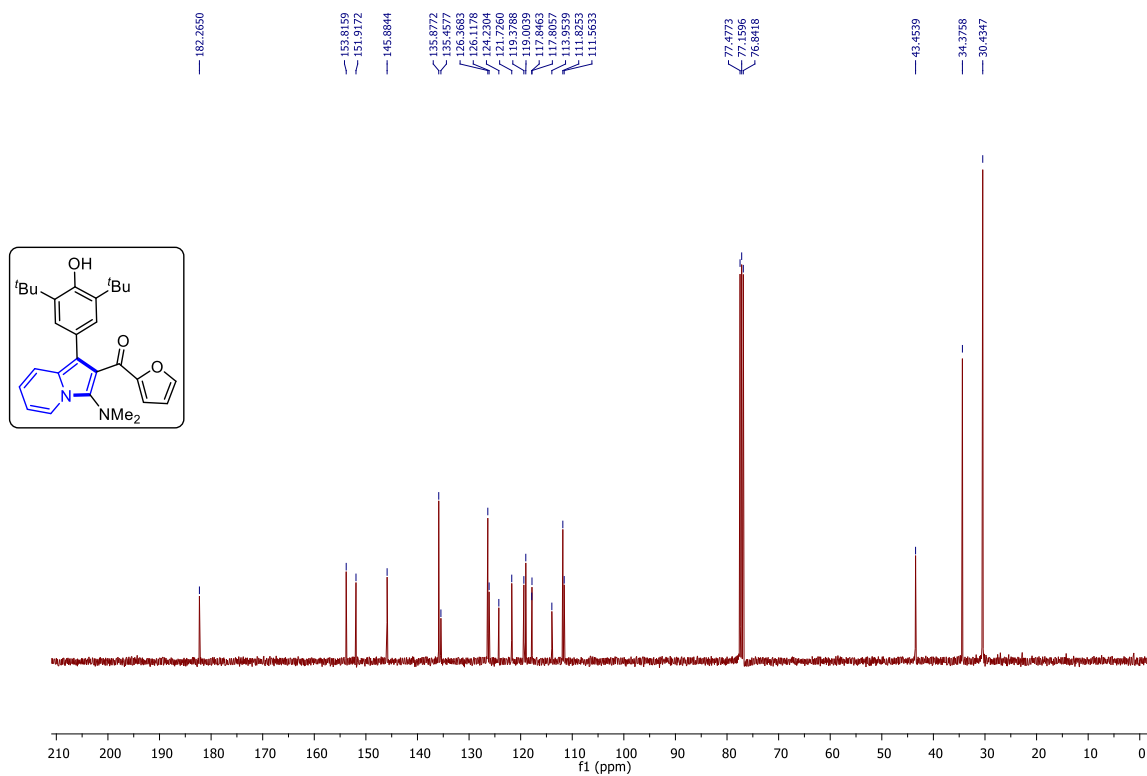
$^{13}\text{C}\{^1\text{H}\}$ NMR (100 MHz, CDCl_3) spectrum of (**42w**)



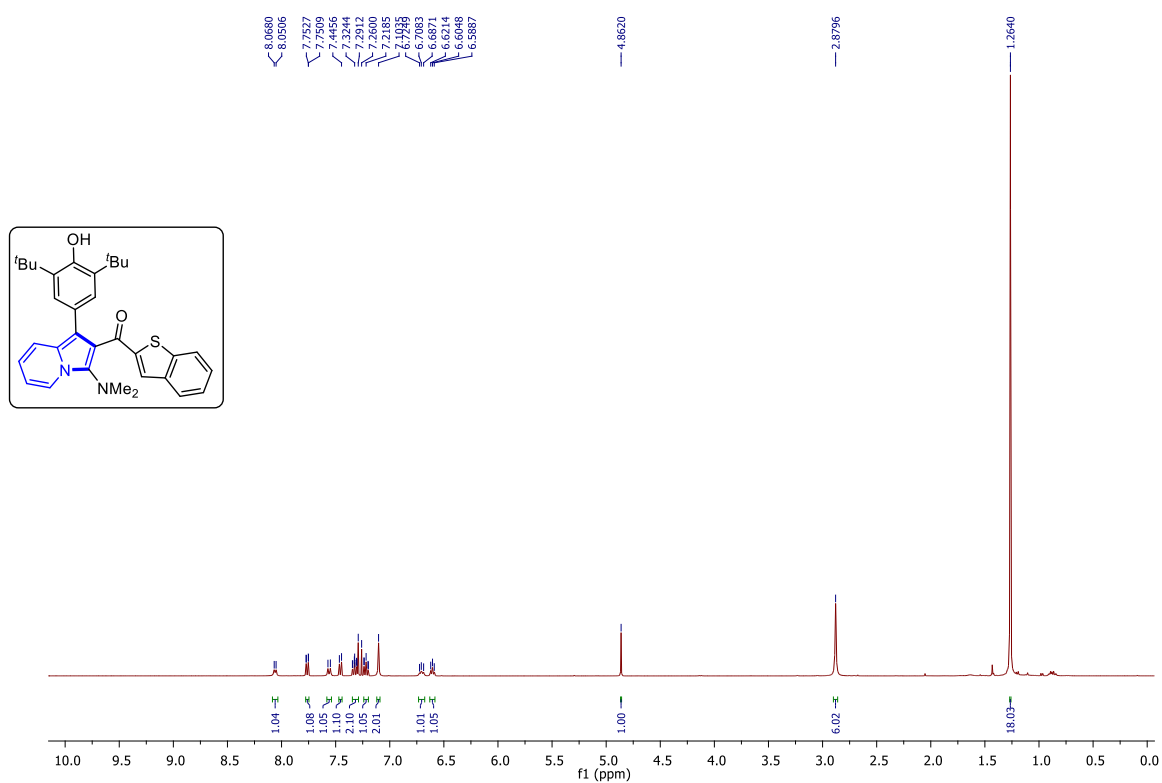
^1H NMR (400 MHz, CDCl_3) spectrum of (**42af**)



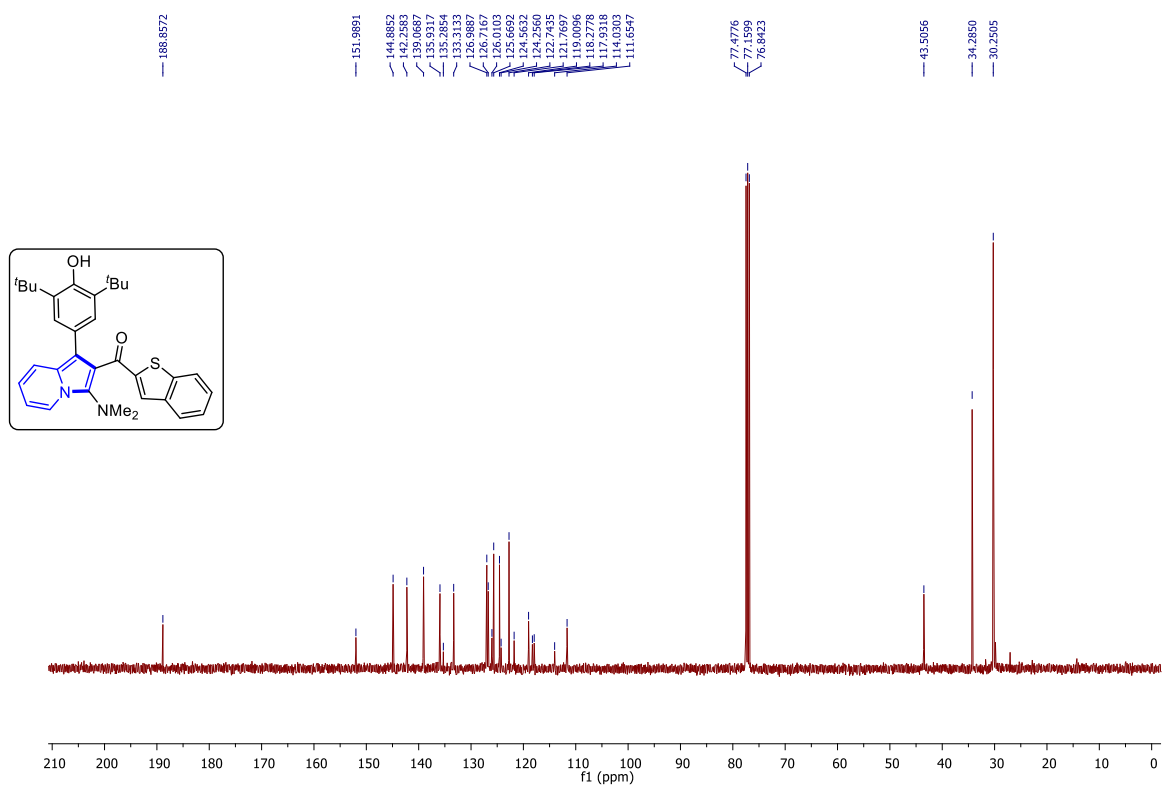
$^{13}\text{C}\{^1\text{H}\}$ NMR (100 MHz, CDCl_3) spectrum of (**42af**)



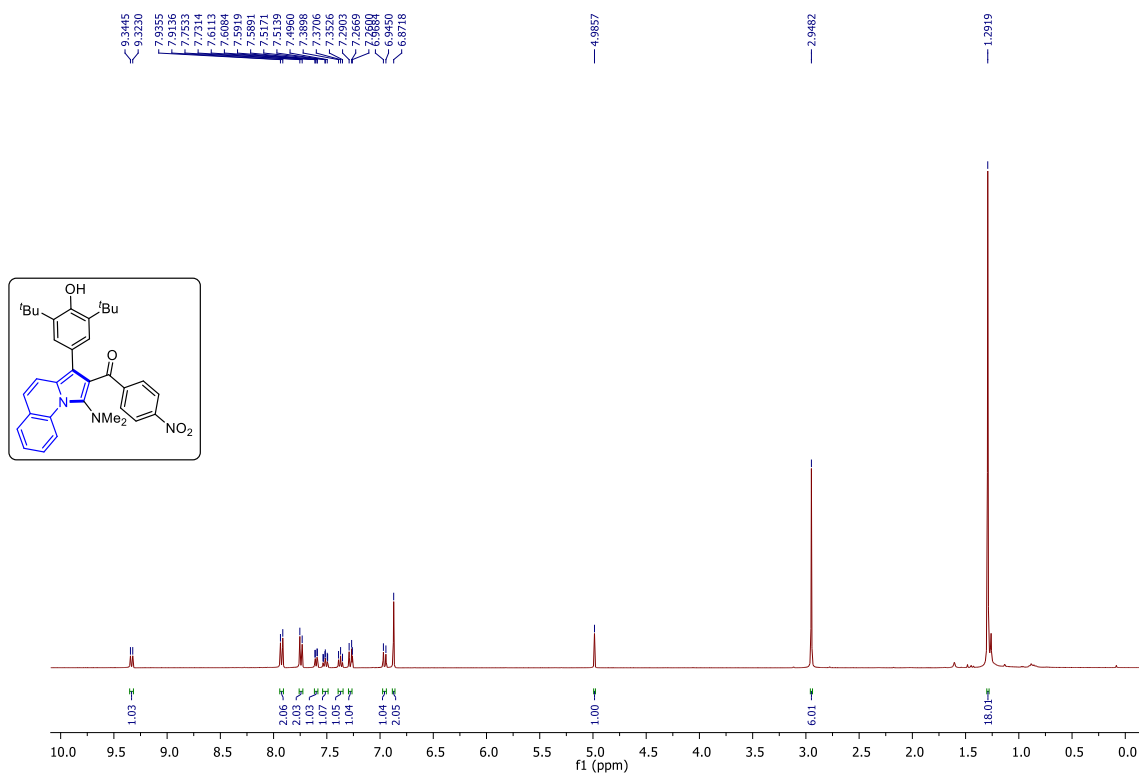
¹H NMR (400 MHz, CDCl₃) spectrum of (**42ai**)



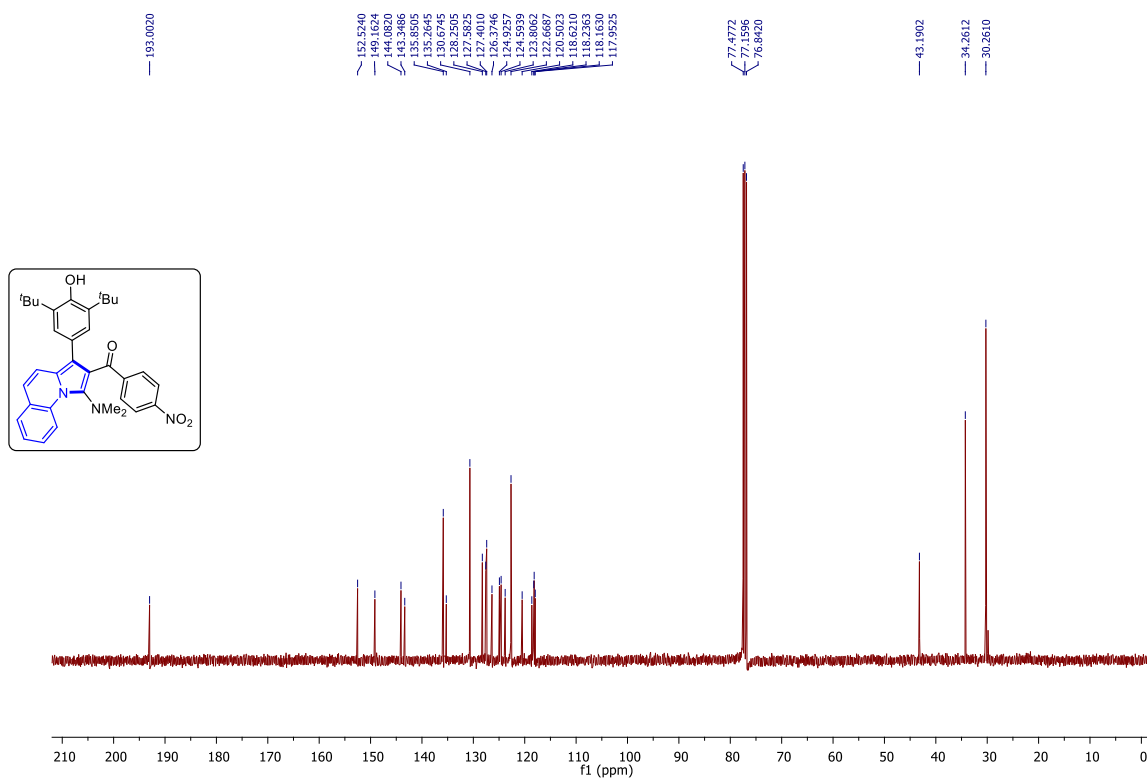
¹³C{¹H} NMR (100 MHz, CDCl₃) spectrum of (**42ai**)

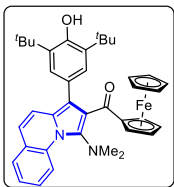
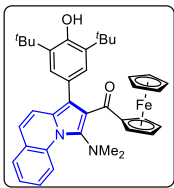


¹H NMR (400 MHz, CDCl₃) spectrum of (**43f**)

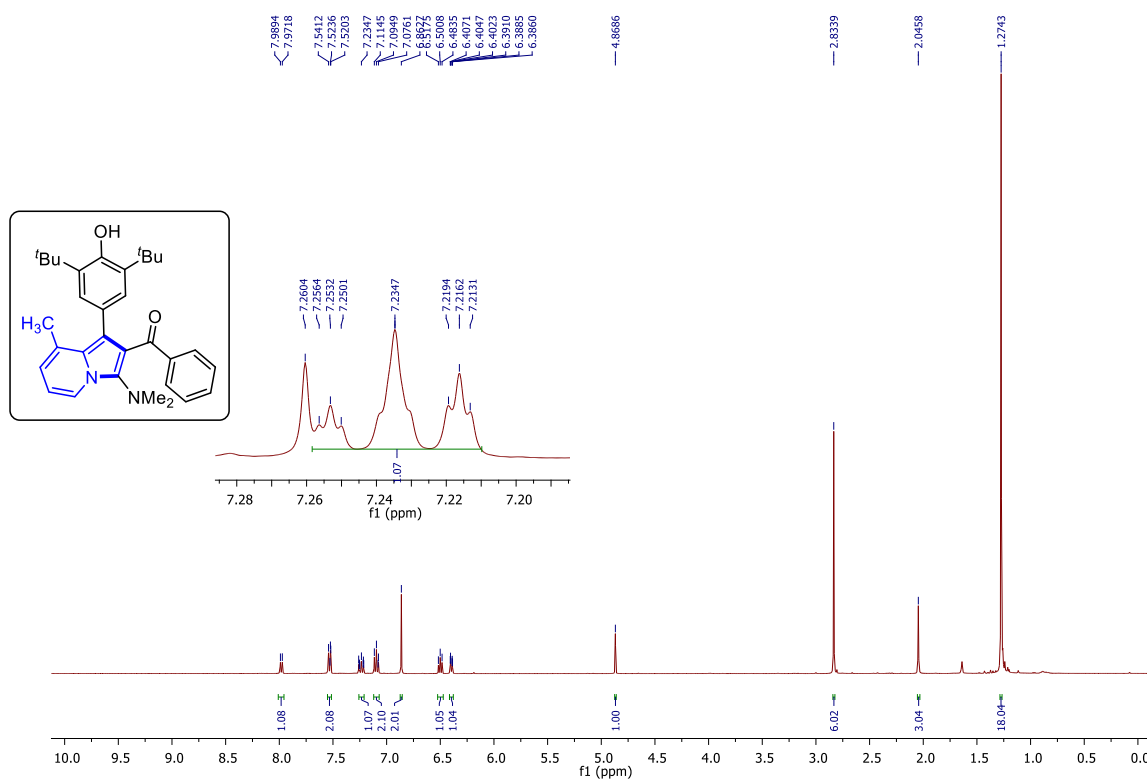


¹³C{¹H} NMR (100 MHz, CDCl₃) spectrum of (**43f**)

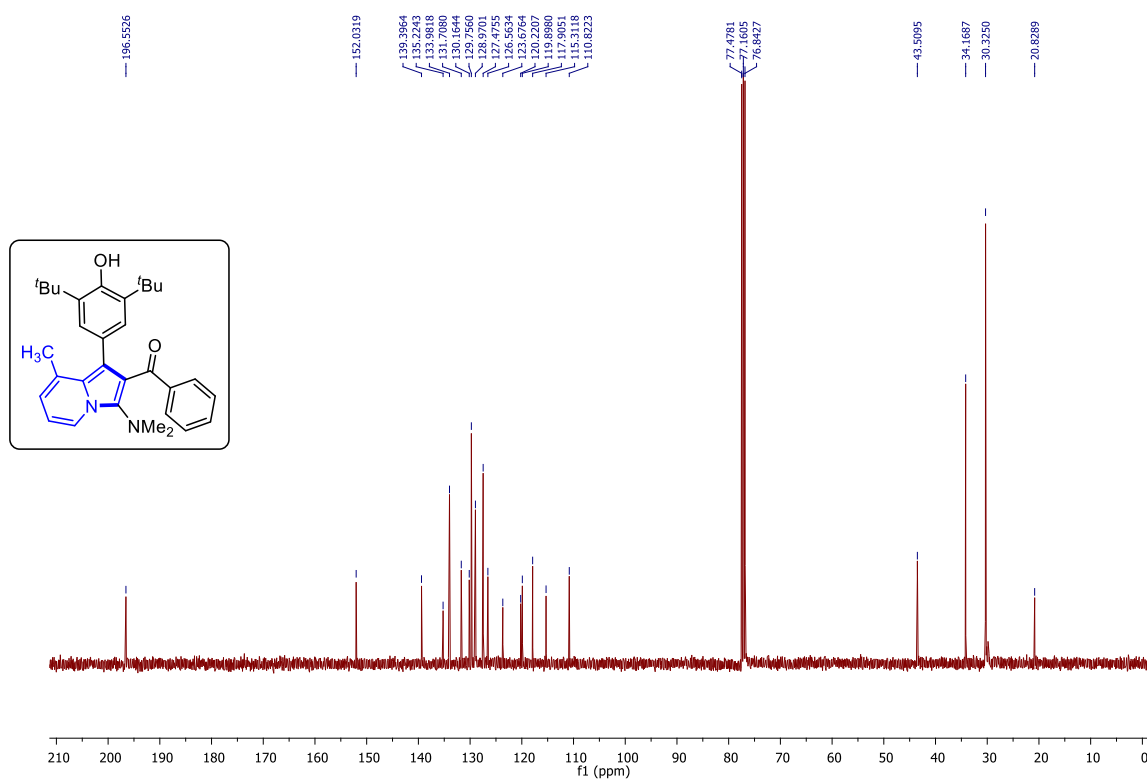


¹H NMR (400 MHz, CDCl₃) spectrum of (**43j**) $^{13}\text{C}\{^1\text{H}\}$ NMR (100 MHz, CDCl_3) spectrum of **(43j)**

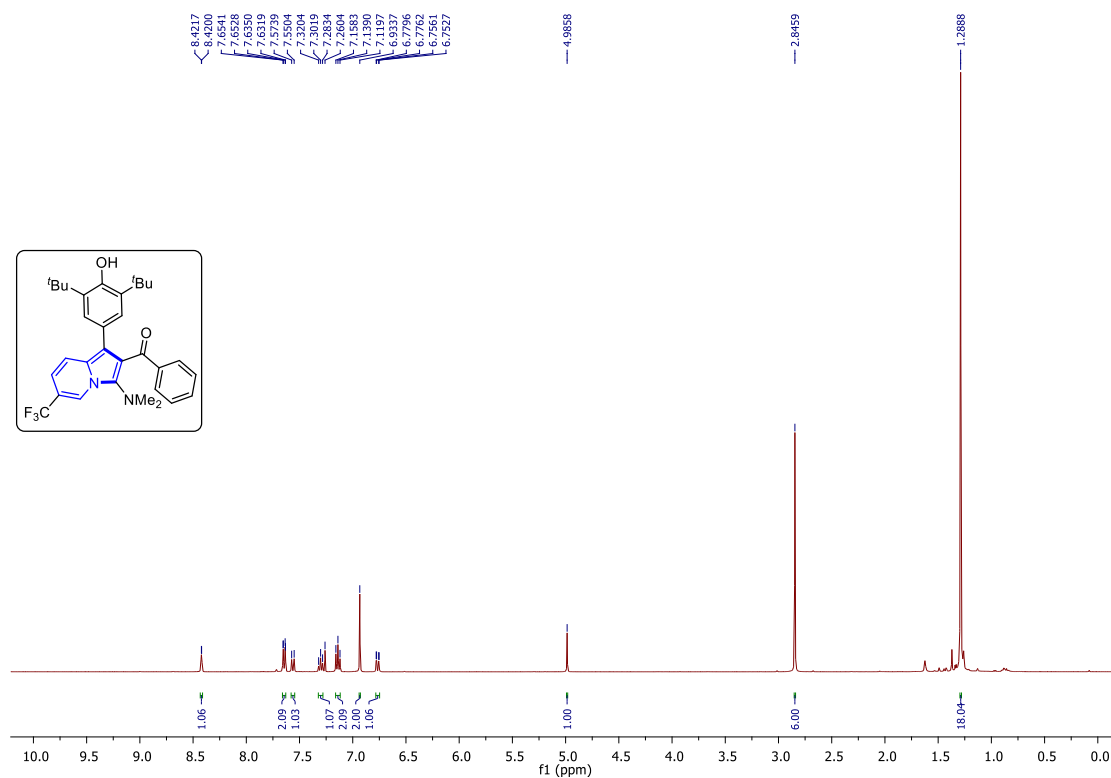
^1H NMR (400 MHz, CDCl_3) spectrum of (**43k**)



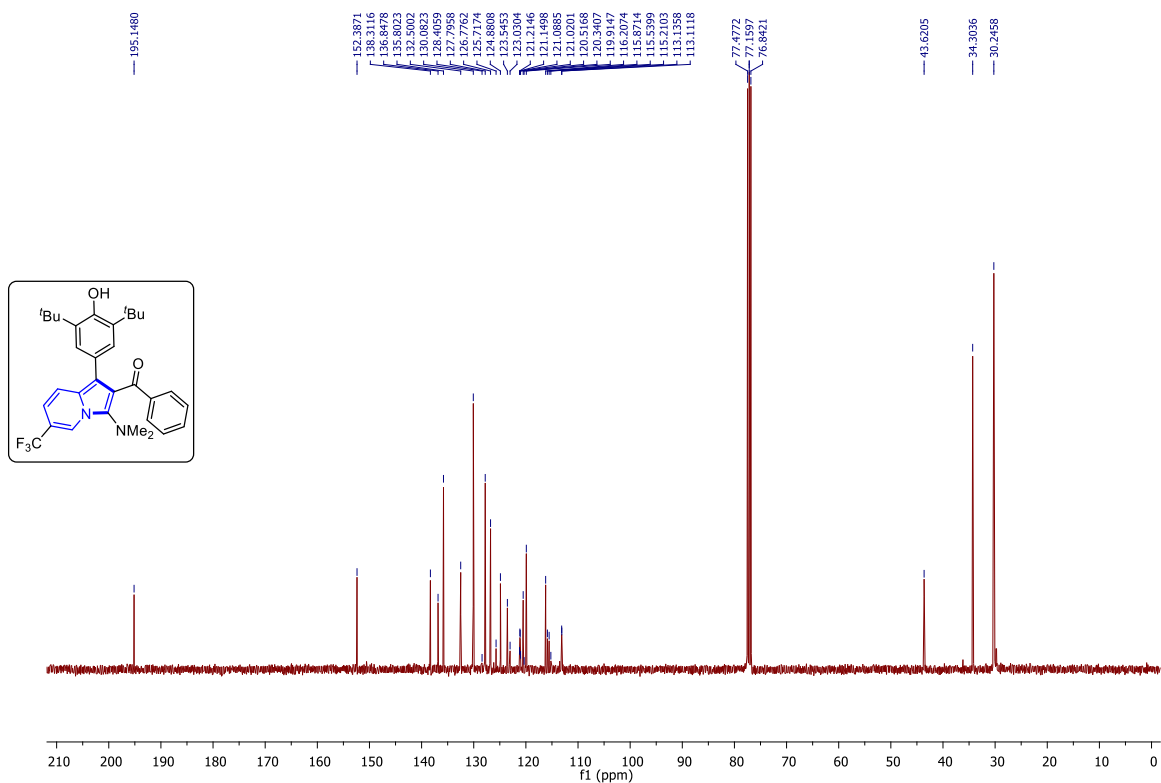
$^{13}\text{C}\{^1\text{H}\}$ NMR (100 MHz, CDCl_3) spectrum of (**43k**)



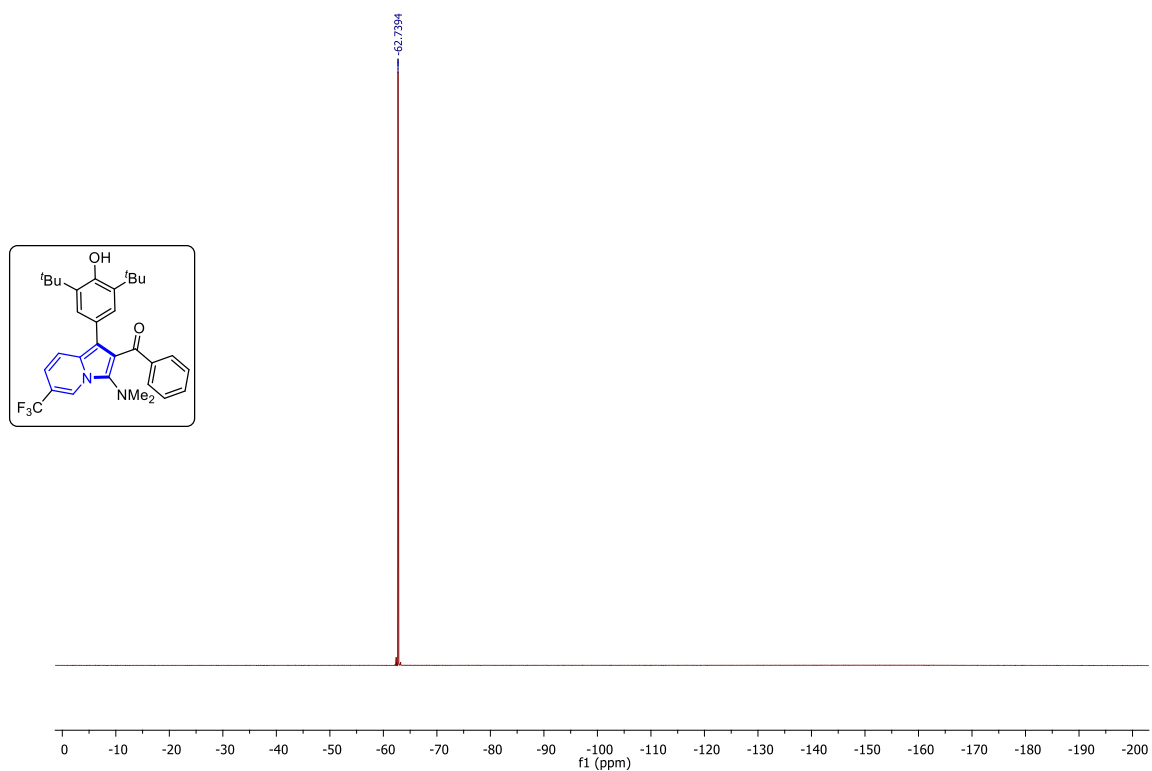
^1H NMR (400 MHz, CDCl_3) spectrum of (**43t**)



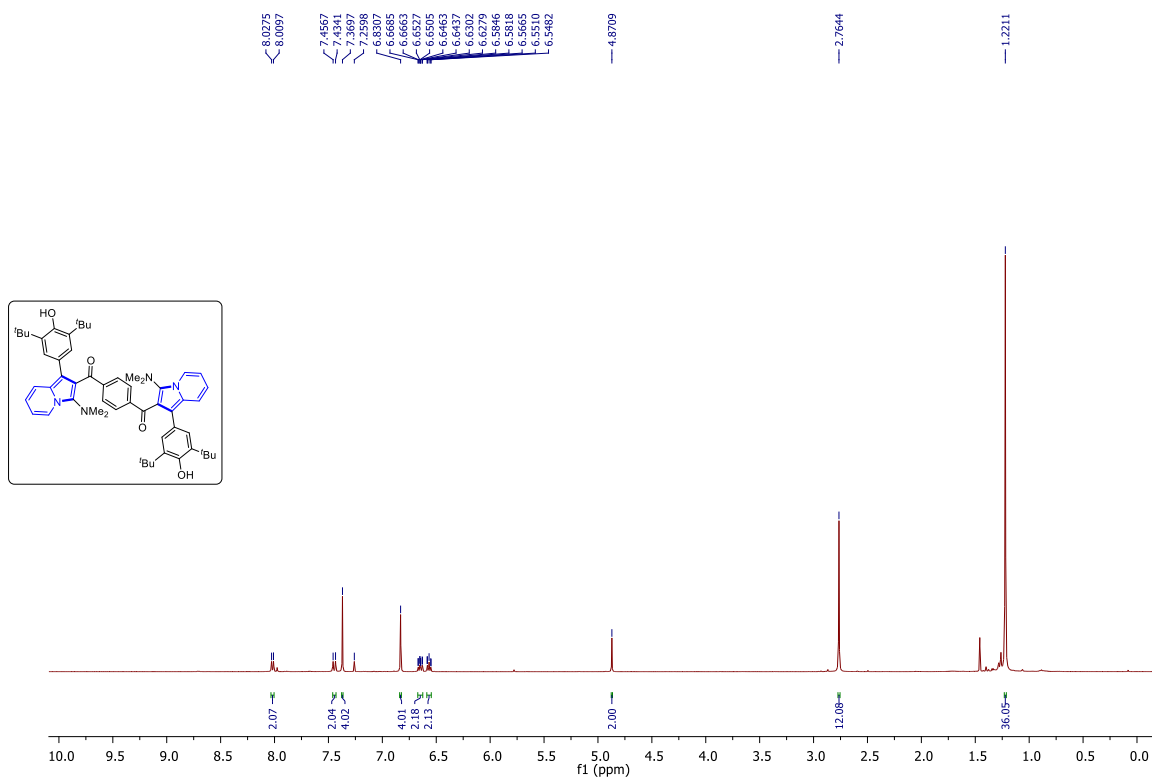
$^{13}\text{C}\{^1\text{H}\}$ NMR (100 MHz, CDCl_3) spectrum of (**43t**)



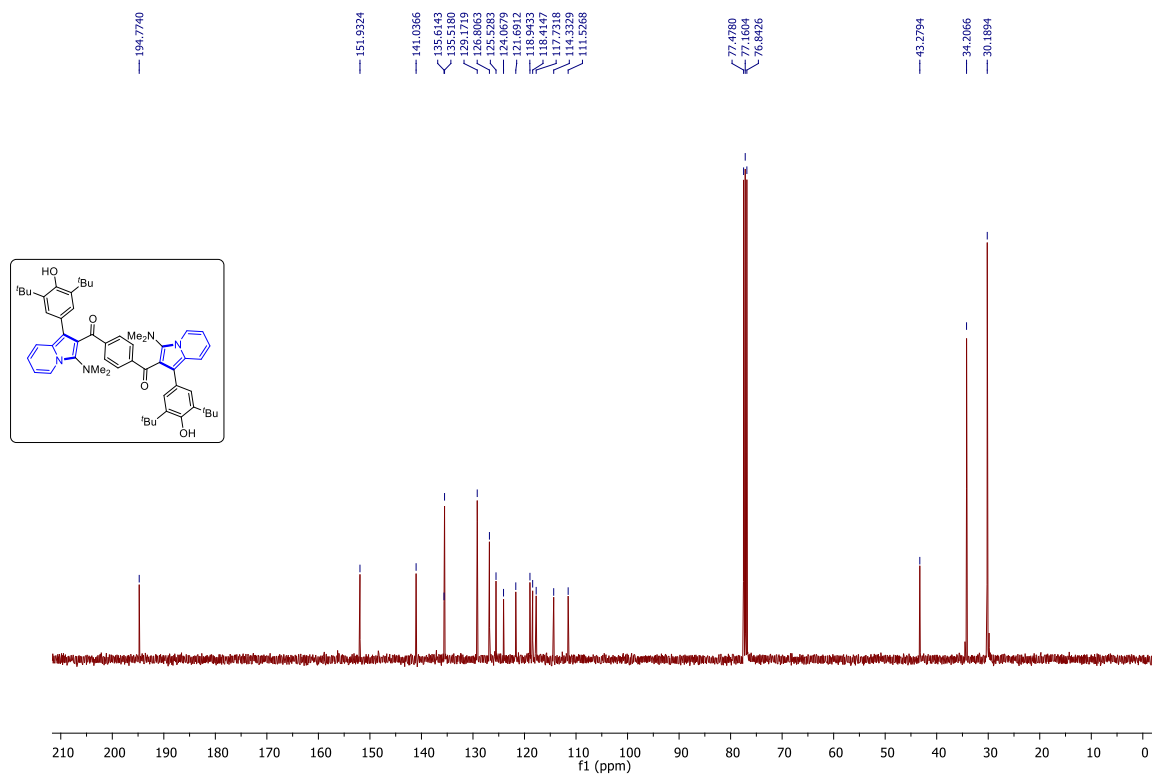
$^{19}\text{F}\{^1\text{H}\}$ NMR (376 MHz, CDCl_3) spectrum of (**43t**)



^1H NMR (400 MHz, CDCl_3) spectrum of (**43u**)



$^{13}\text{C}\{^1\text{H}\}$ NMR (100 MHz, CDCl_3) spectrum of (**43u**)



3.7. References:

1. For selected examples, see: (a) Kerru, N.; Gummidi, L.; Maddila, S.; Gangu, K. K.; Jonnalagadda, S. B. *Molecules* **2020**, *25*, 1909; (b) Gau, M.; Xu, B. *Chem. Rec.* **2016**, *16*, 1701.
2. (a) Michael, J. P. *Nat. Prod. Rep.* **2005**, *22*, 603; (b) Fukuda, T.; Ishibashi, F.; Iwao, M. *Heterocycles* **2011**, *83*, 491; (c) Bailly, C. *Mar. Drugs* **2015**, *13*, 1105.
3. Smith, S. C.; Clarke, E. D.; Ridley, S. M.; Bartlett, D.; Greenhow, D. T.; Glithro, H.; Klong, A. Y.; Mitchell, G.; Mullier, G. W. *Pest Manage. Sci.* **2005**, *61*, 16.
4. (a) Singh, G. S.; Mmatli, E. E. *Eur. J. Med. Chem.* **2011**, *46*, 5237; (b) Xiang, Q.; Wang, C.; Wu, T.; Zhang, C.; Hu, Q.; Luo, G.; Hu, J.; Zhuang, X.; Zou, L.; Shen, H.; Wu, X.; Zhang, Y.; Kong, X.; Liu, J.; Xu, Y. *J. Med. Chem.* **2022**, *65*, 785; (c) Weide, T.; Arve, L.; Prinz, H.; Waldmann, H.; Kessler, H. *Bioorg. Med. Chem. Lett.* **2006**, *16*, 59; (d) Lucescu, L.; Ghinet, A.; Belei, D.; Rigo, D.; Dubois, J.; Bîcu, E. *Bioorg. Med. Chem. Lett.* **2015**, *25*, 3975; (e) Arvin-Berod, M.; Desroches-Castan, A.; Bonte, S.; Brugière, S.; Couté, Y.; Guyon, L.; Feige, J.-J.; Baussanne, I.; Demeunynck, M. *ACS Omega* **2017**, *2*, 9221.
5. (a) Kim, E.; Koh, M.; Lim, B. J.; Park, S. B. *J. Am. Chem. Soc.* **2011**, *133*, 6642; (b) Ge, Y.; Liu, A.; Dong, J.; Duan, G.; Cao, X.; Li, F. *Sens. Actuators B*, **2017**, *247*, 46.
6. For recent reviews see; (a) Sadowski, B.; Klajn, J.; Gryko, D. T. *Org. Biomol. Chem.* **2016**, *14*, 7804; (b) Hui, J.; Ma, Y.; Zhao, J.; Cao, H. *Org. Biomol. Chem.* **2021**, *19*, 10245; (c) Neto, J. S. S.; Zeni, G. *Asian J. Org. Chem.* **2021**, *10*, 1, and references cited therein.
7. For selected recent examples: (a) Escalante, C. H. Hernández, F. A. C.; López, A. H.; Mora, E. I. M.; Delgado, F. Tamariz, J. *Org. Biomol. Chem.* **2022**, *20*, 396; (b) Chen, Y.; Shatskiy, A.; Liu, J. -Q.; Kärkäs, M. D.; Wang, X. -S. *Org. Lett.* **2021**, *23*, 7555; (c) Dong, S.; Huang, J.; Sha, H.; Qiu, L.; Hub, W.; Xu, X. *Org. Biomol. Chem.* **2020**, *18*, 1926; (d) Wang, W.; Han, J.; Sun, J.; Liu, Y. *J. Org. Chem.* **2017**, *82*, 2835; (e) Han, C.; Liu, Y.; Tian, X.; Rominger, F.; Hashmi, A. S. K. *Org. Lett.* **2021**, *23*, 9480; (f) Liu, R.; Wang, Q.; Wei, Y.; Shi, M. *Chem. Commun.* **2018**, *54*, 1225; (g) Liu, R. - R.; Hong, J. -J.; Lu, C. -J.; Xu, M.; Gao, J. -R.; Jia, Y. -X. *Org. Lett.* **2015**, *17*, 3050; (h) Shen, B.; Li, B.; Wang, B. *Org. Lett.* **2016**, *18*, 2816; (i) Hou, X.; Zhou, S.; Li, Y.; Guo, M.; Zhao, W.; Tang, X.; Wang, G. *Org. Lett.* **2020**, *22*, 9313; (j) Douglas, T.; Pordea, A.; Dowden, J. *Org. Lett.* **2017**, *19*, 6396; (k) Xu, X.; Feng, H.; Zhang, X.;

- Song, L.; Meervelt, L. V.; Van der Eycken, J.; Harvey, J. N.; Van der Eycken, E. V. *Org. Lett.* **2022**, *24*, 1232; (l) Briocche, J.; Meyer, C.; Cossy, J. *Org. Lett.* **2015**, *17*, 2800; (m) Roy, D. S. A.; Zgheib, J.; Zhou, C.; Arndtsen, B. A. *Chem. Sci.* **2021**, *12*, 2251; (n) Zhang, D.; Su, Z.; He, Q.; Wu, Z.; Zhou, Y.; Pan, C.; Liu, X.; Feng, X. *J. Am. Chem. Soc.* **2020**, *142*, 15975; (o) Liu, R. R.; Lu, C. J.; Zhang, M. D.; Gao, J. R.; Jia, Y. X. *Chem.-Eur. J.* **2015**, *21*, 7057.
8. For selected examples: (a) Seregin, I. V.; Gevorgyan, V. *J. Am. Chem. Soc.* **2006**, *128*, 12050; (b) Seregin, I.; Schammel, A.; Gevorgyan, V. *Tetrahedron* **2008**, *64*, 6876; (c) Xu, T.; Alper, H. *Org. Lett.* **2015**, *17*, 4526; (d) Oh, K. H.; Kim, S. M.; Park, S. Y.; Park, J. K. *Org. Lett.* **2016**, *18*, 2204; (e) Yan, B.; Zhou, Y.; Zhang, H.; Chen, J.; Liu, Y. *J. Org. Chem.* **2007**, *72*, 7783.
 9. Liu, R. -R.; Lu, C. -J.; Zhang, M. -D.; Gao, J. R.; Jia, Y. -X. *Chem. Eur. J.* **2015**, *21*, 7057; (b) Bagle, P. N.; Mane, M. V.; Venka, K.; Shinde, D. R.; Shaikh, S. R.; Gonnade R. G.; Patil, N. T. *Chem. Commun.* **2016**, *52*, 14462; (c) Pathipati, S. R.; van der Werf, A.; Selander, N. *Org. Lett.* **2018**, *20*, 3691.
 10. (a) Li, Z.; Chernyak, D.; Gevorgyan, V. *Org. Lett.* **2012**, *14*, 6056; (b) Li, Y.; Xiong, W.; Zhang, Z.; Xu, T. *J. Org. Chem.* **2020**, *85*, 6392; (c) Jin, T.; Tang, Z.; Hu, J.; Yuan, H.; Chen, Y.; Li, C.; Jia, X.; Li, J. *Org. Lett.* **2018**, *20*, 413.
 11. For recent reviews on the applications of enamines to the synthesis of heterocycles: (a) Stanovnik, B.; Svete, J. *Chem. Rev.* **2004**, *104*, 2433; (b) Huang, J.; Yu, F. *Synthesis* **2021**, *53*, 587; (c) Wang, Z.; Zhao, B.; Liu, Y.; Wan, J. *Adv. Synth. Catal.* **2022**, *364*, 1508, and references cited therein.
 12. Wan, J. P.; Cao, S.; Liu, Y. *Org. Lett.* **2016**, *18*, 6034.
 13. Zhao, P.; Wu, X.; Zhou, Y.; Geng, X.; Wang, C.; Wu, Y. D.; Wu, A. X. *Org. Lett.* **2019**, *21*, 2708.
 14. Rao, K.; Chai, Z.; Zhou, P.; Liu, D.; Sun, Y.; Yu, F. *Front. Chem.* **2022**, *10*, 1.
 15. Zhang, B.; Zhou, P.; Xu, H.; Huang, J.; Sun, Y.; Liu, D.; Yu, F. *Adv. Synth. Catal.* **2021**, *363*, 4354.
 16. Chen, Z.; Xie, X.; Chen, W.; Luo, N.; Li, X.; Yu, F.; Huang, J. *Org. Biomol. Chem.* **2022**, *20*, 8037.
 17. Li, X.; Chen, Z.; Chen, W.; Xie, X.; Zhou, H.; Liao, Y.; Yu, F.; Huang, J. *Org. Lett.* **2022**, *24*, 7372.
 18. P, R.; S, V.; John, J. *J. Org. Chem.* **2022**, *87*, 13708.

19. For a recent review from our group: Singh, G.; Pandey, R.; Pankhade, Y. A.; Fatma S.; Anand, R. V. *Chem. Rec.* **2021**, *21*, 4150.
20. For recent reviews on *p*-QM chemistry: (a) Li, W.; Xu, X.; Zhang, P.; Li, P. *Chem. Asian J.* **2018**, *17*, 2350; (b) Lima, C. G. S.; Pauli, F. P.; Costa, D. C. S.; de Souza, A. S.; Forezi, L. S. M.; Ferriera, V. F.; de Carvalho da Silva. *Eur. J. Org. Chem.* **2020**, *18*, 2650; (c) Wang, J. -Y.; Hao, W. -J.; Tu, S. -J.; Jiang, B. *Org. Chem. Front.* **2020**, *7*, 1743.
21. (a) Paluru, D. K.; Mahesh, S.; Ahmad F.; Anand, R. V. *Chem. Asian. J.* **2019**, *14*, 4688; (b) Mahesh S.; Anand, R. V. *Eur. J. Org. Chem.* **2017**, 2698; (c) Mahesh, S.; Paluru, D. K.; Ahmad, F.; Patil, S.; Kant G.; Anand, R. V. *Asian J. Org. Chem.* **2017**, *6*, 1857.
22. Ahmad, F.; Ranga, P. K.; Pankhade, Y. A.; Fatma, S.; Gouda, A.; Anand, R. V. *Chem. Commun.* **2022**, 58, 13238.
23. Bedjeguelal, K.; Bienaymé, H.; Dumoulin, A.; Poigny, S.; Schmitt, P.; Tam, E. *Bioorg. Med. Chem. Lett.* **2006**, *16*, 3998.
24. For selected examples: (a) Hickman, J. A.; Wibberley, D. G., *J. Chem. Soc. Perkin Trans I* **1972**, 2954; (b) Yan, B.; Liu, Y., *Org. Lett.* **2007**, *9*, 4323; (c) Bai, Y.; Zeng, J.; Ma, J.; Gorityala, B. K.; Liu, X. -W., *J. Comb. Chem.* **2010**, *12*, 696; (d) Albaladejo, M. J.; Alonso, F.; Yus, M., *Chem. Eur. J.* **2013**, *19*, 5242; (e) Outlaw, V. K.; d'Andrea, F. B.; Townsend, C. A., *Org. Lett.* **2015**, *17*, 1822; (f) Zhang, C.; Wang, W.; Zhu, X.; Chen, L.; Luo, H.; Guo, M.; Liu, D.; Liu, F.; Zhang, H.; Li, Q.; Lin, J., *Org. Lett.* **2023**, *25*, 1192.
25. Singh, G.; Sharm, S.; Rekha; Pandey, R.; Singh, R.; Kumar, T.; Anand, R. V., *Eur. J. Org. Chem.* **2022**, e202200792.
26. For selected recent reviews see: (a) Nambo, M.; Crudden, C. M. *ACS Catal.* **2015**, *5*, 4734; (b) Mondal, S.; Panda, G., *RSC Adv.* **2014**, *4*, 28317; (c) Kshatriya, R.; Jejurkar, V.; Saha, S., *Eur. J. Org. Chem.* **2019**, 3818; (d) Petrini, M., *Adv. Synth. Catal.* **2020**, *362*, 1214.

1. Copper-catalyzed Synthesis of Indolizine Containing Unsymmetrical Triarylmethane Derivatives from 2-(2-Enynyl)pyridines

1.1 Introduction:

The triarylmethanes (TRAMs) are a class of compounds in which the central sp^3 -hybridized carbon atom is linked to three aryl groups. The triarylmethanes could be symmetrically substituted or asymmetrically substituted depending upon the kind of aryl groups attached (Figure 1).

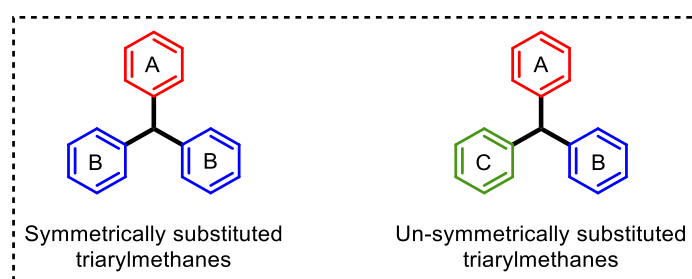


Figure 1: Symmetrically and asymmetrically substituted triarylmethanes (TRAMs).

In recent years, triarylmethanes (TRAMs) have emerged as important and integral scaffolds in many pharmaceuticals and biologically active molecules.¹ Several of them possess

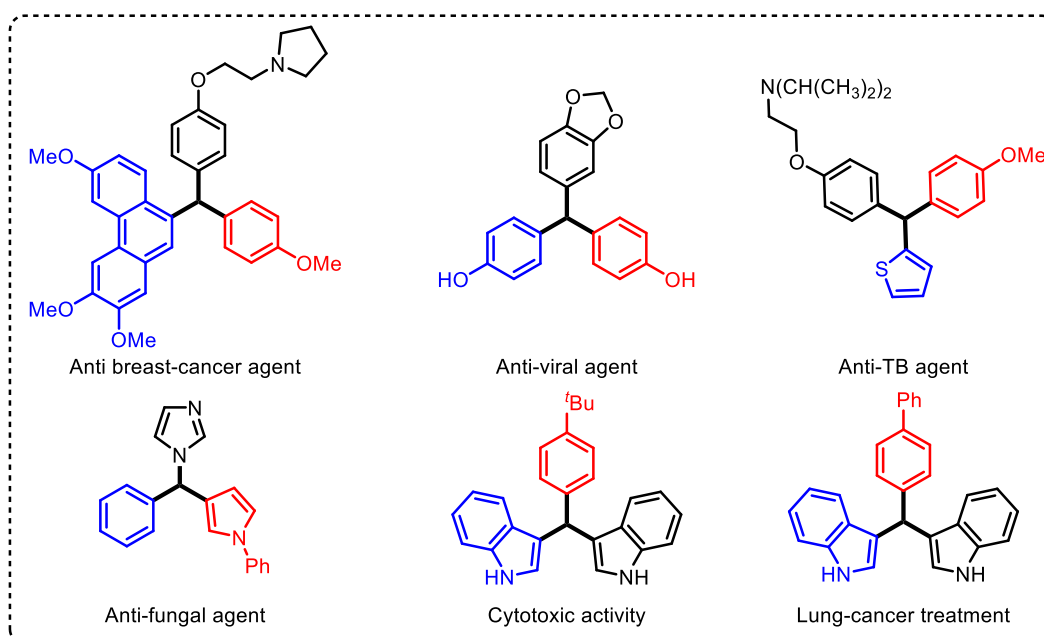


Figure 2. Some biologically significant triarylmethanes (TRAMs)

remarkable biological activities and exhibit important therapeutic applications² and are being explored as anti-breast cancer,^{2b} anti-viral,^{2c} anti-TB agents,^{2d} and anti-fungal agents.^{3a} Furthermore, they are also known to possess significant cytotoxic activity against renal cancer cells^{3b} and lungs cancer cells^{3c} (Figure 2).

Besides the medicinal applications, molecules possessing triarylmethane motifs have also found remarkable applications in various other fields, such as in the dye industry,⁴ materials science^{4b} and some triarylmethane derivatives have been utilized as metal ion sensors⁵ and fluorescent probes.⁶ In addition, in bio-organic chemistry, triarylmethanes are utilized to synthesize polyamide nucleic acid equivalents⁷ (Figure 3).

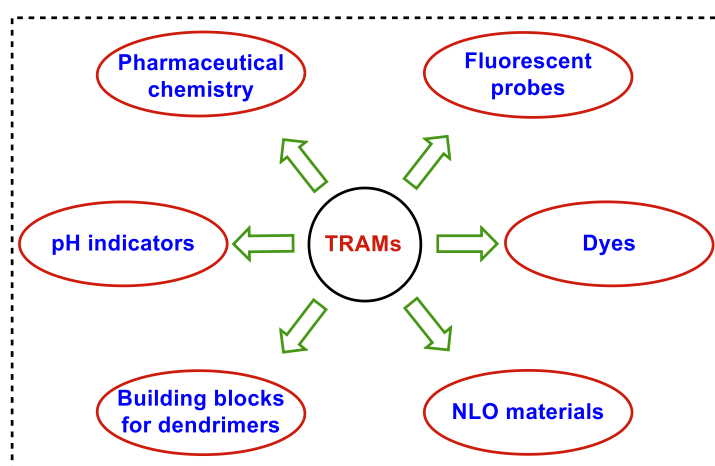


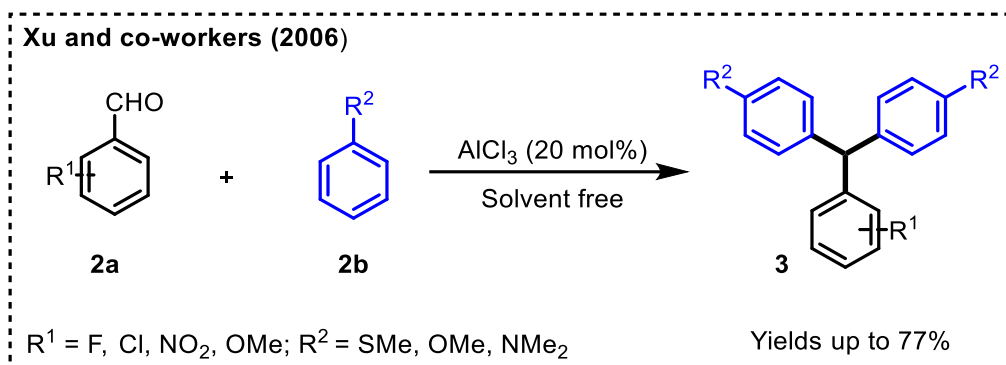
Figure 3: Application of triarylmethanes (TRAMs) in different areas

1.2 Synthesis of Triarylmethanes:

Due to their remarkable chemical and pharmaceutical properties, triarylmethanes (TRAMs) have gained significant attention and attracted the scientific community toward the development of different easily accessible routes for the synthesis of triarylmethanes. Some of the literature reports on the synthesis of (TRAMs) are discussed in this section.

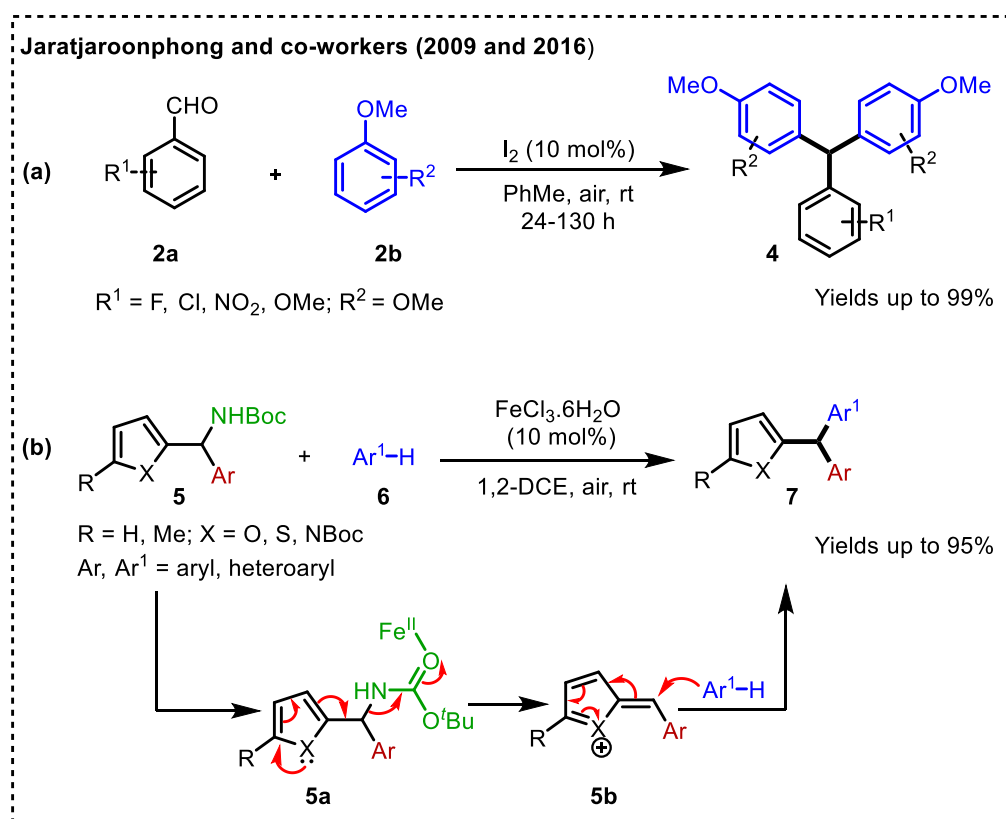
1.2.1 Lewis acid/Bronsted acid-catalyzed Friedel-Crafts approach

Xu and co-workers reported a solvent-free Lewis acid-catalyzed Friedel-Crafts alkylation approach for the synthesis of triarylmethanes.⁸ A wide range of aromatic aldehydes (**2a**) containing electron-poor and electron-rich substituents were reacted with electron-rich arenes (**2b**) in the presence of a catalytic amount of AlCl_3 to undergo a Friedel-Crafts alkylation reaction, and the resultant triarylmethanes (**3**) were isolated in moderate to good yields (Scheme 1).



Scheme 1: Synthesis of triarylmethanes through Friedel-Crafts alkylation

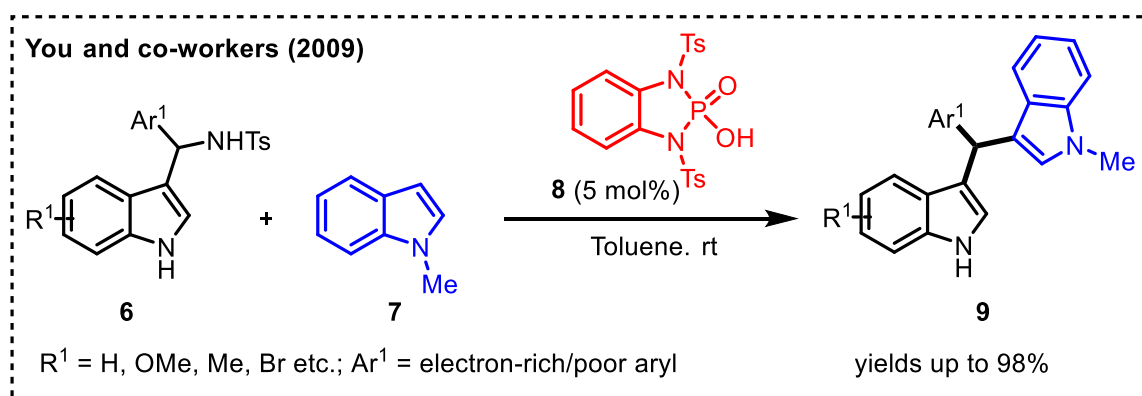
Later, Jaratjaroonphong's group disclosed a molecular iodine-catalyzed mild and efficient Friedel-Crafts alkylation reaction to synthesize triarylmethanes.^{9a} A wide range of electron-rich arenes (**2b**) and aromatic aldehydes (**2a**) were reacted in the presence of 10 mol% of iodine under open flask conditions. Almost in all cases, the corresponding triarylmethanes (**4**) were isolated in good to excellent yields. Both electron-rich and electron-poor aromatic aldehydes were tolerated under the optimized conditions (Scheme 2a).



Scheme 2: Lewis acid catalyzed synthesis of triarylmethanes (TRAMs)

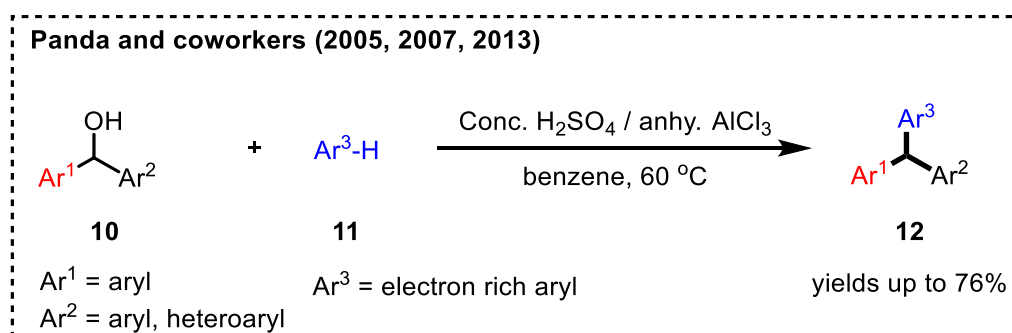
The same group in 2016 reported an atom-economical room temperature synthesis of heteroaryl-substituted TRAMs (**7**) utilizing $\text{FeCl}_3 \cdot 6\text{H}_2\text{O}$ as the catalyst.^{9b} The authors proposed that the activation of the *tert*-butylcarbamate ester by the FeCl_3 catalyst forms the complex **5a**, which leads to the expulsion of *tert*-butyl carbamate from **5** to generate the intermediate **5b** followed by the nucleophilic addition of the heteroarene **6** to produce the desired triarylmethane product **7** (Scheme 2b).

You and co-workers described a Brønsted acid-catalyzed Friedel-Crafts alkylation reaction for the synthesis of unsymmetrical triarylmethanes.¹⁰ Varieties of α -(3-indolyl)benzylamines (**6**) underwent Friedel-Crafts alkylation reaction with *N*-methylindole (**7**) in the presence of a catalytic amount of phosphorodiamidic acid **8** to afford the corresponding triarylmethanes (**9**) in good to excellent yields (Scheme 3).



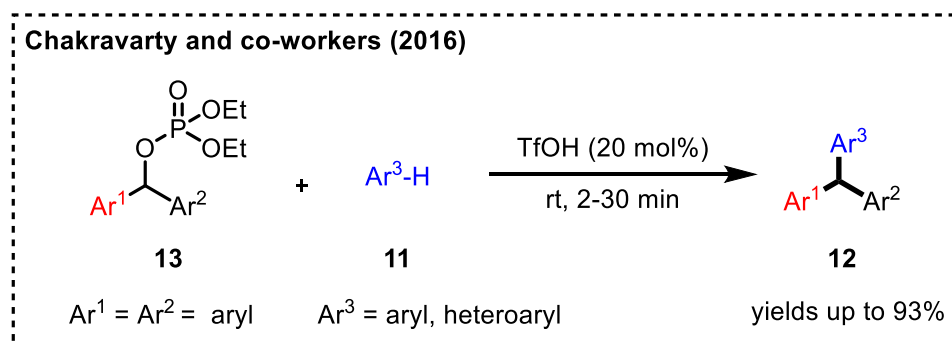
Scheme 3: Brønsted acid catalyzed Friedel-Crafts alkylation approach

Panda and co-workers developed a Friedel-Craft alkylation of diarylcarbinols for the synthesis of unsymmetrical triarylmethanes.¹¹ Different diarylcarbinols (**10**) reacted with electron-rich arenes (**11**) in presence of conc. $\text{H}_2\text{SO}_4/\text{anhy. AlCl}_3$ to furnish the corresponding triarylmethanes (**12**) in good yields (Scheme 4).



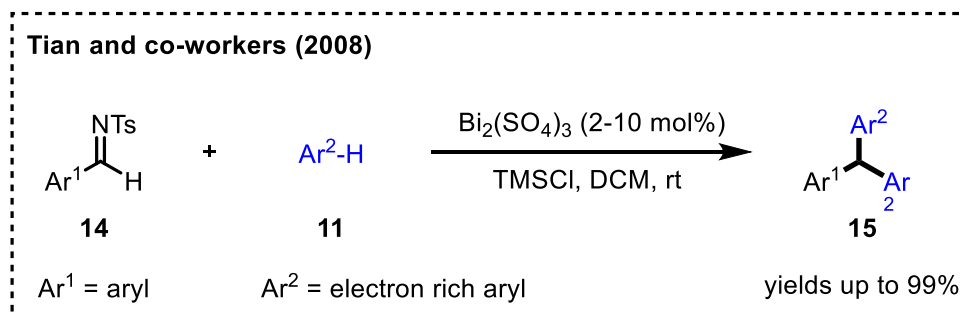
Scheme 4: Brønsted acid catalyzed synthesis of triarylmethanes (TRAMs)

Later, Chakravarty and co-workers reported a triflic acid catalyzed Friedel-Crafts benzylation reaction of secondary benzylic phosphates and arenes.¹² A wide range of electron-rich and electron-poor secondary benzylic phosphates (**13**) reacted efficiently with arenes (**11**) to produce the subsequent unsymmetrical triarylmethanes (**12**) in good to excellent yields. Interestingly, no external solvent was required for this transformation (Scheme 5).



Scheme 5: Friedel-Crafts benzylation of phosphates with arenes

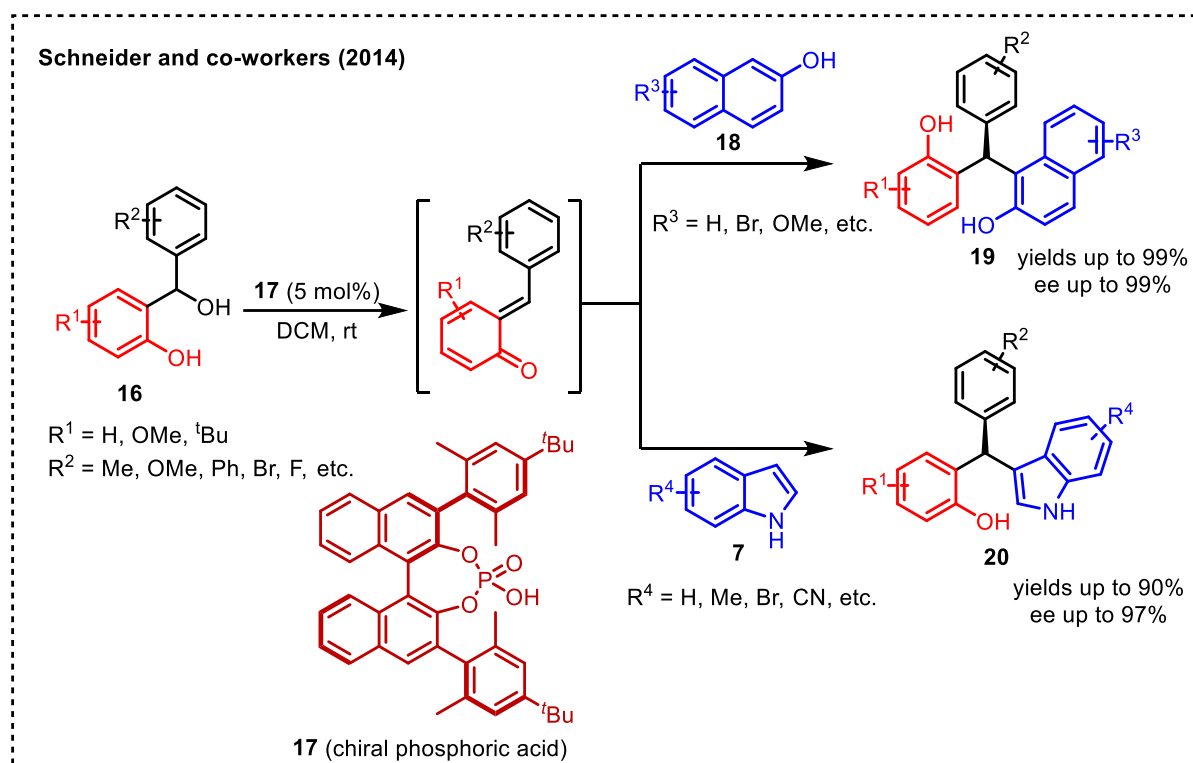
In 2008, Tian's group developed a bismuth catalyzed Friedel-Crafts alkylation approach for the synthesis of symmetrical triarylmethanes.¹³ A wide range of *N*-tosylimines (**14**), derived from aromatic aldehydes, were reacted efficiently with electron-rich arenes (**11**) to produce the resultant symmetrical triarylmethanes (**15**) in a highly regioselective manner (Scheme 6).



Scheme 6: Bi-catalyzed Friedel-Crafts reactions for the synthesis of symmetrical triarylmethanes

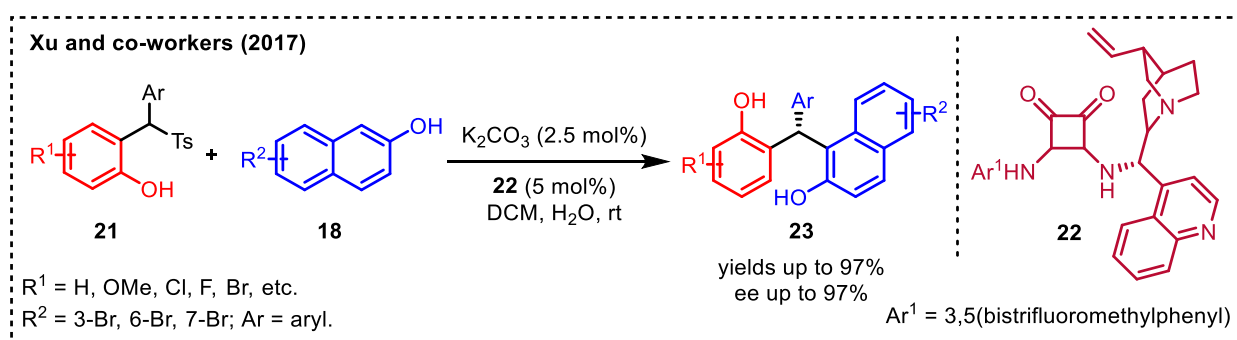
In recent years, quinone methides (QMs) are being utilized as very good precursors for the synthesis of triarylmethane derivatives. For example, Schneider's group accomplished a fascinating approach for the synthesis of chiral triarylmethanes using chiral phosphoric acid as a hydrogen bonding catalyst.¹⁴ A library of 2-naphthols (**18**) and indoles (**7**) were subjected to Friedel-Crafts alkylation reaction with *o*-quinone methides precursors (**16**), respectively

under the optimized conditions and, in most of the cases, the resultant triarylmethanes (**19** & **20**) were isolated in good to excellent yields with excellent *ee* (Scheme 7).



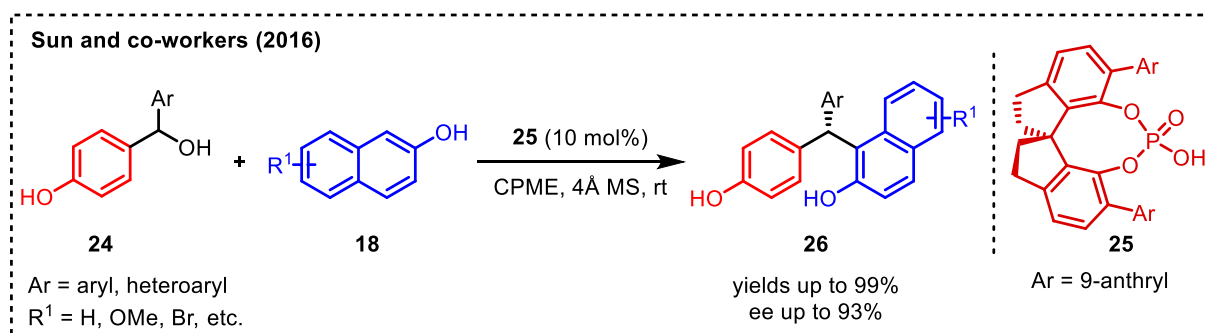
Scheme 7: Chiral phosphoric acid catalyzed synthesis of unsymmetrical triarylmethanes

Very recently, another interesting methodology was disclosed by Xu and co-workers for the synthesis of enantiomerically-enriched triarylmethanes using a chiral bifunctional amine-squaramide catalyst.¹⁵ An array of 2-[phenyl(tosyl)methyl]phenol derivatives (**21**) were reacted with 2-naphthols (**18**) in presence of chiral catalyst (**22**) in an oil-water biphasic medium to furnish the triarylmethanes (**23**) in good to excellent yields with excellent *ee*. The authors believe that oil-water biphasic medium actually increases the effectiveness of the catalytic medium (Scheme 8).



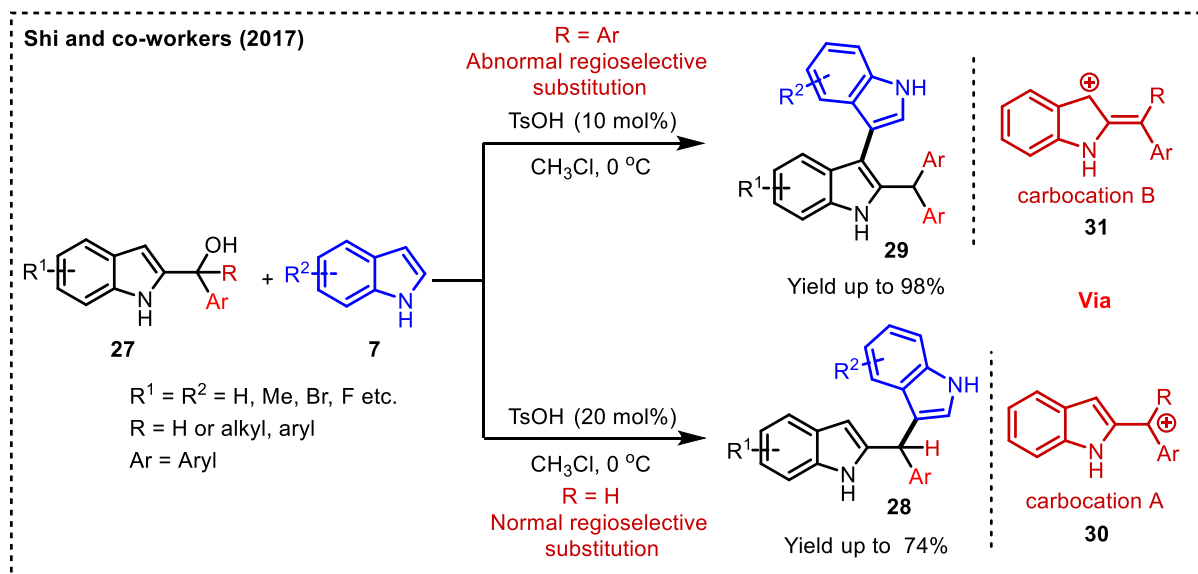
Scheme 8: Synthesis of chiral triarylmethanes in oil-water phase

Sun and co-workers developed a chiral phosphoric acid catalyzed synthesis of enantiomerically enriched triarylmethanes from an *in situ* generated *para*-quinone methides.¹⁶ In presence of chiral phosphoric acid (**25**), 2-naphthols (**18**) underwent 1,6-conjugate addition reactions to *in situ* generated *p*-QMs from a variety of 4-hydroxybenzyl alcohols (**24**) to afford the chiral triarylmethanes (**26**) in excellent yields with very good enantioselectivity (Scheme 9).



Scheme 9: Chiral Brønsted acid catalyzed synthesis of triarylmethanes

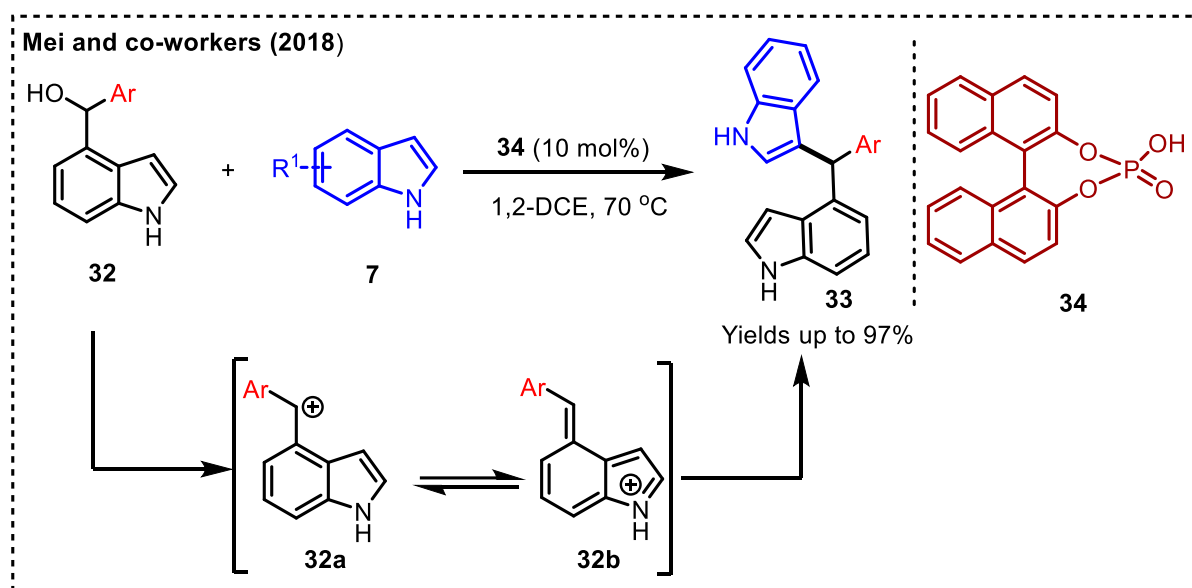
Indolylmethanols (**27**) are considered as versatile building blocks for the synthesis of biologically relevant indole derivatives. In 2017, Shi and co-workers synthesized a variety of bis(indolyl)methanes **28** and 3,3'-bisindole derivatives **29** in excellent yields and high regioselectivities by the regioselective arylation of 2-indolylmethanols (**27**) and indoles (**7**) employing catalytic amount of TsOH.¹⁷ The regioselectivity resulted from the existence of the bulky substituent at the C-3 position of 2-indolyl methanol **27**. When R=H the product **28**



Scheme 10: Regioselective synthesis of bis(indolyl)methanes and 3,3'-bisindole derivatives from indolylmethanols.

bis(indolyl)methane (normal pathway) was the only product formed via vinyliminium/carbocation intermediate **30**; whereas when R = Ar, then 3,3' bisindole **29** became the sole product, formed via carbocation intermediate **31** (abnormal pathway) [Scheme 10].

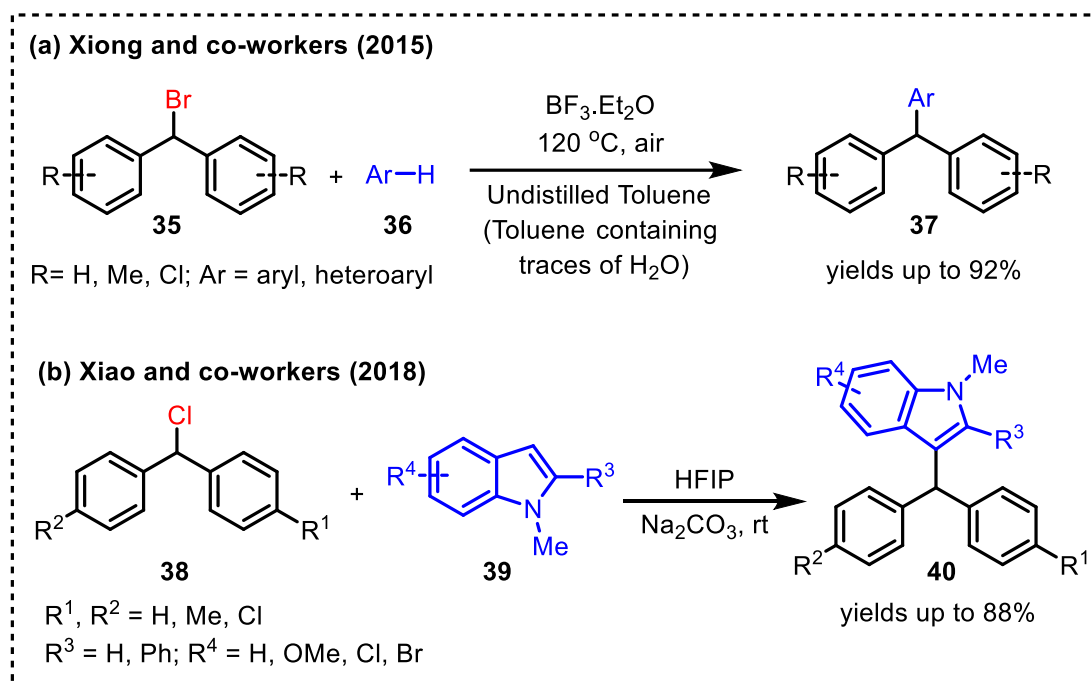
Mei and co-workers in 2018 utilized catalytic amounts of racemic BINOL phosphoric acid (**34**) to synthesize diverse indolyl-substituted triarylmethane derivatives (**33**) in moderate to excellent yields.¹⁸ According to the authors, the reaction is believed to advance through a cascade catalytic dehydration of **32** to generate the carbocation intermediate **32a** followed by the nucleophilic addition of indole **7** to form the desired triarylmethane **33** and, thereby, creating structurally diverse indolyl-substituted triarylmethanes with substituents at the remote C4 position (Scheme 11).



Scheme 11: Synthesis of indolyl-substituted triarylmethanes via Brønsted acid-catalysis

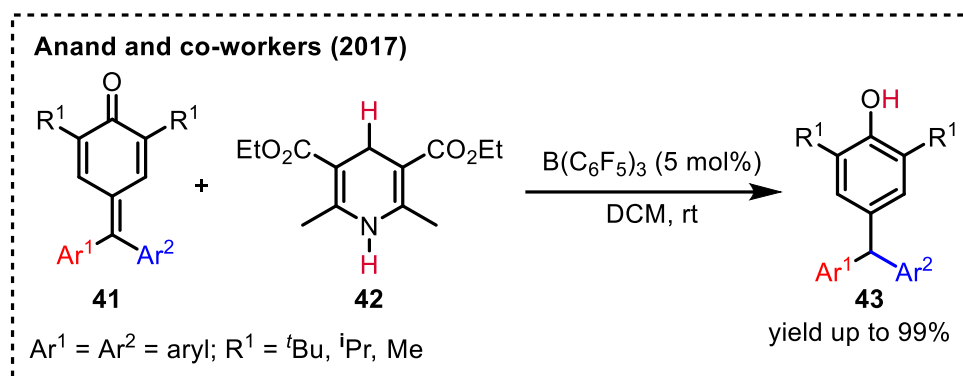
In 2015 Xiong and co-workers developed the synthesis of triarylmethane derivatives (**37**) in excellent yields and regioselectivities via a synergistic metal-free benzylation of (hetero)arenes (**36**) with benzyl bromide **35** utilizing $\text{BF}_3 \cdot \text{H}_2\text{O} / \text{BF}_3 \cdot \text{HX}$ in toluene under an open atmosphere. $\text{BF}_3 \cdot \text{Et}_2\text{O}$ alone was unable to promote the reaction. So, in the presence of water, the precursor $\text{BF}_3 \cdot \text{OEt}_2$ was transformed into super acid $\text{BF}_3 \cdot \text{H}_2\text{O}$. Subsequent ligand exchange between $\text{BF}_3 \cdot \text{OEt}_2$ and HBr, via the cleavage of the C-Br bond, generated $\text{BF}_3 \cdot \text{HBr}$, which then worked as an effective synergistic catalyst for this reaction (Scheme 12a)^{19a}. Later in 2018, Xiao and co-workers reported the synthesis of structurally diverse triarylmethane derivatives (**40**) by reacting various indoles (**39**) with chlorohydrocarbons (**38**) in the presence

of HFIP (hexafluoro2-propanol). Notably, HFIP functions both as the catalyst and solvent in this reaction because of its strong hydrogen bonding capability, which enables the easy dissolution of the substrate as well as activates the C–Halogen bond cleavage (Scheme 12b).^{19b}



Scheme 12: Metal-free benzylation of (hetero)arenes with benzyl halides.

Anand and co-workers in 2017 disclosed an interesting approach for the synthesis of triarylmethanes through a transfer hydrogenation of fuchsones.²⁰ In this method, $\text{B}(\text{C}_6\text{F}_5)_3$ was used as Lewis acid to activate the carbonyl oxygen of fuchsones (**41**). Further, the hydride transfer from the Hantzsch ester (**42**) to the fuchsones in 1,6-fashion leads to the formation of triarylmethanes (**43**) in excellent yields (Scheme 13).

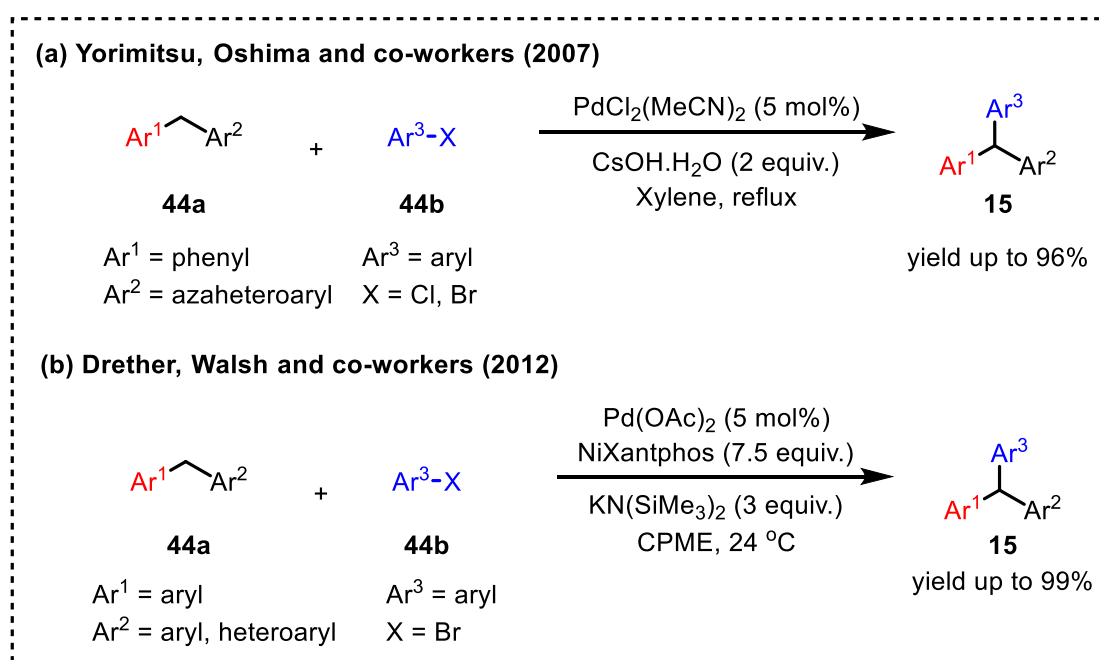


Scheme 13: Reduction of fuchsones for the synthesis of triarylmethanes

1.2.2 Transition metal catalyzed cross-coupling approach for the synthesis of triarylmethanes

Although most of Lewis or Brønsted acid catalyzed approaches are elegant, they suffer from few drawbacks such as poor regioselectivity, harsh reaction conditions and the requirement of electron-rich arenes or heteroarenes. Therefore, to overcome these drawbacks, recently, the transition metal catalyzed cross coupling approach has gained substantial attention from many research groups. Moreover, the transition metal catalyzed cross coupling approaches turn out to be more useful methods for the synthesis of complex unsymmetrical triarylmethanes.²¹ A few of them are discussed in this section.

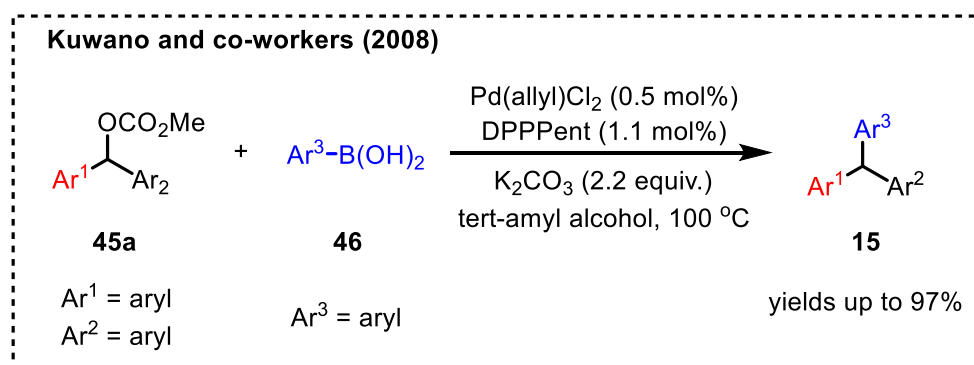
Yorimitsu, Oshima and co-workers reported a palladium catalyzed arylation of aryl(azaaryl)methanes (**44a**) with aryl halides (**44b**) for the first time.^{22a} various unsymmetrical triarylmethanes (**15**) were obtained good to excellent yields (Scheme 14a). Later in 2012, Walsh and co-workers reported a similar palladium catalyzed approach for the synthesis of triarylmethanes **15** through cross coupling of diarylmethanes (**29a**) and aryl halides (**29b**). Different functional groups such as acetal, amide, phenol, and acetyl were well tolerated under the reaction conditions (Scheme 14b).^{22b}



Scheme 14: Pd-catalyzed cross coupling approach for the synthesis of TRAMs

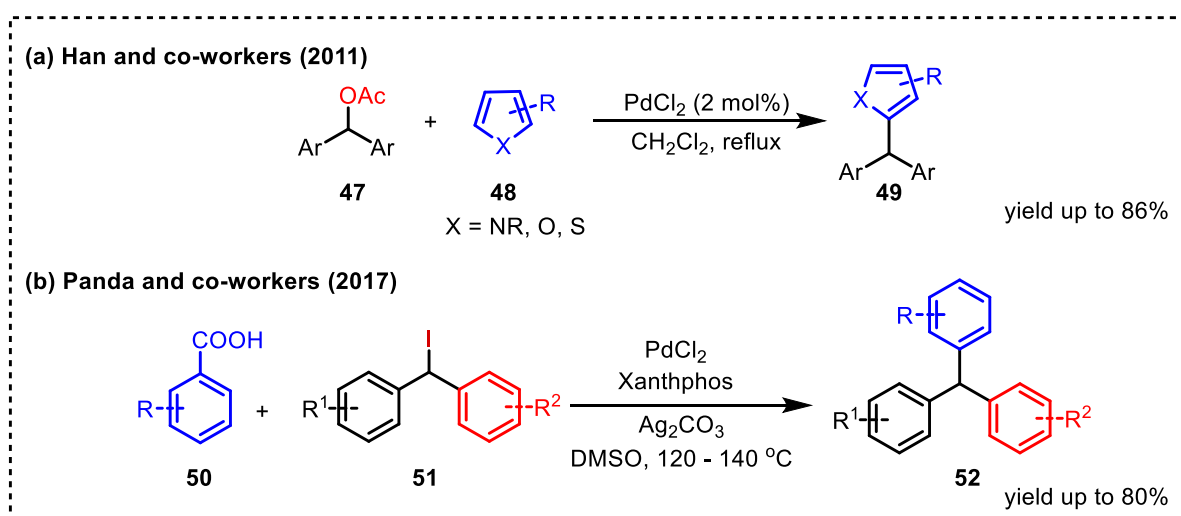
Another interesting approach was discovered by Kuwano and co-workers for the synthesis of unsymmetrical triarylmethanes via a Suzuki-Miyaura cross coupling reaction.²³ Varieties of diarylmethyl carbonates (**45a**) were coupled with arylboronic acid (**46**) under the

optimized conditions to furnish the unsymmetrical triarylmethanes (**15**) in good yields (Scheme 15)



Scheme 15: Pd-catalyzed Suzuki-Miyaura cross coupling approach

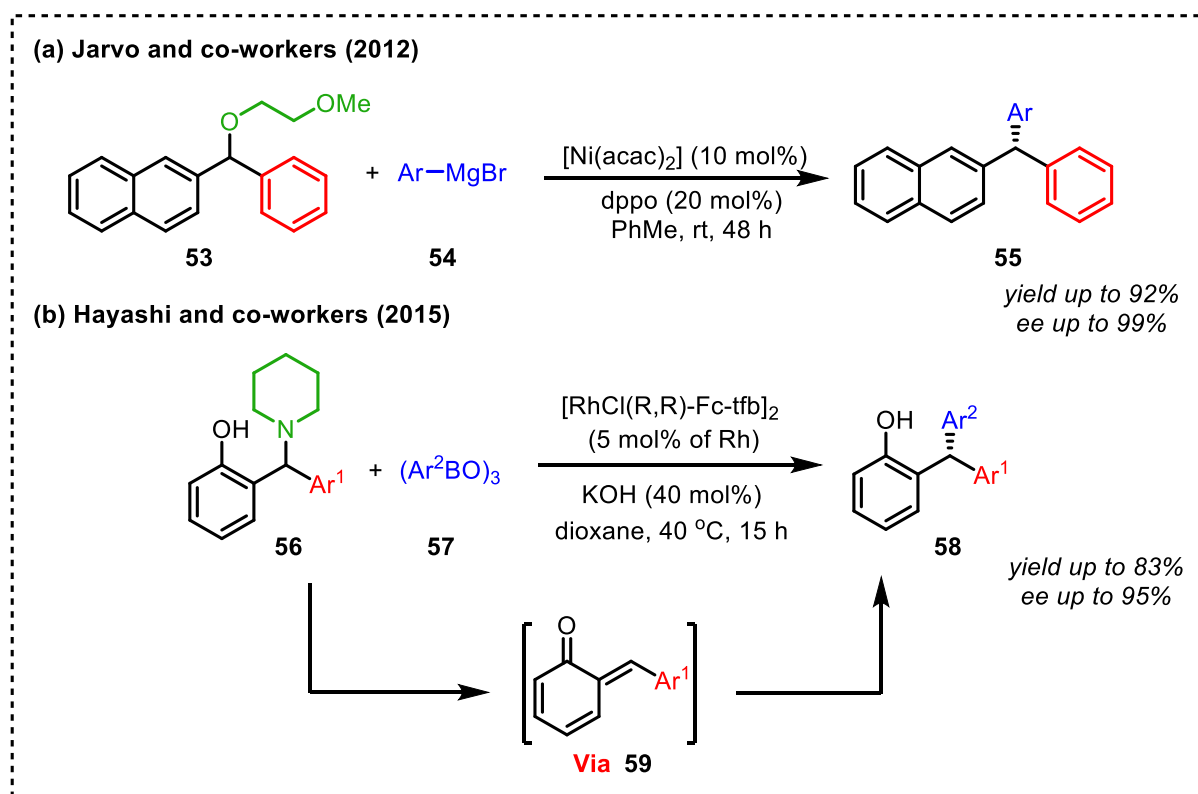
Han and co-workers in the year 2011 developed a PdCl₂-catalyzed protocol for the efficient benzylation of a wide range of -N-, -O-, and -S containing heteroarenes. The benzylation proceeds via the Pd(0)-catalyzed Tsuji–Trost pathway and represents an excellent example of base/acid, additive, and ligand-free cross-coupling approach for the synthesis of TRAMs **49** in moderate to good yields (Scheme 16a).²⁴



Scheme 16: Pd-catalyzed synthesis of TRAMs via cross-coupling reaction.

In 2017, Panda and co-workers reported the synthesis of triarylmethanes (**52**) through a Pd-catalyzed decarboxylative cross-coupling reaction between aryl carboxylic acid **50** and diaryl methyl iodide **51** via expulsion of CO₂. The reaction proceeds through sp²–sp³ coupling via decarboxylation of benzoic acid **50** and subsequent reaction with diaryl methyl iodide **51** leading to the formation of diverse triarylmethane derivatives (**52**) in moderate to good yields (Scheme 16b).²⁵

In 2012 Jarvo and co-workers developed a traceless activation protocol for synthesizing TRAMs derivatives **55** through a nickel-catalyzed cross-coupling reaction between diaryl ether **53** and aryl magnesium bromide **54** employing $\text{Ni}(\text{acac})_2/\text{dppo}$ furnished enantioenriched triarylmethanes (**55**) in good yields and excellent enantioselectivity. Diaryl ethers containing pendant Lewis bases act as coordinating sites for the ligand to direct the approaching nucleophiles and enhance the reaction rate (Scheme 17a).^{26a}

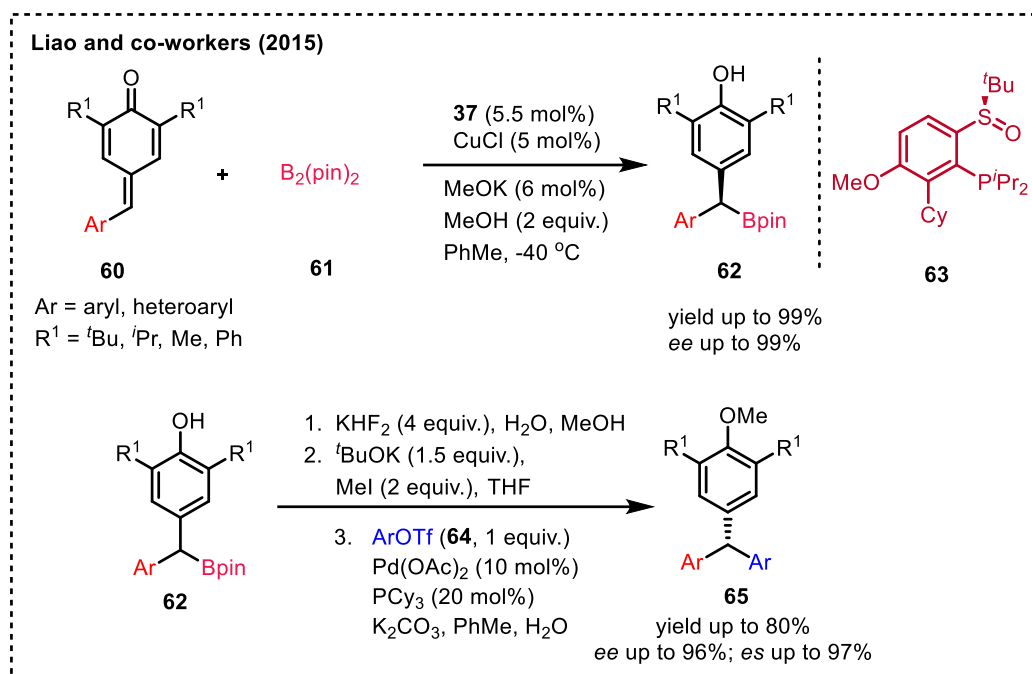


Scheme 17: Nickel and Rhodium-catalyzed synthesis of chiral triarylmethanes

Hayashi and co-workers in 2015 reported an efficient catalytic protocol for the stereoselective construction of chiral TRAMs (**58**), via a rhodium-catalyzed substitution of diarylmethylamines (**56**) with aryl boron reagents (**57**). The reaction proceeds through the conjugate addition of the aryl boron reagent to the in-situ generated *ortho*-quinonemethide intermediate **59** generated from diarylmethylamine **56** in the presence of $[\text{RhCl}(\text{R,R})\text{-Fc-tfb}]_2$ catalysts (Scheme 17b).^{26b}

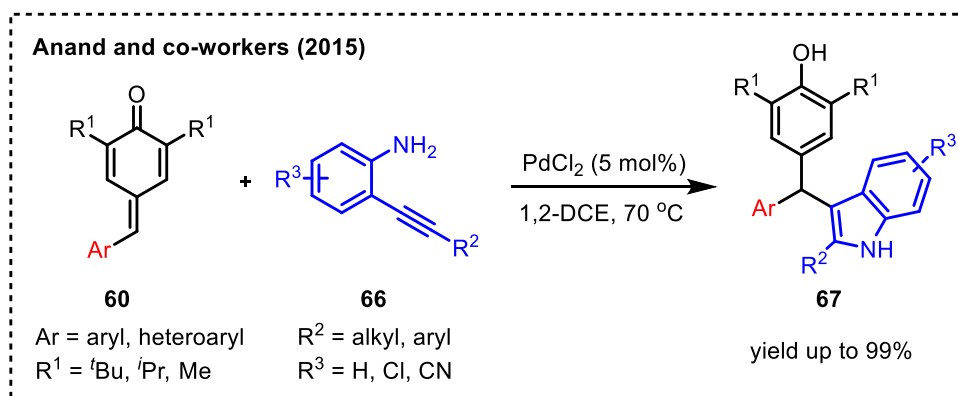
Recently, transition metal catalyzed cross coupling approaches have also applied for the synthesis of triarylmethanes using *p*-QMs as 1,6-acceptor. For example, Liao and coworkers demonstrated a copper-catalyzed asymmetric 1,6-conjugate addition of diborane (**61**) to *p* QMs (**60**) to access *gem*-diarylmethyl boronates (**62**) in excellent yields and enantioselectivity.

Further the chiral *gem*-diarylmethyl boronates (**62**) were subjected to stereospecific Suzuki-Miyaura cross-coupling with aryl triflates (**64**). Notably, in most of the cases, the desired enantioenriched triarylmethanes (**65**) were observed in excellent yields and excellent enantioselectivity (Scheme 18).²⁷



Scheme 18: Asymmetric synthesis of triarylmethanes from *p*-QMs

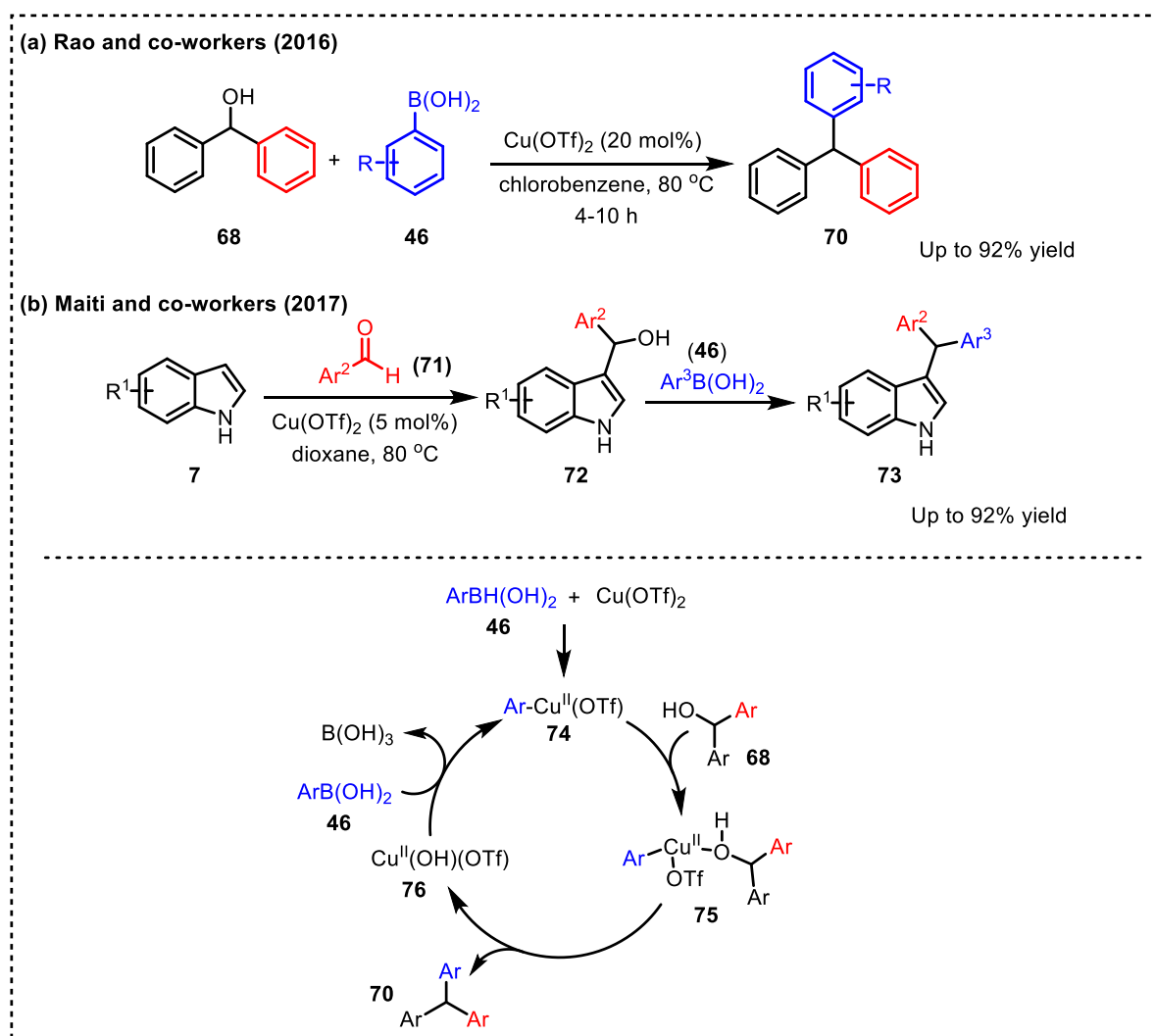
Anand and co-workers in 2015 developed another interesting one-pot approach for the synthesis of unsymmetrical triarylmethanes (**67**) through a palladium catalyzed annulation of *o*-alkynylanilines (**66**) followed by 1,6-conjugate addition to *p*-QMs (**60**). It is noteworthy to mention that, this reaction underwent smoothly without protection of amino group of *o*-alkynylanilines. Most of the unsymmetrical diarylindolylmethanes (**67**) were isolated in good



Scheme 19: Pd-catalyzed domino approach for synthesis of triarylmethanes from *p*-QMs

to excellent yields. Various functional group tolerance, mild reaction conditions, 100% atom economical approach made this transformation very attractive (Scheme 15).²⁸

Besides the use of Pd, Ni and Rh based catalysts, the copper salts, due to their low cost, easy availability, and operational accessibility, have also been utilized as a versatile metal catalysts for various C–C bond forming reactions to synthesize triarylmethanes. For instance in 2016, Rao and co-workers utilized copper (II)-triflate for the synthesis of symmetrical and unsymmetrical triarylmethanes (**70**) in good yields using diarylmethanols (**68**) and arylboronic acid (**46**) as the reaction partners (Scheme 20a).^{29a} Similarly Maiti and co-workers in 2017 utilized Cu(OTf)₂ for the synthesis of unsymmetrical triarylmethane derivatives (**73**) through the initial synthesis of indolylmethanol derivatives (**72**) followed by coupling with arylboronic acids (**46**) (Scheme 20b).^{29b} Both the reaction followed a similar type of mechanism and proceeds via the transmetalation of Cu(OTf)₂ and **46** to form ArCu(OTf) **74**. The reaction of

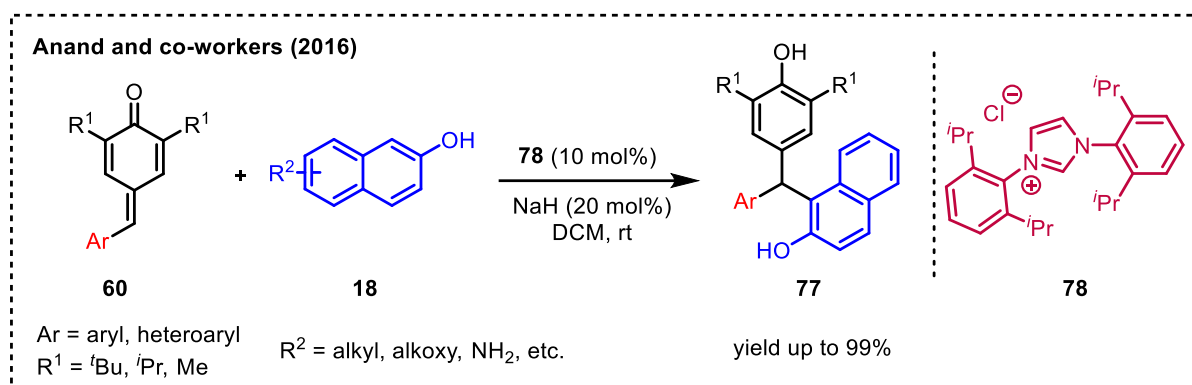


Scheme 20: Copper (II)-catalyzed synthesis of triarylmethanes from diarylmethanols

74 with diarylmethanol **68** advances via the aryl transfer and simultaneous C–O bond cleavage to form the triarylmethane **70** and Cu(OH)(OTf) complex (**76**). The reaction of Cu(OH)(OTf) with aryl boronic acid then regenerates (**72**).

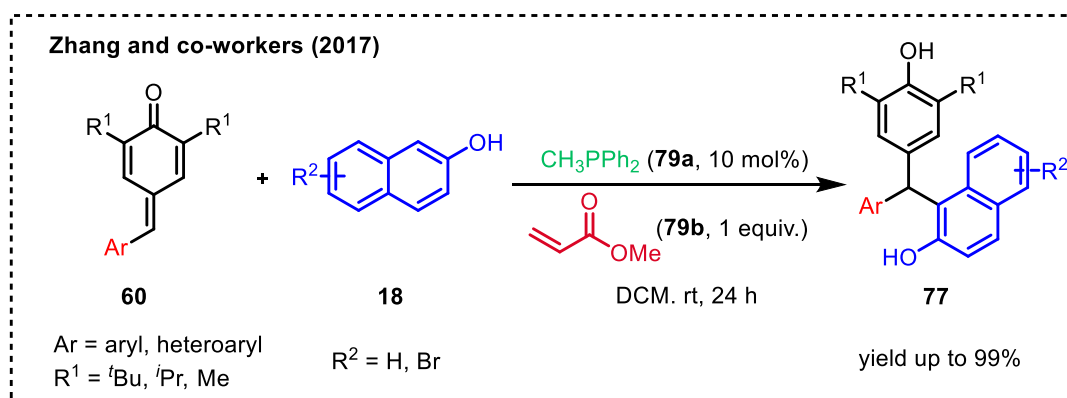
1.2.3 Organocatalytic approaches for the synthesis of triarylmethanes

Apart from Lewis or Brønsted acid catalyzed Friedel-Crafts alkylation approach and transition metal catalyzed cross coupling approaches, there are few organocatalytic approaches known in the literature for the synthesis of unsymmetrical triarylmethanes. For example, Anand and co-workers reported an *N*-heterocyclic carbene catalyzed 1,6-conjugate addition of 2-naphthols (**18**) to *p*-QMs (**60**) for the synthesis of unsymmetrical triarylmethanes. In this method, the *N*-heterocyclic carbene derived from **78** was used as a Brønsted base. An array of unsymmetrical triarylmethanes (**77**) was synthesized in good to excellent yields (Scheme 21).³⁰



Scheme 21: N-heterocyclic carbene catalyzed synthesis of unsymmetrical triarylmethanes

Later, Zhang and co-workers demonstrated an interesting approach for the synthesis of unsymmetrical triarylmethanes. Phosphine catalyzed 1,6-conjugate addition of 2-naphthols (**18**) to *p*-QMs (**60**) was developed and the desired unsymmetrical triarylmethanes (**77**) were isolated in good to excellent yields. Notably, for the first time, phosphine has been utilized for



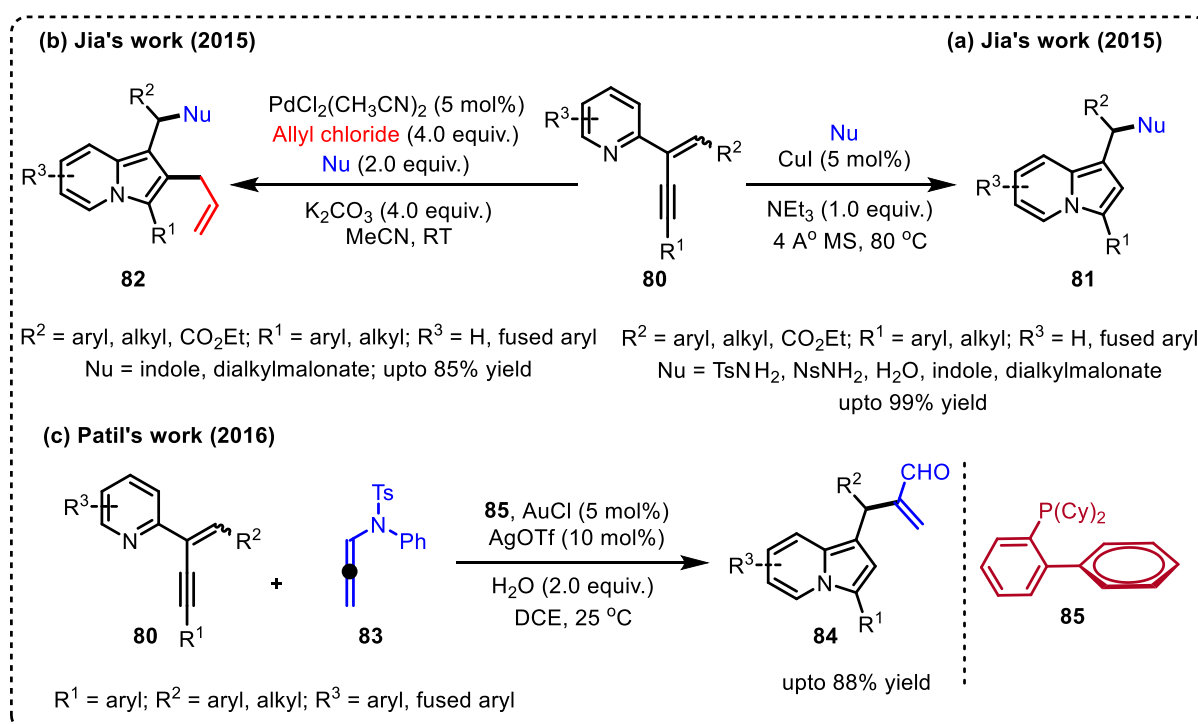
Scheme 22: Phosphine-catalyzed synthesis of unsymmetrical triarylmethanes

the Friedel-Crafts reaction. The authors have explained that the combination of phosphine **79a** and methyl acrylate **79b** generates an active species *in situ*, which actually catalyzes the reaction (Scheme 22).³¹

1.3 Literature reports on 2-(2-enynyl)-pyridines in organic synthesis:

In the past few years, the annulation of 2-(2-enynyl)-pyridines have been utilized for the construction of various nitrogen heterocycles. A few literature reports on the utilization of 2-(2-enynyl)-pyridines have been discussed in this section.

In 2015, Jia and co-workers reported a Cu-catalyzed cyclization of 2-(2-enynyl)-pyridines (**80**) followed by the remote nucleophile addition of different nucleophiles. Various nucleophiles, such as indoles, malonates, amides, alcohols, and even water, were successfully

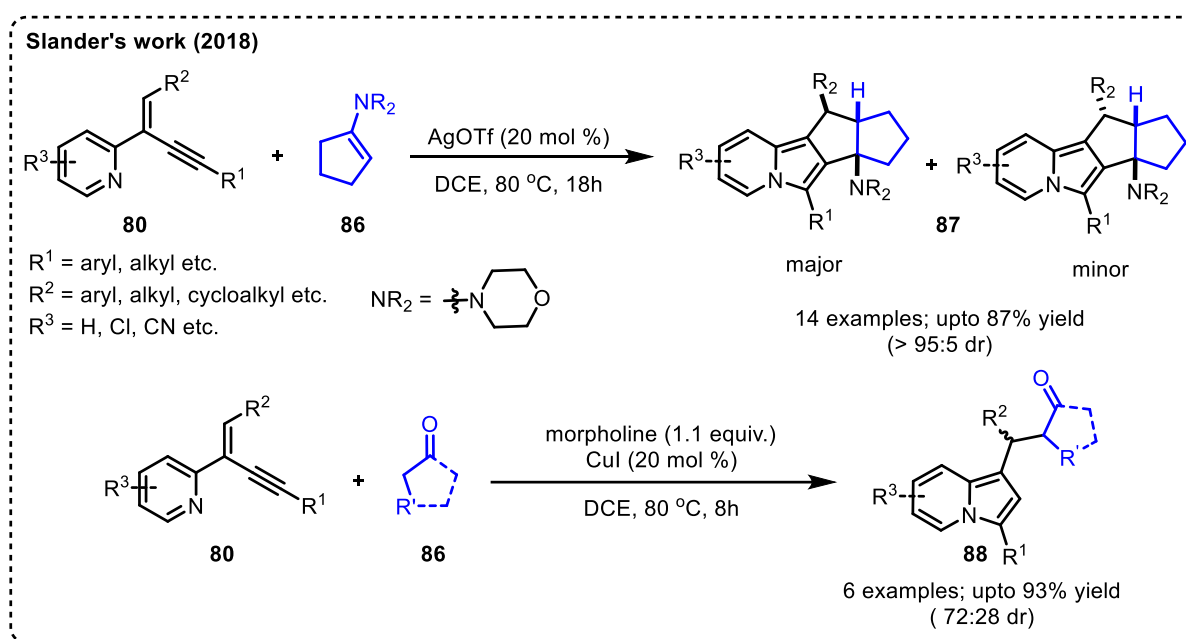


Scheme 23: Indolizine synthesis from 2-(2-enynyl)-pyridines

employed to synthesize a variety of indolizine derivatives **81** (Scheme 23a).^{32a} Further, this protocol was extended to a Pd-catalyzed three-component cascade reaction to synthesize highly substituted indolizine derivatives (**82**). The present cascade reaction unveiled that the cyclization of 2-(2-enynyl)-pyridines (**80**) with a remote nucleophile addition followed by allyl trapping led to indolizines (**82**), in which two C-C and the formation of a C-N bond occur simultaneously (Scheme 23b).^{32b} Later, Patil and co-workers developed a co-operative Au/Ag

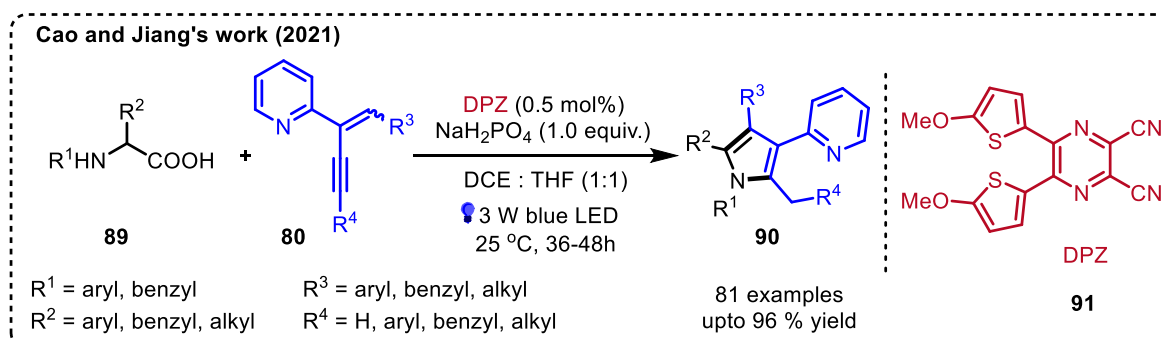
catalyzed protocol for the synthesis of indolizine derivatives (**84**) using 2-(2-enynyl)-pyridines (**80**) and *N*-allenamide (**83**) as a nucleophilic enal equivalent (Scheme 23c).^{32c}

Slander group in 2018 developed a diastereoselective metal-catalyzed synthesis of a variety of polycyclic indolizine derivatives in good to excellent yields by the reaction of 2-(2-enynyl)pyridines (**80**) and cyclic enamines (**86**). When the reaction was performed using enamines, polycyclic indolizines (**87**) were obtained. Whereas with the *in situ*-generated enamines led to the formation of ketone-based indolizine derivatives **88** (Scheme 24).³³



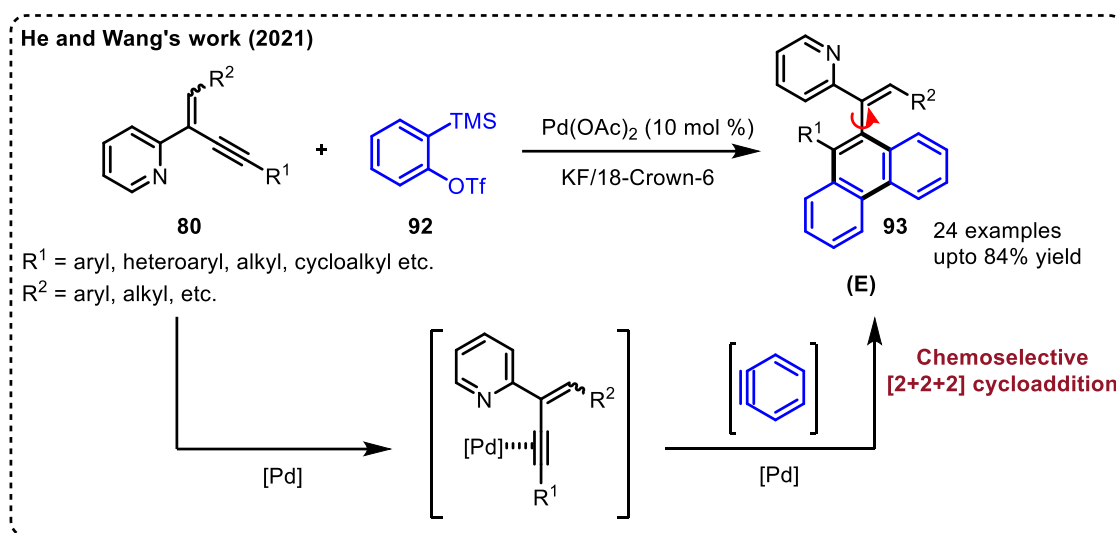
Scheme 24: Synthesis of polycyclic indolizines from 2-(2-enynyl)-pyridines

Very recently, Cao and Jiang's group developed an efficient photoredox catalytic synthetic method to synthesize a variety of azaarene-substituted highly functionalized pyrroles (**90**) from α -amino acids (**89**) and 2-(2-enynyl)-pyridines (**80**) as the reaction partner by utilizing a dicyanopyrazine-derived chromophore (DPZ) as the sensitizer. The reaction



Scheme 25: Synthesis of functionalized pyrroles from 2-(2-enynyl)-pyridines

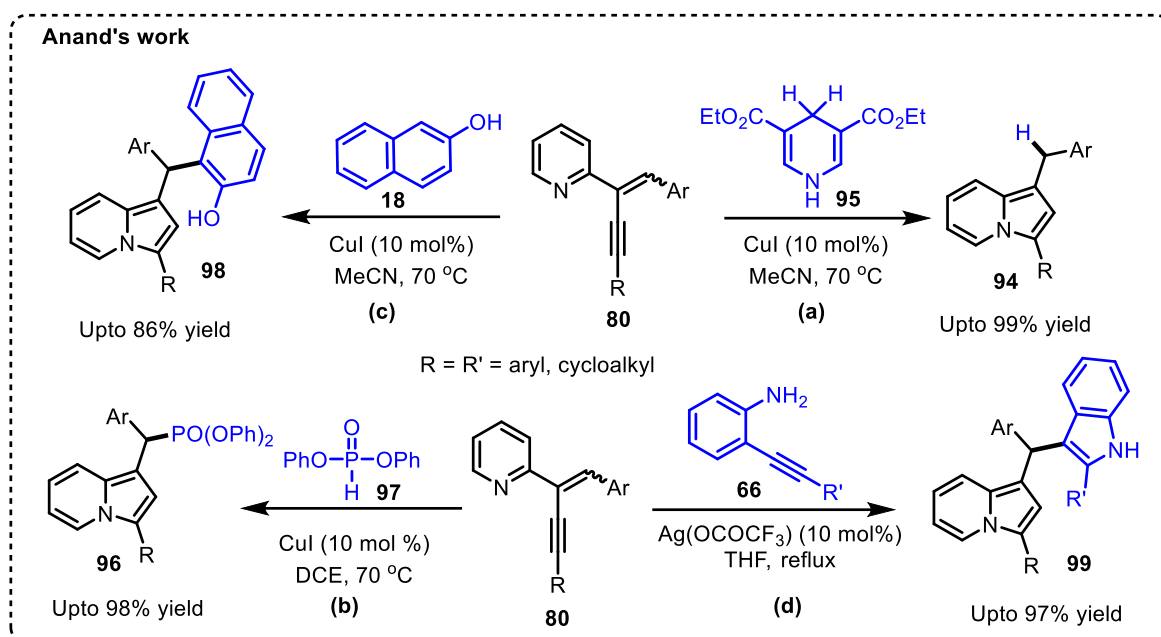
proceeds through the generation of α -amino radical from **89** and a tandem redoxneutral radical addition of α -amino radical to **80**, followed by cyclization and aerobic oxidative aromatization to furnish the desired pyrrole derivatives. In addition, the control experiments and DFT calculations revealed that NaH_2PO_4 is necessary and plays an essential role in protonation and cyclization (Scheme 25).³⁴



Scheme 26: Pd-catalyzed selective [2 + 2 + 2] annulation of 2-(2-Enynyl)pyridines

He and Wang's group reported a palladium-catalyzed chemo- and stereoselective [2+2+2]-annulation reaction of 2-(2-enynyl)pyridines (**80**) with benzyne precursor (**92**) in the presence of KF and 18-crown-6 as an additive. A wide range of (*E*)-phenanthrenylated 2-alkenyl pyridines (**93**) were obtained in moderate to good yields with excellent *E*-selectivity with a chiral axis between an alkene and a phenanthrene ring (Scheme 26).³⁵

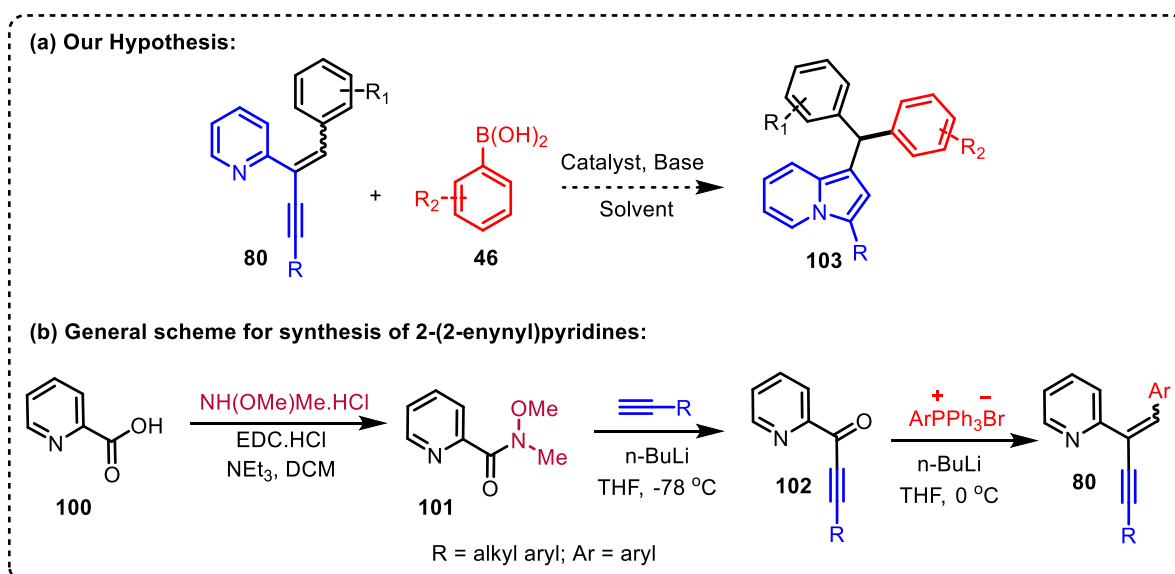
Our group has also contributed in this area, and we have reported the synthesis of a variety of indolizine-containing unsymmetrical diarylmethane derivatives (**94**) in good to excellent yields through a Cu-catalyzed reductive cyclization of 2-(2-enynyl)-pyridines (**80**) using Hantzsch ester (**95**) as a reducing agent (Scheme 27a)^{36a} and the synthesis of indolizine containing diarylmethyl phosphonates (**96**) through a Cu-catalyzed 5-*endo*-dig cyclization of 2-(2-enynyl)-pyridines (**80**) followed by remote hydrophosphonylation (Scheme 27b).^{36b} This protocol was further extended for the synthesis of unsymmetrical triarylmethanes (**98**) through a Cu-catalyzed nucleophilic addition of 2-naphthols (Scheme 27c)^{36a} and Ag-catalyzed double 5-*endo*-dig cyclization of 2-alkynyl anilines (**66**) and 2-(2-enynyl)-pyridines (**80**) to access indolizine containing unsymmetrical triarylmethanes **99** (Scheme 27d).^{36c}



Scheme 27: Metal-catalyzed synthesis of diaryl- and triarylmethanes from 2-(2-Enynyl)pyridines

1.4 Background:

Recently, the 5-*endo*-dig cyclization approach has proven to be an exciting strategy for constructing many valuable bicyclic heterocycles. While working on the development of new protocols to access indolizine-containing diaryl- and triarylmethane derivatives, we envisioned that it could be possible to access indolizine-containing unsymmetrical triarylmethanes from the reaction of 2-(2-enynyl)pyridines (**80**) with organoboronic acids (**46**) as a cheap and readily

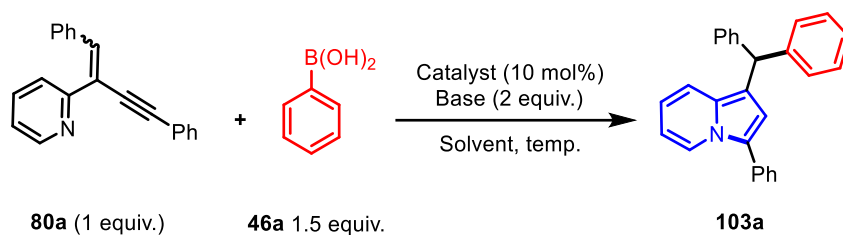


Scheme 28: Our Hypothesis and synthesis of 2-(2-enynyl)-pyridine

available starting material utilizing the 5-*endo-dig* cyclization approach (Scheme 28a). For this purpose, we prepared a broad range of 2-(2-enynyl)-pyridines (**80**) starting from 2-picolinic acid (**100**) by following known literature procedures (Scheme 28b).^{32a-c}

1.5 Results and Discussion:

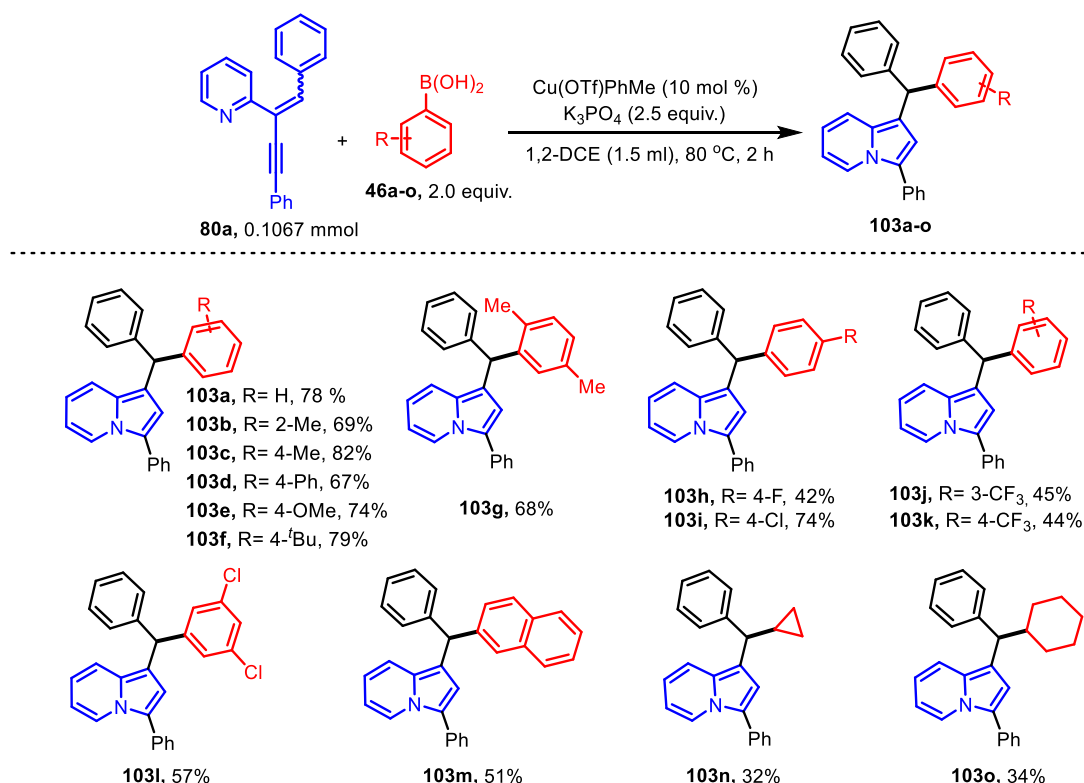
To optimize the reaction conditions, we have chosen readily available phenylboronic acid **46a** and 2-(2-enynyl) pyridine **80a** as model substrates, and the results are shown in Table 1. The preliminary experiment was performed with CuI as the catalyst and KO^tBu as the base in MeCN solvent at room temperature, but no product formation was seen as the starting material was decomposed into many unidentified complex mixtures within 12 hours (Table 1, entry 1). To our pleasure, when the reaction temperature was increased to 70 °C, the desired product **103a** was obtained in 52% yield within 6 hours (Table 1, entry 2). When the reaction was performed in 1,2-DCE as the solvent at 70 °C, the desired product was isolated in 58% yield in just 2 hours (Table 1, entry 3). When the reaction was performed with K₃PO₄ as the base, the yield of the reaction was increased to 62% (table 1, entry 4). Encouraged by this result, further optimization studies were performed using K₃PO₄ as the base in different solvents such as 1,4-dioxane, DMF, etc.; however, the yield of **103a** was lower as compared to 1,2 DCE (Table 1, entries 5 to 7). Further, the reaction was performed with different copper-based catalysts such as Cu(OAc)₂, Cu(OTf)₂, CuBr, etc. (Table 1, entries 8 to 11); out of which Cu(OTf).PhMe was found to be the effective catalyst to drive this transformation as the desired product was obtained in 68% isolated yield (Table 1, entry 11). A considerable improvement in the yield of **103a** was observed when the reaction temperature was raised to 80 °C, and the product was obtained in 78% yield (Table 1, entry 12). Fascinated with these results, we further optimized the reaction conditions using different inorganic and organic bases such as K₂CO₃, NaHCO₃, NEt₃, etc. However, no improvement in the yield was observed (Table 1, entries 13 to 15). When PdCl₂ was used as the catalyst, only trace amounts of product formation was seen even after 24 hours (Table 1, entry 16). The reaction was also performed with various silver salts such as AgOCOCF₃ and AgSbF₆, as well as with Bi(OTf)₃ as the catalyst, but these salts were proven to be ineffective for this transformation as the starting material was decomposed to a complex mixture (Table 1, entries 17-19). No product formation was seen in the absence of the catalyst, which indicates that a catalyst is required to drive this transformation (Table 1, entry 20).

Table 1. Optimization Study^a

S/No	Solvent	Catalyst	Base	Temp. °C	Time (h)	% Yield ^b
01	MeCN	CuI	KO ^t Bu	RT	12	ND
02	MeCN	CuI	KO ^t Bu	70	6	52
03	1,2-DCE	CuI	KO ^t Bu	70	2	58
04	1,2-DCE	CuI	K ₃ PO ₄	70	2	62
05	Toluene	CuI	K ₃ PO ₄	70	12	60
06	1,4-Dioxane	CuI	K ₃ PO ₄	70	36	42
07	DMF	CuI	K ₃ PO ₄	70	12	16
08	1,2-DCE	Cu(OAc) ₂	K ₃ PO ₄	70	24	36
09	1,2-DCE	Cu(OTf) ₂	K ₃ PO ₄	70	2	65
10	1,2-DCE	Cu(OTf).PhMe	K ₃ PO ₄	70	2	68
11	1,2-DCE	CuBr	K ₃ PO ₄	70	3	44
12^c	1,2-DCE	Cu(OTf).PhMe	K₃PO₄	80	2	78
13	1,2-DCE	Cu(OTf).PhMe	K ₂ CO ₃	80	6	63
14	1,2-DCE	Cu(OTf).PhMe	NaHCO ₃	80	6	42
15	1,2-DCE	Cu(OTf).PhMe	NEt ₃	80	12	36
16	1,2-DCE	PdCl ₂	K ₃ PO ₄	80	24	Trace
17	1,2-DCE	AgOCOCF ₃	K ₃ PO ₄	80	24	ND
18	1,2-DCE	AgSbF ₆	K ₃ PO ₄	80	24	ND
19	1,2-DCE	Bi(OTf) ₃	K ₃ PO ₄	80	24	ND
20	1,2-DCE	K ₃ PO ₄	80	24	ND

^a Reaction conditions: All the reactions were carried out with 0.1067 mmol (30 mg) of SM **80a**, 1.5 equiv. of boronic acid, 2.0 equiv. of base and 10 mol % of catalyst in (1.5 ML solvent). ^b Isolated yields; ^c 2.0 equiv. of boronic acid, 2.5 equiv. of base (K₃PO₄) with respect to **80a** and 10 mol % catalyst at 80 °C was found to be optimal.

Table 2 Substrate Scope with different aryl boronic acids

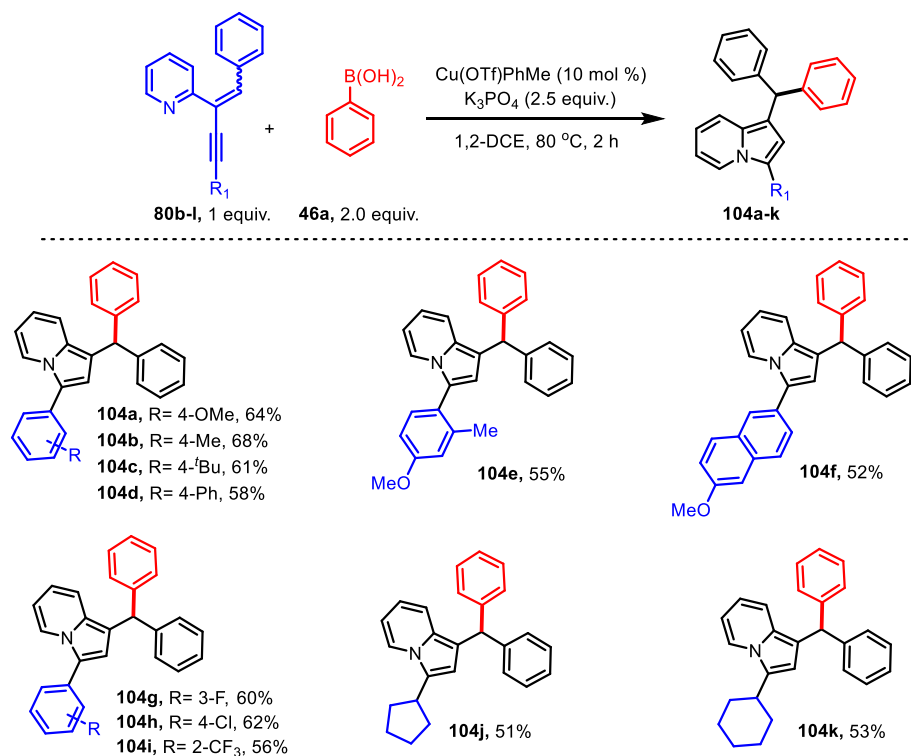


^aReaction conditions: All the reactions were carried out with 0.1067 mmol of (**80a**), 2.0 equiv. of boronic acids (**46a-o**) and 2.5 equiv. K₃PO₄ in (1.5 ML 1,2-DCE). Yields reported are isolated yields.

With the optimized reaction conditions in hands, the generality of this transformation was investigated by employing different (EDG, halo, EWG)-substituted phenylboronic acids **46a-m**, and in all those cases, the desired products **103a-m** were isolated in moderate to good yields (42-82%). This transformation also worked with cyclopropyl and cyclohexyl boronic acids as well. However, the yields were low in those cases as the respective products **103n** and **103o** were isolated in 32 and 34% yields, respectively. Table 2 reveals the substrate scope of this transformation with different boronic acids.

Then, we went on to investigate the substrate scope with 2-(2-enynyl) pyridines **80b-l** having different aryl substituents (both electron-rich and electron-poor) and cycloalkyl groups at the alkyne part and, to our delight, in all those cases, the expected products **104a-k** were obtained in the range of 51-64% yield under the optimized reaction conditions. Table 3 reveals the substrate scope with 2-(2-enynyl) pyridines having different substituents at the alkyne part.

Table 3 Substrate scope with 2-(2- enynyl) pyridines having different substituents at the alkyne part.



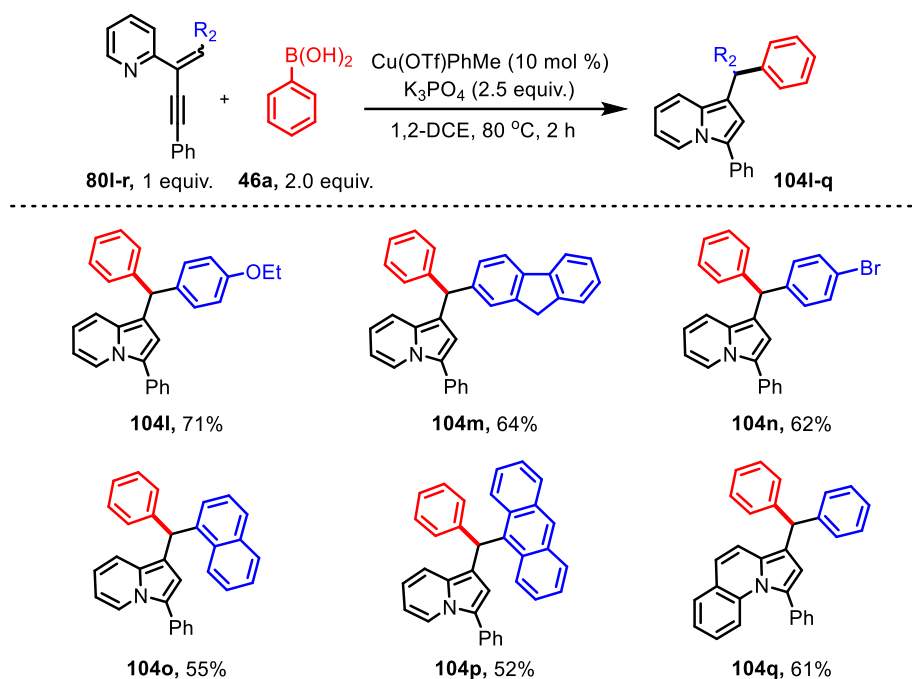
^aReaction conditions: All the reactions were carried out with 0.1067 mmol of (**80b-l**), 2.0 equiv. of bobonic acid (**46a**) and 2.5 equiv. K_3PO_4 in (1.5 ML 1,2-DCE). Yields reported are Isolated yields.

The substrate scope studies were also elaborated to other 2-(2-enynyl) pyridines (**80n-s**) having different aryl substituents at the alkene part under the optimal reaction conditions. 2-(2-enynyl)pyridines (**80n-p**) substituted with electron-rich aryl groups reacted smoothly to afford the corresponding products **104m-o** in moderate yields. 2-(2-enynyl)pyridine **80q**, substituted with halo-group provided the product **104p** in 61% yield. The reaction also worked well with 2-(2-enynyl)pyridine **80r & 80s**, having bulky substituents such as naphthalene and anthracene at the alkene part, and the products were obtained in 55% and 52% respectively. 2-(2-enynyl)pyridine **80t** derived from quinaldic acid afforded the product **104s** in 61% yield. Table 4 reveals the substrate scope with 2-(2-enynyl) pyridines having different substituents at the alkene part.

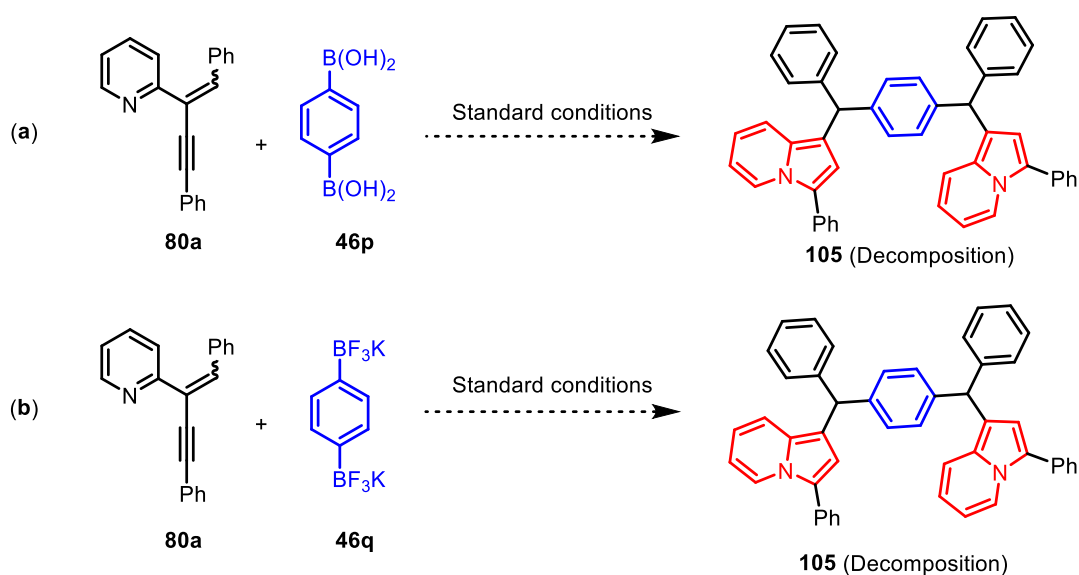
To improve the substrate scope, a couple of reactions were also performed between 2-(2-enynyl)pyridine **80a** (2.2 equiv.) with 1,4-diboronic acid **46p** and also with potassium salt of 1,4-diboronic acid **46q** under the optimized reaction conditions. Unfortunately, the desired

product **105** was not obtained as in both cases, and decomposition of the starting material was observed (Scheme 29).

Table 4 Substrate scope with 2-(2-enynyl) pyridines having different substituents at the alkene part.

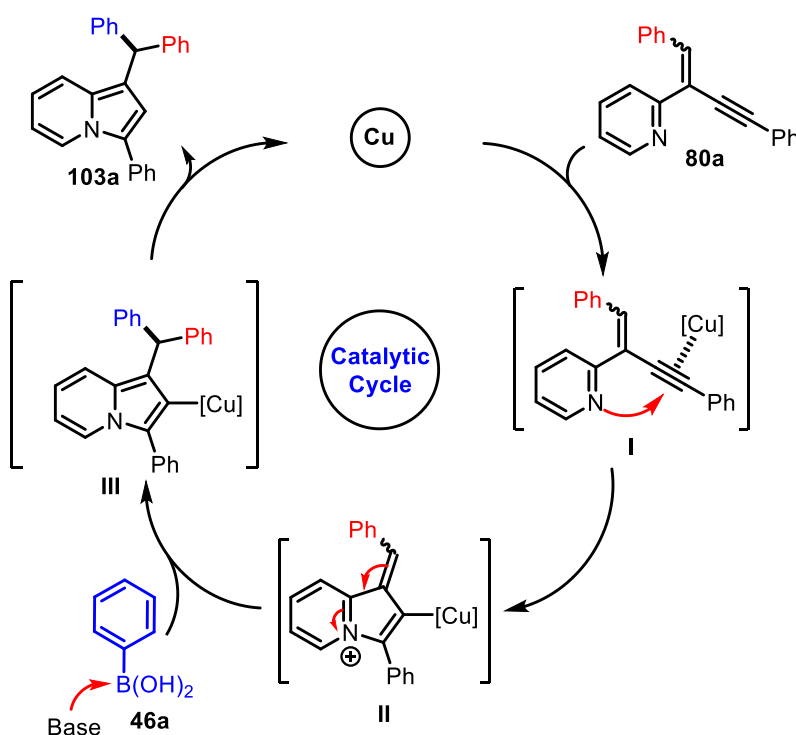


^aReaction conditions: All the reactions were carried out with 0.1067 mmol of (**80l-r**), 2.0 equiv. of bobonic acid (**46a**) and 2.5 equiv. K_3PO_4 in (1.5 mL of 1,2-DCE). Yields reported are Isolated yields.



Scheme 29: Reaction of 2-(2-enynyl)pyridine with 1,4-diboronic acid

Based on the previous literature reports, a plausible mechanism for this transformation was proposed, as shown in (Scheme 30). The reaction begins with the activation of the alkyne part of **80a** by the copper catalyst to generate intermediate **I**, which undergoes 5-*endo*-dig-cyclization to produce the intermediate indolizinium salt **II**, in which the exocyclic alkene-



Scheme 30: Proposed Mechanism

part becomes relatively more electrophilic due to the generation of the positive charge on the nitrogen atom. Subsequently, remote nucleophilic addition of the aryl nucleophile, generated from the boronic acid **46a** to the exocyclic olefinic center of intermediate **II** generates another intermediate **III**, which upon protonation affords the final product **103a** along with the regeneration of the catalyst.

The structure of the final products was confirmed from ^1H NMR, ^{13}C NMR, IR spectroscopy and mass spectrometry. For example, in ^1H NMR of the compound **103c** (see figure 4) the presence of singlet of (3H) at δ 2.33 ppm due to the methyl proton marked as (a), singlet of (1H) at δ 5.72 ppm due to the benzylic $-\text{CH}$ marked as (b) and the singlet of (1H) at δ 6.52 ppm due to the single proton present at the 2-position of indolizine ring marked as (c). In ^{13}C NMR (see figure 5) the disappearance of alkyne peak from **80a**, and the aliphatic peak observed at δ 21.2 ppm for the methyl carbon marked as (a), and the peak at δ 48.3 ppm for the triaryl carbon marked as (b) confirms the formation of product **103c**. Further the formation of

103c was also confirmed by the HRMS (ESI): m/z calcd for $C_{30}H_{22}NO_2$ $[M+H]^+$: 428.1572; found : 427.1572.

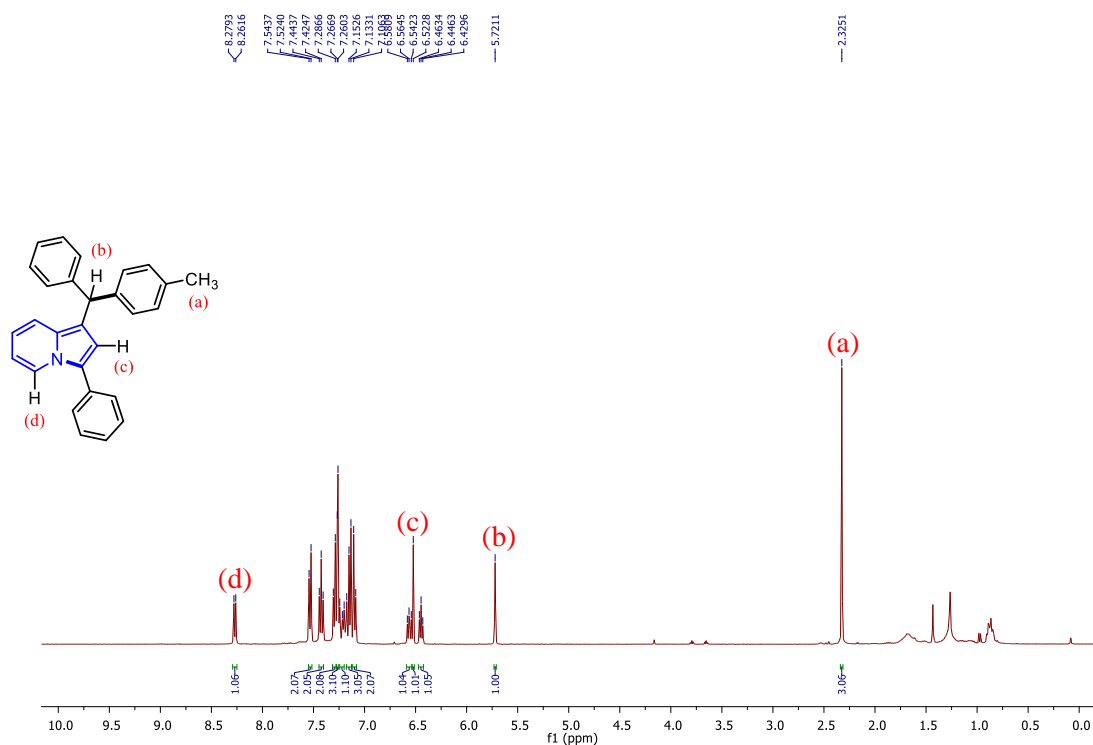


Figure 4: ¹H NMR (400 MHz, CDCl₃) spectrum of **103c**

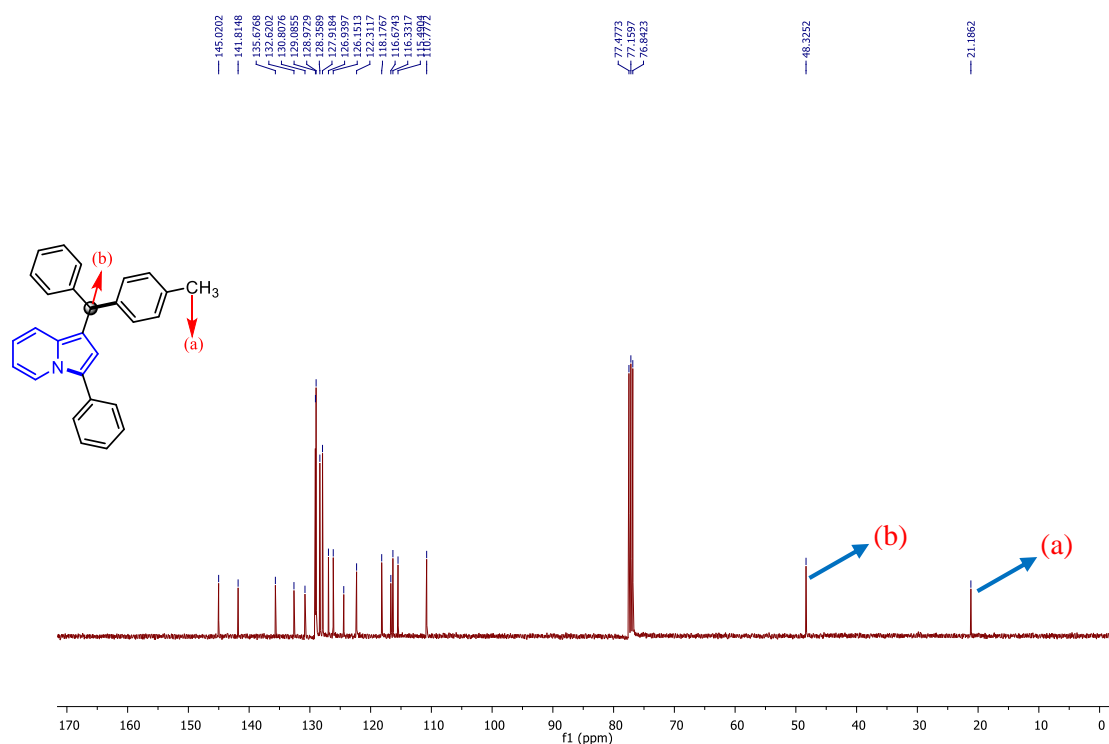


Figure 5: ¹³C{¹H} NMR (100 MHz, CDCl₃) spectrum of **103c**

1.6 Conclusions:

In conclusion, we have developed an efficient protocol for the synthesis of 1,3-disubstituted indolizine containing unsymmetrical triarylmethane derivatives through a copper-catalyzed 5-*endo*-dig cyclization of 2-(2-enynyl)pyridines followed by remote nucleophilic addition of organoboronic acids. The generality of this transformation was examined using a wide range of boronic acid and 2-(2-enynyl) pyridines, and the respective triarylmethanes were obtained in moderate to good yields.

1.7 Experimental Section:

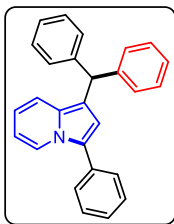
General methods: All reactions were carried out in an oven dried round bottom flask. All the solvents were distilled before use and stored under argon atmosphere. Most of the reagents, starting materials were purchased from commercial sources and used as such. Melting points were recorded on SMP20 melting point apparatus and are uncorrected. ^1H , ^{13}C and ^{19}F spectra were recorded in CDCl_3 (400, 100 and 376 MHz respectively) on Bruker FT-NMR spectrometer. Chemical shift (δ) values are reported in parts per million relative to TMS and the coupling constants (J) are reported in Hz. High resolution mass spectra were recorded on Waters Q-TOF Premier-HAB213 spectrometer. FT-IR spectra were recorded on a Perkin-Elmer FTIR spectrometer. Thin layer chromatography was performed on Merck silica gel 60 F_{254} TLC pellets and visualised by UV irradiation and KMnO_4 stain. Column chromatography was carried out through silica gel (100–200 mesh) using EtOAc/hexane as an eluent.

General procedure for the addition of boronic acids to 2-(2-enynyl)pyridines:

Anhydrous 1,2-DCE (1.5 mL) was added to the mixture of 2-(2-enynyl)pyridine (30 mg, 1.0 equiv.), boronic acid (2.0 equiv.), K_3PO_4 (2.5 equiv.) and $\text{Cu}(\text{OTf})\cdot\text{PhMe}$ (10 mol %) under nitrogen atmosphere and the resulting suspension was stirred at 80 °C until the 2-(2-enynyl)pyridine was completely consumed (based on TLC analysis). The reaction mixture was concentrated under reduced pressure and the residue was purified through a silica gel chromatography, using EtOAc/Hexane mixture as an eluent, to get the pure indolizine based triarylmethanes.

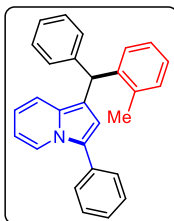
1-benzhydryl-3-phenylindolizine (103a)

The reaction was performed at 0.1067 mmol scale of **80a**; $R_f = 0.8$ (5% EtOAc in hexane); green gummy solid (30.1 mg, 78% yield); ^1H NMR (400 MHz, CDCl_3) δ 8.28 (d, $J = 7.1$ Hz, 1H), 7.54 (d, $J = 8.0$ Hz, 2H), 7.43 (t, $J = 7.6$ Hz, 2H); 7.32 – 7.30 (m, 3H), 7.29 – 7.26 (m,



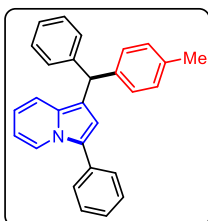
6H), 7.21 (t, $J = 6.9$ Hz, 2H), 7.17 (d, $J = 9.04$ Hz, 1H), 6.60 – 6.55 (m, 1H), 6.54 (s, 1H), 6.46 (t, $J = 6.92$ Hz, 1H), 5.78 (s, 1H); ^{13}C NMR (100 MHz, CDCl_3) δ 144.8, 132.6, 130.8, 129.1, 129.0, 128.4, 128.0, 127.0, 126.2, 124.5, 122.3, 118.1, 116.5, 116.4, 115.5, 110.8, 48.7; FT-IR (thin film, neat): 3028, 1612, 1452, 1250, 736, 696 cm^{-1} ; HRMS (ESI): m/z calcd for $\text{C}_{27}\text{H}_{22}\text{N}$ $[\text{M}+\text{H}]^+$: 360.1752; found : 360.1758.

3-phenyl-1-[phenyl(o-tolyl)methyl]indolizine (103b)



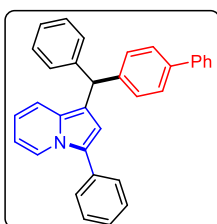
The reaction was performed at 0.1067 mmol scale of **80a**; $R_f = 0.8$ (5% EtOAc in hexane); green gummy solid (27.6 mg, 69% yield); ^1H NMR (400 MHz, CDCl_3) δ 8.30 (d, $J = 7.2$ Hz, 1H), 7.54 (d, $J = 7.6$ Hz, 2H), 7.43 (t, $J = 7.6$ Hz, 2H); 7.31 – 7.28 (m, 3H), 7.24 – 7.17 (m, 4H), 7.15 – 7.10 (m, 3H), 7.04 (d, $J = 7.1$ Hz, 1H), 6.59 – 6.55 (m, 1H), 6.48 – 6.45 (m, 2H), 5.90 (s, 1H), 2.32 (s, 3H); ^{13}C NMR (100 MHz, CDCl_3) δ 144.2, 143.0, 136.4, 132.6, 130.8, 130.4, 129.3, 129.1, 129.0, 128.4, 127.9, 127.0, 126.3, 126.1, 125.9, 124.4, 122.4, 118.1, 116.3, 116.0, 115.9, 110.8, 45.2, 20.0; FT-IR (thin film, neat): 2926, 1601, 1478, 1259, 748, 683 cm^{-1} ; HRMS (ESI): m/z calcd for $\text{C}_{28}\text{H}_{24}\text{N}$ $[\text{M}+\text{H}]^+$: 374.1909; found : 374.1924.

3-phenyl-1-[phenyl(p-tolyl)methyl]indolizine (103c)



The reaction was performed at 0.1067 mmol scale of **80a**; $R_f = 0.8$ (5% EtOAc in hexane); pale yellow solid (32.7 mg, 82% yield); m. p. = 118–120 °C; ^1H NMR (400 MHz, CDCl_3) δ 8.28 (d, $J = 7.2$ Hz, 1H), 7.55 (d, $J = 7.8$ Hz, 2H), 7.44 (t, $J = 7.6$ Hz, 2H); 7.31 (d, $J = 7.4$ Hz, 2H), 7.28 – 7.26 (m, 3H) 7.22 (d, $J = 6.9$ Hz, 1H), 7.19 – 7.15 (m, 3H), 7.11 (d, $J = 7.9$ Hz, 2H), 6.59 – 6.55 (m, 1H), 6.54 (s, 1H), 6.45 (t, $J = 6.76$ Hz, 1H), 5.74 (s, 1H), 2.34 (s, 3H); ^{13}C NMR (100 MHz, CDCl_3) δ 145.0, 141.8, 135.7, 132.6, 130.8, 129.09, 129.08, 129.0 (2C), 128.4, 127.9, 126.9, 126.2, 124.4, 122.3, 118.2, 116.7, 116.3, 115.5, 110.8, 48.3, 21.2; FT-IR (thin film, neat): 2928, 1624, 1482, 1263, 753, 687 cm^{-1} ; HRMS (ESI): m/z calcd for $\text{C}_{28}\text{H}_{24}\text{N}$ $[\text{M}+\text{H}]^+$: 374.1909; found : 374.1916.

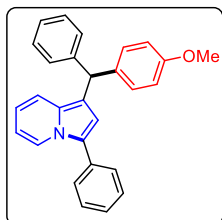
1-[[1,1'-biphenyl]-4-yl(phenyl)methyl]-3-phenylindolizine (103d)



The reaction was performed at 0.1067 mmol scale of **80a**; $R_f = 0.6$ (5% EtOAc in hexane); pale yellow gummy solid (31.3 mg, 67% yield); ^1H NMR (400 MHz, CDCl_3) δ 8.31 (d, $J = 5.9$ Hz, 1H), 7.63 (d, $J = 7.4$ Hz, 2H), 7.58 – 7.55 (m, 4H); 7.47 – 7.43 (m, 4H), 7.37 – 7.30 (m, 8H), 7.26 – 7.22 (m, 2H), 6.62 – 7.59 (m, 2H), 6.48 (t, $J = 6.8$ Hz, 1H), 5.83 (s, 1H); ^{13}C

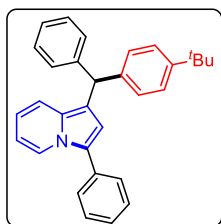
NMR (100 MHz, CDCl₃) δ 144.7, 143.9, 141.1, 139.0, 132.6, 130.9, 129.5, 129.1, 129.0, 128.8, 128.5, 127.9, 127.2, 127.1(2C), 127.0, 126.3, 124.6, 122.4, 118.1, 116.5, 116.4, 115.5, 110.8, 48.4; FT-IR (thin film, neat): 2926, 1610, 1486, 1259, 756, 687 cm⁻¹; HRMS (ESI): m/z calcd for C₃₃H₂₆N [M+H]⁺ : 436.2065; found : 436.2054.

1-[(4-methoxyphenyl)(phenyl)methyl]-3-phenylindolizine (103e)



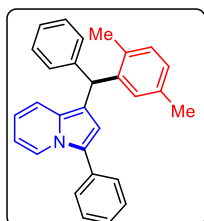
The reaction was performed at 0.1067 mmol scale of **80a**; R_f = 0.5 (5% EtOAc in hexane); pale yellow gummy solid (31.1 mg, 74% yield); ¹H NMR (400 MHz, CDCl₃) δ 8.29 (d, J = 7.12 Hz, 1H), 7.56 – 7.54 (m, 2H), 7.44 (t, J = 7.6 Hz, 2H), 7.33 – 7.29 (m, 3H), 7.28 – 7.26 (m, 2H), 7.24 – 7.20 (m, 2H), 7.18 – 7.16 (m, 2H), 6.87 – 6.84 (m, 2H), 6.60 – 6.56 (m, 1H), 6.54 (s, 1H), 6.46 (t, J = 7.9 Hz, 1H), 5.73 (s, 1H), 3.80 (s, 3H); ¹³C NMR (100 MHz, CDCl₃) δ 158.0, 145.1, 137.0, 132.6, 130.8, 130.0, 129.1, 129.0, 128.4, 127.9, 127.0, 126.2, 124.4, 122.3, 118.2, 116.8, 116.3, 115.5, 113.7, 110.8, 55.4, 47.9; FT-IR (thin film, neat): 2834, 1512, 1436, 1248, 736, 674 cm⁻¹; HRMS (ESI): m/z calcd for C₂₈H₂₄NO [M+H]⁺ : 390.1858; found : 390.1874.

1-[[4-(tert-butyl)phenyl](phenyl)methyl]-3-phenylindolizine (103f)



The reaction was performed at 0.1067 mmol scale of **80a**; R_f = 0.6 (5% EtOAc in hexane); pale yellow gummy solid (35.2 mg, 79% yield); ¹H NMR (400 MHz, CDCl₃) δ 8.27 (d, J = 7.2 Hz, 1H), 7.55 (d, J = 7.8 Hz, 2H), 7.44 (t, J = 7.4 Hz, 2H), 7.32 – 7.26 (m, 7H), 7.21 – 7.18 (m, 4H), 6.59 – 6.55 (m, 2H), 6.45 (t, J = 6.8 Hz, 1H), 5.74 (s, 1H), 1.32 (s, 9H); ¹³C NMR (100 MHz, CDCl₃) δ 148.9, 145.1, 141.6, 132.7, 130.8, 129.1, 129.0, 128.6, 128.3, 127.9, 126.9, 126.1, 125.2, 124.4, 122.3, 118.2, 116.8, 116.3, 115.5, 110.8, 48.2, 34.5, 31.6; FT-IR (thin film, neat): 2964, 1606, 1258, 1388, 752, 699 cm⁻¹; HRMS (ESI): m/z calcd for C₃₁H₃₀N [M+H]⁺ : 416.2378; found : 416.2364.

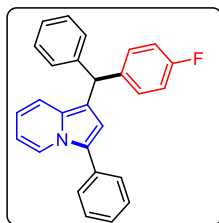
1-[(2,5-dimethylphenyl)(phenyl)methyl]-3-phenylindolizine (103g)



The reaction was performed at 0.1067 mmol scale of **80a**; R_f = 0.6 (5% EtOAc in hexane); pale yellow gummy solid (28.3 mg, 68% yield); ¹H NMR (400 MHz, CDCl₃) δ 8.31 (d, J = 7.1 Hz, 1H), 7.58 – 7.56 (m, 2H), 7.45 (t, J = 7.4 Hz, 2H), 7.33 – 7.29 (m, 3H), 7.24 – 7.22 (m, 3H), 7.15 (d, J = 9.0 Hz, 1H), 7.09 (d, J = 7.6 Hz, 1H), 6.97 (d, J = 7.6 Hz, 1H), 6.88 (s, 1H), 6.58 (t, J = 7.0 Hz, 1H), 6.48 – 6.45 (m, 2H), 6.00 (s, 1H), 2.29 (s, 3H), 2.24 (s, 3H); ¹³C NMR (100 MHz, CDCl₃) δ 144.4, 142.7, 135.2, 133.2, 132.6, 130.9, 130.3, 129.7, 129.3, 129.0, 128.3, 127.9, 127.0, 126.9, 126.1, 124.4, 122.3, 118.1, 116.3, 116.1, 115.9, 110.7, 45.1, 21.4, 19.6;

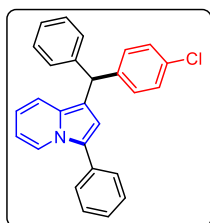
FT-IR (thin film, neat): 2921, 1614, 1492, 1305, 737, 658 cm^{-1} ; HRMS (ESI): m/z calcd for $\text{C}_{29}\text{H}_{26}\text{N}$ $[\text{M}+\text{H}]^+$: 388.2065; found: 388.2058.

1-[(4-fluorophenyl)(phenyl)methyl]-3-phenylindolizine (103h)



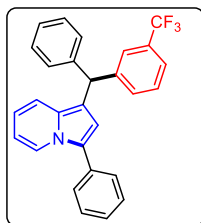
The reaction was performed at 0.1067 mmol scale of **80a**; R_f = 0.8 (5% EtOAc in hexane); green gummy solid (17.1 mg, 42% yield); ^1H NMR (400 MHz, CDCl_3) δ 8.28 (d, J = 7.2 Hz, 1H), 7.54 – 7.52 (m, 2H), 7.44 (t, J = 7.6 Hz, 2H), 7.30 (t, J = 7.4 Hz, 3H), 7.24 – 7.19 (m, 5H), 7.14 (d, J = 9.0 Hz, 1H), 6.98 (t, J = 8.6 Hz, 2H), 6.58 (t, J = 6.4 Hz, 1H), 6.49 – 6.45 (m, 2H), 5.74 (s, 1H); ^{13}C NMR (100 MHz, CDCl_3) δ 161.5 (d, $J_{\text{C-F}}$ = 242.6 Hz), 144.6, 140.5 (d, $J_{\text{C-F}}$ = 3.1 Hz), 132.5, 130.7, 130.5 (d, $J_{\text{C-F}}$ = 7.8 Hz), 129.0, 128.5, 127.9, 127.1, 126.4, 124.6, 122.4, 118.0, 116.6, 116.3, 115.3, 115.2, 115.0, 110.9, 48.0; $^{19}\text{F}\{^1\text{H}\}$ NMR (376 MHz, CDCl_3) δ -117.30; FT-IR (thin film, neat): 3064, 1614, 1582, 1256, 842, 738 cm^{-1} ; HRMS (ESI): m/z calcd for $\text{C}_{27}\text{H}_{21}\text{FN}$ $[\text{M}+\text{H}]^+$: 378.1658; found: 378.1642.

1-[(4-chlorophenyl)(phenyl)methyl]-3-phenylindolizine (103i)



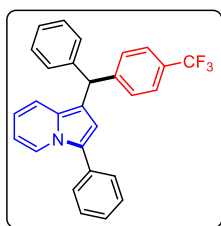
The reaction was performed at 0.1067 mmol scale of **80a**; R_f = 0.7 (5% EtOAc in hexane); pale yellow solid (31.3 mg, 74% yield); m. p. = 114–116 $^{\circ}\text{C}$; ^1H NMR (400 MHz, CDCl_3) δ 8.27 (d, J = 7.1 Hz, 1H), 7.53 (d, J = 7.6 Hz, 2H), 7.43 (t, J = 7.3 Hz, 2H), 7.32 – 7.26 (m, 4H), 7.24 – 7.22 (m, 4H), 7.17 (d, J = 7.7 Hz, 2H), 7.13 (d, J = 9.0 Hz, 1H), 6.58 (t, J = 7.4 Hz, 1H), 6.48 – 6.44 (m, 2H), 5.72 (s, 1H); ^{13}C NMR (100 MHz, CDCl_3) δ 144.3, 143.4, 132.4, 132.0, 130.8, 130.5, 129.0, 128.5, 128.0, 127.1, 126.5, 124.6, 122.4, 118.0, 116.6, 115.9, 115.3, 110.9, 48.1; FT-IR (thin film, neat): 3062, 1496, 1305, 1204, 847 cm^{-1} ; HRMS (ESI): m/z calcd for $\text{C}_{27}\text{H}_{21}\text{ClN}$ $[\text{M}+\text{H}]^+$: 394.1363; found: 394.1377.

3-phenyl-1-{phenyl[3-(trifluoromethyl)phenyl]methyl}indolizine (103j)



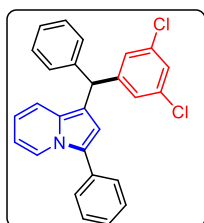
The reaction was performed at 0.1067 mmol scale of **80a**; R_f = 0.6 (5% EtOAc in hexane); pale yellow gummy solid (20.6 mg, 45% yield); ^1H NMR (400 MHz, CDCl_3) δ 8.29 (d, J = 7.2 Hz, 1H), 7.56 – 7.54 (m, 3H), 7.51 – 7.45 (m, 3H), 7.43 – 7.39 (m, 2H), 7.34 – 7.31 (m, 3H), 7.26 – 7.24 (m, 3H), 7.17 (d, J = 9.0 Hz, 1H), 6.61 (t, J = 6.9 Hz, 1H), 6.50 – 6.44 (m, 2H), 5.83 (s, 1H); ^{13}C NMR (100 MHz, CDCl_3) δ 145.8, 143.9, 132.52, 132.50, 132.4, 130.8, 130.7, 130.5 (q, $J_{\text{C-F}}$ = 274 Hz), 129.0, 128.8, 128.6, 128.0, 127.2, 126.6, 125.8 (q, $J_{\text{C-F}}$ = 3.7 Hz), 124.8, 123.2 (q, $J_{\text{C-F}}$ = 3.7 Hz), 122.4, 117.8, 116.8, 115.4, 115.2, 111.0, 48.5; $^{19}\text{F}\{^1\text{H}\}$ NMR (376 MHz, CDCl_3) δ -62.31; FT-IR (thin film, neat): 2934, 1324, 1253, 1121, 867, 762 cm^{-1} ; HRMS (ESI): m/z calcd for $\text{C}_{28}\text{H}_{21}\text{F}_3\text{N}$ $[\text{M}+\text{H}]^+$: 428.1626; found: 428.1647.

3-phenyl-1-{phenyl[4-(trifluoromethyl)phenyl]methyl}indolizine (103k)



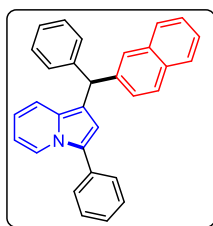
The reaction was performed at 0.1067 mmol scale of **80a**; $R_f = 0.6$ (5% EtOAc in hexane); pale yellow solid (20.2 mg, 44% yield); m. p. = 132–134 °C; ^1H NMR (400 MHz, CDCl_3) δ 8.28 (d, $J = 7.2$ Hz, 1H), 7.56 – 7.53 (m, 4H), 7.44 (t, $J = 7.6$ Hz, 2H), 7.38 – 7.36 (m, 2H), 7.33 – 7.30 (m, 3H), 7.25 (t, $J = 4.9$ Hz, 3H), 7.15 (d, $J = 9.0$ Hz, 1H), 6.61 (t, $J = 6.5$ Hz, 1H), 6.50 – 6.46 (m, 2H), 5.81 (s, 1H); ^{13}C NMR (100 MHz, CDCl_3) δ 148.9, 143.8, 132.4, 130.8, 129.4, 129.08, 129.06, 128.6, 128.4, 128.0, 127.2, 126.6, 125.4 (q, $J_{\text{C-F}} = 3.7$ Hz), 124.8, 124.5 (q, $J_{\text{C-F}} = 270$ Hz), 122.5, 117.9, 116.8, 115.4, 115.3, 111.0, 48.6; $^{19}\text{F}\{^1\text{H}\}$ NMR (376 MHz, CDCl_3) δ –62.23; FT-IR (thin film, neat): 2934, 1428, 1332, 1259, 1126, 867, 756, 642 cm^{-1} ; HRMS (ESI): m/z calcd for $\text{C}_{28}\text{H}_{21}\text{F}_3\text{N}$ $[\text{M}+\text{H}]^+$: 428.1626; found : 428.1634.

1-[(3,5-dichlorophenyl)(phenyl)methyl]-3-phenylindolizine (103l)



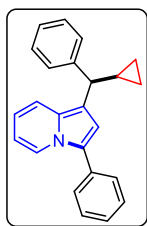
The reaction was performed at 0.1067 mmol scale of **80a**; $R_f = 0.6$ (5% EtOAc in hexane); green gummy solid (26.3 mg, 57% yield); ^1H NMR (400 MHz, CDCl_3) δ 8.27 (d, $J = 7.1$ Hz, 1H), 7.55 – 7.53 (m, 2H), 7.44 (t, $J = 7.4$ Hz, 2H), 7.32 (t, $J = 6.8$ Hz, 3H), 7.24 – 7.21 (m, 4H), 7.16 – 7.13 (m, 3H), 6.62 (t, $J = 7.2$ Hz, 1H), 6.50 – 6.48 (m, 2H), 5.70 (s, 1H); ^{13}C NMR (100 MHz, CDCl_3) δ 148.4, 143.2, 134.9, 132.3, 130.8, 129.1, 129.0, 128.7, 128.0, 127.6, 127.2, 126.8, 126.6, 124.9, 122.5, 117.7, 117.0, 115.1, 114.7, 111.0, 42.8; FT-IR (thin film, neat): 3060, 1492, 1305, 1253, 1154, 867, 737 cm^{-1} ; HRMS (ESI): m/z calcd for $\text{C}_{27}\text{H}_{20}\text{Cl}_2\text{N}$ $[\text{M}+\text{H}]^+$: 428.0973; found : 428.0978.

1-[naphthalen-2-yl(phenyl)methyl]-3-phenylindolizine (103m)



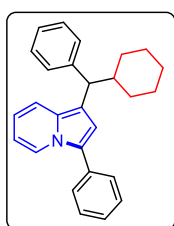
The reaction was performed at 0.1067 mmol scale of **80a**; $R_f = 0.6$ (5% EtOAc in hexane); pale yellow gummy solid (22.5 mg, 51% yield); ^1H NMR (400 MHz, CDCl_3) δ 8.29 (d, $J = 7.1$ Hz, 1H), 7.82 – 7.80 (m, 1H), 7.78 – 7.72 (m, 2H), 7.64 (s, 1H), 7.55 – 7.53 (m, 2H), 7.44 – 7.40 (m, 5H), 7.31 – 7.29 (m, 5H), 7.25 (dd, $J = 8.6, 4.2$ Hz, 1H), 7.20 (d, $J = 9.0$ Hz, 1H), 6.58 – 6.54 (m, 2H), 6.46 (t, $J = 7.0$ Hz, 1H), 5.93 (s, 1H); ^{13}C NMR (100 MHz, CDCl_3) δ 144.6, 142.4, 133.6, 132.5, 132.3, 130.9, 129.2, 129.0, 128.4, 128.05, 128.00, 127.96, 127.92, 127.7, 127.2, 127.0, 126.3, 126.0, 125.5, 124.5, 122.4, 118.2, 116.5, 116.2, 115.6, 110.8, 48.8; FT-IR (thin film, neat): 3056, 1602, 1347, 1264, 847, 732 cm^{-1} ; HRMS (ESI): m/z calcd for $\text{C}_{31}\text{H}_{24}\text{N}$ $[\text{M}+\text{H}]^+$: 410.1909; found : 410.1921.

1-[cyclopropyl(phenyl)methyl]-3-phenylindolizine (103n)



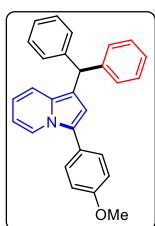
The reaction was performed at 0.1067 mmol scale of **80a**; $R_f = 0.6$ (5% EtOAc in hexane); green gummy solid (11.2 mg, 32% yield); ^1H NMR (400 MHz, CDCl_3) δ 8.25 (d, $J = 7.1$ Hz, 1H), 7.63 – 7.57 (m, 2H), 7.42 (t, $J = 7.6$ Hz, 3H), 7.38 – 7.34 (m, 2H), 7.32 – 7.25 (m, 3H), 6.12 (t, $J = 7.2$ Hz, 1H), 6.90 (s, 1H), 6.52 (t, $J = 7.1$ Hz, 1H), 6.38 (t, $J = 6.6$ Hz, 1H), 3.82 (d, $J = 9.0$ Hz, 1H), 1.87 – 1.76 (m, 1H), 0.98 – 0.93 (m, 2H), 0.67 – 0.64 (m, 2H); ^{13}C NMR (100 MHz, CDCl_3) δ 145.7, 145.6, 132.9, 129.2, 128.5, 128.3, 128.2, 128.0, 127.9, 126.7, 125.6, 125.3, 122.2, 117.6, 112.5, 110.4, 49.5, 16.3, 5.4; FT-IR (thin film, neat): 3032, 1658, 1584, 1316, 748, 712, 657 cm^{-1} ; HRMS (ESI): m/z calcd for $\text{C}_{24}\text{H}_{22}\text{N}$ $[\text{M}+\text{H}]^+$: 324.1752; found : 324.1736.

1-[cyclohexyl(phenyl)methyl]-3-phenylindolizine (103o)



The reaction was performed at 0.1067 mmol scale of **80a**; $R_f = 0.6$ (5% EtOAc in hexane); green gummy solid (13.4 mg, 34% yield); ^1H NMR (400 MHz, CDCl_3) δ 8.23 (d, $J = 7.1$ Hz, 1H), 7.61 – 7.59 (m, 2H), 7.48 (t, $J = 7.6$ Hz, 3H), 7.39 – 7.36 (m, 2H), 7.32 – 7.26 (m, 3H), 6.15 (t, $J = 7.2$ Hz, 1H), 6.93 (s, 1H), 6.62 (t, $J = 7.1$ Hz, 1H), 6.41 (t, $J = 6.6$ Hz, 1H), 3.84 (d, $J = 10.4$ Hz, 1H), 2.15 (q, $J = 10.8$, 21.6 Hz, 1H), 1.72 – 1.46 (m, 6H), 1.32 – 1.11 (m, 4H); ^{13}C NMR (100 MHz, CDCl_3) δ 145.5, 145.4, 132.8, 129.0, 128.6, 128.5, 128.4, 128.2, 127.9, 126.9, 125.8, 125.7, 122.3, 117.8, 112.7, 110.5, 49.8, 42.9, 32.4, 26.8, 26.6; FT-IR (thin film, neat): 2956, 1658, 1496, 1362, 703 cm^{-1} ; HRMS (ESI): m/z calcd for $\text{C}_{27}\text{H}_{28}\text{N}$ $[\text{M}+\text{H}]^+$: 366.2222; found : 366.2208.

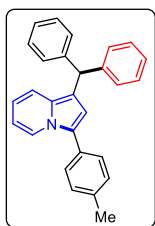
1-benzhydryl-3-(4-methoxyphenyl)indolizine (104a)



The reaction was performed at 0.0964 mmol scale of **80b**; $R_f = 0.5$ (5% EtOAc in hexane); pale yellow gummy solid (24.2 mg, 64% yield); ^1H NMR (400 MHz, CDCl_3) δ 8.17 (d, $J = 7.1$ Hz, 1H), 7.45 (d, $J = 7.6$ Hz, 2H), 7.32 – 7.30 (m, 2H), 7.28 – 7.26 (m, 6H), 7.23 – 7.19 (m, 2H), 7.16 (d, $J = 9.0$ Hz, 1H), 7.98 (d, $J = 7.7$ Hz, 2H), 6.54 (t, $J = 7.2$ Hz, 1H), 6.47 (s, 1H), 6.43 (t, $J = 13.4$ Hz, 1H), 5.77 (s, 1H), 3.84 (s, 1H); ^{13}C NMR (100 MHz, CDCl_3) δ 158.8, 144.9, 130.3, 129.5, 129.1, 128.4, 126.2, 125.1, 124.2, 122.3, 118.1, 116.1, 116.0, 115.0, 114.4, 110.6, 77.5, 77.2, 76.8, 55.5, 48.7; FT-IR (thin film, neat): 2834, 1523, 1364, 1249, 1186, 863, 736 cm^{-1} ; HRMS (ESI): m/z calcd for $\text{C}_{28}\text{H}_{24}\text{NO}$ $[\text{M}+\text{H}]^+$: 390.1858; found : 390.1852.

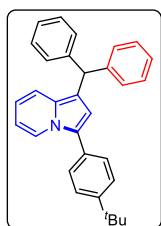
1-benzhydryl-3-(p-tolyl)indolizine (104b)

The reaction was performed at 0.1016 mmol scale of **80c**; $R_f = 0.6$ (5% EtOAc in hexane); pale yellow solid (26.0 mg, 68% yield); m. p. = 122–124 $^{\circ}\text{C}$; ^1H NMR (400 MHz, CDCl_3) δ 8.23 (d, $J = 7.1$ Hz, 1H), 7.42 (d, $J = 7.6$ Hz, 2H), 7.31 – 7.27 (m, 4H), 7.26 – 7.24 (m, 5H), 7.23 – 7.18



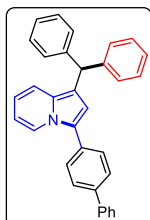
(m, 3H), 7.15 (d, $J = 9.0$ Hz, 1H), 6.55 (t, $J = 6.5$ Hz, 1H), 6.49 (s, 1H), 6.43 (t, $J = 6.9$ Hz, 1H), 5.75 (s, 1H), 2.39 (s, 3H); ^{13}C NMR (100 MHz, CDCl_3) δ 144.8, 136.8, 130.6, 129.7, 129.1, 128.4 (2C), 127.9, 126.2, 124.5, 122.4, 118.1, 116.3, 116.2, 115.2, 110.7, 48.7, 21.4; FT-IR (thin film, neat): 2926, 1486, 1358, 1264, 749 cm^{-1} ; HRMS (ESI): m/z calcd for $\text{C}_{28}\text{H}_{24}\text{N}$ $[\text{M}+\text{H}]^+$: 374.1909; found : 374.1915.

1-benzhydryl-3-[4-(tert-butyl)phenyl]indolizine (104c)



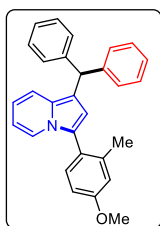
The reaction was performed at 0.0889 mmol scale of **80d**; $R_f = 0.6$ (5% EtOAc in hexane); pale yellow solid (22.7 mg, 61% yield); m. p. = 128–130 $^{\circ}\text{C}$; ^1H NMR (400 MHz, CDCl_3) δ 8.28 (d, $J = 7.2$ Hz, 1H), 7.53 (d, $J = 8.0$ Hz, 2H), 7.42 (t, $J = 7.6$ Hz, 2H), 7.40 – 7.37 (m, 4H), 7.33 – 7.30 (m, 3H), 7.25 – 7.21 (m, 4H), 6.59 – 6.55 (m, 2H), 6.43 (t, $J = 7.0$ Hz, 1H), 5.76 (s, 1H), 1.37 (s, 9H); ^{13}C NMR (100 MHz, CDCl_3) δ 145.1, 132.6, 130.8, 129.1, 129.0, 128.4, 128.0, 127.6, 126.4, 124.5, 122.3, 118.2, 116.6, 116.4, 115.5, 110.8, 48.4, 34.7, 31.5; FT-IR (thin film, neat): 2964, 1495, 1304, 1243, 862, 762, 738 cm^{-1} ; HRMS (ESI): m/z calcd for $\text{C}_{31}\text{H}_{30}\text{N}$ $[\text{M}+\text{H}]^+$: 416.2378; found : 416.2362.

3-([1,1'-biphenyl]-4-yl)-1-benzhydrylindolizine (104d)



The reaction was performed at 0.0839 mmol scale of **80e**; $R_f = 0.6$ (5% EtOAc in hexane); pale yellow gummy solid (21.2 mg, 58% yield); ^1H NMR (400 MHz, CDCl_3) δ 8.28 (d, $J = 7.2$ Hz, 1H), 7.58 (d, $J = 7.4$ Hz, 2H), 7.56 – 7.52 (m, 4H); 7.45 – 7.41 (m, 4H), 7.38 – 7.30 (m, 5H), 7.28 – 7.26 (m, 3H), 7.24 – 7.22 (m, 2H), 6.68 – 7.63 (m, 2H), 6.48 (t, $J = 7.0$ Hz, 1H), 5.78 (s, 1H); ^{13}C NMR (100 MHz, CDCl_3) δ 144.8, 143.6, 141.2, 139.2, 132.4, 131.0, 129.4, 129.0, 128.8, 128.5, 128.1, 127.2, 126.3, 124.6, 122.3, 118.1, 116.5, 116.4, 115.5, 110.8, 48.6; FT-IR (thin film, neat): 3028, 1489, 1239, 1157, 794, 737 cm^{-1} ; HRMS (ESI): m/z calcd for $\text{C}_{33}\text{H}_{26}\text{N}$ $[\text{M}+\text{H}]^+$: 436.2065; found : 436.2047.

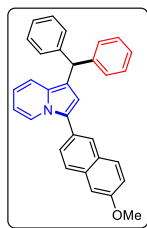
1-benzhydryl-3-(4-methoxy-2-methylphenyl)indolizine (104e)



The reaction was performed at 0.0922 mmol scale of **80f**; $R_f = 0.4$ (5% EtOAc in hexane); pale yellow solid (20.6 mg, 55% yield); m. p. = 124–126 $^{\circ}\text{C}$; ^1H NMR (400 MHz, CDCl_3) δ 7.53 (d, $J = 7.0$ Hz, 1H), 7.33 – 7.31 (m, 2H), 7.29 (brs, 5H), 7.28 – 7.21 (m, 4H), 7.17 (d, $J = 9.0$ Hz, 1H), 6.89 (s, 1H), 6.82 (d, $J = 8.4$ Hz, 1H), 6.55 (t, $J = 7.0$ Hz, 1H), 6.42 – 6.39 (m, 2H), 5.82 (s, 1H), 3.86 (s, 3H), 2.12 (s, 3H); ^{13}C NMR (100 MHz, CDCl_3) δ 159.6, 145.1, 139.9, 132.5, 129.4, 129.1, 128.3, 126.1, 124.2, 123.2, 122.7, 117.8, 115.8, 115.64, 115.60, 115.3, 111.4, 110.2, 55.4, 48.8,

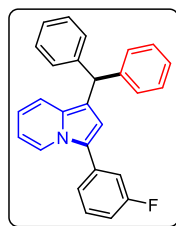
20.2; FT-IR (thin film, neat): 2934, 1606, 1364, 1243, 768, 739 cm^{-1} ; HRMS (ESI): m/z calcd for $\text{C}_{29}\text{H}_{26}\text{NO}$ $[\text{M}+\text{H}]^+$: 404.2014; found : 404.1999.

1-benzhydryl-3-(6-methoxynaphthalen-2-yl)indolizine (104f)



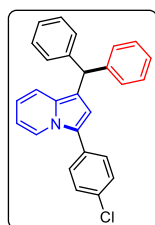
The reaction was performed at 0.0830 mmol scale of **80g**; $R_f = 0.4$ (5% EtOAc in hexane); pale yellow gummy solid (19.2 mg, 52% yield); ^1H NMR (400 MHz, CDCl_3) δ 8.23 (d, $J = 7.1$ Hz, 1H), 7.42 (d, $J = 7.6$ Hz, 2H), 7.41 – 7.39 (m, 2H), 7.34 – 7.30 (m, 2H), 7.31 – 7.27 (m, 4H), 7.26 – 7.24 (m, 3H), 7.23 – 7.18 (m, 3H), 7.15 (d, $J = 9.0$ Hz, 1H), 6.55 (t, $J = 6.5$ Hz, 1H), 6.49 (s, 1H), 6.43 (t, $J = 6.9$ Hz, 1H), 5.75 (s, 1H), 3.72 (s, 3H); ^{13}C NMR (100 MHz, CDCl_3) δ 158.6, 144.8, 136.8, 130.3, 129.7, 129.1, 128.4 (2C), 128.0, 127.6, 126.2, 125.1, 124.5, 123.4, 122.6, 118.1, 116.3, 116.2, 115.3, 113.6, 110.7, 55.6, 48.4; FT-IR (thin film, neat): 2906, 1609, 1359, 1269, 867, 739, 645 cm^{-1} ; HRMS (ESI): m/z calcd for $\text{C}_{32}\text{H}_{26}\text{NO}$ $[\text{M}+\text{H}]^+$: 440.2014; found : 440.1994.

1-benzhydryl-3-(3-fluorophenyl)indolizine (104g)



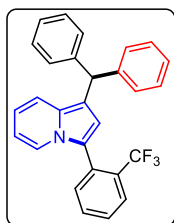
The reaction was performed at 0.1002 mmol scale of **80h**; $R_f = 0.6$ (5% EtOAc in hexane); pale yellow gummy solid (23.0 mg, 60% yield); ^1H NMR (400 MHz, CDCl_3) δ 8.29 (d, $J = 7.2$ Hz, 1H), 7.38 (t, $J = 7.4$ Hz, 1H), 7.34 – 7.30 (m, 5H), 7.28 – 7.22 (m, 7H), 7.19 (d, $J = 9.0$ Hz, 1H), 6.99 (t, $J = 8.3$ Hz, 1H), 6.61 (t, $J = 7.2$ Hz, 1H), 6.56 (s, 1H), 6.51 (t, $J = 6.8$ Hz, 1H), 5.78 (s, 1H); ^{13}C NMR (100 MHz, CDCl_3) δ 163.3 (d, $J_{\text{C-F}} = 244.5$ Hz), 144.6, 134.7 (d, $J_{\text{C-F}} = 33.1$ Hz), 131.3, 130.5 (d, $J_{\text{C-F}} = 8.7$ Hz), 130.2, 128.8 (d, $J_{\text{C-F}} = 66.7$ Hz), 126.3, 123.3 (d, $J_{\text{C-F}} = 2.7$ Hz), 123.2 (d, $J_{\text{C-F}} = 10.0$ Hz), 122.3, 118.3, 116.9, 116.8, 115.9, 114.4 (d, $J_{\text{C-F}} = 21.9$ Hz), 113.7 (d, $J_{\text{C-F}} = 21.1$ Hz), 111.2, 48.7; $^{19}\text{F}\{^1\text{H}\}$ NMR (376 MHz, CDCl_3) δ -112.50; FT-IR (thin film, neat): 3058, 1612, 1583, 1367, 1256, 736, 630 cm^{-1} ; HRMS (ESI): m/z calcd for $\text{C}_{27}\text{H}_{21}\text{FN}$ $[\text{M}+\text{H}]^+$: 378.1658; found : 378.1668.

1-benzhydryl-3-(4-chlorophenyl)indolizine (104h)



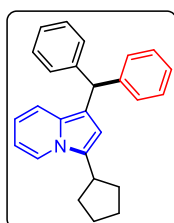
The reaction was performed at 0.0950 mmol scale of **80i**; $R_f = 0.5$ (5% EtOAc in hexane); pale yellow solid (23.3 mg, 62% yield); m. p. = 126–128 $^{\circ}\text{C}$; ^1H NMR (400 MHz, CDCl_3) δ 8.27 (d, $J = 7.1$ Hz, 1H), 7.53 (d, $J = 7.6$ Hz, 2H), 7.43 (t, $J = 7.3$ Hz, 2H), 7.32 – 7.26 (m, 4H), 7.24 – 7.22 (m, 4H), 7.17 (d, $J = 7.7$ Hz, 2H), 7.13 (d, $J = 9.0$ Hz, 1H), 6.58 (t, $J = 7.4$ Hz, 1H), 6.48 – 6.44 (m, 2H), 5.72 (s, 1H); ^{13}C NMR (100 MHz, CDCl_3) δ 144.3, 143.4, 132.4, 132.0, 130.8, 130.5, 129.0, 128.5, 128.0, 127.1, 126.5, 124.6, 122.4, 118.0, 116.6, 115.9, 115.3, 110.9, 48.1; FT-IR (thin film, neat): 3060, 1494, 1309, 1204, 847, 739, 697 cm^{-1} ; HRMS (ESI): m/z calcd for $\text{C}_{27}\text{H}_{21}\text{ClN}$ $[\text{M}+\text{H}]^+$: 394.1363; found : 394.1347.

1-benzhydryl-3-[2-(trifluoromethyl)phenyl]indolizine (104i)



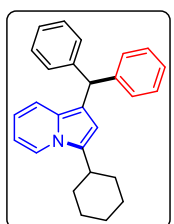
The reaction was performed at 0.0859 mmol scale of **80j**; $R_f = 0.6$ (5% EtOAc in hexane); pale green gummy solid (20.6 mg, 56% yield); ^1H NMR (400 MHz, CDCl_3) δ 8.26 (d, $J = 7.1$ Hz, 1H), 7.62 – 7.58 (m, 3H), 7.53 – 7.47 (m, 3H), 7.46 – 7.39 (m, 2H), 7.34 – 7.31 (m, 2H), 7.28 (t, $J = 7.4$ Hz, 2H), 7.26 – 7.24 (m, 2H), 7.18 (d, $J = 9.0$ Hz, 1H), 6.66 (t, $J = 7.6$ Hz, 1H), 6.54 – 6.47 (m, 2H), 5.86 (s, 1H); ^{13}C NMR (100 MHz, CDCl_3) δ 145.6, 132.5, 132.4 (q, $J_{\text{C-F}} = 2.9$ Hz), 130.8, 130.5, 129.0, 128.8, 128.6 (q, $J_{\text{C-F}} = 276.4$ Hz), 128.0, 127.2, 126.6, 126.4 (q, $J_{\text{C-F}} = 5.2$ Hz), 124.8, 123.2, 122.4, 117.8, 116.8, 115.4, 111.0, 48.6; $^{19}\text{F}\{^1\text{H}\}$ NMR (376 MHz, CDCl_3) δ –60.13; FT-IR (thin film, neat): 2934, 1438, 1326, 1178, 866, 763 cm^{-1} ; HRMS (ESI): m/z calcd for $\text{C}_{28}\text{H}_{21}\text{F}_3\text{N}$ $[\text{M}+\text{H}]^+$: 428.1626; found : 428.1642.

1-benzhydryl-3-cyclopentylindolizine (104j)



The reaction was performed at 0.1097 mmol scale of **80k**; $R_f = 0.6$ (5% EtOAc in hexane); pale green solid (19.7 mg, 51% yield); m. p. = 110–112 $^\circ\text{C}$; ^1H NMR (400 MHz, CDCl_3) δ 7.74 (d, $J = 7.0$ Hz, 1H), 7.32 – 7.30 (m, 3H), 7.29 – 7.27 (m, 2H), 7.26 – 7.22 (m, 2H), 7.21 – 7.18 (m, 3H), 7.12 (d, $J = 8.7$ Hz, 1H), 6.52 – 6.45 (m, 2H), 6.27 (s, 1H), 5.77 (s, 1H), 3.24 (quintet, $J = 8.0$ Hz, 1H), 1.83 – 1.64 (m, 8H); ^{13}C NMR (100 MHz, CDCl_3) δ 145.3, 132.4, 129.1, 129.0, 128.4, 126.1, 121.6, 118.2, 114.4, 115.3, 110.6, 109.4, 48.7, 36.6, 31.3, 25.1; FT-IR (thin film, neat): 2954, 1656, 1493, 1326, 1259, 701 cm^{-1} ; HRMS (ESI): m/z calcd for $\text{C}_{27}\text{H}_{28}\text{N}$ $[\text{M}+\text{H}]^+$: 366.2222; found : 352.2080.

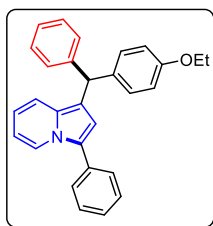
1-benzhydryl-3-cyclohexylindolizine (104k)



The reaction was performed at 0.1044 mmol scale of **80l**; $R_f = 0.6$ (5% EtOAc in hexane); pale green gummy solid (20.4 mg, 53% yield); ^1H NMR (400 MHz, CDCl_3) δ 7.76 (d, $J = 6.6$ Hz, 1H), 7.33 – 7.29 (m, 4H), 7.26 – 7.21 (m, 6H), 7.12 (d, $J = 8.7$ Hz, 1H), 6.52 – 6.45 (m, 2H), 6.27 (s, 1H), 5.77 (s, 1H), 2.84 – 2.80 (m, 1H), 2.09 (d, $J = 9.6$ Hz, 2H), 1.89 – 1.79 (m, 3H), 1.45 (q, $J = 9.1$ Hz, 4H) 1.35 – 1.30 (m, 1H); ^{13}C NMR (100 MHz, CDCl_3) δ 145.2, 129.14, 129.10, 128.3 (2C), 126.1, 121.8, 118.0, 114.6, 114.5, 110.7, 109.8, 48.9, 35.4, 31.8, 26.7, 26.5; FT-IR (thin film, neat): 2953, 1656, 1494, 1256, 863, 724, cm^{-1} ; HRMS (ESI): m/z calcd for $\text{C}_{27}\text{H}_{28}\text{N}$ $[\text{M}+\text{H}]^+$: 366.2222; found : 366.2234.

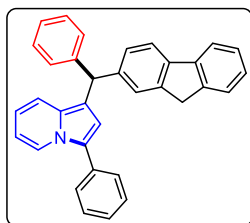
1-[(4-ethoxyphenyl)(phenyl)methyl]-3-phenylindolizine (104l)

The reaction was performed at 0.0922 mmol scale of **80m**; $R_f = 0.4$ (5% EtOAc in hexane); pale yellow gummy solid (26.5 mg, 71% yield); ^1H NMR (400 MHz, CDCl_3) δ 8.28 (d, $J = 7.2$



Hz, 1H), 7.56 – 7.53 (m, 2H), 7.44 (t, $J = 7.5$ Hz, 2H), 7.32 – 7.30 (m, 2H), 7.28 – 7.26 (m, 3H), 7.24 – 7.20 (m, 1H), 7.18 – 7.15 (m, 3H), 6.86 – 6.82 (m, 2H), 6.57 (ddd, $J = 7.4, 6.4, 1.0$ Hz, 1H), 6.53 (s, 1H), 6.45 (td, $J = 7.3, 1.3$ Hz, 1H), 5.72 (s, 1H), 4.02 (q, $J = 7.0$ Hz, 2H), 1.41 (t, $J = 7.0$ Hz, 3H); ^{13}C NMR (100 MHz, CDCl_3) δ 157.4, 145.2, 136.8, 132.6, 130.8, 130.0, 129.1, 129.0, 128.4, 127.9, 126.9, 126.1, 124.4, 122.3, 118.2, 116.9, 116.3, 115.5, 114.3, 110.8, 63.5, 47.9, 15.1; FT-IR (thin film, neat): 2963, 1604, 1436, 1267, 754, 701 cm^{-1} ; HRMS (ESI): m/z calcd for $\text{C}_{29}\text{H}_{26}\text{NO}$ $[\text{M}+\text{H}]^+$: 404.2014; found : 404.2027.

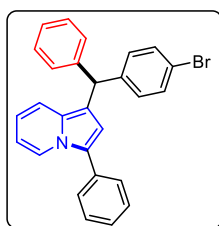
1-[(9H-fluoren-2-yl)(phenyl)methyl]-3-phenylindolizine (104m)



The reaction was performed at 0.0812 mmol scale of **80n**; $R_f = 0.5$ (5% EtOAc in hexane); pale yellow solid (23.4 mg, 64% yield); ^1H NMR (400 MHz, CDCl_3) δ 8.31 (d, $J = 7.1$ Hz, 1H), 7.77 (d, $J = 7.5$ Hz, 1H), 7.73 (d, $J = 7.9$ Hz, 1H); 7.57 (d, $J = 7.6$ Hz, 2H), 7.53 (d, $J = 7.4$ Hz, 1H); 7.46 – 7.43 (m, 3H), 7.37 (t, $J = 7.4$ Hz, 1H), 7.35 – 7.26 (m, 8H), 7.21

(d, $J = 9.1$ Hz, 1H), 6.60 – 6.57 (m, 2H), 6.47 (t, $J = 6.8$ Hz, 1H), 5.87 (s, 1H), 3.86 (s, 1H); ^{13}C NMR (100 MHz, CDCl_3) δ 145.0, 143.7, 143.6, 143.9, 141.8, 140.0, 132.6, 130.9, 129.2, 129.0, 128.4, 127.9, 127.9, 127.0, 126.8, 126.5, 126.3, 125.8, 125.1, 124.5, 122.4, 119.9, 119.8, 118.2, 116.7, 116.4, 115.6, 110.9, 48.9, 37.1; FT-IR (thin film, neat): 2962, 1604, 1434, 1267, 846, 753, cm^{-1} ; HRMS (ESI): m/z calcd for $\text{C}_{34}\text{H}_{26}\text{N}$ $[\text{M}+\text{H}]^+$: 448.2065; found : 448.2052.

1-[(4-bromophenyl)(phenyl)methyl]-3-phenylindolizine (104n)

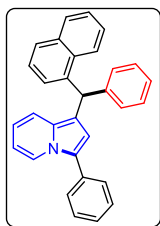


The reaction was performed at 0.0833 mmol scale of **80o**; $R_f = 0.5$ (5% EtOAc in hexane); pale green gummy solid (22.7 mg, 62% yield); ^1H NMR (400 MHz, CDCl_3) δ 8.28 (d, $J = 8.3$ Hz, 1H), 7.54 (d, $J = 7.7$ Hz, 2H), 7.43 (dd, $J = 14.5, 7.4$ Hz, 4H); 7.33 – 7.29 (m, 3H), 7.26 – 7.23 (m, 3H), 7.15 – 7.12 (m, 3H), 6.60 (t, $J = 7.4$ Hz, 1H), 6.49 – 6.45 (m, 2H), 5.72 (s, 1H); ^{13}C

NMR (100 MHz, CDCl_3) δ 144.2, 143.9, 132.4, 131.5, 130.9, 130.8, 129.0 (2C), 128.5, 128.0, 127.1, 126.5, 124.6, 122.4, 120.1, 118.0, 116.7, 115.8, 115.3, 110.9, 48.2; FT-IR (thin film, neat): 3056, 1601, 1496, 1306, 737, 687 cm^{-1} ; HRMS (ESI): m/z calcd for $\text{C}_{27}\text{H}_{21}\text{BrN}$ $[\text{M}+\text{H}]^+$: 438.0857; found : 438.0838.

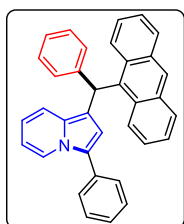
1-[naphthalen-1-yl(phenyl)methyl]-3-phenylindolizine (104o)

The reaction was performed at 0.0905 mmol scale of **80p**; $R_f = 0.5$ (5% EtOAc in hexane); pale yellow gummy solid (20.5 mg, 55% yield); ^1H NMR (400 MHz, CDCl_3) δ 8.29 (d, $J = 7.1$ Hz,



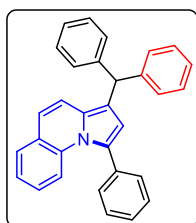
1H), 7.82 – 7.80 (m, 1H), 7.78 – 7.72 (m, 2H), 7.64 (s, 1H), 7.55 – 7.53 (m, 2H), 7.44 – 7.40 (m, 5H), 7.31 – 7.29 (m, 5H), 7.25 (dd, $J = 8.6, 4.2$ Hz, 1H), 7.20 (d, $J = 9.0$ Hz, 1H), 6.58 – 6.54 (m, 2H), 6.46 (t, $J = 7.0$ Hz, 1H), 5.93 (s, 1H); ^{13}C NMR (100 MHz, CDCl_3) δ 144.6, 142.4, 133.6, 132.5, 132.3, 130.9, 129.2, 129.0, 128.4, 128.05, 128.00, 127.96, 127.92, 127.7, 127.2, 127.0, 126.3, 126.0, 125.5, 124.5, 122.4, 118.2, 116.5, 116.2, 115.6, 110.8, 48.8; FT-IR (thin film, neat): 2923, 1600, 1487, 1336, 1254, 757, 687 cm^{-1} ; HRMS (ESI): m/z calcd for $\text{C}_{31}\text{H}_{24}\text{N}$ $[\text{M}+\text{H}]^+$: 410.1909; found : 410.1917.

1-[anthracen-9-yl(phenyl)methyl]-3-phenylindolizine (104p)



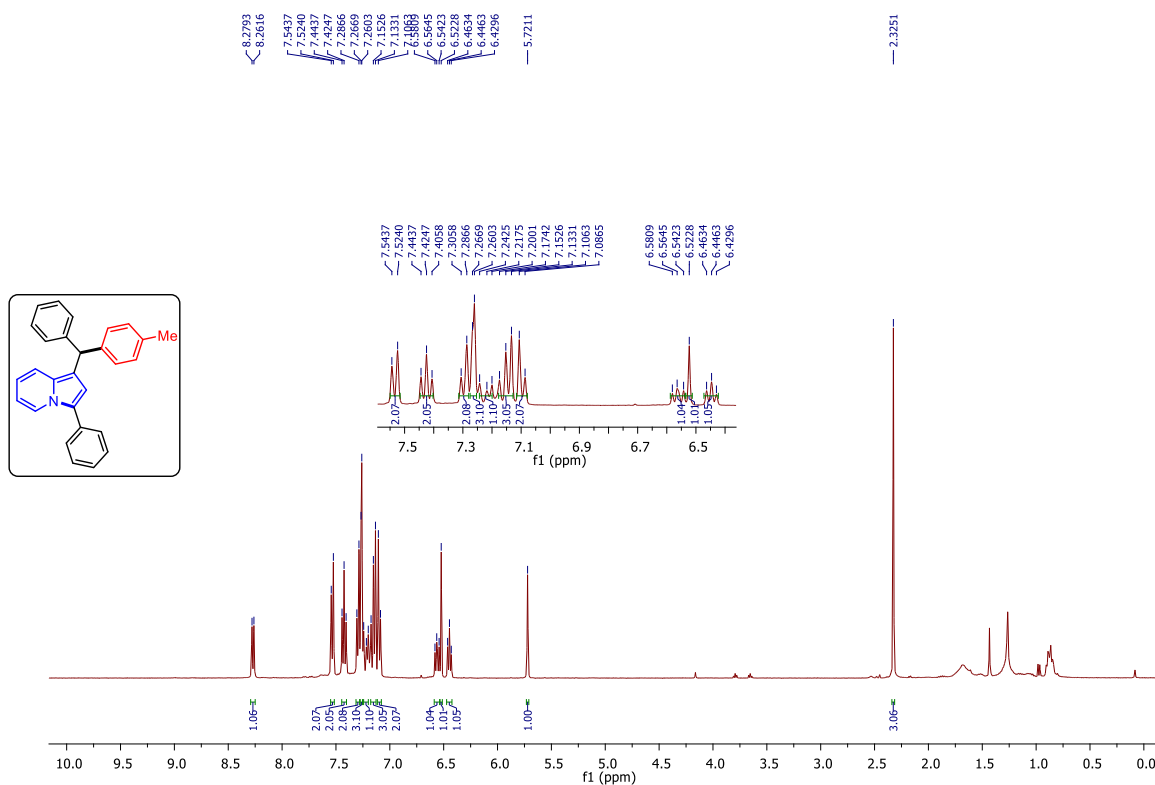
The reaction was performed at 0.0786 mmol scale of **80q**; $R_f = 0.5$ (5% EtOAc in hexane); pale yellow solid (19.0 mg, 52% yield); m. p. = 156–158 $^{\circ}\text{C}$; ^1H NMR (400 MHz, CDCl_3) δ 8.47 (s, 1H), 8.37 (d, $J = 8.9$ Hz, 2H), 8.30 (d, $J = 7.1$ Hz, 1H); 8.03 (d, $J = 8.4$ Hz, 1H); 7.46 – 7.43 (m, 2H), 7.41 – 7.37 (m, 4H) 7.35 – 7.28 (m, 4H), 7.26 – 7.18 (m, 6H), 6.64 – 6.60 (m, 2H), 6.48 (t, $J = 6.8$ 1H); ^{13}C NMR (100 MHz, CDCl_3) δ 145.1, 136.6, 132.5, 132.2, 131.5, 130.7, 129.3, 128.9, 128.4, 128.0, 127.5, 126.9, 125.8, 125.4, 124.8, 124.6, 122.5, 118.2, 116.7, 115.9, 114.5, 110.8, 41.9; FT-IR (thin film, neat): 3057, 1607, 1473, 1348, 1187, 863, 734 cm^{-1} ; HRMS (ESI): m/z calcd for $\text{C}_{35}\text{H}_{26}\text{N}$ $[\text{M}+\text{H}]^+$: 460.2065; found : 460.2045.

3-benzhydryl-1-phenylpyrrolo[1,2-a]quinoline (104q)

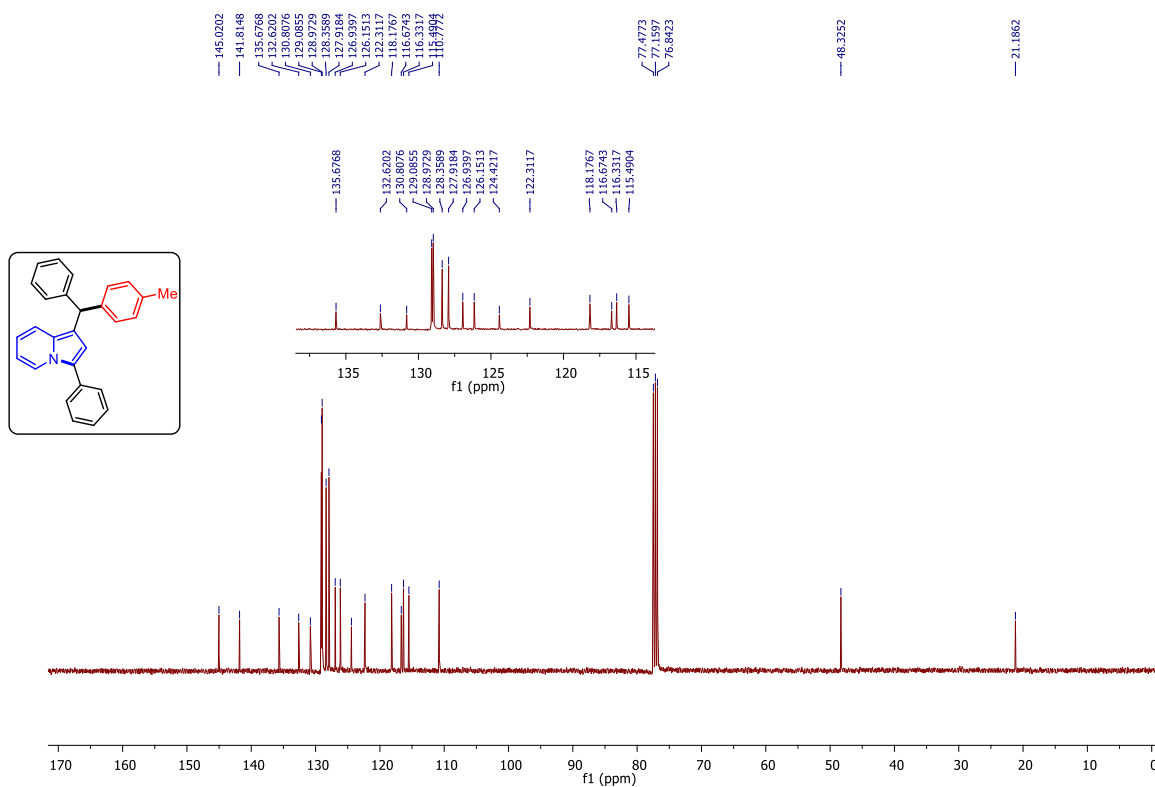


The reaction was performed at 0.0905 mmol scale of **80r**; $R_f = 0.5$ (5% EtOAc in hexane); pale yellow solid (22.7 mg, 61% yield); ^1H NMR (400 MHz, CDCl_3) δ 7.58 (d, $J = 7.7$ Hz, 1H), 7.51 – 7.50 (m, 3H), 7.44 – 7.41 (m, 2H), 7.40 – 7.36 (m, 1H), 7.33 – 7.28 (m, 8H), 7.25 – 7.21 (m, 3H), 7.19 – 7.17 (m, 1H), 7.11 (t, $J = 7.8$ Hz, 1H), 6.92 (d, $J = 9.3$ Hz, 1H); 6.38 (s, 1H), 5.80 (s, 1H); ^{13}C NMR (100 MHz, CDCl_3) δ 144.7, 135.7, 134.7, 129.7, 129.4, 129.3, 129.2 (2C), 128.6, 128.5, 128.4, 127.6, 126.4, 126.3, 125.6, 123.4, 119.3, 118.7, 117.8, 117.6, 48.5; FT-IR (thin film, neat): 3059, 1599, 1448, 1327, 1257, 753 cm^{-1} ; HRMS (ESI): m/z calcd for $\text{C}_{31}\text{H}_{24}\text{N}$ $[\text{M}+\text{H}]^+$: 410.1909; found : 410.1924.

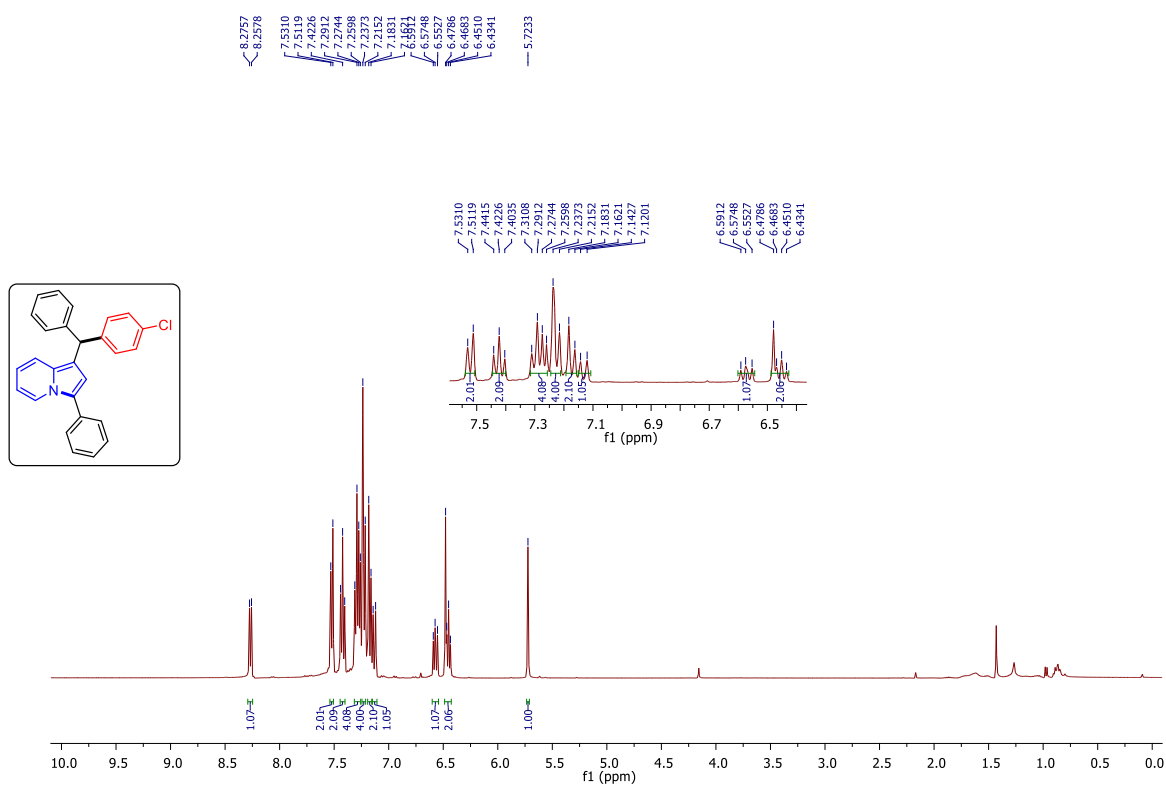
^1H NMR (400 MHz, CDCl_3) spectrum of (**103c**)



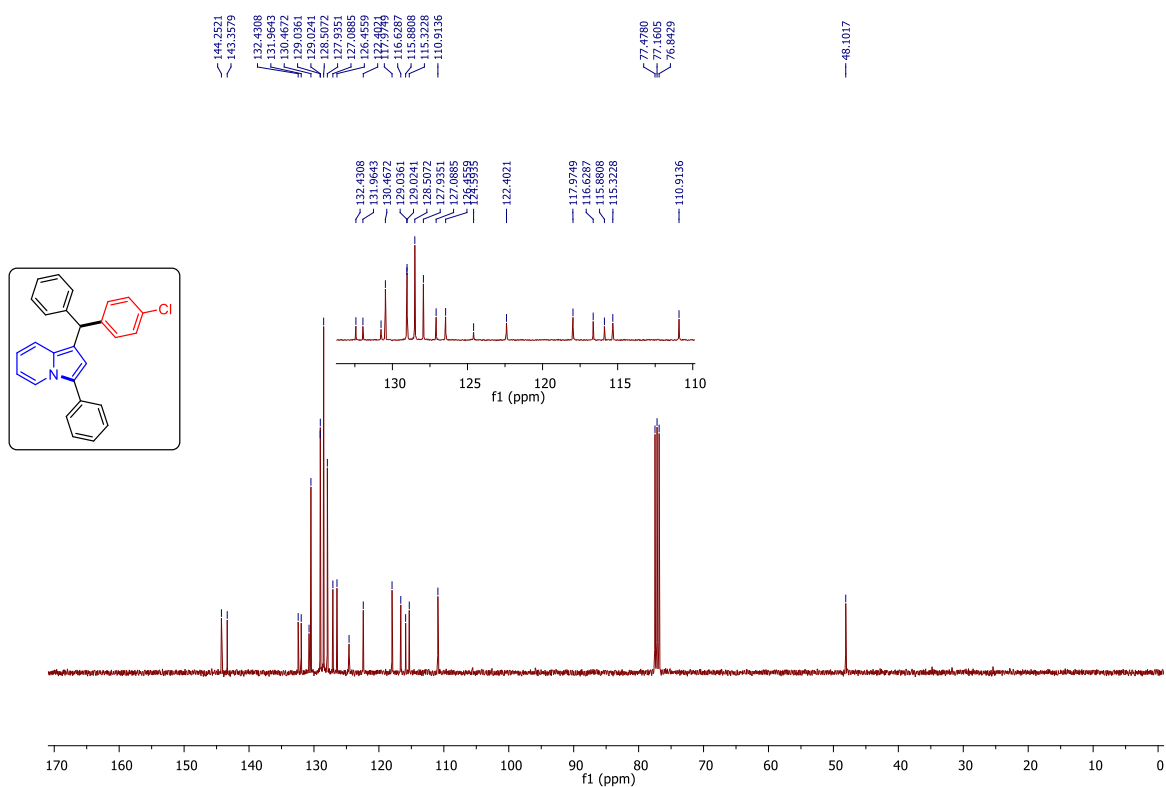
$^{13}\text{C}\{^1\text{H}\}$ NMR (400 MHz, CDCl_3) spectrum of (**103c**)



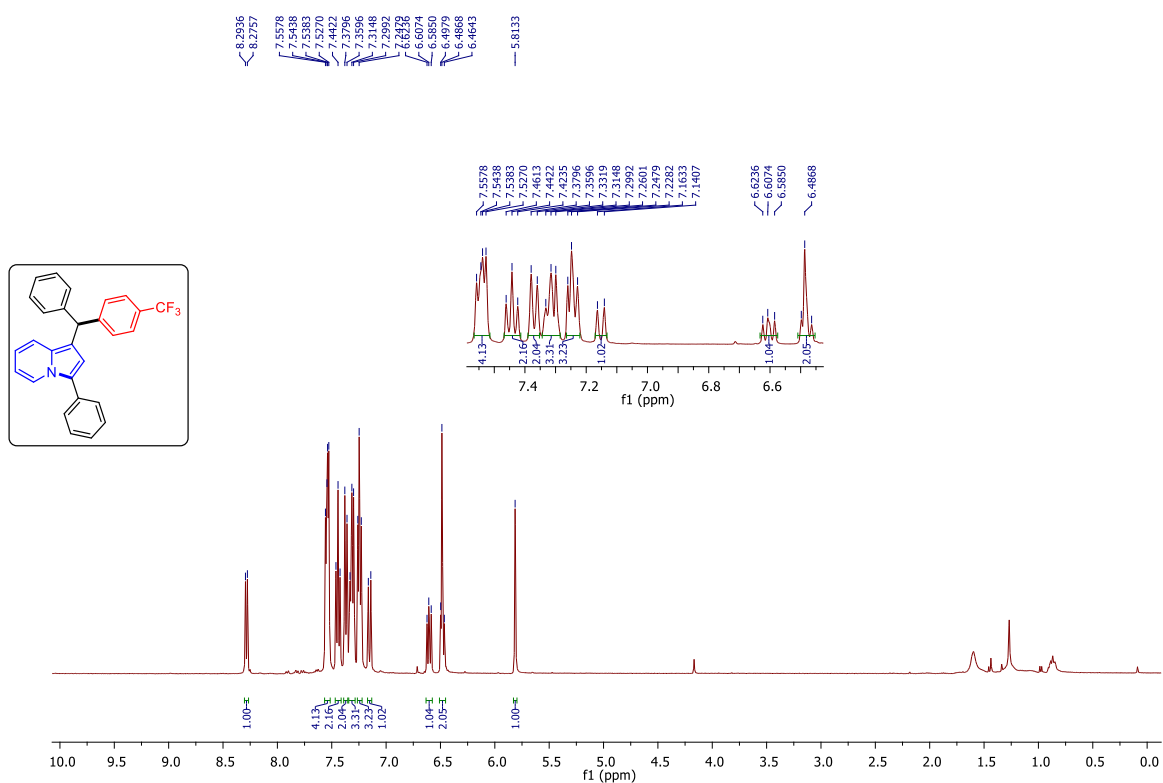
¹H NMR (400 MHz, CDCl₃) spectrum of (**103i**)



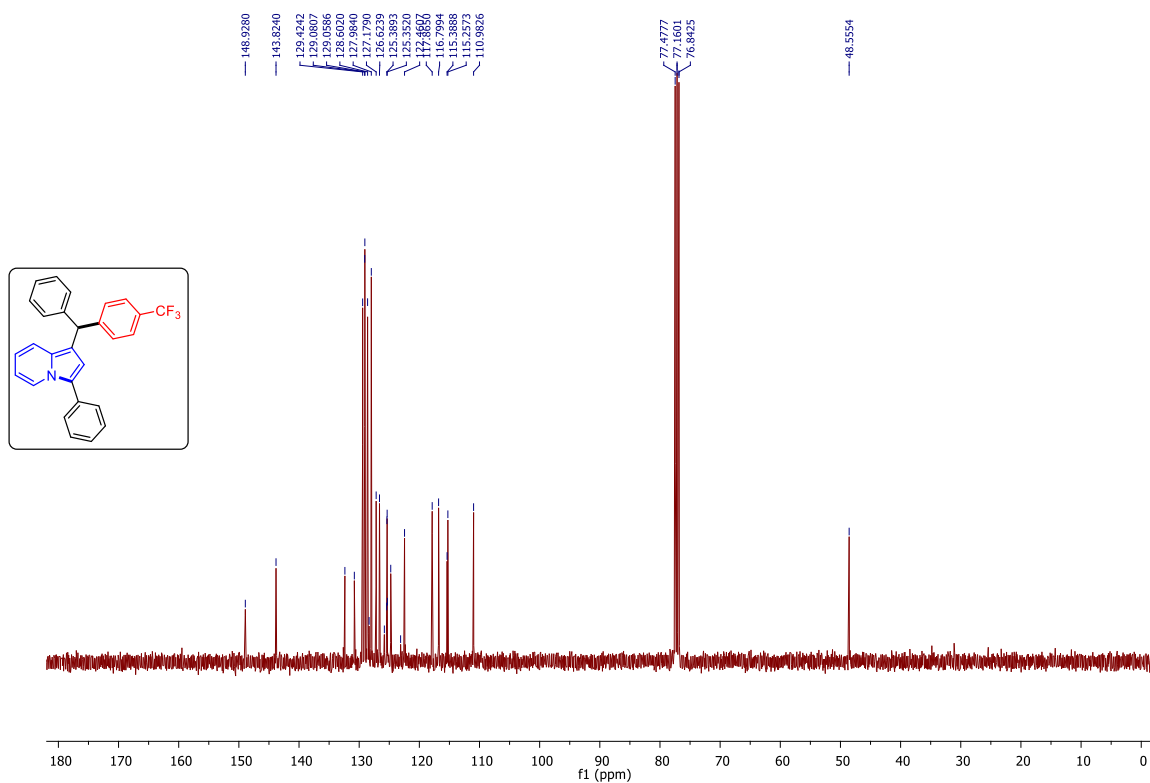
¹³C{¹H} NMR (400 MHz, CDCl₃) spectrum of (**103i**)



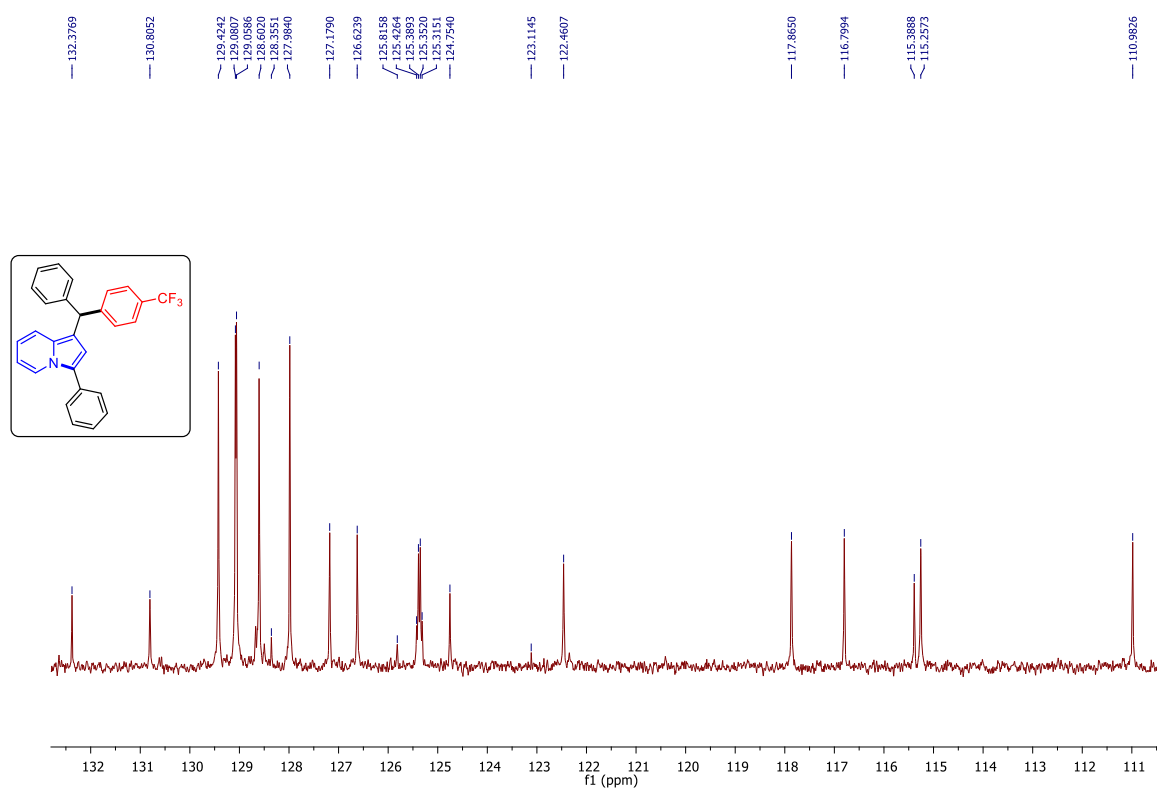
^1H NMR (400 MHz, CDCl_3) spectrum of (**103k**)



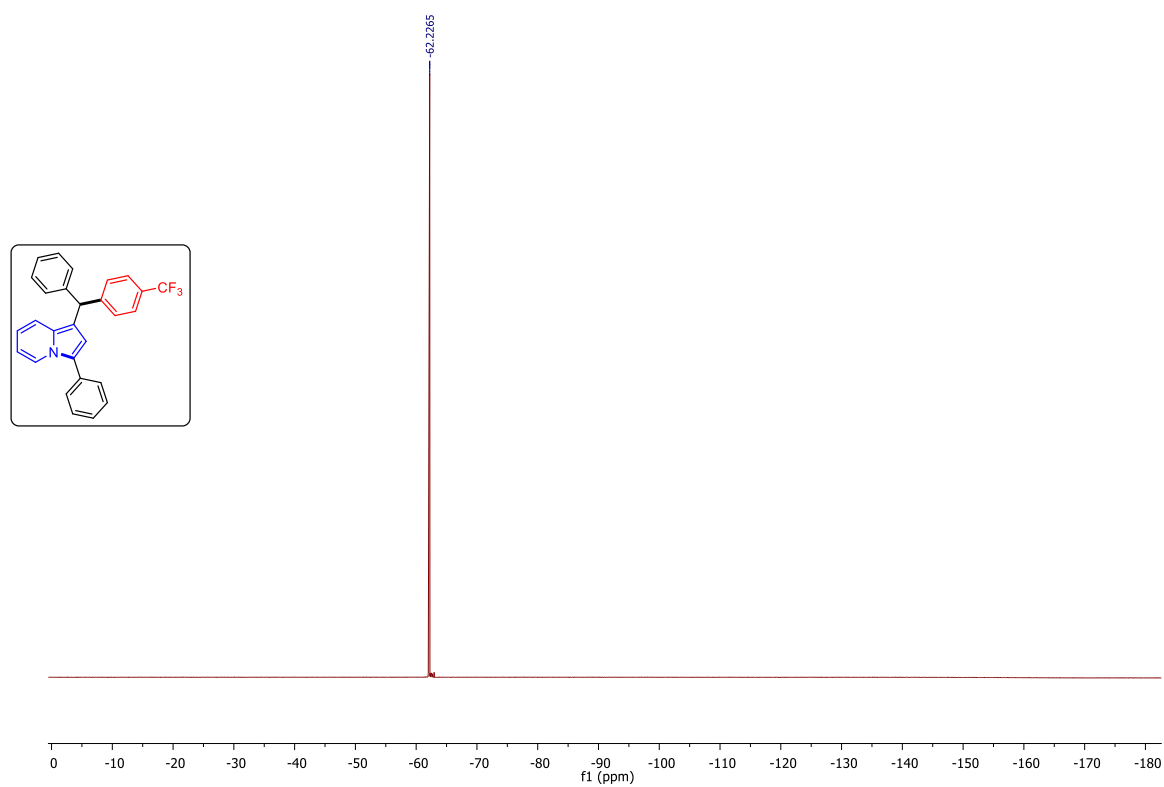
$^{13}\text{C}\{^1\text{H}\}$ NMR (400 MHz, CDCl_3) spectrum of (**103k**)

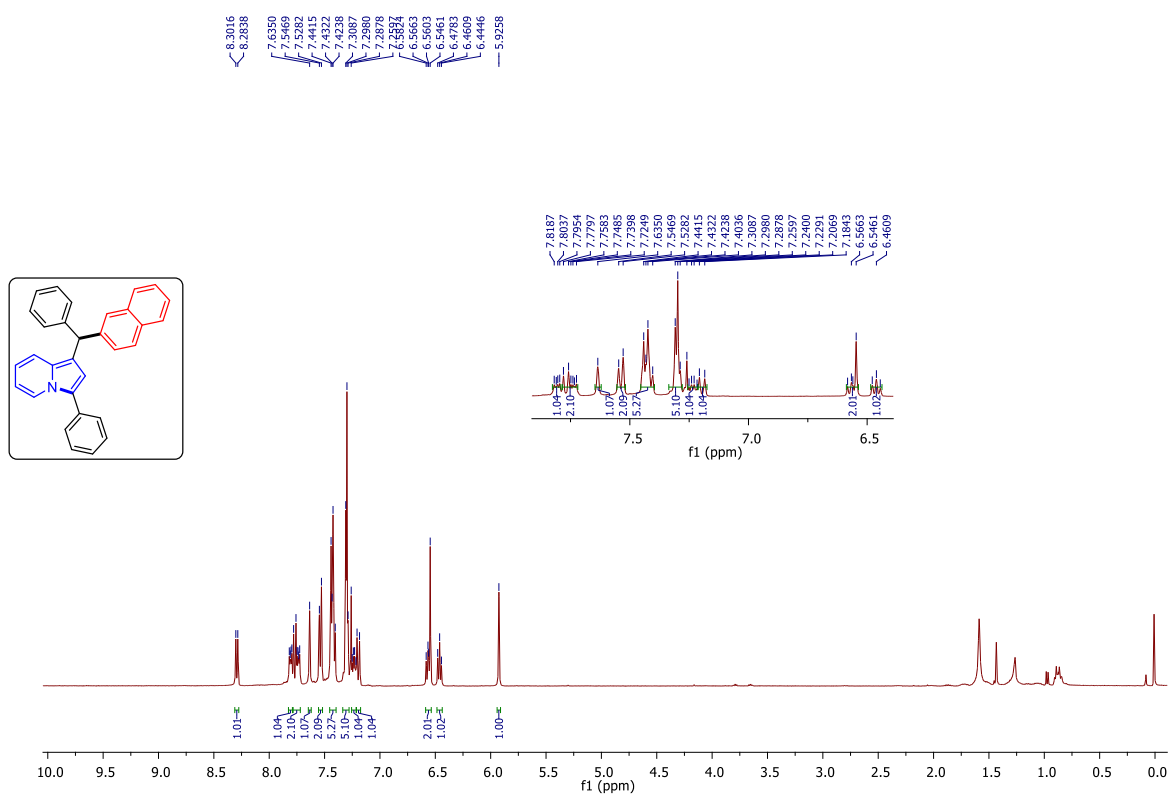
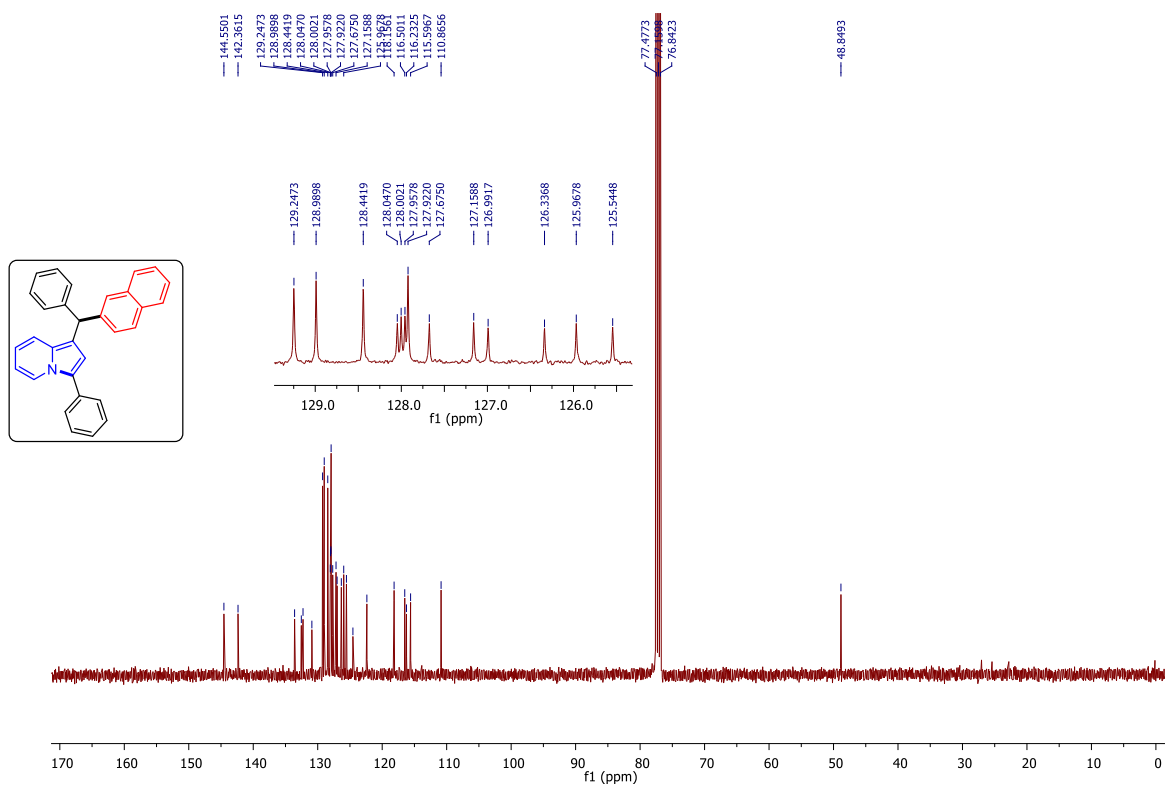


Expanded $^{13}\text{C}\{^1\text{H}\}$ NMR (400 MHz, CDCl_3) spectrum of (**103k**)

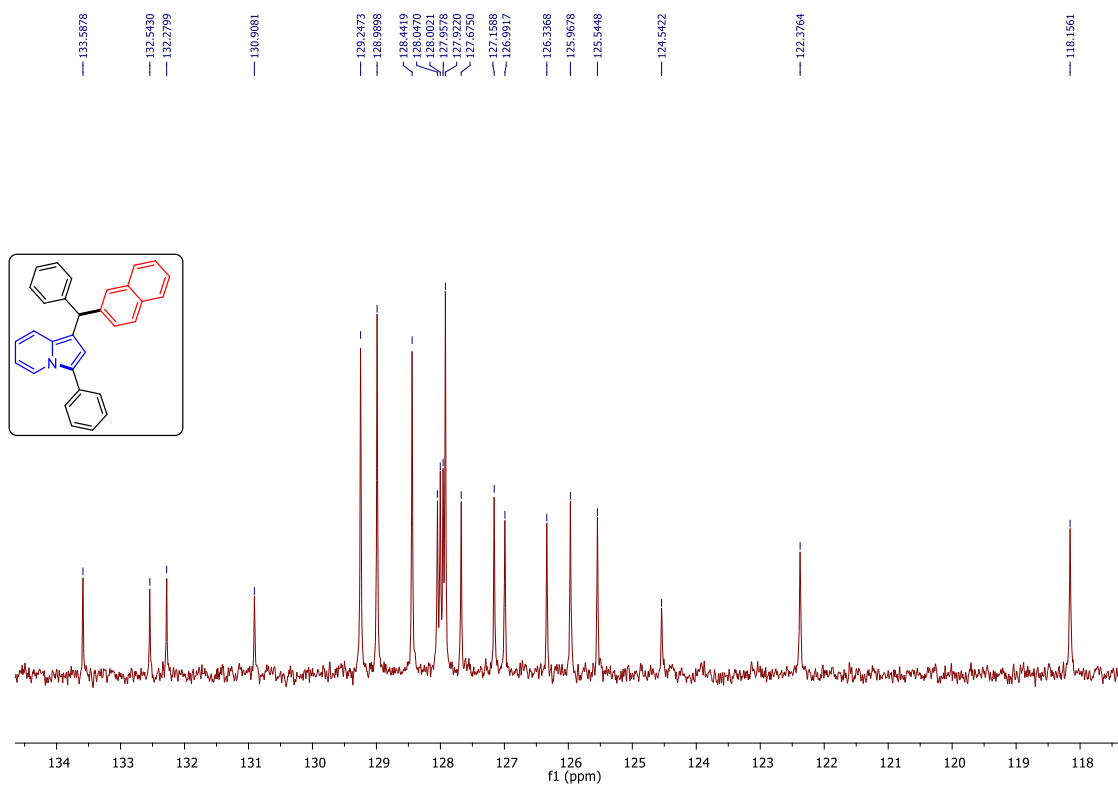


$^{19}\text{F}\{^1\text{H}\}$ NMR (376 MHz, CDCl_3) spectrum of (**103k**)

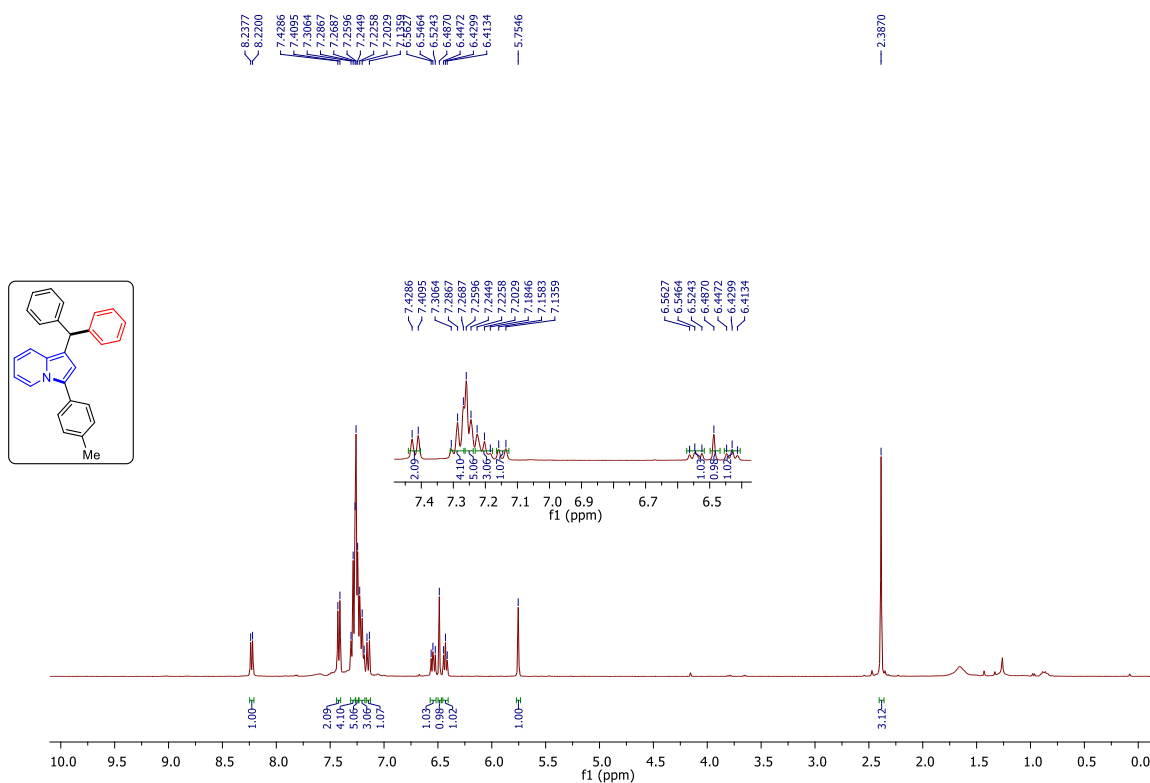


¹H NMR (400 MHz, CDCl₃) spectrum of (**103m**) $^{13}\text{C}\{^1\text{H}\}$ NMR (400 MHz, CDCl_3) spectrum of (**103m**)

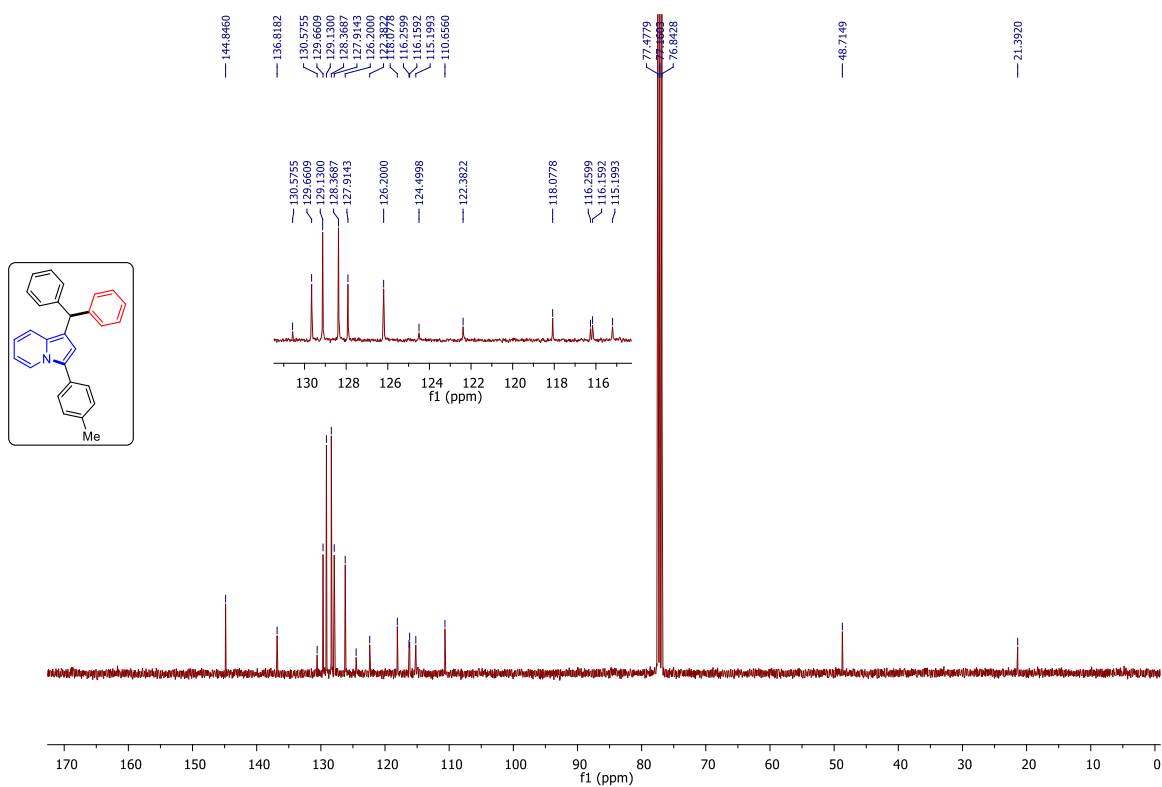
Expanded $^{13}\text{C}\{^1\text{H}\}$ NMR (400 MHz, CDCl_3) spectrum of (**103m**)



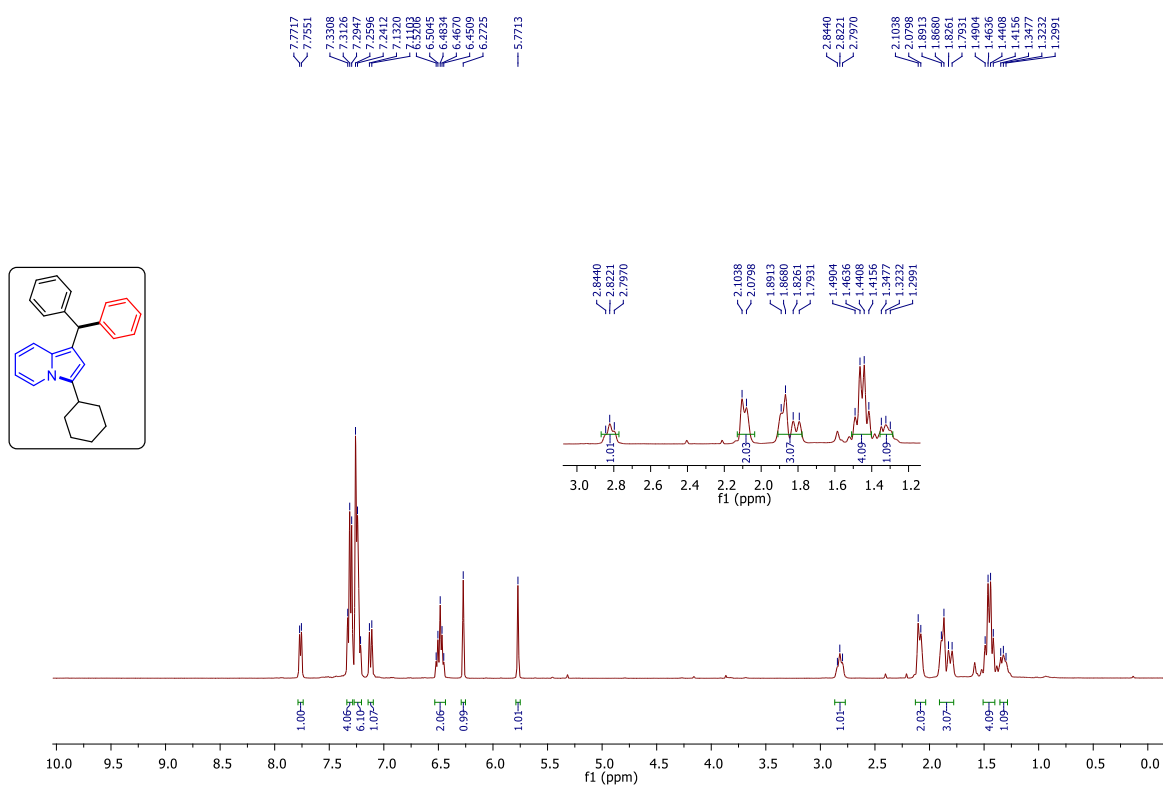
^1H NMR (400 MHz, CDCl_3) spectrum of (**104b**)



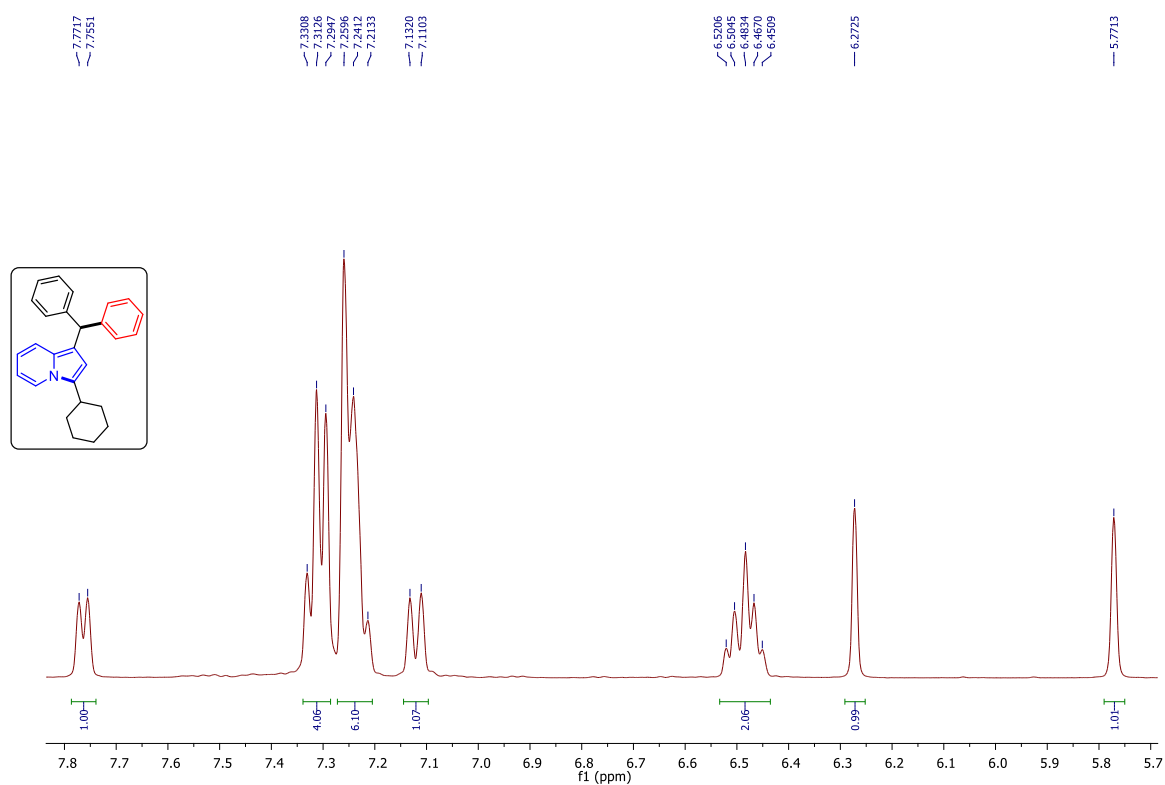
$^{13}\text{C}\{^1\text{H}\}$ NMR (400 MHz, CDCl_3) spectrum of (**104b**)



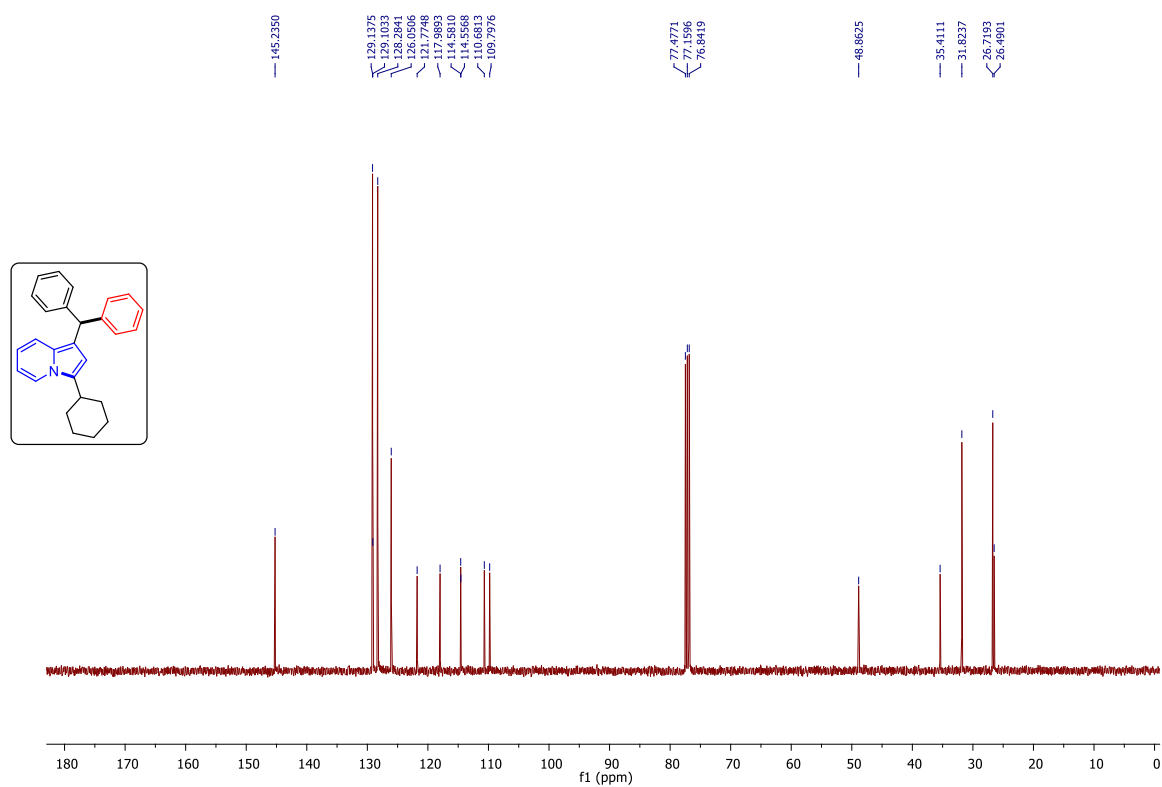
^1H NMR (400 MHz, CDCl_3) spectrum of (**104k**)



Expanded ^1H NMR (400 MHz, CDCl_3) spectrum of (**104k**)



$^{13}\text{C}\{^1\text{H}\}$ NMR (400 MHz, CDCl_3) spectrum of (**104k**)



1.8 References:

1. For selected examples: (a) Bindal, R. D.; Golab, J. T.; Katzenellenbogen, J. A. *J. Am Chem. Soc.* **1990**, *112*, 7861. (b) Wang, P.; Kozlowski, J.; Cushman, M. *J. Org. Chem.* **1992**, *57*, 3861. (c) Benzaquen, L. R.; Brugnara, C.; Byers, H. R.; Gattoni-Celli, S.; Halperin, J. A. *Nat. Med.* **1995**, *1*, 534. (d) Bai, L.; Masukawa, N.; Yamaki, M.; Takagi, S. *Phytochemistry* **1998**, *47*, 1637. (e) Al-awasmeh, R. A.; Lee, Y.; Cao, M. Y.; Gu, X.; Vassilakos, A.; Wright, J. A.; Young, A. *Bioorg. Med. Chem. Lett.* **2004**, *14*, 347.
2. (a) Rauer, H.; Lanigan, M. D.; Pennington, M. W.; Aiyar, J.; Ghanshani, S.; Cahalan, M. D.; Norton, R. S.; Chandy, K. G. *J. Biol. Chem.* **2000**, *275*, 1201. (b) Shagufta; Srivastava, A. K.; Sharma, R.; Mishra, R.; Balapure, A. K.; Murthy, P. S. R.; Panda, G. *Bioorg. Med. Chem.* **2006**, *14*, 1497. (c) Mibu, N.; Yokomizo, K.; Miyata, T.; Sumoto, K. *J. Heterocyclic Chem.* **2010**, *47*, 1434. (d) Singh, P.; Manna, S. K.; Jana, A. K.; Saha, T.; Mishra, P.; Bera, S.; Parai, M. K.; Kumar M, S. L.; Mondal, S.; Trivedi, P.; Chaturvedi, V.; Singh, S.; Sinha, S.; Panda, G. *Eur. J. Med. Chem.* **2015**, *95*, 357. (e) Mondal, S.; Panda, G. *RSC Adv.* **2014**, *4*, 28317.
3. (a) Tafi, A.; Costi, R.; Botta, M.; Santo, R. D.; Corelli, F.; Massa, S.; Ciacci, A.; Manetti, F.; Artico, M. *J. Med. Chem.* **2002**, *45*, 2720. (b) York, M.; Abdelrahim, M.; Chintharlapalli, S.; Lucero, S. D.; Safe, S. *Clin Cancer Res* **2007**, *13*, 6743. (c) Ichite, N.; Chougule, M. B.; Jackson, T.; Fulzele, S. V.; Safe, S.; Singh, M. *Clin Cancer Res* **2009**, *15*, 543.
4. (a) Rys, P.; Zollinger, H. *Fundamentals of the Chemistry and Application of Dyes*; Wiley-Interscience: New York, NY, **1972**. (b) Duxbury, D. F. *Chem. Rev.* **1993**, *93*, 381. (c) Muthyala, R.; Kartritzky, A. R.; Lan, X. F. *Dyes Pigm.* **1994**, *25*, 303.
5. (a) Ota, M.; Ootani, S. *Chem. Lett.* **1989**, 1179. (b) Gindre, C. A.; Screttas, C. G.; Fiorini, C.; Schmidt, C.; Nunzi, J. M. *Tetrahedron Lett* **1999**, *40*, 7413. (c) Strekowski, L.; Lee, H.; Lin, S. Y.; Czarny, A.; Deerveer, D. V. *J. Org. Chem.* **2000**, *65*, 7703. (d) Noack, A.; Schroder, A.; Hartmann, H. *Angew. Chem., Int. Ed.* **2001**, *40*, 3008. (e) Kim, H. N.; Lee, H. M.; Kim, H. J.; Kim, J. S.; Yoon, J. *Chem. Soc. Rev.* **2008**, *37*, 1465.
6. Beija, M.; Afonso, C. A. M.; Martinho, J. M. G. *Chem. Soc. Rev.* **2009**, *38*, 2410.
7. (a) Stetsenko, D. A.; Lubyako, E. N.; Potapov, V. K.; Azhikina, T. L.; Sverdiov, E. D. *Tetrahedron Lett.* **1996**, *37*, 3571. (b) Shchepinov, M. S.; Case-Green, S. C.; Southern, E. M. *Nucl. Acids Res.* **1997**, *25*, 1155.
8. Wang, X.; Wang, Y.; Du, D. M.; Xu, J. *J. Mol. Catal. A. Chem.* **2006**, *255*, 31.

9. (a) Jaratjaroonphong, J.; Sathalalai, S.; Techasauvapak, P.; Reutrakul, V. *Tetrahedron Lett.* **2009**, *50*, 6012. (b) Ruengsangtongkul, S.; Taprasert, P.; Sirion, U.; Jaratjaroonphong, J. *Org. Biomol. Chem.*, **2016**, *14*, 8493.
10. He, Q. –L.; Sun, F. –L.; Zheng, X. –J.; You, S. –L. *Synlett* **2009**, 1111.
11. (a) Singh, P.; Dinda, S. K.; Shagufta; Panda, G. *RSC Adv.* **2013**, *3*, 12100. (b) Das, S. K.; Panda, G.; Chaturvedi, V.; Manju, Y. S.; Gaikwad, A. K.; Sinha, S. *Bioorg. Med. Chem. Lett.* **2007**, *17*, 5586. (c) Das, S. K.; Shagufta, Panda, G. *Tetrahedron Lett.* **2005**, *46*, 3097.
12. Pallikonda, G.; Chakravarty, M. *J. Org. Chem.* **2016**, *81*, 2135.
13. Liu, C. R.; Li, M. B.; Yang, C. –F.; Tian, S. –K. *Chem. Commun.* **2008**, 1249.
14. Saha, S.; Alamsetti, S. K.; Schneider, C. *Chem. Commun.* **2015**, *51*, 1461.
15. Wang, Y.; Zhang, C.; Wang, H.; Jiang, Y.; Du, X.; Xu, D. *Adv. Synth. Catal.* **2017**, *359*, 791.
16. Wong, Y. F.; Wang, Z.; Sun, J. *Org. Biomol. Chem.* **2016**, *14*, 5751.
17. He, Y. Y.; Sun, X. X.; Li, G. H.; Mei, G. J.; Shi, F. *J. Org. Chem.* **2017**, *82*, 2462.
18. Liu, J. X.; Zhu, Z. Q.; Yu, L.; Du; Mei, G. J.; Shi, F. *Synthesis*, **2018**, *50*, 3436.
19. (a) Huang, R.; Zhang, X.; Pan, J.; Li, J.; Shen, H.; Ling, X.; Xiong, Y. *Tetrahedron*, **2015**, *71*, 1540. (b) Li, S.-S.; Yu, L.; Li, W.; Yu, S.; Liu, Q.; Xiao, J. *J. Org. Chem.*, **2018**, *83*, 15277.
20. Mahesh, S.; Anand, R. V. *Org. Biomol. Chem.* **2017**, *15*, 8393.
21. Nambo, M.; Crudden, C. M. *ACS Catal.* **2015**, *5*, 4734.
22. (a) Nawa, T.; Yorimitsu, H.; Oshima, K. *Org. Lett.* **2007**, *9*, 2373. (b) Zhang, J.; Bellomo, A.; Creamer, A. D.; Dreher, S. D.; Walsh, P. J. *J. Am. Chem. Soc.* **2012**, *134*, 13765.
23. Yu, J. –Y.; Kuwano, R. *Org. Lett.* **2008**, *10*, 973.
24. Yuan, F. Q.; Gao, L. X.; Han, F. S. *Chem. Commun.*, **2011**, *47*, 5289.
25. Saha, T.; Kumar, M. S. L.; Bera, S.; Karkara, B. B.; Panda, G. *RSC Adv.*, **2017**, *7*, 6966.
26. (a) Zhou, Q.; Srinivas, H. D.; Dasgupta, S.; Watson, M. P. *J. Am. Chem. Soc.*, **2013**, *135*, 3307. (b) Huang, Y.; Hayashi, T. *J. Am. Chem. Soc.*, **2015**, *137*, 7556.
27. Lou, Y.; Cao, P.; Jia, T.; Zhang, Y.; Wang, M.; Liao, J. *Angew. Chem., Int. Ed.* **2015**, *54*,

28. Reddy, V.; Anand, R. V. *Org. Lett.* **2015**, *17*, 3390.
29. (a) Rao, H. S. P.; Rao, A. V. B. *Beilstein J. Org. Chem.*, **2016**, *12*, 496. (b) Das, T.; Debnath, S.; Maiti, R.; Maiti, D. K. *J. Org. Chem.*, **2017**, *82*, 688.
30. Arde, P.; Anand, R. V. *RSC Adv.* **2016**, *6*, 77111.
31. Zhou, T.; Li, S.; Huang, B.; Li, C.; Zhao, Y.; Chen, J.; Chen, A.; Xiao, Y.; Liu, L.; Zhang, J. *Org. Biomol. Chem.* **2017**, *15*, 4941.
32. (a) Liu, R. -R.; Cai, Z. -Y.; Lu, C. -J.; Ye, S. -C.; Xiang, B.; Gao, J.; Jia, Y. -X. *Org. Chem. Front.* **2015**, *2*, 226. (b) Liu, R. -R.; Lu, C. -J.; Zhang, M. -D.; Gao, J. -R.; Jia, Y. -X. *Chem. Eur. J.* **2015**, *21*, 7057. (c) Bagle, P. N.; Mane, M. V.; Vanka, K.; Shinde, D. R.; Shaikh, S. R.; Gonnade, R. G.; Patil, N. T. *Chem. Commun.* **2016**, *52*, 14462.
33. Pathipati, S. R.; van der Werf, A.; Selander, N. *Org. Lett.* **2018**, *20*, 3691.
34. Hu, W.; Zhan, Q.; Zhou, H.; Cao, S.; Jiang, Z. *Chem. Sci.* **2021**, *12*, 6543.
35. Hu, W.; Zhan, Q.; Zhou, H.; Cao, S.; Jiang, Z. *Chem. Sci.* **2021**, *12*, 6543.
36. (a) Mahesh, S.; Paluru, D. K.; Ahmad, F.; Patil, S.; Kant, G.; Anand, R. V. *Asian J. Org. Chem* **2017**, *6*, 1857; (b) Mahesh, S.; Anand, R. V. *Eur. J. Org. Chem.* **2017**, *2017*, 2698; (c) Paluru, D. K.; Mahesh, S.; Ahmad, F.; Anand, R. V. *Chem. Asian J.* **2019**, *14*, 4688.

2. Copper-catalyzed Synthesis of Chromone and Indolizine-based Unsymmetrical Triarylmethanes from 2-(2-Enynyl)pyridines

2.1 Introduction:

The heterocyclic compound Chromone is considered to be a privileged core and found as an integral part of many natural products, bio-active molecules, clinical medicines, and lead compounds.^[1] Flavones and isoflavones, for instance, being the most common chromone-based natural compounds (Figure 1), have made significant contributions to a variety of various scientific and industrial fields, including medicinal chemistry, biochemistry, health care, and organic synthesis.^[2] In addition, functionalized chromones have recently been found to have a variety of bioactivities, including anti-virus, anti-bacterial, anti-oxidant, anti-fungal, and anti-tumour properties, etc.^[3]

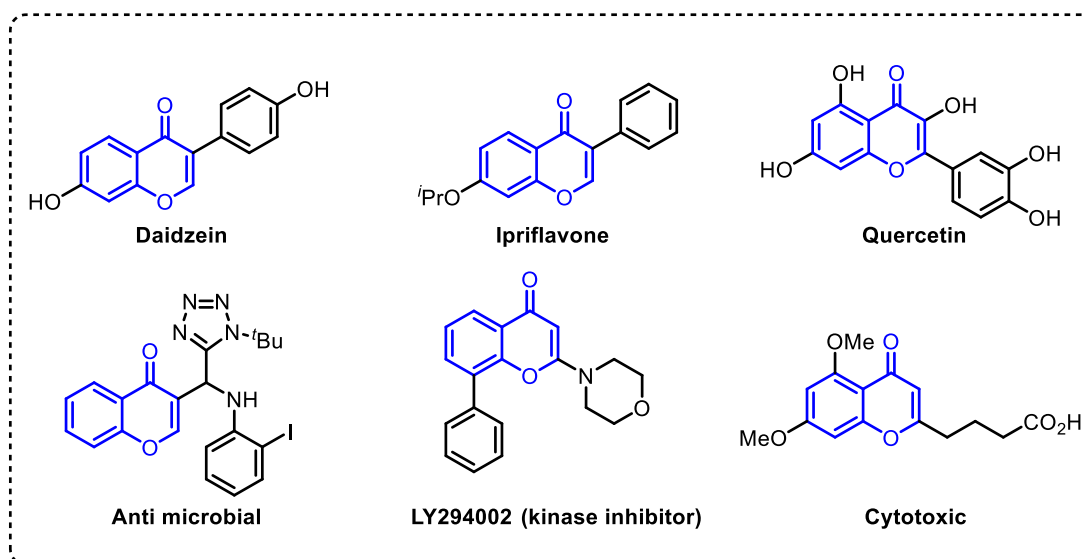


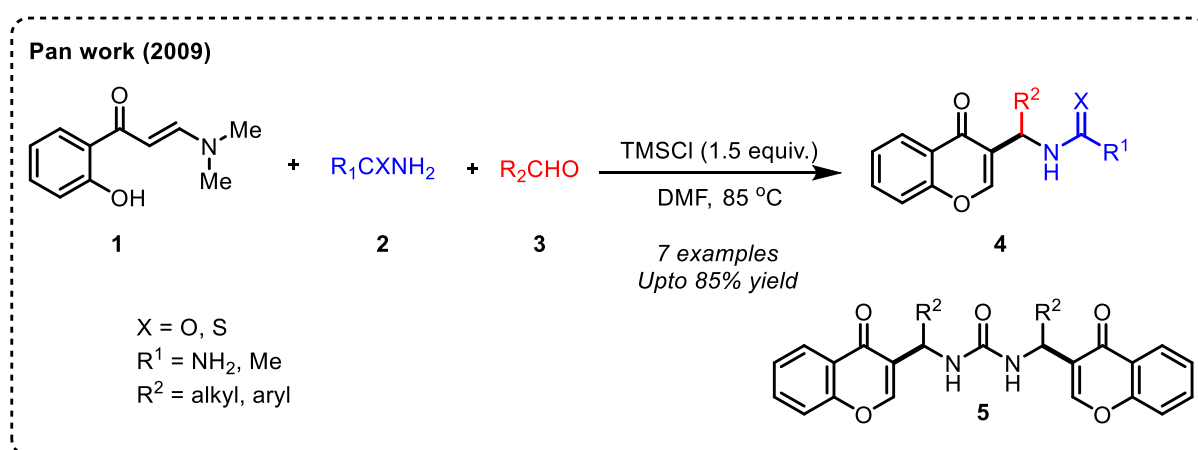
Figure 1: Chromone-Based Natural Products and Bioactive Compounds

Due to the importance of these heterocyclic compounds, research works focusing on the synthesis of chromones continue to be of great interest and attracted many synthetic chemists to develop various synthetic protocols for their syntheses. In general, two main strategies are employed for the synthesis of chromone scaffolds. The first method is the direct elaboration of the naturally occurring chromone, which results in chromone derivatives with various substructures.^[4] As natural chromone is expensive, as well as due to the limited availability of

natural chromones, this method has limited applications. The other approach shows a much broader application and involves synthesizing chromone rings having enhanced structural diversity from various acyclic building blocks.^[5-14] In recent years, the domino reactions initiated by the cyclization of *N,N*-disubstituted 2-hydroxyphenyl enaminone have been realized as a reliable and easy method for synthesizing 3-substituted chromones.^[15,16] It involves the formation of new carbon-carbon and carbon-heteroatom bonds *via* direct functionalization of the enaminone C-H bond. A few literature reports for synthesizing 3-substituted chromones, through domino cyclization of 2-hydroxyphenyl enaminones and its C-H elaboration, have been summarized below.

2.2 Literature reports on synthesis of 3-substituted chromones:

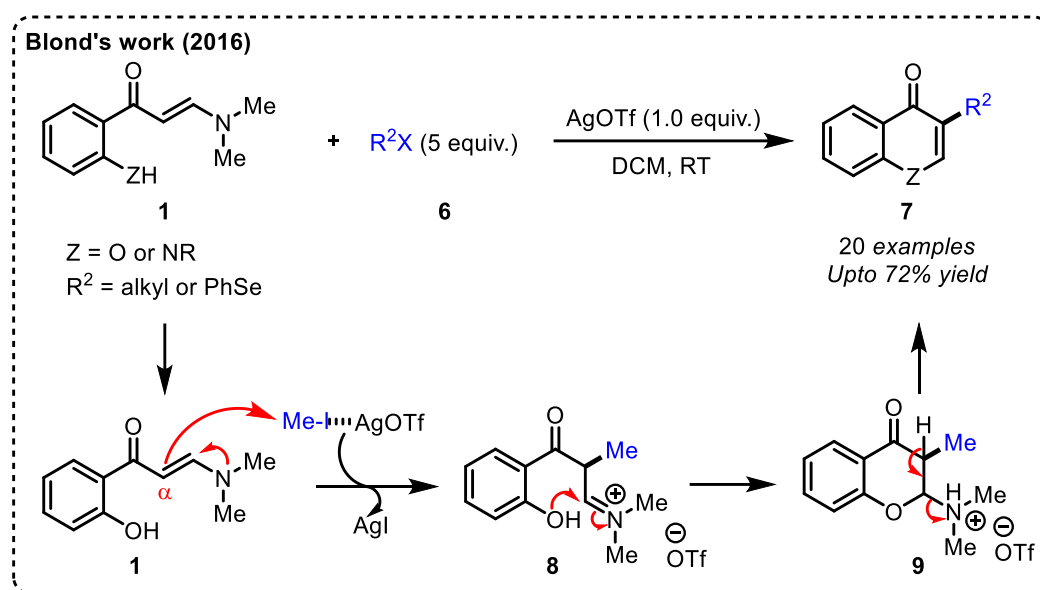
In recent years various carbon-based coupling reagents have been effectively used to react with 2-hydroxyphenyl enaminones to access a variety of C3-substituted chromone derivatives. For example, in the year 2009, Pan and co-workers reported a TMS-Cl promoted multicomponent reaction of 2-hydroxyphenyl enaminones (**1**), urea/thiourea (**2**), and aldehydes (**3**) to synthesize 3-aminoalkylated chromones (**4**). According to the authors, the reaction proceeds through the cyclization of enaminone **1** to form chromone, followed by the nucleophilic attack on the *in situ* generated imine from the condensation reaction of **2** and **3** to access the final 3-substituted chromone product **4**. In some cases, the urea-bridged bisalkylchromone **5** was formed as a side product when urea was used as one of the substrates (Scheme 1).^[17]



Scheme 1: Synthesis of 3-aminoalkylated chromones

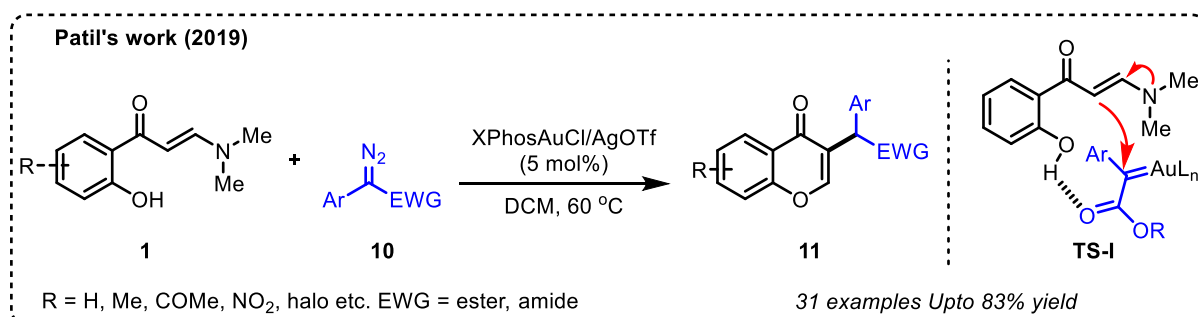
Later in 2016, Blond's group reported the synthesis of 3-alkyl chromones (**7**) in moderate yields by the reaction of enaminones (**1**) and excess of alkyl halides (**6**) in the

presence of a stoichiometric amount of AgOTf. In addition, 3-phenylselenenylated chromones were obtained when phenylselenenyl chloride was used as the electrophile. According to their proposed mechanism, the reaction proceeds through the activation of the alkyl halide **6** by the Ag(I) salt, followed by nucleophilic attack from the α -position of enaminone **1** to generate the alkylated iminium salt **8**. The subsequent cyclization of the intermediate **8** produces another intermediate **9**, which upon amine elimination, affords the desired product **7** (Scheme 2).^[18]



Scheme 2: Synthesis of 3-alkyl chromones

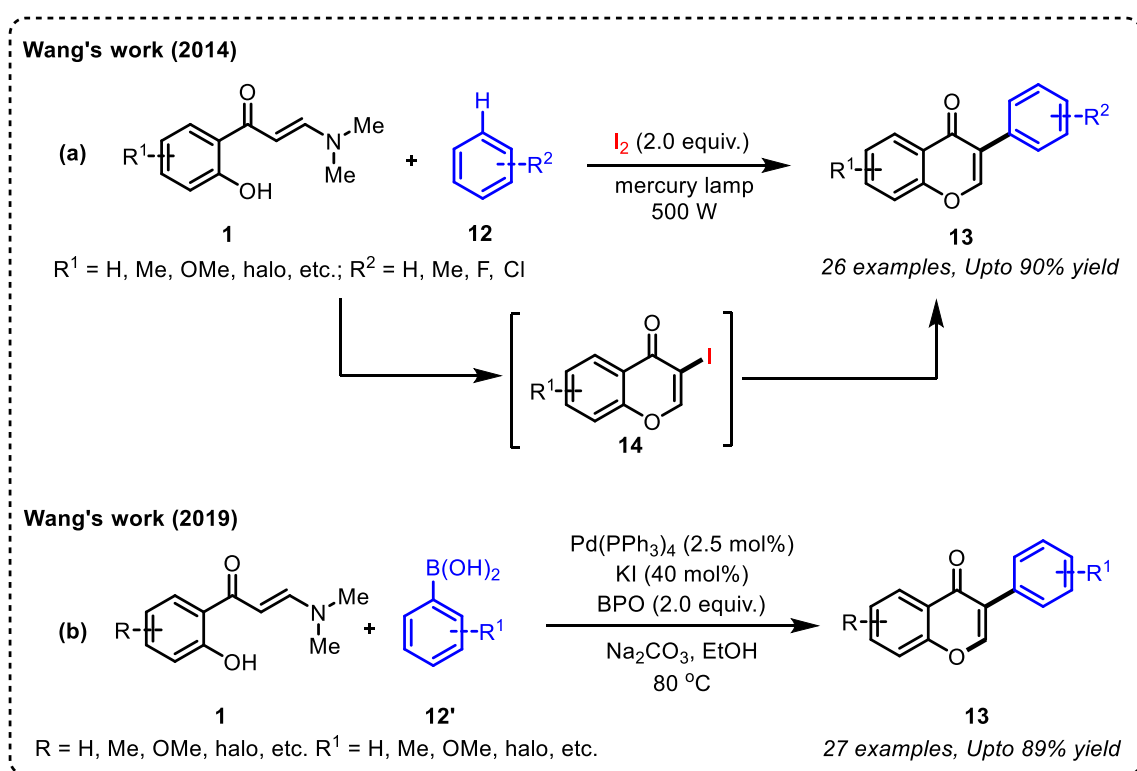
In 2019, Patil and co-workers developed an interesting protocol for synthesizing 3-alkylated chromones through the reaction of enaminone (**1**) and diazo compounds (**10**) catalyzed by a dual XPhosAuCl/AgOTf catalyst. A variety of substituted enaminones and functionalized diazo compounds, were well tolerated while delivering the corresponding 3-alkylated chromones (**11**) in moderate to good yields. Computational studies revealed that the



Scheme 3: Au catalysed synthesis of 3-alkylated chromones

hydroxyl group of the reactant **1** (in the transition state TS-I) assists the alkylation reaction by promoting the incorporation of the enaminone into the Au-carbene intermediate during the formation of the desired product (Scheme 3).^[19]

In 2014, Wang's group reported a photochemical approach for the synthesis of isoflavone derivatives (**13**) by the reactions of enaminone (**1**) and benzene derivatives (**12**) in the presence of 2 equivalents of molecular iodine under the irradiation of a 500W mercury lamp. This transformation proceeds through the formation of 3-iodochromone **14** as the reaction intermediate. The benzene substrates **12** need to be used as a solvent, and when unsymmetrical benzene derivatives were used as the reagent, a mixture of regioisomers was

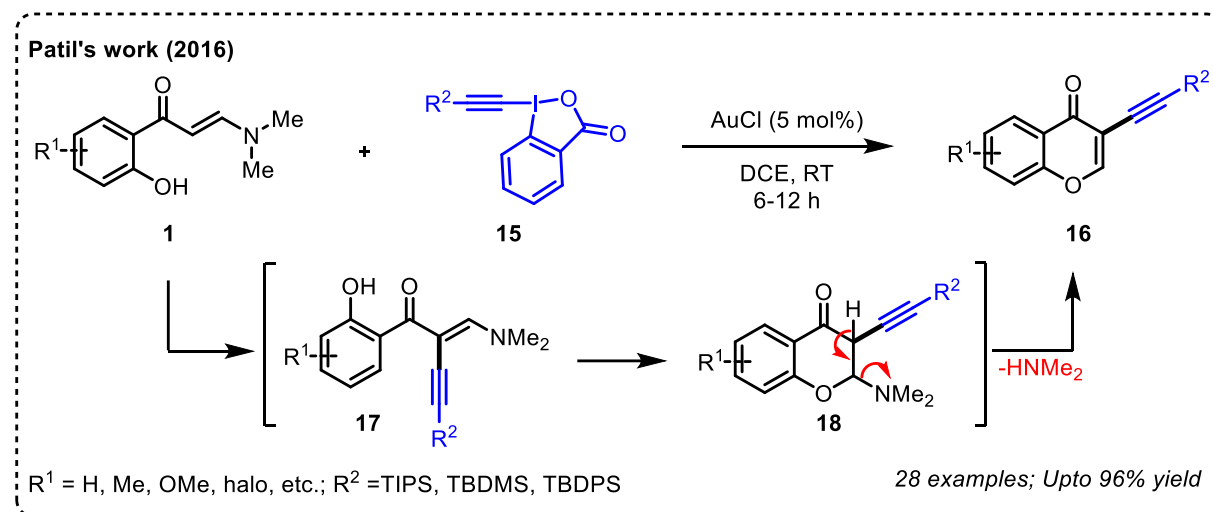


Scheme 4: Synthesis of isoflavones through C3- arylation of chromones

obtained, resulting from the transformation of different C-H bonds (Scheme 4a).^[20a] Later, in 2019, the same group reported a BPO-promoted one-pot approach for the synthesis of 3-arylchromones from *o*-hydroxyphenyl enaminones and aryl boronic acids (**12'**). A wide range of 3-halochromones was synthesized and then, *in-situ*, transformed into 3-arylchromones through palladium cross-couplings. The advantage of this approach over the previous report is that it does not require any pre-functionalization of the enaminone (Scheme 4b)^[20b]

In 2016, Patil group reported a AuCl catalyzed synthesis of 3-alkynyl chromones (**16**) through a C-H alkynylation from the reaction of enaminones (**1**) and the alkynyl cation

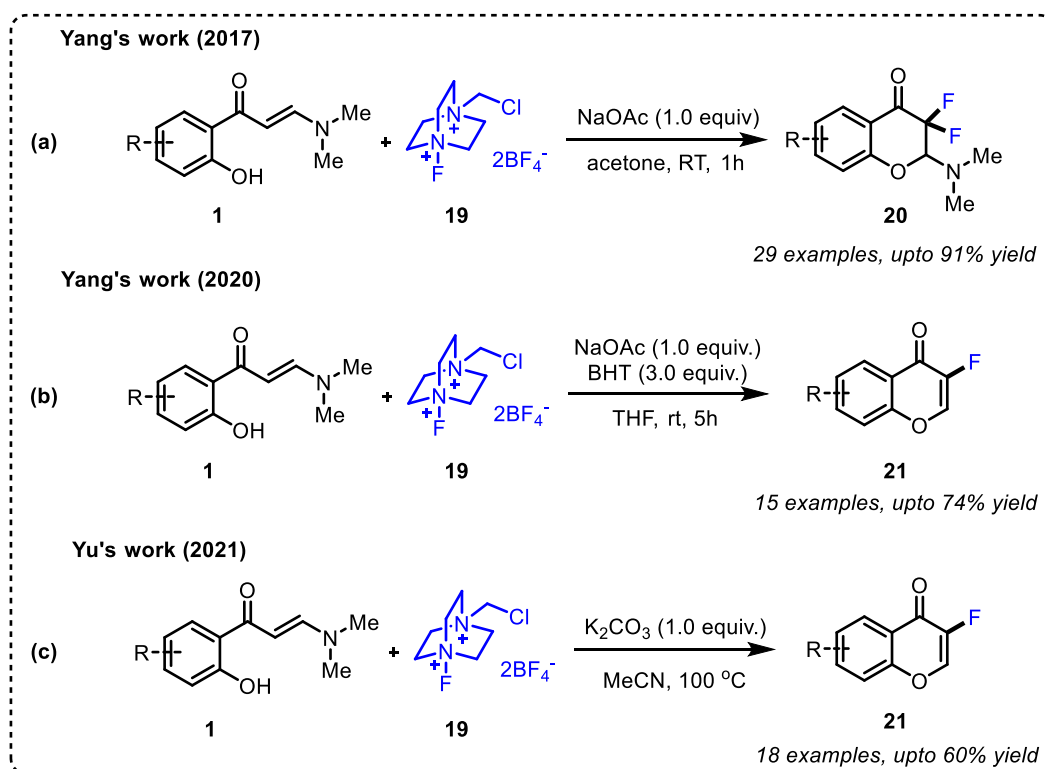
precursors (**15**). This transformation worked well at room temperature, and the 3-alkynyl chromones (**16**) were obtained in good to excellent yields. Control experiments revealed that



Scheme 5: Synthesis of 3-alkynyl chromones

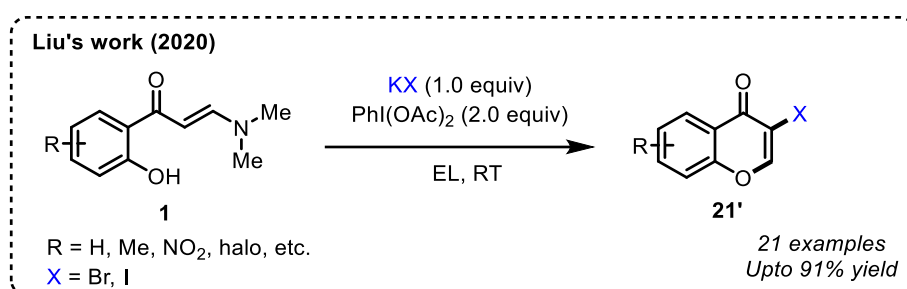
the reaction proceeds through the C-H alkylation to give alkynyl enaminone **17**. The cyclization of **17** generates the dihydrochromone **18**, which upon amine elimination, gives the final product **16** (Scheme 5).^[21]

In 2017, Yang's group developed a Selectfluor-triggered tandem cyclization of *o*-hydroxyarylenaminone **1** for the construction of a variety of difluorinated 2-amino-substituted



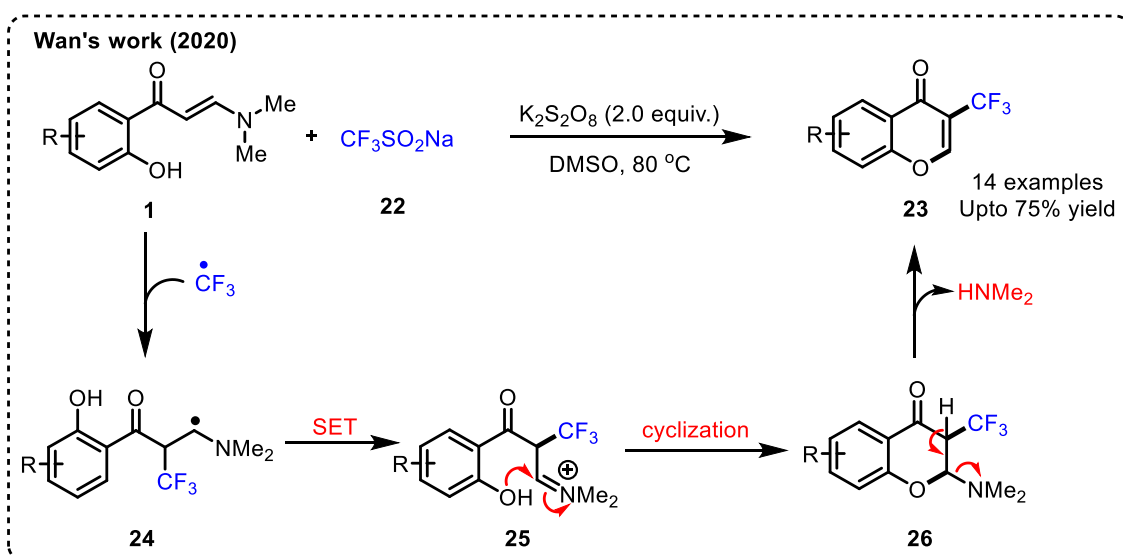
Scheme 6: Synthesis of 3-fluorinated chromones

chromanones **20** in good yields (Scheme 6a).^[22a] Later in 2020, the same group extended this protocol for the one-pot synthesis of monofluorinated chromones **21** by the cyclization of 2-hydroxyphenyl enaminones **1** initiated by fluorination with Selectfluor **19** in the presence of the radical scavenger BHT or TEMPO and a diverse range of 3-fluorochromones were obtained in moderate to good yields (Scheme 6b).^[22b] In 2021, Yu and co-workers reported a similar protocol in the absence of the radical scavenger BHT or TEMPO for the synthesis of 3-fluorinated chromones **21** via a K₂CO₃-promoted C–H fluorination and subsequent intramolecular cyclization and deamination by using *o*-hydroxyarylenaminones **1** and Selectfluor **19** as reaction partners in MeCN at 100 °C (Scheme 6c).^[22c]



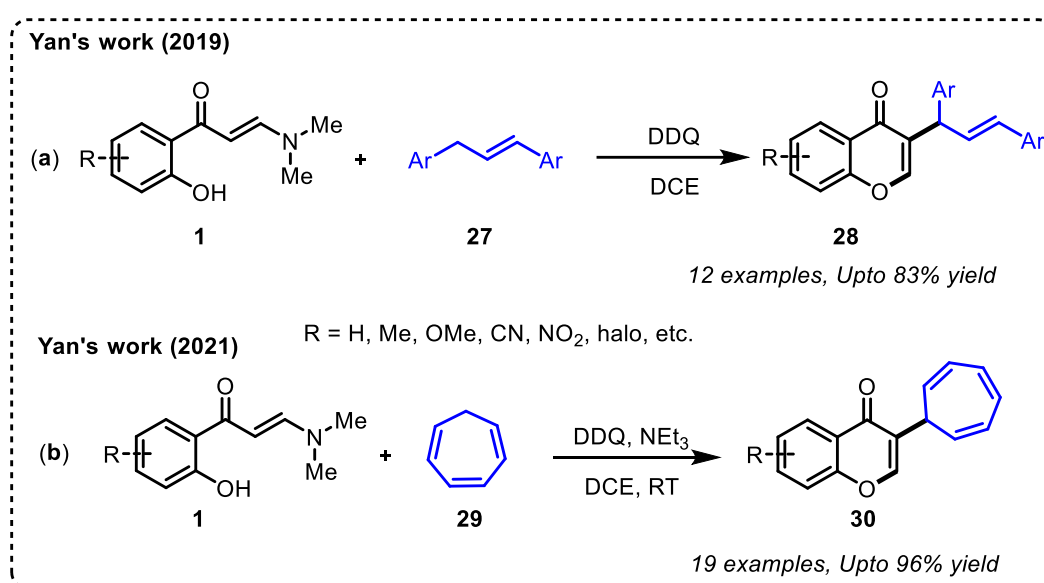
Scheme 7: Synthesis of 3-halo chromones from 2-hydroxyphenyl substituted enaminone

In 2020, Liu and co-workers reported the synthesis of 3-Br/I chromones **21'** from 2-hydroxyphenyl enaminones **1** using a combination of simple and nontoxic KBr/KI with the oxidant $PhI(OAc)_2$ as the halogenating reagent and ethyl lactate (EL) as the solvent. Although this protocol was successfully utilized for the synthesis of 3-Br/I chromones, the 3-Cl chromones could not be prepared using this transformation (Scheme 7).^[23]



Scheme 8: K₂S₂O₈ promoted synthesis of 3-trifluoromethyl chromones

In 2020, the Wan group developed a transition metal-free protocol for the synthesis of 3-trifluoromethyl chromones (**23**) by the reaction of 2-hydroxyphenyl enaminones (**1**) and $\text{CF}_3\text{SO}_2\text{Na}$ **22** as a source of CF_3 radical. The reaction proceeds through a $\text{K}_2\text{S}_2\text{O}_8$ -promoted radical addition of CF_3 radical **24'** to enaminone **1** to generate the intermediate **24** followed by a SET to give another intermediate **25**, which upon intramolecular cyclization and amine elimination produces the final product **23**. A variety of trifluoromethyl chromones (**23**) were synthesized in moderate to good yields. Furthermore, the 3-trifluoromethyl chromone products were successfully used for the synthesis of 3-trifluoromethyl pyrimidines by reacting with guanidine/amidine substrates. (Scheme 8).^[24]

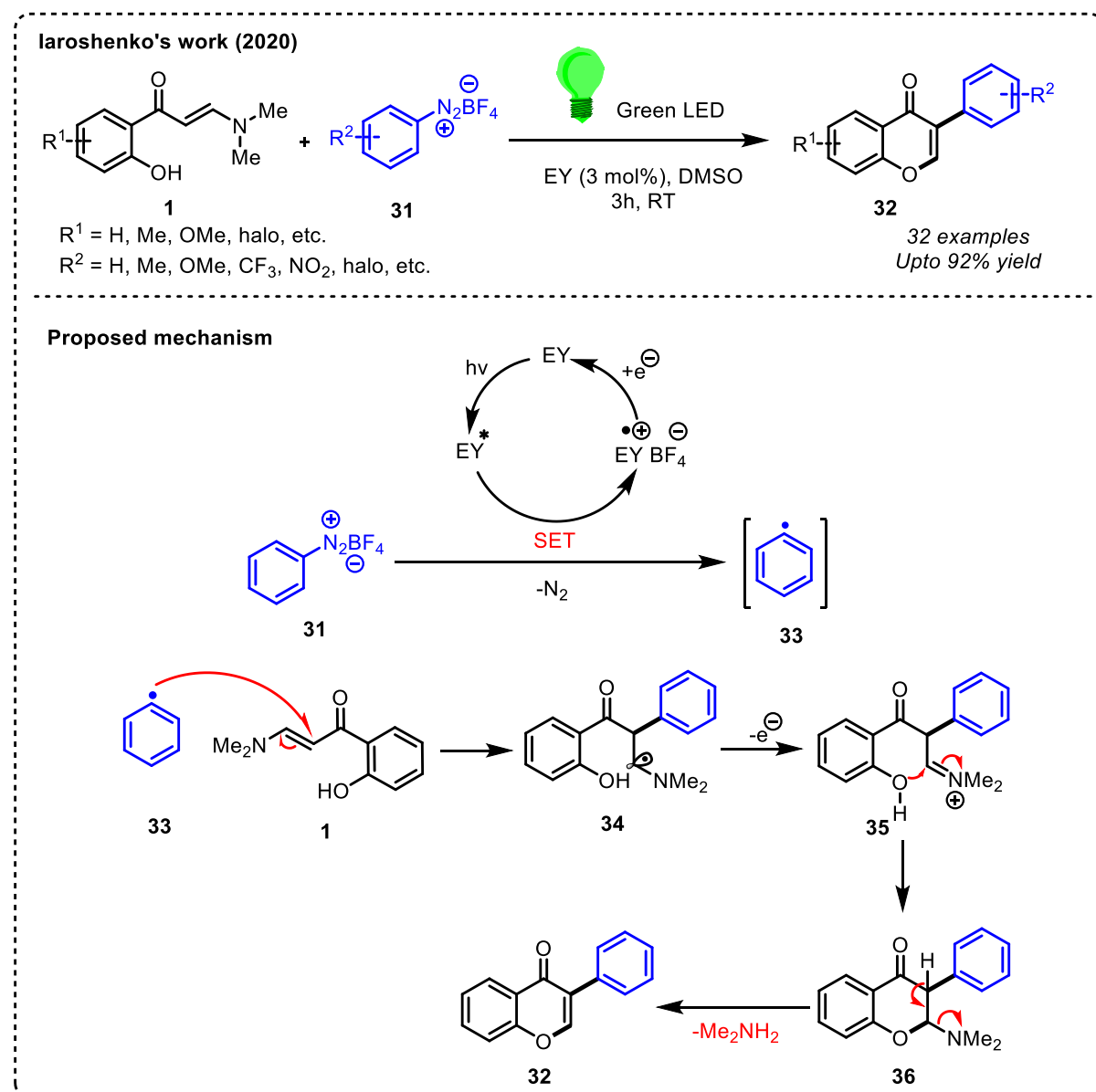


Scheme 9: DDQ-promoted synthesis of 3-allyl chromones

In 2019, the Yan and co-workers developed a DDQ-mediated oxidative allylation subsequent intramolecular cyclization followed by deamination to synthesize a variety of 3-allyl chromones (**28**) in moderate to good yields from *o*-hydroxyaryl enaminones (**1**) with 1,3-diarylpropenes (**27**) as the reaction partners (Scheme 9a).^[25a] Due to the high efficiency, transition metals free, and mild reaction conditions, this methodology demonstrated a broad range of potential applications for synthesizing bioactive chemicals. Later in 2021, the same group reported the same protocol for the reaction of enaminones (**1**) with cycloheptatriene **29** as the reaction partner for synthesizing 3-cycloheptatrienyl chromones (**30**) in good to excellent yields (Scheme 9b).^[25b]

Iaroshenko and co-workers recently developed a photo-induced route to access 3-arylchromones by the reaction of orthohydroxyaryl enaminones (**1**) and aryldiazonium

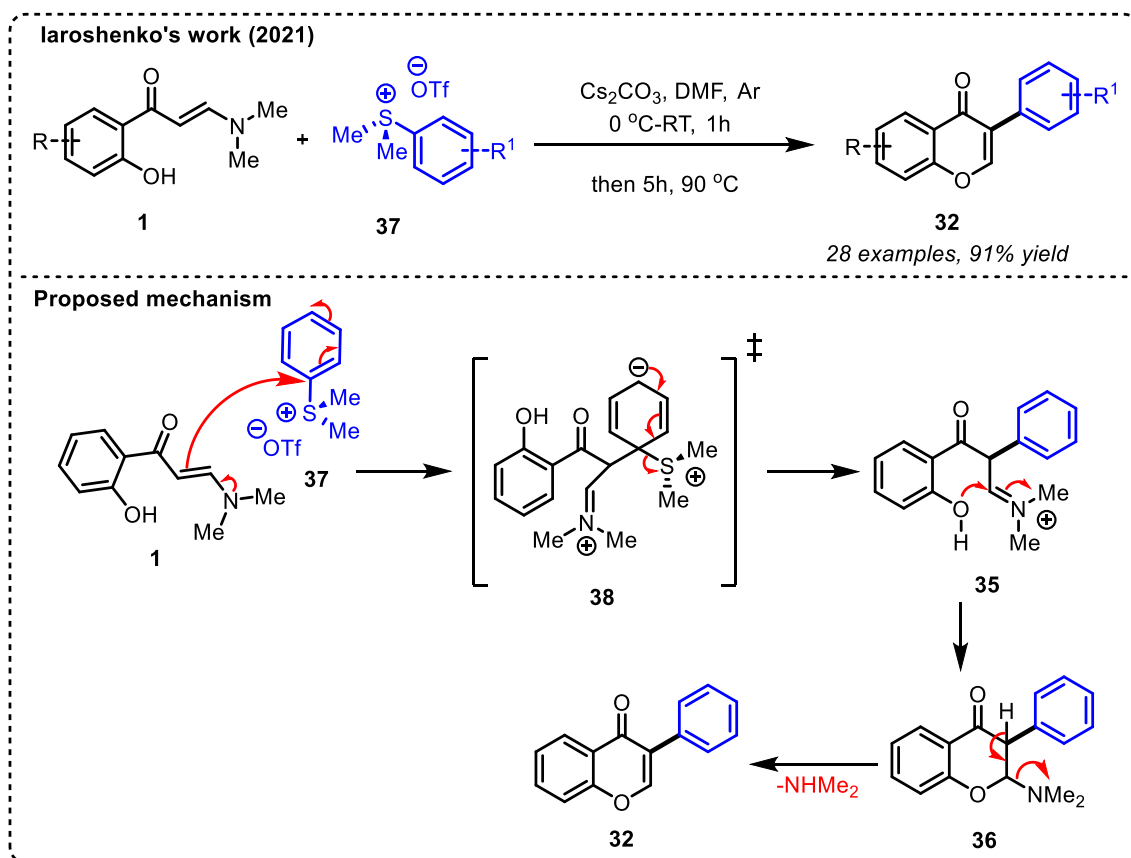
tetrafluoroborates (**31**) as the aryl radical source. The reaction proceeds through the generation of the aryl radical **33** through a SET from the irradiation of aryldiazonium tetrafluoroborates **31** in the presence of the photocatalyst Eosin Y. The radical addition of **33** to enaminone **1** generates intermediate **34**, which upon SET produces another intermediate **35**. The intermediate **35** undergoes intramolecular cyclization to generate **36**, which upon the elimination of dimethylamine, gives the product **32** (Scheme 10).^[26]



Scheme 10: Synthesis of 3-aryl chromones

Later, in 2021, they also developed another straightforward and efficient protocol for the synthesis of 3-arylchromones by the electrophilic arylation of 2-hydroxyaryl enaminones (**1**) using dimethyl(aryl)sulfonium salts (**37**) as the reaction partner and a wide

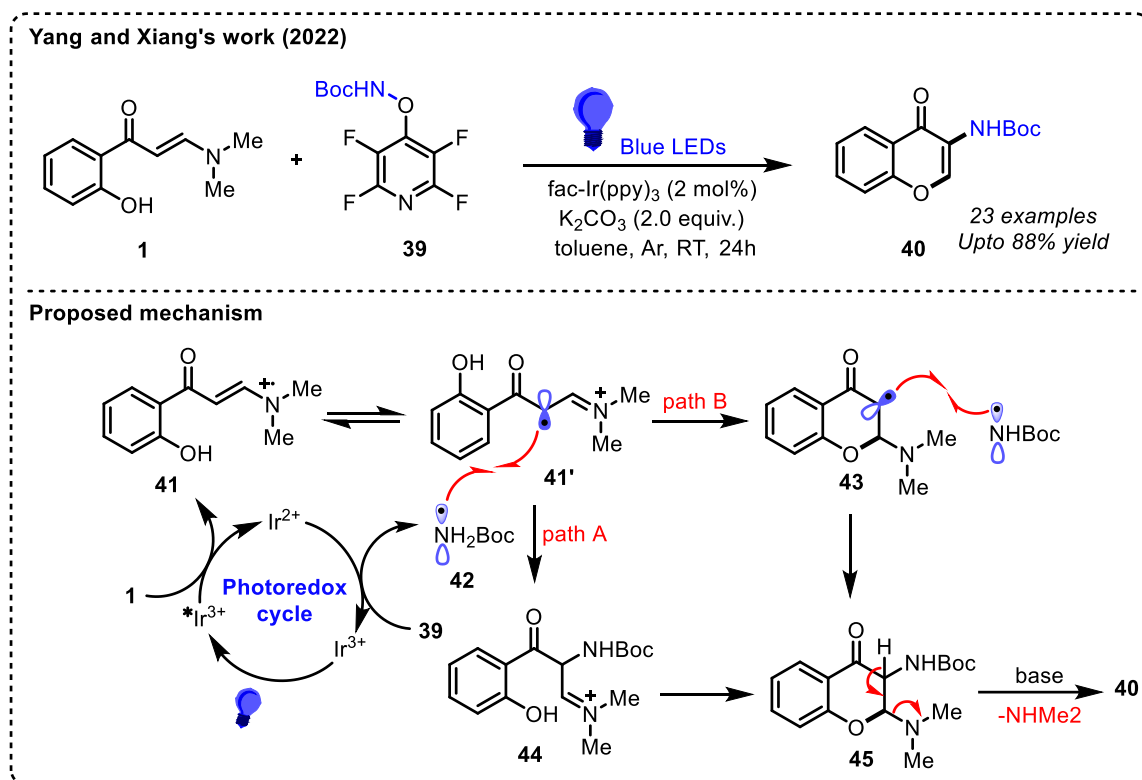
range of 3-arylchromones (**32**) were prepared in good to excellent yields. According to the proposed mechanism, the reaction starts with the initial electrophilic attack of the enaminone **1** on the sulfonium salt **37** followed by the S_NAr nucleophilic substitution to produce the intermediate **35** through the transition state **38**. The intermediate **35**, upon intramolecular cyclization and dimethylamine elimination, gives the final product **32** (Scheme 11).^[27]



Scheme 11: Synthesis of 3-aryl chromones using dimethyl(aryl)sulfonium salts

In 2022, Xiang and co-workers developed a photoredox-catalyzed amination of *o*-hydroxyaryl enaminones with tert-butyl ((perfluoropyridin-4-yl)oxy)carbamate as an amidyl-radical precursor to access a range of 3-aminochromones (Scheme 12). Based on the experimental results, the authors proposed that the reaction starts with the photoexcitation of the fac-Ir(ppy)₃ catalyst to *fac-Ir(ppy)₃ using a blue LED. The photo-excited *fac-Ir(ppy)₃ is then reductively quenched to Ir(II) through a single-electron transfer (SET) by the enaminone **1**, generating the nitrogen-center radical **41**. The radical intermediate **41** produces the carbon-center radical **41'** through a radical transposition. Meanwhile, the Ir(II) species is oxidized to Ir(III) by **39** to produce the amidyl radical **42**, which combines with **41'** to generate **44**. Intramolecular cyclization of **44** gives intermediate **45** (path A). Alternatively, the radical intermediate **41'** first undergoes intramolecular cyclization to produce another radical **43**,

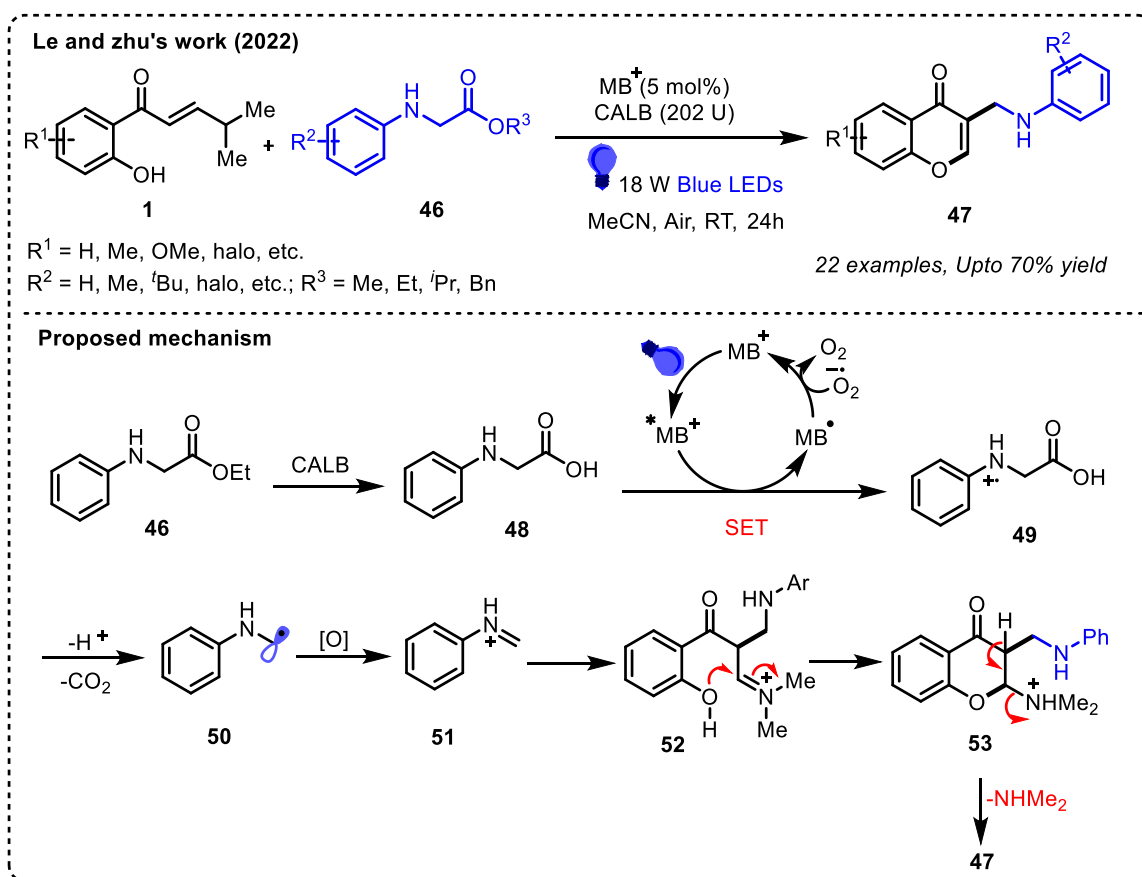
which is captured by the amidyl radical **42** to generate **45** (path B). The final elimination of dimethylamine from **45** produces the final product (Scheme 12).^[28]



Scheme 12: Photoredox-catalyzed synthesis of 3-aminated chromones

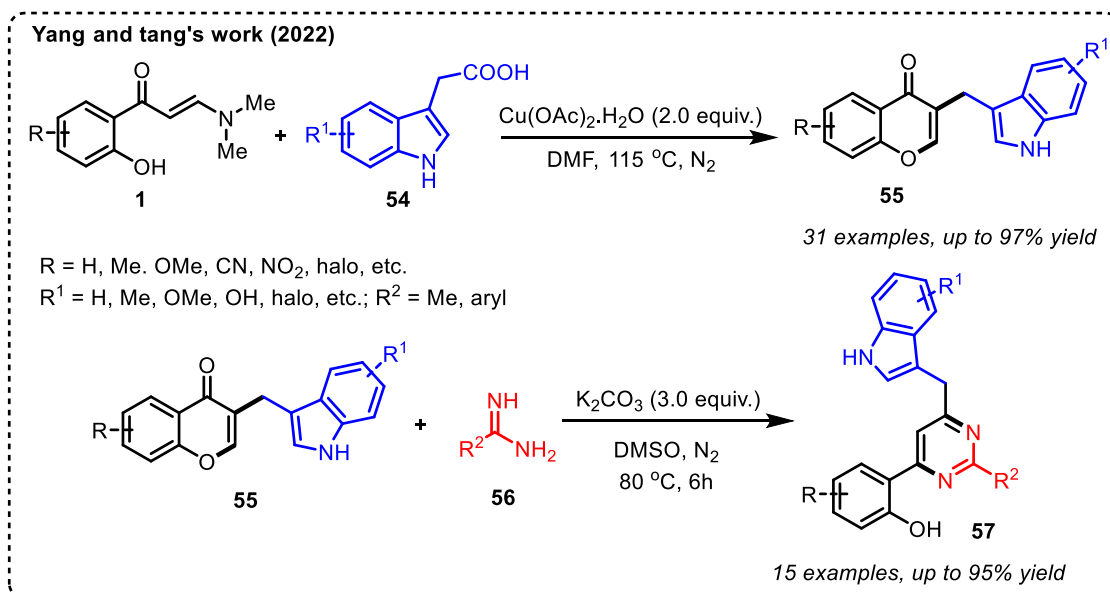
In 2022, Zhu and co-workers reported a combination of photoredox and enzyme catalysis for synthesizing 3-aminoalkyl chromones from *o*-hydroxyaryl enaminones and *N*-arylglycine esters as the reaction partners (Scheme 13). A variety of 3-aminoalkyl chromones (**47**) were obtained in moderate to good yields in one pot using this protocol. Based on the control experiments, the authors proposed that this cooperative photo-enzymatic reaction proceeds through the hydrolysis of *N*-arylglycine ester **46** into *N*-arylglycine **48** by the enzyme CALB. Then, *N*-arylglycine **46** undergoes single electron transfer (SET) with the photocatalyst MB⁺ to produce radical cation **49** under visible-light irradiation. Subsequently, the free radical intermediate **49** undergoes decarboxylation to give amine alkyl radicals **50**, which is oxidized to the imine intermediate **51**. The intermediate **51** then reacts with the enaminone **1** to generate the iminium intermediate **52**. Finally, intermediate **52** undergoes intramolecular cyclization followed by elimination of dimethylamine to generate the desired product **47** (Scheme 13).^[29]

Very recently, Tang and co-workers reported an efficient copper-mediated decarboxylative coupling/annulation protocol to access a wide range of 3-indolmethyl-chromones **55** in good to excellent yields by the reaction of *o*-hydroxyaryl enaminones (**1**) with



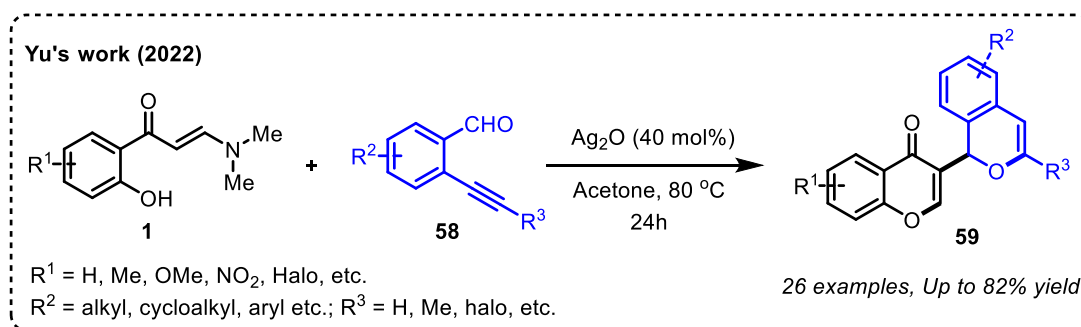
Scheme 13: Cooperative photoenzymatic synthesis of 3-aminoalkyl chromones

3-indoleacetic acids (**54**). Furthermore, the products were derivatized into various indolmethyl-substituted pyrimidines (**57**) by treating them with amidines (**56**) in the presence of an excess of base K_2CO_3 (**Scheme 14**).^[30]



Scheme 14: Cu-mediated synthesis of 3-indolmethyl chromones

In 2022 Yu's group developed a silver-catalyzed cascade protocol for the synthesis of 3-(1*H*-isochromen)-chromones derivatives (**59**) in good yields from *o*-hydroxyaryl enaminones (**1**) and 2-alkynyl benzaldehydes (**58**) as the starting materials. This method enables the installation of 1*H*-isochromen and chromone in a single structure via an initial 6-*endo*-dig cyclization of *o*-alkynyl benzaldehydes and a subsequent C-H alkylation/chromone annulation of the ortho-hydroxyaryl enaminones (Scheme 15).^[31]



Scheme 15: Ag₂O-mediated cascade cyclization of ortho-hydroxyarylenaminones

2.3 Background:

As a part of our current ongoing research on the development of new protocols to synthesize indolizine based unsymmetrical diaryl and triarylmethanes, we envisioned that it

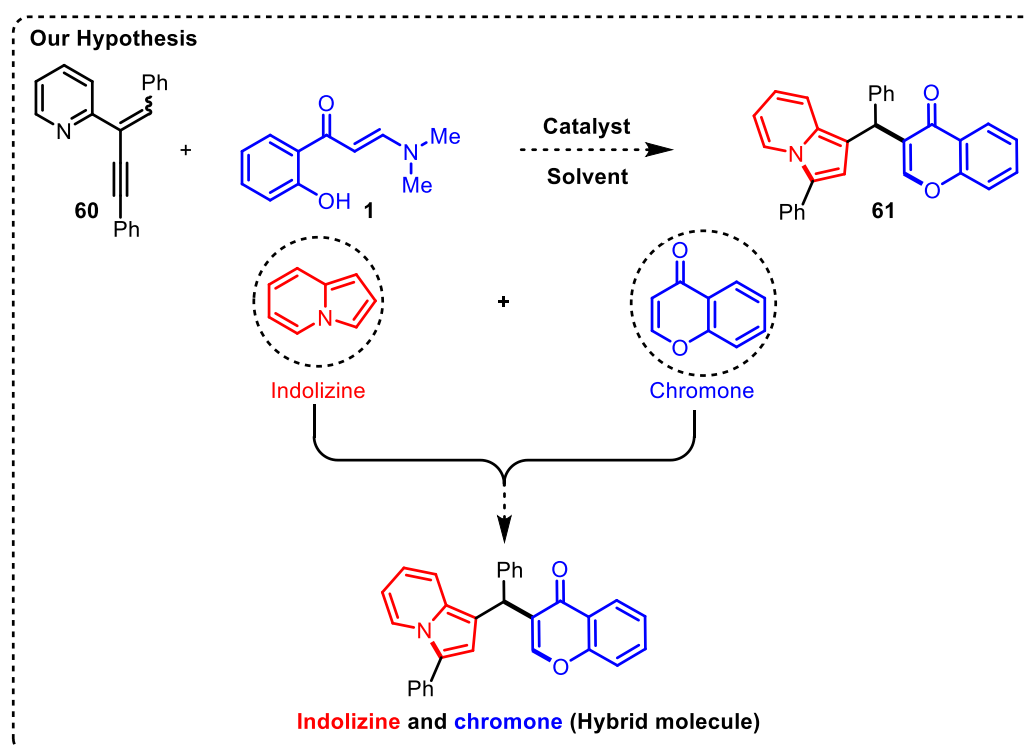
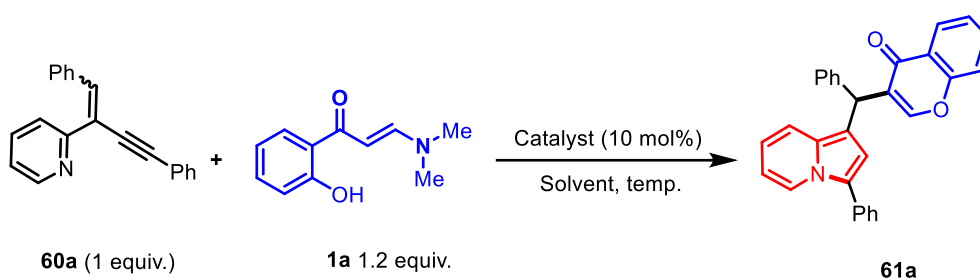


Figure 2: Our hypothesis for the synthesis of indolizine and chromone based TRAMs

could be possible to synthesize indolizine and chromone based triarylmethanes through the addition of *N,N*-dimethyl-2-hydroxyphenyl enaminone **1** to 2-(2-enynyl)-pyridines (**60**) through the initial 5-*endo*-dig cyclization 2-(2-enynyl)-pyridines followed by remote addition of 2-hydroxyphenyl enaminone to afford unsymmetrical triarylmethanes **61** containing both indolizine and chromone in the same molecule (Figure 2).

2.4 Results and Discussions:

To optimize the reaction conditions, we have chosen 2-(2-enynyl)-pyridine **60a** and *o*-hydroxyphenylenaminone **1a** as model substrates, and the results are shown in **Table 1**. First, we went for the optimization of the solvent for this reaction, and the preliminary experiment was performed with CuI as a catalyst in THF solvent at 50 °C, and the product **61a** was isolated in 89% yield after 8 hours (table 1, entry 1). However, when the reaction was conducted in PhMe, a slight increase in the yield of the reaction was observed, but it took a long time for the completion of the reaction, and the product **61a** was obtained in 91% yield after 18 hours (table 2, entry 2). The reaction was then optimized in other solvents such as 1,4-dioxane, CHCl₃, and ethyl acetate, although in these cases, the desired products were isolated in better yield (up to 94% in 1,4-dioxane); the reactions took longer time for completion (table 1, entry 3,4 & 5). The yield of the reaction was increased to 98% when the reaction was conducted in MeCN as a polar aprotic solvent, and it took only 3 hours to complete. (table 1, entry 6). The reaction was also conducted in chlorinated solvent 1,2-DCE and polar protic solvent EtOH, but in those solvents, the yield of **61a** was decreased to 79% and 72%, respectively (table 1, entries 7 & 8). The desired product **61a** was obtained in 80% yield after 40 hours when the reaction was conducted at room temperature (table 1, entry 9). The yield of **61a** was decreased to 80% after 6 hours when the catalyst loading was decreased to 5 mol% (table 1, entry 10). Then we went for screening other catalysts for this transformation; the reaction was conducted with different catalysts in MeCN as the solvent (table 1, entry 11-18). The reaction worked well with Cu(OTf)₂ as the catalyst, and 97% yield of **61a** was obtained after 4 hours (table 1, entry 11). With Cu(OTf).PhMe as the catalyst, the product was isolated in 85% yield after 10 hours (table 1, entry 12). CuBr and CuCl also worked well and yielded the product in 94% and 90%, respectively (table 1, entries 13 & 14). The reaction was also performed with various other copper salts as well such as Cu(SO₄).5H₂O and Cu(OAc)₂, but these salts were proven to be less effective for this transformation as compared to CuI and Cu(OTf)₂ as with these salts the reaction took a long time for completion and the yield was also

Table 1. Optimization Study^a

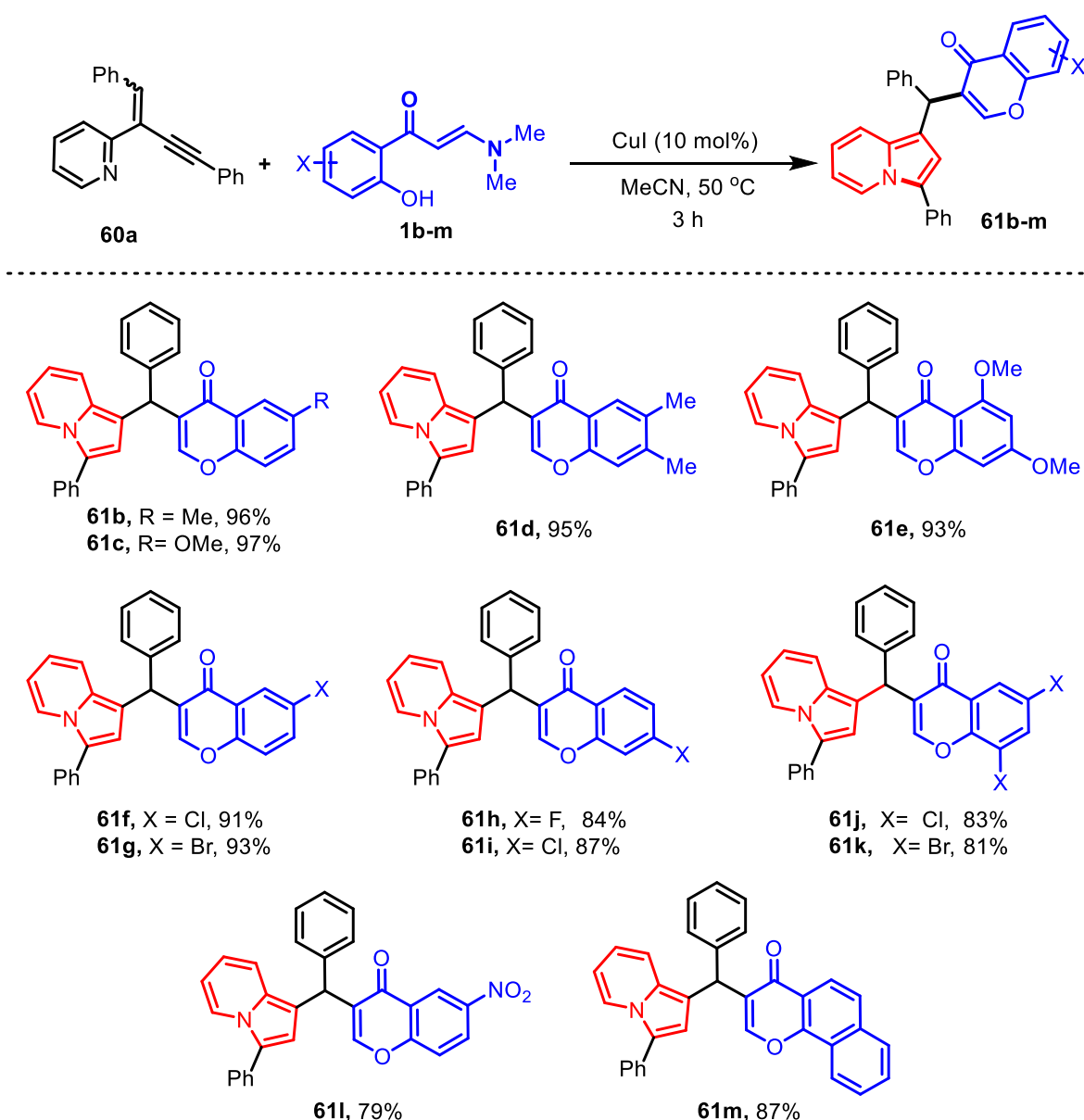
S/No	Solvent	Catalyst	Temp. °C	Time (h)	% Yield ^b
01	THF	CuI	50	8	89
02	Toluene	CuI	50	18	91
03	1,4-Dioxane	CuI	50	16	94
04	CHCl ₃	CuI	50	10	93
05	EtOAc	CuI	50	18	90
06^c	MeCN	CuI	50	3	98
07	1,2-DCE	CuI	50	6	79
08	EtOH	CuI	50	24	72
09	MeCN	CuI	RT	40	82
10 ^d	MeCN	CuI	50	6	80
11	MeCN	Cu(OTf) ₂	50	4	97
12	MeCN	Cu(OTf).toul.	50	10	85
13	MeCN	CuBr	50	8	94
14	MeCN	CuCl	50	12	90
15	MeCN	Cu(SO ₄).5H ₂ O	50	36	68
16	MeCN	Cu(OAc) ₂	50	12	76
17	MeCN	Bi(OTf) ₃	50	24	Trace
18	MeCN	Sc(OTf) ₃	50	24	Trace
19	MeCN	50	24	NR

^a Reaction conditions: All the reactions were carried out with 0.1423 mmol (40 mg) of SM **60a**, 1.2 equiv. of enaminone and 10 mol % of catalyst in (1.5 ML solvent). ^b Isolated yields; ^c 1.2 equiv. of enaminone with respect to **1a** and 10 mol % catalyst at 50 °C was found to be optimal. ^d with 5 mol% CuI as catalyst.

decreased (table 1, entries 15 & 16). The reaction was also performed with other Lewis acids, such as Bi(OTf)₃ and Sc(OTf)₃, but these catalysts were proven to be ineffective for this

transformation as only a trace amounts of the product formation was seen after 24 hours (table 1, entries 17 & 18). In the absence of the catalyst, no product formation was seen, which confirms that a catalyst is needed for this transformation. Although this protocol worked well with most of the catalysts and solvents screened, CuI in MeCN was found to be the best condition to drive this transformation. (table 1, entry 6). So further studies were carried out with CuI as the catalyst in MeCN as the optimized condition.

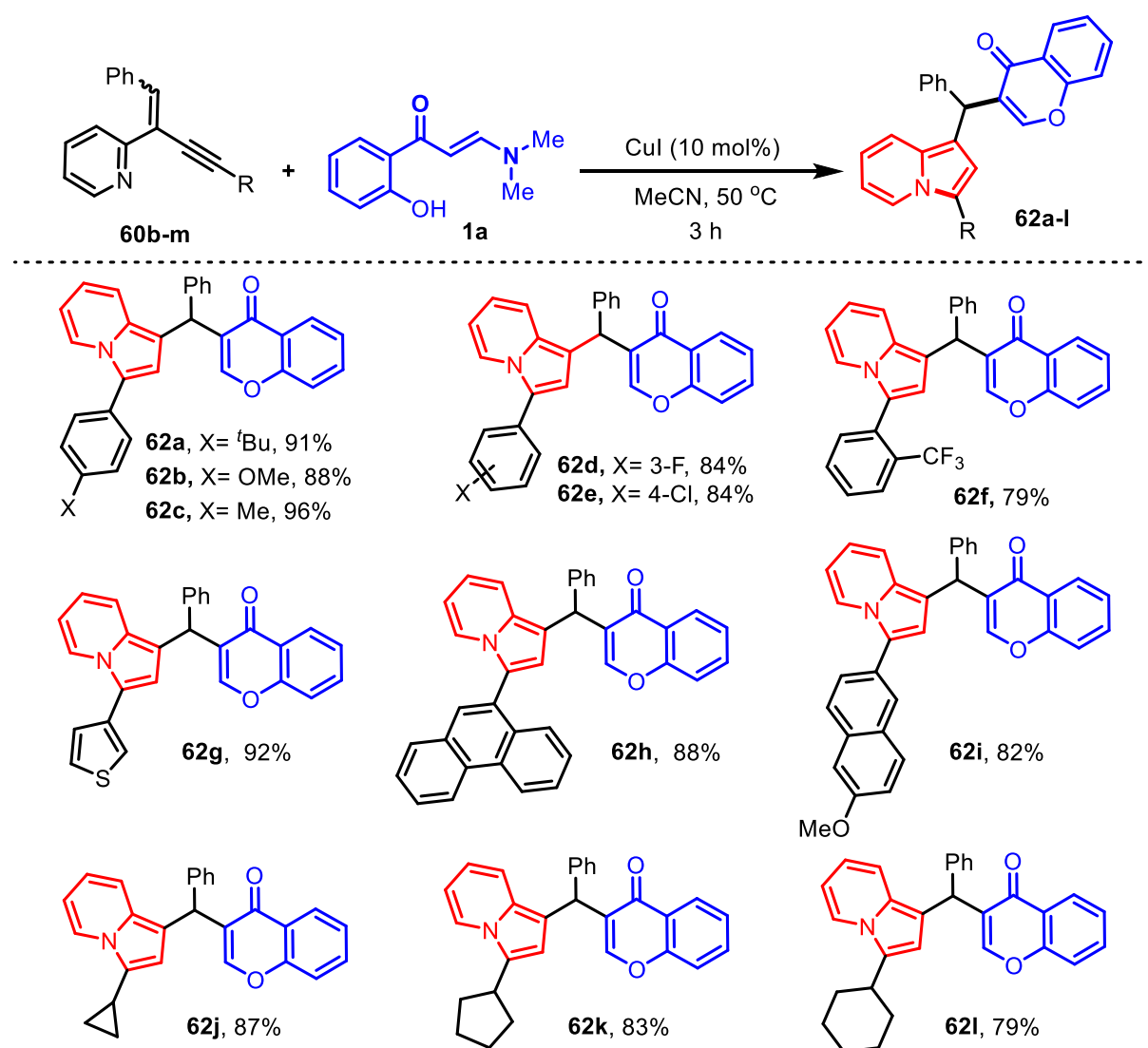
Table 2. Substrate Scope^b



^aReactions were carried out with 40 mg of **60a** and 1.2 equiv. of **1b-m** in 1.5 mL of MeCN. ^bYields reported are isolated yields.

With the optimal conditions in hand, first, we investigated the scope of this transformation with different *o*-hydroxyphenyl enaminones **1b-m** and 2-(2-enynyl)pyridine **60a**. A wide range of *o*-hydroxyphenyl enaminones containing different substituents on the phenyl ring were well tolerated, and the corresponding products **61b-m** were isolated in good to excellent yields (Table 2). The reaction worked well with enaminone-substituted with electron-donating groups (**1b-e**), and their respective products **61b-e** were isolated in excellent yield (93-97%). Halo-substituted enaminones **1f-k** also reacted efficiently with **60a**, and their respective products **61f-k** were obtained in the range of 81-93% isolated yield. *o*-Hydroxyphenyl enaminone **1l**, substituted with an electron-withdrawing (5-NO₂) group also

Table 3. Substrate Scope^b

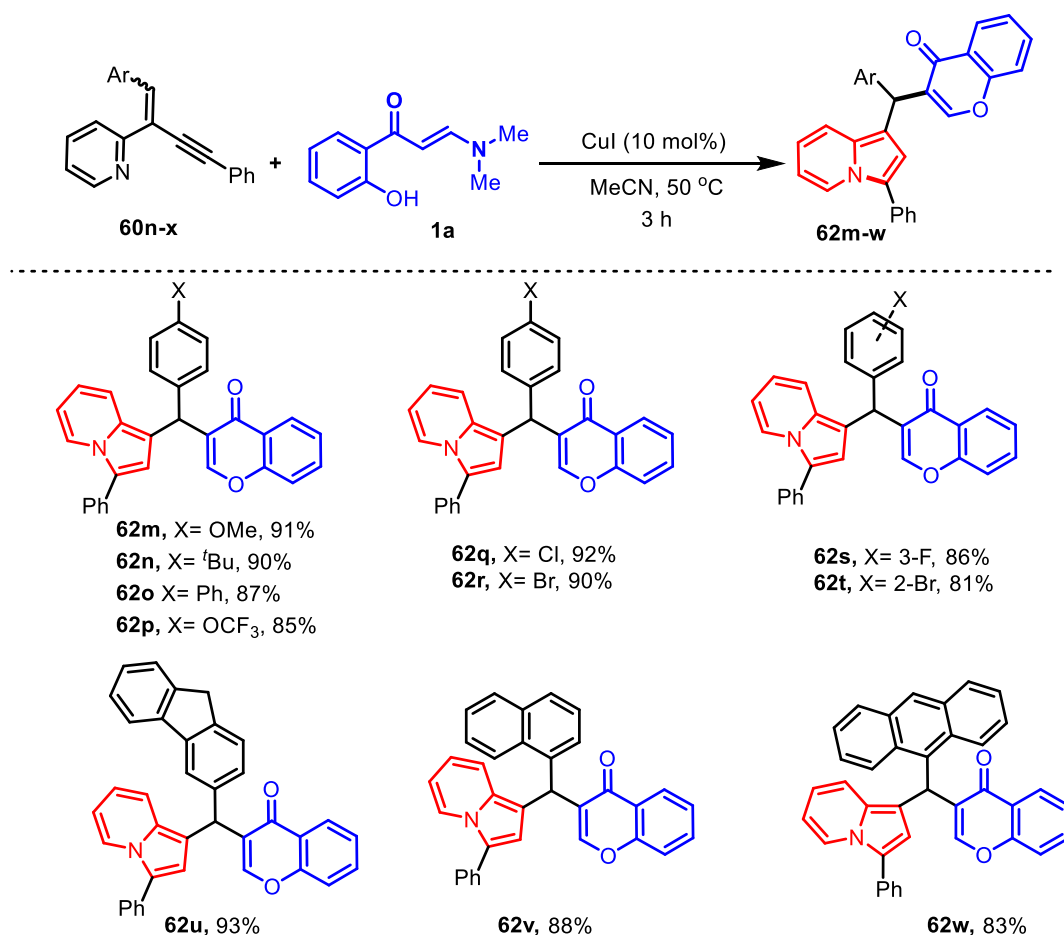


^aReactions were carried out with 40 mg of **60b-m** and 1.2 equiv. of **1a** in 1.5 mL of MeCN. ^bYields reported are isolated yields.

reacted smoothly, affording the corresponding product **61l** in 79% yield. The reaction of **60a** with a bulky naphthalene-based *o*-hydroxyphenyl enaminone **1m** afforded the product **61m** in 87% yield.

Next, we evaluated the substrate scope of this protocol with 2-(2-enynyl)pyridines **60b–m** having different aryl substituents (both electron-rich and electron-poor) at the alkyne part and, in all those cases, the expected products **62a–l** were obtained in the range of 78–96% yield. 2-(2-enynyl)pyridines **60k–m**, substituted with alicyclic compounds (such as cyclopropyl, cyclopentyl, and cyclohexyl), were also found to be suitable for this reaction, and the respective products **62j–l** were obtained in 79–87% isolated yields under optimized reaction conditions (table 3). Then, we went on to investigate the substrate scope with other 2-(2-enynyl)pyridines **60n–v**, having different aryl substituents (such as Me, OMe, halo, etc.) at

Table 4. Substrate Scope^b

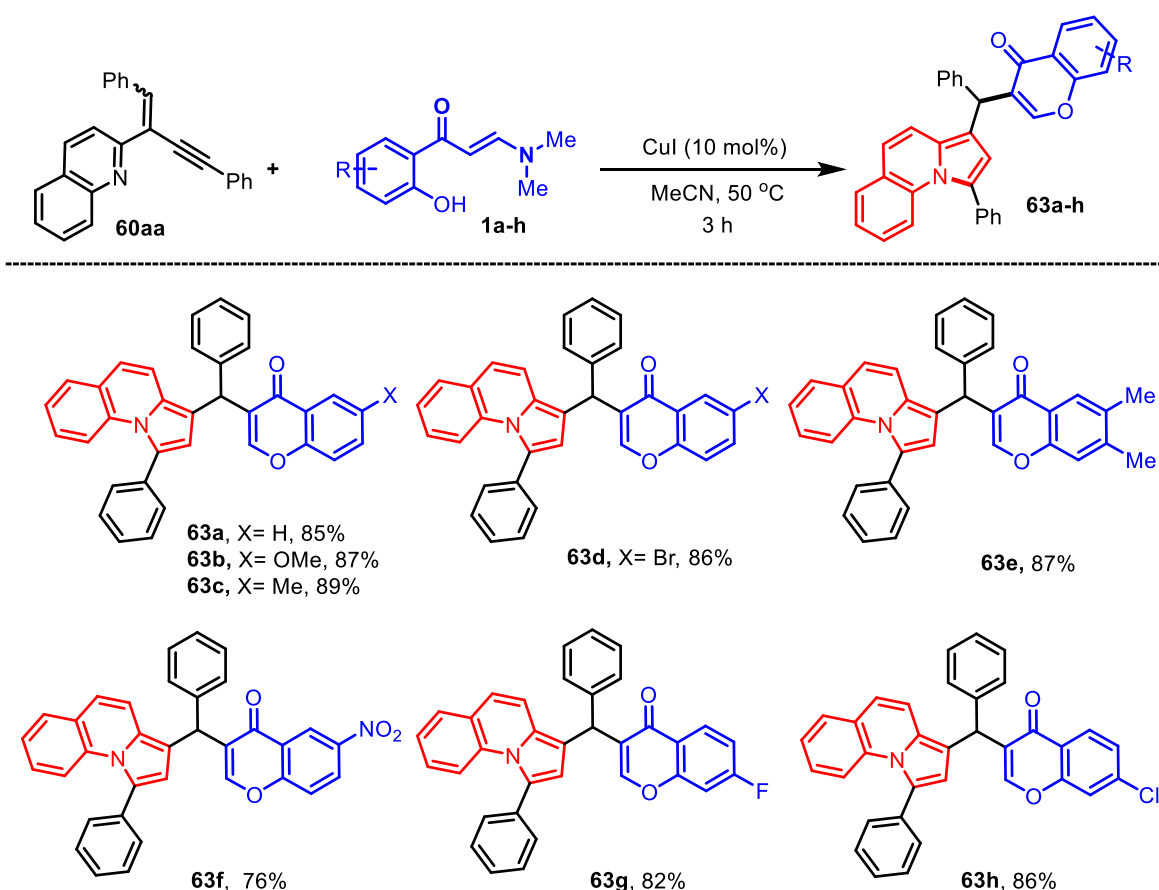


^aReactions were carried out with 40 mg of **60n-x** and 1.2 equiv. of **1a** in 1.5 mL of MeCN. ^bYields reported are isolated yields.

the alkene part. To our delight, in all those cases, the expected products **62m–t** were formed in the range of 81–92% yields. The reaction with fluorene based 2-(2-enynyl)pyridine provided the desired product **62u** in 93% yield. 2-(2-enynyl)pyridine **60w** & **60x**, containing electronically bulky substituents like naphthalene and anthracene at the alkene part, also reacted smoothly to generate the products **62v** & **62w** in 88% and 83% yield, respectively (table 4).

The reaction also worked well with 2-(2-enynyl)pyridine **60aa** derived from quinoline-2-carboxylic acid. Differently substituted *o*-hydroxyphenyl enaminones were subjected to react with **60aa** under the optimized reaction conditions, and the corresponding products **63a–h** were obtained in 76–89% yields (table 5).

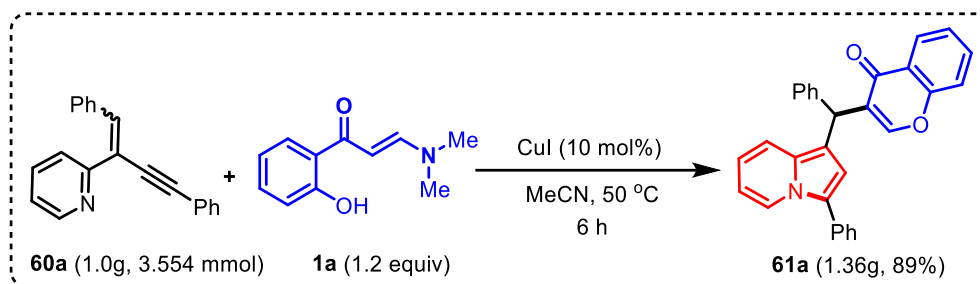
Table 5. Substrate Scope^b



^aReactions were carried out with 40 mg of **1aa** and 1.2 equiv. of **1a–h** in 1.5 mL of MeCN . ^bYields reported are isolated yields.

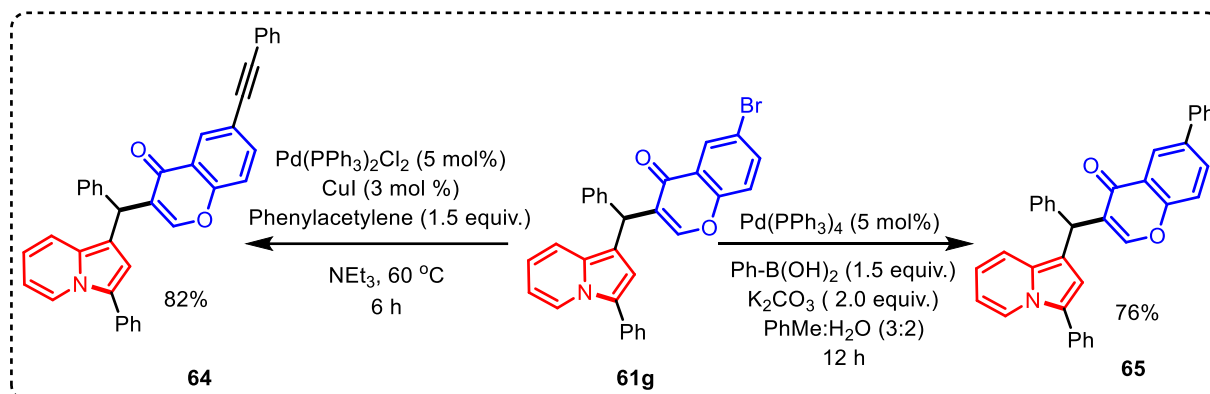
To show the practical applicability of this transformation, a gram-scale reaction of **60a** with **1a** was performed under the standard reaction conditions. The desired product was

obtained in 89% yield after 6 hours, indicating that this transformation has the potential feasibility for practical applications (Scheme 22).



Scheme 22. Gram Scale Reaction of **61a**

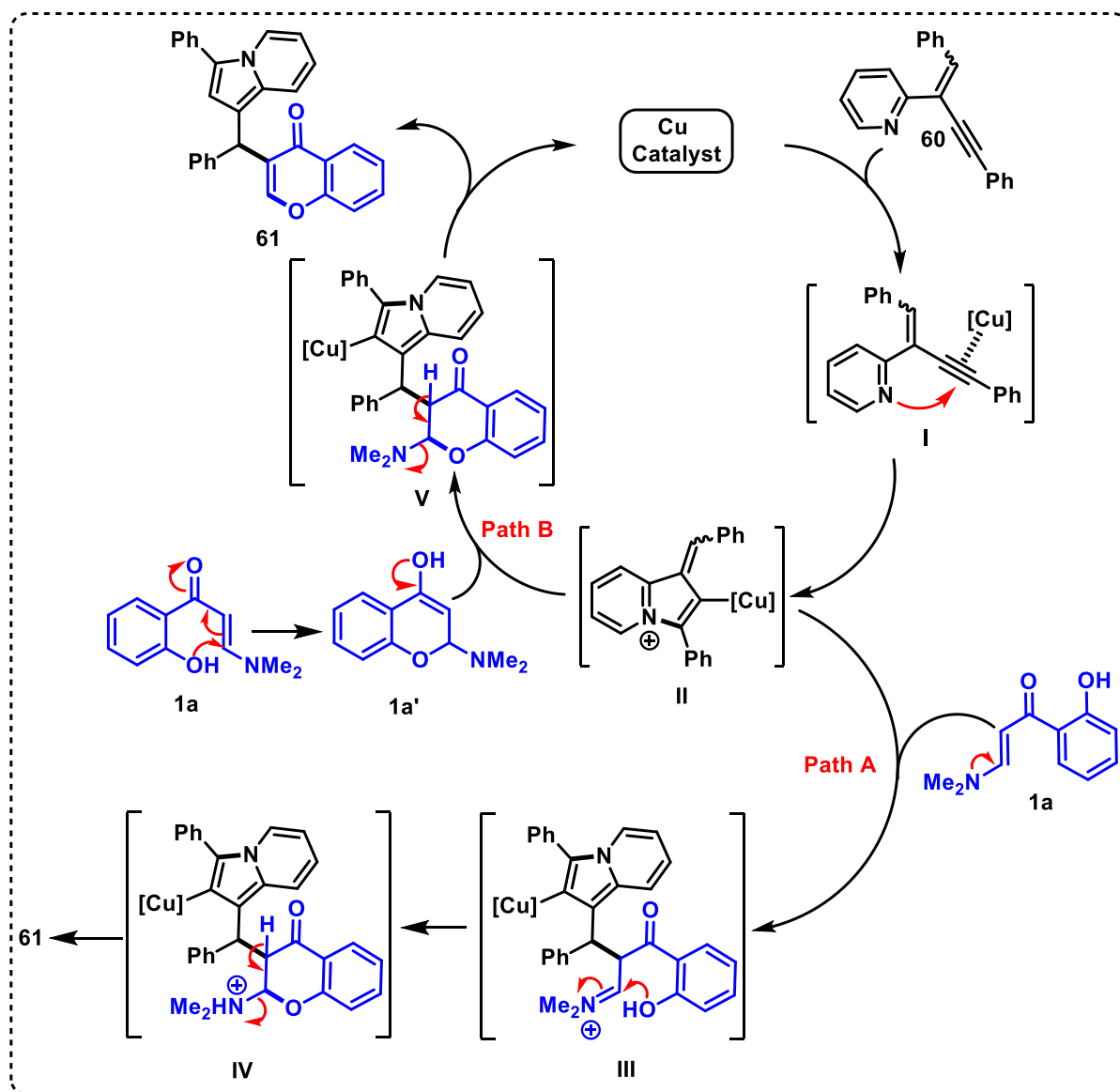
In general, converting products containing a Br group into valuable compounds is very easy, so to further demonstrate the synthetic potential of this protocol, compound **61g** was reacted with phenylacetylene under Sonogashira coupling reaction conditions, and the alkynylated product **64** was obtained in 82% yield (Scheme 23a). In another experiment, **61g** was subjected to react with phenyl boronic acid under Suzuki coupling reaction conditions, and the arylated product **65** was isolated in 76% yield after 12 hours (Scheme 23b).



Scheme 23. Synthetic elaboration of compound **61g**

Based on previous literature reports involving *o*-hydroxyaryl enaminones, a plausible mechanism for this transformation was proposed (Scheme 24). Initially, CuI activates the alkyne of the 2-(2-enynyl) pyridine (**60**) to generate the intermediate **I**, followed by the 5-*endo*-dig cyclization to produce the indozolinium salt **II**. Then, the nucleophilic α -C of the *o*-hydroxyphenyl enaminone **1a** attacks the electrophilic exocyclic double bond of the intermediate **II**, leading to the formation of intermediate **III**, which upon intramolecular cyclization produces **IV**. Finally, **IV** upon protonation and a β -elimination of NHMe₂, generates the desired product **61** (path A). Alternatively, *o*-hydroxyphenyl enaminone **1a** first undergoes

intramolecular cyclization to give the enolate **1a'**, which attacks the intermediate **II** to produce **V**. Finally, **V** undergoes the elimination of NHMe_2 and protonation leads to the formation of the product (path B).



Scheme 24. Plausible Mechanism

The structure of **61a** was confirmed from ^1H NMR, ^{13}C NMR, IR spectroscopy and mass spectrometry. In ^1H NMR (see figure 3) the presence of singlet of (1H) at δ 5.93 ppm due to benzylic $-\text{CH}$ marked as (a), singlet of (1H) at δ 6.76 ppm due to the single proton present at C-2 position of indolizine ring marked as (b) and the singlet of (1H) at δ 7.94 ppm due to the single protons present at β -carbon of chromone ring marked as (c). In ^{13}C NMR (see figure 4) the disappearance of alkyne peak from **60a**, and the aliphatic peak observed at δ 37.8 ppm for the methyl carbon marked as (a), the appearance of carbonyl peak at δ 175.6 ppm for carbonyl

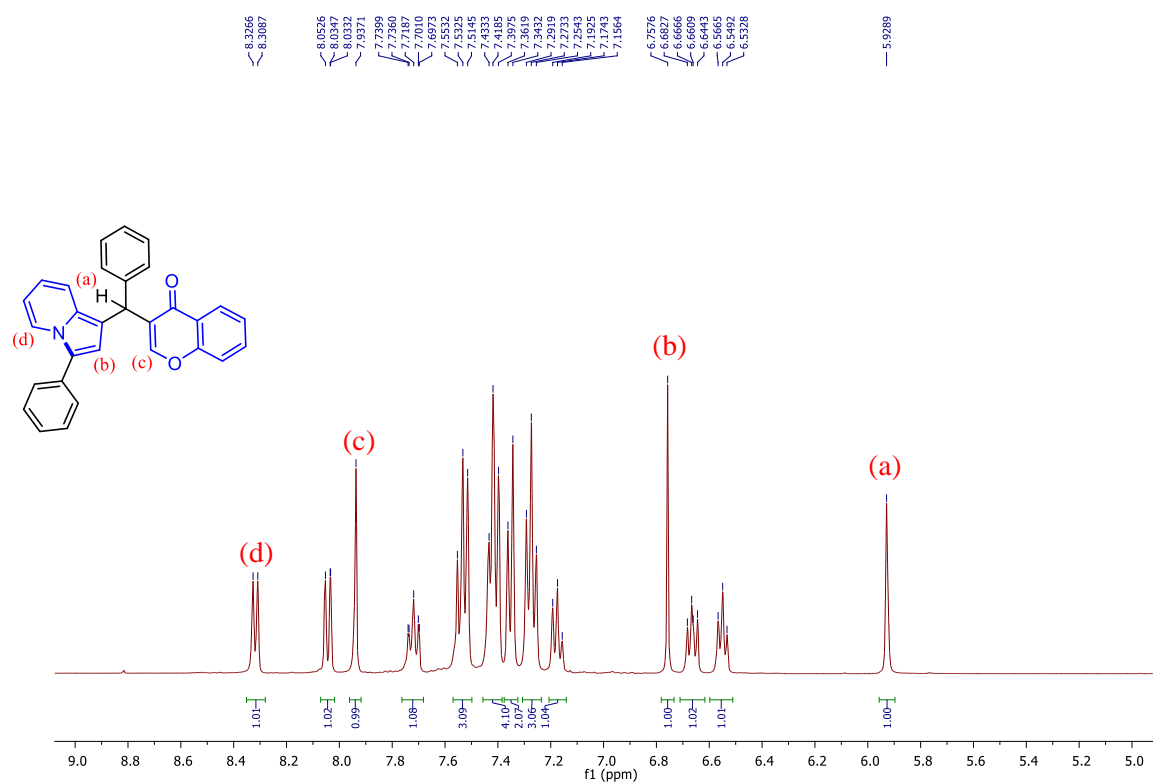


Figure 3: ¹H NMR (400 MHz, CDCl₃) spectrum of **61a**

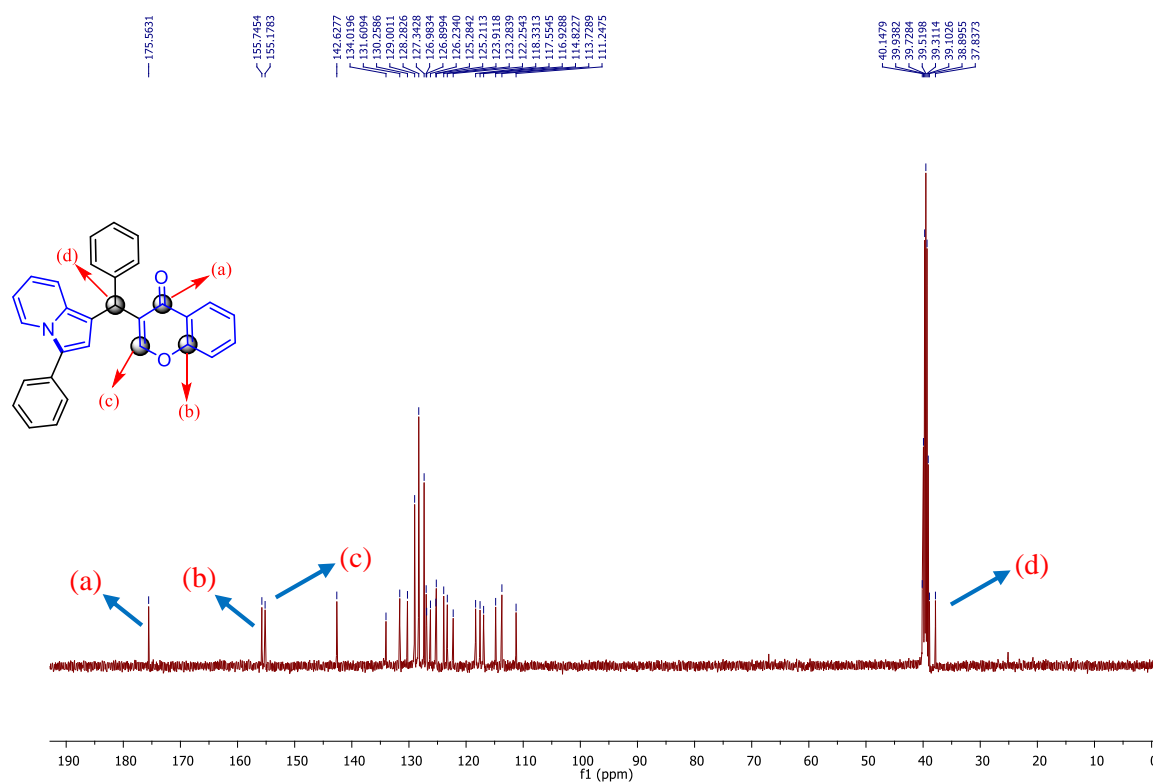


Figure 4: ¹³C{¹H} NMR (100 MHz, CDCl₃) spectrum of **42a**

carbon of chromone marked as (a) and the disappearance of -N(Me)₂ peak from **1a** also supported the formation of **61a**. Further in IR peak observed at 1642 cm⁻¹ supported the presence of carbonyl carbon in product **61a**. Further the formation of **61a** was also confirmed by the HRMS (ESI): *m/z* calcd for C₃₀H₂₂NO₂ [M+H]⁺ : 428.1651; found : 428.1637.

2.5 conclusion:

In conclusion, we have developed an efficient copper-catalyzed protocol for synthesizing indolizine and chromone containing unsymmetrical triarylmethane derivatives. This transformation proceeds through an initial Cu-catalyzed 5-*endo*-dig cyclization of 2-(2-enynyl) pyridines followed by a domino C-H alkylation and chromone annulation of the *o*-hydroxyarylenaminones, which provides a straightforward route to access unsymmetrical triarylmethanes enabling the installation of indolizine and chromone rings in the same compound. The generality of this transformation was examined using a wide range of 2-(2-enynyl) pyridines and *o*-hydroxyphenylenaminones, and a gram-scale reaction was also conducted to show the practical applicability of this transformation.

2.6 Experimental Section:

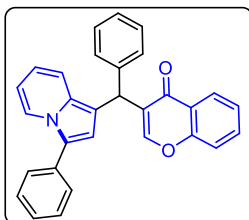
General information: All reactions were carried out in an oven dried round bottom flask. All the solvents were distilled before use and stored under argon atmosphere. Most of the reagents, starting materials were purchased from commercial sources and used as such. Melting points were recorded on SMP20 melting point apparatus and are uncorrected. ¹H, ¹³C and ¹⁹F spectra were recorded in CDCl₃ (400, 100 and 376 MHz respectively) on Bruker FT-NMR spectrometer. Chemical shift (δ) values are reported in parts per million relative to TMS and the coupling constants (*J*) are reported in Hz. High resolution mass spectra were recorded on Waters Q-TOF Premier-HAB213 spectrometer. FT-IR spectra were recorded on a Perkin-Elmer FTIR spectrometer. Thin layer chromatography was performed on Merck silica gel 60 F₂₅₄ TLC pellets and visualised by UV irradiation and KMnO₄ stain. Column chromatography was carried out through silica gel (100–200 mesh) using EtOAc/hexane as an eluent.

General procedure for addition of *o*-hydroxyphenylenaminones to 2-(2-enynyl)pyridines

Anhydrous MeCN (1.5 mL) was added to the mixture of 2-(2-enynyl)pyridine (40 mg, 1.0 equiv.), *o*-hydroxyphenyl enaminone (1.2 equiv.) and CuI (10 mol %) under nitrogen atmosphere and the resulting suspension was stirred at 50 °C until the 2-(2-enynyl)pyridine was completely consumed (based on TLC analysis). The reaction mixture was concentrated under

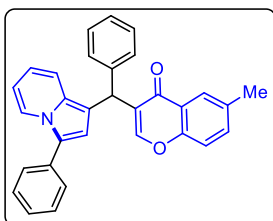
reduced pressure and the residue was purified through a silica gel chromatography, using EtOAc/Hexane mixture as an eluent, to get the pure indolizine and chromone based triarylmethanes.

3-(phenyl(3-phenylindolizin-1-yl)methyl)-4H-chromen-4-one (61a)



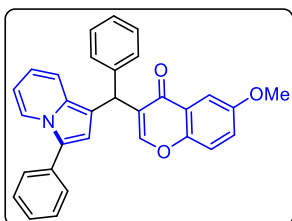
The reaction was performed at 0.1422 mmol scale of **60a**; $R_f = 0.4$ (20% EtOAc in hexane); brown solid (59.7 mg, 98% yield); M.P. 118–120 °C; ^1H NMR (400 MHz, DMSO- d_6) δ 8.32 (d, $J = 7.2$ Hz, 1H), 8.05 – 8.03 (m, 1H), 7.94 (s, 1H), 7.74 – 7.70 (m, 1H), 7.56 – 7.51 (m, 3H), 7.43 – 7.40 (m, 4H), 7.36 – 7.34 (m, 2H), 7.29 – 7.25 (m, 3H), 7.19 – 7.16 (m, 1H), 6.76 (s, 1H), 6.68 – 6.64 (m, 1H), 6.57 – 6.53 (m, 1H), 5.93 (s, 1H); $^{13}\text{C}\{^1\text{H}\}$ NMR (100 MHz, DMSO- d_6) δ 175.6, 155.7, 155.2, 142.6, 134.0, 131.6, 130.3, 129.0, 128.3, 127.3, 127.0, 126.9, 126.2, 125.3, 125.2, 123.9, 123.3, 122.3, 118.3, 117.6, 116.9, 114.8, 113.7, 111.2, 37.8; FT-IR (thin film, neat): 3060, 2926, 1642, 1609, 1465, 1348, 1242, 1141, 1034, 836 cm^{-1} ; HRMS (ESI): m/z calcd for $\text{C}_{30}\text{H}_{22}\text{NO}_2$ $[\text{M}+\text{H}]^+$: 428.1651; found : 428.1637.

6-methyl-3-(phenyl(3-phenylindolizin-1-yl)methyl)-4H-chromen-4-one (61b)



The reaction was performed at 0.1422 mmol scale of **60a**; $R_f = 0.4$ (20% EtOAc in hexane); brown solid (60.4 mg, 96% yield); M.P. 126–128 °C; ^1H NMR (400 MHz, DMSO- d_6) δ 8.33 (d, $J = 6.8$ Hz, 1H), 7.92 (s, 1H), 7.82 (s, 1H), 7.55 – 7.53 (m, 3H), 7.48 – 7.39 (m, 4H), 7.35 – 7.28 (m, 5H), 7.20 – 7.18 (m, 1H), 6.74 (s, 1H), 6.70 – 6.66 (m, 1H), 6.58 – 6.57 (m, 1H), 5.91 (s, 1H), 2.37 (s, 3H); $^{13}\text{C}\{^1\text{H}\}$ NMR (100 MHz, DMSO- d_6) δ 175.5, 155.1, 154.0, 142.7, 135.1, 134.8, 131.6, 130.3, 129.0, 128.3, 128.2, 127.3, 126.9, 126.8, 126.2, 124.4, 123.9, 123.0, 122.3, 118.1, 117.6, 116.9, 114.8, 113.9, 111.3, 37.8, 20.5; FT-IR (thin film, neat): 3062, 2926, 1640, 1467, 1392, 873 cm^{-1} ; HRMS (ESI): m/z calcd for $\text{C}_{31}\text{H}_{24}\text{NO}_2$ $[\text{M}+\text{H}]^+$: 442.1807; found : 442.1787.

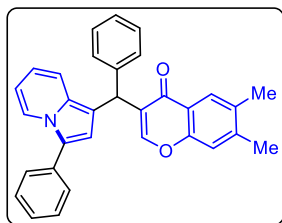
6-methoxy-3-(phenyl(3-phenylindolizin-1-yl)methyl)-4H-chromen-4-one (61c)



The reaction was performed at 0.1422 mmol scale of **60a**; $R_f = 0.3$ (20% EtOAc in hexane); pale yellow solid (63.2 mg, 97% yield); M.P. 128–130 °C; ^1H NMR (400 MHz, DMSO- d_6) δ 8.33 (d, $J = 7.2$ Hz, 1H), 7.94 (s, 1H), 7.55 – 7.52 (m, 3H), 7.45 – 7.40 (m, 4H), 7.36 – 7.32 (m, 3H), 7.31 – 7.26 (m, 3H), 7.20 – 7.16 (m, 1H), 6.76 (s, 1H), 6.70 – 6.66 (m, 1H), 6.58 – 6.55 (m, 1H), 5.92 (s, 1H), 3.79 (s, 3H); $^{13}\text{C}\{^1\text{H}\}$ NMR (100 MHz,

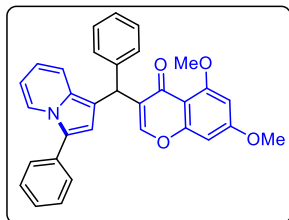
DMSO- d_6) δ 175.3, 156.4, 154.9, 150.5, 142.7, 131.6, 130.3, 129.0, 128.3, 127.4, 126.9, 126.2 (2C), 123.9 (2C), 123.3, 122.3, 119.9, 117.6, 117.5, 117.0, 114.9, 113.8, 111.3, 104.8, 55.6, 37.9; FT-IR (thin film, neat): 3058, 2924, 1639, 1585, 1484, 1220, 1029 cm^{-1} ; HRMS (ESI): m/z calcd for $\text{C}_{31}\text{H}_{24}\text{NO}_3$ $[\text{M}+\text{H}]^+$: 458.1756; found : 458.1743.

6,7-dimethyl-3-(phenyl(3-phenylindolizin-1-yl)methyl)-4H-chromen-4-one (61d)



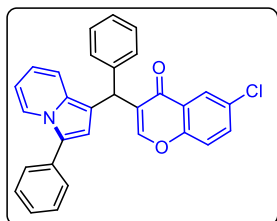
The reaction was performed at 0.1422 mmol scale of **60a**; R_f = 0.4 (20% EtOAc in hexane); pale yellow solid (61.8 mg, 95% yield); M.P. 134–136 °C; ^1H NMR (400 MHz, DMSO- d_6) δ 8.32 (d, J = 7.2 Hz, 1H), 7.86 (d, J = 0.6 Hz, 1H), 7.75 (s, 1H), 7.54 – 7.53 (m, 2H), 7.44 – 7.38 (m, 3H), 7.34 – 7.32 (m, 3H), 7.30 – 7.25 (m, 3H), 7.19 – 7.15 (m, 1H), 6.74 (s, 1H), 6.68 – 6.64 (m, 1H), 6.57 – 6.53 (m, 1H), 5.91 (s, 1H), 2.28 (s, 3H), 2.25 (s, 3H); $^{13}\text{C}\{^1\text{H}\}$ NMR (100 MHz, DMSO- d_6) δ 175.3, 154.7, 154.3, 144.2, 142.8, 134.3, 131.6, 130.2, 129.0, 128.27, 128.26, 127.3, 127.1, 126.9, 126.7, 126.2, 124.6, 123.9, 122.3, 121.2, 118.1, 117.6, 116.9, 114.8, 114.0, 111.2, 37.8, 19.8, 18.9; FT-IR (thin film, neat): 3056, 2934, 1748, 1524, 1284, 1156, 1037, 860, 712 cm^{-1} ; HRMS (ESI): m/z calcd for $\text{C}_{32}\text{H}_{26}\text{NO}_2$ $[\text{M}+\text{H}]^+$: 456.1964; found : 456.1966.

5,7-dimethoxy-3-(phenyl(3-phenylindolizin-1-yl)methyl)-4H-chromen-4-one (61e)



The reaction was performed at 0.1422 mmol scale of **60a**; R_f = 0.3 (20% EtOAc in hexane); pale yellow solid (64.6 mg, 93% yield); M.P. 138–140 °C; ^1H NMR (400 MHz, CDCl_3) δ 8.24 (d, J = 7.2 Hz, 1H), 7.53 – 7.51 (m, 2H), 7.44 – 7.40 (m, 3H), 7.36 – 7.33 (m, 3H), 7.28 (t, J = 7.4 Hz, 3H), 7.21 – 7.17 (m, 1H), 6.62 – 6.58 (m, 1H), 6.55 (s, 1H), 6.46 – 6.43 (m, 1H), 6.38 (d, J = 2.3 Hz, 1H), 6.33 (d, J = 2.3 Hz, 1H), 6.03 (s, 1H), 3.89 (s, 3H), 3.85 (s, 3H); $^{13}\text{C}\{^1\text{H}\}$ NMR (100 MHz, CDCl_3) δ 175.6, 163.9, 161.3, 160.1, 152.7, 142.8, 132.5, 130.7, 129.1, 129.0, 128.7, 128.5, 127.9, 127.0, 126.4, 124.4, 122.2, 118.2, 116.6, 115.1, 114.3, 111.0, 109.5, 96.0, 92.5, 56.3, 55.8, 38.1; FT-IR (thin film, neat): 3064, 2927, 1736, 1601, 1255, 1032, 864, 749 cm^{-1} ; HRMS (ESI): m/z calcd for $\text{C}_{32}\text{H}_{26}\text{NO}_4$ $[\text{M}+\text{H}]^+$: 488.1862; found : 488.1852.

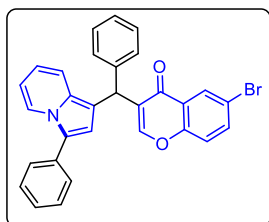
6-chloro-3-(phenyl(3-phenylindolizin-1-yl)methyl)-4H-chromen-4-one (61f)



The reaction was performed at 0.1422 mmol scale of **60a**; R_f = 0.4 (20% EtOAc in hexane); pale yellow solid (59.8 mg, 91% yield); M.P. 126–128 °C; ^1H NMR (400 MHz, DMSO- d_6) δ 8.31 (s, 1H), 7.94 (s, 2H), 7.72 – 7.70 (m, 1H), 7.61 – 7.51 (m, 3H), 7.41 – 7.40 (m, 3H), 7.35 – 7.33 (m, 2H), 7.27 (s, 3H), 7.17 (s, 1H), 6.76 (s, 1H), 6.67 – 6.65

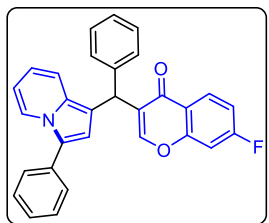
(m, 1H), 6.54 (d, $J = 5.0$ Hz 1H), 5.90 (s, 1H); $^{13}\text{C}\{^1\text{H}\}$ NMR (100 MHz, DMSO- d_6) δ 174.5, 155.4, 154.3, 142.4, 133.9, 131.6, 130.3, 129.8, 129.0, 128.3, 127.3, 127.0, 126.9, 126.3, 124.3, 124.2, 123.9, 122.2, 120.84, 120.78, 117.5, 116.9, 114.8, 113.5, 111.2, 37.9 ; FT-IR (thin film, neat): 3056, 2921, 1724, 1612, 1554, 1262, 1176, 824, 742 cm^{-1} ; HRMS (ESI): m/z calcd for $\text{C}_{30}\text{H}_{21}\text{ClNO}_2$ $[\text{M}+\text{H}]^+$: 462.1261; found : 462.1247.

6-bromo-3-(phenyl(3-phenylindolizin-1-yl)methyl)-4H-chromen-4-one (61g)



The reaction was performed at 0.1422 mmol scale of **60a**; $R_f = 0.4$ (20% EtOAc in hexane); pale yellow solid (67.1 mg, 93% yield); m.p. = 136–138 $^{\circ}\text{C}$; ^1H NMR (400 MHz, DMSO- d_6) δ 8.33 (d, $J = 6.8$ Hz, 1H), 8.09 (d, $J = 2.4$ Hz, 1H), 7.98 (s, 1H), 7.91 – 7.87 (m, 1H), 7.59 – 7.53 (m, 3H), 7.45 – 7.40 (m, 3H), 7.35 – 7.26 (m, 5H), 7.19 (t, $J = 7.1$ Hz, 1H), 6.76 (s, 1H), 6.68 (t, $J = 7.8$ Hz, 1H), 6.57 (t, $J = 6.8$ Hz, 1H), 5.89 (s, 1H); $^{13}\text{C}\{^1\text{H}\}$ NMR (100 MHz, DMSO- d_6) δ 174.4, 155.5, 154.7, 142.4, 136.6, 131.6, 130.3, 129.0, 128.30, 128.26, 127.34, 127.30, 127.1, 126.9, 126.3, 124.7, 123.9, 122.3, 121.1, 117.7, 117.5, 117.0, 114.8, 113.5, 111.3, 37.9; FT-IR (thin film, neat): 3062, 2943, 1732, 1521, 1467, 1176, 1037, 842, 738 cm^{-1} ; HRMS (ESI): m/z calcd for $\text{C}_{30}\text{H}_{21}\text{BrNO}_2$ $[\text{M}+\text{H}]^+$: 506.0756; found : 506.0753.

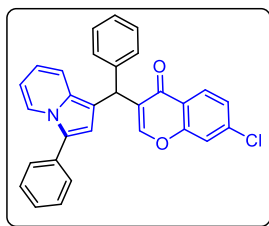
7-fluoro-3-(phenyl(3-phenylindolizin-1-yl)methyl)-4H-chromen-4-one (61h)



The reaction was performed at 0.1422 mmol scale of **60a**; $R_f = 0.4$ (20% EtOAc in hexane); pale yellow semi-solid (53.2 mg, 84% yield); ^1H NMR (400 MHz, DMSO- d_6) δ 8.32 (d, $J = 7.1$ Hz, 1H), 8.11 – 8.07 (m, 1H), 7.95 (s, 1H), 7.54 – 7.52 (m, 3H), 7.45 – 7.40 (m, 3H), 7.36 – 7.26 (m, 6H), 7.20 – 7.16 (m, 1H), 6.76 (s, 1H), 6.70 – 6.66 (m, 1H), 6.56 (t, $J = 6.8$ Hz, 1H), 5.90 (s, 1H); $^{13}\text{C}\{^1\text{H}\}$ NMR (100 MHz, DMSO- d_6) δ 174.8, 166.2, 163.7, 156.8 (d, $J = 13.9$ Hz), 155.4, 142.5, 131.6, 130.3, 129.0, 128.3 (d, $J = 4.4$ Hz), 128.1 (d, $J = 11.0$ Hz), 127.4, 127.1, 126.6 (d, $J = 64.7$ Hz), 123.9, 122.3, 120.5 (d, $J = 2.0$ Hz), 117.3 (d, $J = 57.5$ Hz), 114.8, 114.1, 114.0, 113.6, 111.3, 105.0 (d, $J = 25.5$ Hz), 104.9, 37.8; $^{19}\text{F}\{^1\text{H}\}$ NMR (376 MHz, CDCl_3) δ -103.7; FT-IR (thin film, neat): 3067, 2928, 1746, 1614, 1318, 1259, 1036, 858, 748 cm^{-1} ; HRMS (ESI): m/z calcd for $\text{C}_{30}\text{H}_{21}\text{FNO}_2$ $[\text{M}+\text{H}]^+$: 446.1556; found : 446.1551.

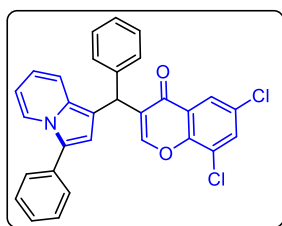
7-chloro-3-(phenyl(3-phenylindolizin-1-yl)methyl)-4H-chromen-4-one (61i)

The reaction was performed at 0.1422 mmol scale of **60a**; $R_f = 0.4$ (20% EtOAc in hexane); pale yellow solid (57.3 mg, 87% yield); M.P. 124–126 $^{\circ}\text{C}$; ^1H NMR (400 MHz, DMSO- d_6) δ 8.31 (d, $J = 7.2$ Hz, 1H), 8.00 (d, $J = 8.6$ Hz, 1H), 7.92 (s, 1H), 7.72 (s, 1H), 7.53 – 7.51 (m, 2H), 7.46 – 7.39 (m, 4H), 7.35 – 7.33 (m, 2H), 7.27 (t, $J = 7.4$ Hz, 3H), 7.17 (t, $J = 7.2$ Hz,



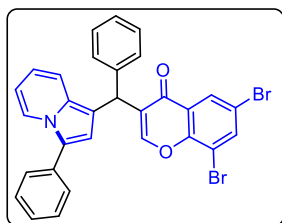
1H), 6.76 (s, 1H), 6.66 (t, $J = 6.7$ Hz, 1H), 6.55 (t, $J = 6.9$ Hz, 1H), 5.89 (s, 1H); $^{13}\text{C}\{^1\text{H}\}$ NMR (100 MHz, DMSO- d_6) δ 174.9, 155.9, 155.3, 142.4, 138.4, 131.6, 130.3, 129.0, 128.3, 128.2, 127.3, 127.1, 126.9, 126.3, 125.8, 123.9, 122.2, 122.1, 118.2, 117.5, 116.9, 114.80, 114.79, 113.5, 111.2, 37.8; FT-IR (thin film, neat): 3062, 2915, 1725, 1624, 1432, 1267, 742 cm^{-1} ; HRMS (ESI): m/z calcd for $\text{C}_{30}\text{H}_{21}\text{ClNO}_2$ $[\text{M}+\text{H}]^+$: 462.1261; found : 462.1248.

6,8-dichloro-3-(phenyl(3-phenylindolizin-1-yl)methyl)-4H-chromen-4-one (61j)



The reaction was performed at 0.1422 mmol scale of **60a**; $R_f = 0.4$ (20% EtOAc in hexane); pale yellow semi-solid (58.6 mg, 83% yield); ^1H NMR (400 MHz, CDCl_3) δ 8.26 (d, $J = 7.2$ Hz, 1H), 8.09 (s, 1H), 7.70 (s, 2H), 7.53 – 7.51 (m, 2H), 7.43 (t, $J = 7.6$ Hz, 2H), 7.36 – 7.30 (m, 6H), 7.24 – 7.22 (m, 1H), 6.65 (t, $J = 7.5$ Hz, 1H), 6.55 (s, 1H), 6.49 (t, $J = 6.9$ Hz, 1H), 6.01 (s, 1H); $^{13}\text{C}\{^1\text{H}\}$ NMR (100 MHz, CDCl_3) δ 175.2, 155.2, 150.8, 141.7, 133.7, 132.3, 130.7, 130.6, 129.0, 128.7, 128.6, 128.5, 128.0, 127.2, 126.8, 125.8, 124.8, 124.4, 124.3, 117.8, 117.1, 114.9, 112.9, 111.1, 38.7; FT-IR (thin film, neat): 3055, 2928, 1756, 1615, 1486, 1262, 1037, 842, 752 cm^{-1} ; HRMS (ESI): m/z calcd for $\text{C}_{30}\text{H}_{20}\text{Cl}_2\text{NO}_2$ $[\text{M}+\text{H}]^+$: 496.0871; found : 496.0876.

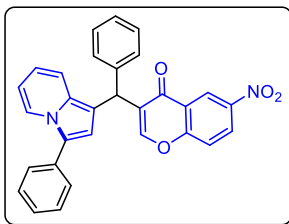
6,8-dibromo-3-(phenyl(3-phenylindolizin-1-yl)methyl)-4H-chromen-4-one (61k)



The reaction was performed at 0.1422 mmol scale of **60a**; $R_f = 0.4$ (20% EtOAc in hexane); pale yellow solid (67.6 mg, 81% yield); m.p. = 138 – 140 $^\circ\text{C}$; ^1H NMR (400 MHz, DMSO- d_6) δ 8.33 (d, $J = 7.2$ Hz, 1H), 8.28 (d, $J = 1.9$ Hz, 1H), 8.05 (s, 2H), 7.55 (d, $J = 7.8$ Hz, 1H), 7.45 – 7.41 (m, 3H), 7.36 – 7.34 (m, 2H), 7.32 – 7.26 (m, 3H), 7.21 – 7.17 (m, 1H), 6.78 (s, 1H), 6.71 – 6.67 (m, 1H), 6.58 (t, $J = 6.8$ Hz, 1H), 5.86 (s, 1H); $^{13}\text{C}\{^1\text{H}\}$ NMR (100 MHz, DMSO- d_6) δ 174.0, 155.6, 151.6, 142.1, 138.8, 131.6, 130.3, 129.0, 128.3, 128.2, 127.4, 127.3, 127.1, 126.9, 126.3, 125.5, 124.0, 122.3, 117.6, 117.5, 117.0, 114.8, 113.2, 113.0, 111.3, 37.9; FT-IR (thin film, neat): 3052, 2964, 1760, 1614, 1424, 1242, 874, 732 cm^{-1} ; HRMS (ESI): m/z calcd for $\text{C}_{30}\text{H}_{20}\text{Br}_2\text{NO}_2$ $[\text{M}+\text{H}]^+$: 583.9861; found : 583.9857.

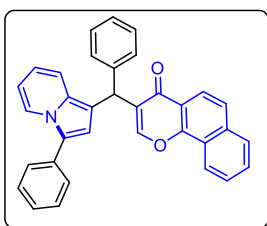
6-nitro-3-(phenyl(3-phenylindolizin-1-yl)methyl)-4H-chromen-4-one (61l)

The reaction was performed at 0.1422 mmol scale of **60a**; $R_f = 0.3$ (20% EtOAc in hexane); pale yellow solid (53.2 mg, 79% yield); m.p. = 140 – 142 $^\circ\text{C}$; ^1H NMR (400 MHz, CDCl_3) δ 9.09 (d, $J = 2.7$ Hz, 1H), 8.46 (dd, $J = 9.2, 2.7$ Hz, 1H), 8.27 (d, $J = 7.2$ Hz, 1H), 7.68 (s, 1H), 7.57 – 7.54 (m, 2H), 7.52 (s, 1H), 7.44 (t, $J = 7.6$ Hz, 2H), 7.38 – 7.31 (m, 6H), 7.29 – 7.24 (m,



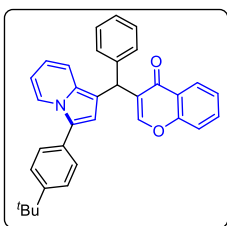
1H), 6.68 – 6.64 (m, 1H), 6.58 (s, 1H), 6.50 (t, $J = 6.7$ Hz, 1H), 6.04 (s, 1H); $^{13}\text{C}\{^1\text{H}\}$ NMR (100 MHz, CDCl_3) δ 175.6, 159.2, 155.3, 144.7, 141.6, 132.2, 130.7, 129.1, 129.0, 128.7, 128.5, 128.0, 127.8, 127.2, 126.9, 124.9, 124.0, 123.1, 122.5, 120.0, 117.8, 117.1, 114.8, 112.7, 111.2, 38.6; FT-IR (thin film, neat): 3058, 2956, 1714, 1525, 1432, 1240, 842, 745 cm^{-1} ; HRMS (ESI): m/z calcd for $\text{C}_{30}\text{H}_{21}\text{N}_2\text{O}_4$ $[\text{M}+\text{H}]^+$: 473.1501; found : 473.1506.

3-(phenyl(3-phenylindolizin-1-yl)methyl)-4H-benzo[h]chromen-4-one (61m)



The reaction was performed at 0.1422 mmol scale of **60a**; $R_f = 0.4$ (20% EtOAc in hexane); pale yellow semi-solid (59.2 mg, 87% yield); ^1H NMR (400 MHz, $\text{DMSO}-d_6$) δ 9.92 (d, $J = 8.6$ Hz, 1H), 8.34 (d, $J = 7.1$ Hz, 1H), 8.27 – 8.24 (m, 1H), 8.04 (d, $J = 8.0$ Hz, 1H), 7.99 – 7.98 (m, 1H), 7.72 – 7.69 (m, 1H), 7.65 – 7.60 (m, 2H), 7.54 (d, $J = 7.7$ Hz, 1H), 7.46 – 7.38 (m, 5H), 7.29 (t, $J = 7.4$ Hz, 3H), 7.19 (t, $J = 7.4$ Hz, 1H), 6.78 (s, 1H), 6.69 (t, $J = 6.8$ Hz, 1H), 6.58 (t, $J = 6.7$ Hz, 1H), 6.04 (s, 1H); $^{13}\text{C}\{^1\text{H}\}$ NMR (100 MHz, $\text{DMSO}-d_6$) δ 177.3, 157.1, 153.0, 142.8, 135.7, 131.6, 130.29, 130.27, 129.9, 129.6, 129.1, 129.0, 128.6, 128.3, 127.4, 126.9, 126.5, 126.2, 126.1, 123.9, 122.3, 118.0, 117.6, 117.0, 116.0, 114.8, 113.9, 111.3, 37.8; FT-IR (thin film, neat): 3057, 2924, 1762, 1436, 1257, 1156, 1037, 842, 684 cm^{-1} ; HRMS (ESI): m/z calcd for $\text{C}_{34}\text{H}_{24}\text{NO}_2$ $[\text{M}+\text{H}]^+$: 478.1807; found : 478.1812.

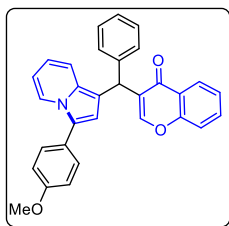
3-((3-(4-(tert-butyl)phenyl)indolizin-1-yl)(phenyl)methyl)-4H-chromen-4-one (62a)



The reaction was performed at 0.1185 mmol scale of **60b**; $R_f = 0.4$ (20% EtOAc in hexane); pale yellow gummy solid (52.4 mg, 91% yield); ^1H NMR (400 MHz, CDCl_3) δ 8.28 – 8.24 (m, 2H), 7.66 – 7.62 (m, 2H), 7.49 – 7.45 (m, 4H), 7.42 (d, $J = 8.4$ Hz, 1H), 7.40 – 7.37 (m, 3H), 7.34 (d, $J = 4.08$ Hz, 1H), 7.32 – 7.30 (m, 2H), 7.23 (t, $J = 7.2$ Hz, 1H), 6.64 – 7.60 (m, 1H), 6.55 (s, 1H), 6.49 – 6.45 (m, 1H), 6.07 (s, 1H), 1.37 (s, 9H); $^{13}\text{C}\{^1\text{H}\}$ NMR (100 MHz, CDCl_3) δ 176.9, 156.5, 155.1, 150.2, 142.5, 133.5, 130.5, 129.5, 128.6, 128.5, 127.6, 126.6, 126.3, 125.9, 125.0, 124.7, 124.1, 122.5, 118.1, 118.0, 116.6, 114.9, 113.5, 110.9, 38.6, 34.7, 31.4; FT-IR (thin film, neat): 3059, 2966, 1752, 1513, 1438, 1247, 842, 741 cm^{-1} ; HRMS (ESI): m/z calcd for $\text{C}_{34}\text{H}_{30}\text{NO}_2$ $[\text{M}+\text{H}]^+$: 484.2277; found : 484.2255.

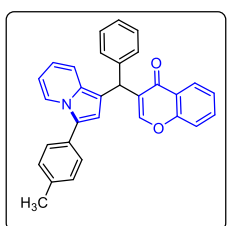
3-((3-(4-methoxyphenyl)indolizin-1-yl)(phenyl)methyl)-4H-chromen-4-one (62b)

The reaction was performed at 0.1285 mmol scale of **60c**; $R_f = 0.3$ (20% EtOAc in hexane); pale yellow semi-solid (52.1 mg, 88% yield); ^1H NMR (400 MHz, CDCl_3) δ 8.21 – 8.19 (m, 1H), 8.05 – 8.02 (m, 1H), 7.94 – 7.91 (m, 1H), 7.76 – 7.71 (m, 1H), 7.48 – 7.36 (m, 5H), 7.34



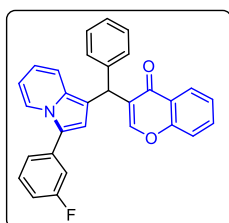
– 7.33 (m, 2H), 7.29 – 7.14 (m, 3H), 7.01 – 6.97 (m, 2H), 6.65 (s, 1H), 6.63 – 6.49 (m, 2H), 5.90 (s, 1H), 3.75 (s, 3H); $^{13}\text{C}\{^1\text{H}\}$ NMR (100 MHz, CDCl_3) δ 175.6, 158.4, 155.8, 155.2, 142.8, 134.3, 129.7, 129.1, 128.34, 128.31, 127.1, 126.3, 125.3, 125.0, 124.1, 123.9, 123.3, 122.2, 118.4, 117.5, 116.5, 114.5, 113.3, 112.3, 111.6, 55.2, 37.9; FT-IR (thin film, neat): 3058, 1757, 1624, 1436, 1264, 1142, 737, 632 cm^{-1} ; HRMS (ESI): m/z calcd for $\text{C}_{31}\text{H}_{24}\text{NO}_3$ $[\text{M}+\text{H}]^+$: 458.1756; found : 458.1742.

3-(phenyl(3-(p-tolyl)indolizin-1-yl)methyl)-4H-chromen-4-one (62c)



The reaction was performed at 0.1353 mmol scale of **60d**; R_f = 0.4 (20% EtOAc in hexane); pale yellow gummy solid (57.6 mg, 96% yield); ^1H NMR (400 MHz, DMSO-d_6) δ 8.28 (d, J = 7.0 Hz, 1H), 8.05 – 8.02 (m, 1H), 7.95 (s, 1H), 7.77 – 7.73 (m, 1H), 7.58 (d, J = 8.2 Hz, 1H), 7.46 – 7.38 (m, 4H), 7.35 – 7.33 (m, 2H), 7.29 – 7.23 (m, 4H), 7.20 – 7.16 (m, 1H), 6.71 (s, 1H), 6.68 – 6.64 (m, 1H), 6.55 (t, J = 6.5 Hz, 1H), 5.90 (s, 1H), 2.31 (s, 3H); $^{13}\text{C}\{^1\text{H}\}$ NMR (100 MHz, DMSO-d_6) δ 175.6, 155.8, 155.2, 142.7, 136.3, 134.1, 130.0, 129.6, 128.7, 128.3, 128.2, 127.4, 127.0, 126.2, 125.3, 125.2, 124.0, 123.3, 122.3, 118.4, 117.5, 116.7, 114.4, 113.6, 111.1, 37.8, 20.8; FT-IR (thin film, neat): 3064, 2921, 1764, 1514, 1235, 1037 cm^{-1} ; HRMS (ESI): m/z calcd for $\text{C}_{31}\text{H}_{24}\text{NO}_2$ $[\text{M}+\text{H}]^+$: 442.1807; found : 442.1803.

3-((3-(3-fluorophenyl)indolizin-1-yl)(phenyl)methyl)-4H-chromen-4-one (62d)

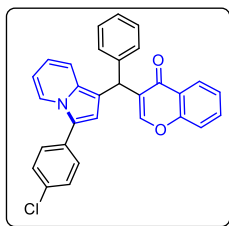


The reaction was performed at 0.1336 mmol scale of **60e**; R_f = 0.4 (20% EtOAc in hexane); pale yellow solid (50.2 mg, 84% yield); m.p. = 104 – 106 $^{\circ}\text{C}$; ^1H NMR (400 MHz, CDCl_3) δ 8.29 – 8.26 (m, 2H), 7.65 – 7.61 (m, 2H), 7.43 – 7.40 (m, 2H), 7.39 – 7.37 (m, 3H), 7.37 – 7.31 (m, 4H), 7.28 – 7.27 (m, 1H), 7.26 – 7.23 (m, 1H), 7.01 – 6.96 (m, 1H), 6.69 – 6.66

(m, 1H), 6.65 – 6.64 (m, 1H), 6.54 – 6.50 (m, 1H), 6.11 (s, 1H); $^{13}\text{C}\{^1\text{H}\}$ NMR (100 MHz, CDCl_3) δ 176.8, 163.1 (d, J = 244.6 Hz), 156.3, 155.0, 142.2, 134.4 (d, J = 8.3 Hz), 133.5, 131.1, 130.5 (d, J = 8.7 Hz), 128.5, 127.9, 126.6, 126.2, 125.0, 123.9, 123.3, 123.25, 123.20, 123.17, 122.2, 118.1, 118.0, 115.4 (d, J = 1.4 Hz), 114.4 (J = 21.9 Hz), 114.0, 113.7 (d, J = 21.0 Hz), 111.4, 38.5; $^{19}\text{F}\{^1\text{H}\}$ NMR (376 MHz, CDCl_3) δ –112.22; FT-IR (thin film, neat): 3062, 2934, 1622, 1434, 1262, 746 cm^{-1} ; HRMS (ESI): m/z calcd for $\text{C}_{30}\text{H}_{21}\text{FNO}_2$ $[\text{M}+\text{H}]^+$: 446.1556; found : 446.1548.

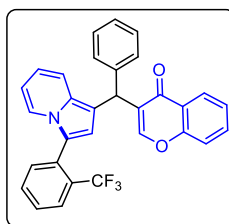
3-((3-(4-chlorophenyl)indolizin-1-yl)(phenyl)methyl)-4H-chromen-4-one (62e)

The reaction was performed at 0.1267 mmol scale of **60f**; R_f = 0.4 (20% EtOAc in hexane); pale yellow gummy solid (49.3 mg, 84% yield); ^1H NMR (400 MHz, DMSO-d_6) δ 8.33 – 8.30



(m, 1H), 8.04 – 8.02 (m, 1H), 7.95 – 7.93 (m, 1H), 7.78 – 7.72 (m, 1H), 7.60 – 7.53 (m, 3H), 7.48 – 7.41 (m, 4H), 7.35 – 7.33 (m, 2H), 7.30 – 7.25 (m, 2H), 7.20 – 7.16 (m, 1H), 6.78 (s, 1H), 6.73 – 6.67 (m, 1H), 6.61 – 6.56 (m, 1H), 5.90 (s, 1H); $^{13}\text{C}\{^1\text{H}\}$ NMR (100 MHz, DMSO- d_6) δ 175.6, 155.8, 155.3, 142.6, 134.1, 131.2, 130.6, 130.5, 129.0, 128.98, 128.8, 128.3, 126.9, 126.3, 125.4, 125.2, 123.3, 122.7, 122.4, 118.4, 117.6, 117.3, 115.2, 114.0, 111.6, 37.9; FT-IR (thin film, neat): 3062, 2974, 1742, 1467, 1258, 1037, 842 cm^{-1} ; HRMS (ESI): m/z calcd for $\text{C}_{30}\text{H}_{21}\text{ClNO}_2$ $[\text{M}+\text{H}]^+$: 462.1261; found : 462.1241.

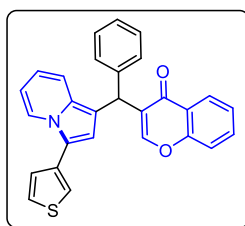
3-(phenyl(3-(2-(trifluoromethyl)phenyl)indolizin-1-yl)methyl)-4H-chromen-4-one (62f)



The reaction was performed at 0.1145 mmol scale of **60g**; R_f = 0.4 (20% EtOAc in hexane); pale yellow gummy solid (45.1 mg, 79% yield); ^1H NMR (400 MHz, DMSO- d_6) δ 8.04 (d, J = 7.9 Hz, 1H), 7.90 (d, J = 7.8 Hz, 1H), 7.83 – 7.73 (m, 3H), 7.66 (t, J = 7.6 Hz, 1H), 7.62 – 7.58 (m, 3H), 7.47 – 7.41 (m, 2H), 7.34 – 7.33 (m, 2H), 7.28 (t, J = 7.4 Hz, 2H), 7.20 –

7.16 (m, 1H), 6.72 – 6.68 (m, 1H), 6.60 (s, 1H), 6.51 (t, J = 6.8 Hz, 1H) 5.93 (s, 1H); $^{13}\text{C}\{^1\text{H}\}$ NMR (100 MHz, DMSO- d_6) δ 175.5, 155.8, 154.9 (q, $J_{\text{C-F}}$ = 2.9 Hz), 142.6, 134.1, 133.3, 132.8, 129.2, 129.1, 128.6 (q, $J_{\text{C-F}}$ = 278.4 Hz), 128.2, 128.1, 127.2, 126.8 (q, $J_{\text{C-F}}$ = 5.2 Hz), 126.2, 125.4, 125.2, 125.0, 123.3, 122.6, 122.5, 119.0, 118.4, 117.1, 117.0, 116.0, 112.7, 111.0, 37.9; $^{19}\text{F}\{^1\text{H}\}$ NMR (376 MHz, DMSO- d_6) δ –58.1; FT-IR (thin film, neat): 3064, 2956, 1735, 1601, 1436, 1257, 1037, 750 cm^{-1} ; HRMS (ESI): m/z calcd for $\text{C}_{31}\text{H}_{21}\text{F}_3\text{NO}_2$ $[\text{M}+\text{H}]^+$: 496.1524; found : 496.1521.

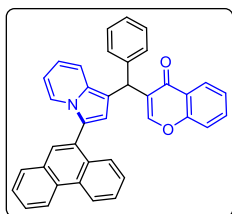
3-(phenyl(3-(thiophen-3-yl)indolizin-1-yl)methyl)-4H-chromen-4-one (62g)



The reaction was performed at 0.1392 mmol scale of **60h**; R_f = 0.4 (20% EtOAc in hexane); pale yellow semi-solid (55.6 mg, 92% yield); ^1H NMR (400 MHz, DMSO- d_6) δ 8.37 (d, J = 7.1 Hz, 1H), 8.04 (dd, J = 8.0, 1.5 Hz, 1H), 7.93 (s, 1H), 7.79 – 7.73 (m, 2H), 7.65 – 7.63 (m, 1H), 7.61 – 7.56 (m, 1H), 7.46 – 7.40 (m, 3H), 7.35 – 7.33 (m, 2H), 7.28, (t, J = 7.4

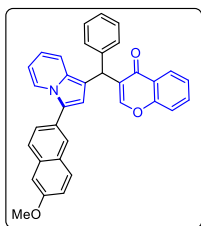
Hz, 2H), 7.21 – 7.17 (m, 1H), 6.84 (s, 1H), 6.71 – 6.67 (m, 1H), 6.64 – 6.61 (m, 1H), 5.92 (s, 1H); $^{13}\text{C}\{^1\text{H}\}$ NMR (100 MHz, DMSO- d_6) δ 175.5, 155.7, 155.2, 142.6, 134.1, 131.9, 130.0, 128.31, 128.27, 127.4, 127.0, 126.6, 126.2, 125.3, 125.2, 123.3, 123.0, 120.1, 119.8, 118.4, 117.4, 116.6, 114.7, 113.4, 111.4, 37.8; FT-IR (thin film, neat): 3064, 2932, 2852, 1421, 1268, 1029 cm^{-1} ; HRMS (ESI): m/z calcd for $\text{C}_{28}\text{H}_{20}\text{NO}_2\text{S}$ $[\text{M}+\text{H}]^+$: 434.1215; found : 434.1212.

3-((3-(phenanthren-9-yl)indolizin-1-yl)(phenyl)methyl)-4H-chromen-4-one (62h)



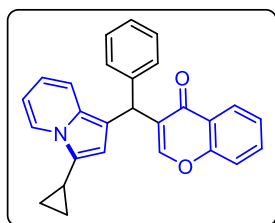
The reaction was performed at 0.1049 mmol scale of **60i**; $R_f = 0.4$ (20% EtOAc in hexane); pale yellow solid (48.7 mg, 88% yield); m.p. = 132 – 134 °C; ^1H NMR (400 MHz, CDCl_3) δ 8.78 (d, $J = 8.3$ Hz, 1H), 8.73 (d, $J = 8.2$ Hz, 1H), 8.28 – 8.26 (m, 1H), 7.86 (t, $J = 7.0$ Hz, 2H), 7.72 – 7.69 (m, 2H), 7.68 – 7.60 (m, 3H), 7.51 – 7.49 (m, 3H), 7.44 – 7.39 (m, 5H), 7.37 – 7.33 (m, 2H), 7.26 – 7.21 (m, 1H), 6.73 (s, 1H), 6.66 (dd, $J = 8.7, 6.6$ Hz, 1H), 6.38 – 6.35 (m, 1H), 6.18 (s, 1H); $^{13}\text{C}\{^1\text{H}\}$ NMR (100 MHz, CDCl_3) δ 177.0, 156.5, 155.1, 142.6, 133.5, 132.0, 131.0, 130.8, 130.5, 130.3, 130.2, 130.1, 128.9, 128.7, 128.6, 128.3, 127.2, 127.1, 127.0, 126.9, 126.6, 126.3, 125.1, 124.1, 123.4, 123.3, 123.2, 122.7, 118.2, 117.8, 116.7, 116.4, 116.3, 113.1, 110.7, 38.7; FT-IR (thin film, neat): 3058, 2924, 1764, 1601, 1424, 1252, 1028 cm^{-1} ; HRMS (ESI): m/z calcd for $\text{C}_{38}\text{H}_{26}\text{NO}_2$ $[\text{M}+\text{H}]^+$: 528.1964; found : 528.1958.

3-((3-(6-methoxynaphthalen-2-yl)indolizin-1-yl)(phenyl)methyl)-4H-chromen-4-one (62i)



The reaction was performed at 0.1107 mmol scale of **60j**; $R_f = 0.3$ (20% EtOAc in hexane); pale yellow semi-solid (46.2 mg, 82% yield); ^1H NMR (400 MHz, CDCl_3) δ 8.32 (d, $J = 3.6$ Hz, 1H), 8.23 (td, $J = 8.3, 1.6$ Hz, 2H), 7.89 (d, $J = 1.2$ Hz, 1H), 7.85 (d, $J = 6.0$ Hz, 1H), 7.79 – 7.77 (m, 1H), 7.73 (d, $J = 8.7$ Hz, 1H), 7.65 – 7.61 (m, 2H), 7.47 – 7.43 (m, 2H), 7.41 – 7.39 (m, 2H), 7.38 – 7.36 (m, 2H), 7.34 – 7.30 (m, 2H), 7.15 (s, 1H), 6.64 (s, 1H), 6.51 – 6.47 (m, 1H), 6.35 (d, $J = 6.0$ Hz, 1H), 6.08 (s, 1H), 3.93 (s, 3H); $^{13}\text{C}\{^1\text{H}\}$ NMR (100 MHz, CDCl_3) δ 176.0, 157.9, 156.5, 155.4, 155.2, 142.5, 134.0, 133.5, 129.5, 129.2, 128.64, 128.60, 128.1, 127.4, 126.9, 126.6, 126.3, 126.2, 125.9, 125.4, 125.1, 124.1, 122.4, 119.4, 118.3, 118.2, 116.8, 113.8, 113.1, 111.1, 105.8, 55.5, 38.6; FT-IR (thin film, neat): 3058, 2954, 1762, 1624, 1268, 1027 cm^{-1} ; HRMS (ESI): m/z calcd for $\text{C}_{35}\text{H}_{26}\text{NO}_3$ $[\text{M}+\text{H}]^+$: 508.1913; found : 508.1892.

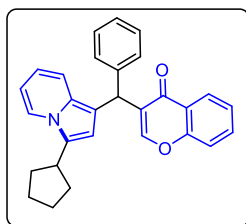
3-(3-cyclopropylindolizin-1-yl)(phenyl)methyl)-4H-chromen-4-one (62j)



The reaction was performed at 0.1630 mmol scale of **60k**; $R_f = 0.5$ (20% EtOAc in hexane); pale yellow solid (55.6 mg, 87% yield); m.p. = 128 – 130 °C; ^1H NMR (400 MHz, CDCl_3) δ 8.24 (dd, $J = 8.0, 1.6$ Hz, 1H), 8.03 (d, $J = 7.0$ Hz, 1H), 7.65 – 7.60 (m, 1H), 7.56 (d, $J = 0.9$ Hz, 1H), 7.42 – 7.37 (m, 2H), 7.35 – 7.33 (m, 3H), 7.31 – 7.28 (m, 2H), 7.25 – 7.20 (m, 1H), 6.62 – 6.58 (m, 1H), 6.53 (td, d, $J = 7.00, 1.3$ Hz, 1H), 6.25 (s, 1H), 6.03 (s, 1H), 1.85 – 1.78 (m, 1H), 0.96 – 0.91 (m, 2H), 0.65 – 0.62 (m, 2H); $^{13}\text{C}\{^1\text{H}\}$ NMR (100 MHz, CDCl_3) δ 176.9, 156.4, 155.1, 142.7, 133.4, 129.2, 128.5, 128.4, 128.2, 126.4, 126.2, 125.2, 124.9, 124.0, 122.3, 118.1, 117.5, 115.8, 112.4, 111.3, 110.1, 38.6, 6.3, 5.4; FT-

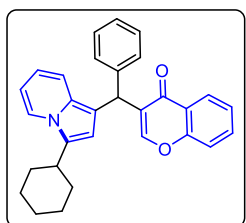
IR (thin film, neat): 3061, 2956, 1734, 1428, 1226, 1036, 738 cm^{-1} ; HRMS (ESI): m/z calcd for $\text{C}_{27}\text{H}_{22}\text{NO}_2$ $[\text{M}+\text{H}]^+$: 392.1651; found : 392.1653.

3-((3-cyclopentylindolizin-1-yl)(phenyl)methyl)-4H-chromen-4-one (62k)



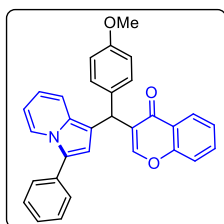
The reaction was performed at 0.1463 mmol scale of **60l**; $R_f = 0.5$ (20% EtOAc in hexane); pale yellow gummy solid (54.2 mg, 83% yield); ^1H NMR (400 MHz, CDCl_3) δ 8.22 (dd, $J = 8.0, 1.5$ Hz, 1H), 7.75 (d, $J = 7.1$, Hz, 1H), 7.64 – 7.60 (m, 1H), 7.57 (d, $J = 0.8$ Hz, 1H), 7.41 – 7.38 (m, 2H), 7.35 – 7.33 (m, 2H), 7.31 – 7.29 (m, 2H), 7.26 (s, 1H), 7.24 – 7.22 (m, 1H), 6.56 – 6.52 (m, 1H), 6.46 (dt, $J = 7.9, 1.3$ Hz, 1H), 6.30 (s, 1H), 6.03 (s, 1H), 3.22 (quintet, $J = 8.0$ Hz, 1H), 1.78 – 1.59 (m, 8H); $^{13}\text{C}\{^1\text{H}\}$ NMR (100 MHz, CDCl_3) δ 176.9, 156.4, 155.1, 142.8, 133.4, 129.3, 128.5, 128.4, 128.2, 128.0, 126.4, 126.2, 124.9, 124.0, 122.2, 118.1, 117.6, 115.0, 111.5, 110.4, 110.0, 38.6, 36.6, 31.3, 25.1; FT-IR (thin film, neat): 3062, 2963, 1722, 1452, 1210, 1028, 778 cm^{-1} ; HRMS (ESI): m/z calcd for $\text{C}_{29}\text{H}_{26}\text{NO}_2$ $[\text{M}+\text{H}]^+$: 420.1964; found : 420.1969.

3-((3-cyclohexylindolizin-1-yl)(phenyl)methyl)-4H-chromen-4-one (62l)



The reaction was performed at 0.1392 mmol scale of **60m**; $R_f = 0.5$ (20% EtOAc in hexane); pale yellow solid (47.8 mg, 79% yield); m.p. = 130 – 132 $^{\circ}\text{C}$; ^1H NMR (400 MHz, CDCl_3) δ 8.24 (dd, $J = 8.00, 1.6$ Hz, 1H), 7.74 (d, $J = 7.2$, Hz, 1H), 7.65 – 7.60 (m, 1H), 7.57 (s, 1H), 7.42 – 7.37 (m, 2H), 7.36 – 7.32 (m, 3H), 7.31 (s, 1H), 7.29 (d, $J = 1.5$ Hz, 1H), 7.24 – 7.20 (m, 1H), 6.56 – 6.52 (m, 1H), 6.49 – 6.45 (m, 1H), 6.28 (s, 1H), 6.04 (s, 1H), 2.82 – 2.76 (m, 1H), 2.08 – 2.04 (m, 2H), 1.86 – 1.76 (m, 3H), 1.49 – 1.36 (m, 5H); $^{13}\text{C}\{^1\text{H}\}$ NMR (100 MHz, CDCl_3) δ 176.9, 156.4, 155.1, 142.8, 133.4, 129.3, 129.0, 128.5, 128.4, 128.3, 126.4, 126.3, 124.9, 124.0, 121.8, 118.1, 117.8, 115.0, 111.7, 110.2, 110.0, 38.6, 35.3, 31.8, 31.7, 26.65, 26.62, 26.4 ; FT-IR (thin film, neat): 3062, 2952, 1764, 1434, 1216, 1030, 734 cm^{-1} ; HRMS (ESI): m/z calcd for $\text{C}_{30}\text{H}_{28}\text{NO}_2$ $[\text{M}+\text{H}]^+$: 434.2120; found : 434.2113.

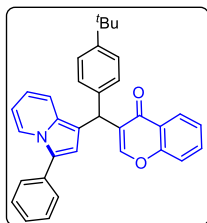
3-[(4-methoxyphenyl)(3-phenylindolizin-1-yl)methyl]-4H-chromen-4-one (62m)



The reaction was performed at 0.128 mmol scale of **60n**; $R_f = 0.3$ (20% EtOAc in hexane); light yellow solid (53.5 mg, 91% yield); m. p. = 108 – 110 $^{\circ}\text{C}$; ^1H NMR (400 MHz, CDCl_3) δ 8.27 – 8.25 (m, 1H), 8.24 – 8.22 (m, 1H), 7.66 – 7.62 (m, 1H), 7.61 (d, $J = 0.9$ Hz, 1H), 7.54 – 7.52 (m, 2H), 7.45 – 7.43 (m, 2H), 7.41 (s, 1H), 7.40 – 7.38 (m, 1H), 7.33 – 7.29 (m, 2H), 7.29 – 7.28 (m, 1H), 7.28 – 7.27 (m, 1H), 6.88 – 6.84 (m, 2H), 6.64 – 6.00 (m, 1H), 6.49 – 6.45 (m, 1H), 6.00 (s, 1H), 3.78 (s, 3H); $^{13}\text{C}\{^1\text{H}\}$ NMR (100 MHz, CDCl_3) δ 177.0, 158.2, 156.5,

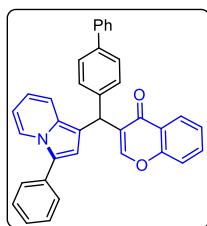
155.0, 134.5, 133.5, 132.4, 130.6, 129.6, 129.0, 128.3, 127.9, 127.1, 126.3, 125.0, 124.6, 124.1, 122.4, 118.2, 118.1, 116.7, 115.0, 114.0 (2C), 111.0, 55.4, 37.8; FT-IR (thin film, neat): 3058, 1745, 1626, 1432, 1272, 1029, 874 cm^{-1} ; HRMS (ESI): m/z calcd for $\text{C}_{31}\text{H}_{24}\text{NO}_3$ $[\text{M}+\text{H}]^+$: 458.1756; found : 458.1737.

3-([4-(*tert*-butyl)phenyl](3-phenylindolizin-1-yl)methyl)-4H-chromen-4-one (62n)



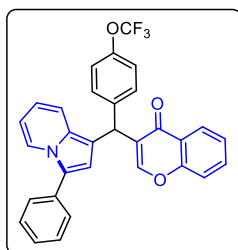
The reaction was performed at 0.1185 mmol scale of **60o**; $R_f = 0.4$ (20% EtOAc in hexane); pale yellow gummy solid (51.8 mg, 90% yield); ^1H NMR (400 MHz, CDCl_3) δ 8.27 – 8.23 (m, 2H), 7.65 – 7.62 (m, 2H), 7.54 – 7.23 (m, 2H), 7.45 – 7.41 (m, 3H), 7.41 – 7.33 (m, 3H), 7.31 – 7.22 (m, 5H), 6.61 (s, 1H), 6.47 (t, $J = 6.9$ Hz, 1H), 6.05 (s, 1H), 1.30 (s, 9H); $^{13}\text{C}\{^1\text{H}\}$ NMR (100 MHz, CDCl_3) δ 177.0, 156.5, 155.1, 149.2, 139.2, 133.5, 132.5, 130.7, 129.0, 128.3, 128.2, 128.0, 127.1, 126.3, 125.5, 125.0, 124.6, 124.1, 122.3, 118.2, 118.1, 116.7, 115.0, 114.0, 111.0, 37.9, 34.5, 31.5; FT-IR (thin film, neat): 3058, 2963, 1758, 1513, 1421, 1033, 752 cm^{-1} ; HRMS (ESI): m/z calcd for $\text{C}_{34}\text{H}_{30}\text{NO}_2$ $[\text{M}+\text{H}]^+$: 484.2277; found : 484.2247.

3-([1,1'-biphenyl]-4-yl(3-phenylindolizin-1-yl)methyl)-4H-chromen-4-one (62o)



The reaction was performed at 0.112 mmol scale of **60p**; $R_f = 0.4$ (20% EtOAc in hexane); pale yellow gummy solid (49.2 mg, 87% yield); m.p. = 142 – 144 $^{\circ}\text{C}$; ^1H NMR (400 MHz, CDCl_3) δ 8.29 – 8.25 (m, 2H), 7.68 – 7.63 (m, 2H), 7.60 – 7.58 (m, 2H), 7.57 – 7.54 (m, 4H), 7.46 – 7.41 (m, 7H), 7.40 – 7.36 (m, 2H), 7.34 – 7.28 (m, 2H), 6.67 – 6.63 (m, 1H), 6.62 (s, 1H), 6.51 – 6.48 (m, 1H), 6.11 (s, 1H); $^{13}\text{C}\{^1\text{H}\}$ NMR (100 MHz, CDCl_3) δ 177.0, 156.5, 155.2, 141.6, 141.1, 139.4, 133.6, 132.4, 130.7, 129.0 (2C), 128.9, 128.8 (2C), 128.0, 127.4, 127.2, 127.1, 126.3, 125.1, 124.7, 124.1, 122.4, 118.2, 118.0, 116.9, 115.1, 113.6, 111.1, 38.3; FT-IR (thin film, neat): 3058, 2923, 1730, 1601, 1438, 1206, 1030, 754 cm^{-1} ; HRMS (ESI): m/z calcd for $\text{C}_{36}\text{H}_{26}\text{NO}_2$ $[\text{M}+\text{H}]^+$: 504.1964; found : 504.1948.

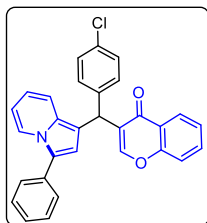
3-((3-phenylindolizin-1-yl)(4-(trifluoromethoxy)phenyl)methyl)-4H-chromen-4-one (62p)



The reaction was performed at 0.1095 mmol scale of **60q**; $R_f = 0.4$ (20% EtOAc in hexane); pale yellow gummy solid (48.0 mg, 85% yield); ^1H NMR (400 MHz, $\text{DMSO}-d_6$) δ 8.34 (d, $J = 7.2$ Hz, 1H), 8.05 – 8.02 (m, 2H), 7.77 – 7.73 (m, 1H), 7.59 – 7.54 (m, 3H), 7.48 – 7.46 (m, 4H), 7.44 – 7.42 (m, 2H), 7.32 – 7.25 (m, 3H), 6.78 (s, 1H), 6.72 – 6.69 (m, 1H), 6.60 – 6.57 (m, 1H), 5.95 (s, 1H); $^{13}\text{C}\{^1\text{H}\}$ NMR (100 MHz, $\text{DMSO}-d_6$) δ 175.6, 155.8, 155.3, 146.7, 142.2, 134.1, 131.5, 130.3, 130.0, 129.0, 127.4, 127.0, 126.5, 125.3, 125.2, 124.1, 123.3,

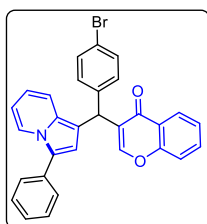
122.3, 120.8, 120.1 (q, $J_{\text{C-F}} = 254.2$ Hz), 118.4, 117.5, 117.1, 114.70, 113.1, 111.3, 37.4 ; $^{19}\text{F}\{^1\text{H}\}$ NMR (376 MHz, DMSO- d_6) δ -56.84; FT-IR (thin film, neat): 3061, 2987, 1746, 1596, 1436, 1225, 1037, 842 cm^{-1} ; HRMS (ESI): m/z calcd for $\text{C}_{31}\text{H}_{21}\text{F}_3\text{NO}_3$ $[\text{M}+\text{H}]^+$: 512.1474; found : 512.1478.

3-((4-chlorophenyl)(3-phenylindolizin-1-yl)methyl)-4H-chromen-4-one (62q)



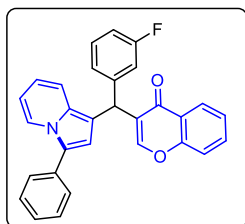
The reaction was performed at 0.1267 mmol scale of **60r**; $R_f = 0.4$ (20% EtOAc in hexane); pale yellow gummy solid (54.2 mg, 92% yield); ^1H NMR (400 MHz, DMSO- d_6) δ 8.32 (d, $J = 7.1$ Hz, 1H), 8.02 (dd, $J = 7.9, 1.6$ Hz, 1H), 7.94 (s, 1H), 7.75 – 7.72 (m, 1H), 7.56 – 7.54 (m, 3H), 7.46 – 7.38 (m, 6H), 7.27 (d, $J = 8.5$ Hz, 3H), 6.72 (s, 1H), 6.70 – 6.64 (m, 1H), 6.56 (t, $J = 7.0$ Hz, 1H), 5.85 (s, 1H); $^{13}\text{C}\{^1\text{H}\}$ NMR (100 MHz, DMSO- d_6) δ 175.5, 155.6, 155.2, 142.0, 134.2, 131.8, 131.4, 130.4, 130.1, 129.2, 127.5, 127.0, 126.5, 125.4, 125.1, 124.3, 123.2, 122.6, 119.2, 118.5, 117.3, 117.1, 114.2, 113.0, 111.1, 37.5; FT-IR (thin film, neat): 3058, 1756, 1467, 1241, 1028 cm^{-1} ; HRMS (ESI): m/z calcd for $\text{C}_{30}\text{H}_{21}\text{ClNO}_2$ $[\text{M}+\text{H}]^+$: 462.1261; found : 462.1249.

3-((4-bromophenyl)(3-phenylindolizin-1-yl)methyl)-4H-chromen-4-one (62r)



The reaction was performed at 0.111 mmol scale of **60s**; $R_f = 0.4$ (20% EtOAc in hexane); pale yellow solid (50.7 mg, 90% yield); m. p. = 126–128 °C; ^1H NMR (400 MHz, DMSO- d_6) δ 8.32 (d, $J = 7.2$ Hz, 1H), 8.03 (dd, $J_1 = 8.0$ Hz, $J_2 = 1.5$ Hz, 1H), 7.96 (s, 1H), 7.76 – 7.70 (m, 1H), 7.57 – 7.52 (m, 3H), 7.46 – 7.40 (m, 6H), 7.29 (d, $J = 8.5$ Hz, 3H), 6.74 (s, 1H), 6.70 – 6.67 (m, 1H), 6.57 (t, $J = 7.0$ Hz, 1H), 5.87 (s, 1H); $^{13}\text{C}\{^1\text{H}\}$ NMR (100 MHz, DMSO- d_6) δ 175.6, 155.8, 155.3, 142.2, 134.1, 131.6, 131.2, 130.5, 130.3, 129.0, 127.4, 127.0, 126.5, 125.4, 125.2, 124.1, 123.3, 122.3, 119.4, 118.4, 117.5, 117.1, 114.7, 113.0, 111.4, 37.6; FT-IR (thin film, neat): 3066, 2956, 1734, 1464, 1223, 1028, 842, 736 cm^{-1} ; HRMS (ESI): m/z calcd for $\text{C}_{30}\text{H}_{21}\text{BrNO}_2$ $[\text{M}+\text{H}]^+$: 506.0756; found : 506.0739.

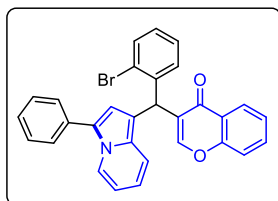
3-((3-fluorophenyl)(3-phenylindolizin-1-yl)methyl)-4H-chromen-4-one (62s)



The reaction was performed at 0.1336 mmol scale of **60t**; $R_f = 0.4$ (20% EtOAc in hexane); pale yellow solid (51.3 mg, 86% yield); m.p. = 134 – 136 °C; ^1H NMR (400 MHz, CDCl_3) δ 8.29 – 8.26 (m, 2H), 7.65 – 7.61 (m, 2H), 7.43 – 7.40 (m, 2H), 7.39 – 7.37 (m, 3H), 7.37 – 7.31 (m, 4H), 7.28 – 7.27 (m, 1H), 7.26 – 7.23 (m, 1H), 7.01 – 6.96 (m, 1H), 6.69 – 6.66 (m, 1H), 6.65 – 6.64 (m, 1H), 6.54 – 6.50 (m, 1H), 6.11 (s, 1H); $^{13}\text{C}\{^1\text{H}\}$ NMR (100 MHz,

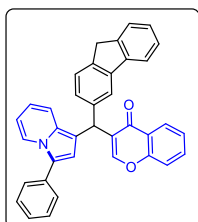
CDCl₃) δ 176.7, 163.0 (d, J = 244.1 Hz), 156.4, 155.1, 145.3 (d, J = 6.7 Hz), 133.6, 132.2, 130.6, 129.9 (d, J = 8.2 Hz), 129.0, 127.9, 127.4, 127.2, 126.2, 125.1, 124.8, 124.3 (d, J = 2.4 Hz), 123.9, 122.4, 118.1, 117.7, 117.0, 115.4 (d, J = 21.5 Hz), 114.8 (d, J = 1.3 Hz), 113.5 (d, J = 21.0 Hz), 112.8, 111.1, 38.3; $^{19}\text{F}\{^1\text{H}\}$ NMR (376 MHz, CDCl₃) δ -112.22; FT-IR (thin film, neat): 3062, 2945, 1754, 1596, 1436, 1254, 1028, 842 cm⁻¹; HRMS (ESI): m/z calcd for C₃₀H₂₁FNO₂ [M+H]⁺ : 446.1556; found : 446.1546.

3-((2-bromophenyl)(3-phenylindolizin-1-yl)methyl)-4H-chromen-4-one (62t)



The reaction was performed at 0.111 mmol scale of **60u**; R_f = 0.4 (20% EtOAc in hexane); pale yellow semi-solid (45.6 mg, 81% yield); ^1H NMR (400 MHz, DMSO-*d*₆) δ 8.36 (d, J = 7.2 Hz, 1H), 8.04 (dd, J = 8.0, 1.6 Hz, 1H), 7.79 – 7.75 (m, 2H), 7.63 – 7.55 (m, 4H), 7.48 – 7.42 (m, 3H), 7.38 – 7.34 (m, 2H), 7.32 – 7.27 (m, 2H), 7.18 – 7.14 (m, 1H), 6.74 – 6.71 (m, 1H), 6.68 (s, 1H), 6.60 (t, J = 7.0 Hz, 1H), 6.18 (s, 1H); $^{13}\text{C}\{^1\text{H}\}$ NMR (100 MHz, CDCl₃) δ 175.4, 155.8, 155.1, 141.5, 134.2, 132.9, 131.5, 130.3, 129.6, 129.0, 128.5, 127.7, 127.4, 127.0, 126.0, 125.4, 125.2, 124.3, 124.1, 123.1, 122.4, 118.4, 117.4, 117.3, 114.9, 111.5, 111.4, 37.8; FT-IR (thin film, neat): 3060, 2961, 1736, 1446, 1258, 1032, 856, 732 cm⁻¹; HRMS (ESI): m/z calcd for C₃₀H₂₁BrNO₂ [M+H]⁺ : 506.0756; found : 506.0768.

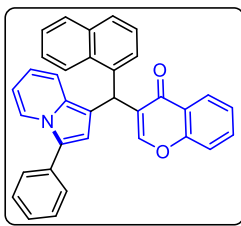
3-((9H-fluoren-3-yl)(3-phenylindolizin-1-yl)methyl)-4H-chromen-4-one (62u)



The reaction was performed at 0.1083 mmol scale of **60v**; R_f = 0.4 (20% EtOAc in hexane); pale yellow gummy solid (52.1 mg, 93% yield); ^1H NMR (400 MHz, CDCl₃) δ 8.30 – 8.25 (m, 2H), 7.75 (t, J = 6.6 Hz, 2H), 7.68 – 7.63 (m, 2H), 7.56 – 7.51 (m, 4H), 7.45 – 7.41 (m, 4H), 7.39 – 7.35 (m, 3H), 7.34 – 7.25 (m, 2H), 6.66 – 6.62 (m, 2H), 6.51 – 6.48 (m, 1H), 6.15 (s, 1H), 3.87 (s, 2H); $^{13}\text{C}\{^1\text{H}\}$ NMR (100 MHz, CDCl₃) δ 177.0, 156.5, 155.2, 143.7, 143.4, 141.7, 141.2, 140.4, 133.5, 132.4, 130.7, 129.0, 128.2, 127.9, 127.2, 127.1, 126.8, 126.5, 126.3, 125.3, 125.1, 124.7, 124.1, 122.4, 119.9, 119.8, 118.2, 118.1, 116.8, 115.12, 115.11, 113.9, 111.1, 38.8, 37.0; FT-IR (thin film, neat): 3056, 2957, 1734, 1445, 1265, 1032, 832, 738 cm⁻¹; HRMS (ESI): m/z calcd for C₃₇H₂₆NO₂ [M+H]⁺ : 516.1964; found : 516.1940.

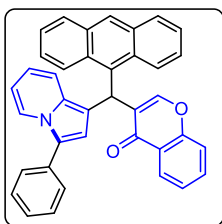
3-(naphthalen-1-yl)(3-phenylindolizin-1-yl)methyl)-4H-chromen-4-one (62v)

The reaction was performed at 0.121 mmol scale of **60w**; R_f = 0.4 (20% EtOAc in hexane); pale yellow solid (50.7 mg, 88% yield); m. p. = 120–122 °C; ^1H NMR (400 MHz, CDCl₃) δ 8.30 – 8.28 (m, 2H), 8.18 – 8.15 (m, 1H), 7.91 – 7.87 (m, 1H), 7.77 (d, J = 7.6 Hz, 1H), 7.66 –



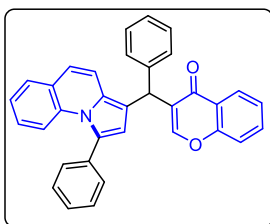
7.62 (m, 1H), 7.54 – 7.52 (m, 3H), 7.50 – 7.45 (m, 2H), 7.44 – 7.34 (m, 7H), 7.31 – 7.26 (m, 1H), 6.86 (s, 1H), 6.64 – 6.60 (m, 2H), 6.50 – 6.47 (m, 1H); $^{13}\text{C}\{^1\text{H}\}$ NMR (100 MHz, CDCl_3) δ 176.8, 156.5, 155.2, 138.5, 134.2, 133.6, 132.4, 131.6, 130.9, 129.0, 128.8, 128.0, 127.9 (2C), 127.6, 127.0, 126.5, 126.4, 125.7, 125.3, 125.1, 124.6, 124.1, 124.0, 122.4, 118.2, 118.0, 116.8, 115.3, 113.1, 111.1, 34.3; FT-IR (thin film, neat): 3054, 2956, 1732, 1436, 1266, 1028, 736, 645 cm^{-1} ; HRMS (ESI): m/z calcd for $\text{C}_{34}\text{H}_{24}\text{NO}_2$ $[\text{M}+\text{H}]^+$: 478.1807; found : 478.1787.

3-(anthracen-9-yl(3-phenylindolizin-1-yl)methyl)-4H-chromen-4-one (62w)



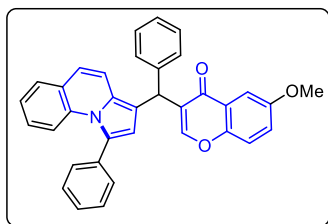
The reaction was performed at 0.1049 mmol scale of **60x**; R_f = 0.4 (20% EtOAc in hexane); pale yellow solid (46.2 mg, 83% yield); m. p. = 122–124 $^{\circ}\text{C}$; ^1H NMR (400 MHz, CDCl_3) δ 8.27 – 8.23 (m, 2H), 8.08 – 8.06 (m, 1H), 7.84 (d, J = 7.6 Hz, 1H), 7.67 – 7.63 (m, 3H), 7.56 (s, 1H), 7.54 – 7.52 (m, 1H), 7.50 – 7.42 (m, 5H), 7.35 – 7.33 (m, 2H), 7.30 (s, 1H), 7.25 – 7.16 (m, 4H), 7.05 (s, 1H), 6.83 – 6.79 (m, 1H), 6.57 – 6.54 (m, 1H), 5.78 (s, 1H); $^{13}\text{C}\{^1\text{H}\}$ NMR (100 MHz, CDCl_3) δ 177.1, 156.1, 153.3, 140.7, 139.0, 136.7, 136.2, 134.2, 133.4, 131.8, 130.2, 129.1, 128.9, 128.6, 128.3, 128.2, 127.7, 127.6, 127.3, 127.2, 126.6, 126.5, 126.1, 126.0, 124.9, 124.2, 123.4, 123.1, 118.8, 118.3, 118.0, 117.8, 113.0, 111.7, 110.5, 29.9; FT-IR (thin film, neat): 3058, 2924, 1736, 1428, 1265, 1036, 738 cm^{-1} ; HRMS (ESI): m/z calcd for $\text{C}_{38}\text{H}_{26}\text{NO}_2$ $[\text{M}+\text{H}]^+$: 528.1964; found : 528.1951.

3-(phenyl(1-phenylpyrrolo[1,2-a]quinolin-3-yl)methyl)-4H-chromen-4-one (63a)



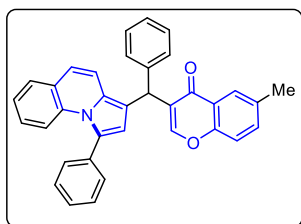
The reaction was performed at 0.1207 mmol scale of **60aa**; R_f = 0.4 (20% EtOAc in hexane); pale yellow gummy solid (49.2 mg, 85% yield); ^1H NMR (400 MHz, CDCl_3) δ 8.24 (dd, J = 8.0 Hz, 1.6 Hz, 1H), 7.67 – 7.62 (m, 2H), 7.59 (dd, J = 6.4 Hz, 1.4 Hz, 1H), 7.49 – 7.47 (m, 3H), 7.43 – 7.37 (m, 7H), 7.33 – 7.30 (m, 3H), 7.25 – 7.19 (m, 2H), 7.12 – 7.08 (m, 1H), 6.97 (d, J = 9.4 Hz, 1H), 6.41 (s, 1H), 6.08 (s, 1H); $^{13}\text{C}\{^1\text{H}\}$ NMR (100 MHz, CDCl_3) δ 176.9, 156.5, 155.2, 142.3, 135.5, 134.3, 133.6, 129.6, 129.4, 129.3, 128.7, 128.62, 128.58, 128.1, 127.7, 126.7, 126.5, 126.3 (2C), 125.6, 125.1, 124.1, 123.5, 119.1, 118.2, 117.8, 117.3, 117.2, 116.6, 38.4; FT-IR (thin film, neat): 3057, 2850, 1756, 1448, 1036, 737 cm^{-1} ; HRMS (ESI): m/z calcd for $\text{C}_{34}\text{H}_{24}\text{NO}_2$ $[\text{M}+\text{H}]^+$: 478.1807; found : 478.1789.

6-methoxy-3-(phenyl(1-phenylpyrrolo[1,2-a]quinolin-3-yl)methyl)-4H-chromen-4-one (63b)



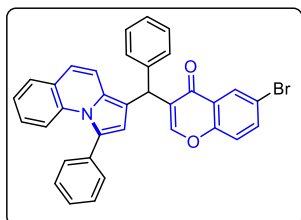
The reaction was performed at 0.1207 mmol scale of **60aa**; $R_f = 0.3$ (20% EtOAc in hexane); pale yellow solid (53.6 mg, 87% yield); m.p. = 160 – 162 °C; ^1H NMR (400 MHz, CDCl_3) δ 7.66 – 7.65 (m, 1H), 7.63 (d, $J = 3.0$ Hz, 1H), 7.60 (dd, $J = 7.8, 1.3$ Hz, 1H), 7.52 – 7.50 (m, 3H), 7.45 – 7.38 (m, 5H), 7.37 – 7.32 (m, 4H), 7.26 – 7.20 (m, 3H), 7.13 – 7.09 (m, 1H), 7.00, (d, $J = 9.3$ Hz, 1H), 6.45 (s, 1H), 6.13 (s, 1H), 3.88 (s, 3H); $^{13}\text{C}\{^1\text{H}\}$ NMR (100 MHz, CDCl_3) δ 176.6, 156.8, 154.9, 151.3, 142.3, 135.5, 134.3, 129.6, 129.4, 129.3, 128.6, 128.55, 128.53 (2C), 127.6, 127.3, 126.6, 126.4, 125.6, 124.5, 123.8, 123.5, 119.5, 119.1, 117.7, 117.3, 117.2, 116.6, 105.1, 55.9, 38.4; FT-IR (thin film, neat): 3058, 2971, 1754, 1443, 1256, 1047, 842, 736 cm^{-1} ; HRMS (ESI): m/z calcd for $\text{C}_{35}\text{H}_{25}\text{NNaO}_3$ $[\text{M}+\text{Na}]^+$: 530.1732; found : 530.1736.

6-methyl-3-(phenyl(1-phenylpyrrolo[1,2-a]quinolin-3-yl)methyl)-4H-chromen-4-one (63c)



The reaction was performed at 0.1207 mmol scale of **60aa**; $R_f = 0.4$ (20% EtOAc in hexane); pale yellow solid (53.1 mg, 89% yield); m.p. = 158 – 160 °C; ^1H NMR (400 MHz, CDCl_3) δ 8.04 (d, $J = 1.0$ Hz, 1H), 7.64 – 7.63 (m, 1H), 7.59 (dd, $J = 7.8, 1.3$ Hz, 1H), 7.51 – 7.49 (m, 3H), 7.46 – 7.42 (m, 2H), 7.41 – 7.38 (m, 4H), 7.36 – 7.31 (m, 4H), 7.26 – 7.20 (m, 2H), 7.13 – 7.08 (m, 1H), 6.98 (d, $J = 9.3$ Hz, 1H), 6.44 (s, 1H), 6.12 (s, 1H), 2.45 (s, 3H); $^{13}\text{C}\{^1\text{H}\}$ NMR (100 MHz, CDCl_3) δ 176.8, 155.0, 154.7, 142.4, 135.5, 134.9, 134.8, 134.3, 129.6, 129.3 (2C), 129.2, 128.6, 128.55, 128.54, 127.8, 127.6, 126.6, 126.4, 125.6, 125.5, 123.7, 123.5, 119.0, 117.9, 117.7, 117.4, 117.2, 116.7, 38.3, 27.0; FT-IR (thin film, neat): 3060, 2954, 1734, 1472, 1199, 1029, 841 cm^{-1} ; HRMS (ESI): m/z calcd for $\text{C}_{35}\text{H}_{25}\text{NNaO}_2$ $[\text{M}+\text{Na}]^+$: 514.1783; found : 514.1789.

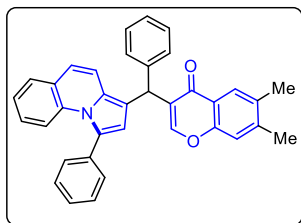
6-bromo-3-(phenyl(1-phenylpyrrolo[1,2-a]quinolin-3-yl)methyl)-4H-chromen-4-one (63d)



The reaction was performed at 0.1207 mmol scale of **60aa**; $R_f = 0.4$ (20% EtOAc in hexane); pale yellow solid (57.8 mg, 86% yield); m.p. = 128 – 130 °C; ^1H NMR (400 MHz, CDCl_3) δ 8.36 (d, $J = 2.4$ Hz, 1H), 7.70 (dd, $J = 8.9, 2.4$ Hz, 1H), 7.64 (s, 1H), 7.59 (dd, $J = 7.7, 0.8$ Hz, 1H), 7.50 – 7.48 (m, 3H), 7.42 – 7.38 (m, 3H), 7.36 – 7.29 (m, 6H), 7.24 – 7.20 (m, 2H), 7.12 – 7.08 (m, 1H), 6.98, (d, $J = 9.4$ Hz, 1H), 6.41 (s, 1H), 6.07 (s, 1H); $^{13}\text{C}\{^1\text{H}\}$ NMR (100 MHz, CDCl_3) δ 175.5, 155.2, 155.1, 142.0, 136.5, 135.4, 134.3, 129.6, 129.5, 129.3, 128.9, 128.6, 128.5 (2C), 128.4, 127.7, 126.8, 126.5, 125.6, 125.3, 123.5,

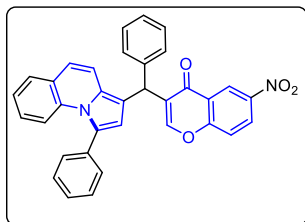
120.1, 119.2, 118.5, 117.7 (2C), 117.2, 117.1, 116.2, 38.4; FT-IR (thin film, neat): 3058, 2924, 1736, 1447, 1320, 1029 cm^{-1} ; HRMS (ESI): m/z calcd for $\text{C}_{34}\text{H}_{23}\text{BrNO}_2$ $[\text{M}+\text{H}]^+$: 556.0912; found : 556.0918.

6,7-dimethyl-3-(phenyl(1-phenylpyrrolo[1,2-a]quinolin-3-yl)methyl)-4H-chromen-4-one (63e)



The reaction was performed at 0.1207 mmol scale of **60aa**; R_f = 0.4 (20% EtOAc in hexane); pale yellow solid (53.1 mg, 87% yield); m.p. = 148 – 150 $^{\circ}\text{C}$; ^1H NMR (400 MHz, CDCl_3) δ 7.98 (s, 1H), 7.60 – 7.57 (m, 2H), 7.50 – 7.48 (m, 3H), 7.44 – 7.39 (m, 3H), 7.38 – 7.37 (m, 2H), 7.35 – 7.33 (m, 1H), 7.32 – 7.30 (m, 2H), 7.24 – 7.19 (m, 3H), 7.12 – 7.08 (m, 1H), 6.96 (d, J = 9.3 Hz, 1H), 6.42 (s, 1H), 6.10 (s, 1H), 2.36 (s, 3H), 2.34 (s, 3H); $^{13}\text{C}\{^1\text{H}\}$ NMR (100 MHz, CDCl_3) δ 176.7, 155.0, 154.8, 144.0, 142.5, 135.5, 134.3, 134.28, 129.6, 129.3 (2C), 129.28, 128.6, 128.5 (2C), 127.7, 127.6, 126.5, 126.4, 125.8, 125.6, 123.4, 121.9, 119.0, 118.2, 117.7, 117.4, 117.3, 116.9, 38.3, 20.5, 19.4; FT-IR (thin film, neat): 3058, 2924, 1639, 1447, 1224, 1140, 1032 cm^{-1} ; HRMS (ESI): m/z calcd for $\text{C}_{36}\text{H}_{28}\text{NO}_2$ $[\text{M}+\text{H}]^+$: 506.2120; found : 506.2126.

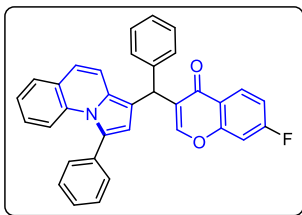
6-nitro-3-(phenyl(1-phenylpyrrolo[1,2-a]quinolin-3-yl)methyl)-4H-chromen-4-one (63f)



The reaction was performed at 0.1207 mmol scale of **60aa**; R_f = 0.3 (20% EtOAc in hexane); pale yellow solid (48.2 mg, 76% yield); m.p. = 152 – 154 $^{\circ}\text{C}$; ^1H NMR (400 MHz, CDCl_3) δ 9.09 (d, J = 2.7 Hz, 1H), 8.45 (dd, J = 9.2, 2.8 Hz, 1H), 7.69 (d, J = 0.64 Hz, 1H), 7.59 (dd, J = 7.7, 1.2 Hz, 1H), 7.55 (d, J = 9.2 Hz, 1H), 7.49 – 7.47 (m, 3H), 7.44 – 7.39 (m, 4H), 7.37 – 7.34 (m, 3H), 7.33 – 7.30 (m, 1H), 7.27 – 7.26 (m, 1H), 7.24 – 7.20 (m, 1H), 7.12 – 7.08 (m, 1H), 7.00 (d, J = 9.4 Hz, 1H), 6.41 (s, 1H), 6.06 (s, 1H); $^{13}\text{C}\{^1\text{H}\}$ NMR (100 MHz, CDCl_3) δ 175.5, 159.2, 155.4, 144.7, 141.5, 135.4, 134.2, 129.65, 129.60, 129.3, 129.2, 128.8, 128.62 (2C), 128.57, 127.9, 127.8, 127.0, 126.7, 125.5, 124.0, 123.7, 123.1, 120.0, 119.4, 117.7, 117.0, 116.9, 115.6, 38.4; FT-IR (thin film, neat): 3058, 2964, 1738, 1556, 1436, 1367, 1267, 1032, 742 cm^{-1} ; HRMS (ESI): m/z calcd for $\text{C}_{34}\text{H}_{22}\text{NNaO}_4$ $[\text{M}+\text{Na}]^+$: 545.1477; found : 545.1474.

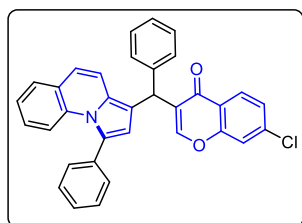
7-fluoro-3-(phenyl(1-phenylpyrrolo[1,2-a]quinolin-3-yl)methyl)-4H-chromen-4-one (63g)

The reaction was performed at 0.1207 mmol scale of **60aa**; R_f = 0.4 (20% EtOAc in hexane); pale yellow solid (49.3 mg, 82% yield); m.p. = 130 – 138 $^{\circ}\text{C}$; ^1H NMR (400 MHz, CDCl_3) δ 8.29 – 8.25 (m, 1H), 7.64 (s, 1H), 7.61 (dd, J = 7.8, 0.3 Hz, 1H), 7.52 – 7.50 (m, 3H), 7.46 –



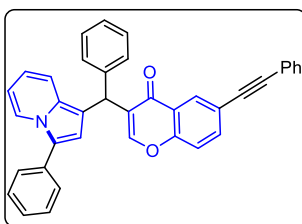
7.43 (m, 1H), 7.41 – 7.39 (m, 4H), 7.36 – 7.32 (m, 3H), 7.27 – 7.25 (m, 1H), 7.24 – 7.20 (m, 1H), 7.15 – 7.09 (m, 3H), 7.00 (d, $J = 2.3$ Hz, 1H), 6.44 (s, 1H), 6.10 (s, 1H); $^{13}\text{C}\{^1\text{H}\}$ NMR (100 MHz, CDCl_3) δ 175.9, 165.6 (d, $J = 253.1$ Hz), 157.4 (d, $J = 13.3$ Hz), 155.2, 142.1, 135.5, 134.3, 129.6, 129.4, 129.3, 128.9, 128.8, 128.6, 128.5, 128.3, 127.7, 126.7, 126.5, 125.6, 123.5, 120.9, 120.8, 119.2, 117.7, 117.2, 117.1, 116.3, 113.9, (d, $J = 22.8$ Hz), 104.7 (d, $J = 25.0$ Hz), 38.3; $^{19}\text{F}\{^1\text{H}\}$ NMR (376 MHz, CDCl_3) δ -103.13; FT-IR (thin film, neat): 3058, 2952, 1736, 1432, 1257, 1042, 842, 742 cm^{-1} ; HRMS (ESI): m/z calcd for $\text{C}_{34}\text{H}_{23}\text{FNO}_2$ $[\text{M}+\text{H}]^+$: 496.1713; found: 496.1724.

7-chloro-3-(phenyl(1-phenylpyrrolo[1,2-a]quinolin-3-yl)methyl)-4H-chromen-4-one (63h)



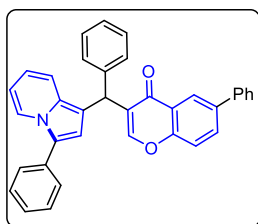
The reaction was performed at 0.1207 mmol scale of **60aa**; $R_f = 0.4$ (20% EtOAc in hexane); pale yellow gummy solid (53.3 mg, 86% yield); ^1H NMR (400 MHz, CDCl_3) δ 8.21 (d, $J = 2.6$ Hz, 1H), 7.66 (s, 1H), 7.61 – 7.55 (m, 2H), 7.51 – 7.49 (m, 3H), 7.45 – 7.37 (m, 6H), 7.36 – 7.34 (m, 2H), 7.32 (s, 1H), 7.27 – 7.24 (m, 1H), 7.22 – 7.20 (m, 1H), 7.13 – 7.09 (m, 1H), 7.00 (d, $J = 9.4$ Hz, 1H), 6.43 (s, 1H), 6.09 (s, 1H); $^{13}\text{C}\{^1\text{H}\}$ NMR (100 MHz, CDCl_3) δ 175.7, 155.2, 154.7, 142.0, 135.4, 134.2, 133.8, 130.9, 129.6, 129.4, 129.3, 128.6, 128.5 (2C), 128.2, 127.7, 126.7, 126.5, 125.6, 125.5, 124.9, 123.5, 119.9, 119.2, 117.7 (2C), 117.2, 117.1, 116.2, 38.4; FT-IR (thin film, neat): 3061, 2956, 1732, 1437, 1252, 1176, 1037, 738 cm^{-1} ; HRMS (ESI): m/z calcd for $\text{C}_{34}\text{H}_{23}\text{ClNO}_2$ $[\text{M}+\text{H}]^+$: 512.1417; found: 512.1410.

3-(phenyl(3-phenylindolizin-1-yl)methyl)-6-(phenylethynyl)-4H-chromen-4-one (64)



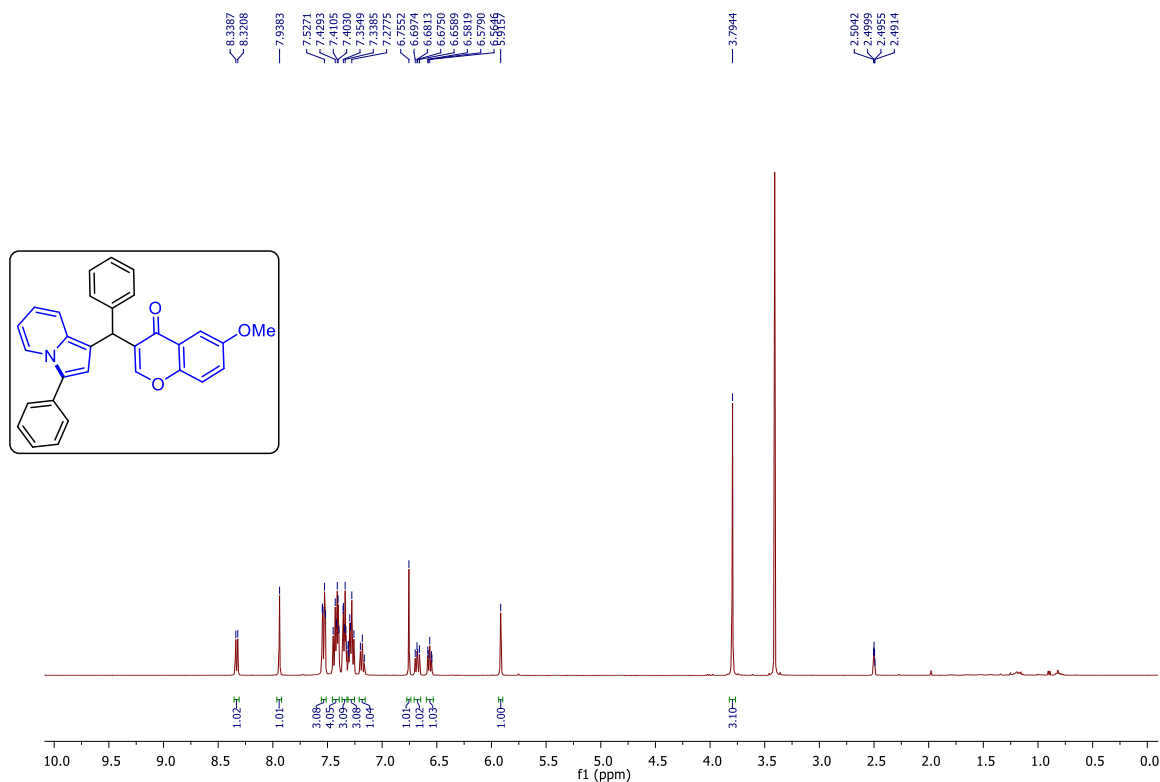
The reaction was performed at 0.1975 mmol scale of **61g**; $R_f = 0.4$ (20% EtOAc in hexane); pale yellow solid (85.6 mg, 82% yield); m.p. = 162 – 164 $^{\circ}\text{C}$; ^1H NMR (400 MHz, CDCl_3) δ 8.41 (d, $J = 1.8$ Hz, 1H), 8.28 (d, $J = 7.2$ Hz, 1H), 7.77 (dd, $J = 8.7, 2.1$ Hz, 1H), 7.63 (d, $J = 0.5$ Hz, 1H), 7.57 – 7.54 (m, 4H), 7.46 – 7.44 (m, 2H), 7.42 – 7.39 (m, 3H), 7.38 – 7.36 (m, 4H), 7.34 – 7.31 (m, 3H), 7.29 – 7.24 (m, 1H), 6.67 – 6.63 (m, 1H), 6.59 (s, 1H), 6.51 – 6.47 (m, 1H), 6.09 (s, 1H); $^{13}\text{C}\{^1\text{H}\}$ NMR (100 MHz, CDCl_3) δ 176.1, 155.8, 155.1, 142.3, 136.3, 132.3, 131.8, 130.7, 129.6, 129.0, 128.7, 128.6 (2C), 128.5, 128.3, 127.9, 127.1, 126.7, 124.7, 124.0, 122.9, 122.4, 120.5, 118.5, 118.0, 116.9, 115.0, 113.5, 111.1, 90.3, 88.0, 38.5; FT-IR (thin film, neat): 3061, 2926, 2360, 2214, 1741, 1494, 1321, 1145, 1028 cm^{-1} ; HRMS (ESI): m/z calcd for $\text{C}_{38}\text{H}_{26}\text{NO}_2$ $[\text{M}+\text{H}]^+$: 528.1964; found: 528.1957.

6-phenyl-3-(phenyl(3-phenylindolizin-1-yl)methyl)-4H-chromen-4-one (**65**)

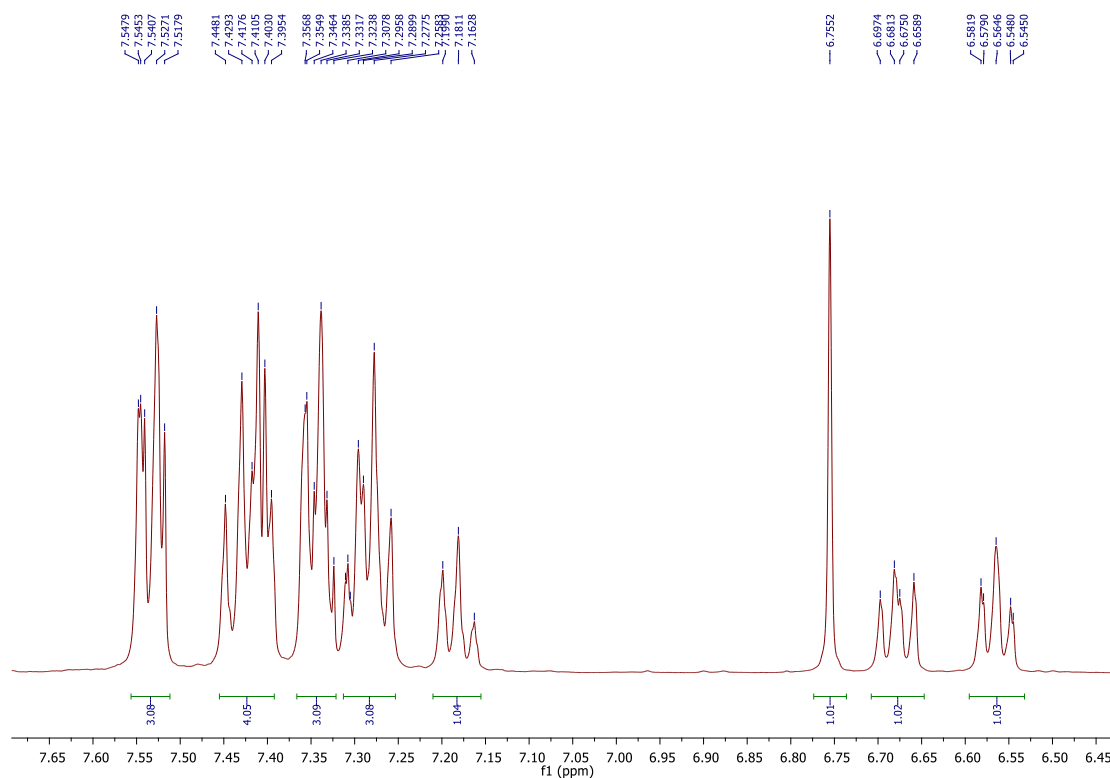


The reaction was performed at 0.1975 mmol scale of **61g**; $R_f = 0.4$ (20% EtOAc in hexane); pale yellow solid (76.1 mg, 76% yield); m.p. = 170 – 172 °C; ^1H NMR (400 MHz, CDCl_3) δ 8.47 (d, $J = 2$ Hz, 1H), 8.28 (d, $J = 7.2$ Hz, 1H), 7.89 (dd, $J = 8.7, 2.3$ Hz, 1H), 7.65 – 7.64 (m, 3H), 7.55 – 7.54 (m, 2H), 7.51 – 7.49 (m, 2H), 7.47 – 7.44 (m, 3H), 7.42 – 7.38 (m, 4H), 7.36 – 7.31 (m, 3H), 7.29 – 7.23 (m, 1H), 6.67 – 6.63 (m, 1H), 6.60 (s, 1H), 6.51 – 6.47 (m, 1H), 6.12 (s, 1H); $^{13}\text{C}\{^1\text{H}\}$ NMR (100 MHz, CDCl_3) δ 177.0, 155.9, 155.1, 142.4, 139.5, 138.2, 132.5, 132.4, 130.7, 129.1, 129.0, 128.6, 128.5, 128.1, 127.9, 127.8, 127.2, 127.1, 126.6, 124.7, 124.2, 124.1, 122.4, 118.7, 118.0, 116.8, 115.0, 113.7, 111.1, 38.6; FT-IR (thin film, neat): 3061, 2924, 1724, 1337, 1252, 1023 cm^{-1} ; HRMS (ESI): m/z calcd for $\text{C}_{36}\text{H}_{26}\text{NO}_2$ $[\text{M}+\text{H}]^+$: 504.1964; found : 504.1967.

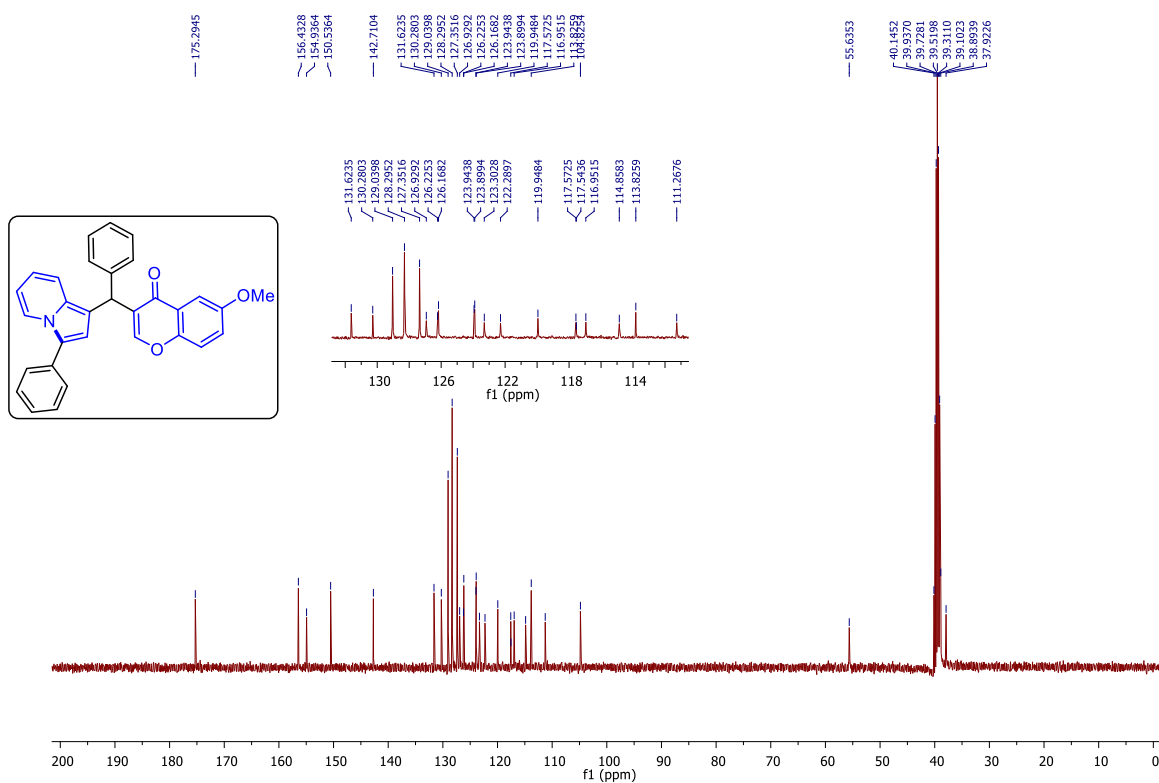
^1H NMR (400 MHz, DMSO-d_6) spectrum of (**61c**)



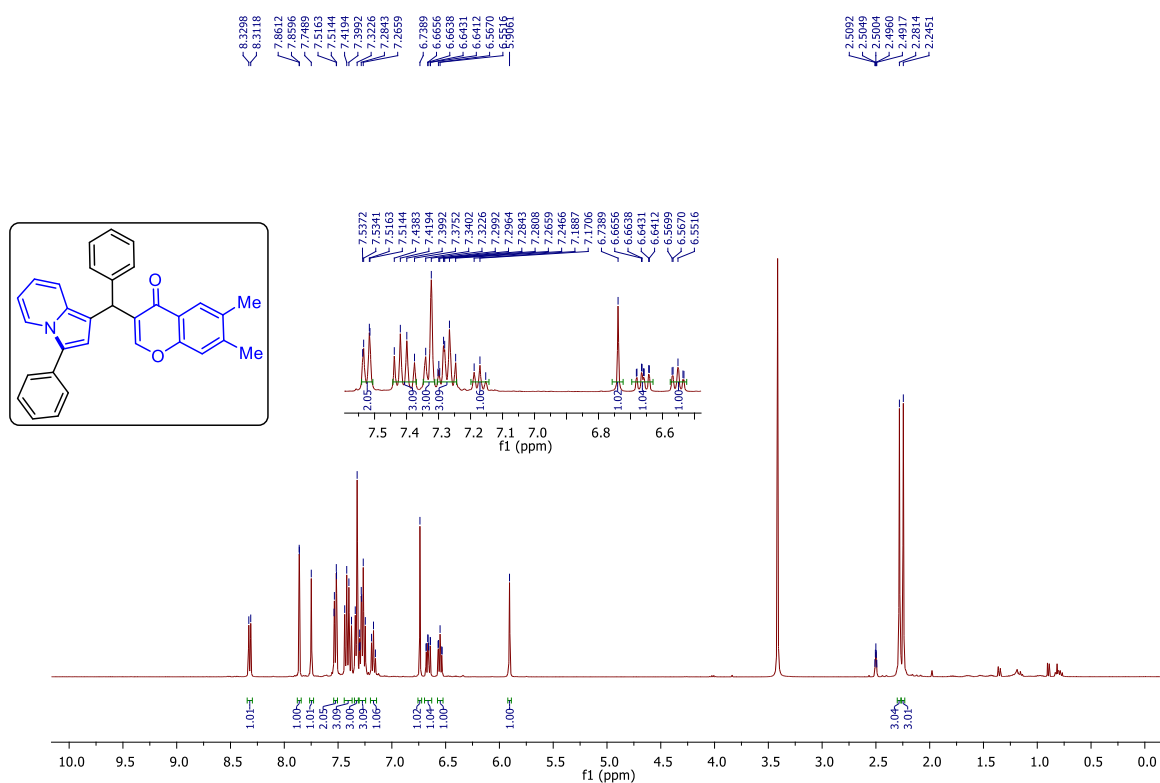
Expanded ^1H NMR (400 MHz, DMSO- d_6) spectrum of (**61c**)



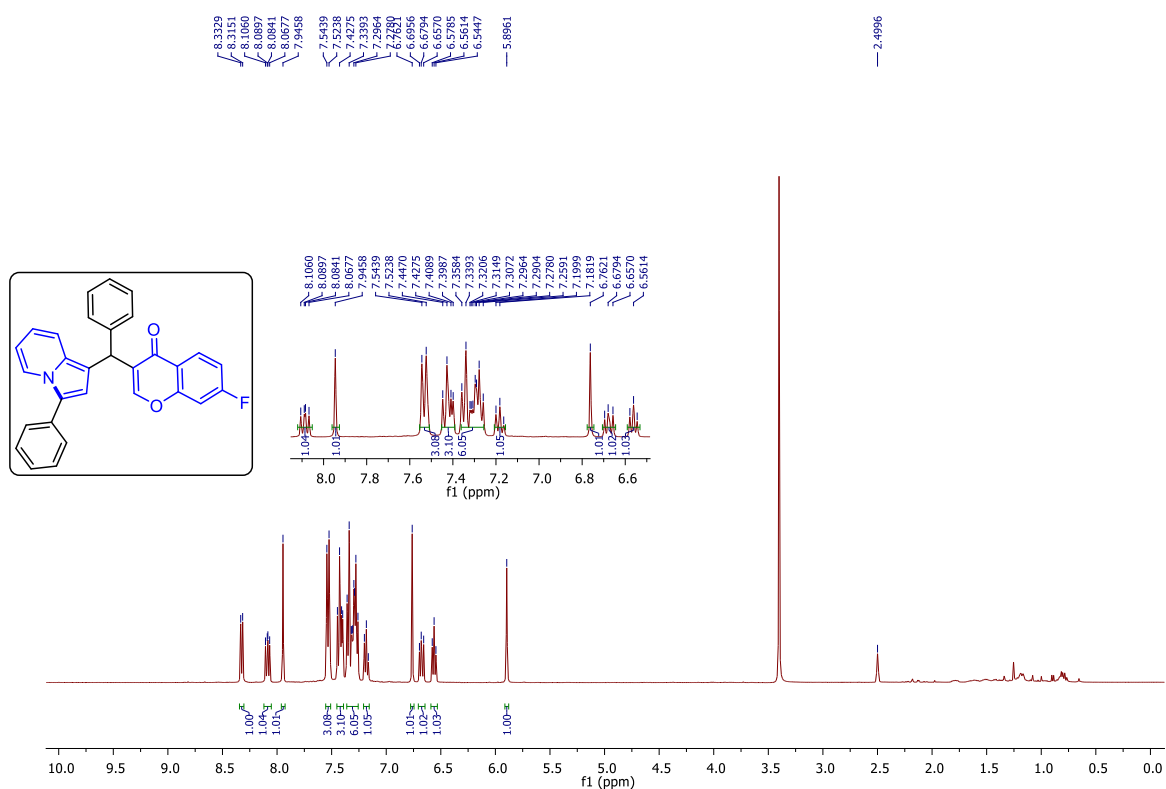
$^{13}\text{C}\{^1\text{H}\}$ NMR (100 MHz, DMSO- d_6) spectrum of (**61c**)



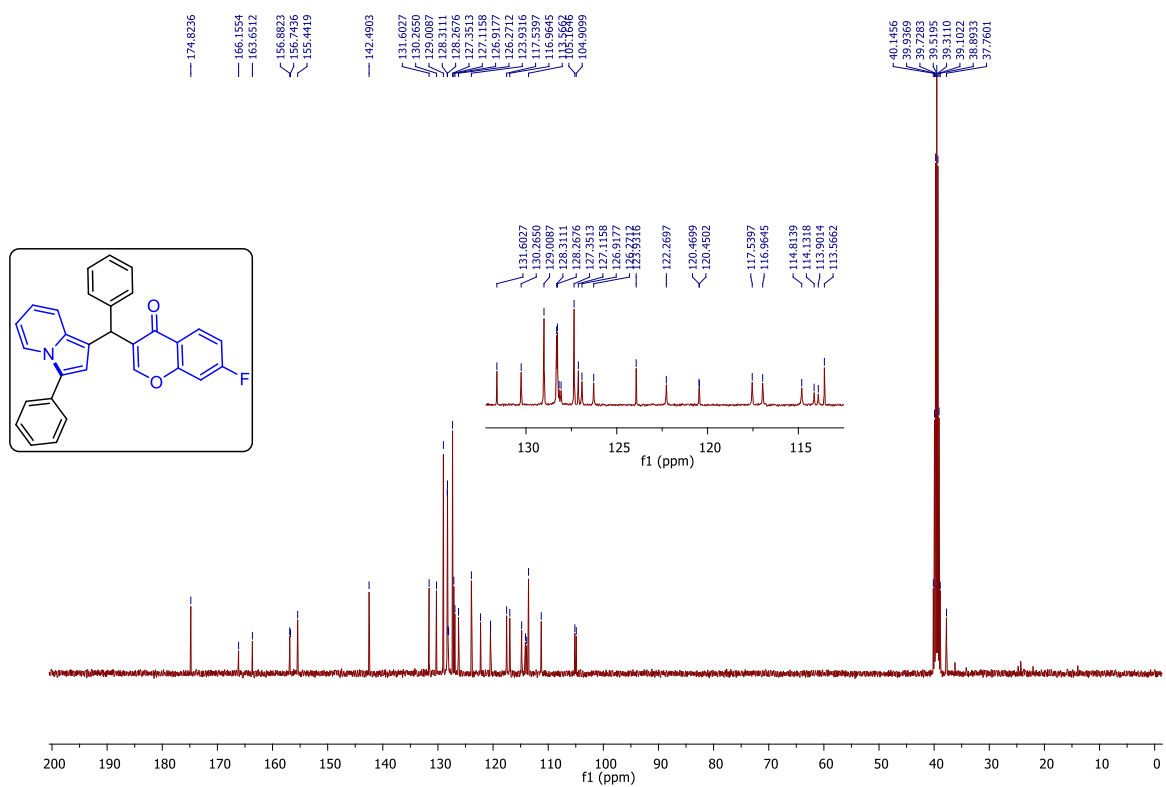
^1H NMR (400 MHz, DMSO- d_6) spectrum of (**61d**)



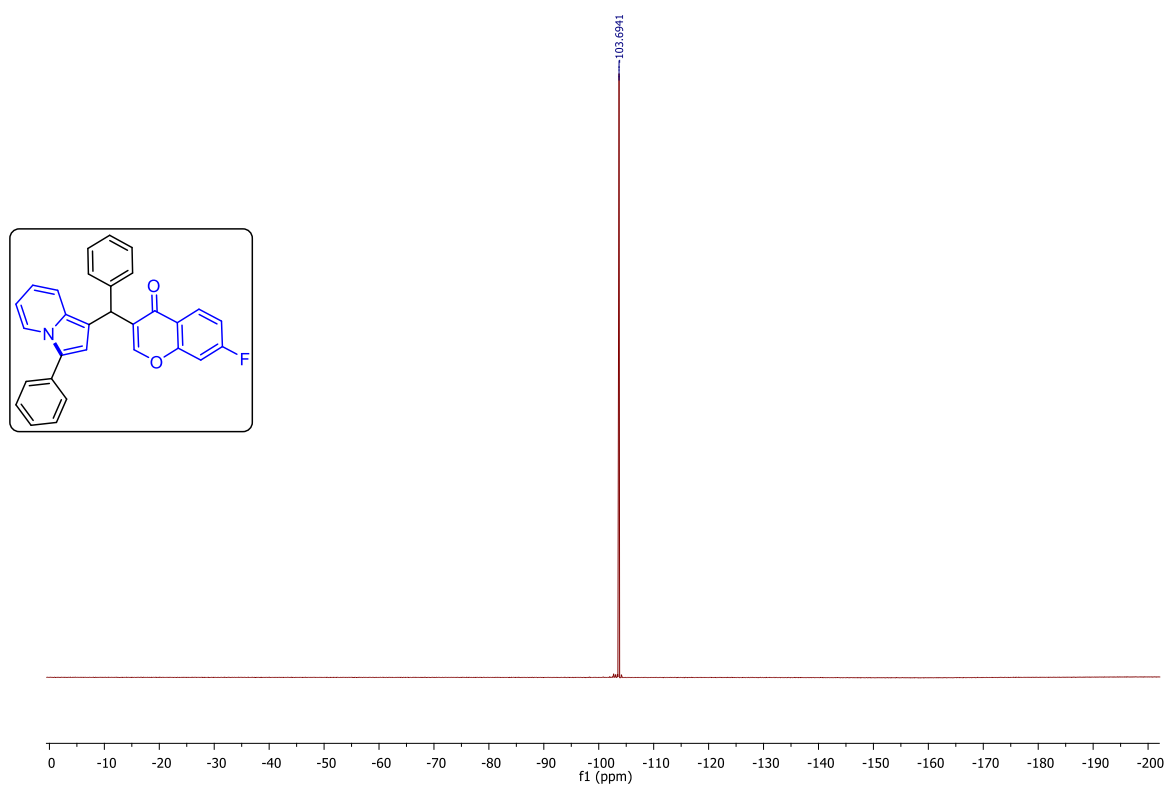
^1H NMR (400 MHz, DMSO- d_6) spectrum of (**61h**)



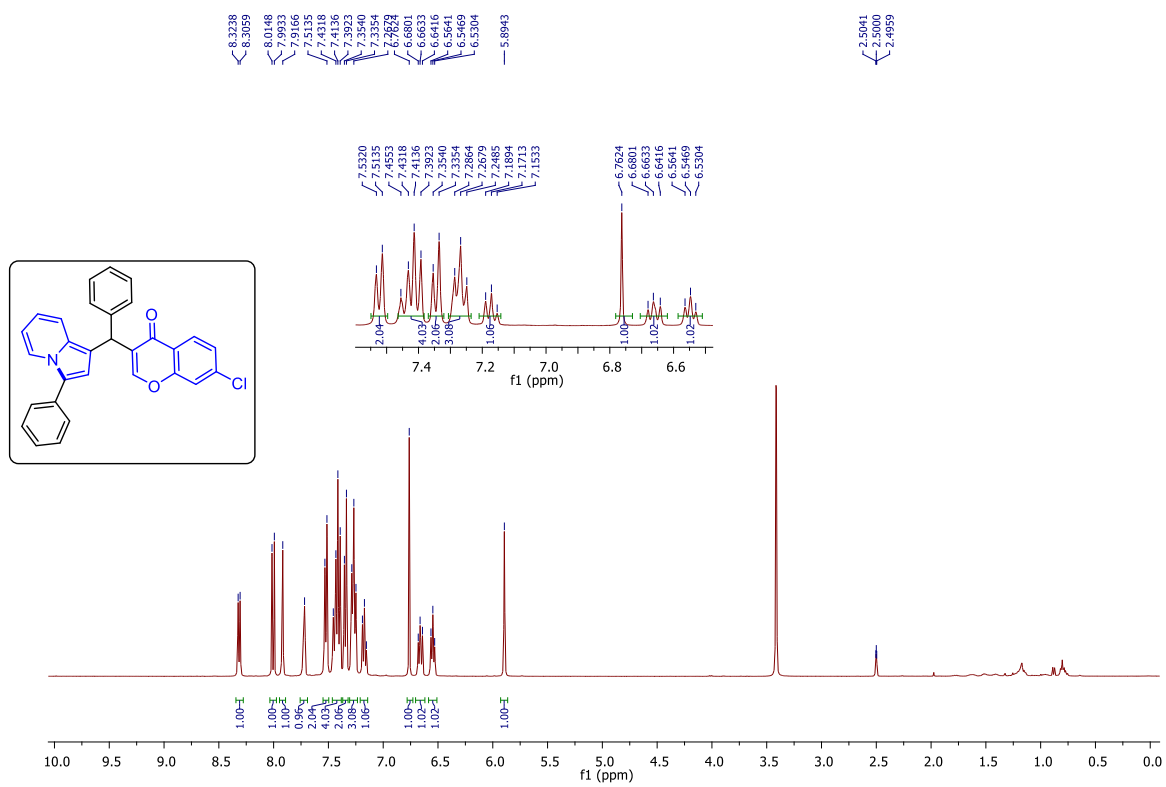
$^{13}\text{C}\{^1\text{H}\}$ NMR (100 MHz, DMSO- d_6) spectrum of (**61h**)



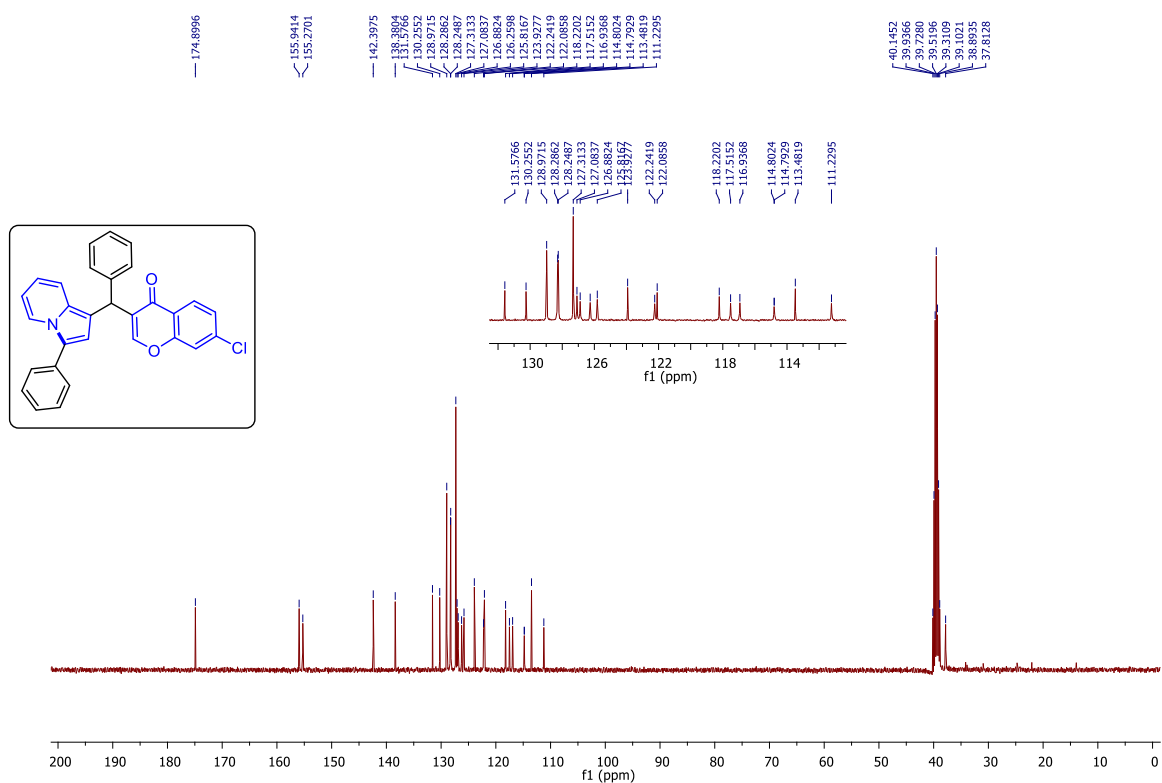
$^{19}\text{F}\{^1\text{H}\}$ NMR (376 MHz, DMSO- d_6) spectrum of (**61h**)



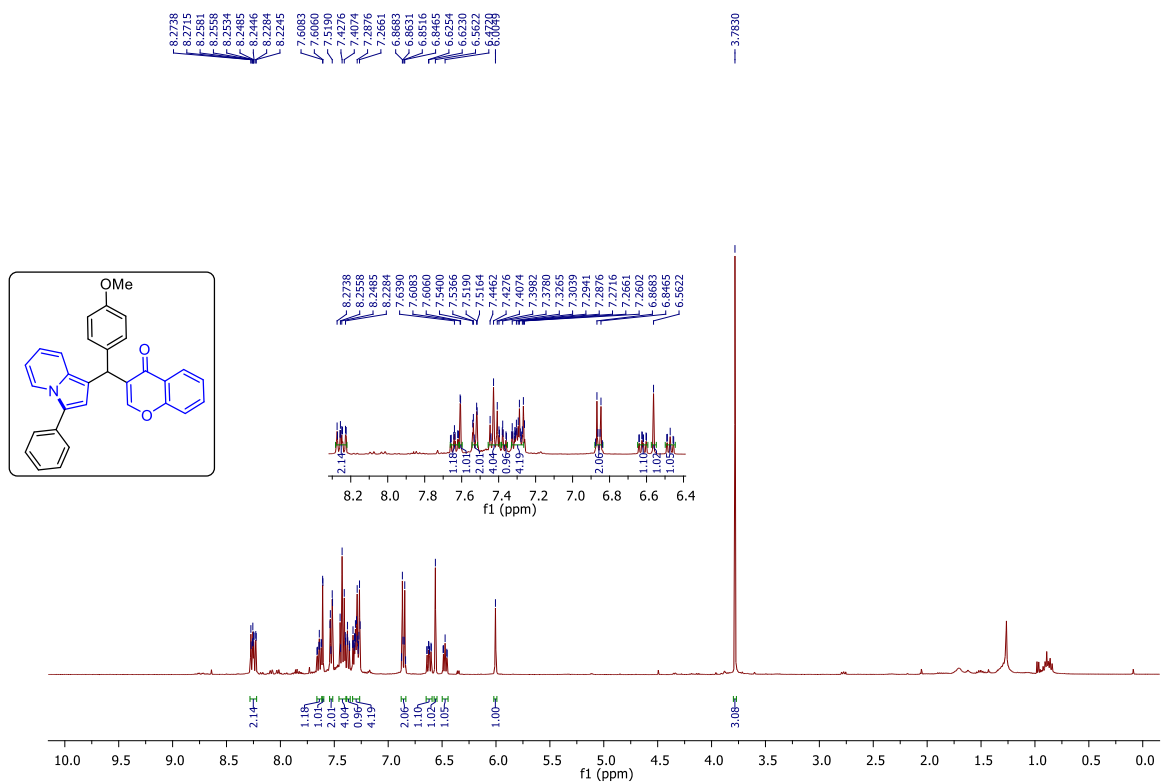
^1H NMR (400 MHz, DMSO- d_6) spectrum of (**61i**)



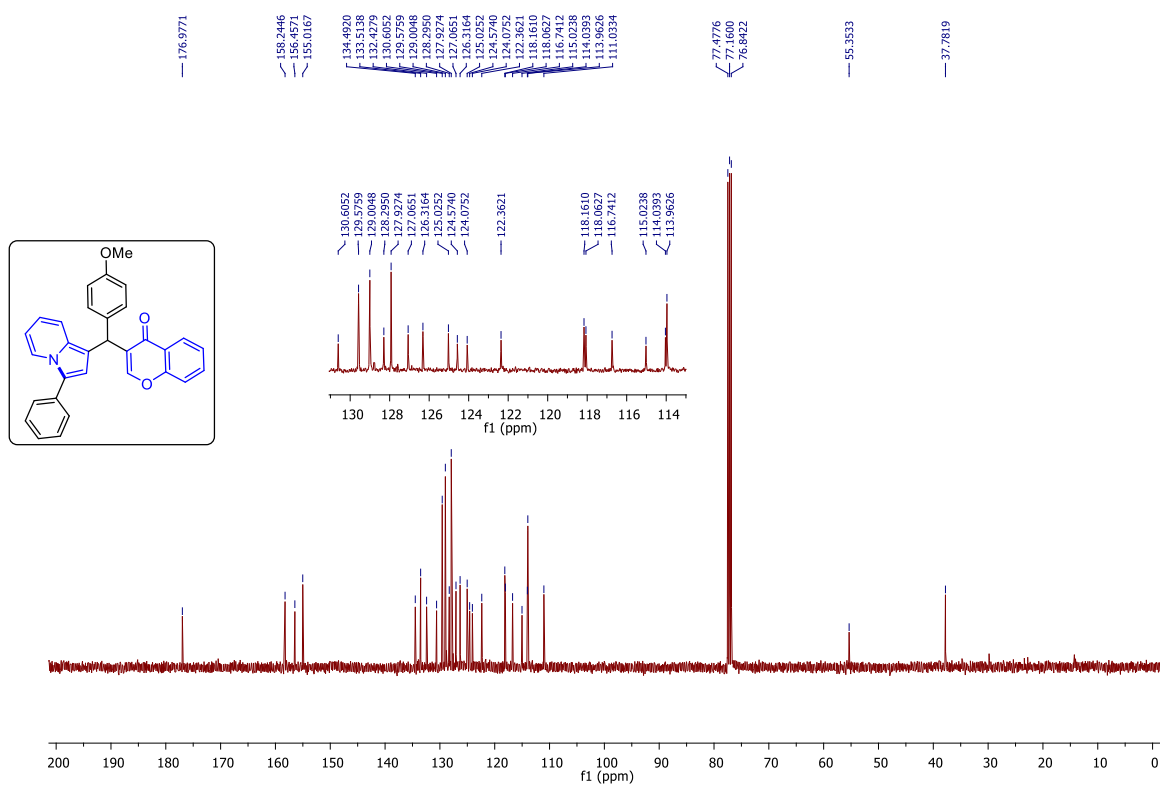
$^{13}\text{C}\{^1\text{H}\}$ NMR (100 MHz, DMSO- d_6) spectrum of (**61i**)



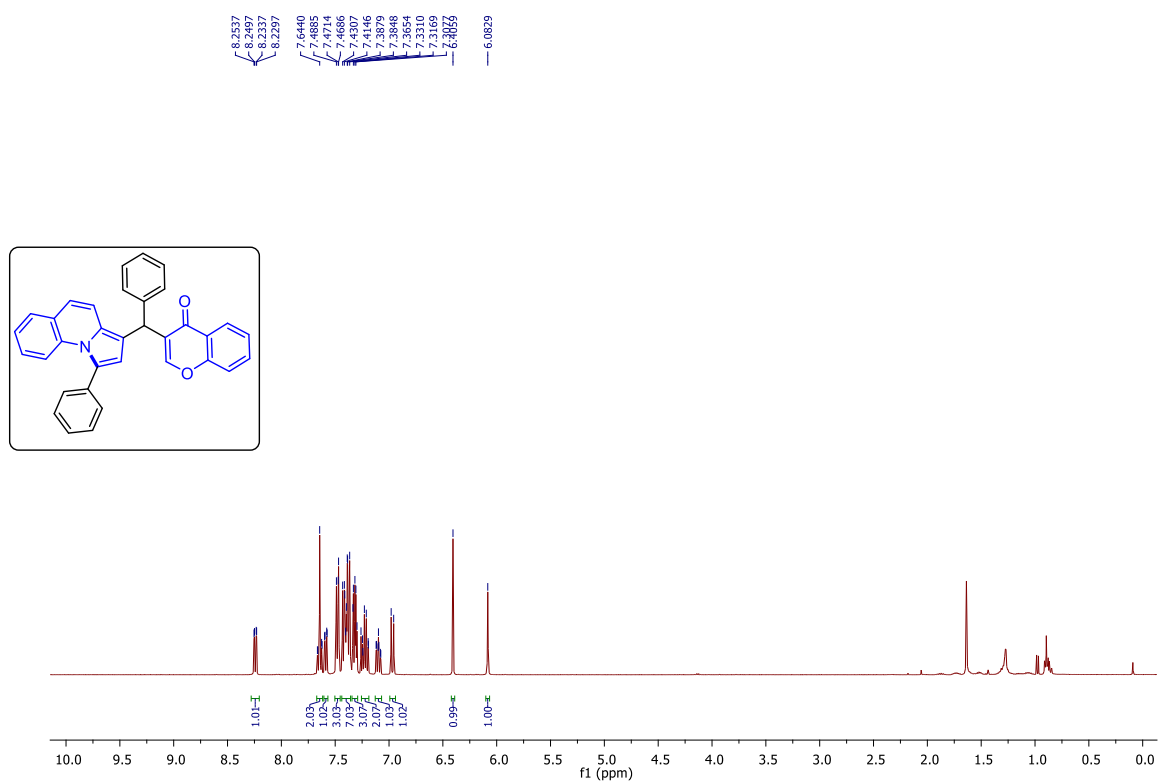
^1H NMR (400 MHz, CDCl_3) spectrum of (**62m**)



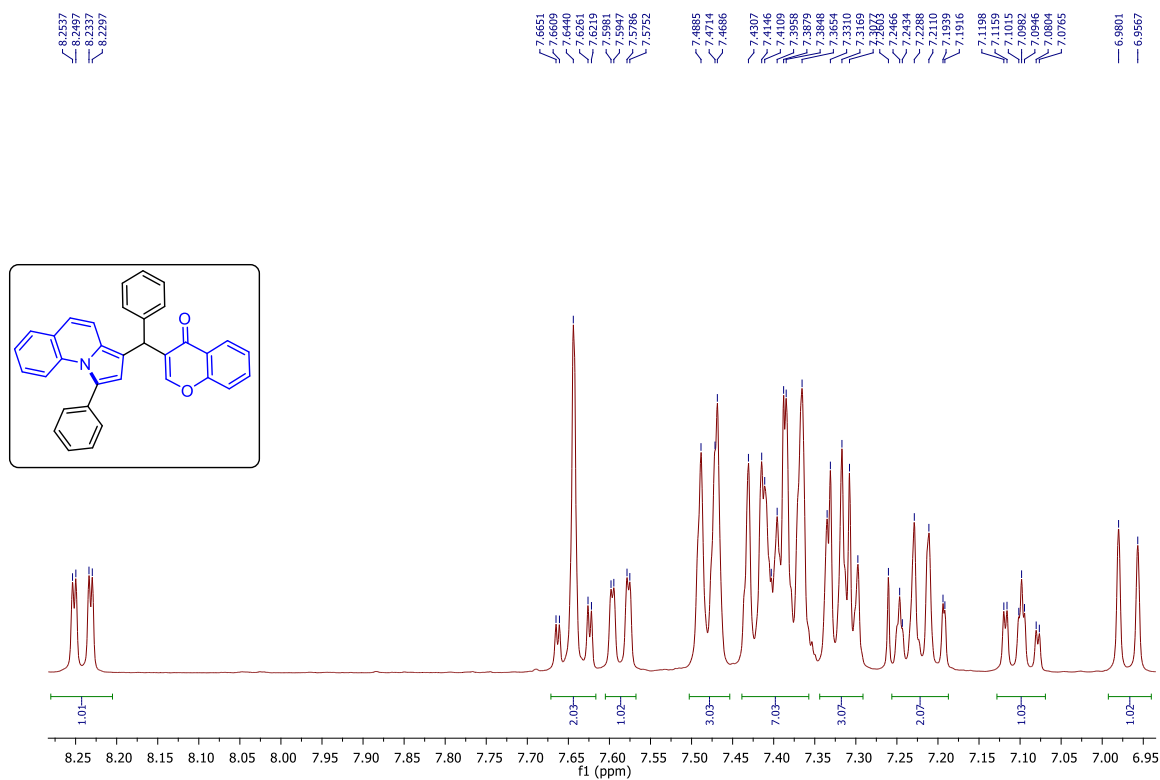
$^{13}\text{C}\{^1\text{H}\}$ NMR (100 MHz, CDCl_3) spectrum of (**62m**)



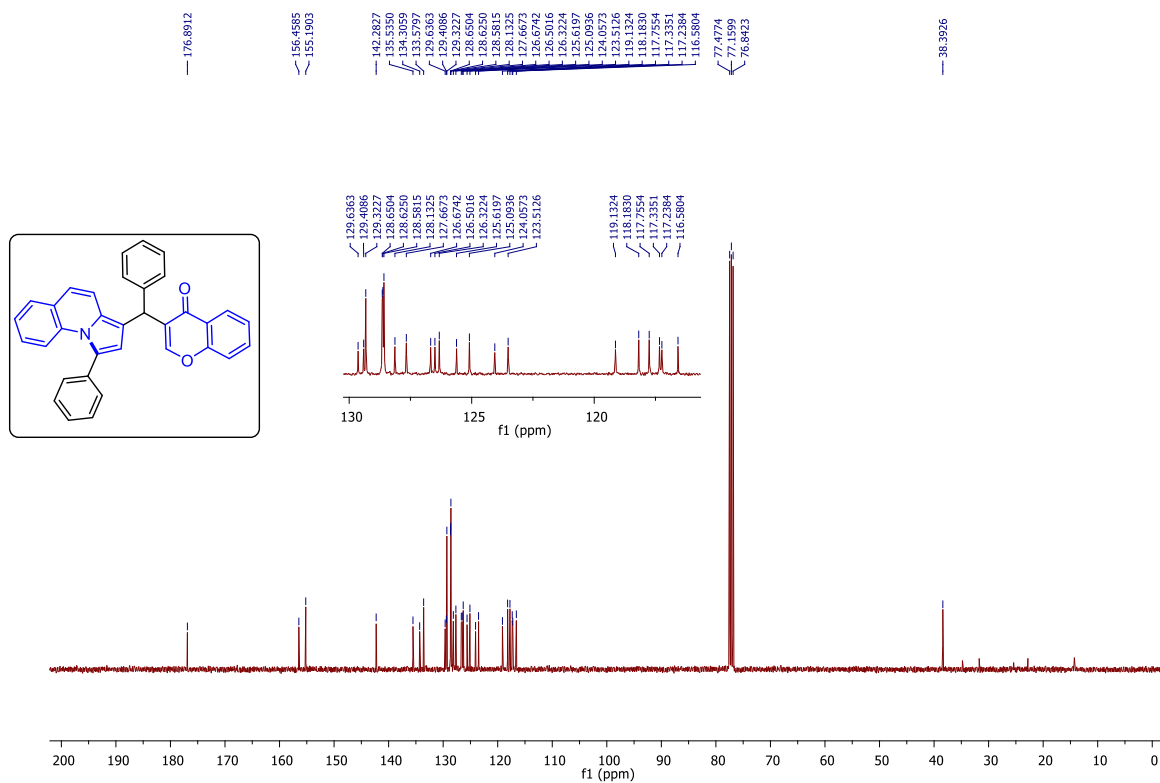
^1H NMR (400 MHz, CDCl_3) spectrum of (**63a**)



Expanded ^1H NMR (400 MHz, CDCl_3) spectrum of (**63a**)



$^{13}\text{C}\{^1\text{H}\}$ NMR (100 MHz, CDCl_3) spectrum of (**63a**)



2.7 References:

1. (a) Nohara, H. Kuriki, T. Saijo, H. Sugihara, M. Kanno, Y. Sanno, *J. Med. Chem.* **1997**, 20, 141; (b) W. Huang, Y. Ding, M.-Z. Liu, Y. Li, G.-F. Yang, *Eur. J. Med. Chem.* **2009**, 44, 3687; (c) S. K. Sharma, S. Kumar, K. Chand, A. Kathuria, A. Gupta, R. Jain, *Curr. Med. Chem.* **2011**, 18, 3825; (d) M. Mohadeszadeh, M. Iranshahi, *Mini-Rev. Med. Chem.* **2017**, 17, 1377; (e) S. R. M. Ibrahim, G. A. Mohamed, *Nat. Prod. Res.* **2015**, 29, 1489.
2. (a) S. Sabatini, F. Gosetto, G. Manfroni, O. Tabarrini, G. W. Kaatz, D. Patel, V. Cecchetti, *J. Med. Chem.* **2011**, 54, 5722; (b) G. Lewin, A. Maciuk, S. Thore, G. Aubert, J. Dubois, T. Cresteil, *J. Nat. Prod.* **2010**, 73, 702; (c) C. Echeverry, F. Arredondo, J. A. Abin-Carriquiry, J. O. Midiwo, C. Ochieng, L. Kerubo, F. Dajas, *J. Agric. Food. Chem.* **2010**, 58, 2111; (d) R. Kshatriya, V. P. Jejurkar, S. Saha, *Tetrahedron* **2018**, 74, 811; (e) D. F. Birt, S. Hendrich, W. Wang, *Pharmacol. Therapeut.* **2001**, 90, 157.
3. (a) S. Kawai, Y. Ishikawa, Y. Yoshizawa, *Anticancer Res.* **2018**, 38, 5679; (b) M. Waheed, N. Ahmed, M. A. Alsharif, M. I. Alahmadi, *Chemistry Select* **2019**, 4, 1872; (c) Y. Li, H. Zhang, *Food Funct.* **2017**, 8, 2935; (d) Y. Li, Y. Meng, Y. Yang, Y. Qin, C. Xia, Y. Ye, X. Gao, Q. Hu, *Photochem. Lett.* **2014**, 10, 46; (e) W. Huang, Y. Ding, Y. Miao, M.-Z. Liu, Y. Li, G.-F. Yang, *Eur. J. Med. Chem.* **2009**, 44, 3687; (f) M. Kuroda, S. Uchida, K. Watanabe, Y. Mimaki, *Phytochemistry* **2009**, 70, 288.
4. (a) L. Klier, T. Bresser, T. A. Nigst, K. Karaghiosoff, P. Knochel, *J. Am. Chem. Soc.* **2012**, 134, 13584; (b) K. Kim, H. Choe, Y. Jeong, J. H. Lee, S. Hong, *Org. Lett.* **2015**, 17, 2550; (c) I. Vints, S. Rozen, *J. Org. Chem.* **2014**, 79, 7261; (d) M. Spadafora, V. Y. Postupalenko, V. V. Shvadchak, A. S. Klymchenko, Y. Mély, A. Burger, R. Benhida, *Tetrahedron* **2009**, 65, 7809; (e) Q. Tang, Z. Bian, W. Wu, J. Wang, P. Xie, C. U. Pittman Jr, A. Zhou, *J. Org. Chem.* **2017**, 82, 10617; (f) D. Kang, K. Ahn, S. Hong, *Asian J. Org. Chem.* **2018**, 7, 1136; (g) R. Samanta, R. Narayan, J. O. Bauer, C. Strohmman, S. Sievers, A. P. Antonchick, *Chem. Commun.* **2015**, 51, 925.
5. A. St-Gelais, J. Alsarraf, J. Legault, C. Gauthier, A. Pichette, *Org. Lett.* **2018**, 20, 7424.
6. (a) Z. Zheng, Y. Wang, M. Xu, L. Kong, M. Wang, Y. Li, *Chem. Commun.* **2018**, 54, 6192; (b) X. Wang, G. Cheng, X. Cui, *Chem. Commun.* **2014**, 50, 652.
7. R. J. Smith, D. Nhu, M. R. Clark, S. Gai, N. T. Lucas, B. C. Hawkins, *J. Org. Chem.* **2017**, 82, 5317.
8. P. Sun, S. Gao, C. Yang, S. Guo, A. Lin, H. Yao, *Org. Lett.* **2016**, 18, 6464.

9. M. Wang, B.-C. Tang, J.-T. Ma, Z.-X. Wang, J.-C. Xiang, Y.-D. Wu, J.-G. Wang, A.-X. Wu, *Org. Biomol. Chem.* **2019**, *17*, 1535.
10. (a) J. Zhao, Y. Zhao, H. Fu, *Org. Lett.* **2012**, *14*, 2710; (b) J. A. Seijas, M. P. Vázquez-Tato, R. Carballido-Reboredo, *J. Org. Chem.* **2005**, *70*, 2855.
11. S. Vedachalam, Q.-L. Wong, B. Maji, J. Zeng, J. Ma, X.-W. Liu, *Adv. Synth. Catal.* **2011**, *353*, 219.
12. L. Wang, S. Peng, J. Wang, *Chem. Commun.* **2011**, *47*, 5422.
13. B. Liang, M. Huang, Z. You, Z. Xiong, K. Lu, R. Fathi, J. Chen, Z. Yang, *J. Org. Chem.* **2005**, *70*, 6097.
14. T. Yatabe, X. Jin, K. Yamaguchi, N. Mizuno, *Angew. Chem. Int. Ed.* **2015**, *54*, 13302.
15. (a) B. Föhlisch, *Chem. Ber.* **1971**, *104*, 348; (b) C. Balakrishna, V. Kandula, R. Gudipati, S. Yennam, P. U. Devi, M. Behera, *Synlett.* **2018**, *29*, 1087; (c) V. O. Iaroshenko, S. Mkrtchyan, A. Gevorgyan, M. Miliutina, A. Villinger, D. Volochnyuk, V. Y. Sosnovskikh, P. Langer, *Org. Biomol. Chem.* **2012**, *10*, 890.
16. For recent references, see: (a) P. Gandeepan, T. Müller, D. Zell, G. Cera, S. Warratz, L. Ackermann, *Chem. Rev.* **2019**, *119*, 2192; (b) D. J. Abrams, P. A. Provencher, E. J. Sorensen, *Chem. Soc. Rev.* **2018**, *47*, 8925; (c) W. Hao, Y. Liu, *Beilstein J. Org. Chem.* **2015**, *11*, 2132; (d) Z.-K. Li, X.-S. Jia, L. Yin, *Synthesis* **2018**, *50*, 4165; (e) Y. Liu, J. Xiong, L. Wei, *Chin. J. Org. Chem.* **2017**, *37*, 1667; (f) G.-H. Li, D.-Q. Dong, Y. Yang, X.-Y. Yu, Z.-L. Wang, *Adv. Synth. Catal.* **2019**, *361*, 832; (g) F. Bai, S. Zhang, L. Wei, Y. Liu, *Asian J. Org. Chem.* **2018**, *7*, 371; (h) J. Xiong, Y. Liu, *Chemistry Select* **2019**, *4*, 693; (i) L.-Y. Xie, S. Peng, F. Liu, G.-R. Chen, W. Xia, X. Yu, W.-F. Li, Z. Cao, W.-M. He, *Org. Chem. Front.* **2018**, *5*, 2604; (j) X. Chen, Y. Liu, *RSC Adv.* **2017**, *7*, 37839; (k) L. Deng, Y. Liu, *ACS Omega* **2018**, *3*, 11890.
17. J.-P. Wan, Y.-J. Pan, *Chem. Commun.* **2009**, 2768.
18. J. Joussot, A. Schoenfelder, L. Larquetoux, M. Nicolas, J. Suffert, G. Blond, *Synthesis* **2016**, *48*, 3364.
19. P. N. Bagle, M. V. Mane, S. P. Sancheti, A. B. Gade, S. R. Shaikh, M.-H. Baik, N. T. Patil, *Org. Lett.* **2019**, *21*, 335.
20. (a) L. Liu, Q. Wang, Z. Zhang, Q. Zhang, Z. Du, D. Xue, T. Wang, *Mol. Divers.* **2014**, *18*, 777. (b) J. P. Wan, Z. Tu, Y. Wang, *Chem. Eur. J.* **2019**, *25*, 6907.
21. M. O. Akram, S. Bera, N. T. Patil, *Chem. Commun.* **2016**, *52*, 12306.
22. (a) Q. Zhao, H. Xiang, J. A. Xiao, P. J. Xia, J. J. Wang, X. Chen, H. Yang, *J. Org. Chem.* **2017**, *82*, 9837; (b) Q.-L. Zhao, P.-J. Xia, L. Zheng, Z.-Z. Xie, Y.-Z. Hu, G.-J.

- Chen, X.-Q. Chen, H.-Y. Xiang and H. Yang, *Tetrahedron*, **2020**, 76, 130833; (c) Y. Wang, B. Hu, Q. Zhang, S. Zhao, Y. Zhao, B. Zhang, and F. Yu, *J. Chem. Res.*, **2021**, 45, 95.
23. Y. Lin, J.-P. Wan and Y. Liu, *New J. Chem.*, **2020**, 44, 8120.
24. Q. Yu, Y. Liu and J.-P. Wan, *Org. Chem. Front.*, **2020**, 7, 2770.
25. (a) D. Cheng, M. Wang, Z. Deng, X. Yan, X. Xu and J. Yan, *Eur. J. Org. Chem.*, **2019**, 4589; (b) D. Cheng, Y. Pu, M. Wang, Y. Shen, J. Shen, X. Xu and J. Yan, *Synthesis*, **2021**, 1372.
26. S. Mkrtchyan, V. O. Iaroshenko, *Chem. Commun.*, **2020**, 56, 2606.
27. S. Mkrtchyan, V. O. Iaroshenko, *J. Org. Chem.* **2021**, 86, 4896
28. Z. W. Wang, Y. Zheng, Y. E. Qian, J. P. Guan, W. D. Lu, C. P. Yuan, J. A. Xiao, K. Chen, H. Y. Xiang, H. Yang, *J. Org. Chem.* **2022**, 87, 1477.
29. J. -Y. Hu, Z. -B. Xie, J. Tang, Z. -G. Le, Z. -Q. Zhu, *J. Org. Chem.* **2022** 87, 21, 14965.
30. K. Wen, Y. Li, Q. Gao, J. Chen, J. Yang, X. Tang, *J. Org. Chem.* **2022**, 87, 9270.
31. M. Zhang, Z. Liu, L. Chen, D. Liu, Y. Sun, Z. Chai, X. -B. Chen, F. Yua, *Adv. Synth. Catal.* **2022**, 364, 4440.

Summary

In summary, the research work presented in this thesis describes the design and development of transition metal catalysed synthesis of functionalized indolizine derivatives (**Figure 1**). These compounds are fundamental in nature, being prevalent in various natural products and biologically active molecules, and also found applications in material sciences. Therefore, the development of efficient and straightforward protocols for accessing indolizine derivatives is of great significance.

This thesis has been divided into two main parts:

Part A: The first part of this research work mainly focuses on the synthesis of functionalized indolizine derivatives through a [3+2]-annulation of 2-pyridinyl substituted *para*-quinone methides (*p*-QMs) as a three-atom synthon with suitable coupling partners, including terminal alkynes and *N,N*-dimethyl enaminones. This method is significant because it offers a practical means to create diverse derivatives of indolizines, allowing for the introduction of various functional groups and modifications.

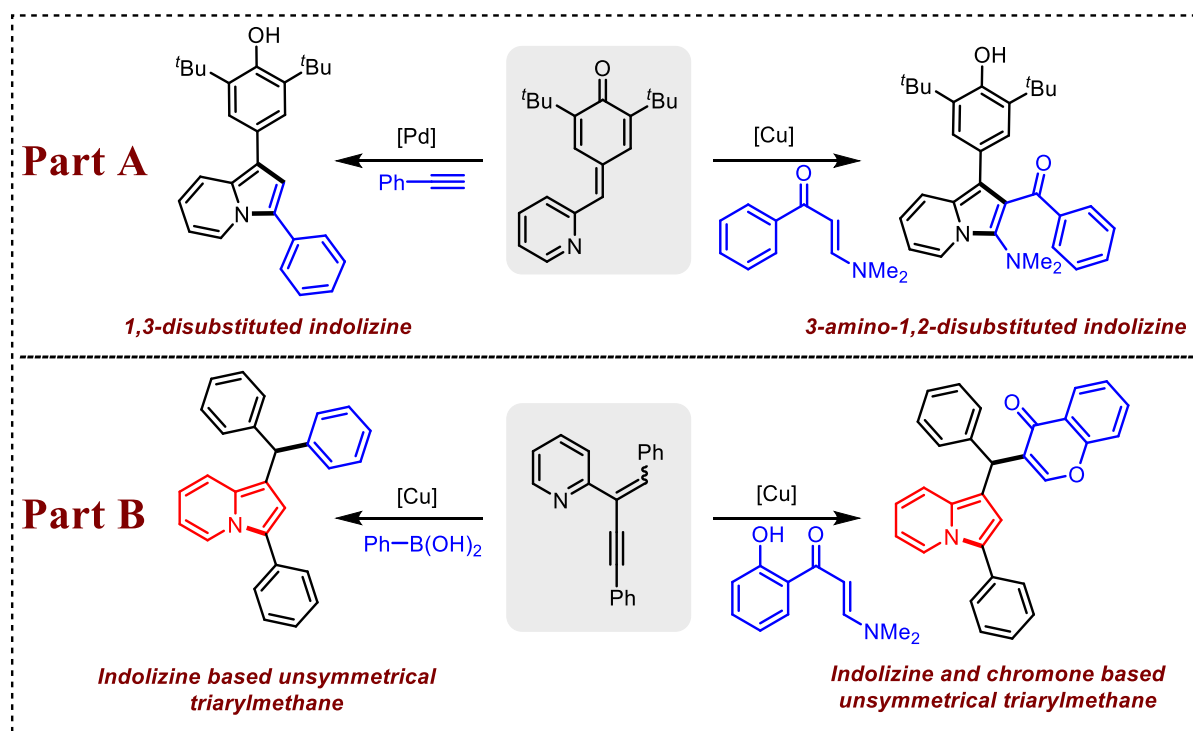


Figure 1: Summary of The Thesis

Part B: The second part of this research work focuses on the copper-catalyzed synthesis of indolizine-containing unsymmetrical triarylmethanes. This is achieved through the reaction of 2-(2-enynyl) pyridines with boronic acids and 2-hydroxyaryl substituted *N,N*-dimethyl

enaminones. The resulting compounds represent another class of indolizine derivatives, with the potential for unique properties and applications. In most of the methodologies a scale up reaction is also conducted to show the practical applicability of these transformations. Since indolizines are considered as an important class of heterocycles from medicinal chemistry to materials science, we believe that the products originating from these methods would contribute to potential bioactivities in pharmaceutical field and in the field of material science, and many of these compounds were found to be very fluorescent, that may be of importance to future studies (**Figure 2**).



Figure 2: Few of The Synthesized Products under UV-light

CURRICULUM VITAE

Mr. Feroz Ahmad

Department of Chemical Science, Indian Institute
of Science Education and Research Mohali

E-mail: ahmadferoz29@gmail.com

Mob: +91-9779924906



Experimental Organic Chemistry Skill: Firsthand experience in setting up a synthetic organic chemistry lab and designing projects. Good knowledge of organic and organometallic chemistry, performing reactions in a continuous-flow microreactor, microwave reactor, and Schlenk line. Furthermore, I have Excellent practical skills in handling air/moisture sensitive reagents/reactions and gram/milligram scale reactions. Good knowledge of multi-step synthesis. Experience in modern chromatographic and spectroscopic (IR, UV, NMR, and HRMS) techniques. Proficiency in handling HPLC and Biotage-Isolera One flash column chromatography.

Research Expertise: Synthetic Organic Chemistry, Organocatalysis.

Education and Research Training

- **2016 – 2023: Ph. D. in Synthetic Organic Chemistry**, Department of Chemical Sciences, Indian Institute of Science Education and Research (IISER) Mohali, 140306, Punjab, India.
 - **Thesis Title:** “*Metal-catalyzed Approaches to the synthesis of Indolizine Derivatives from 2-pyridinyl-substituted para-Quinone Methides and/or 2-(2-enynyl)pyridines*”
 - **Ph.D. Thesis Supervisor:** Prof. R. Vijaya Anand
- **2013 – 2014: M.Sc. in Chemistry**, Rashtrasant Tukadoji Maharaj Nagpur University, Maharashtra, India with CGPA **7.84**.
 - **M.Sc. Thesis Title:** “*Quality assessment of coal from kanhan valley coalfield Maharashtra*” carried out at CSIR-Central Institute of Mining and fuel Research, Nagpur Unit II.

- **M.Sc. Thesis Supervisor:** Dr. S. P. Singh (Officer-in-charge & head CSIR-CIMFR, Nagpur unit II)
- **2010 – 2012: Bachelor of Science**, Govt. Degree College kargil, (Affiliated with University of Kashmir, srinagar), with **First Division (61.33%)**.

Awards/Scholarships and Grants

- Awarded **Senior Research Fellowship** and **Junior Research Fellowship** (MHRD Fellowship) from University Grants Commission (UGC)-New Delhi from August 2016 to July 2021.
- Qualified **UGC-NET/JRF** with all India 96th rank in **CSIR-UGC NET** (Council of Scientific and Industrial Research-University Grants Commission National Eligibility Test) examination held on June 2015.

List of Publications

1. [Ahmad, F.;](#) Ranga, P. K.; Fatma, S.; Kumar, A.; Anand, R. V.*

“Cu(II)-Catalysed [3+2]-Annulation of 2-Pyridinyl-substituted *p*-Quinone Methides with Enaminones: Access to Functionalized Indolizine Derivatives” *Adv. Synth. Catal.* **2023**, 365, 3271 – 3276.

2. [Ahmad, F.;](#) Ranga, P. K.; Fatma, S.; Pankhade, Y. A.; Gauda, A.; Anand, R. V.*

“Pd(II)-catalysed annulation of terminal alkynes with 2-pyridinyl-substituted *p*-quinone methides: direct access to indolizines” *Chem. Comm.* **2022**, 58, 13238 – 13241.

3. [Ahmad, F.;](#) Ranga, P. K.; Singh, G.; Tyagi, A.; Anand, R. V.*

“Recent Advances in the Organocatalytic Applications of Cyclopropene- and Cyclopropenium-based Small Molecules” *Org. Biomol. Chem.*, **2021**, 19, 9541 – 9564.

4. [Ahmad, F.;](#) Ranga, P. K.; Fatma, S.; Anand, R. V.*

“Cu-Catalysed Synthesis of Chromone and Indolizine Based Unsymmetrical Triarylmethanes From 2-(2-enynyl)Pyridines” (*Manuscript under Preparation*).

5. [Ahmad, F.;](#) Ranga, P. K.; Fatma, S.; Anand, R. V.*

“Cu-Catalysed Synthesis of Indolizine Containing Unsymmetrical Triarylmethanes From 2-(2-enynyl)Pyridines” (*Manuscript under Preparation*).

6. Pankhade, Y. A.; Pandey, R.; Fatma, S.; [Ahmad, F.;](#) Anand, R. V.*

“TfOH-Catalyzed Intramolecular Annulation of 2-(Aryl)-Phenyl-Substituted *p*-Quinone Methides under Continuous Flow: Total Syntheses of Selaginpulvin I and Isoselagintamarlin A” *J. Org. Chem.* **2022**, 87, 3363 – 3377.

7. Ranga, P. K.; [Ahmad, F.](#); Nager, P.; Rana, P. S.; Anand, R. V.*

“Bis(amino)cyclopropenium Ion as a Hydrogen-bond Donor Catalyst for 1,6-Conjugate Addition Reactions” *J. Org. Chem.* **2021**, 86, 4994 – 5010.

8. Paluru, D. K.; Mahesh, S.; [Ahmad, F.](#); Anand, R. V.*

“A Cascade Synthesis of Hetero-arylated Triarylmethanes Through a Double 5-endo-dig Cyclization Sequence” *Chem. Asian. J.* **2019**, 14, 4688.

9. Mahesh, S.; Paluru, D. K.; [Ahmad, F.](#); Patil, S.; Kant, G.; Anand, R. V.*

“Synthesis of indolizine containing diaryl- and triarylmethanes through a Cu-catalyzed domino cyclization of 2-(2-enynyl)-pyridines” *Asian J. Org. Chem.* **2017**, 6, 1857 – 1866.

Conferences/Symposia

- Participated in the *National Symposium In Chemical Sciences* organized by Royal Society of Chemistry West India held at Hislop College Nagpur, India (14th September, 2013).
- Participated in the 24th *National Conference on Liquid Crystals* held at the Department of Chemical Sciences, Indian Institute of Science Education and Research (IISER) Mohali, S. A. S. Nagar, India (11 – 13th October, 2017).
- Presented a poster on “One-pot synthesis of heteroarylated triarylmethanes through a double 5-endo-dig cyclization cascade” [Ahmad F.](#); Anand, R. V. in the *Recent Advances in Organic and Bioorganic Chemistry* (RAOBC) held at the Department of Chemical Sciences, Indian Institute of Science Education and Research (IISER) Mohali, S. A. S. Nagar, India (22nd – 24th March, 2019).
- Presented a poster on “One-pot synthesis of heteroarylated triarylmethanes through a double 5-endo-dig cyclization cascade” [Ahmad F.](#); Anand, R. V. in the “*National Conference On Recent Trends in Chemical Sciences*” & *RSC Workshop On “Periodic Table: Boon for Mankind*” organized by Department of Chemistry, University of Delhi, India (30th August – 1st September 2019)
- Presented a poster on “Synthesis of heteroarylated triarylmethanes through a copper-catalyzed 5-endo-dig cyclization” [Ahmad F.](#); Anand, R. V. in the *1st Crikc Chemistry*

Symposium (CCS 2019) held at the Department of Chemical Sciences, Indian Institute of Science Education and Research (IISER) Mohali, S. A. S. Nagar, India (2nd & 3rd November, 2019).

- Presented a poster on “An Efficient Metal Catalyzed Approach for the Synthesis of Indolizine-Containing Unsymmetrical Triarylmethanes” [Ahmad F.](#); Anand, R. V. in the *16th Junior National Organic Symposium (J-NOST)* organized by Indian Institute of Science, Bangalore, India (31st October – 1st November 2020).
- Participated in the *ACS Publications Symposium: The Power of Chemical Transformations* virtual event organized by ACS Publications in partnership with the university of Hong Kong (20th – 21st May, 2021).
- Participated in the *2nd International Conference on Main Group Molecules to Materials* (MMM-II) held at the Department of Chemical Sciences, National Institute of Science Education and Research (NISER) Bhubaneswar, Odisha, India (13th – 15th December, 2021).
- Participated in the *Online Faculty Development Program on “Research Methodology: Tools & Techniques”* organized by IES University and IES College of Technology, Bhopal, India (20th – 22nd January, 2022).
- Presented a poster on “An efficient metal-catalyzed approaches for the synthesis of indolizine-containing triarylmethanes” [Ahmad F.](#); Anand, R. V. in the *International Symposium On Recent Advances In Self-Assembled Materials and Supramolecular Chemistry* held at Department of Chemistry, Guru Nanak Dev University, Amritsar, India on 19th March 2022.
- Participated in the *29th CRSI-National Symposium in Chemistry & CRSI-ACS Symposium Series in Chemistry* held at the Department of Chemical Sciences, Indian Institute of Science Education and Research (IISER) Mohali, S. A. S. Nagar, India (07-09th July, 2022).